Real-Time Multiprocessor Locks with Nesting: Optimizing the Common Case

Catherine E. Nemitz, Tanya Amert, and James H. Anderson
Department of Computer Science, University of North Carolina at Chapel Hill

ABSTRACT

In prior work on multiprocessor real-time locking protocols, only protocols within the RNLP family support unrestricted lock nesting while guaranteeing asymptotically optimal priority-inversion blocking bounds. However, these protocols support nesting at the expense of increasing the cost of processing non-nested lock requests, which tend to be the common case in practice. To remedy this situation, a new *fast-path mechanism* is presented herein that extends prior RNLP variants by ensuring that non-nested requests are processed efficiently. This mechanism yields overhead and blocking costs for such requests that are nearly identical to those seen in the most efficient single-resource locking protocols. In experiments, the proposed fast-path mechanism enabled observed blocking times for non-nested requests that were up to 17 times lower than under an existing RNLP variant.

CCS CONCEPTS

• **Computer systems organization → Real-time systems**; *Embedded and cyber-physical systems*; *Embedded software*; • **Software and its engineering → Mutual exclusion**; **Real-time systems software**; **Synchronization**; *Scheduling*; *Process synchronization*;

KEYWORDS

multiprocess locking protocols, nested locks, priority-inversion blocking, reader/writer locks, real-time locking protocols

ACM Reference format:
Catherine E. Nemitz, Tanya Amert, and James H. Anderson. 2017. Real-Time Multiprocessor Locks with Nesting: Optimizing the Common Case. In *Proceedings of RTNS '17, Grenoble, France, October 4–6, 2017,* 274 pages.
https://doi.org/10.1145/3139258.3139262

1 INTRODUCTION

Multicore technologies have the potential to enable a wealth of new computationally intensive embedded real-time applications, provided efficient resource-allocation infrastructure is available. Such infrastructure must necessarily include support for multiprocessor real-time locking protocols. Evidence suggests that the ability to nest lock requests to allow a task to access multiple resources simultaneously is commonly required in practice, even though non-nested requests predominate [1, 3]. However, only a few protocols exist that support unrestricted nesting, and of those that do, only those in the RNLP (real-time nested locking protocol) family provide asymptotically optimal priority-inversion blocking (pi-blocking) bounds.

The RNLP family includes the basic RNLP [14], which provides mutex sharing, the RW-RNLP [13], which provides reader/writer sharing, and the C-RNLP [10], which provides contention-sensitive mutex sharing. A locking protocol is *contention-sensitive* if a task's pi-blocking time is $O(C)$, where C is the number of tasks actually contending for the same resources [10]. The key to ensuring contention-sensitivity is to avoid *transitive blocking chains*, which are caused by nested requests and may create blocking relationships between otherwise non-conflicting tasks.

To support nested requests, each RNLP variant employs logic more complicated than that of single-resource protocols. This logic is the most complex in the C-RNLP because it ensures contention-sensitivity. The RNLP and the RW-RNLP employ simpler logic but sacrifice contention-sensitive pi-blocking, even for non-nested requests. Thus, these protocols support nesting (the *less common* case) at the expense of increased processing costs and/or pi-blocking bounds for non-nested requests (the *more common* case).

Contributions. Motivated by this observation, we propose a new *fast-path mechanism* for the RNLP family that was designed with the twin goals of ensuring non-nested lock requests are **(i)** contention-sensitive and **(ii)** incur low lock/unlock overheads comparable to those of single-resource protocols. We present this fast-path mechanism in the context of a new reader/writer RNLP variant, which we call the *fast* RW-RNLP.[1] In reader/writer sharing, read requests can execute concurrently but write requests require exclusive access [6]. Since reader/writer sharing subsumes mutex sharing, the fast RW-RNLP can be applied to support the latter.

We build directly on two prior protocols. The first is the *phase-fair ticket lock (PF-TL)*, which is used to provide reader/writer access to a single resource [4]. The PF-TL is a non-preemptive spin-lock. The protected resource has two FIFO request queues, one for reads and one for writes. If both kinds of requests are queued concurrently, the protocol alternates between *read phases* wherein read requests are given preference, and corresponding *write phases*. The PF-TL has asymptotically optimal pi-blocking bounds and very low runtime overheads (and is trivially contention-sensitive).

The other protocol we build on is the RW-RNLP. At this point, it suffices to know that the RW-RNLP uses two queues per resource, one for readers and one for writers, like the PF-TL does for a single resource. However, additional complications arise because tasks can hold multiple resources at the same time. This affects the queueing logic and the orchestration of phases. The latter becomes more difficult because different resources may be in different phases.

Work supported by NSF grants CNS 1409175, CPS 1446631, and CNS 1563845, AFOSR grant FA9550-14-1-0161, ARO grant W911NF-14-1-0499, and funding from General Motors. This material is based upon work supported by the National Science Foundation Graduate Research Fellowship Program under Grant No. DGS-1650116. Any opinions, findings, and conclusions or recommendations expressed in this material are those of the author(s) and do not necessarily reflect the views of the National Science Foundation.

RTNS '17, October 4–6, 2017, Grenoble, France

ACM ISBN 978-1-4503-5286-4/17/10…$15.00
https://doi.org/10.1145/3139258.3139262

[1] The terminology "fast-*in-the-common-case* RW-RNLP," which is obviously too verbose, would be more technically precise.

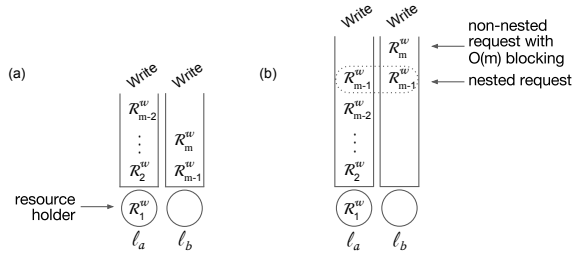

Figure 1: Impact of transitive blocking on non-nested requests. In (b), $\mathcal{R}_{m-1}$ requests ℓ_a and ℓ_b together using a DGL, as allowed by the RW-RNLP.

The more complicated queueing logic of the RW-RNLP causes even non-nested requests to incur higher lock/unlock overheads. Additionally, such requests do not have contention-sensitive pi-blocking bounds because they may become part of transitive blocking chains caused by nested requests. A simple example is given in Fig. 1, which depicts two resources ℓ_a and ℓ_b, on m processors, accessed by m write requests, $\mathcal{R}_1, \ldots, \mathcal{R}_m$, issued in this order. Two scenarios are shown that result in different pi-blocking times for request $\mathcal{R}_m$. In inset (a), there are no nested requests, and each resource is protected by a PF-TL. Here, $\mathcal{R}_m$ is pi-blocked by only one other request, which is clearly in accordance with the definition of contention-sensitivity. In inset (b), request $\mathcal{R}_{m-1}$ accesses both resources, and the RW-RNLP is used. Here, the nested request $\mathcal{R}_{m-1}$ forces $\mathcal{R}_m$ to be pi-blocked by all other requests, which is clearly not contention-sensitive.

In our fast RW-RNLP, non-nested requests are immune from the effects for transitive blocking chains caused by nesting. This is achieved by employing a modular design that mostly separates concerns related to handling nested and non-nested requests. This modular design also facilitates applying the protocol in different contexts. For example, one of the components we introduce directly supports constant-time access for all requests in systems of single-writer, multiple-reader resources, a common use case in embedded systems [9]. Also, by altering one of the components, contention-sensitivity can also be ensured for nested requests (like with the C-RNLP, but at the expense of greater overheads for such requests). Waiting in the fast RNLP can be realized by either spinning or suspension, though we consider only the former in detail due to space constraints. When no nested requests occur, the fast RW-RNLP functions nearly identically to a set of per-resource PF-TLs.

This similarity is borne out in experiments we conducted in which lock/unlock overheads and observed pi-blocking times were recorded for non-nested requests. We found that lock/unlock overheads for such requests were nearly identical under the fast RW-RNLP and PF-TLs. We also found that observed pi-blocking times for such requests were reduced compared to the RW-RNLP. This is because such requests require less overhead and are immune to transitive blocking effects under the fast RW-RNLP.

Organization. In the rest of the paper, we give needed background (Sec. 2), describe the fast RW-RNLP in detail (Sec. 3), discuss our experiments (Sec. 4), and conclude (Sec. 5).

2 BACKGROUND

In this section, we present relevant background material.

Task model. We consider the classic sporadic real-time task model (we assume familiarity with this model) and focus on a system $\Gamma = \{\tau_1, \ldots, \tau_n\}$ of n tasks scheduled on m processors by a job-level fixed-priority scheduler (*e.g.* partitioned, global, or clustered earliest-deadline-first). We denote an arbitrary job of task τ_i as J_i.

Resource model. We assume the existence of n_r shared resources, denoted $\mathcal{L} = \{\ell_1, \ldots, \ell_{n_r}\}$. When a job J_i requires access to one or more of these resources, it *issues* a *request* $\mathcal{R}_i$ for its needed resources by invoking a locking protocol. We say that $\mathcal{R}_i$ is *satisfied* as soon as J_i *holds* its requested resources and that it has *completed* once J_i has *released* all of those resources. A request $\mathcal{R}_i$ is considered to be *active* during the time interval that begins with its issuance and ends with its completion. Whenever job J_i holds any resources, it is said to be executing within a *critical section*. We let L_i denote the maximum duration of a critical section of J_i and define $L_{max} = \max_{1 \le i \le n}\{L_i\}$.

We allow requests to be nested. The essence of nesting is that jobs are allowed to hold multiple resources simultaneously. Ordinarily, nesting is realized by allowing jobs to request different resources individually. Instead, we assume that such a job requests all of its needed resources via one request. The resulting functionality is equivalent to a mechanism called a *dynamic group lock* (*DGL*) [12], which allows groups of resources to be coalesced under one lock dynamically at runtime. (This is different from ordinary group locks, which are used to coordinate access to groups of resources that are statically determined offline.)

The usage of DGLs avoids deadlock. Another way to avoid deadlock is by requiring resources to be acquired according to some prescribed ordering. When using DGLs instead of this approach, jobs may sometimes have to request resources that are not actually needed if conditional code exists. For example, if after acquiring resource ℓ_a, job J_i acquires one of resources ℓ_b and ℓ_c based on some condition, it would have to acquire all three resources via one request. While this functionality may seem to put DGLs at a disadvantage, the usage of DGLs results in the same worst-case pi-blocking bounds (see below) under all existing RNLP variants as when resource orderings are enforced.

Given our focus on reader/writer sharing, we classify resource accesses as either *reads* or *writes*: a resource may be accessed by multiple jobs concurrently for reading but by only one job at a time for writing. If a job requests multiple resources via one request, we assume that all such resources are requested for either reading or writing. Mechanisms for handling mixed requests, comprised of both read and write accesses, have been presented in prior work [12]; our focus is efficiently processing *non-nested* requests.

If a request $\mathcal{R}_i$ is a read (resp., write) request, then we will often use the notation $\mathcal{R}_i^r$ (resp., $\mathcal{R}_i^w$) to emphasize its type. If its type is not relevant, then we will simply use $\mathcal{R}_i$. We let D_i denote the set of resources requested by $\mathcal{R}_i$. Additionally, we denote the maximum critical-section length over all read (resp., write) requests by any task as L_{max}^r (resp., L_{max}^w).

Pi-blocking. When designing a real-time locking protocol, the primary goal is to enable pi-blocking to be bounded. In the multiprocessor case, the precise definition of pi-blocking is subtle as it depends on how waiting is realized (spinning vs. suspension) and on certain analysis assumptions [2]. Due to space constraints, we limit our attention to protocols that use spinning to realize blocking and that are invoked non-preemptively (*i.e.*, a resource-requesting job is non-preemptive for the entire time it is executing code involving the acquisition, use, and release of resources), but

suspension-based variants of our fast RW-RNLP can be obtained by slightly altering the spin-based version presented later. (We are nearing the completion of a suspension-based implementation and intend to release it soon.) Non-preemptive execution is an example of a *progress mechanism* [2]: it ensures that lock-holding tasks are not delayed by untimely preemptions and thus make progress. With spin-based waiting, a job can be considered to be *pi-blocked* if it is spinning.[2]

Analysis assumptions. In our analysis of pi-blocking, we consider critical-section lengths and the number of critical sections per job to be constants, and m and n to be variables, as in prior work [2]. If t is the time at which request $\mathcal{R}_i$ is issued, then we define the *contention* C_i of $\mathcal{R}_i$ to be the number of other active requests at time t that require resources in common with $\mathcal{R}_i$. A reader/writer locking protocol ensures *contention-sensitivity* for a request $\mathcal{R}_i$ if the worst-case pi-blocking for $\mathcal{R}_i$ is $O(1)$ if it is a read request, and $O(C_i)$ if it is a write request. These pi-blocking bounds are asymptotically optimal for non-preemptive, spin-based locking protocols [12].

Related work. In recent years, a number of locking protocols have been presented that are asymptotically optimal with respect to pi-blocking. These include RNLP variants [10, 13, 14] that provide *fine-grained* lock nesting, meaning that each resource is protected by its own lock. The only other protocols known to us that provide fine-grained lock nesting are the multiprocessor bandwidth inheritance protocol [7] and MrsP [5]; however, neither is optimal in any sense. To our knowledge, the only existing protocols that distinguish between read and write requests are single-resource phase-fair locks and the RW-RNLP, both discussed next.

Phase-fair locks. Given our focus (non-preemptive spin locks), phase-fair reader/writer locks are perhaps the best contention-sensitive option in terms of lock/unlock costs (*i.e.*, the time required to acquire or release a lock) if all requests are single-resource requests [4]. As noted earlier, a phase-fair lock utilizes two FIFO queues, one for read requests and one for write requests, and alternates between read phases and write phases. Several possible implementations of phase-fair locks were considered by Brandenburg and Anderson [4]. They found the phase-fair ticket-lock (PF-TL) to be comparable to or better than other phase-fair implementations from the perspective of lock/unlock costs.

The RW-RNLP. As mentioned earlier, the RW-RNLP uses two per-resource FIFO queues, one for read requests and one for write requests. Furthermore, it uses a mechanism called *request entitlement* to orchestrate reader and writer phases; the entitlement rules determine "who" (reader or writer) must concede to "whom": entitled requests do not concede. In Sec. 3, we consider in detail a new variant of the RW-RNLP, which we call the RW-RNLP*, that is useful for our purposes. We carefully explain there the concept of entitlement. The RW-RNLP is actually a family of protocols because waiting can be realized by spinning or suspension and because different mechanisms for dealing with priority inversions are required depending on how tasks are scheduled. For the non-preemptive, spin-based variant of the RW-RNLP (our focus), worst-case pi-blocking is $O(1)$ for read requests and $O(m)$ for write requests. These bounds are asymptotically optimal, assuming contention for write requests is $\Omega(m)$.

[2] A job can be pi-blocked at release by lower-priority jobs executing non-preemptively. By our analysis assumptions, this *release blocking* is asymptotically upper bounded by the maximum spin blocking for any such jobs, so we focus on spin blocking.

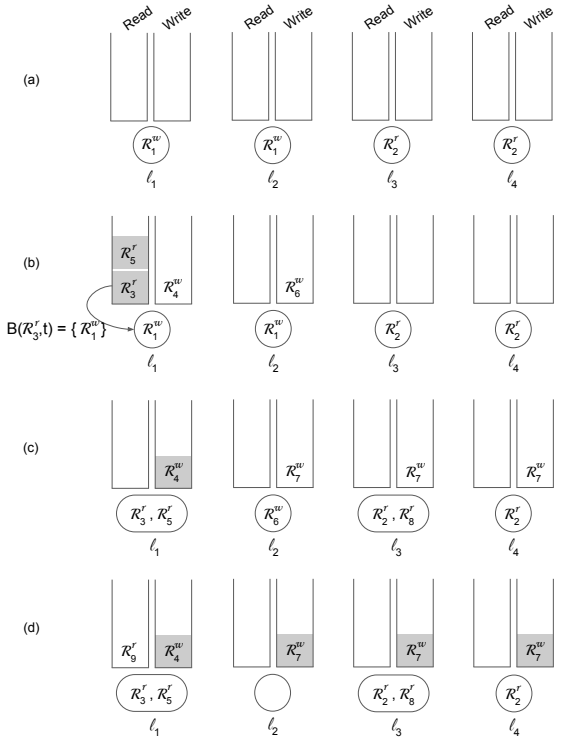

Figure 2: Example illustrating the rules of the RW-RNLP*.

3 THE FAST RW-RNLP

Our proposed fast RW-RNLP is constructed based on a new variant of the RW-RNLP called the RW-RNLP* and existing locking protocols. In this section, we describe the RW-RNLP* and its pi-blocking analysis and then present the fast RW-RNLP.

3.1 The RW-RNLP*

The RW-RNLP* is obtained from the RW-RNLP by altering one aspect of its design and changing the context in which it is applied. For each resource ℓ_a, the RW-RNLP* maintains two queues Q_a^r and Q_a^w, for unsatisfied read and write requests, respectively.

Example 3.1. We will use Fig. 2 as a continuing example to illustrate important concepts in the design of the RW-RNLP*. Each inset of this figure shows read and write queues for four resources: ℓ_1, ℓ_2, ℓ_3, and ℓ_4. At the time illustrated in Fig. 2(a), the write request $\mathcal{R}_1^w$ is satisfied for its requested resources $D_1 = \{\ell_1, \ell_2\}$, as indicated by being positioned within the circles denoting the resources ℓ_1 and ℓ_2. Because $\mathcal{R}_1^w$ is satisfied, it is not in any of the queues. Similarly, the read request $\mathcal{R}_2^r$ for $D_2 = \{\ell_3, \ell_4\}$ is satisfied.

Basic RW-RNLP rules.* We describe the RW-RNLP* via a set of rules to which an implementation must conform. With the exception of Rule P3, all of the rules below are taken directly from [13]. As we shall see in Sec. 3.2, Rule P3 enables tighter pi-blocking bounds to be computed in our context.

The first three rules place constraints on how the protocol is used; the first two essentially enforce non-preemptive scheduling and the third introduces our specific restricted context.

P1 A resource-holding job is always scheduled.

P2 At most m jobs may have incomplete resource requests at any time, at most one per processor.

P3 There is at most one incomplete non-nested write request and one incomplete nested write request per resource at any time.

While Rule P3 may seem restrictive, it will be upheld by definition when the RW-RNLP* is applied in the context of the fast RW-RNLP. It is also trivially upheld in systems with only single-writer resources, which is common use case we consider later. The following are general rules that define how requests are processed.

G1 When J_i issues $\mathcal{R}_i$ at time t, the timestamp of the request is recorded: $ts(\mathcal{R}_i) := t$.

G2 When $\mathcal{R}_i$ is satisfied, it is dequeued from either Q_a^r (if it is a read request) or Q_a^w (if it is a write request) for each $\ell_a \in D_i$.

G3 When $\mathcal{R}_i$ completes, it unlocks all resources in D_i.

G4 Each request issuance or completion occurs atomically. Therefore, there is a total order on timestamps, and a request cannot be issued at the same time that a critical section completes.

Example 3.1 (cont'd). Moving from inset (a) to inset (b) in Fig. 2, four additional requests have been issued. Timestamps are determined for these requests when they are issued (Rule G1). (In our examples, jobs issue requests in increasing index order.) The issuance of each request occurs atomically (Rule G4), so it is not possible for two requests to obtain the same timestamp.

The arrow from $\mathcal{R}_3^r$ to $\mathcal{R}_1^w$ indicates that $\mathcal{R}_3^r$ is blocked by $\mathcal{R}_1^w$. This blocking relationship is formally defined later and serves to represent just one such relationship in the system.

Fig. 2(c) depicts the system after $\mathcal{R}_1^w$ has completed. By Rule G3, it released resources ℓ_1 and ℓ_2. This enabled both $\mathcal{R}_3^r$ and $\mathcal{R}_5^r$ to be satisfied for ℓ_1 and dequeued from Q_1^r (Rule G2). Similarly, $\mathcal{R}_6^w$ became satisfied for ℓ_2.

In moving from inset (b) to inset (c), $\mathcal{R}_7^w$ and $\mathcal{R}_8^r$ have been issued, and $\mathcal{R}_8^r$ was satisfied immediately. Notice that request $\mathcal{R}_7^w$ for resources $D_7 = \{\ell_2, \ell_3, \ell_4\}$ was atomically enqueued on Q_2^w, Q_3^w, and Q_4^w. Because such an action is atomic, no cycles among blocked requests can exist. In an actual implementation, the issuance and completion of a request would not really occur atomically. However, an implementation must ensure that these actions have the "effect" of being atomic. We consider such issues later.

Read and write entitlement. Like the RW-RNLP, the RW-RNLP* functions by alternating read and write phases. The mechanism for orchestrating these phases is *entitlement*, which is defined separately for read and write requests below (these definitions are taken directly from [13]). Intuitively, a request is entitled when it should be satisfied in the next phase, thus only *unsatisfied* requests may be entitled. Together with the reader and writer rules presented later, the definition of entitlement ensures progress and allows us to bound pi-blocking times. Below, we use $E(Q_a^w)$ to denote the earliest-timestamped unsatisfied write request for resource ℓ_a.

Example 3.1 (cont'd). In Fig. 2(b), $E(Q_2^w) = \mathcal{R}_6^w$.

Definition 3.1. An unsatisfied read request $\mathcal{R}_i^r$ becomes *entitled* when there exists $\ell_a \in D_i$ that is write locked, and for each resource $\ell_a \in D_i$, $E(Q_a^w)$ is not entitled (see Def. 3.2).[3] (Note that $E(Q_a^w) = \emptyset$ could hold. In this case, we consider $E(Q_a^w) = \emptyset$ to be a "null" request that is not entitled.) $\mathcal{R}_i^r$ remains entitled until it is satisfied.

[3]Entitlement is a property of a request, and Def. 3.1 and Def. 3.2 give conditions upon which a request becomes entitled in terms of the entitlement of other requests. Therefore, while Def. 3.1 and Def. 3.2 reference each other parenthetically to aid the reader, they are not in fact circularly defined.

Example 3.1 (cont'd). In Fig. 2(b), $\mathcal{R}_3^r$ and $\mathcal{R}_5^r$ are both entitled (Def. 3.1): ℓ_1 is write locked, and there exists no resource ℓ_a in D_3 or D_5 for which $E(Q_a^w)$ is entitled (Def. 3.2, below). Entitled requests are indicated in Fig. 2 by a light gray shading.

Definition 3.2. An unsatisfied write request $\mathcal{R}_i^w$ becomes *entitled* when for each $\ell_a \in D_i$, $\mathcal{R}_i^w = E(Q_a^w)$, no read request in Q_a^r is entitled (see Def. 3.1),[3] and ℓ_a is not write locked. $\mathcal{R}_i^w$ remains entitled until it is satisfied.

Example 3.1 (cont'd). In Fig. 2(c), $\mathcal{R}_4^w$ is entitled: ℓ_1 is the only resource in D_4, $E(Q_1^w) = \mathcal{R}_4^w$ holds, there is no entitled read in Q_1^r, and ℓ_1 is not write locked. In moving from inset (c) to inset (d), $\mathcal{R}_6^w$ completed and released ℓ_2. In Fig. 2(d), $\mathcal{R}_7^w$ is entitled: $\mathcal{R}_7^w$ was at the head of each of its queues and there were no entitled read requests in the corresponding read queues, so the only condition that prevented $\mathcal{R}_7^w$ from being entitled earlier was $\mathcal{R}_6^w$'s lock on ℓ_2.

Rules for read and write requests. We complete our specification of the RW-RNLP* by stating rules that govern how read and write requests are processed. To state these rules, we introduce notation to allow us identify the set of requests on which an entitled request $\mathcal{R}_i$ (a read or a write) is blocked. Specifically, we let $B(\mathcal{R}_i, t)$ denote the set of requests on which such a request $\mathcal{R}_i$ is blocked at time t.

Example 3.1 (cont'd). In Fig. 2(b), there are two entitled requests, $\mathcal{R}_3^r$ and $\mathcal{R}_5^r$, both waiting on the satisfied write request $\mathcal{R}_1^w$. If inset (b) reflects the system state at time t, then $B(\mathcal{R}_3^r, t) = \{\mathcal{R}_1^w\}$ and $B(\mathcal{R}_5^r, t) = \{\mathcal{R}_1^w\}$. Only one of these relationships is depicted with an arrow in the diagram to avoid clutter. Similarly, if Fig. 2(c) reflects the system state at time t', then $B(\mathcal{R}_4^w, t') = \{\mathcal{R}_3^r, \mathcal{R}_5^r\}$. Note that there are other blocking relationships throughout Fig. 2, but $B(\mathcal{R}_i, t)$ is only defined for $\mathcal{R}_i$ at a time t when $\mathcal{R}_i$ is entitled.

The rules for read requests are as follows.

R1 When $\mathcal{R}_i^r$ is issued, for each $\ell_a \in D_i$, $\mathcal{R}_i^r$ is enqueued in Q_a^r. If $\mathcal{R}_i^r$ does not conflict with any entitled or satisfied write requests, then it is satisfied immediately.

R2 An entitled read request $\mathcal{R}_i^r$ is satisfied at the first time instant t such that $B(\mathcal{R}_i^r, t) = \emptyset$.

Example 3.1 (cont'd). When $\mathcal{R}_3^r$ and $\mathcal{R}_5^r$ were issued, by Rule R1, each was enqueued in Q_1^r, as shown in Fig. 2(b). When $\mathcal{R}_1^w$ later completed at some time t, as shown in Fig. 2(c), $B(\mathcal{R}_3^r, t) = \emptyset$ and $B(\mathcal{R}_5^r, t) = \emptyset$ were both established and $\mathcal{R}_3^r$ and $\mathcal{R}_5^r$ were both satisfied immediately, by Rule R2. Fig. 2(c) also shows $\mathcal{R}_8^r$ being satisfied immediately after being issued. This occurred by Rule R1, as no satisfied or entitled write requests for ℓ_3 existed at that time.

The rules for write requests are as follows.

W1 When $\mathcal{R}_i^w$ is issued, for each $\ell_a \in D_i$, $\mathcal{R}_i^w$ is enqueued in timestamp order in the write queue Q_a^w. If $\mathcal{R}_i^w$ does not conflict with any entitled or satisfied requests (read or write), then it is satisfied immediately.

W2 An entitled write request $\mathcal{R}_i^w$ is satisfied at the first time instant t such that $B(\mathcal{R}_i^w, t) = \emptyset$.

Example 3.1 (cont'd). When $\mathcal{R}_6^w$ was issued prior to the system state depicted in Fig. 2(b), it was enqueued in Q_2^w, and because it conflicted with the satisfied request $\mathcal{R}_1^w$, by Rule W1, it was not satisfied immediately. Request $\mathcal{R}_1^w$ later completed at some time t, as shown in Fig. 2(c), and at that time t, $B(\mathcal{R}_6^w, t) = \emptyset$ held, so $\mathcal{R}_6^w$ became satisfied, by Rule W2.

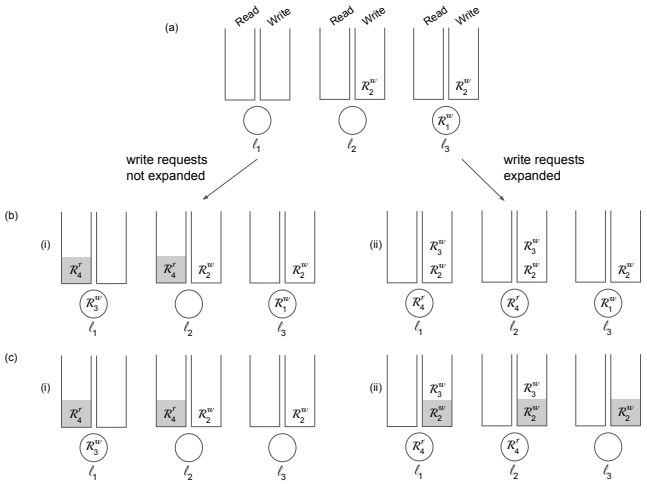

Figure 3: System states without write expansion are labeled (i), and states with write expansion (used in the RW-RNLP) are labeled (ii).

Write expansion. Aside from Rule P3, the only other difference between the RW-RNLP* and the RW-RNLP is with regard to a technique called *write expansion*, which is employed by the latter but not the former. Since the RW-RNLP* does not employ write expansion, we have chosen to avoid introducing the necessary formal machinery to completely define this technique, opting instead for conveying the general idea behind it with an example.

Example 3.2. The general idea behind write expansion is as follows. If a write request $\mathcal{R}_i^w$ is issued, and if a read request $\mathcal{R}_j^r$ that accesses resources in common with $\mathcal{R}_i^w$ could *possibly* be active concurrently, then the set of resources requested by $\mathcal{R}_i^w$, D_i, must be expanded to include all resources in D_j. An example is given in Fig. 3. In inset (a), a write request $\mathcal{R}_1^w$ is satisfied, holding the lock for ℓ_3. Inset (b) shows two possible scenarios after the issuance of $\mathcal{R}_2^w$, $\mathcal{R}_3^w$, and $\mathcal{R}_4^r$, with $D_2 = \{\ell_2, \ell_3\}$, $D_3 = \{\ell_1\}$, and $D_4 = \{\ell_1, \ell_2\}$. Inset (b)(i), on the left, shows the situation with no write expansion. $\mathcal{R}_3^w$ requires only resource ℓ_1 and thus is immediately satisfied. $\mathcal{R}_4^r$ is then entitled. In inset (b)(ii), $\mathcal{R}_2^w$ and $\mathcal{R}_3^w$ are expanded: because there exists a read request (namely, $\mathcal{R}_4^r$) in the system that requires ℓ_1 and ℓ_2, $\mathcal{R}_2^w$ must be issued for $D_2 = \{\ell_1, \ell_2, \ell_3\}$ and $\mathcal{R}_3^w$ must be issued for $D_3 = \{\ell_1, \ell_2\}$. Therefore, in inset (b)(ii), $\mathcal{R}_3^w$ cannot be satisfied until $\mathcal{R}_2^w$ completes, though they do not share resources.

Inset (c) shows the situation after $\mathcal{R}_1^w$ has completed. As seen in inset (c)(i), in the scenario without write expansion, nothing new happens to the other requests, as $\mathcal{R}_2^w$ cannot proceed ahead of the entitled read $\mathcal{R}_4^r$. However, as seen in inset (c)(ii), in the scenario with write expansion, the completion of $\mathcal{R}_1^w$ makes $\mathcal{R}_2^w$ entitled.

One reason write expansion is used in the RW-RNLP is because it makes reasoning about the largest possible pi-blocking for write requests easier. With write expansion, if $\mathcal{R}_i^w$ is the earliest-timestamped write among *all* write requests, then it is either entitled or satisfied, as illustrated in Ex. 3.2 and proven in [13]. Additionally, write expansion eases certain implementation challenges.

In our setting, write expansion is problematic, as our ultimate intent is to speed the processing of non-nested requests. With write expansion, these could be converted into nested requests. However, removing write expansion under the RW-RNLP* creates additional complexity with respect to the pi-blocking scenarios that can occur, and increases worst-case pi-blocking bounds for write requests by a constant factor compared to the bounds under the RW-RNLP.

3.2 RW-RNLP* Pi-Blocking Bounds

In this section, we derive bounds on the worst-case *acquisition delay* experienced by a request under the RW-RNLP*, *i.e.*, the worst-case time between the issuance and satisfaction of a request. Occasionally, we will find it convenient to distinguish whether a read request $\mathcal{R}_i^r$ or a write request $\mathcal{R}_i^w$ is nested or non-nested. For this purpose, we will use the notation $\mathcal{R}_i^{r,n}$, $\mathcal{R}_i^{r,nn}$, $\mathcal{R}_i^{w,n}$, and $\mathcal{R}_i^{w,nn}$, where the superscript "n" (resp., "nn") means "nested" (resp., "non-nested"). As in [13], we assume that all lock and unlock invocations take no time.

The properties needed to derive acquisition-delay bounds are stated below. Lemma 3.1 and Theorem 3.1 were proved in [13] (appearing as "Lemma 1" and "Theorem 1" there), and those proofs are not affected by the changes we made to the RW-RNLP to obtain the RW-RNLP*. We illustrate each of these properties by referring to our prior example. The remaining properties either require new proofs or are entirely new.

Lemma 3.1. *A write request $\mathcal{R}_i^w$ experiences acquisition delay of at most L_{max}^r time units after becoming entitled.*

Example 3.1 (cont'd). In insets (c) and (d) of Fig. 2, $\mathcal{R}_4^w$ is simply waiting for all requests in $B(\mathcal{R}_4^w, t_e)$ to complete, where t_e is the time when $\mathcal{R}_4^w$ became entitled. It can be shown that no new requests can be added to $B(\mathcal{R}_4^w, t_e)$ until $\mathcal{R}_4^w$ is satisfied. Furthermore, by Def. 3.2, all of the requests in this set are read requests. In this scenario, $\mathcal{R}_4^w$ waits for two requests to complete before becoming satisfied, as $B(\mathcal{R}_4^w, t_e) = \{\mathcal{R}_3^r, \mathcal{R}_5^r\}$. In the worst case, $\mathcal{R}_4^w$ must wait for L_{max}^r time units. Note that having multiple reads in the set $B(\mathcal{R}_4^w, t_e)$ does not increase this worst-case acquisition delay.

Theorem 3.1. *The worst-case acquisition delay of a read request $\mathcal{R}_i^r$ is at most $L_{max}^w + L_{max}^r$ time units.*

Example 3.1 (cont'd). Consider $\mathcal{R}_9^r$ in Fig. 2(d). Resource ℓ_1 is currently in a read phase, as $\mathcal{R}_3^r$ and $\mathcal{R}_5^r$ are in their critical sections, and there is an entitled write request, $\mathcal{R}_4^w$. Therefore, before $\mathcal{R}_9^r$ is satisfied, the read requests $\mathcal{R}_3^r$ and $\mathcal{R}_5^r$ could take up to L_{max}^r time units, and then the write request $\mathcal{R}_4^w$ could take up to L_{max}^w additional time units.

Lemma 3.2 below is very similar to Lemma 2 in [13] and much of the proof given for it is taken verbatim from there. However, new reasoning is required as we do not employ write expansion.

Lemma 3.2. *If $\mathcal{R}_i^w$ is the earliest-timestamped active write request for each resource in D_i, then $\mathcal{R}_i^w$ will be satisfied within $L_{max}^w + L_{max}^r$ time units.*

Proof. An unsatisfied write request $\mathcal{R}_i^w$ is either entitled or not. If $\mathcal{R}_i^w$ is entitled, then by Lemma 3.1, it will become satisfied within L_{max}^r time units. Otherwise, by Def. 3.2, for some resource $\ell_a \in D_i$, either **(i)** $\mathcal{R}_i^w \neq E(Q_a^w)$, **(ii)** some request $\mathcal{R}_x^r \in Q_a^r$ is entitled, or **(iii)** ℓ_a is write locked by some other request. By Rule W1, Cases (i) and (iii) are not possible because the write queues are timestamp ordered, and $\mathcal{R}_i^w$ is the earliest-timestamped active write request for each resource in D_i. For Case (ii), assume that $\mathcal{R}_x^r$ is entitled and $\ell_a \in D_i \cap D_x$. Then, by Def. 3.1, $\mathcal{R}_x^r$ is blocked by at least one satisfied write request $\mathcal{R}_j^w$. By Rule P1 (a resource-holding job is continually scheduled), all such write requests will complete within

L^w_{max} time units. At the time t when all such write requests have completed, by Rule R2, each $\mathcal{R}^r_x$ in $B(\mathcal{R}^w_i, t)$ will be satisfied, and by Def. 3.2, $\mathcal{R}^w_i$ will be entitled. By Lemma 3.1, $\mathcal{R}^w_i$ will subsequently experience at most L^r_{max} additional time units of delay before being satisfied. □

In systems for which each resource is a single-writer resource, each write request is the earliest-timestamped active write request for all of its required resources upon release.

Corollary 3.1. *If all resources are single-writer resources, then the worst-case acquisition delay of a write request $\mathcal{R}^w_i$ is at most $L^w_{max} + L^r_{max}$ time units.*

Lemma 3.3. *If no nested write requests are active while the non-nested request $\mathcal{R}^{w,nn}_i$ is active, and if $\mathcal{R}^{w,nn}_i$ is the earliest-timestamped active write request for its lone requested resource ℓ_a in D_i, then $\mathcal{R}^{w,nn}_i$ will be satisfied within L^r_{max} time units.*

Proof. The proof of this lemma differs from that given above for Lemma 3.2 only in how Case (ii) in that proof is addressed. For Case (ii) in the context of Lemma 3.3, if the non-nested request $\mathcal{R}^{r,nn}_x$ is entitled, then by Def. 3.1, it must blocked by a satisfied write request $\mathcal{R}^{w,nn}_j$ for resource ℓ_a. However, $\mathcal{R}^{w,nn}_i$ is the earliest-timestamped request for ℓ_a, so Case (ii) is actually impossible in the context of Lemma 3.3. Therefore, $\mathcal{R}^{w,nn}_i$ must be either satisfied or entitled, and in the latter case, it becomes satisfied within L^r_{max} time units, by Lemma 3.1. □

The next two lemmas heavily exploit Rule P3.

Lemma 3.4. *After being issued, a nested write request $\mathcal{R}^{w,n}_i$ will become the earliest-timestamped active write request for all of the resources in D_i within $2L^w_{max} + L^r_{max}$ time units.*

Proof. For any resource in D_i for which $\mathcal{R}^{w,n}_i$ is not the earliest-timestamped write request, by Rule P3, the earliest-timestamped write is a non-nested write request. By Lemma 3.2, each such request is satisfied within $L^w_{max} + L^r_{max}$ time units. By Rule P1, once satisfied, all such non-nested write requests will complete within L^w_{max} time units. Summing these two bounds yields the worst-case bound of $2L^w_{max} + L^r_{max}$ time units stated in the lemma. □

Lemma 3.5. *After being issued, a non-nested write request $\mathcal{R}^{w,nn}_i$ will become the earliest-timestamped active write request for its lone requested resource ℓ_a in D_i:* **(i)** *immediately, if no nested requests are active while $\mathcal{R}^{w,nn}_i$ is active;* **(ii)** *within $4L^w_{max} + 2L^r_{max}$ time units, if nested requests may be active while $\mathcal{R}^{w,nn}_i$ is active.*

Proof. In Case (i), by Rule P3, there are no other write requests accessing ℓ_a, so $\mathcal{R}^{w,nn}_i$ immediately becomes the earliest-timestamped request for that resource.

In Case (ii), if $\mathcal{R}^{w,nn}_i$ is not immediately the earliest-timestamped write request for ℓ_a, then there exists exactly one nested write request $\mathcal{R}^{w,n}_x$ that is the earliest-timestamped write request for ℓ_a. By Lemma 3.4, $\mathcal{R}^{w,n}_x$ will be the earliest-timestamped request for *all* of its requested resources within $2L^w_{max} + L^r_{max}$ time units. By Lemma 3.2, $\mathcal{R}^{w,n}_x$ will be satisfied within an additional $L^w_{max} + L^r_{max}$ time units. Once it is satisfied, by Rule P1, it will complete within L^w_{max} time units. At that time, $\mathcal{R}^{w,nn}_i$ will be the earliest-timestamped write request for its requested resource. Summing all the bounds just stated, this occurs within $4L^w_{max} + 2L^r_{max}$ time units in the worst case. □

Theorem 3.2, given next, provides our desired delay-acquisition bounds. Together with Theorem 3.1, this theorem implies that all pi-blocking bounds under the RW-RNLP* are $O(1)$.

Theorem 3.2. *The worst-case acquisition delay of a write request $\mathcal{R}^w_i$ is:* **(i)** *L^r_{max} time units, if $\mathcal{R}^{w,nn}_i$ is a non-nested request and no nested requests are active while $\mathcal{R}^{w,nn}_i$ is active;* **(ii)** *$5L^w_{max} + 3L^r_{max}$ time units, if $\mathcal{R}^{w,nn}_i$ is a non-nested request and nested requests may be active while $\mathcal{R}^{w,nn}_i$ is active;* **(iii)** *$3L^w_{max} + 2L^r_{max}$ time units, if $\mathcal{R}^{w,n}_i$ is a nested request.*

Proof. In Case (i), by Lemma 3.5(i), $\mathcal{R}^{w,nn}_i$ will be the earliest-timestamped active write request for its lone requested resource as soon as it is issued. By Lemma 3.3, it will be satisfied within L^r_{max} time units.

In Case (ii), by Lemma 3.5(ii), $\mathcal{R}^{w,nn}_i$ will be the earliest-timestamped active write request for its lone requested resource within $4L^w_{max} + 2L^r_{max}$ time units. By Lemma 3.2, it will then be satisfied within $L^w_{max} + L^r_{max}$ time units, resulting in a worst-case acquisition delay of $5L^w_{max} + 3L^r_{max}$ time units.

In Case (iii), by Lemma 3.4, $\mathcal{R}^{w,n}_i$ will be the earliest-timestamped active write request for all of its requested resources within $2L^w_{max} + L^r_{max}$ time units. By Lemma 3.2, it is then satisfied within $L^w_{max} + L^r_{max}$ time units, resulting in a worst-case acquisition delay of $3L^w_{max} + 2L^r_{max}$ time units. □

It can be shown that all of the blocking bounds in Theorem 3.2 are *tight*, *i.e.*, scenarios exist in which these exact bounds occur.[4] Notice that, by Theorem 3.1 and Theorem 3.2(i), if non-nested requests are not affected by nested requests, then read and write requests have worst-case pi-blocking bounds of only $L^w_{max} + L^r_{max}$ and L^r_{max} time units, respectively.

3.3 Putting the Pieces Together

In this section, we describe our proposed fast RW-RNLP protocol. Our goals for this protocol are threefold: **(i)** non-nested requests should have low lock/unlock overheads; **(ii)** such requests should have contention-sensitive worst-case pi-blocking bounds; **(iii)** nested requests should have worst-case pi-blocking bounds that are asymptotically the same as under the RW-RNLP. In describing the fast RW-RNLP below, we verify that Goals (ii) and (iii) are met. We address Goal (i) later when we discuss an implementation of the protocol and an experimental evaluation of that implementation.

The fast RW-RNLP is defined by using the lock and unlock routines of the RNLP, the RW-RNLP*, and ordinary (not phase-fair) mutex ticket locks (TLs) [11] as subroutines, as shown in Fig. 4.[5] Recall that the RNLP provides mutex sharing and supports nested requests. Under it, the worst-case pi-blocking of any request is $O(m)$ [14]. A TL provides mutex sharing for a single resource and ensures contention-sensitive pi-blocking.

Referring to the fast RW-RNLP structure in Fig. 4, notice that all read requests (both nested and non-nested) directly invoke the RW-RNLP*. Furthermore, any nested write request that requires access to a resource ℓ_a must first "acquire" that resource within the context of the RNLP and then invoke the RW-RNLP*. Also, any non-nested write request for that resource must first "acquire" that resource within the context of a TL associated with that resource and then

[4] See online appendix: http://www.cs.unc.edu/anderson/papers.html.

[5] The lock and unlock routines for the RW-RNLP* routines have been denoted in a slightly abbreviated way. For example, W*_Lock^{nn} denotes the lock routine invoked by non-nested write requests under the RW-RNLP*.

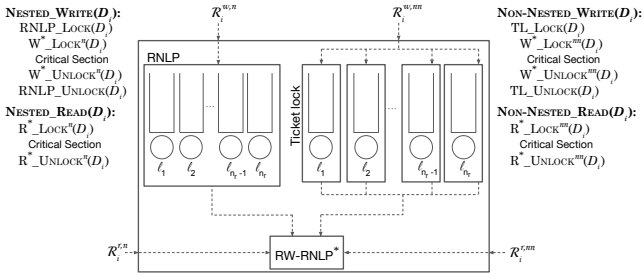

Figure 4: Fast RW-RNLP structure.

invoke the RW-RNLP*. This overall protocol structure ensures that Rule P3 is upheld from the perspective of the RW-RNLP*.

Because read requests directly invoke the RW-RNLP*, by Theorem 3.1, the pi-blocking incurred by them is $O(1)$ in the worst case (we consider L_{max} to be constant). Thus, Goals (ii) and (iii) above are met for read requests. The following theorem shows that these goals are also met for write requests; the pi-blocking incurred by a non-nested write request $\mathcal{R}_i^{w,nn}$ is $O(C_i)$ in the worst case (recall that C_i is the contention experienced by request $\mathcal{R}_i$), and the pi-blocking incurred by a nested write request is $O(m)$ in the worst case. (Referring to Goal (iii), we note that the worst-case pi-blocking for write requests under the RW-RNLP is $O(m)$ [13].[6])

Theorem 3.3. *Under the fast RW-RNLP, the worst-case acquisition delay for a write request $\mathcal{R}_i^w$ is:* **(i)** $C_i(L_{max}^w+L_{max}^r)+L_{max}^r$ *time units, if $\mathcal{R}_i^{w,nn}$ is a non-nested request and no nested requests are active while $\mathcal{R}_i^{w,nn}$ is active;* **(ii)** $C_i\cdot(6L_{max}^w+3L_{max}^r)+5L_{max}^w+3L_{max}^r$ *time units, if $\mathcal{R}_i^{w,nn}$ is a non-nested request and nested requests may be active while $\mathcal{R}_i^{w,nn}$ is active;* **(iii)** $(m-1)\cdot(4L_{max}^w+2L_{max}^r)+3L_{max}^w+2L_{max}^r$ *time units, if $\mathcal{R}_i^{w,n}$ is a nested request.*

Proof. In Case (i), $\mathcal{R}_i^{w,nn}$ must wait for up to C_i contending write requests ahead of it in the TL associated with its lone requested resource. By Theorem 3.2(i), each of these write requests may face an acquisition delay of up to L_{max}^r time units within the RW-RNLP* and then execute its critical section for up to L_{max}^w time units. Thus, within $C_i\cdot(L_{max}^w+L_{max}^r)$ time units after being issued, $\mathcal{R}_i^{w,nn}$ will not be blocked by any write requests in the TL associated with its requested resource. At that time, $\mathcal{R}_i^{w,nn}$ will invoke the RW-RNLP* and, again by Theorem 3.2(i), experience an acquisition delay of up to L_{max}^r time units. In total, this yields a worst-case acquisition delay of $C_i\cdot(L_{max}^w+L_{max}^r)+L_{max}^r$ time units for $\mathcal{R}_i^{w,nn}$.

Case (ii) is similar to Case (i) except that Theorem 3.2(ii) is applied instead of Theorem 3.2(i). Thus, the worst-case acquisition delay is $C_i\cdot(6L_{max}^w+3L_{max}^r)+5L_{max}^w+3L_{max}^r$ time units.

In Case (iii), $\mathcal{R}_i^{w,n}$ must wait within the RNLP for up to $m-1$ other requests to complete before it can invoke the RW-RNLP*. Arguing as in the cases above, but this time using Theorem 3.2(iii), a worst-case acquisition delay of $(m-1)\cdot(4L_{max}^w+2L_{max}^r)+3L_{max}^w+2L_{max}^r$ time units results. □

Note that, in a system with only single-writer resources, the RW-RNLP* alone is sufficient and Cor. 3.1 can be applied to show that all requests incur $O(1)$ pi-blocking with very low constant factors.

To this point, we have fully specified the RW-RNLP* abstractly. What remains is to devise an actual implementation of it with reasonable overheads. We consider this issue next.

[6]More precisely, the bound presented is $(m-1)(L_{max}^w+L_{max}^r)$.

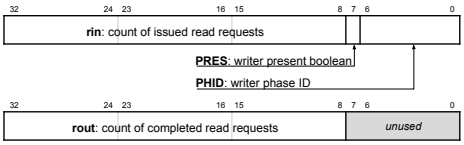

Figure 5: Bits in the per-resource *rin* and *rout* variables. (A very similar figure appears in [4].)

4 IMPLEMENTATION AND EVALUATION

Of the building blocks used to construct the fast RW-RNLP, the TL and the RNLP have existing implementations [4, 13]. Therefore, it remains for us to provide an implementation of the RW-RNLP* as well as an experimental evaluation of the overall fast RW-RNLP. Recall that we focus on the user-level, spin-based version.

4.1 Implementation

The main challenge in implementing the RW-RNLP* lies in supporting the atomicity assumptions inherent in the rule-based specification of it. Such assumptions could be supported by encapsulating certain code regions within lock and unlock calls to an underlying mutex. Indeed, this approach was taken in implementing the rules of the RW-RNLP [13]. While such an approach introduces additional pi-blocking, the protected critical sections are usually very short, so we consider such blocking to be part of the lock and unlock overhead of the protocol being implemented. Still, we would like to avoid relying on the use of mutex protocols in this way if possible, and we want to *categorically preclude* their use in implementing the lock and unlock routines for non-nested requests, as efficiently implementing such routines is the emphasis of this paper.

With these concerns in mind, we now describe our implementation of the RW-RNLP*.

Shared variables of the RW-RNLP.* From the point of view of our implementation, each shared resource ℓ_a is viewed as pointer to a structure called *res_state*, which consists of four shared counters, *rin*, *rout*, *win*, and *wout*, as shown in Listing 1. Almost identical counters to these are used in the PF-TL [4]. Counters *win* and *wout* track the number of write requests for resource ℓ_a that have been issued and completed, respectively. Counters *rin* and *rout* similarly count read requests, with the added complexity of storing information about writes in the bottom byte, as shown in Fig. 5. Listing 1 shows various constant bit vectors used in our code to access and manipulate certain bits in *rin* and *rout*.

Listing 1 RW-RNLP* Definitions

```
type res_state: record
  rin, rout: unsigned integer initially 0
  win, wout: unsigned integer initially 0
constant
 RINC 0x100 // reader increment value
 WBITS 0xff // writer bits in rin
 PRES 0x80 // writer present bit
 PHID 0x7f // writer phase ID bits
```

Non-nested requests in the RW-RNLP.* The lock and unlock routines for non-nested requests in our implementation are shown in Listing 2. These are *nearly identical to those for the PF-TL* [4], which to our knowledge is *the most efficient reader/writer lock for single-resource requests proposed to date.* A non-nested read $\mathcal{R}_i^{r,nn}$ of a resource ℓ_a is performed by simply incrementing the number of readers for ℓ_a (Line 3) and then spinning if necessary (Line 4). In

particular, if ℓ_a is currently being written, then $\mathcal{R}_i^{r,nn}$ waits for a single write request to complete as indicated by either the PRES bit being cleared or the PHID bits being changed, which indicates that a new writer has set those bits, and thus a write has completed. To unlock ℓ_a, $\mathcal{R}_i^{r,nn}$ simply increments *rout* by RINC (Line 6).

A non-nested write $\mathcal{R}_i^{w,nn}$ of a resource ℓ_a waits until it holds the earliest ticket among all write requests for ℓ_a (Lines 9–10). It then atomically sets the last byte of ℓ_a's *rin* variable and determines the number of read requests for ℓ_a upon which it must block (Lines 11–12). Next, it waits until those reads (if any) are complete (Line 13). When $\mathcal{R}_i^{w,nn}$ completes, it clears the writer byte of ℓ_a's *rin* variable (Line 15) and increments its *wout* counter (Line 16).

Listing 2 RW-RNLP* Routines for Non-Nested Reqs.

```
1:  procedure R*_Lock^nn(ℓ: ptr to res_state)
2:      var w: unsigned int
3:      w := fetch&add(ℓ→rin, RINC) & WBITS                    ▷ In read queue
4:      await (w = 0) or (w ≠ (ℓ→rin & WBITS))                 ▷ Satisfied
5:  procedure R*_Unlock^nn(ℓ: ptr to res_state)
6:      atomic_add(ℓ→rout, RINC)
7:  procedure W*_Lock^nn(ℓ: ptr to res_state)
8:      var rticket, wticket, w: unsigned int
9:      wticket := fetch&add(ℓ→win, 1)                         ▷ In write queue
10:     await (wticket = ℓ→wout)                               ▷ Head of write queue
11:     w := PRES | (wticket & PHID)
12:     rticket := fetch&add(ℓ→rin, w)
                                   ▷ Marked entitled now for all reads to see
13:     await (rticket = ℓ→rout)                               ▷ Satisfied
14: procedure W*_Unlock^nn(ℓ: ptr to res_state)
15:     fetch&and(ℓ→rin, 0xFFFFFF00)                           ▷ Clear WBITS
16:     ℓ→wout := ℓ→wout + 1
```

Nested requests in the RW-RNLP.* The lock and unlock routines for nested requests are shown in Listing 3. These routines are very similar to those in Listing 2, with two notable exceptions. First, an extra phase has been added to the lock routine for read requests (Lines 19–21). Introducing this extra phase eliminates unnecessary writer blocking in one particular corner case.[4] Second, because requests are now for *sets* of resources, we need to ensure that such sets can be enqueued atomically to prevent potential deadlock. (This is why, as discussed in Sec. 2, resources must be acquired according to a predetermined order in the variant of the RNLP that does not use DGLs.) However, it turns out that the only potential deadlock situation that can occur involves a race condition between nested readers and nested writers. Furthermore, we discovered that this race condition can be eliminated by requiring each nested read request to hold a global PF-TL for *writing* when updating multiple read queues (Lines 22–25) and by requiring each nested write request to hold this PF-TL for *reading* when it updates multiple write queues (Lines 36–40). (The calls to the phase-fair lock and unlock routines in Lines 22, 25, 36, and 40 do not specify input parameters because we have no need to distinguish different shared resources protected by these routines.) While using a PF-TL introduces blocking overhead, this overhead is only $O(1)$ for write requests, which require only read access. This is preferable to the blocking overhead that would result from using a mutex lock.

Clearly, the routines in our implementation are not actually atomic: each executes over durations of time, not instantaneously. However, it can be formally shown that each routine is linearizable.[4] That is, for each routine, an instantaneous *linearization point* can be defined at which the routine "appears" to take effect atomically. When viewing these routines in this way, they can be shown to support the rule-based specification of the RW-RNLP* given earlier.

Listing 3 RW-RNLP* Routines for Nested Reqs.

```
17: procedure R*_Lock^n(D: set of ptr to res_state)
18:     var w_ℓ: unsigned int for each ℓ in D
19:     for each ℓ in D:
20:         w_ℓ := ℓ→rin & WBITS
21:         await (w_ℓ = 0) or (w_ℓ ≠ (ℓ→rin & WBITS))
22:     PFTL_W_Lock()                                  ▷ Write-lock global PFTL
23:     for each ℓ in D:
24:         w_ℓ := fetch&add(ℓ→rin, RINC) & WBITS
25:     PFTL_W_Unlock()                                ▷ Unlock global PFTL
26:     for each ℓ in D:
27:         await (w_ℓ = 0) or (w_ℓ ≠ (ℓ→rin & WBITS))          ▷ Satisfied
28: procedure R*_Unlock^n(D: set of ptr to res_state)
29:     for each ℓ in D:
30:         atomic_add(ℓ→rout, RINC)
31: procedure W*_Lock^n(D: set of ptr to res_state)
32:     var rticket_ℓ, wticket_ℓ, w_ℓ: unsigned int for each ℓ in D
33:     for each ℓ in D:
34:         wticket_ℓ := fetch&add(ℓ→win, 1)                 ▷ In write queue
35:         await (wticket_ℓ = ℓ→wout)
                                   ▷ Head of all requested write queues now
36:     PFTL_R_Lock()                                  ▷ Read-lock global PFTL
37:     for each ℓ in D:
38:         w_ℓ := PRES | (wticket_ℓ & PHID)
39:         rticket_ℓ := fetch&add(ℓ→rin, w_ℓ)
                                   ▷ Marked entitled now for all reads to see
40:     PFTL_R_Unlock()                                ▷ Unlock global PFTL
41:     for each ℓ in D:
42:         await (rticket_ℓ = ℓ→rout)                       ▷ Satisfied
43: procedure W*_Unlock^n(D: set of ptr to res_state)
44:     for each ℓ in D:
45:         fetch&and(ℓ→rin, 0xFFFFFF00)                     ▷ Clear WBITS
46:         ℓ→wout := ℓ→wout + 1
```

4.2 Evaluation

We conducted a user-space experimental evaluation of the fast RW-RNLP in which lock/unlock overheads and observed blocking times were recorded under a variety of scenarios. Given the focus of this paper, we were particularly interested in overheads and blocking times for non-nested requests. We conducted our experiments on a dual-socket, 18-cores-per-socket Intel Xeon E5-2699 platform.

In our experiments, we varied a number of experimental parameters including the numbers of tasks and resources, nesting depths and critical-section lengths of requests, and ratios of non-nested to nested requests and of read to write requests. Each task was pinned to a single core, and for task counts of up to 18, all tasks were assigned to the same socket. Each task was configured to issue lock and unlock calls 1,000 times to simulate behavior that would generate the worst-case lock overhead and blocking times. In all of our graphs, we plot these worst-case values, which were obtained by computing the 99^{th} percentile of all recorded results in order to filter out any spurious measurements (our measurements were taken at user level, so we have no other means for filtering results impacted by interrupts).

Overheads and blocking. We compared the considered protocols on the basis of overhead and blocking: the *overhead* incurred by a resource request is the total time spent by it executing lock logic within lock and unlock routines (including any time spent waiting to access underlying locks used to enforce atomicity properties required by that logic); the *blocking* incurred by the request is the total time spent by it waiting to access its requested resources. We measured both overhead and blocking for a number of different scenarios. Each such scenario was defined by specifying particular values or ranges for the experimental parameters mentioned above.

In designing the fast RW-RNLP, we have sought to ensure that **(i)** non-nested requests have low overhead and experience contention-sensitive pi-blocking and **(ii)** nested requests experience pi-blocking

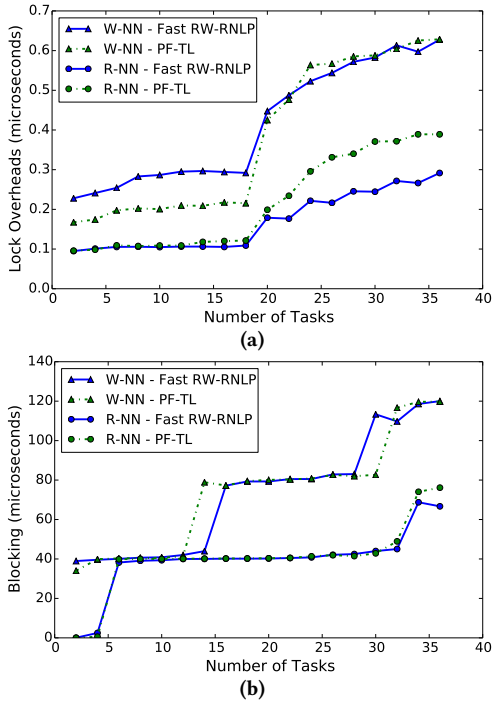

Figure 6: (a) Lock overheads and (b) blocking for non-nested read and write requests when using PF-TLs versus the fast RW-RNLP. For each request $\mathcal{R}_i$, $L_i^r = 40\mu$s, $L_i^w = 40\mu$s, $n_r = 64$, $|D_i| = 1$. Requests were randomly chosen to be a read (or a write) with probability 0.5.

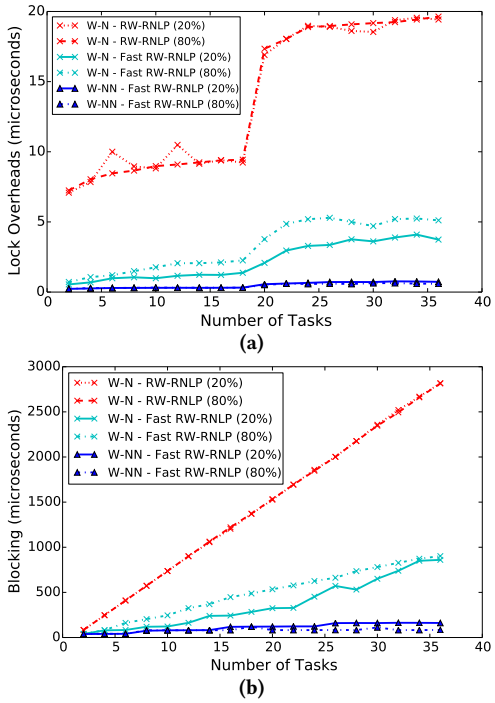

Figure 7: (a) Overhead and (b) blocking for nested and non-nested write requests under the RW-RNLP and the fast RW-RNLP. Here, $L_i^r = 40\mu$s, $L_i^w = 40\mu$s, $n_r = 64$, $|D_i| = 1$, for non-nested requests, and $|D_i| = 4$, for nested requests. Requests were chosen to be a read (or write) with probability 0.5. Data is plotted for the cases of 20% and 80% of requests being nested. Due to write expansion (recall Fig. 3), D_i was inflated to include all 64 resources for writes under the RW-RNLP.

that is no worse (and hopefully better) than that under the RW-RNLP. Accordingly, as standards for comparison, we considered the use of per-resource PF-TLs (which exhibit very low overhead and are contention-sensitive) in assessing (i) and the RW-RNLP (of course) in assessing (ii). In the course of our experiments, we produced hundreds of graphs. The full set of graphs can be found online.[4] A few graphs that are exemplars of trends seen generally are discussed in the following observations.

Obs. 1. *For non-nested read and write requests, the fast RW-RNLP and PF-TLs exhibited comparable overheads.*

This observation is supported by Fig. 6(a), which plots lock overheads for both reads and writes under both the fast RW-RNLP and PF-TLs as a function of the task count, n. The data in this figure corresponds to a scenario in which all requests were non-nested, evenly distributed between reads and writes, and the total number of resources, n_r, was set to 64. The critical section of each request was configured to have a duration of 40μs. For comparison, lock overheads for both protocols hold steady in the range of around 1.0μs to 2.5μs for up to 18 tasks, with the fast RW-RNLP having a slightly higher write-lock overhead than PF-TLs. Beyond 18 tasks, lock overheads increase under both protocols. This is because, beyond a task count of 18, tasks are executing on both sockets of the considered platform. Notice that, beyond a task count of 18, the write-lock overheads of both protocols converge, and the read-lock overhead of the fast RW-RNLP becomes slightly better. We suspect that the better read-lock overhead of the fast RW-RNLP is due to reduced cache invalidations of shared lock state caused by contending write requests, which must first acquire a ticket lock under the fast RW-RNLP. We omit graphs showing unlock overheads due to space constraints, but they showed similar trends.

Obs. 2. *In general, overheads increased when using two sockets instead of one.*

This trend is seen in Fig. 6(a), discussed earlier, and also in Fig. 7(a), considered in detail below. When tasks execute on two sockets instead of one, overheads due to maintaining cache coherency increase. Observe that, in Fig. 6(a), lock overheads under the fast RW-RNLP are never more than around 0.6μs. This value is quite small compared to the 40μs critical-section length. Note that any blocking is mostly a function of critical-section lengths.

Obs. 3. *In scenarios with only non-nested requests, the fast RW-RNLP and PF-TLs exhibited nearly identical blocking.*

This observation is clearly supported by Fig. 6(b). Together with Obs. 1, this observation suggests the viability of providing the fast RW-RNLP as a general synchronization solution. It can even be used in systems in which nested requests do not occur with no detrimental impacts of note.

Obs. 4. *In scenarios with both nested and non-nested requests, overheads for write requests tended to be much lower under the fast RW-RNLP than under the RW-RNLP.*

This observation is supported by Fig. 7(a), which depicts data from two different scenarios as detailed in the figure's caption. The higher overheads under the RW-RNLP are partially due to the use of write expansion (recall Fig. 3), which increases resource contention. This increased contention impacts the overhead of write requests, as they write-lock an underlying PF-TL to update all relevant resource

queues atomically. Note that, under the RW-RNLP, write expansion forces non-nested write requests to be processed like nested ones.

Notice that Fig. 7 pertains to write requests. The corresponding read request results at $m = 36$ show overheads of around 0.3μs for non-nested requests under the fast RW-RNLP compared to around 0.8μs under the RW-RNLP. Under the fast RW-RNLP, non-nested requests had higher blocking by about one critical-section length, and nested read requests had higher overhead (of around 3μs) and higher blocking by a few critical-section lengths.

Obs. 5. *In scenarios with both nested and non-nested requests, blocking for write requests tended to be much lower under the fast RW-RNLP than under the RW-RNLP.*

This observation is supported by Fig. 7(b), which plots recorded worst-case blocking times associated with the scenarios in Fig. 7(a). For $m = 36$, blocking was 17 times lower under the fast RW-RNLP than under the RW-RNLP; write expansion increases resource contention, which increases blocking times of the RW-RNLP.

Obs. 6. *Non-nested requests exhibited contention-sensitive blocking under the fast RW-RNLP but not the RW-RNLP.*

This observation is also supported by Fig. 7(b). Notice that, as the task count increases, the potential for additional blocking increases due to transitive blocking, which negatively impacts any protocol that provides no mechanisms for eliminating transitive blocking. Blocking for non-nested requests under the fast RW-RNLP increases slowly as the task count increases; with more tasks, more contention is possible. In contrast, non-nested write requests are converted to nested ones under the RW-RNLP due to write expansion. As a result, their blocking under that protocol is not $O(C)$.

Of relevance to the analysis presented in Sec. 3, Fig. 8 demonstrates the results of varying the critical-section length while holding the number of tasks n constant (in our experiments, m and n are equal). In contrast, in Fig. 7(b) the number of tasks was varied, and the critical-section length was held constant; the points in Fig. 7(b) at $m = 36$ are the same as those in Fig. 8 for $L_i = 40\mu$s. Note that varying m effectively modifies the term C_i for each request $\mathcal{R}_i$.

Obs. 7. *Blocking time scaled linearly with critical-section length for both the fast RW-RNLP and the RW-RNLP.*

Fig. 8 illustrates this observation, which reflects expected behavior based on the blocking analysis; for each type of request, the worst-case blocking bound contains both L^w_{max} and L^r_{max} terms with different coefficients depending on the request type.

Although our approach results in higher coefficients for the nested write requests than the bounds proven for the RW-RNLP, lower blocking times were generally seen under the fast RW-RNLP. We suspect this difference is because, under the RW-RNLP, write expansion guarantees that all write requests conflict.

We also noted differences between nested and non-nested write requests under the fast RW-RNLP, highlighting the improvement of $O(C)$ over $O(m)$ blocking. Under the fast RW-RNLP, the $O(C)$ blocking of non-nested write requests was almost identical to the $O(1)$ blocking of nested read requests. Thus, there is a significant benefit that can be gained when contention is guaranteed to be low.

5 CONCLUSION

We have presented a new RNLP variant, the fast RW-RNLP, which employs a fast-path mechanism to provide contention-sensitive pi-blocking and low processing costs for non-nested lock requests,

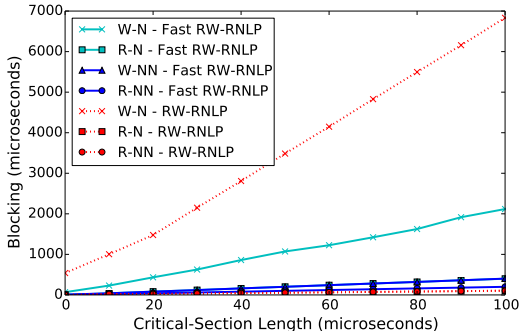

Figure 8: Blocking for nested and non-nested write requests under the RW-RNLP and the fast RW-RNLP. The critical-section length varies, $m = 36$, $n_r = 64$, $|D_i| = 1$, for non-nested requests, and $|D_i| = 4$, for nested requests. ($|D_i|$ is inflated to 64 under the RW-RNLP as above.) A request was chosen to be a write with probability 0.5.

while preserving the RW-RNLP's asymptotic pi-blocking bounds for nested requests. While the goal of ensuring contention sensitivity *efficiently* in the general case (nested requests) has so far proven to be elusive, we have shown that it is at least possible to do so for the common case of non-nested requests even when nested requests exist. To ensure contention-sensitivity for non-nested requests, we had to eliminate the write-expansion rule of the RW-RNLP. In our experiments, this had a positive impact on blocking for all requests.

The fast RW-RNLP has a modular structure that enables different variants to be applied in different contexts. For example, the RW-RNLP* gives constant-time access to all resource requests in systems comprised of single-writer, multiple-reader resources. Additionally, the RNLP component in Fig. 4 could be replaced by the C-RNLP to obtain contention-sensitive pi-blocking for nested requests (at the expense of higher overheads for such requests). Further variants realize task waiting by suspending tasks rather than by requiring them to block by spinning; the implementation of one such variant is in progress. In a future expanded version of this paper, we will discuss these variants in full. We plan to compare the fast RW-RNLP to other alternatives by conducting a large-scale overhead-aware schedulability study. Such a study will allow us to assess the extent to which the more efficient processing of non-nested requests affects the ability to ensure timing correctness in a holistic sense.

REFERENCES

[1] D. Bacon, R. Konuru, C. Murthy, and M. Serrano. Thin locks: Featherweight synchronization for java. In *PLDI 1998*.

[2] B. Brandenburg. *Scheduling and Locking in Multiprocessor Real-Time Operating Systems*. PhD thesis, University of North Carolina, Chapel Hill, NC, 2011.

[3] B. Brandenburg and J. Anderson. Feather-trace: A lightweight event tracing toolkit. In *OSPERT 2007*.

[4] B. Brandenburg and J. Anderson. Spin-based reader-writer synchronization for multiprocessor real-time systems. *Real-Time Systems*, 46(1), 2010.

[5] A. Burns and A. Wellings. A schedulability compatible multiprocessor resource sharing protocol - MrsP. In *ECRTS 2013*.

[6] P. Courtois, F. Heymans, and D. Parnas. Concurrent control with readers and writers. *CACM*, 14(10), 1971.

[7] D. Faggioli, G. Lipari, and T. Cucinotta. Analysis and implementation of the multiprocessor bandwidth inheritance protocol. *Real-Time Systems*, 48(6), 2012.

[8] M. Herlihy and J. Wing. Linearizability: A correctness condition for concurrent objects. *ACM Trans. Program. Lang. Syst.*, 12(3):463–492, July 1990.

[9] H. Huang, P. Pillai, and K. Shin. Improving wait-free algorithms for interprocess communication in embedded real-time systems. In *Proceedings of the General Track of the Annual Conference on USENIX Annual Technical Conference*, 2002.

[10] C. Jarrett, B. Ward, and J. Anderson. A contention-sensitive fine-grained locking protocol for multiprocessor real-time systems. In *RTNS 2015*.

[11] J. Mellor-Crummey and M. Scott. Algorithms for scalable synchronization of shared-memory multiprocessors. *Transactions on Computer Systems*, 9(1), 1991.

[12] B. Ward. *Sharing Non-Processor Resources in Multiprocessor Real-Time Systems*. PhD thesis, University of North Carolina, Chapel Hill, NC, 2016.

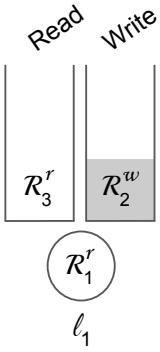

Figure 9: A simple example that shows worst case acquisition delay for a read request and the acquisition delay a write may experience after becoming entitled.

[13] B. Ward and J. Anderson. Multi-resource real-time reader/writer locks for multiprocessors. In *IPDPS 2014*.

[14] B. Ward and J. Anderson. Supporting nested locking in multiprocessor real-time systems. In *ECRTS 2012*.

A ADDITIONAL DETAILS

This appendix provides additional details for which the full explanation, given here, would not reasonably fit within the body of the paper.

A.1 Tight Blocking Bounds

To show that each blocking bound is tight, we show that each worst-case bound can actually occur by means of examples. An example corresponding to each lemma and theorem up through Theorem 3.2 is presented below in the order in which the lemmas and theorems appear in Sec. 3. In each example, requests are numbered in the order in which they were issued.

Lemma 3.1 bounds the acquisition delay that a write request can experience after becoming entitled to L_{max}^r.

Example A.1. As shown in Fig. 9, write request $\mathcal{R}_2^w$, issued just after $\mathcal{R}_1^r$, is immediately entitled and can experience L_{max}^r acquisition delay. This is exactly the upper bound presented in Lemma 3.1.

Theorem 3.1 bounds the acquisition delay a read request can experience to $L_{max}^w + L_{max}^r$.

Example A.2. As Fig. 9 demonstrates, read request $\mathcal{R}_3^r$ could experience the worst-case acquisition delay if it were issued just after the issuance of requests $\mathcal{R}_1^r$ and $\mathcal{R}_2^w$, all for the same resource. It cannot be satisfied initially as $\mathcal{R}_2^w$ is entitled, and once $\mathcal{R}_2^w$ is satisfied, $\mathcal{R}_3^r$ becomes entitled and may need to wait for another L_{max}^w time units before acquiring the resource.

A write request $\mathcal{R}_i^w$ may experience up to $L_{max}^w + L_{max}^r$ blocking after becoming the earliest-timestamped active write request for each resource in D_i, as stated in Lemma 3.2.

Example A.3. Similarly to the previous examples, in Fig. 10, write request $\mathcal{R}_3^w$ can experience the worst-case delay stated in Lemma 3.2 if issued just after $\mathcal{R}_1^w$ and $\mathcal{R}_2^r$. It is immediately the earliest-timestamped active write request for $D_3 = \{\ell_2\}$, and must wait both for $\mathcal{R}_1^w$ to complete (L_{max}^w) and for the entitled $\mathcal{R}_2^r$ to become satisfied and then complete (L_{max}^r) before it can be satisfied.

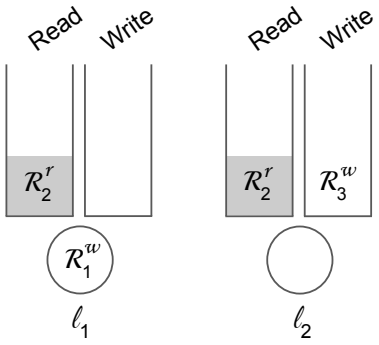

Figure 10: An issuance order which may cause the maximum blocking after a write request $\mathcal{R}_3^w$ becomes the earliest-timestamped active write request for each of its resources, here simply ℓ_2.

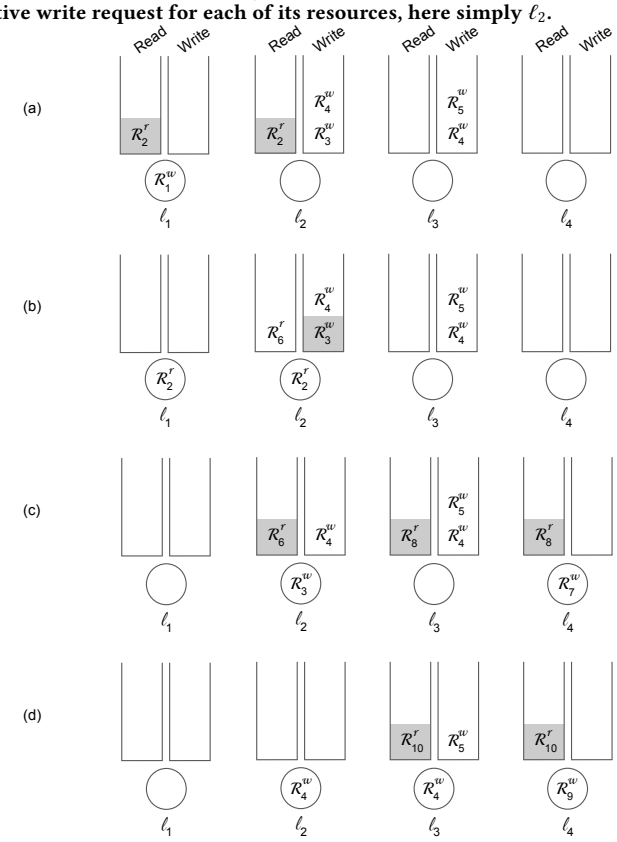

Figure 11: A series of read and write requests that illustrate the worst-case acquisition delay for nested and non-nested write requests.

Example A.1 can also be used to demonstrate a scenario in which a non-nested write request experiences the worst-case acquisition delay of L_{max}^r, proven in Lemma 3.3.

Lemma 3.4 bounds the time a nested write request must wait before becoming the earliest-timestamped write request for all of its resources to $2L_{max}^w + L_{max}^r$.

Example A.4. As shown in Fig. 11(a), $\mathcal{R}_4^{w,n}$ is not the earliest-timestamped active write request for each of $D_4 = \{\ell_2, \ell_3\}$ when it is issued. In fact, it must wait until $\mathcal{R}_3^w$ has completed execution. Given that each of these requests could have been issued just after each other, $\mathcal{R}_4^w$ will need to wait for the completion of $\mathcal{R}_1^w$, $\mathcal{R}_2^r$,

and $\mathcal{R}_3^w$, which may take up to $2L_{max}^w + L_{max}^r$ time units, to be the earliest-timestamped active write request.

Lemma 3.5 has two cases for how soon a non-nested write request $\mathcal{R}_i^{w,nn}$ will become the earliest-timestamped request for each of its resources. Case (i) does not need an example; the worst-case delay for $\mathcal{R}_i^{w,nn}$ becoming the earliest-timestamped active write request in the RW-RNLP* for D_i is none at all when no nested requests are active. Case (ii) bounds this time to $4L_{max}^w + 2L_{max}^r$ in the presence of nested requests.

Example A.5. Consider $\mathcal{R}_5^w$ in Fig. 11 as the non-nested write request that is seeking to become the earliest-timestamped request for $D_5 = \{\ell_3\}$. $\mathcal{R}_3^w$ may wait for up to $L_{max}^w + L_{max}^r$ time units to become entitled as shown in (a) and (b). $\mathcal{R}_4^w$ must complete before $\mathcal{R}_5^w$ will be the earliest-timestamped request for ℓ_3, and it must wait for $\mathcal{R}_3^w$ to complete. If read request $\mathcal{R}_6^r$ for ℓ_2 is issued as shown in (b), then in (c), $\mathcal{R}_4^w$ can be waiting behind the entitled read $\mathcal{R}_6^r$. In fact, after just under L_{max}^w time units of $\mathcal{R}_3^w$ executing, $\mathcal{R}_7^w$ and $\mathcal{R}_8^r$ could be issued as shown in (c). Thus, $\mathcal{R}_4^w$ could wait an additional $L_{max}^w + L_{max}^r$ time units for those two request to finish before it is satisfied. Once it is satisfied, our request of interest $\mathcal{R}_5^w$ may wait up to L_{max}^w time units for $\mathcal{R}_4^w$ to complete, at which point $\mathcal{R}_5^w$ is finally the earliest-timestamped request for ℓ_3 after waiting for $4L_{max}^w + 2L_{max}^r$ time units.

Theorem 3.2 presents three bounds for write requests. Non-nested write requests may experience up to L_{max}^r time units of acquisition delay if no nested requests are active (illustrated in Fig. 9 and described in Ex. A.1). Non-nested write requests in the presence of nested requests may experience up $5L_{max}^w + 3L_{max}^r$ time units of acquisition delay (described below). Finally, nested write requests may experience acquisition delay of up to $3L_{max}^w + 2L_{max}^r$ (also described below).

Example A.6. As illustrated by Fig. 11, $\mathcal{R}_5^w$ may wait for $4L_{max}^w + 2L_{max}^r$ time units to become the earliest-timestamped request for its resources. Suppose just before $\mathcal{R}_4^w$ completes, $\mathcal{R}_9^w$ and $\mathcal{R}_{10}^r$ are issued, as illustrated in Fig. 11(d). $\mathcal{R}_5^w$ may indeed need to wait an additional $L_{max}^w + L_{max}^r$ time units before being satisfied, making its total acquisition delay $5L_{max}^w + 3L_{max}^r$ time units.

Fig. 11 also illustrates that a nested write request, namely $\mathcal{R}_4^w$, may experience acquisition delay of $3L_{max}^w + 2L_{max}^r$. Indeed, $\mathcal{R}_4^w$ waits for the completion of three write requests ($\mathcal{R}_1^w$, $\mathcal{R}_3^w$, and $\mathcal{R}_7^w$), which may only barely overlap, and two read phases ($\mathcal{R}_2^r$'s and $\mathcal{R}_8^r$'s read phases) that do not overlap with any of the write requests.

A.2 Linearizability

Herlihy and Wing presented linearizability as a new correctness condition for concurrent objects that "provides the illusion that each operation applied by concurrent processes takes effect instantaneously at some point between its invocation and its response." Linearizability is a local property; if the operations on each object can be linearized, the system as a whole is considered to be linearizable [8].

In the body of the paper, we claim that each routine we presented has a linearization point; this is the point at which the routine can be considered to take effect (atomically). For the non-nested routines, these points are clear. A read request enqueues atomically at Line 3 (Listing 2) and can be viewed as executing the lock function as a whole atomically at the end of the procedure. Similarly for R*_Unlock^{nn}, the routine's linearization point can be considered to be at its invocation. The non-nested write routines function similarly, with linearization points at the end of the lock routine's execution and the beginning of the execution of the unlock routine.

The nested routines grant access to groups of resources at a time (Listing 3). Considering the routines themselves, each call of the lock routine can be said to linearize to the last point in its execution. That is, no access to any of the requested resources occurs before that point in time, and the order of request accesses to those resources is exactly the order of termination of the lock routines. (Recall that linearization is defined relative to a specific resource; there may be requests for other resources occurring concurrently. These requests are not granted access clearly before or after the non-conflicting request. Again, linearization is a local property and there may be multiple legal sequential histories [8].) Just like non-nested requests, the invocation of each unlock routine can be considered to be the linearization point of the entire routine.

An example of the linearization of several objects is shown in Fig. 12. An operation invocation *op* on a set of shared resources D_i by request $\mathcal{R}_i$ is indicated by D_i *op* $\mathcal{R}_i$ above a line whose length corresponds to the duration of time each invocation takes. The linearization point of each operation's execution is indicated with a circle at some point during its execution. As discussed above, this point can always be selected at the end of the execution of a `lock` operation and at the beginning of the execution of an `unlock` operation. In Fig. 12, time moves forward to the right.

Example A.7. In Fig. 12, $\mathcal{R}_1^{w,n}$ is the first to begin executing the lock logic to gain mutual exclusion access to $D_1 = \{\ell_1, \ell_2\}$. Then $\mathcal{R}_2^{w,nn}$ is issued for $D_2 = \{\ell_2\}$. $\mathcal{R}_2^{w,nn}$ calls `lock` for ℓ_2. It is granted access to ℓ_2 first (at the end of the lock routine), and then enters its critical section before calling `unlock`.

During $\mathcal{R}_2^{w,nn}$'s execution of the lock operation, $\mathcal{R}_3^{r,n}$ invoked the lock call for $D_3 = \{\ell_1, \ell_2\}$.

At some point $\mathcal{R}_2^{w,nn}$ completes its critical section and invokes the unlock routine. The unlock routine can be linearized to the point indicated in the Fig. 12, which clearly comes before the point at which $\mathcal{R}_1^{w,n}$ or $\mathcal{R}_3^{r,nn}$ has linearized its respective lock call. Note that this properly reflects the mutually exclusive access for $\mathcal{R}_2^{w,n}$ for ℓ_2; a request is considered to access the resource between the linearization point for its call to the lock routine and the linearization point for its call to the unlock routine.

At a later point in time, $\mathcal{R}_1^{w,n}$ finishes execution of the lock routine, enters its critical section, and then calls the unlock routine.

While $\mathcal{R}_1^{w,n}$ is executing the unlock routine for $D_1 = \{\ell_1, \ell_2\}$, $\mathcal{R}_4^{r,nn}$ and $\mathcal{R}_5^{w,nn}$ are issued for $D_4 = \{\ell_1\}$ and $D_5 = \{\ell_1\}$, respectively.

At some point in time after $\mathcal{R}_1^{w,nn}$ has updated the writer bits of ℓ_1's *rin* variable, $\mathcal{R}_4^{r,nn}$ becomes satisfied and completes its call to the lock routine. Similarly, after $\mathcal{R}_1^{w,nn}$ has updated ℓ_2's *rin* variable, $\mathcal{R}_3^{r,nn}$ becomes satisfied and completes its call to the lock routine. Note that overlapping critical sections for ℓ_1 is expected behavior for these requests; read requests may overlap.

Once the read requests finish accessing their respective resources, they both call the unlock routine. At a future point in time, $\mathcal{R}_5^{w,nn}$ completes its call to the lock routine and can begin its critical section. Note that the linearization points correctly reflect mutually exclusive access for this request for ℓ_1.

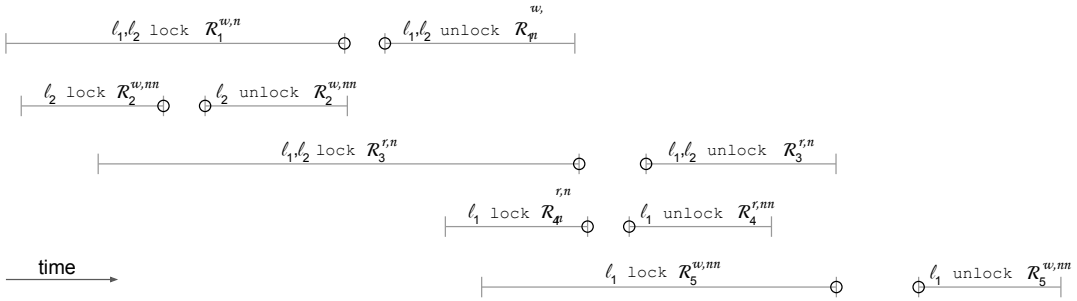

Figure 12: Illustration of a series of lock and unlock calls by requests $\mathcal{R}_1$ through $\mathcal{R}_5$ with the linearization point of each operation shown with a circle.

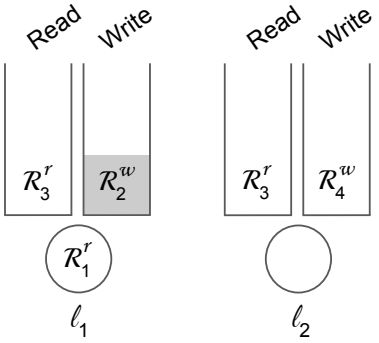

Figure 13: Illustrates the edge case in which a write request ($\mathcal{R}_4^w$) would need to wait unnecessarily behind a nested read request ($\mathcal{R}_3^r$) if the extra code step had not been added in Listing 3.

A.3 Corner Case for Nested Reads

In an initial implementation of the R*_Lock^n routine in Listing 3, we did not include the extra phase in Lines 19-21. Unfortunately, this allows a potential edge case, as demonstrated in Fig. 13, in which write requests suffer unnecessary transitive blocking caused by read requests incorrectly marking themselves entitled.

In this scenario, read request $\mathcal{R}_1^{r,nn}$ is satisfied and write request $\mathcal{R}_2^{w,nn}$ is entitled when read request $\mathcal{R}_3^{r,n}$ is issued. At this point, $\mathcal{R}_1^{r,nn}$ has completed the R*_Lock^{nn} routine and $\mathcal{R}_2^{w,nn}$ is waiting at Line 13 for its requested resource to become available.

Without Lines 19-21, $\mathcal{R}_3^{r,n}$ immediately modifies ℓ_1's *rin* variable, effectively marking itself entitled, and waits at Line 27 for $\mathcal{R}_2^{w,nn}$ to complete. When $\mathcal{R}_4^{w,nn}$ is released, it must wait at Line 13 (Listing 2) for $\mathcal{R}_3^{r,n}$ to complete, even though it should have been immediately satisfied following the rules of the fast RW-RNLP.

Using the implementation given in Listing 3, however, $\mathcal{R}_3^{r,n}$ must wait at Line 21 due to $\mathcal{R}_2^{w,nn}$ having marked itself present in the bottom byte of ℓ_1's *rin* variable. This prevents $\mathcal{R}_3^{r,n}$ from modifying ℓ_1's *rin* variable before it should become entitled. Therefore, when $\mathcal{R}_4^{w,nn}$ is released, the condition at Line 13 is true for its single resource ℓ_2, so it is immediately satisfied.

A.4 Use of a PF-TL in Nested Routines

In the lock and unlock routines for nested requests (Listing 3), we use a single PF-TL to provide reader/writer-like sharing for nested requests to enqueue themselves for their respective resources. We do this because we need to guarantee that read and write requests enqueue atomically with respect to each other (guaranteed by accessing the PF-TL for a write and read, respectively). Because no two nested writes are at the heads of queues for overlapping resource sets, no two nested writes can concurrently modify the same *rin* values on Line 39. Therefore, the read-lock functionality of the PF-TL provides access to these values that is mutually exclusive with regards to nested read requests and nested write requests. The write-lock functionality of the PF-TL alone guarantees mutually exclusive access for read requests in Listing 3.

Our only challenge here was providing mutually exclusive access for all nested requests to the *rin* variables. A non-nested read or write that modifies the some *rin* variable will linearize before or after the nested request (see Sec. A.2), so this does not present an issue.

Finally, although nested read requests experience additional overhead incurred by waiting for the write-lock of the PF-TL, this overhead is small, as each nested request $\mathcal{R}_i$ only modifies $|D_i|$ *rin* values while holding the PF-TL (no blocking is done while holding the PF-TL); our experiments still showed very low lock overhead and blocking times for nested read requests under the fast RW-RNLP.

B ADDITIONAL GRAPHS

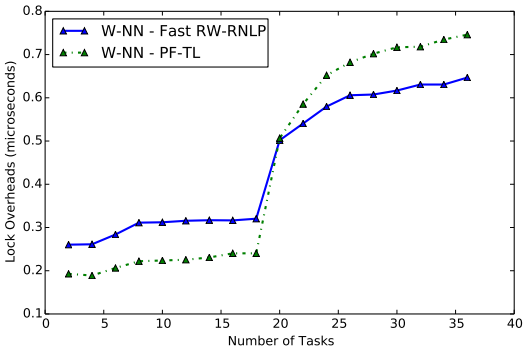

(a) Lock overhead.

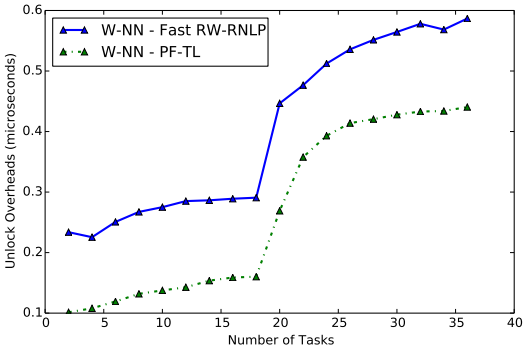

(b) Unlock overhead.

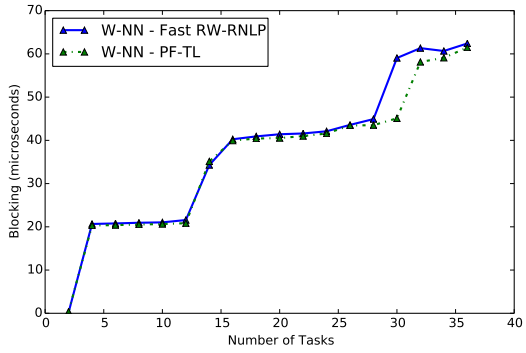

(c) Blocking.

Figure 14: (a) Lock and (b) unlock overheads and (c) blocking for non-nested read and write requests under the PF-TL and the fast RW-RNLP. Here, $L_i^w = 20\mu$s, $n_r = 56$, and $|D_i| = 1$ for each request $\mathcal{R}_i$. Each request was randomly chosen to be a read (as opposed to a write) with probability 0.

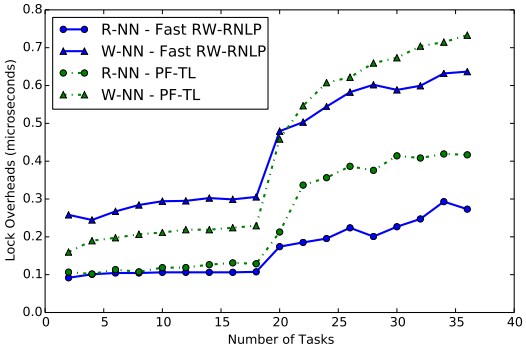

(a) Lock overhead.

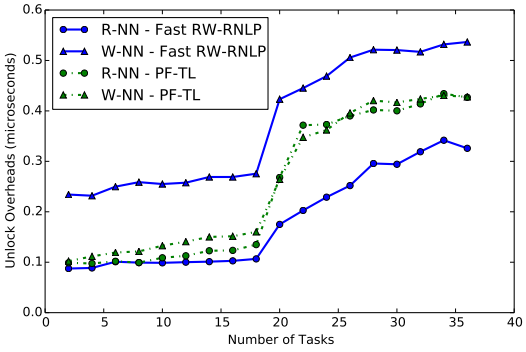

(b) Unlock overhead.

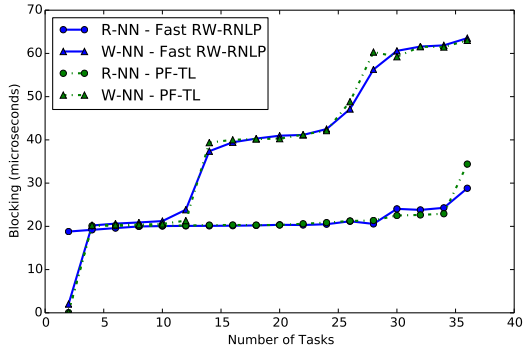

(c) Blocking.

Figure 15: (a) Lock and (b) unlock overheads and (c) blocking for non-nested read and write requests under the PF-TL and the fast RW-RNLP. Here, $L_i^r = 20\mu$s, $L_i^w = 20\mu$s, $n_r = 56$, and $|D_i| = 1$ for each request $\mathcal{R}_i$. Each request was randomly chosen to be a read (as opposed to a write) with probability 0.2.

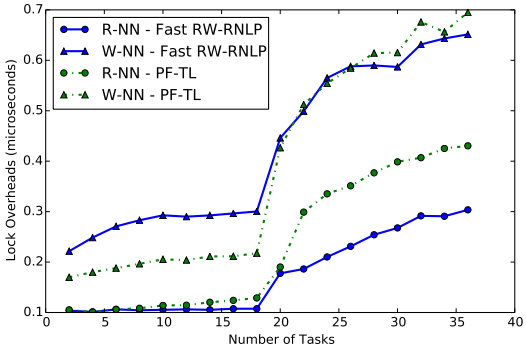

(a) Lock overhead.

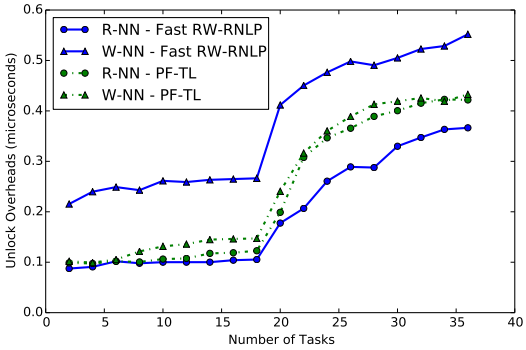

(b) Unlock overhead.

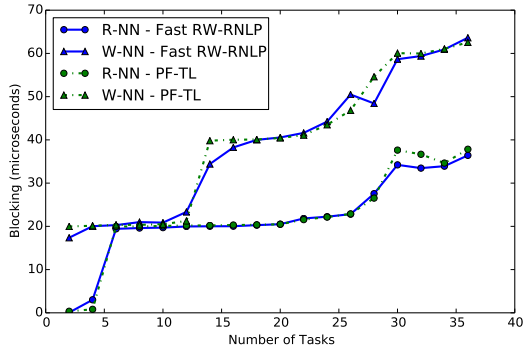

(c) Blocking.

Figure 16: (a) Lock and (b) unlock overheads and (c) blocking for non-nested read and write requests under the PF-TL and the fast RW-RNLP. Here, $L_i^r = 20\mu$s, $L_i^w = 20\mu$s, $n_r = 56$, and $|D_i| = 1$ for each request $\mathcal{R}_i$. Each request was randomly chosen to be a read (as opposed to a write) with probability 0.5.

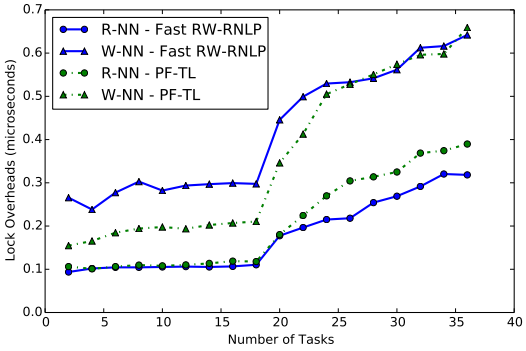

(a) Lock overhead.

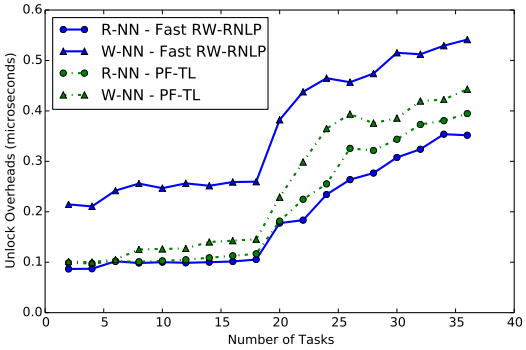

(b) Unlock overhead.

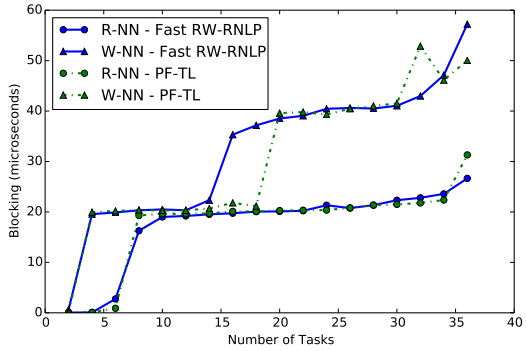

(c) Blocking.

Figure 17: (a) Lock and (b) unlock overheads and (c) blocking for non-nested read and write requests under the PF-TL and the fast RW-RNLP. Here, $L_i^r = 20\mu$s, $L_i^w = 20\mu$s, $n_r = 56$, and $|D_i| = 1$ for each request $\mathcal{R}_i$. Each request was randomly chosen to be a read (as opposed to a write) with probability 0.8.

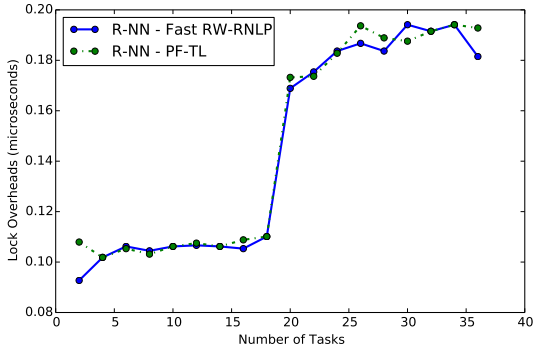

(a) Lock overhead.

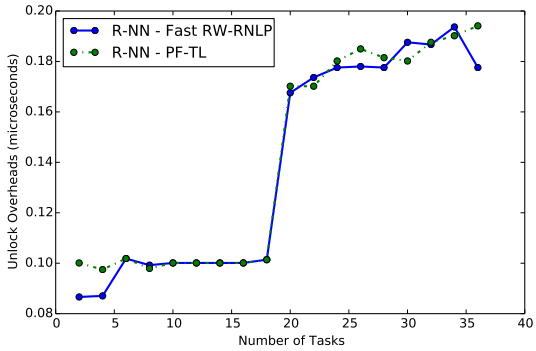

(b) Unlock overhead.

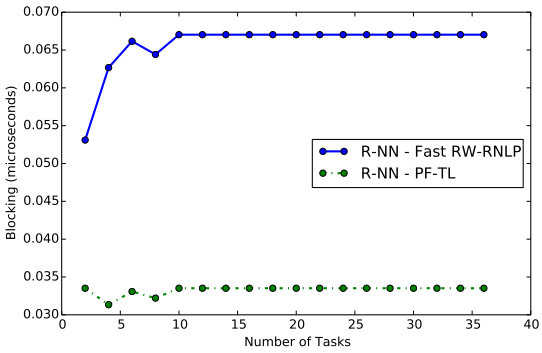

(c) Blocking.

Figure 18: (a) Lock and (b) unlock overheads and (c) blocking for non-nested read and write requests under the PF-TL and the fast RW-RNLP. Here, $L_i^r = 20\mu$s, $n_r = 56$, and $|D_i| = 1$ for each request $\mathcal{R}_i$. Each request was randomly chosen to be a read (as opposed to a write) with probability 1.

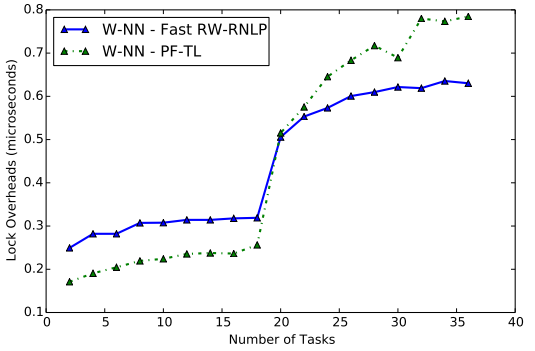

(a) Lock overhead.

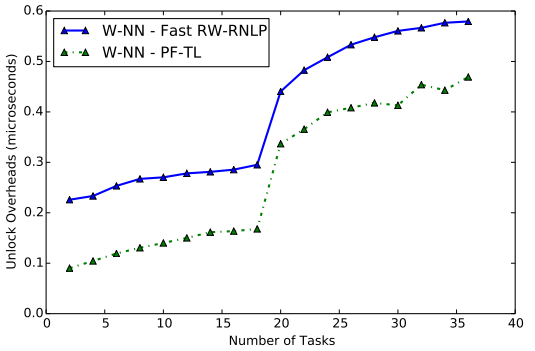

(b) Unlock overhead.

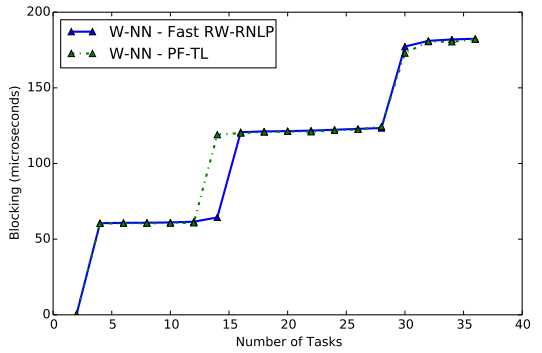

(c) Blocking.

Figure 19: (a) Lock and (b) unlock overheads and (c) blocking for non-nested read and write requests under the PF-TL and the fast RW-RNLP. Here, $L_i^w = 60\mu$s, $n_r = 56$, and $|D_i| = 1$ for each request $\mathcal{R}_i$. Each request was randomly chosen to be a read (as opposed to a write) with probability 0.

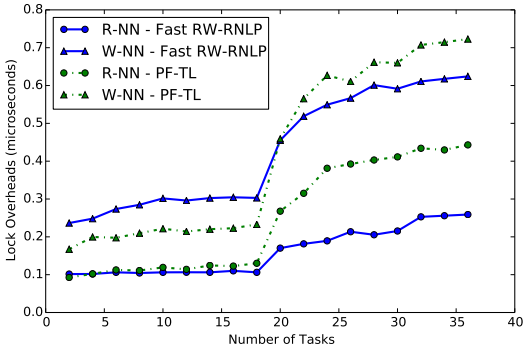

(a) Lock overhead.

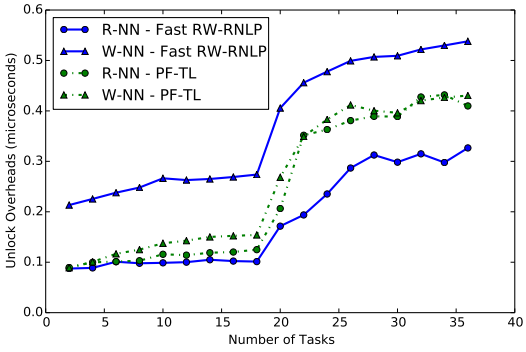

(b) Unlock overhead.

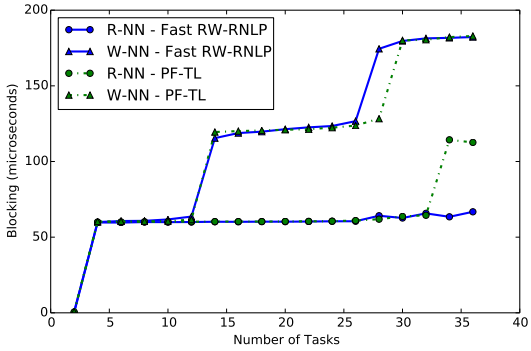

(c) Blocking.

Figure 20: (a) Lock and (b) unlock overheads and (c) blocking for non-nested read and write requests under the PF-TL and the fast RW-RNLP. Here, $L_i^r = 60\mu$s, $L_i^w = 60\mu$s, $n_r = 56$, and $|D_i| = 1$ for each request $\mathcal{R}_i$. Each request was randomly chosen to be a read (as opposed to a write) with probability 0.2.

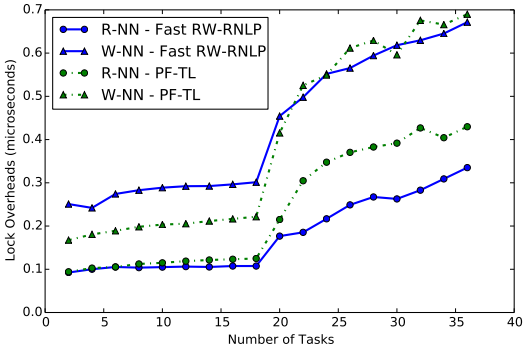

(a) Lock overhead.

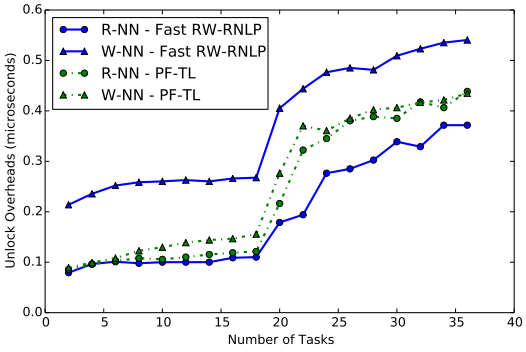

(b) Unlock overhead.

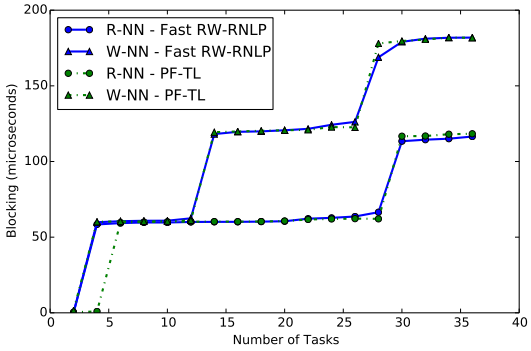

(c) Blocking.

Figure 21: (a) Lock and (b) unlock overheads and (c) blocking for non-nested read and write requests under the PF-TL and the fast RW-RNLP. Here, $L_i^r = 60\mu$s, $L_i^w = 60\mu$s, $n_r = 56$, and $|D_i| = 1$ for each request $\mathcal{R}_i$. Each request was randomly chosen to be a read (as opposed to a write) with probability 0.5.

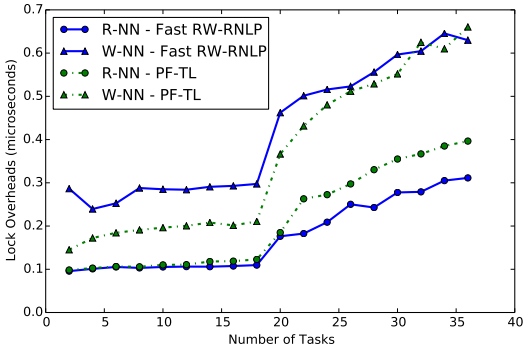

(a) Lock overhead.

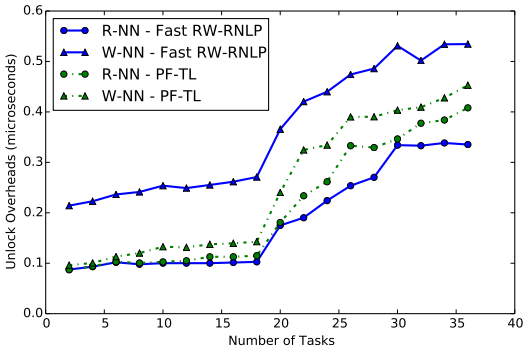

(b) Unlock overhead.

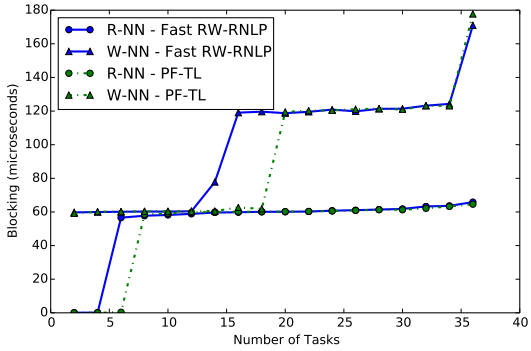

(c) Blocking.

Figure 22: (a) Lock and (b) unlock overheads and (c) blocking for non-nested read and write requests under the PF-TL and the fast RW-RNLP. Here, $L_i^r = 60\mu$s, $L_i^w = 60\mu$s, $n_r = 56$, and $|D_i| = 1$ for each request $\mathcal{R}_i$. Each request was randomly chosen to be a read (as opposed to a write) with probability 0.8.

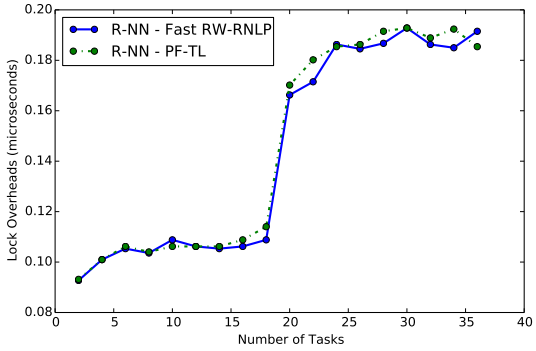

(a) Lock overhead.

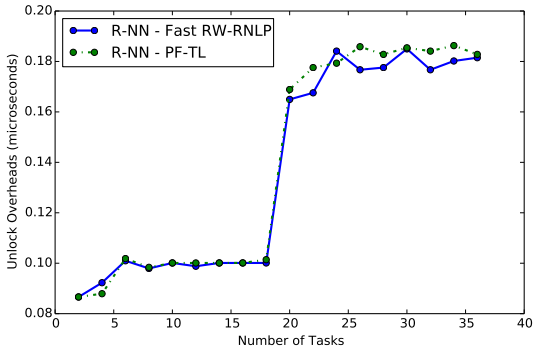

(b) Unlock overhead.

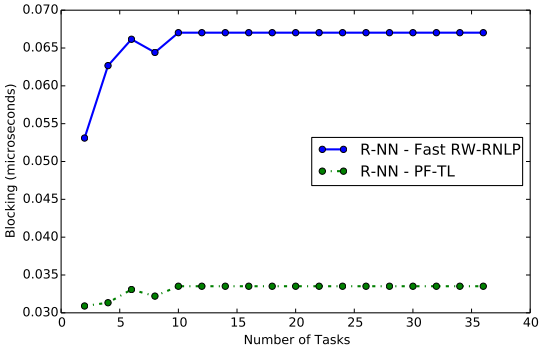

(c) Blocking.

Figure 23: (a) Lock and (b) unlock overheads and (c) blocking for non-nested read and write requests under the PF-TL and the fast RW-RNLP. Here, $L_i^r = 60\mu$s, $n_r = 56$, and $|D_i| = 1$ for each request $\mathcal{R}_i$. Each request was randomly chosen to be a read (as opposed to a write) with probability 1.

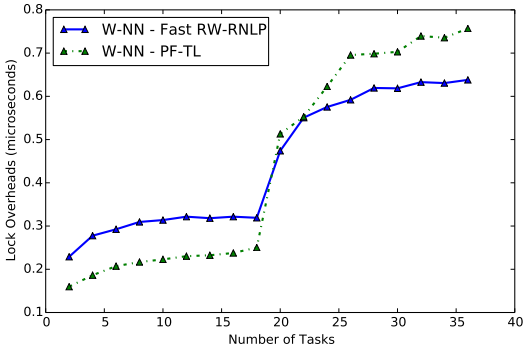

(a) Lock overhead.

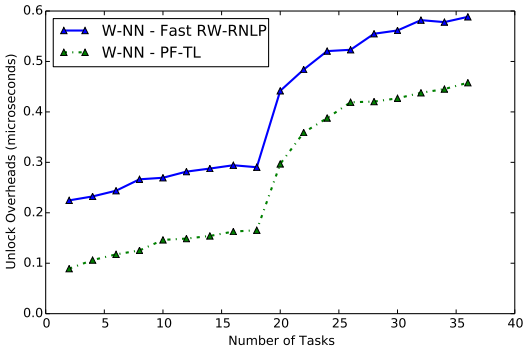

(b) Unlock overhead.

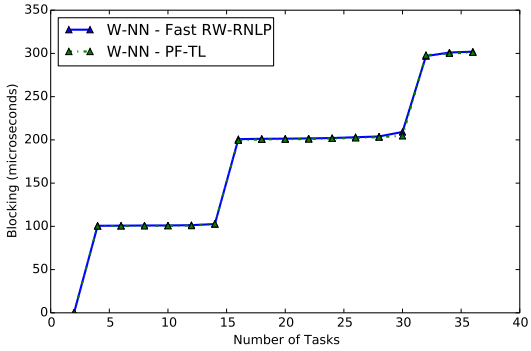

(c) Blocking.

Figure 24: (a) Lock and (b) unlock overheads and (c) blocking for non-nested read and write requests under the PF-TL and the fast RW-RNLP. Here, $L_i^w = 100\mu$s, $n_r = 56$, and $|D_i| = 1$ for each request $\mathcal{R}_i$. Each request was randomly chosen to be a read (as opposed to a write) with probability 0.

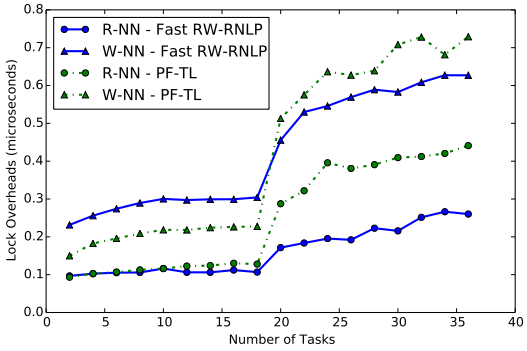

(a) Lock overhead.

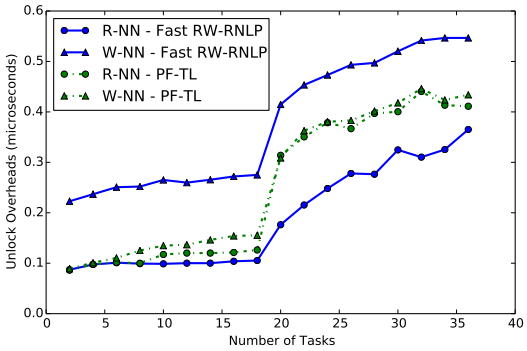

(b) Unlock overhead.

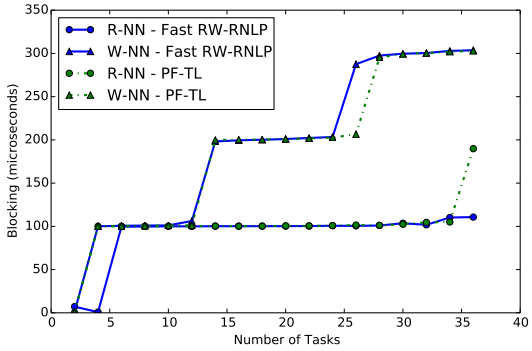

(c) Blocking.

Figure 25: (a) Lock and (b) unlock overheads and (c) blocking for non-nested read and write requests under the PF-TL and the fast RW-RNLP. Here, $L_i^r = 100\mu$s, $L_i^w = 100\mu$s, $n_r = 56$, and $|D_i| = 1$ for each request $\mathcal{R}_i$. Each request was randomly chosen to be a read (as opposed to a write) with probability 0.2.

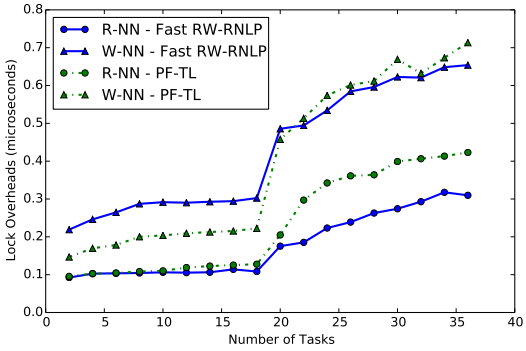

(a) Lock overhead.

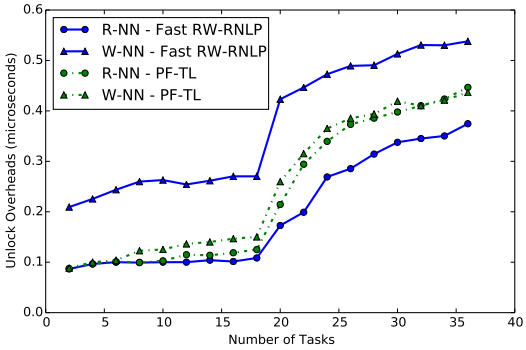

(b) Unlock overhead.

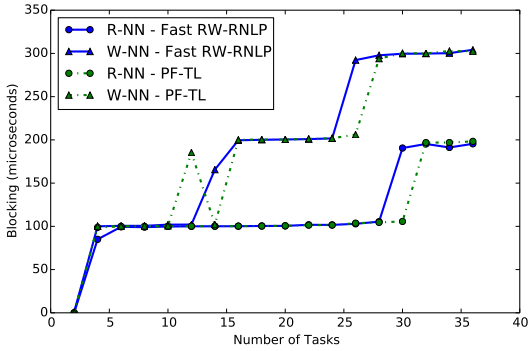

(c) Blocking.

Figure 26: (a) Lock and (b) unlock overheads and (c) blocking for non-nested read and write requests under the PF-TL and the fast RW-RNLP. Here, $L_i^r = 100\mu$s, $L_i^w = 100\mu$s, $n_r = 56$, and $|D_i| = 1$ for each request $\mathcal{R}_i$. Each request was randomly chosen to be a read (as opposed to a write) with probability 0.5.

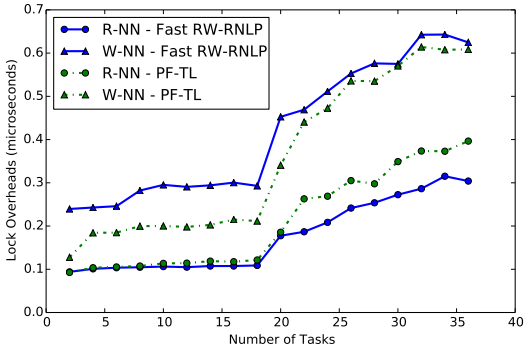

(a) Lock overhead.

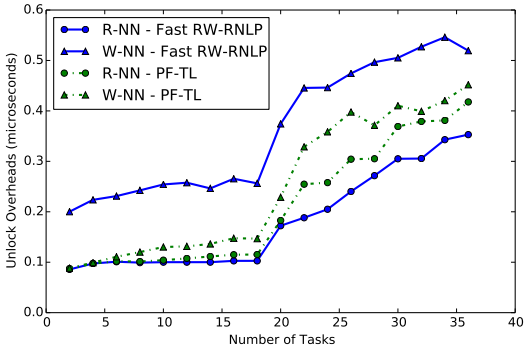

(b) Unlock overhead.

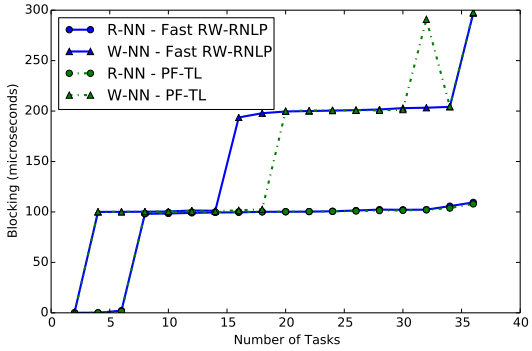

(c) Blocking.

Figure 27: (a) Lock and (b) unlock overheads and (c) blocking for non-nested read and write requests under the PF-TL and the fast RW-RNLP. Here, $L_i^r = 100\mu$s, $L_i^w = 100\mu$s, $n_r = 56$, and $|D_i| = 1$ for each request $\mathcal{R}_i$. Each request was randomly chosen to be a read (as opposed to a write) with probability 0.8.

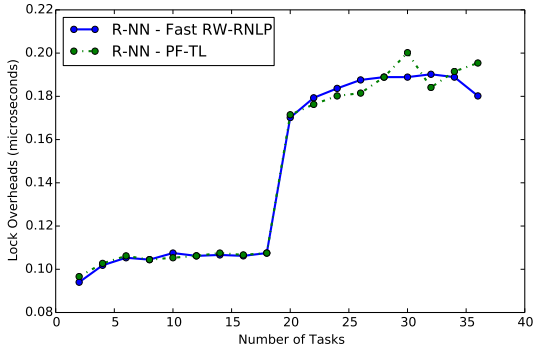

(a) Lock overhead.

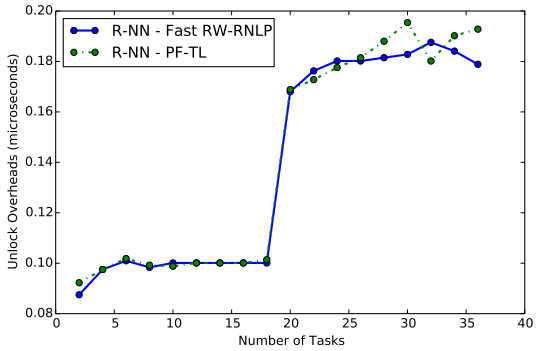

(b) Unlock overhead.

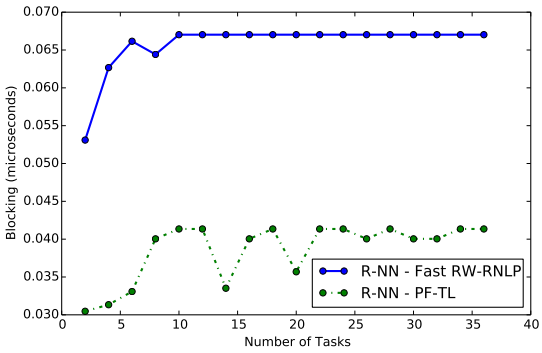

(c) Blocking.

Figure 28: (a) Lock and (b) unlock overheads and (c) blocking for non-nested read and write requests under the PF-TL and the fast RW-RNLP. Here, $L_i^r = 100\mu$s, $n_r = 56$, and $|D_i| = 1$ for each request $\mathcal{R}_i$. Each request was randomly chosen to be a read (as opposed to a write) with probability 1.

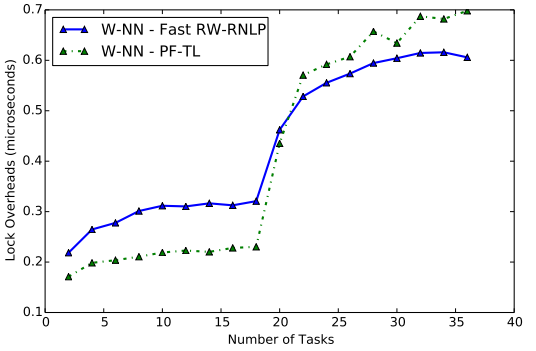

(a) Lock overhead.

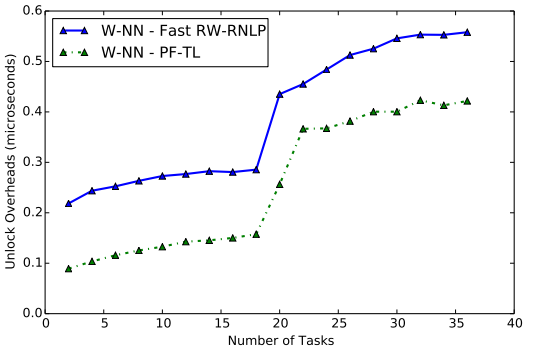

(b) Unlock overhead.

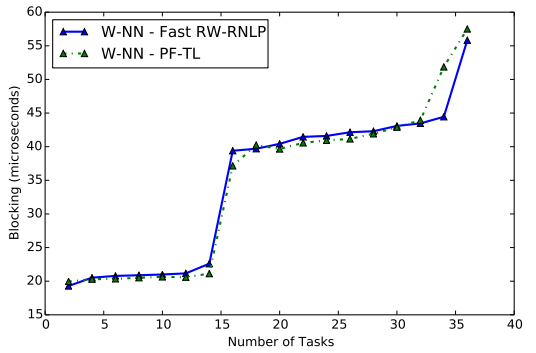

(c) Blocking.

Figure 29: (a) Lock and (b) unlock overheads and (c) blocking for non-nested read and write requests under the PF-TL and the fast RW-RNLP. Here, $L_i^w = 20\mu$s, $n_r = 64$, and $|D_i| = 1$ for each request $\mathcal{R}_i$. Each request was randomly chosen to be a read (as opposed to a write) with probability 0.

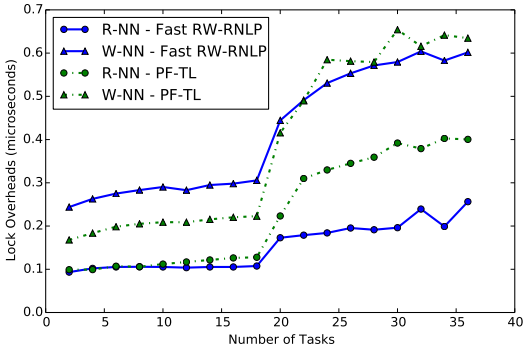

(a) Lock overhead.

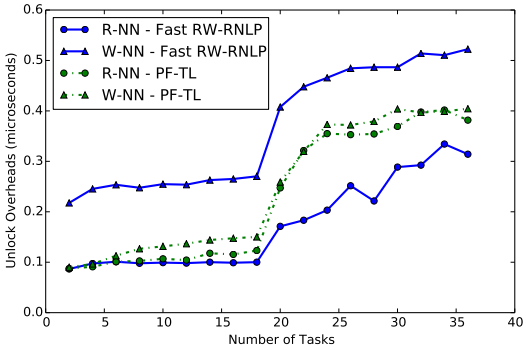

(b) Unlock overhead.

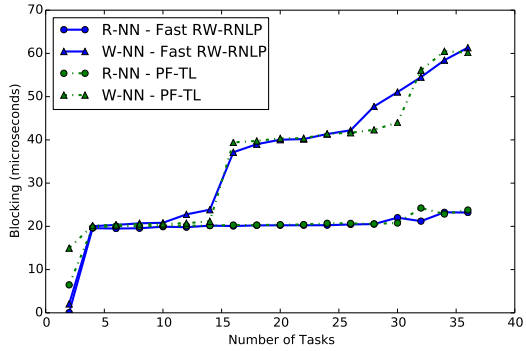

(c) Blocking.

Figure 30: (a) Lock and (b) unlock overheads and (c) blocking for non-nested read and write requests under the PF-TL and the fast RW-RNLP. Here, $L_i^r = 20\mu$s, $L_i^w = 20\mu$s, $n_r = 64$, and $|D_i| = 1$ for each request $\mathcal{R}_i$. Each request was randomly chosen to be a read (as opposed to a write) with probability 0.2.

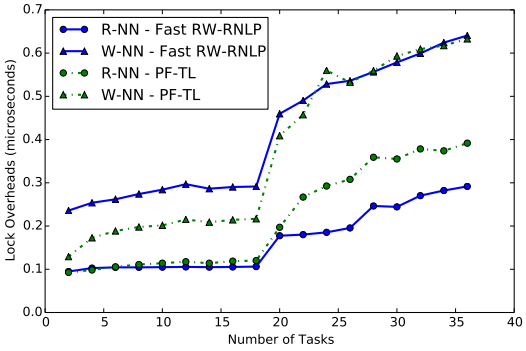

(a) Lock overhead.

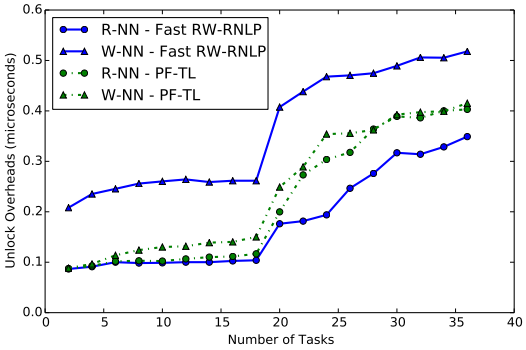

(b) Unlock overhead.

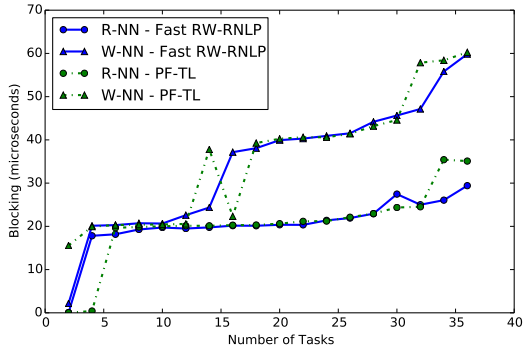

(c) Blocking.

Figure 31: (a) Lock and (b) unlock overheads and (c) blocking for non-nested read and write requests under the PF-TL and the fast RW-RNLP. Here, $L_i^r = 20\mu$s, $L_i^w = 20\mu$s, $n_r = 64$, and $|D_i| = 1$ for each request $\mathcal{R}_i$. Each request was randomly chosen to be a read (as opposed to a write) with probability 0.5.

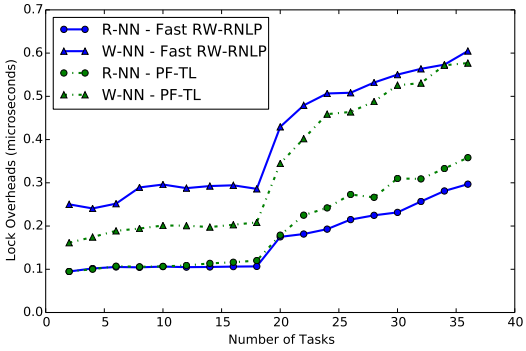

(a) Lock overhead.

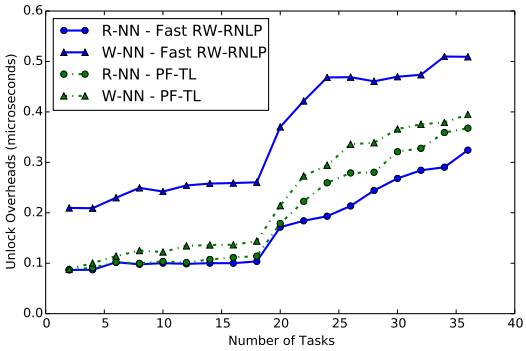

(b) Unlock overhead.

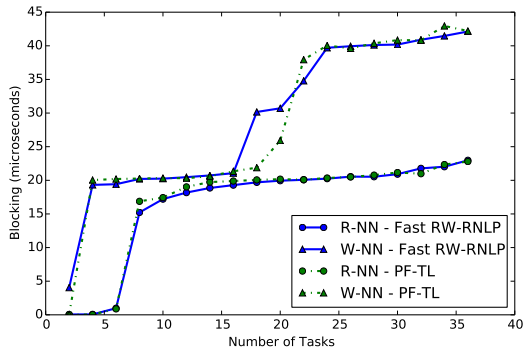

(c) Blocking.

Figure 32: (a) Lock and (b) unlock overheads and (c) blocking for non-nested read and write requests under the PF-TL and the fast RW-RNLP. Here, $L_i^r = 20\mu$s, $L_i^w = 20\mu$s, $n_r = 64$, and $|D_i| = 1$ for each request $\mathcal{R}_i$. Each request was randomly chosen to be a read (as opposed to a write) with probability 0.8.

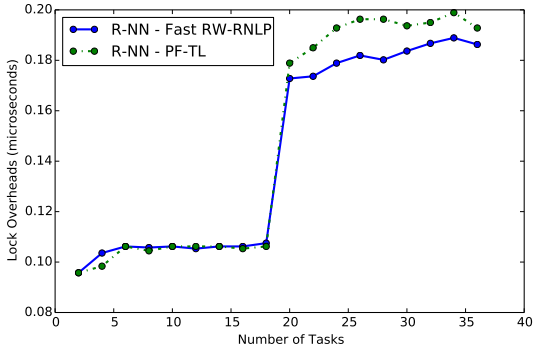

(a) Lock overhead.

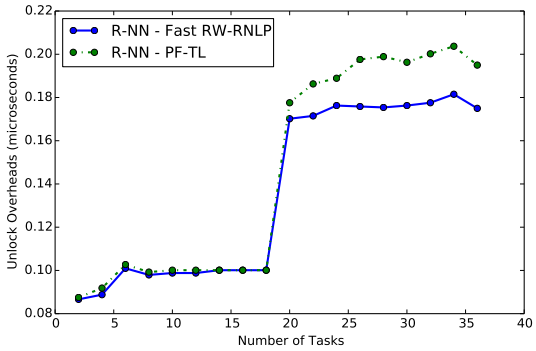

(b) Unlock overhead.

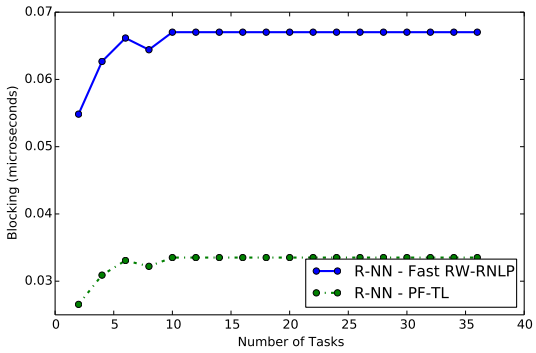

(c) Blocking.

Figure 33: (a) Lock and (b) unlock overheads and (c) blocking for non-nested read and write requests under the PF-TL and the fast RW-RNLP. Here, $L_i^r = 20\mu$s, $n_r = 64$, and $|D_i| = 1$ for each request $\mathcal{R}_i$. Each request was randomly chosen to be a read (as opposed to a write) with probability 1.

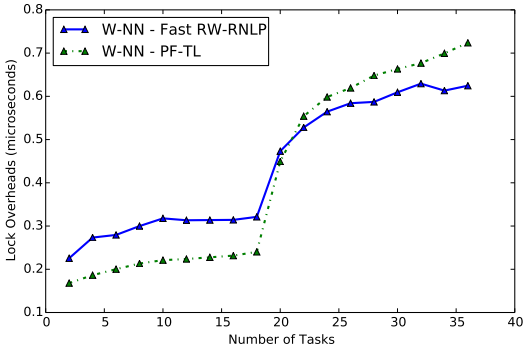

(a) Lock overhead.

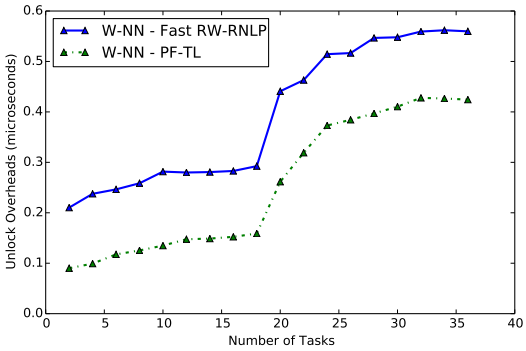

(b) Unlock overhead.

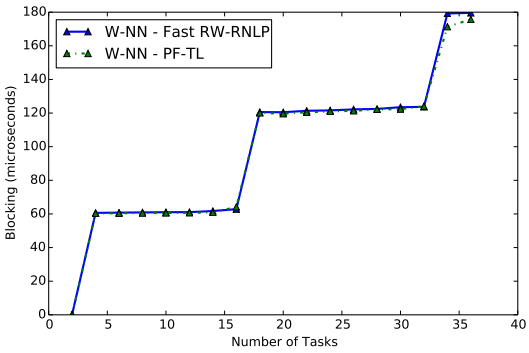

(c) Blocking.

Figure 34: (a) Lock and (b) unlock overheads and (c) blocking for non-nested read and write requests under the PF-TL and the fast RW-RNLP. Here, $L_i^w = 60\mu$s, $n_r = 64$, and $|D_i| = 1$ for each request $\mathcal{R}_i$. Each request was randomly chosen to be a read (as opposed to a write) with probability 0.

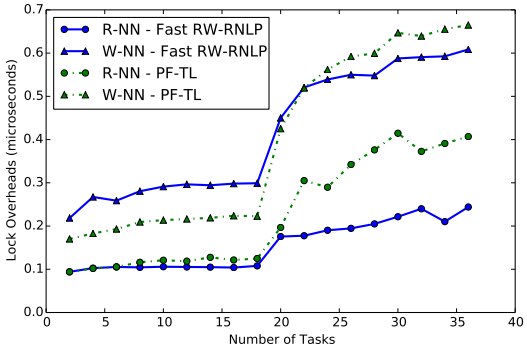

(a) Lock overhead.

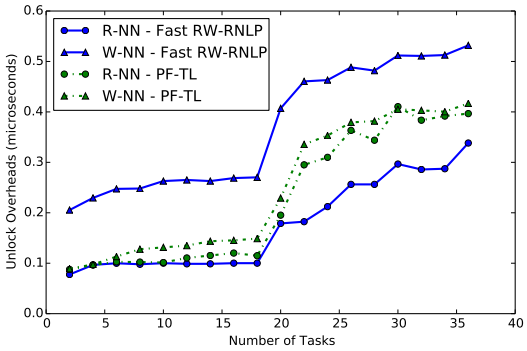

(b) Unlock overhead.

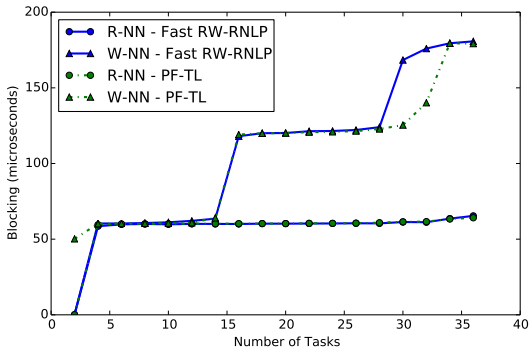

(c) Blocking.

Figure 35: (a) Lock and (b) unlock overheads and (c) blocking for non-nested read and write requests under the PF-TL and the fast RW-RNLP. Here, $L_i^r = 60\mu$s, $L_i^w = 60\mu$s, $n_r = 64$, and $|D_i| = 1$ for each request $\mathcal{R}_i$. Each request was randomly chosen to be a read (as opposed to a write) with probability 0.2.

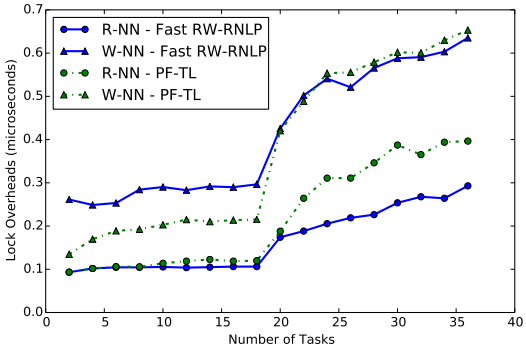

(a) Lock overhead.

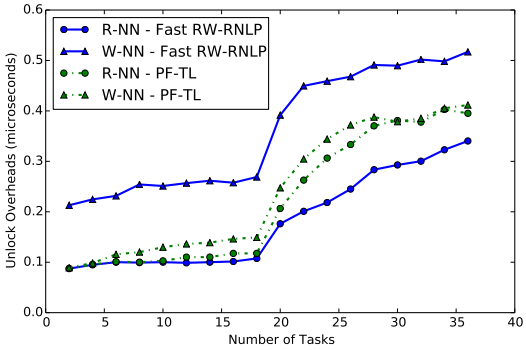

(b) Unlock overhead.

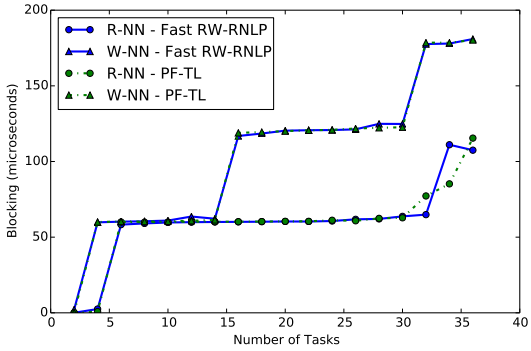

(c) Blocking.

Figure 36: (a) Lock and (b) unlock overheads and (c) blocking for non-nested read and write requests under the PF-TL and the fast RW-RNLP. Here, $L_i^r = 60\mu$s, $L_i^w = 60\mu$s, $n_r = 64$, and $|D_i| = 1$ for each request $\mathcal{R}_i$. Each request was randomly chosen to be a read (as opposed to a write) with probability 0.5.

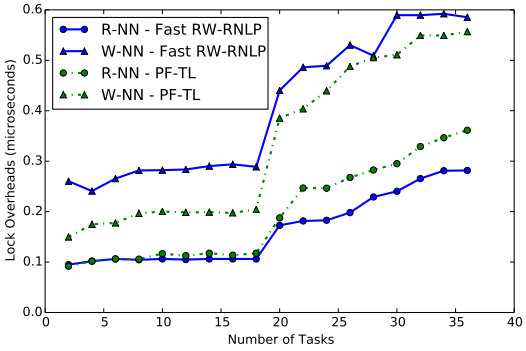

(a) Lock overhead.

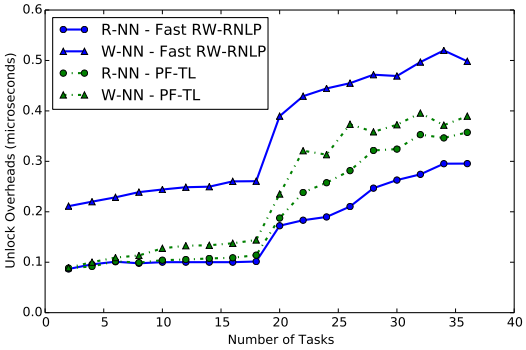

(b) Unlock overhead.

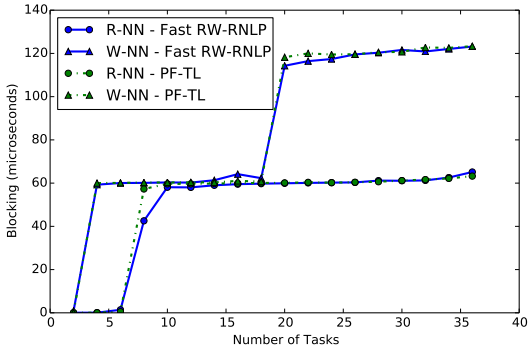

(c) Blocking.

Figure 37: (a) Lock and (b) unlock overheads and (c) blocking for non-nested read and write requests under the PF-TL and the fast RW-RNLP. Here, $L_i^r = 60\mu$s, $L_i^w = 60\mu$s, $n_r = 64$, and $|D_i| = 1$ for each request $\mathcal{R}_i$. Each request was randomly chosen to be a read (as opposed to a write) with probability 0.8.

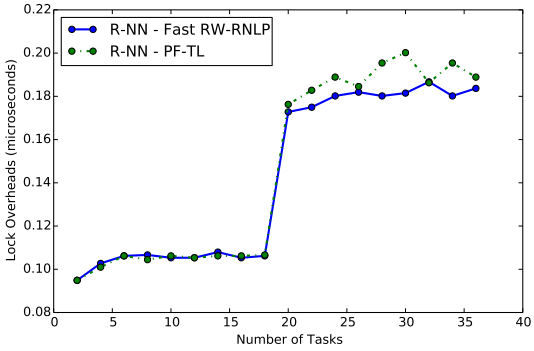

(a) Lock overhead.

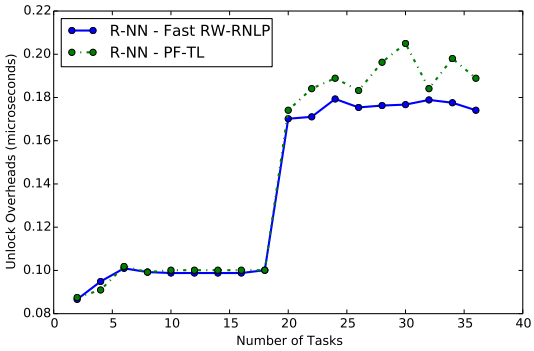

(b) Unlock overhead.

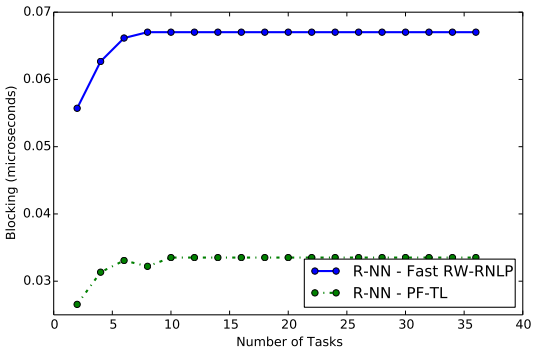

(c) Blocking.

Figure 38: (a) Lock and (b) unlock overheads and (c) blocking for non-nested read and write requests under the PF-TL and the fast RW-RNLP. Here, $L_i^r = 60\mu$s, $n_r = 64$, and $|D_i| = 1$ for each request $\mathcal{R}_i$. Each request was randomly chosen to be a read (as opposed to a write) with probability 1.

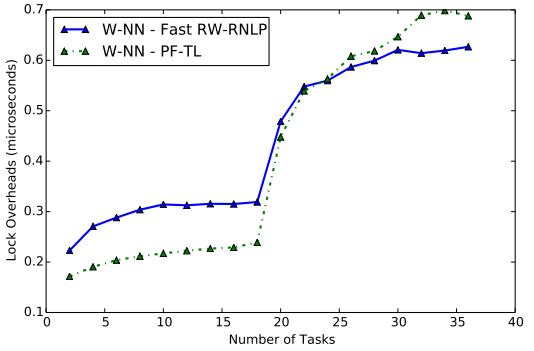

(a) Lock overhead.

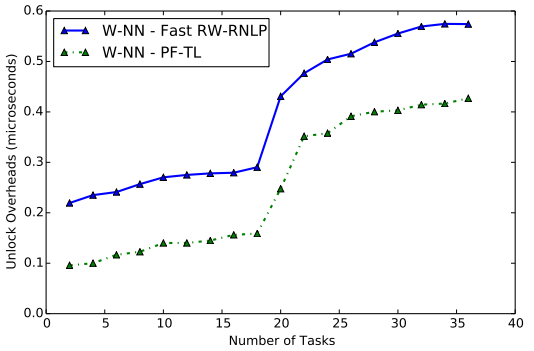

(b) Unlock overhead.

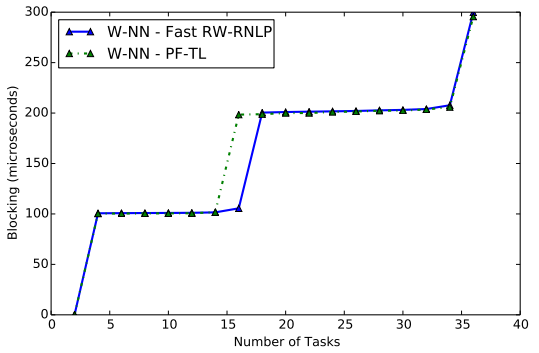

(c) Blocking.

Figure 39: (a) Lock and (b) unlock overheads and (c) blocking for non-nested read and write requests under the PF-TL and the fast RW-RNLP. Here, $L_i^w = 100\mu$s, $n_r = 64$, and $|D_i| = 1$ for each request $\mathcal{R}_i$. Each request was randomly chosen to be a read (as opposed to a write) with probability 0.

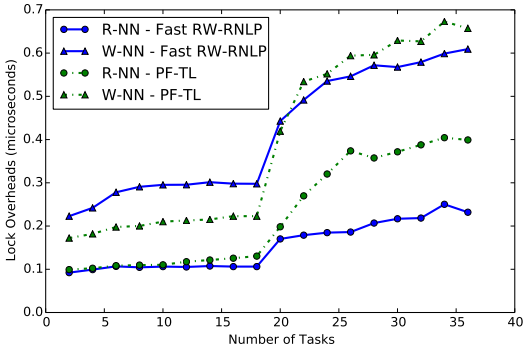

(a) Lock overhead.

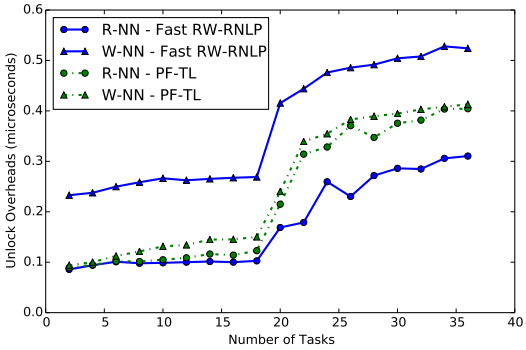

(b) Unlock overhead.

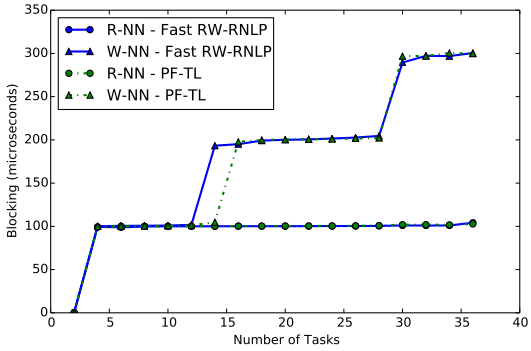

(c) Blocking.

Figure 40: (a) Lock and (b) unlock overheads and (c) blocking for non-nested read and write requests under the PF-TL and the fast RW-RNLP. Here, $L_i^r = 100\mu$s, $L_i^w = 100\mu$s, $n_r = 64$, and $|D_i| = 1$ for each request $\mathcal{R}_i$. Each request was randomly chosen to be a read (as opposed to a write) with probability 0.2.

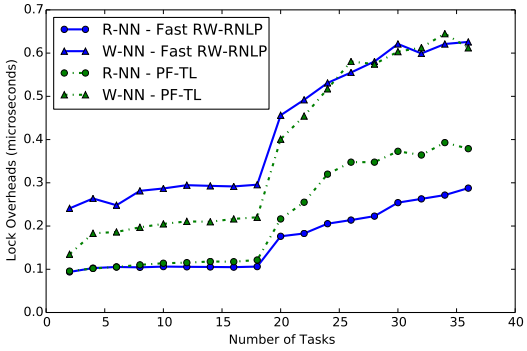

(a) Lock overhead.

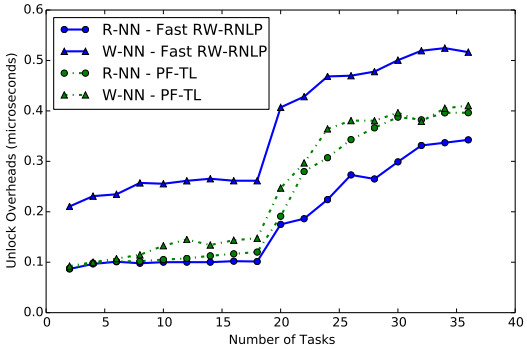

(b) Unlock overhead.

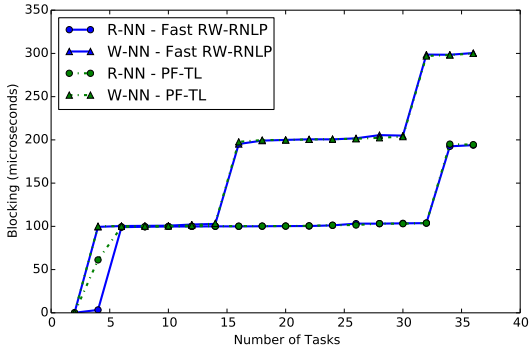

(c) Blocking.

Figure 41: (a) Lock and (b) unlock overheads and (c) blocking for non-nested read and write requests under the PF-TL and the fast RW-RNLP. Here, $L_i^r = 100\mu$s, $L_i^w = 100\mu$s, $n_r = 64$, and $|D_i| = 1$ for each request $\mathcal{R}_i$. Each request was randomly chosen to be a read (as opposed to a write) with probability 0.5.

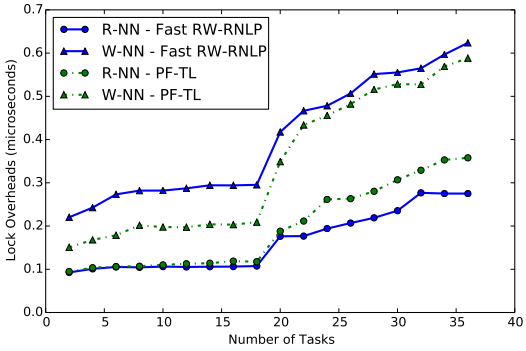

(a) Lock overhead.

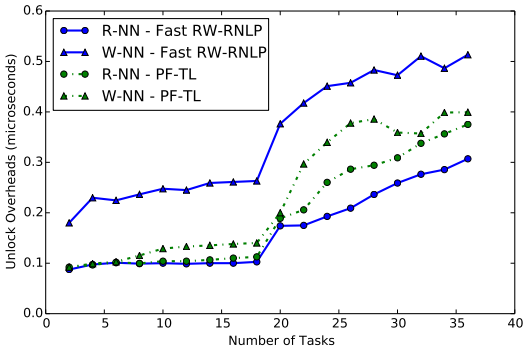

(b) Unlock overhead.

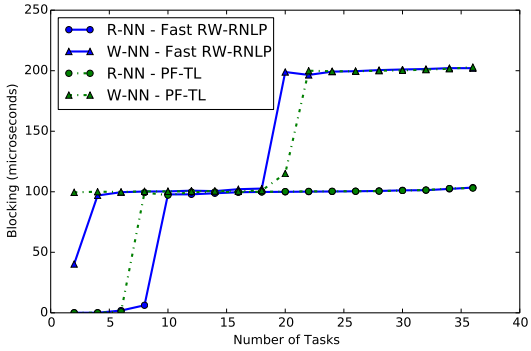

(c) Blocking.

Figure 42: (a) Lock and (b) unlock overheads and (c) blocking for non-nested read and write requests under the PF-TL and the fast RW-RNLP. Here, $L_i^r = 100\mu$s, $L_i^w = 100\mu$s, $n_r = 64$, and $|D_i| = 1$ for each request $\mathcal{R}_i$. Each request was randomly chosen to be a read (as opposed to a write) with probability 0.8.

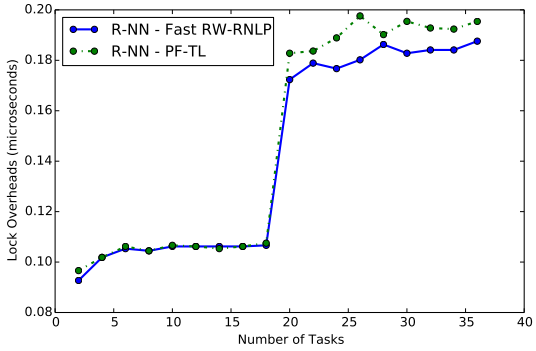

(a) Lock overhead.

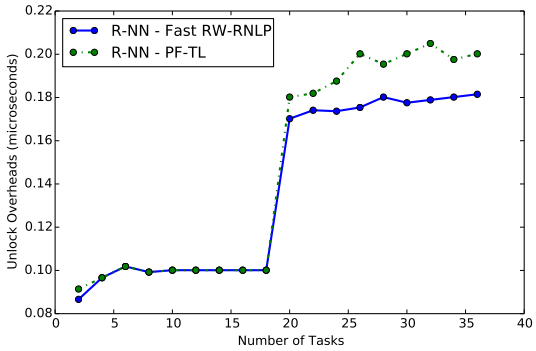

(b) Unlock overhead.

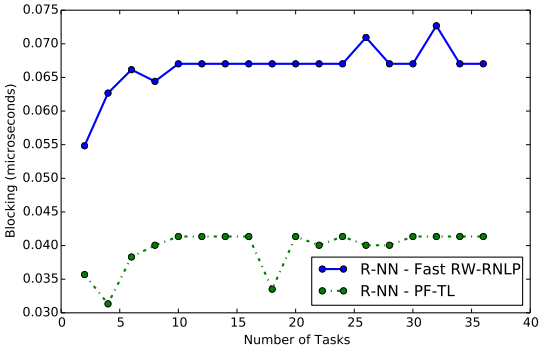

(c) Blocking.

Figure 43: (a) Lock and (b) unlock overheads and (c) blocking for non-nested read and write requests under the PF-TL and the fast RW-RNLP. Here, $L_i^r = 100\mu$s, $n_r = 64$, and $|D_i| = 1$ for each request $\mathcal{R}_i$. Each request was randomly chosen to be a read (as opposed to a write) with probability 1.

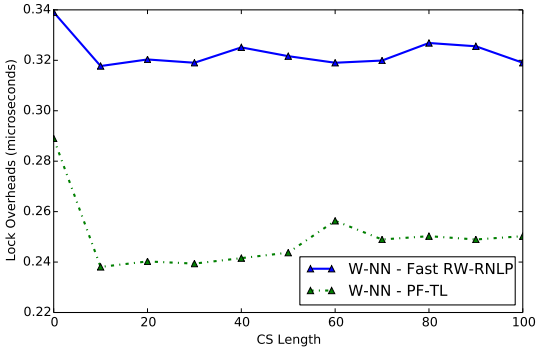

(a) Lock overhead.

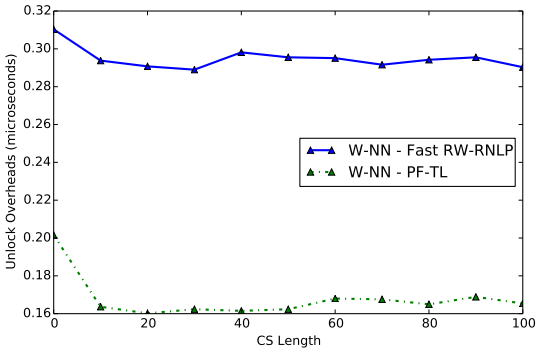

(b) Unlock overhead.

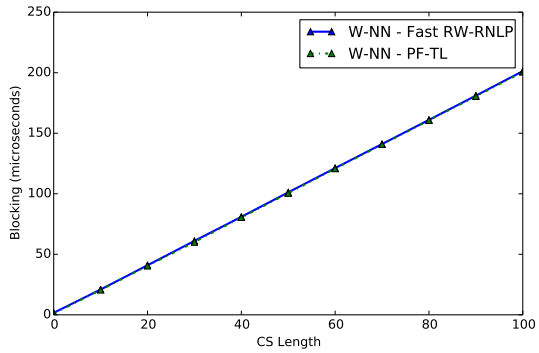

(c) Blocking.

Figure 44: (a) Lock and (b) unlock overheads and (c) blocking for non-nested read and write requests under the PF-TL and the fast RW-RNLP. Here, $m = 18$, $n_r = 56$, and $|D_i| = 1$ for each request $\mathcal{R}_i$. Each request was randomly chosen to be a read (as opposed to a write) with probability 0.

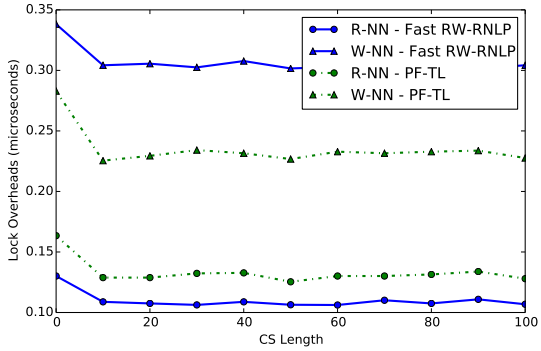

(a) Lock overhead.

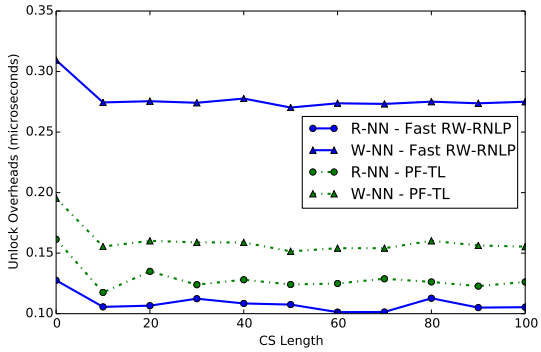

(b) Unlock overhead.

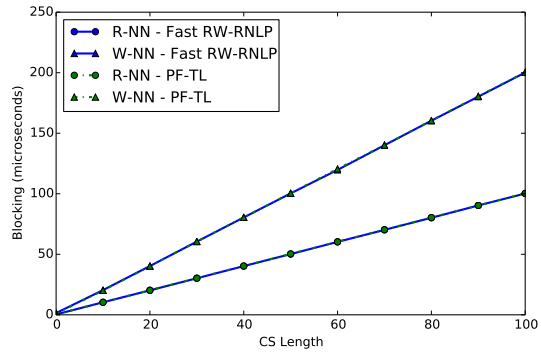

(c) Blocking.

Figure 45: (a) Lock and (b) unlock overheads and (c) blocking for non-nested read and write requests under the PF-TL and the fast RW-RNLP. Here, $m = 18$, $n_r = 56$, and $|D_i| = 1$ for each request $\mathcal{R}_i$. Each request was randomly chosen to be a read (as opposed to a write) with probability 0.2.

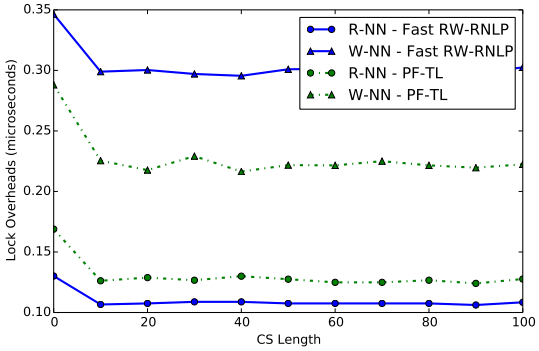

(a) Lock overhead.

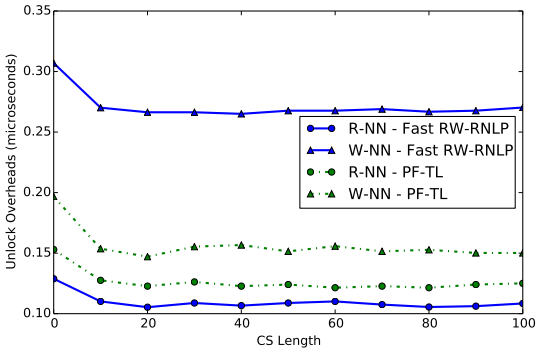

(b) Unlock overhead.

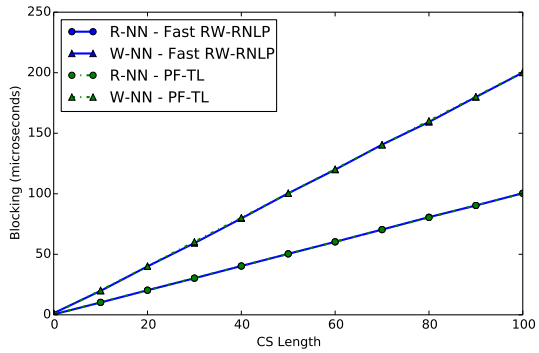

(c) Blocking.

Figure 46: (a) Lock and (b) unlock overheads and (c) blocking for non-nested read and write requests under the PF-TL and the fast RW-RNLP. Here, $m = 18$, $n_r = 56$, and $|D_i| = 1$ for each request $\mathcal{R}_i$. Each request was randomly chosen to be a read (as opposed to a write) with probability 0.5.

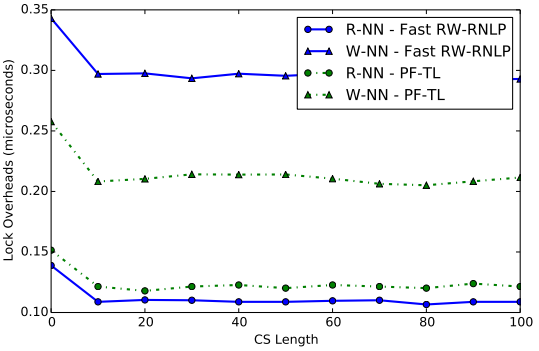

(a) Lock overhead.

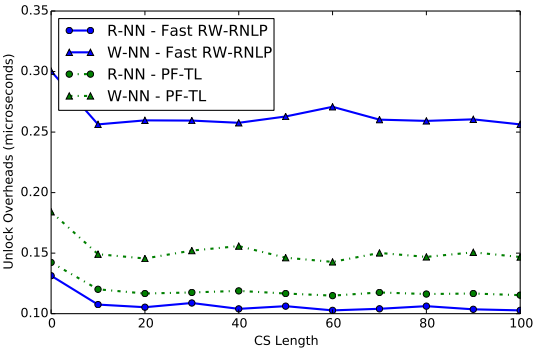

(b) Unlock overhead.

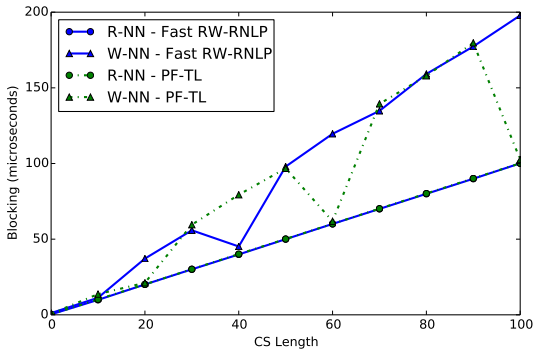

(c) Blocking.

Figure 47: (a) Lock and (b) unlock overheads and (c) blocking for non-nested read and write requests under the PF-TL and the fast RW-RNLP. Here, $m = 18$, $n_r = 56$, and $|D_i| = 1$ for each request $\mathcal{R}_i$. Each request was randomly chosen to be a read (as opposed to a write) with probability 0.8.

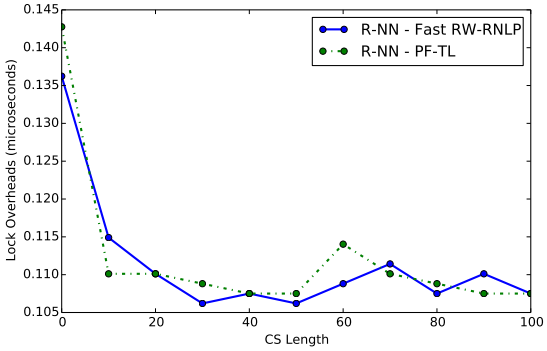

(a) Lock overhead.

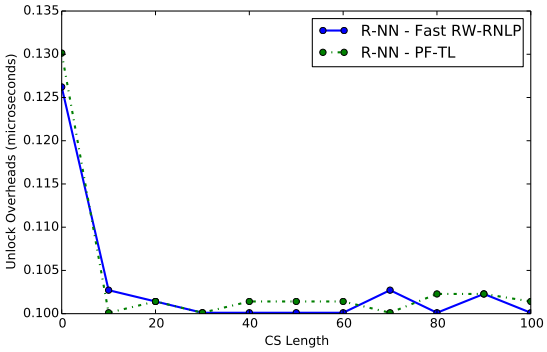

(b) Unlock overhead.

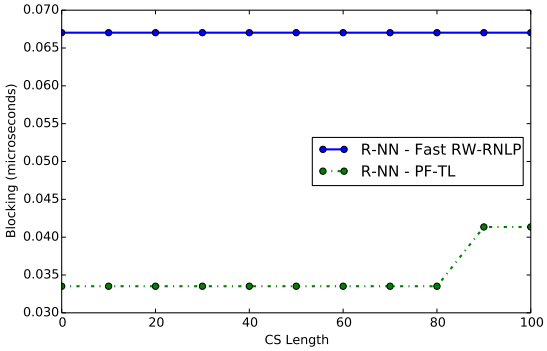

(c) Blocking.

Figure 48: (a) Lock and (b) unlock overheads and (c) blocking for non-nested read and write requests under the PF-TL and the fast RW-RNLP. Here, $m = 18$, $n_r = 56$, and $|D_i| = 1$ for each request $\mathcal{R}_i$. Each request was randomly chosen to be a read (as opposed to a write) with probability 1.

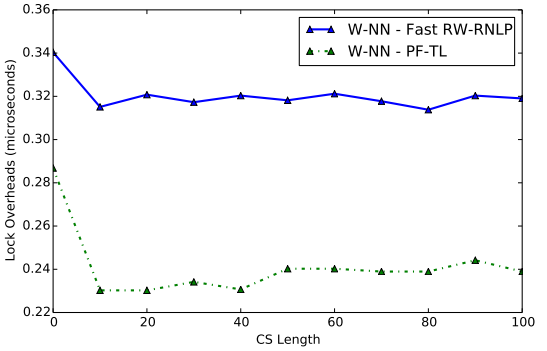

(a) Lock overhead.

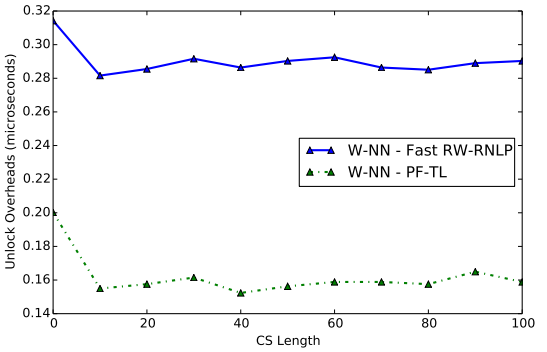

(b) Unlock overhead.

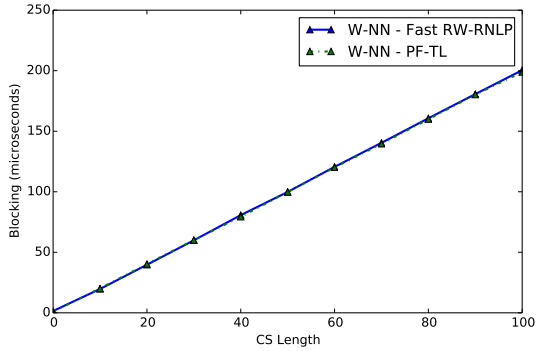

(c) Blocking.

Figure 49: (a) Lock and (b) unlock overheads and (c) blocking for non-nested read and write requests under the PF-TL and the fast RW-RNLP. Here, $m = 18$, $n_r = 64$, and $|D_i| = 1$ for each request $\mathcal{R}_i$. Each request was randomly chosen to be a read (as opposed to a write) with probability 0.

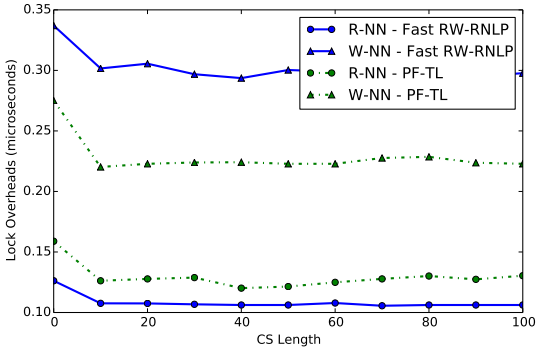

(a) Lock overhead.

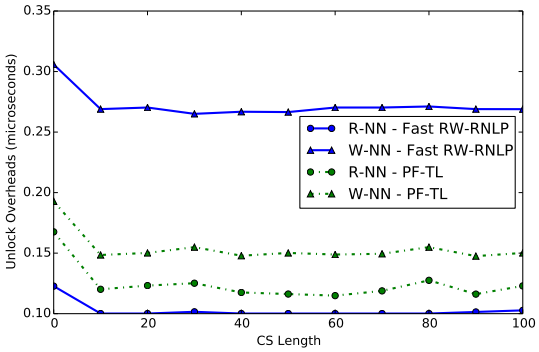

(b) Unlock overhead.

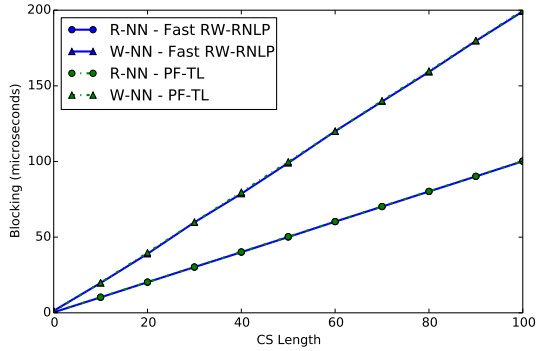

(c) Blocking.

Figure 50: (a) Lock and (b) unlock overheads and (c) blocking for non-nested read and write requests under the PF-TL and the fast RW-RNLP. Here, $m = 18$, $n_r = 64$, and $|D_i| = 1$ for each request $\mathcal{R}_i$. Each request was randomly chosen to be a read (as opposed to a write) with probability 0.2.

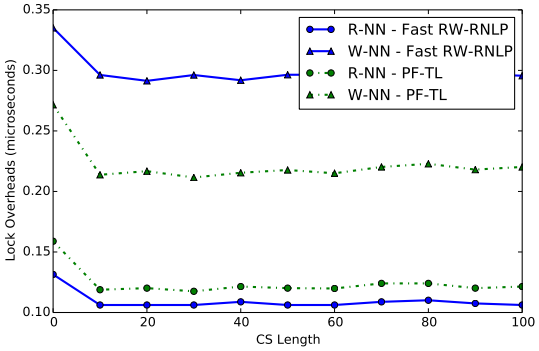

(a) Lock overhead.

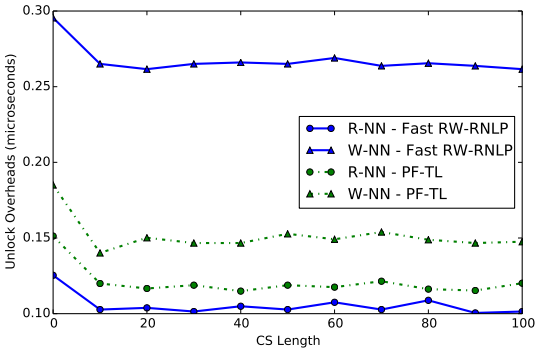

(b) Unlock overhead.

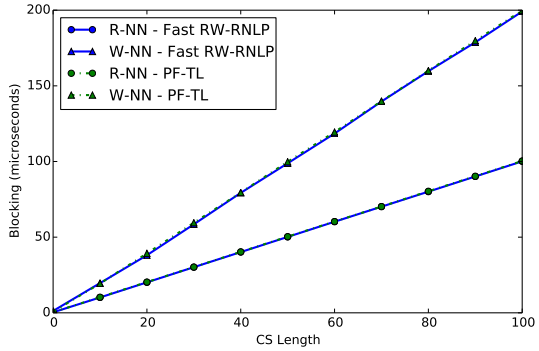

(c) Blocking.

Figure 51: (a) Lock and (b) unlock overheads and (c) blocking for non-nested read and write requests under the PF-TL and the fast RW-RNLP. Here, $m = 18$, $n_r = 64$, and $|D_i| = 1$ for each request $\mathcal{R}_i$. Each request was randomly chosen to be a read (as opposed to a write) with probability 0.5.

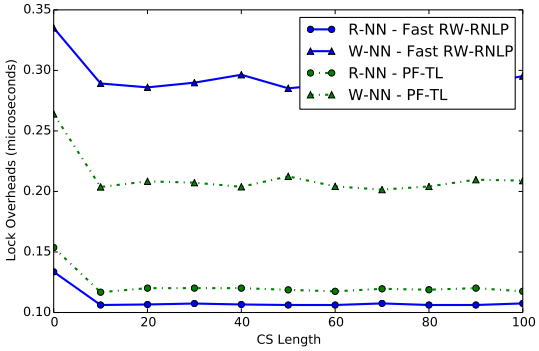

(a) Lock overhead.

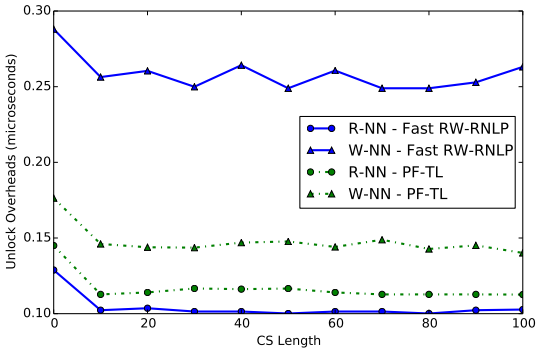

(b) Unlock overhead.

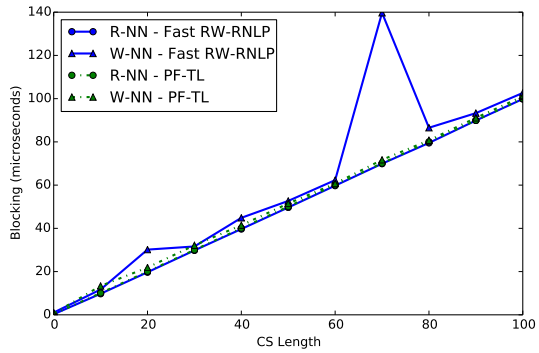

(c) Blocking.

Figure 52: (a) Lock and (b) unlock overheads and (c) blocking for non-nested read and write requests under the PF-TL and the fast RW-RNLP. Here, $m = 18$, $n_r = 64$, and $|D_i| = 1$ for each request $\mathcal{R}_i$. Each request was randomly chosen to be a read (as opposed to a write) with probability 0.8.

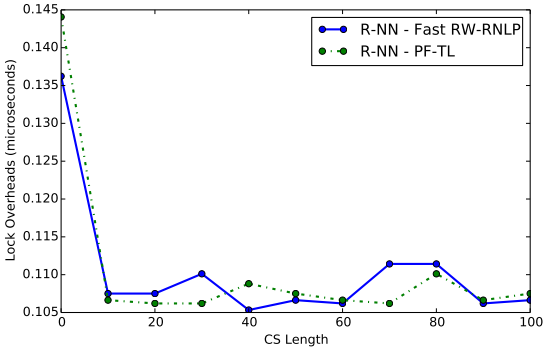

(a) Lock overhead.

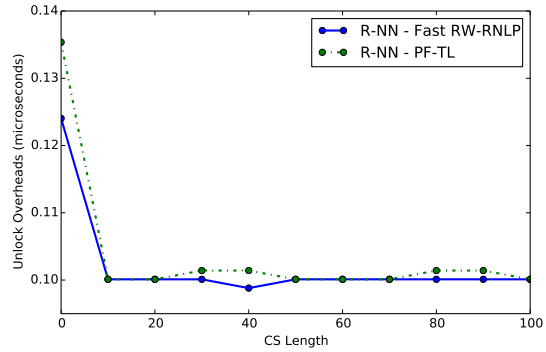

(b) Unlock overhead.

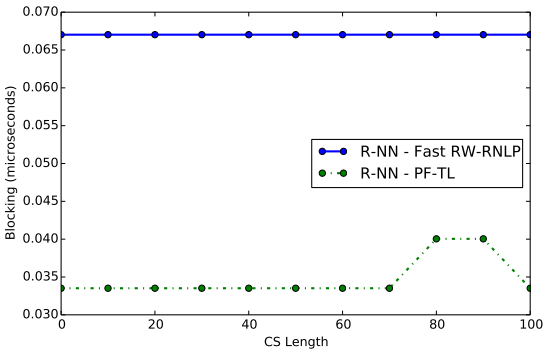

(c) Blocking.

Figure 53: (a) Lock and (b) unlock overheads and (c) blocking for non-nested read and write requests under the PF-TL and the fast RW-RNLP. Here, $m = 18$, $n_r = 64$, and $|D_i| = 1$ for each request $\mathcal{R}_i$. Each request was randomly chosen to be a read (as opposed to a write) with probability 1.

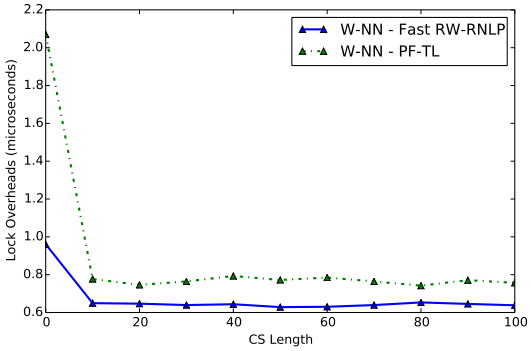

(a) Lock overhead.

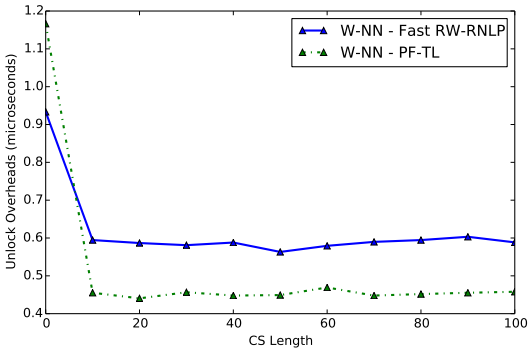

(b) Unlock overhead.

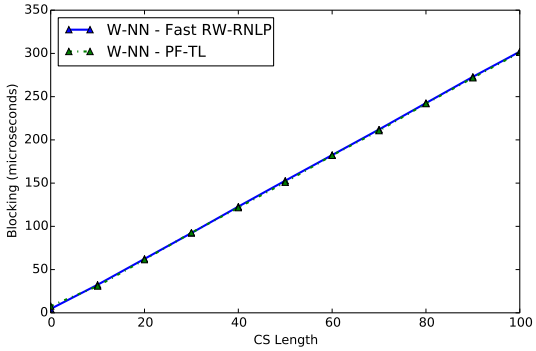

(c) Blocking.

Figure 54: (a) Lock and (b) unlock overheads and (c) blocking for non-nested read and write requests under the PF-TL and the fast RW-RNLP. Here, $m = 36$, $n_r = 56$, and $|D_i| = 1$ for each request $\mathcal{R}_i$. Each request was randomly chosen to be a read (as opposed to a write) with probability 0.

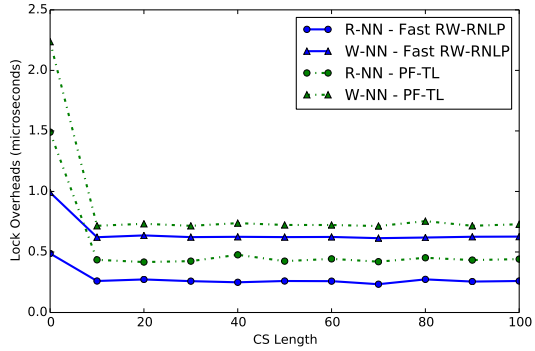

(a) Lock overhead.

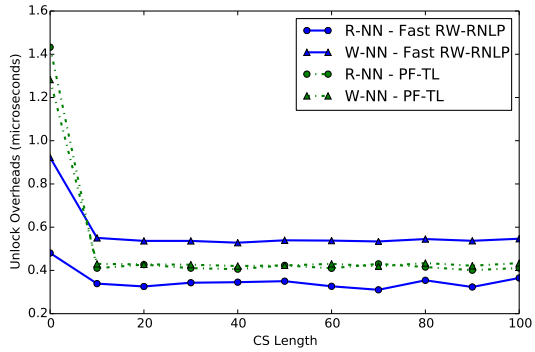

(b) Unlock overhead.

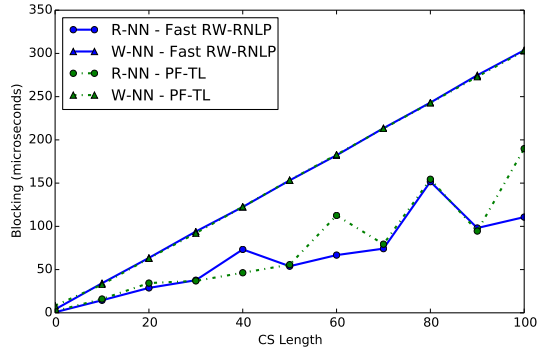

(c) Blocking.

Figure 55: (a) Lock and (b) unlock overheads and (c) blocking for non-nested read and write requests under the PF-TL and the fast RW-RNLP. Here, $m = 36$, $n_r = 56$, and $|D_i| = 1$ for each request $\mathcal{R}_i$. Each request was randomly chosen to be a read (as opposed to a write) with probability 0.2.

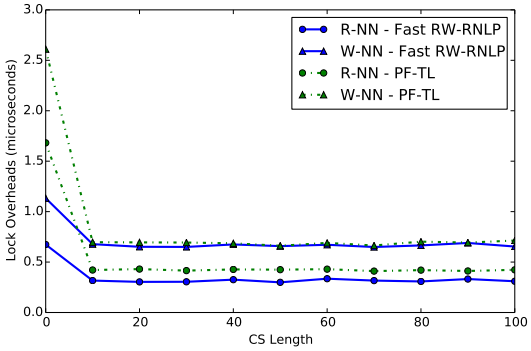

(a) Lock overhead.

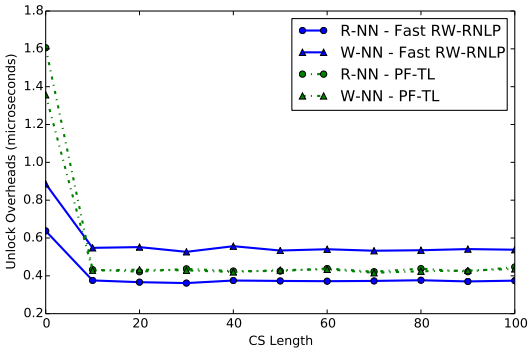

(b) Unlock overhead.

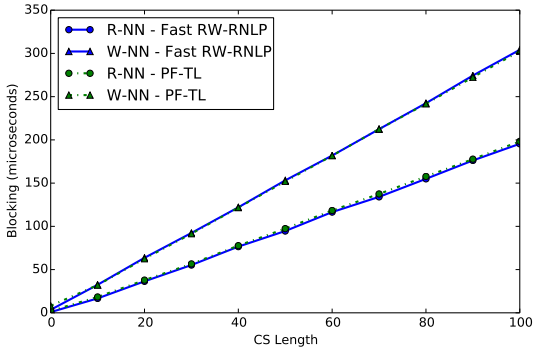

(c) Blocking.

Figure 56: (a) Lock and (b) unlock overheads and (c) blocking for non-nested read and write requests under the PF-TL and the fast RW-RNLP. Here, $m = 36$, $n_r = 56$, and $|D_i| = 1$ for each request $\mathcal{R}_i$. Each request was randomly chosen to be a read (as opposed to a write) with probability 0.5.

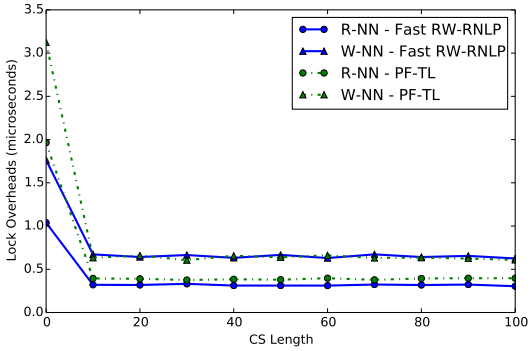

(a) Lock overhead.

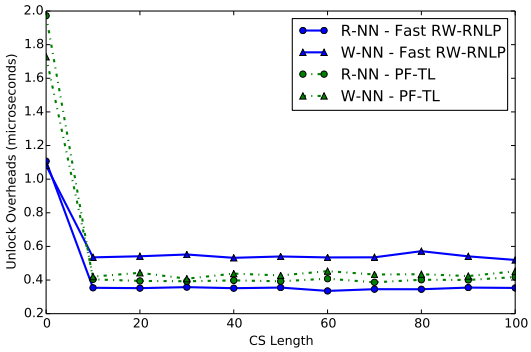

(b) Unlock overhead.

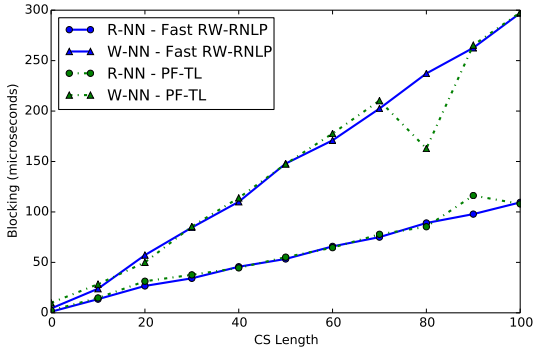

(c) Blocking.

Figure 57: (a) Lock and (b) unlock overheads and (c) blocking for non-nested read and write requests under the PF-TL and the fast RW-RNLP. Here, $m = 36$, $n_r = 56$, and $|D_i| = 1$ for each request $\mathcal{R}_i$. Each request was randomly chosen to be a read (as opposed to a write) with probability 0.8.

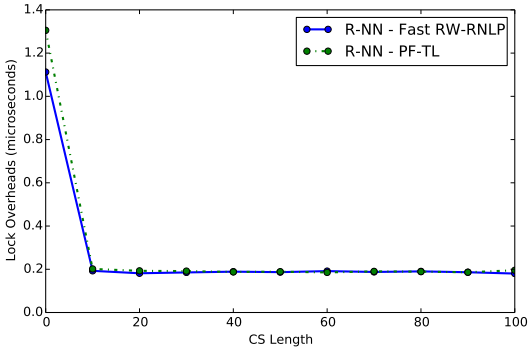

(a) Lock overhead.

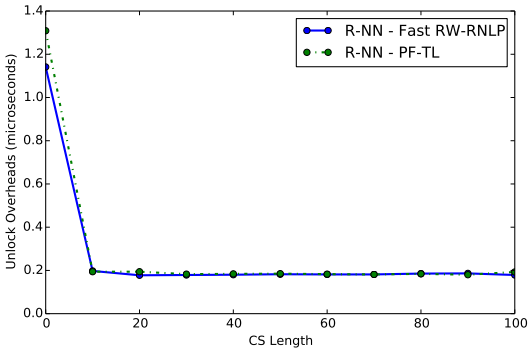

(b) Unlock overhead.

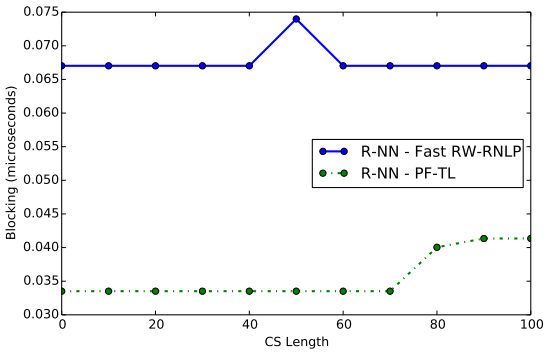

(c) Blocking.

Figure 58: (a) Lock and (b) unlock overheads and (c) blocking for non-nested read and write requests under the PF-TL and the fast RW-RNLP. Here, $m = 36$, $n_r = 56$, and $|D_i| = 1$ for each request $\mathcal{R}_i$. Each request was randomly chosen to be a read (as opposed to a write) with probability 1.

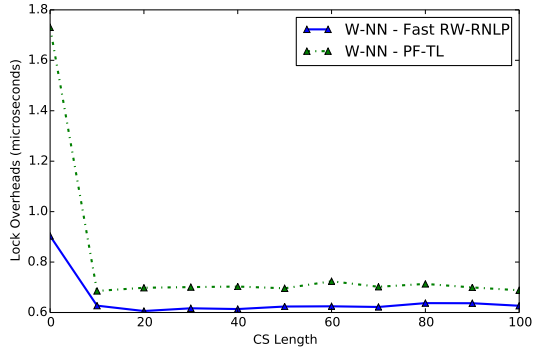

(a) Lock overhead.

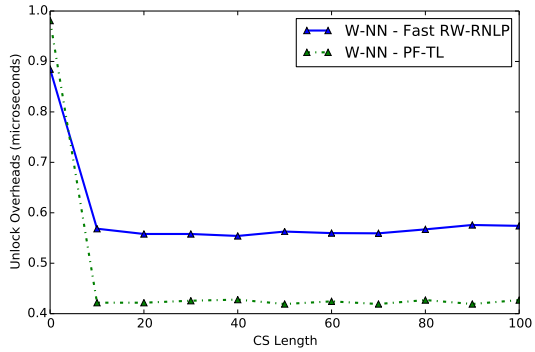

(b) Unlock overhead.

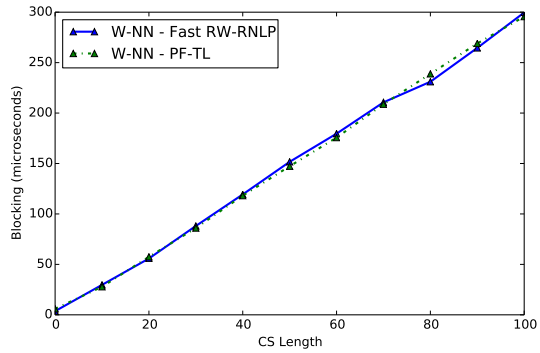

(c) Blocking.

Figure 59: (a) Lock and (b) unlock overheads and (c) blocking for non-nested read and write requests under the PF-TL and the fast RW-RNLP. Here, $m = 36$, $n_r = 64$, and $|D_i| = 1$ for each request $\mathcal{R}_i$. Each request was randomly chosen to be a read (as opposed to a write) with probability 0.

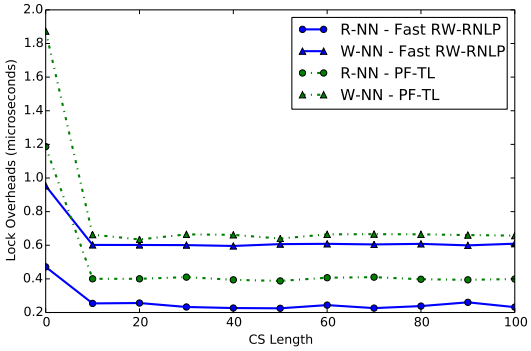

(a) Lock overhead.

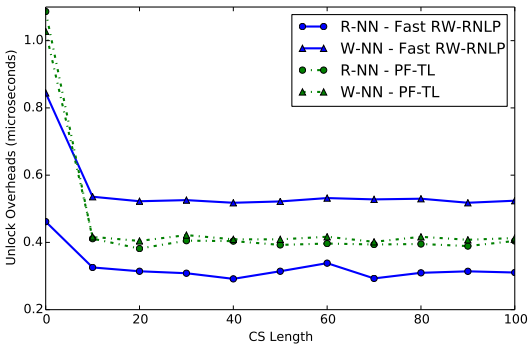

(b) Unlock overhead.

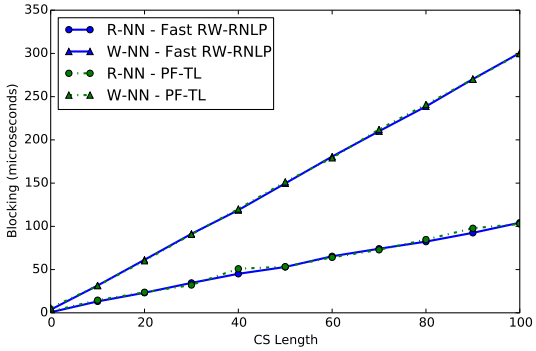

(c) Blocking.

Figure 60: (a) Lock and (b) unlock overheads and (c) blocking for non-nested read and write requests under the PF-TL and the fast RW-RNLP. Here, $m = 36$, $n_r = 64$, and $|D_i| = 1$ for each request $\mathcal{R}_i$. Each request was randomly chosen to be a read (as opposed to a write) with probability 0.2.

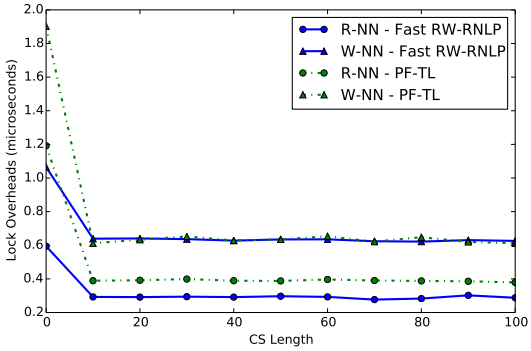

(a) Lock overhead.

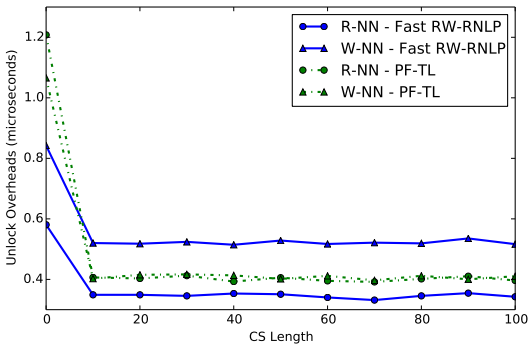

(b) Unlock overhead.

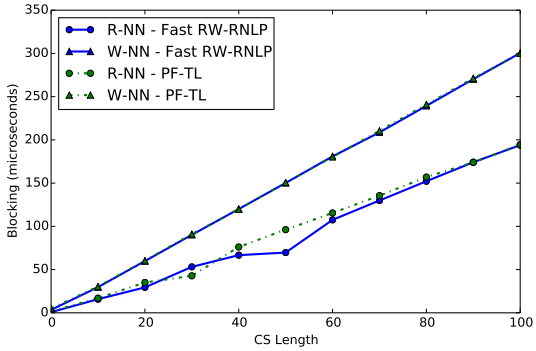

(c) Blocking.

Figure 61: (a) Lock and (b) unlock overheads and (c) blocking for non-nested read and write requests under the PF-TL and the fast RW-RNLP. Here, $m = 36$, $n_r = 64$, and $|D_i| = 1$ for each request $\mathcal{R}_i$. Each request was randomly chosen to be a read (as opposed to a write) with probability 0.5.

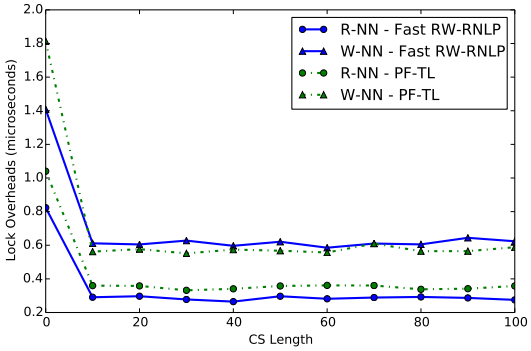

(a) Lock overhead.

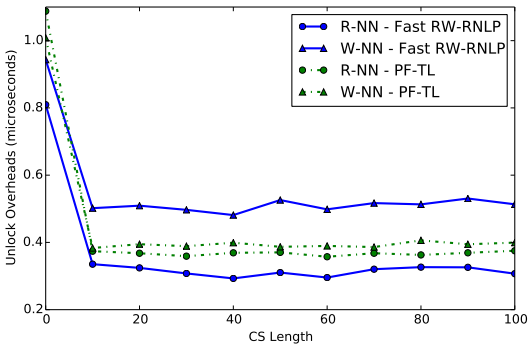

(b) Unlock overhead.

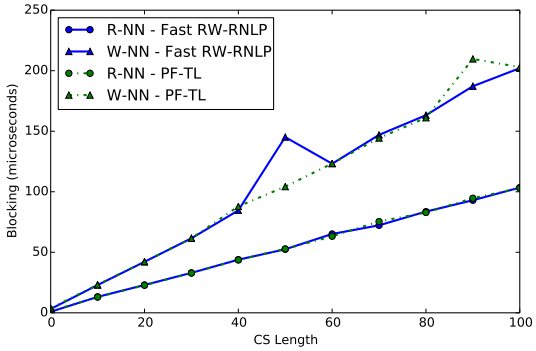

(c) Blocking.

Figure 62: (a) Lock and (b) unlock overheads and (c) blocking for non-nested read and write requests under the PF-TL and the fast RW-RNLP. Here, $m = 36$, $n_r = 64$, and $|D_i| = 1$ for each request $\mathcal{R}_i$. Each request was randomly chosen to be a read (as opposed to a write) with probability 0.8.

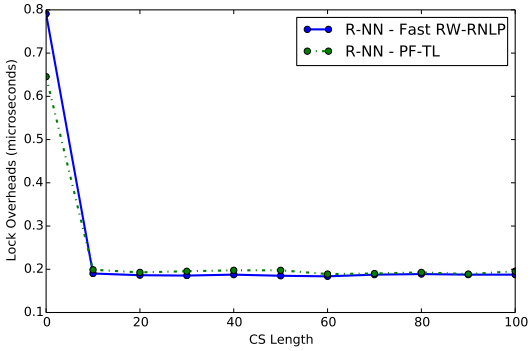

(a) Lock overhead.

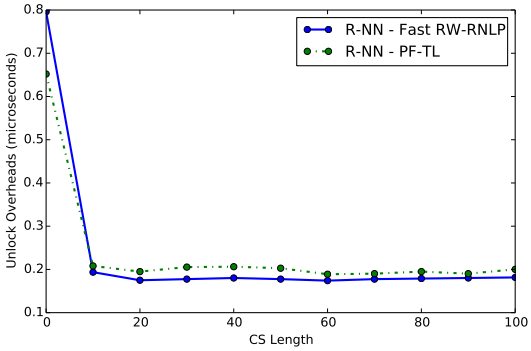

(b) Unlock overhead.

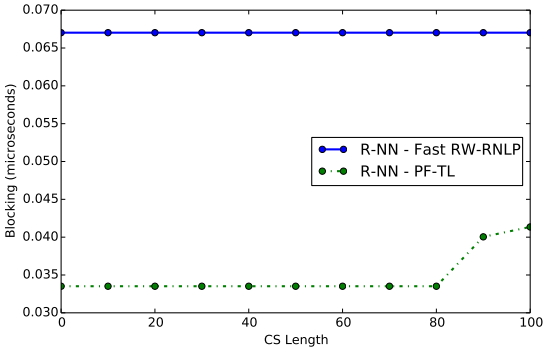

(c) Blocking.

Figure 63: (a) Lock and (b) unlock overheads and (c) blocking for non-nested read and write requests under the PF-TL and the fast RW-RNLP. Here, $m = 36$, $n_r = 64$, and $|D_i| = 1$ for each request $\mathcal{R}_i$. Each request was randomly chosen to be a read (as opposed to a write) with probability 1.

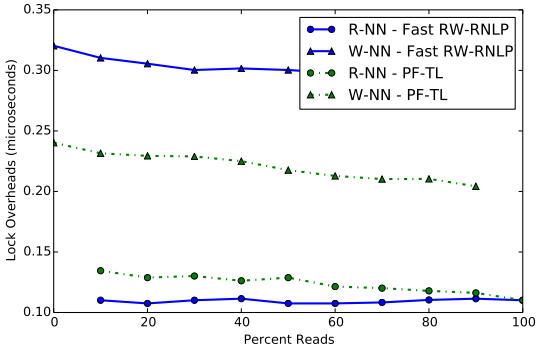

(a) Lock overhead.

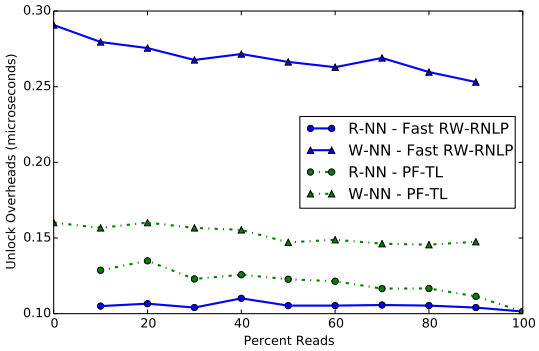

(b) Unlock overhead.

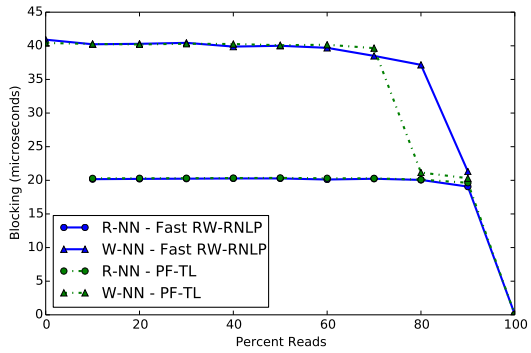

(c) Blocking.

Figure 64: (a) Lock and (b) unlock overheads and (c) blocking for non-nested read and write requests under the PF-TL and the fast RW-RNLP. Here, $m = 18$, $L_i^r = 20\mu$s, $L_i^w = 20\mu$s, $n_r = 56$, and $|D_i| = 1$ for each request $\mathcal{R}_i$. Each request was randomly chosen to be a read (as opposed to a write) with probability as shown.

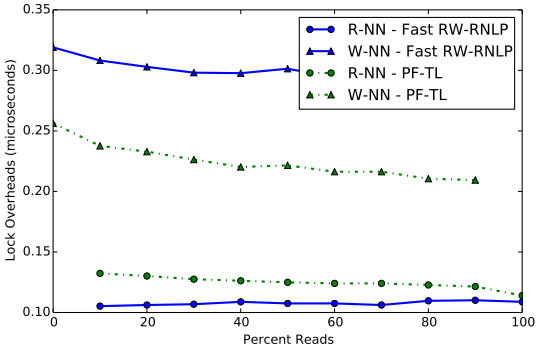

(a) Lock overhead.

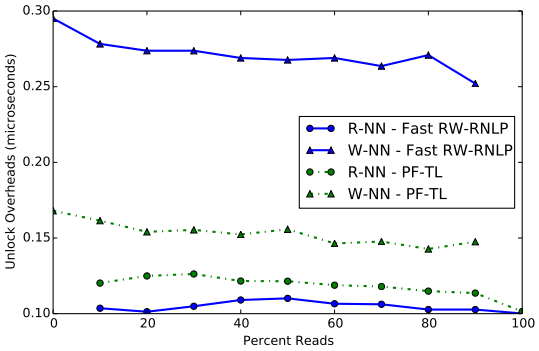

(b) Unlock overhead.

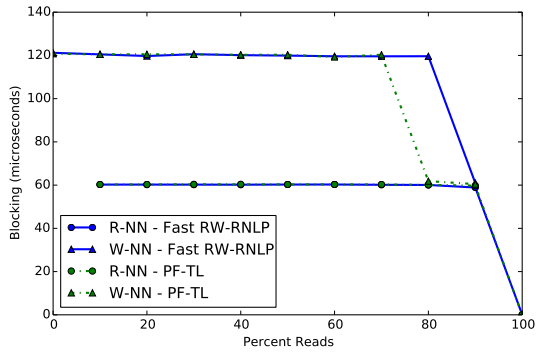

(c) Blocking.

Figure 65: (a) Lock and (b) unlock overheads and (c) blocking for non-nested read and write requests under the PF-TL and the fast RW-RNLP. Here, $m = 18$, $L_i^r = 60\mu$s, $L_i^w = 60\mu$s, $n_r = 56$, and $|D_i| = 1$ for each request $\mathcal{R}_i$. Each request was randomly chosen to be a read (as opposed to a write) with probability as shown.

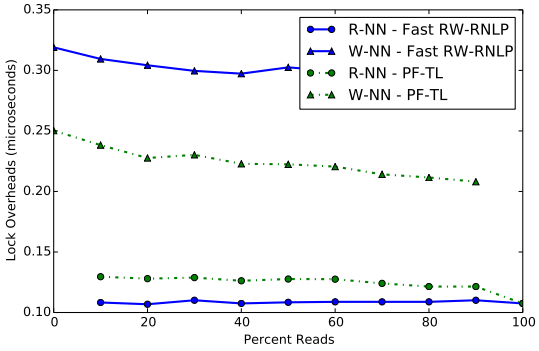

(a) Lock overhead.

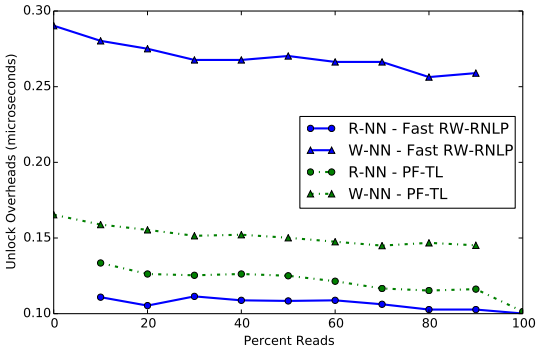

(b) Unlock overhead.

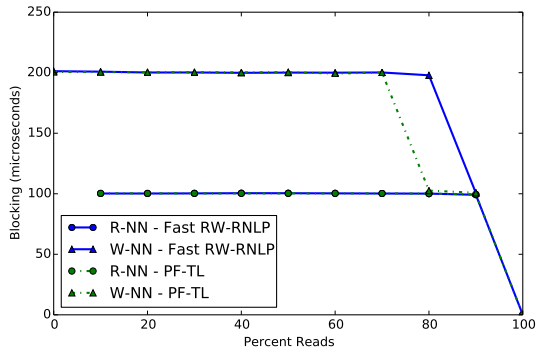

(c) Blocking.

Figure 66: (a) Lock and (b) unlock overheads and (c) blocking for non-nested read and write requests under the PF-TL and the fast RW-RNLP. Here, $m = 18$, $L_i^r = 100\mu$s, $L_i^w = 100\mu$s, $n_r = 56$, and $|D_i| = 1$ for each request $\mathcal{R}_i$. Each request was randomly chosen to be a read (as opposed to a write) with probability as shown.

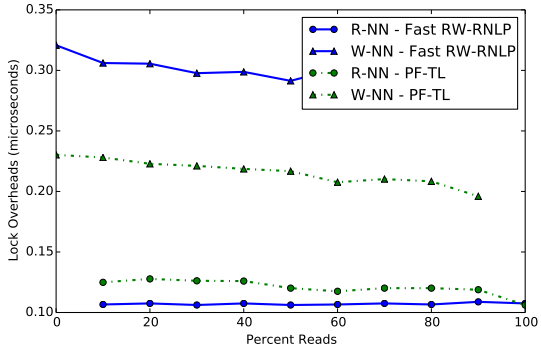

(a) Lock overhead.

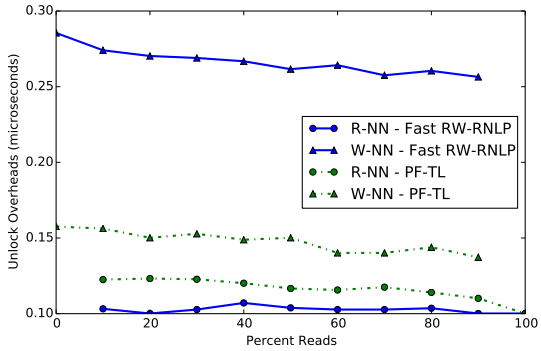

(b) Unlock overhead.

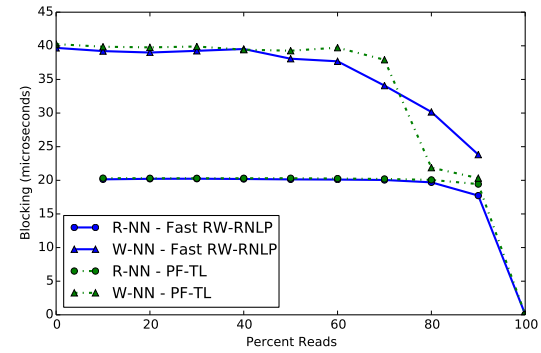

(c) Blocking.

Figure 67: (a) Lock and (b) unlock overheads and (c) blocking for non-nested read and write requests under the PF-TL and the fast RW-RNLP. Here, $m = 18$, $L_i^r = 20\mu$s, $L_i^w = 20\mu$s, $n_r = 64$, and $|D_i| = 1$ for each request $\mathcal{R}_i$. Each request was randomly chosen to be a read (as opposed to a write) with probability as shown.

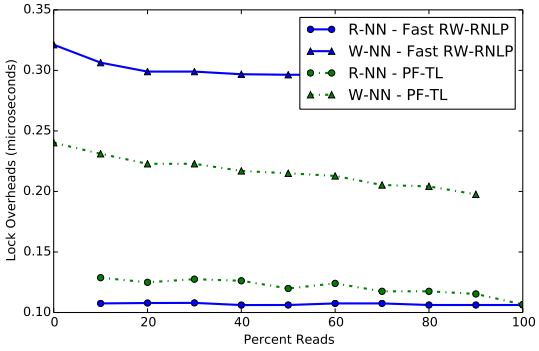

(a) Lock overhead.

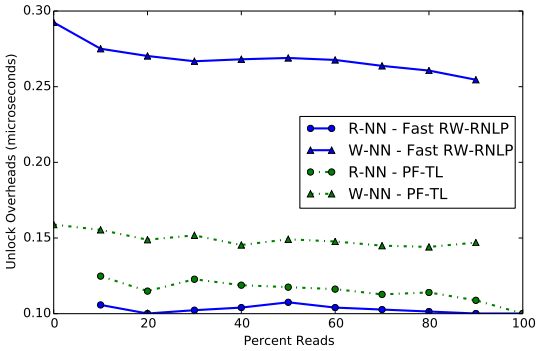

(b) Unlock overhead.

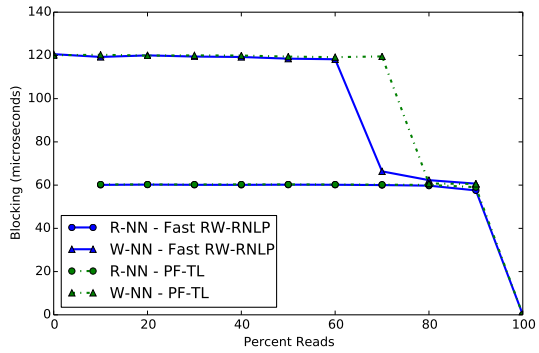

(c) Blocking.

Figure 68: (a) Lock and (b) unlock overheads and (c) blocking for non-nested read and write requests under the PF-TL and the fast RW-RNLP. Here, $m = 18$, $L_i^r = 60\mu$s, $L_i^w = 60\mu$s, $n_r = 64$, and $|D_i| = 1$ for each request $\mathcal{R}_i$. Each request was randomly chosen to be a read (as opposed to a write) with probability as shown.

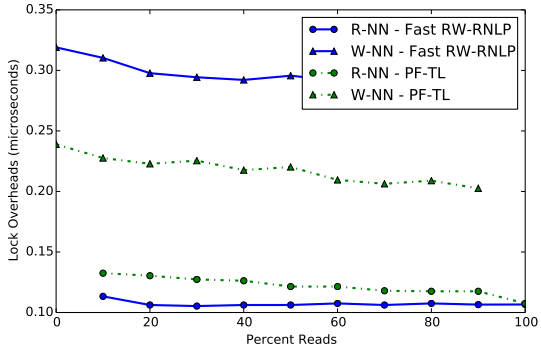

(a) Lock overhead.

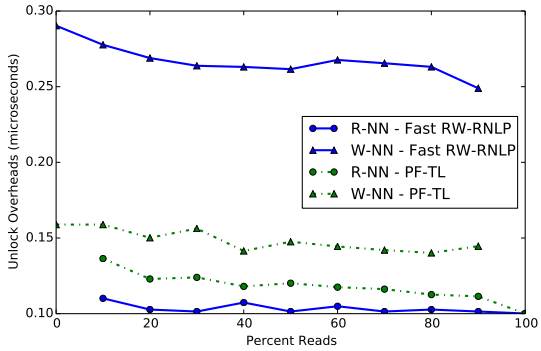

(b) Unlock overhead.

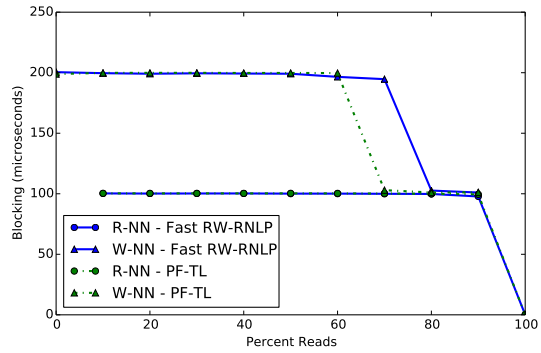

(c) Blocking.

Figure 69: (a) Lock and (b) unlock overheads and (c) blocking for non-nested read and write requests under the PF-TL and the fast RW-RNLP. Here, $m = 18$, $L_i^r = 100\mu$s, $L_i^w = 100\mu$s, $n_r = 64$, and $|D_i| = 1$ for each request $\mathcal{R}_i$. Each request was randomly chosen to be a read (as opposed to a write) with probability as shown.

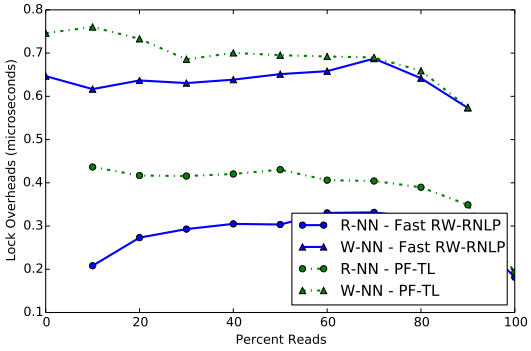

(a) Lock overhead.

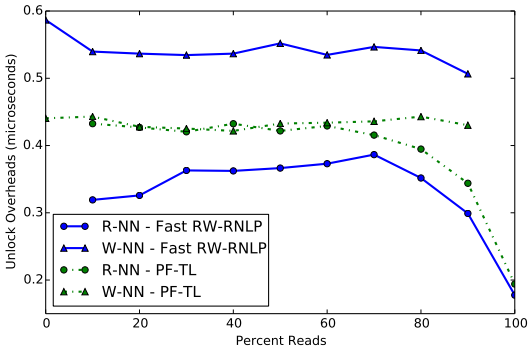

(b) Unlock overhead.

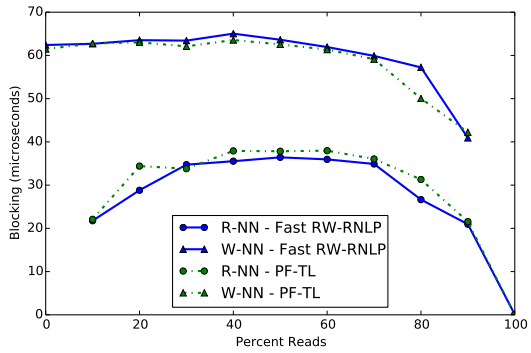

(c) Blocking.

Figure 70: (a) Lock and (b) unlock overheads and (c) blocking for non-nested read and write requests under the PF-TL and the fast RW-RNLP. Here, $m = 36$, $L_i^r = 20\mu$s, $L_i^w = 20\mu$s, $n_r = 56$, and $|D_i| = 1$ for each request $\mathcal{R}_i$. Each request was randomly chosen to be a read (as opposed to a write) with probability as shown.

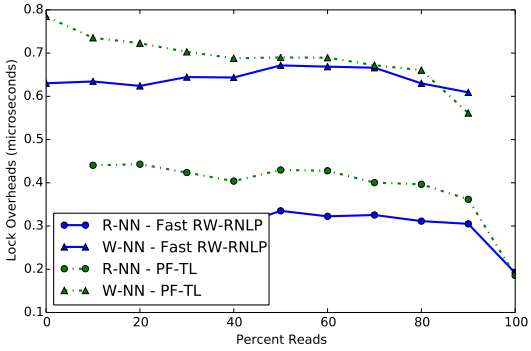

(a) Lock overhead.

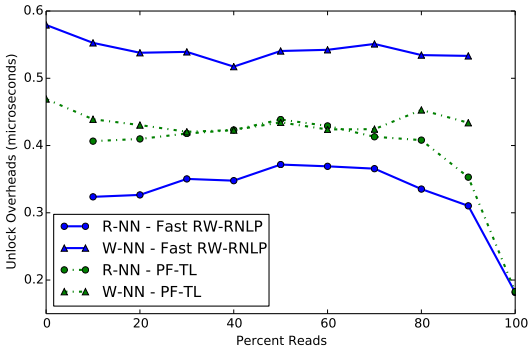

(b) Unlock overhead.

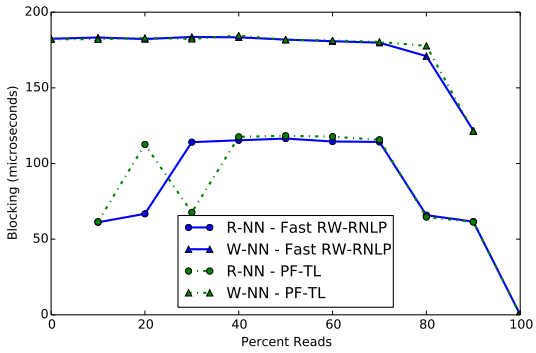

(c) Blocking.

Figure 71: (a) Lock and (b) unlock overheads and (c) blocking for non-nested read and write requests under the PF-TL and the fast RW-RNLP. Here, $m = 36$, $L_i^r = 60\mu$s, $L_i^w = 60\mu$s, $n_r = 56$, and $|D_i| = 1$ for each request $\mathcal{R}_i$. Each request was randomly chosen to be a read (as opposed to a write) with probability as shown.

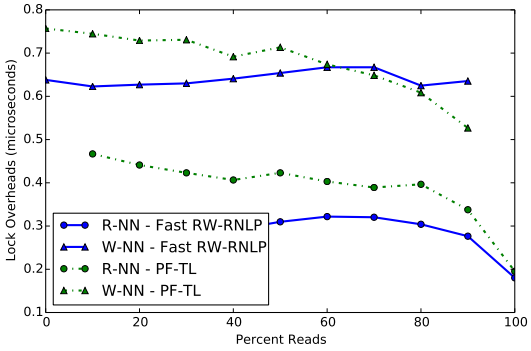

(a) Lock overhead.

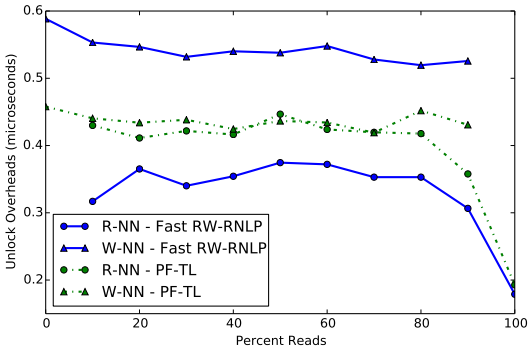

(b) Unlock overhead.

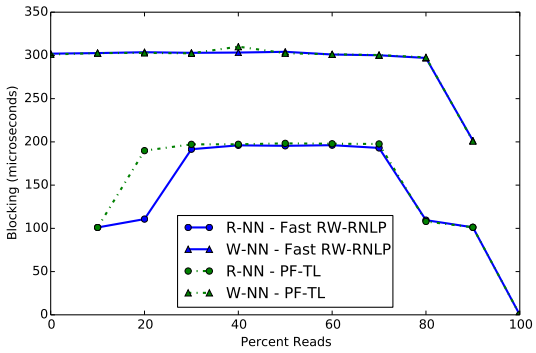

(c) Blocking.

Figure 72: (a) Lock and (b) unlock overheads and (c) blocking for non-nested read and write requests under the PF-TL and the fast RW-RNLP. Here, $m = 36$, $L_i^r = 100\mu$s, $L_i^w = 100\mu$s, $n_r = 56$, and $|D_i| = 1$ for each request $\mathcal{R}_i$. Each request was randomly chosen to be a read (as opposed to a write) with probability as shown.

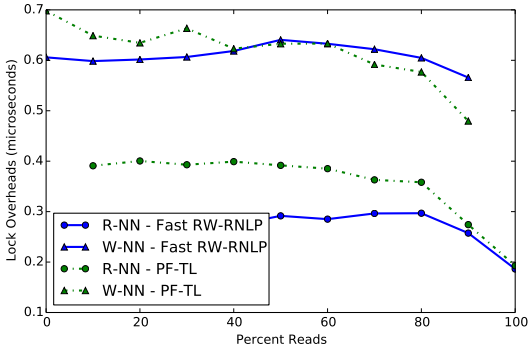

(a) Lock overhead.

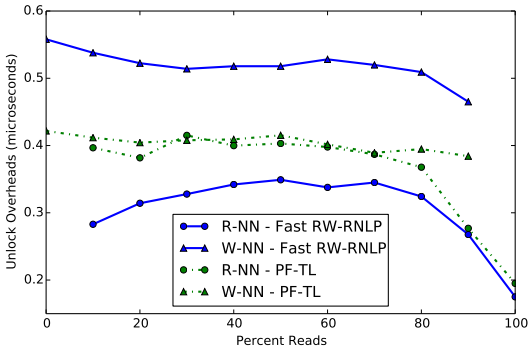

(b) Unlock overhead.

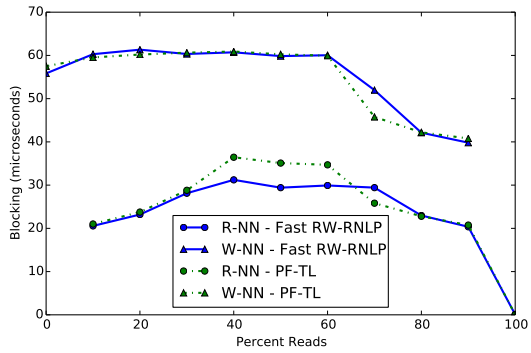

(c) Blocking.

Figure 73: (a) Lock and (b) unlock overheads and (c) blocking for non-nested read and write requests under the PF-TL and the fast RW-RNLP. Here, $m = 36$, $L_i^r = 20\mu$s, $L_i^w = 20\mu$s, $n_r = 64$, and $|D_i| = 1$ for each request $\mathcal{R}_i$. Each request was randomly chosen to be a read (as opposed to a write) with probability as shown.

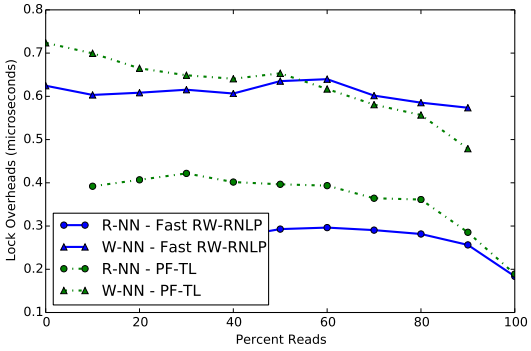

(a) Lock overhead.

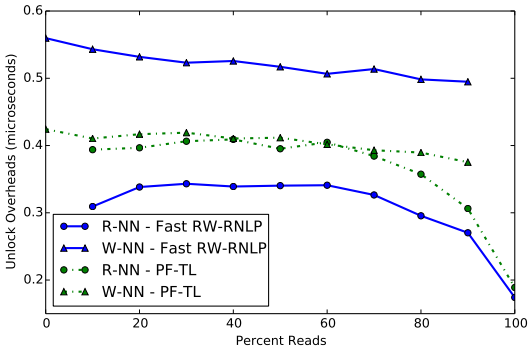

(b) Unlock overhead.

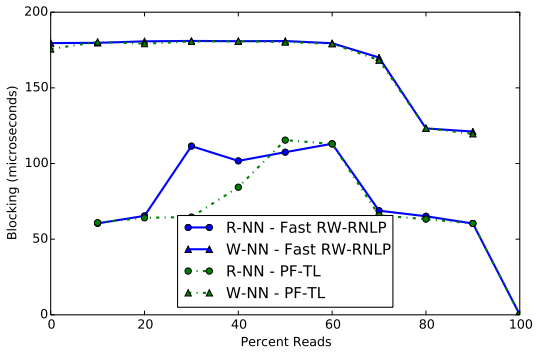

(c) Blocking.

Figure 74: (a) Lock and (b) unlock overheads and (c) blocking for non-nested read and write requests under the PF-TL and the fast RW-RNLP. Here, $m = 36$, $L_i^r = 60\mu$s, $L_i^w = 60\mu$s, $n_r = 64$, and $|D_i| = 1$ for each request $\mathcal{R}_i$. Each request was randomly chosen to be a read (as opposed to a write) with probability as shown.

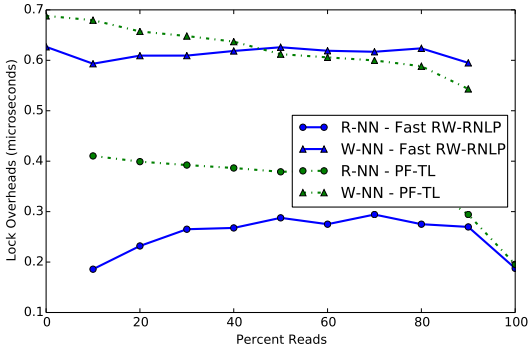

(a) Lock overhead.

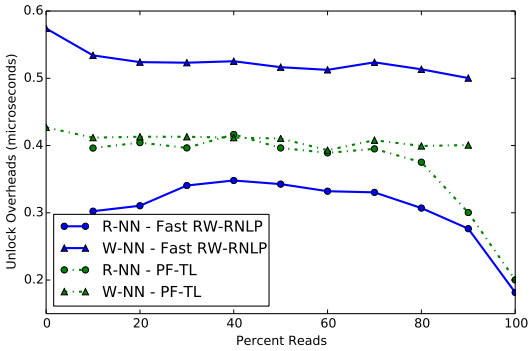

(b) Unlock overhead.

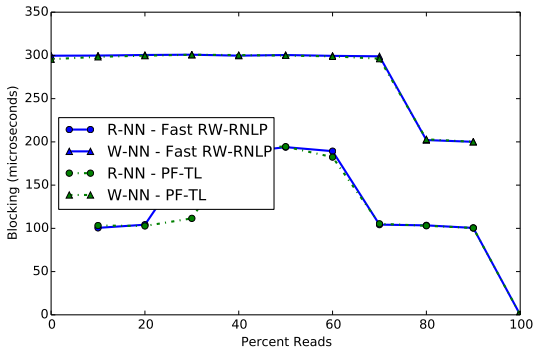

(c) Blocking.

Figure 75: (a) Lock and (b) unlock overheads and (c) blocking for non-nested read and write requests under the PF-TL and the fast RW-RNLP. Here, $m = 36$, $L_i^r = 100\mu$s, $L_i^w = 100\mu$s, $n_r = 64$, and $|D_i| = 1$ for each request $\mathcal{R}_i$. Each request was randomly chosen to be a read (as opposed to a write) with probability as shown.

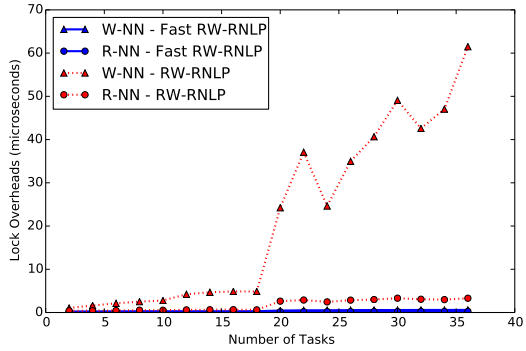

(a) Lock overhead.

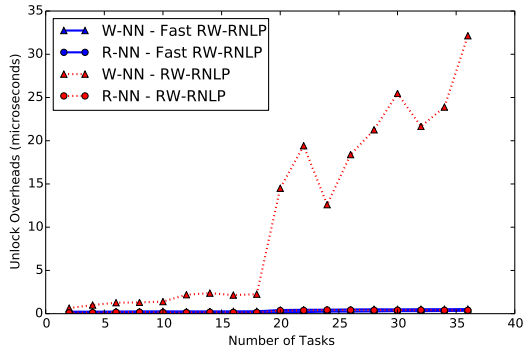

(b) Unlock overhead.

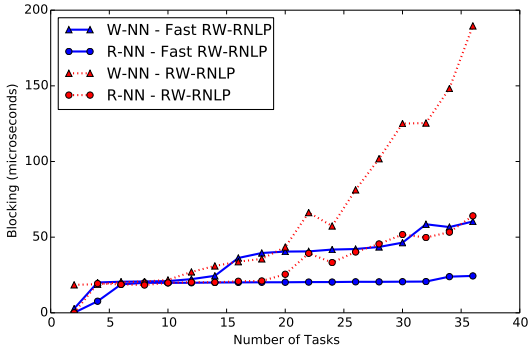

(c) Blocking.

Figure 76: (a) Lock and (b) unlock overheads and (c) blocking for non-nested read and write requests under the RW-RNLP and the fast RW-RNLP. Here, for each request $\mathcal{R}_i$, $L_i = 20\mu$s, $n_r = 64$, and $|D_i| = 1$. Each request was randomly chosen to be a read (as opposed to a write) with probability 0.2 and to be a nested request with probability 0.

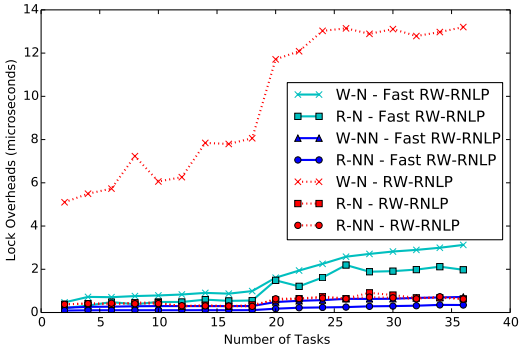

(a) Lock overhead.

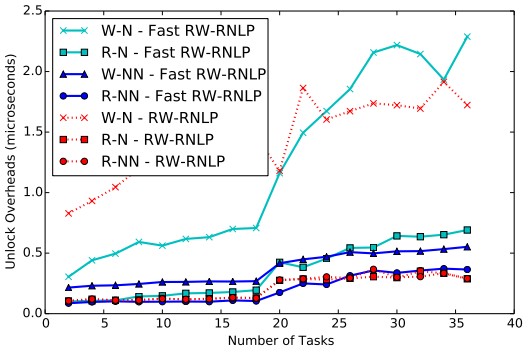

(b) Unlock overhead.

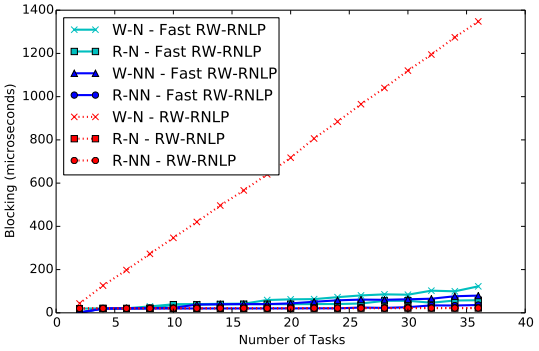

(c) Blocking.

Figure 77: (a) Lock and (b) unlock overheads and (c) blocking for nested and non-nested read and write requests under the RW-RNLP and the fast RW-RNLP. Here, for each request $\mathcal{R}_i$, $L_i = 20\mu$s, $n_r = 64$, $|D_i| = 1$ for non-nested requests, and $|D_i| = 2$ for nested requests. Each request was randomly chosen to be a read (as opposed to a write) with probability 0.2 and to be a nested request with probability 0.2. Due to write expansion, $|D_i|$ was inflated to 64 for all write requests under the RW-RNLP, as read requests can access any resource.

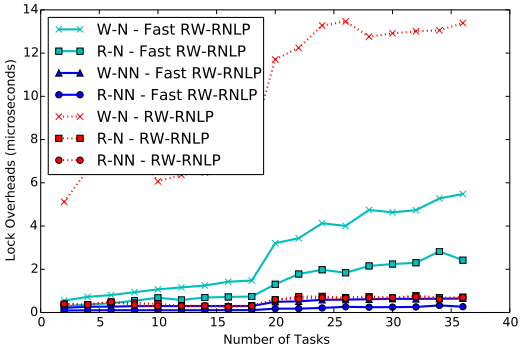

(a) Lock overhead.

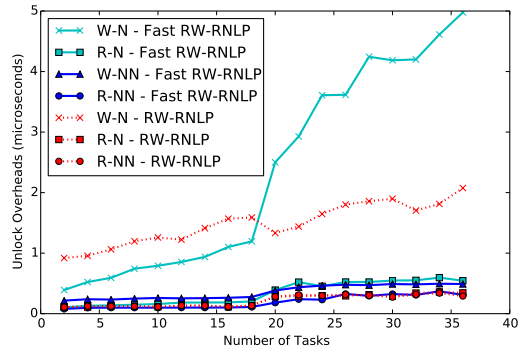

(b) Unlock overhead.

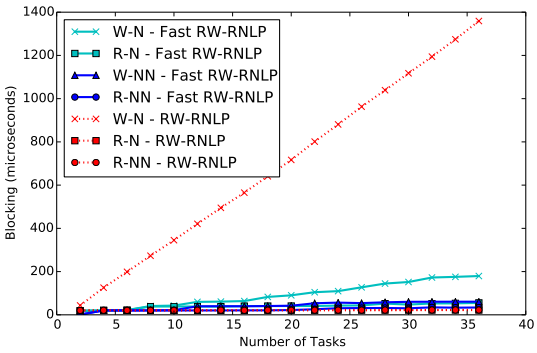

(c) Blocking.

Figure 78: (a) Lock and (b) unlock overheads and (c) blocking for nested and non-nested read and write requests under the RW-RNLP and the fast RW-RNLP. Here, for each request $\mathcal{R}_i$, $L_i = 20\mu$s, $n_r = 64$, $|D_i| = 1$ for non-nested requests, and $|D_i| = 2$ for nested requests. Each request was randomly chosen to be a read (as opposed to a write) with probability 0.2 and to be a nested request with probability 0.5. Due to write expansion, $|D_i|$ was inflated to 64 for all write requests under the RW-RNLP, as read requests can access any resource.

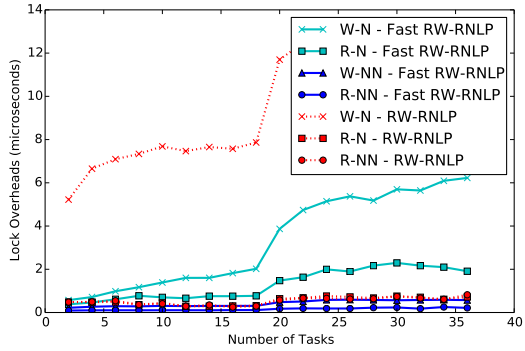

(a) Lock overhead.

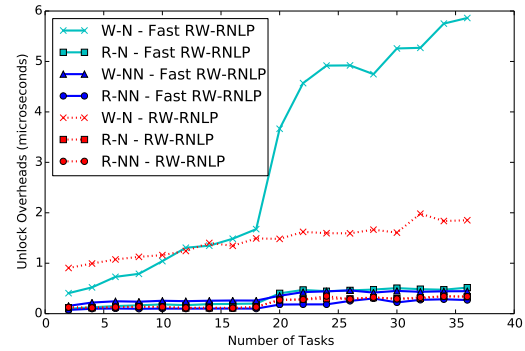

(b) Unlock overhead.

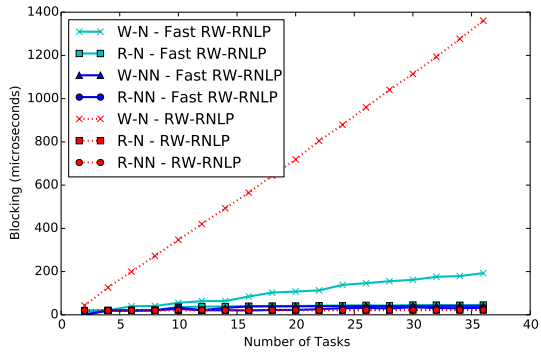

(c) Blocking.

Figure 79: (a) Lock and (b) unlock overheads and (c) blocking for nested and non-nested read and write requests under the RW-RNLP and the fast RW-RNLP. Here, for each request $\mathcal{R}_i$, $L_i = 20\mu$s, $n_r = 64$, $|D_i| = 1$ for non-nested requests, and $|D_i| = 2$ for nested requests. Each request was randomly chosen to be a read (as opposed to a write) with probability 0.2 and to be a nested request with probability 0.8. Due to write expansion, $|D_i|$ was inflated to 64 for all write requests under the RW-RNLP, as read requests can access any resource.

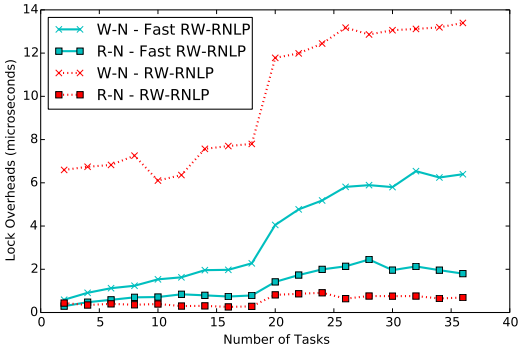

(a) Lock overhead.

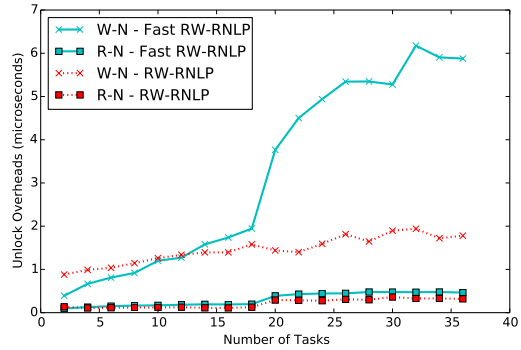

(b) Unlock overhead.

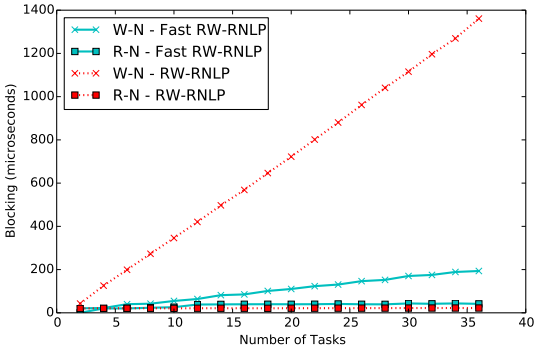

(c) Blocking.

Figure 80: (a) Lock and (b) unlock overheads and (c) blocking for nested read and write requests under the RW-RNLP and the fast RW-RNLP. Here, for each request $\mathcal{R}_i$, $L_i = 20\mu$s, $n_r = 64$, and $|D_i| = 2$. Each request was randomly chosen to be a read (as opposed to a write) with probability 0.2 and to be a nested request with probability 1. Due to write expansion, $|D_i|$ was inflated to 64 for all write requests under the RW-RNLP, as read requests can access any resource.

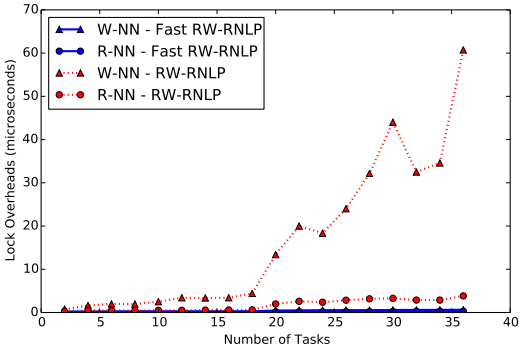

(a) Lock overhead.

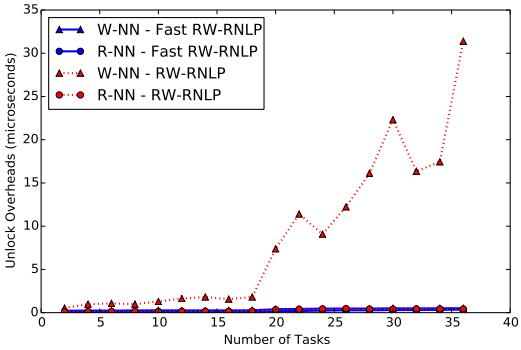

(b) Unlock overhead.

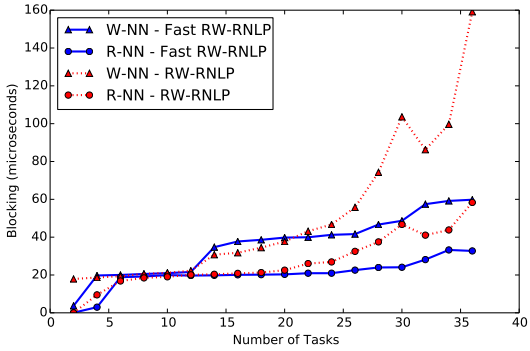

(c) Blocking.

Figure 81: (a) Lock and (b) unlock overheads and (c) blocking for non-nested read and write requests under the RW-RNLP and the fast RW-RNLP. Here, for each request $\mathcal{R}_i$, $L_i = 20\mu$s, $n_r = 64$, and $|D_i| = 1$. Each request was randomly chosen to be a read (as opposed to a write) with probability 0.5 and to be a nested request with probability 0.

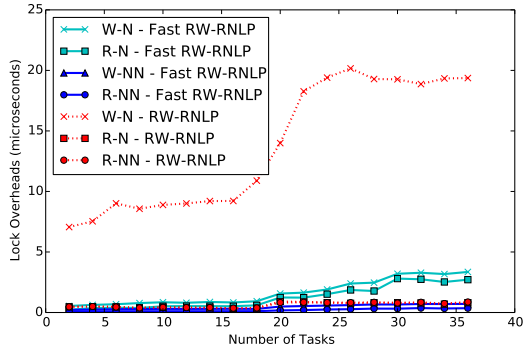

(a) Lock overhead.

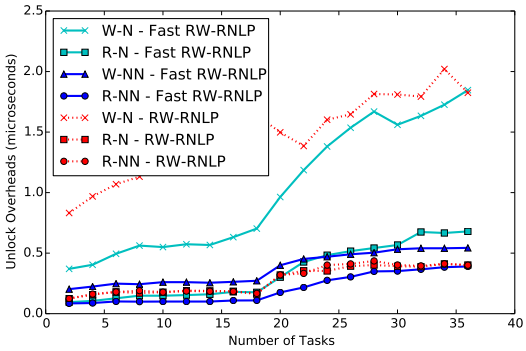

(b) Unlock overhead.

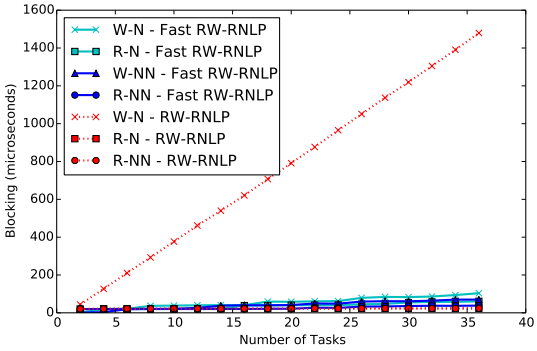

(c) Blocking.

Figure 82: (a) Lock and (b) unlock overheads and (c) blocking for nested and non-nested read and write requests under the RW-RNLP and the fast RW-RNLP. Here, for each request $\mathcal{R}_i$, $L_i = 20\mu$s, $n_r = 64$, $|D_i| = 1$ for non-nested requests, and $|D_i| = 2$ for nested requests. Each request was randomly chosen to be a read (as opposed to a write) with probability 0.5 and to be a nested request with probability 0.2. Due to write expansion, $|D_i|$ was inflated to 64 for all write requests under the RW-RNLP, as read requests can access any resource.

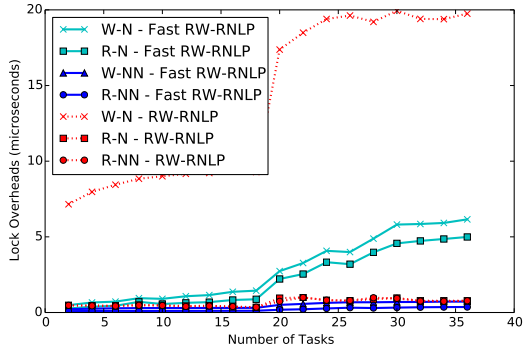

(a) Lock overhead.

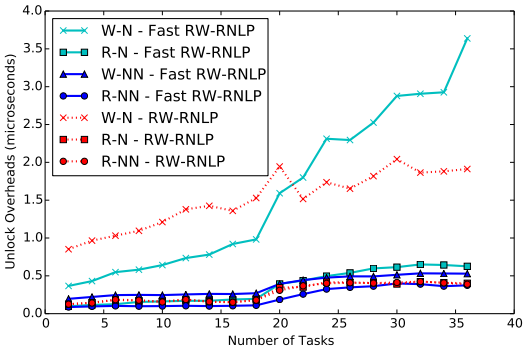

(b) Unlock overhead.

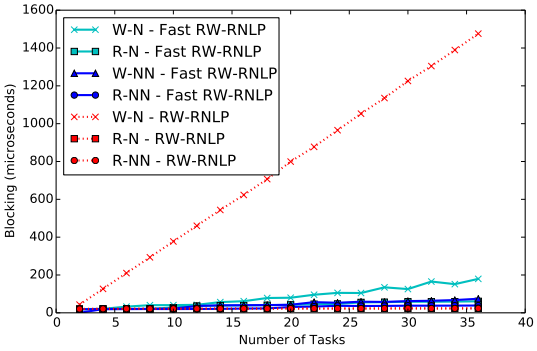

(c) Blocking.

Figure 83: (a) Lock and (b) unlock overheads and (c) blocking for nested and non-nested read and write requests under the RW-RNLP and the fast RW-RNLP. Here, for each request $\mathcal{R}_i$, $L_i = 20\mu$s, $n_r = 64$, $|D_i| = 1$ for non-nested requests, and $|D_i| = 2$ for nested requests. Each request was randomly chosen to be a read (as opposed to a write) with probability 0.5 and to be a nested request with probability 0.5. Due to write expansion, $|D_i|$ was inflated to 64 for all write requests under the RW-RNLP, as read requests can access any resource.

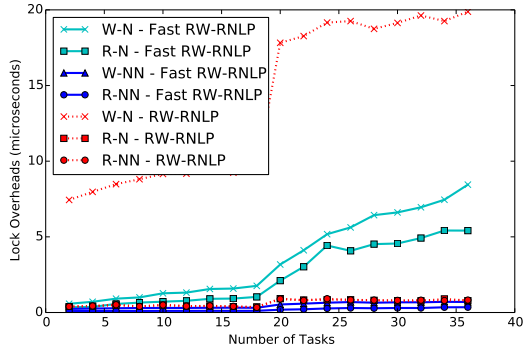

(a) Lock overhead.

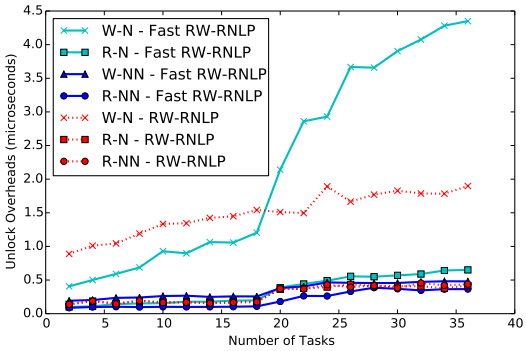

(b) Unlock overhead.

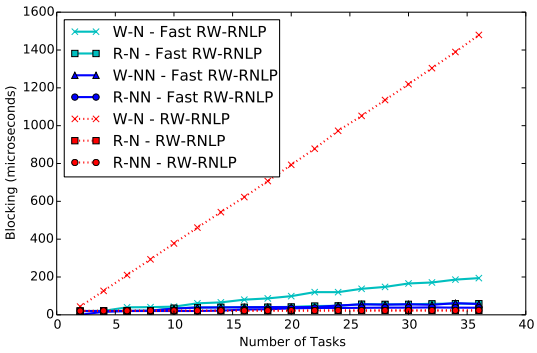

(c) Blocking.

Figure 84: (a) Lock and (b) unlock overheads and (c) blocking for nested and non-nested read and write requests under the RW-RNLP and the fast RW-RNLP. Here, for each request $\mathcal{R}_i$, $L_i = 20\mu$s, $n_r = 64$, $|D_i| = 1$ for non-nested requests, and $|D_i| = 2$ for nested requests. Each request was randomly chosen to be a read (as opposed to a write) with probability 0.5 and to be a nested request with probability 0.8. Due to write expansion, $|D_i|$ was inflated to 64 for all write requests under the RW-RNLP, as read requests can access any resource.

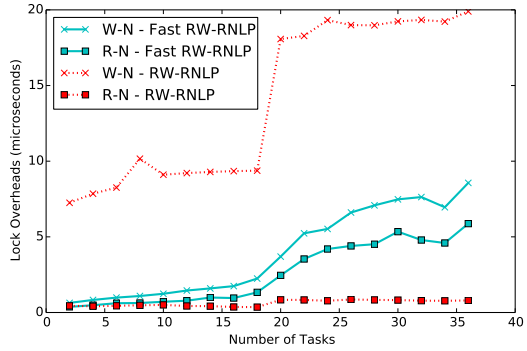

(a) Lock overhead.

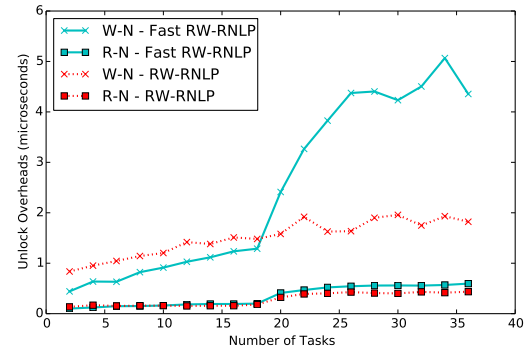

(b) Unlock overhead.

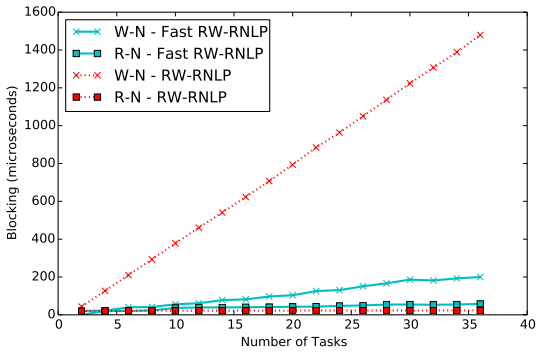

(c) Blocking.

Figure 85: (a) Lock and (b) unlock overheads and (c) blocking for nested read and write requests under the RW-RNLP and the fast RW-RNLP. Here, for each request $\mathcal{R}_i$, $L_i = 20\mu$s, $n_r = 64$, and $|D_i| = 2$. Each request was randomly chosen to be a read (as opposed to a write) with probability 0.5 and to be a nested request with probability 1. Due to write expansion, $|D_i|$ was inflated to 64 for all write requests under the RW-RNLP, as read requests can access any resource.

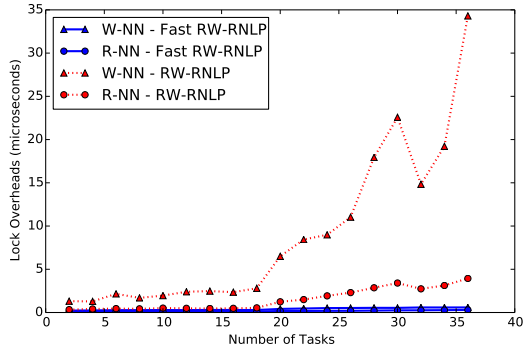

(a) Lock overhead.

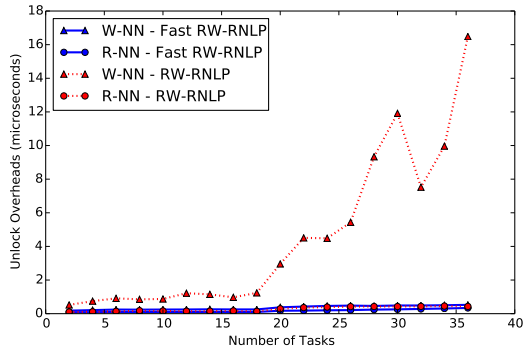

(b) Unlock overhead.

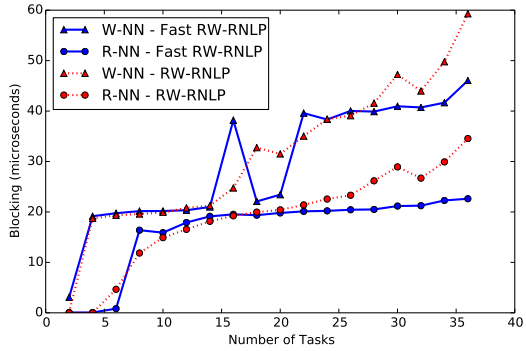

(c) Blocking.

Figure 86: (a) Lock and (b) unlock overheads and (c) blocking for non-nested read and write requests under the RW-RNLP and the fast RW-RNLP. Here, for each request $\mathcal{R}_i$, $L_i = 20\mu$s, $n_r = 64$, and $|D_i| = 1$. Each request was randomly chosen to be a read (as opposed to a write) with probability 0.8 and to be a nested request with probability 0.

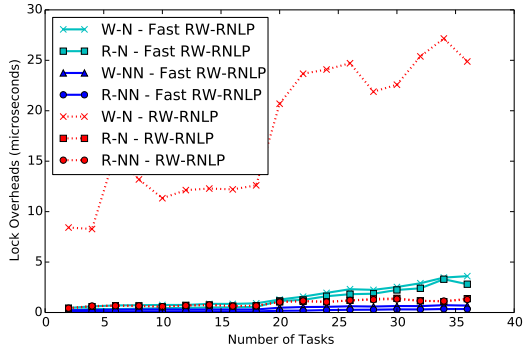

(a) Lock overhead.

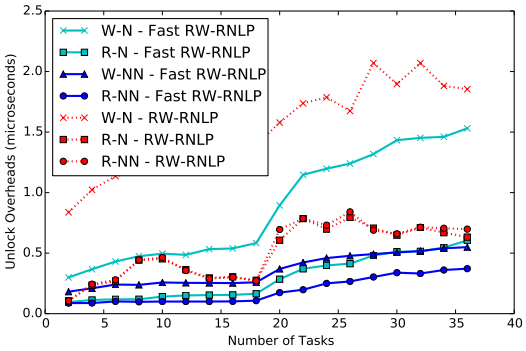

(b) Unlock overhead.

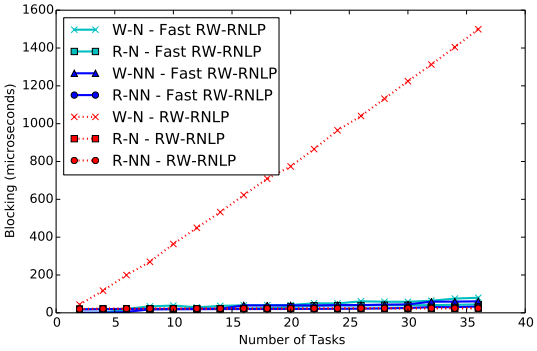

(c) Blocking.

Figure 87: (a) Lock and (b) unlock overheads and (c) blocking for nested and non-nested read and write requests under the RW-RNLP and the fast RW-RNLP. Here, for each request $\mathcal{R}_i$, $L_i = 20\mu$s, $n_r = 64$, $|D_i| = 1$ for non-nested requests, and $|D_i| = 2$ for nested requests. Each request was randomly chosen to be a read (as opposed to a write) with probability 0.8 and to be a nested request with probability 0.2. Due to write expansion, $|D_i|$ was inflated to 64 for all write requests under the RW-RNLP, as read requests can access any resource.

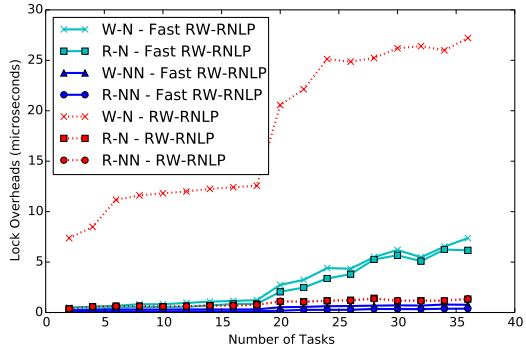

(a) Lock overhead.

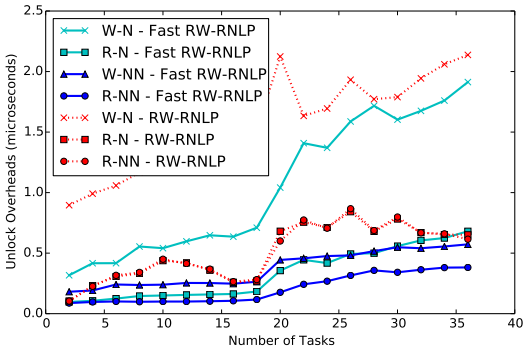

(b) Unlock overhead.

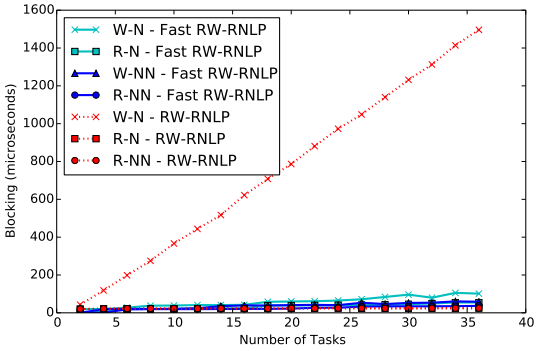

(c) Blocking.

Figure 88: (a) Lock and (b) unlock overheads and (c) blocking for nested and non-nested read and write requests under the RW-RNLP and the fast RW-RNLP. Here, for each request $\mathcal{R}_i$, $L_i = 20\mu$s, $n_r = 64$, $|D_i| = 1$ for non-nested requests, and $|D_i| = 2$ for nested requests. Each request was randomly chosen to be a read (as opposed to a write) with probability 0.8 and to be a nested request with probability 0.5. Due to write expansion, $|D_i|$ was inflated to 64 for all write requests under the RW-RNLP, as read requests can access any resource.

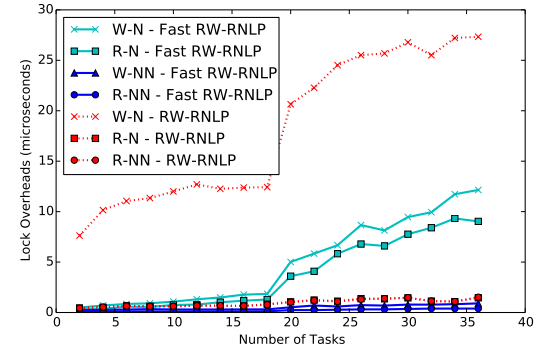

(a) Lock overhead.

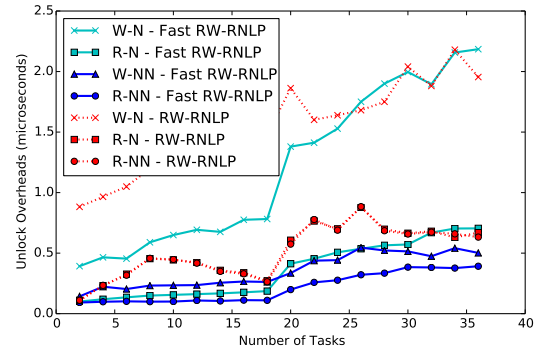

(b) Unlock overhead.

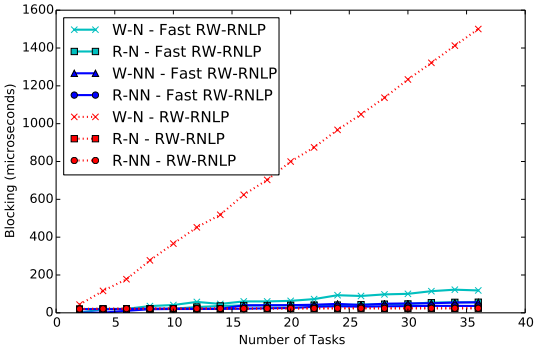

(c) Blocking.

Figure 89: (a) Lock and (b) unlock overheads and (c) blocking for nested and non-nested read and write requests under the RW-RNLP and the fast RW-RNLP. Here, for each request $\mathcal{R}_i$, $L_i = 20\mu$s, $n_r = 64$, $|D_i| = 1$ for non-nested requests, and $|D_i| = 2$ for nested requests. Each request was randomly chosen to be a read (as opposed to a write) with probability 0.8 and to be a nested request with probability 0.8. Due to write expansion, $|D_i|$ was inflated to 64 for all write requests under the RW-RNLP, as read requests can access any resource.

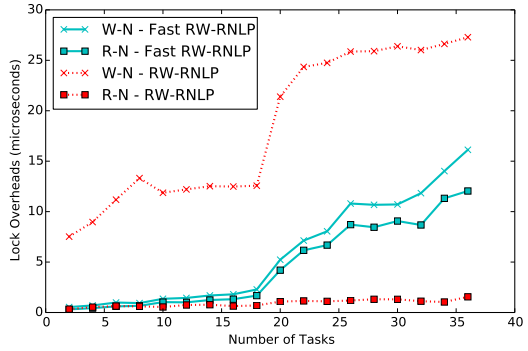

(a) Lock overhead.

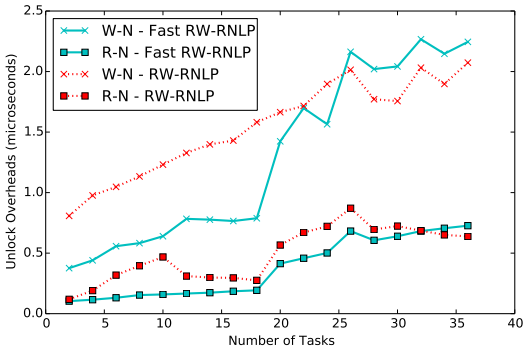

(b) Unlock overhead.

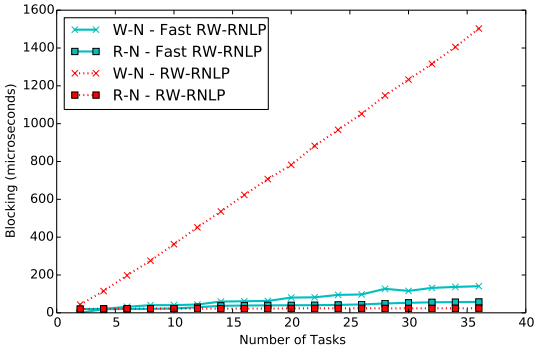

(c) Blocking.

Figure 90: (a) Lock and (b) unlock overheads and (c) blocking for nested read and write requests under the RW-RNLP and the fast RW-RNLP. Here, for each request $\mathcal{R}_i$, $L_i = 20\mu$s, $n_r = 64$, and $|D_i| = 2$. Each request was randomly chosen to be a read (as opposed to a write) with probability 0.8 and to be a nested request with probability 1. Due to write expansion, $|D_i|$ was inflated to 64 for all write requests under the RW-RNLP, as read requests can access any resource.

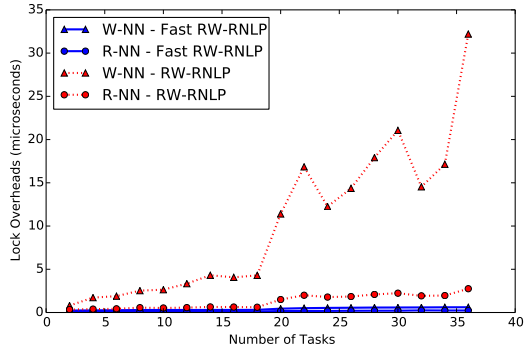

(a) Lock overhead.

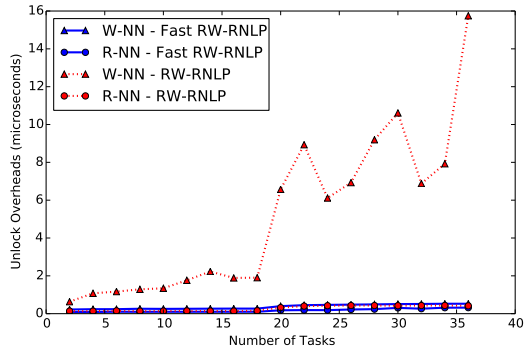

(b) Unlock overhead.

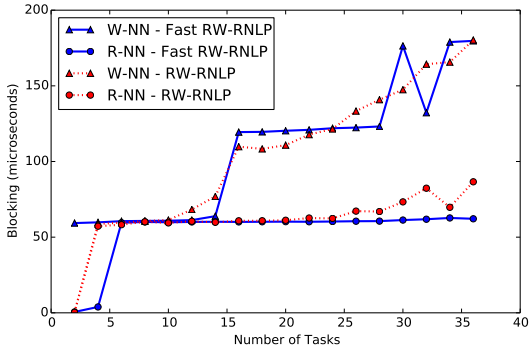

(c) Blocking.

Figure 91: (a) Lock and (b) unlock overheads and (c) blocking for non-nested read and write requests under the RW-RNLP and the fast RW-RNLP. Here, for each request $\mathcal{R}_i$, $L_i = 60\mu$s, $n_r = 64$, and $|D_i| = 1$. Each request was randomly chosen to be a read (as opposed to a write) with probability 0.2 and to be a nested request with probability 0.

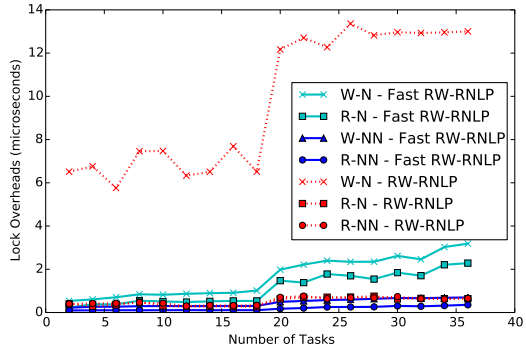

(a) Lock overhead.

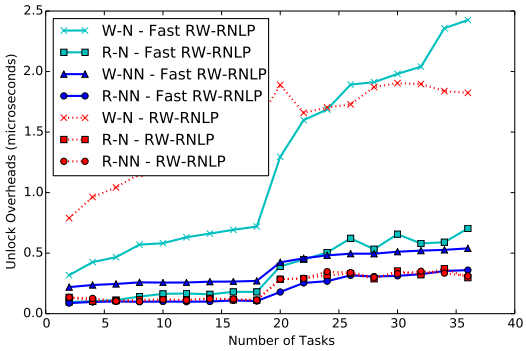

(b) Unlock overhead.

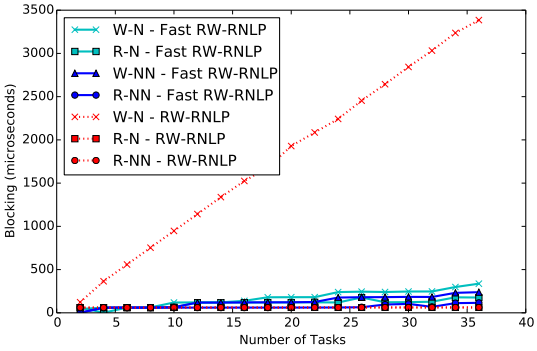

(c) Blocking.

Figure 92: (a) Lock and (b) unlock overheads and (c) blocking for nested and non-nested read and write requests under the RW-RNLP and the fast RW-RNLP. Here, for each request $\mathcal{R}_i$, $L_i = 60\mu$s, $n_r = 64$, $|D_i| = 1$ for non-nested requests, and $|D_i| = 2$ for nested requests. Each request was randomly chosen to be a read (as opposed to a write) with probability 0.2 and to be a nested request with probability 0.2. Due to write expansion, $|D_i|$ was inflated to 64 for all write requests under the RW-RNLP, as read requests can access any resource.

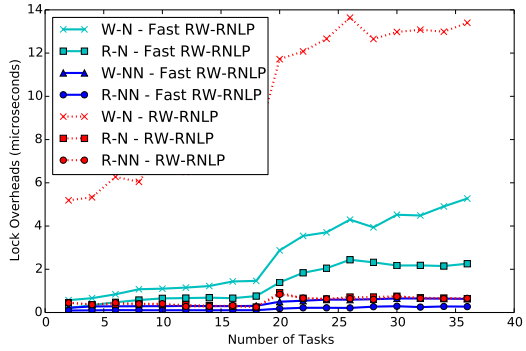

(a) Lock overhead.

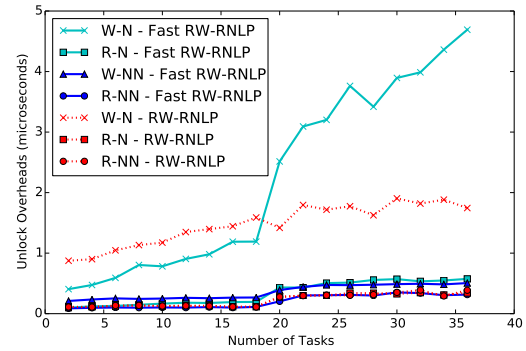

(b) Unlock overhead.

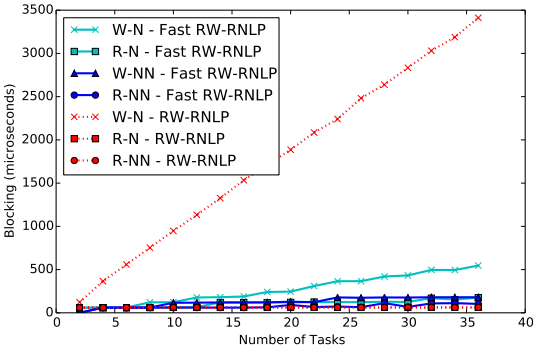

(c) Blocking.

Figure 93: (a) Lock and (b) unlock overheads and (c) blocking for nested and non-nested read and write requests under the RW-RNLP and the fast RW-RNLP. Here, for each request $\mathcal{R}_i$, $L_i = 60\mu$s, $n_r = 64$, $|D_i| = 1$ for non-nested requests, and $|D_i| = 2$ for nested requests. Each request was randomly chosen to be a read (as opposed to a write) with probability 0.2 and to be a nested request with probability 0.5. Due to write expansion, $|D_i|$ was inflated to 64 for all write requests under the RW-RNLP, as read requests can access any resource.

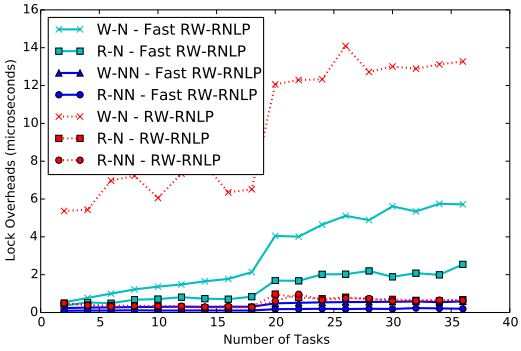

(a) Lock overhead.

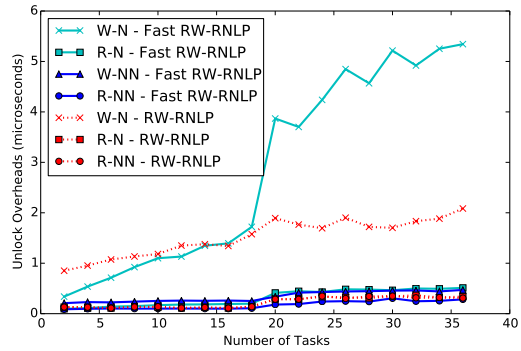

(b) Unlock overhead.

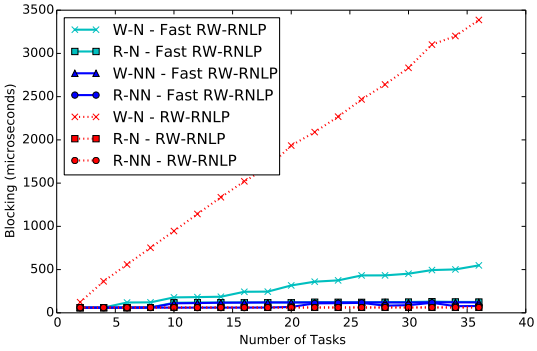

(c) Blocking.

Figure 94: (a) Lock and (b) unlock overheads and (c) blocking for nested and non-nested read and write requests under the RW-RNLP and the fast RW-RNLP. Here, for each request $\mathcal{R}_i$, $L_i = 60\mu$s, $n_r = 64$, $|D_i| = 1$ for non-nested requests, and $|D_i| = 2$ for nested requests. Each request was randomly chosen to be a read (as opposed to a write) with probability 0.2 and to be a nested request with probability 0.8. Due to write expansion, $|D_i|$ was inflated to 64 for all write requests under the RW-RNLP, as read requests can access any resource.

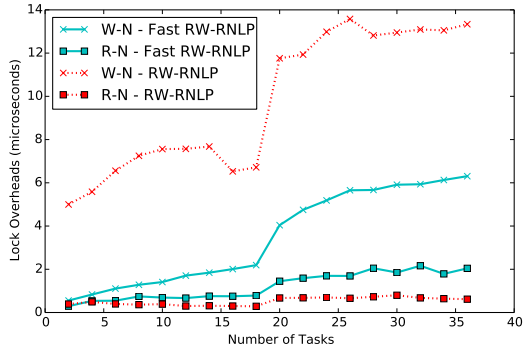

(a) Lock overhead.

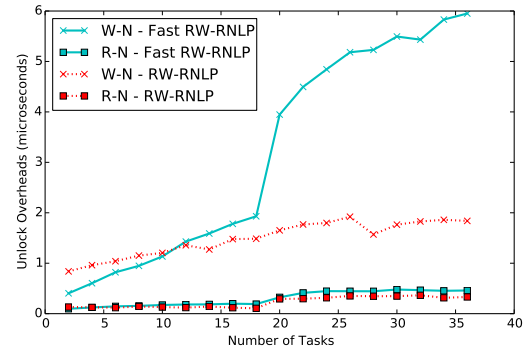

(b) Unlock overhead.

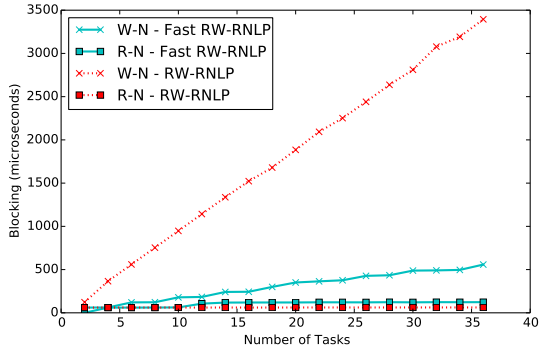

(c) Blocking.

Figure 95: (a) Lock and (b) unlock overheads and (c) blocking for nested read and write requests under the RW-RNLP and the fast RW-RNLP. Here, for each request $\mathcal{R}_i$, $L_i = 60\mu$s, $n_r = 64$, and $|D_i| = 2$. Each request was randomly chosen to be a read (as opposed to a write) with probability 0.2 and to be a nested request with probability 1. Due to write expansion, $|D_i|$ was inflated to 64 for all write requests under the RW-RNLP, as read requests can access any resource.

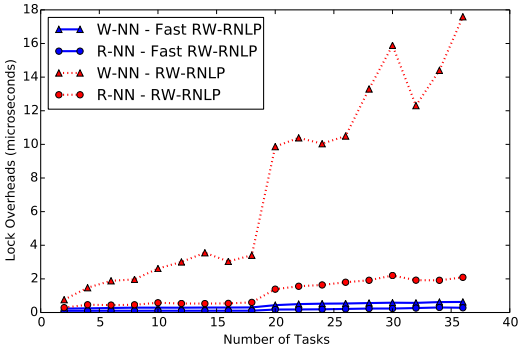

(a) Lock overhead.

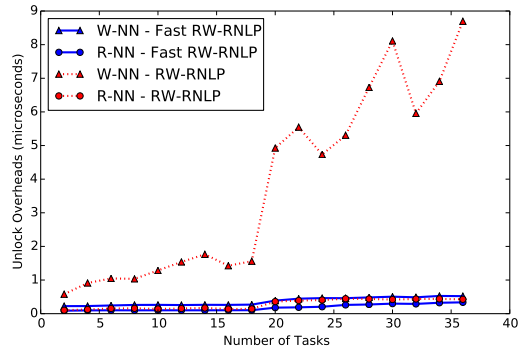

(b) Unlock overhead.

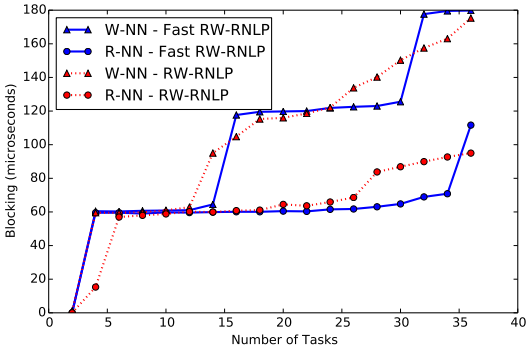

(c) Blocking.

Figure 96: (a) Lock and (b) unlock overheads and (c) blocking for non-nested read and write requests under the RW-RNLP and the fast RW-RNLP. Here, for each request $\mathcal{R}_i$, $L_i = 60\mu$s, $n_r = 64$, and $|D_i| = 1$. Each request was randomly chosen to be a read (as opposed to a write) with probability 0.5 and to be a nested request with probability 0.

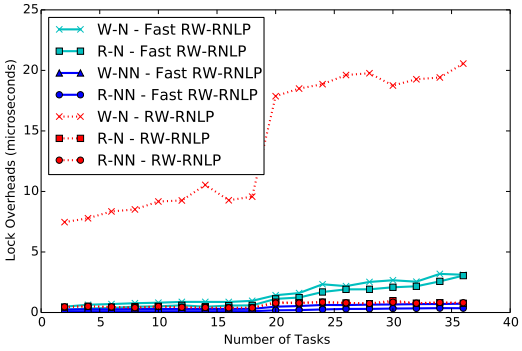

(a) Lock overhead.

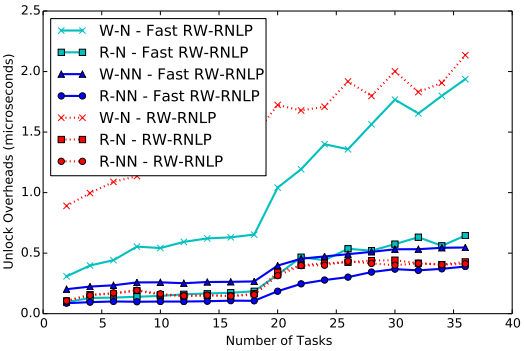

(b) Unlock overhead.

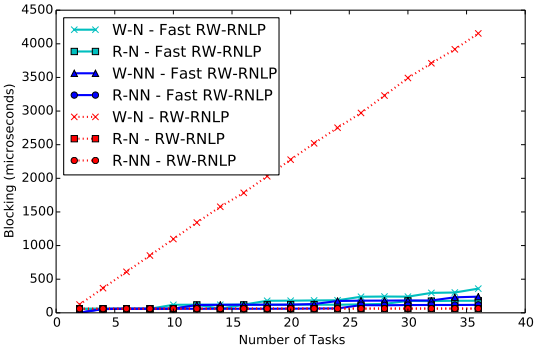

(c) Blocking.

Figure 97: (a) Lock and (b) unlock overheads and (c) blocking for nested and non-nested read and write requests under the RW-RNLP and the fast RW-RNLP. Here, for each request $\mathcal{R}_i$, $L_i = 60\mu$s, $n_r = 64$, $|D_i| = 1$ for non-nested requests, and $|D_i| = 2$ for nested requests. Each request was randomly chosen to be a read (as opposed to a write) with probability 0.5 and to be a nested request with probability 0.2. Due to write expansion, $|D_i|$ was inflated to 64 for all write requests under the RW-RNLP, as read requests can access any resource.

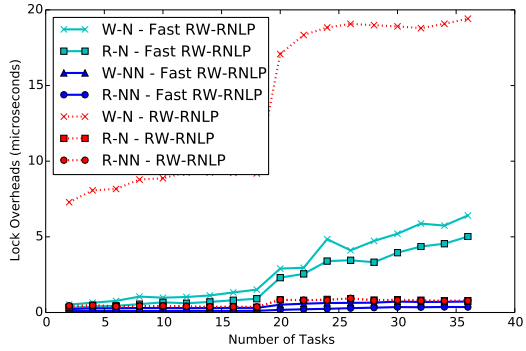

(a) Lock overhead.

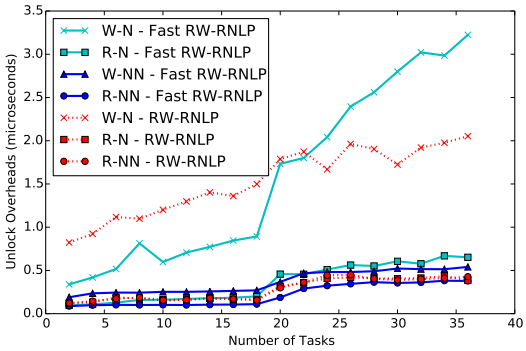

(b) Unlock overhead.

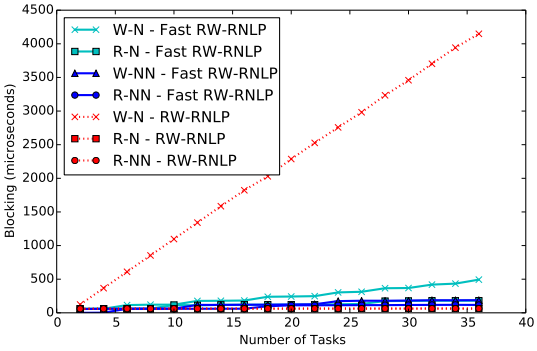

(c) Blocking.

Figure 98: (a) Lock and (b) unlock overheads and (c) blocking for nested and non-nested read and write requests under the RW-RNLP and the fast RW-RNLP. Here, for each request $\mathcal{R}_i$, $L_i = 60\mu$s, $n_r = 64$, $|D_i| = 1$ for non-nested requests, and $|D_i| = 2$ for nested requests. Each request was randomly chosen to be a read (as opposed to a write) with probability 0.5 and to be a nested request with probability 0.5. Due to write expansion, $|D_i|$ was inflated to 64 for all write requests under the RW-RNLP, as read requests can access any resource.

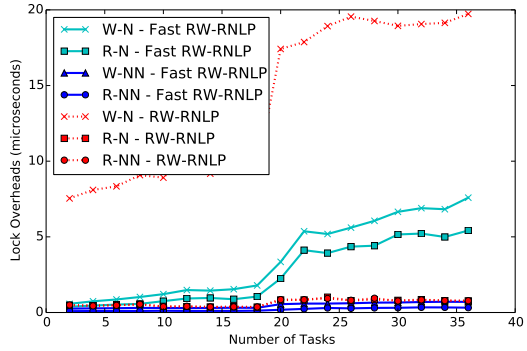

(a) Lock overhead.

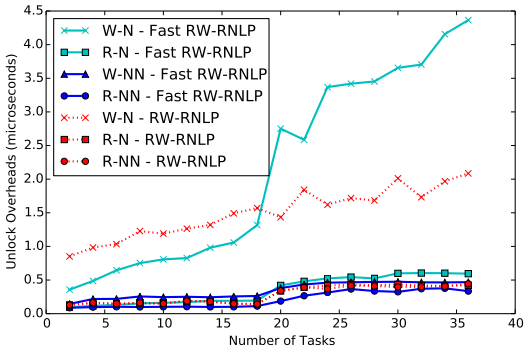

(b) Unlock overhead.

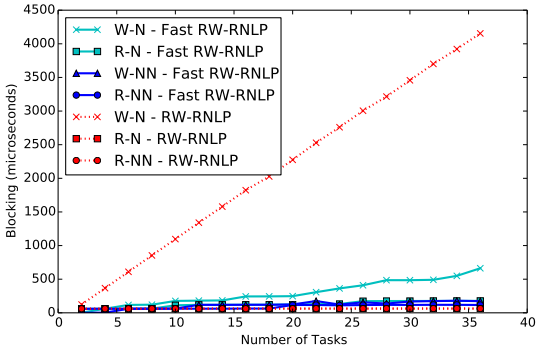

(c) Blocking.

Figure 99: (a) Lock and (b) unlock overheads and (c) blocking for nested and non-nested read and write requests under the RW-RNLP and the fast RW-RNLP. Here, for each request $\mathcal{R}_i$, $L_i = 60\mu$s, $n_r = 64$, $|D_i| = 1$ for non-nested requests, and $|D_i| = 2$ for nested requests. Each request was randomly chosen to be a read (as opposed to a write) with probability 0.5 and to be a nested request with probability 0.8. Due to write expansion, $|D_i|$ was inflated to 64 for all write requests under the RW-RNLP, as read requests can access any resource.

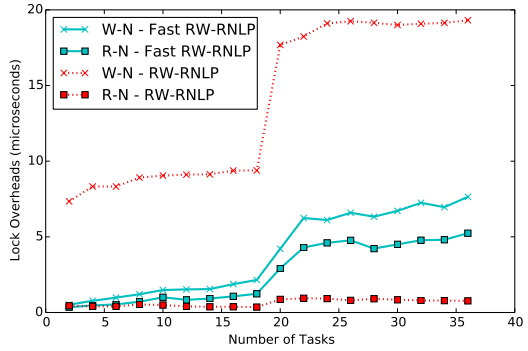

(a) Lock overhead.

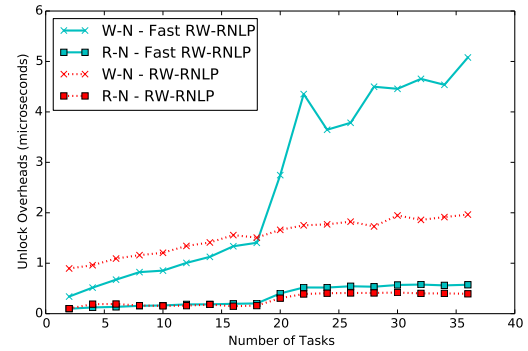

(b) Unlock overhead.

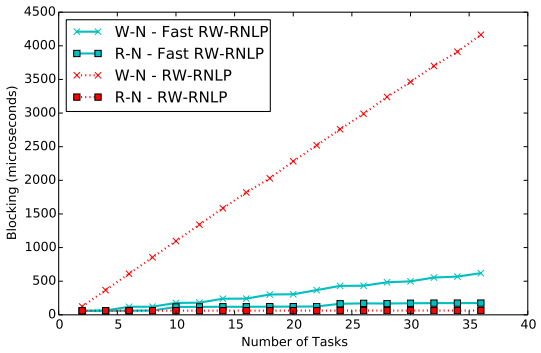

(c) Blocking.

Figure 100: (a) Lock and (b) unlock overheads and (c) blocking for nested read and write requests under the RW-RNLP and the fast RW-RNLP. Here, for each request $\mathcal{R}_i$, $L_i = 60\mu$s, $n_r = 64$, and $|D_i| = 2$. Each request was randomly chosen to be a read (as opposed to a write) with probability 0.5 and to be a nested request with probability 1. Due to write expansion, $|D_i|$ was inflated to 64 for all write requests under the RW-RNLP, as read requests can access any resource.

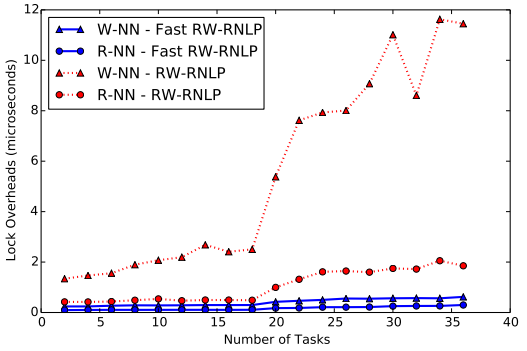

(a) Lock overhead.

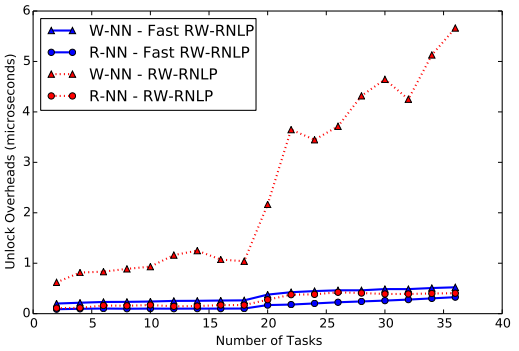

(b) Unlock overhead.

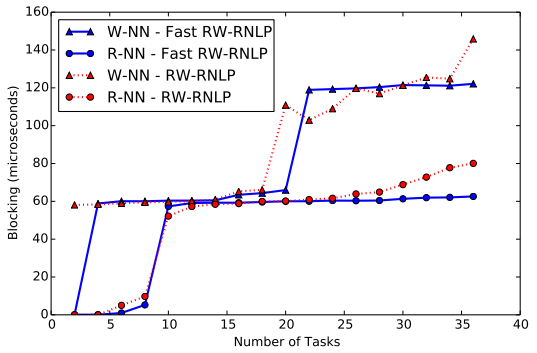

(c) Blocking.

Figure 101: (a) Lock and (b) unlock overheads and (c) blocking for non-nested read and write requests under the RW-RNLP and the fast RW-RNLP. Here, for each request $\mathcal{R}_i$, $L_i = 60\mu$s, $n_r = 64$, and $|D_i| = 1$. Each request was randomly chosen to be a read (as opposed to a write) with probability 0.8 and to be a nested request with probability 0.

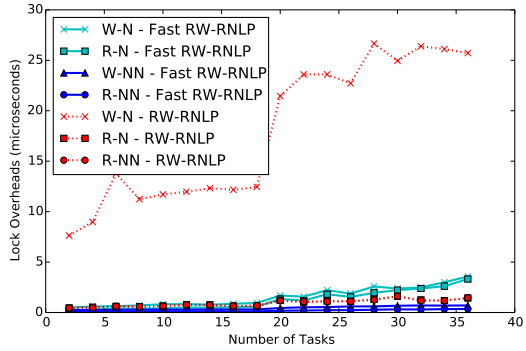

(a) Lock overhead.

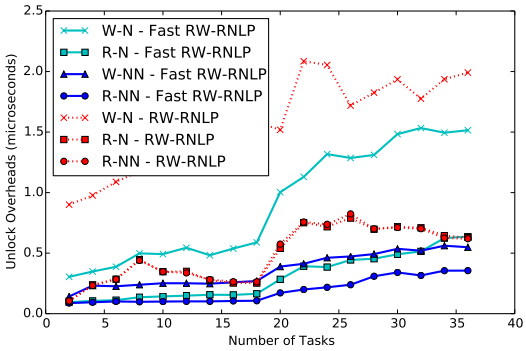

(b) Unlock overhead.

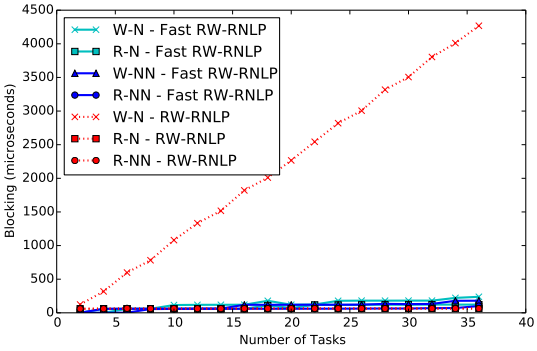

(c) Blocking.

Figure 102: (a) Lock and (b) unlock overheads and (c) blocking for nested and non-nested read and write requests under the RW-RNLP and the fast RW-RNLP. Here, for each request $\mathcal{R}_i$, $L_i = 60\mu$s, $n_r = 64$, $|D_i| = 1$ for non-nested requests, and $|D_i| = 2$ for nested requests. Each request was randomly chosen to be a read (as opposed to a write) with probability 0.8 and to be a nested request with probability 0.2. Due to write expansion, $|D_i|$ was inflated to 64 for all write requests under the RW-RNLP, as read requests can access any resource.

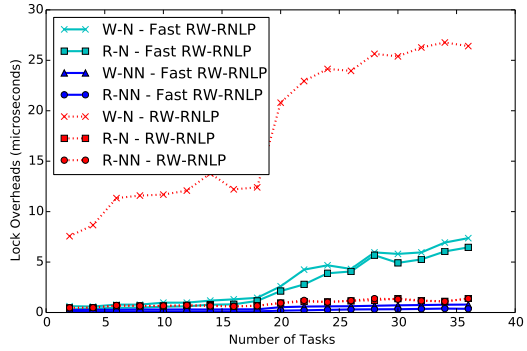

(a) Lock overhead.

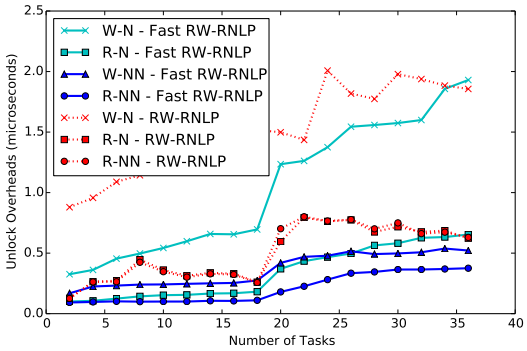

(b) Unlock overhead.

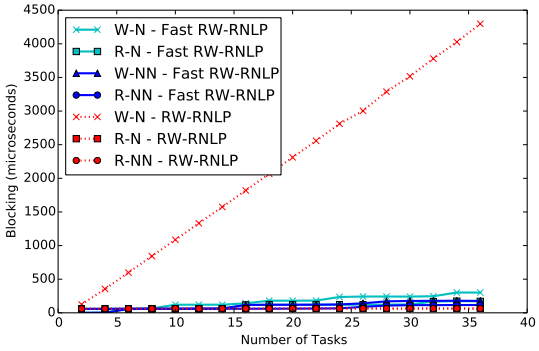

(c) Blocking.

Figure 103: (a) Lock and (b) unlock overheads and (c) blocking for nested and non-nested read and write requests under the RW-RNLP and the fast RW-RNLP. Here, for each request $\mathcal{R}_i$, $L_i = 60\mu$s, $n_r = 64$, $|D_i| = 1$ for non-nested requests, and $|D_i| = 2$ for nested requests. Each request was randomly chosen to be a read (as opposed to a write) with probability 0.8 and to be a nested request with probability 0.5. Due to write expansion, $|D_i|$ was inflated to 64 for all write requests under the RW-RNLP, as read requests can access any resource.

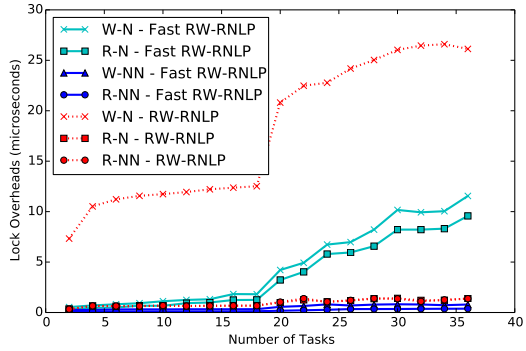

(a) Lock overhead.

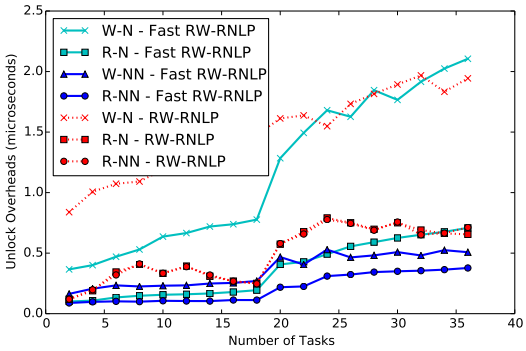

(b) Unlock overhead.

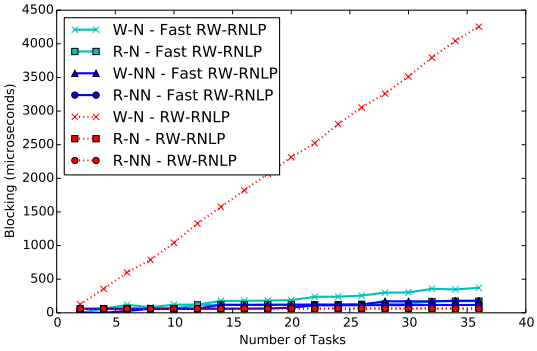

(c) Blocking.

Figure 104: (a) Lock and (b) unlock overheads and (c) blocking for nested and non-nested read and write requests under the RW-RNLP and the fast RW-RNLP. Here, for each request $\mathcal{R}_i$, $L_i = 60\mu$s, $n_r = 64$, $|D_i| = 1$ for non-nested requests, and $|D_i| = 2$ for nested requests. Each request was randomly chosen to be a read (as opposed to a write) with probability 0.8 and to be a nested request with probability 0.8. Due to write expansion, $|D_i|$ was inflated to 64 for all write requests under the RW-RNLP, as read requests can access any resource.

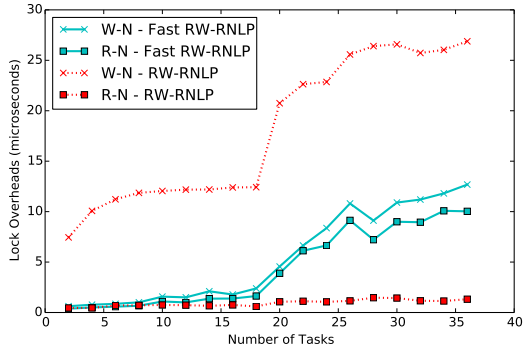

(a) Lock overhead.

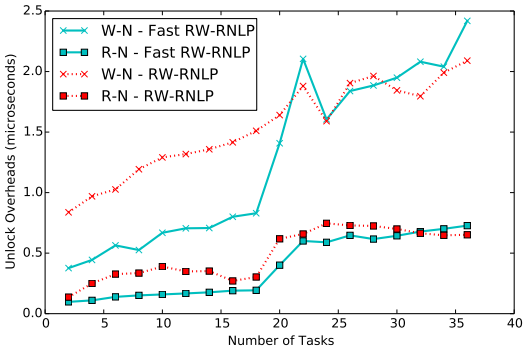

(b) Unlock overhead.

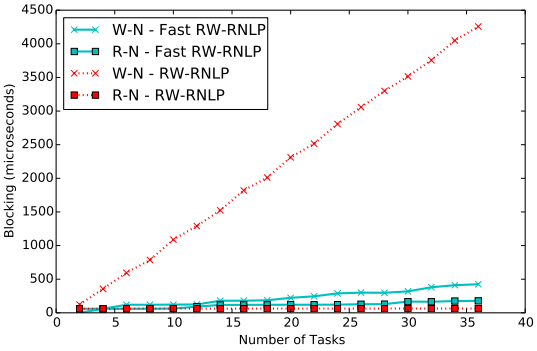

(c) Blocking.

Figure 105: (a) Lock and (b) unlock overheads and (c) blocking for nested read and write requests under the RW-RNLP and the fast RW-RNLP. Here, for each request $\mathcal{R}_i$, $L_i = 60\mu$s, $n_r = 64$, and $|D_i| = 2$. Each request was randomly chosen to be a read (as opposed to a write) with probability 0.8 and to be a nested request with probability 1. Due to write expansion, $|D_i|$ was inflated to 64 for all write requests under the RW-RNLP, as read requests can access any resource.

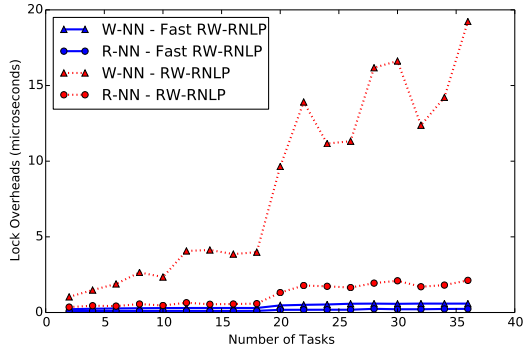

(a) Lock overhead.

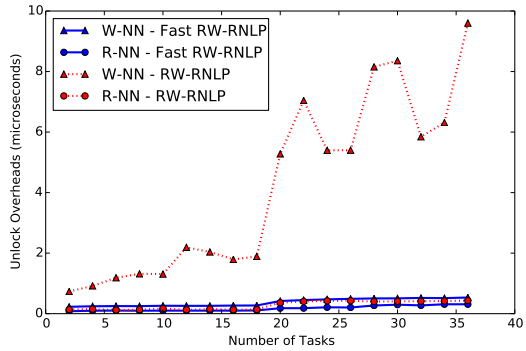

(b) Unlock overhead.

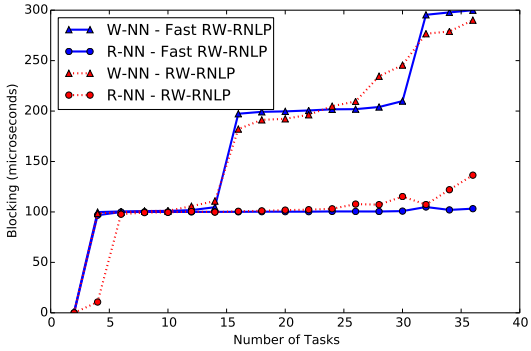

(c) Blocking.

Figure 106: (a) Lock and (b) unlock overheads and (c) blocking for non-nested read and write requests under the RW-RNLP and the fast RW-RNLP. Here, for each request $\mathcal{R}_i$, $L_i = 100\mu$s, $n_r = 64$, and $|D_i| = 1$. Each request was randomly chosen to be a read (as opposed to a write) with probability 0.2 and to be a nested request with probability 0.

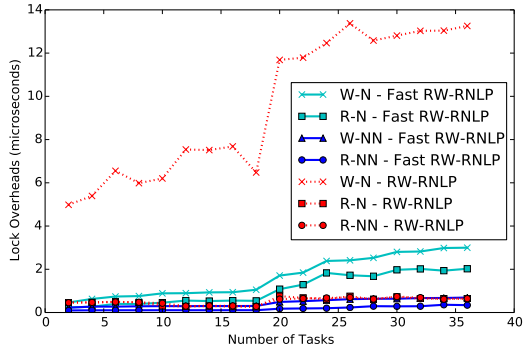

(a) Lock overhead.

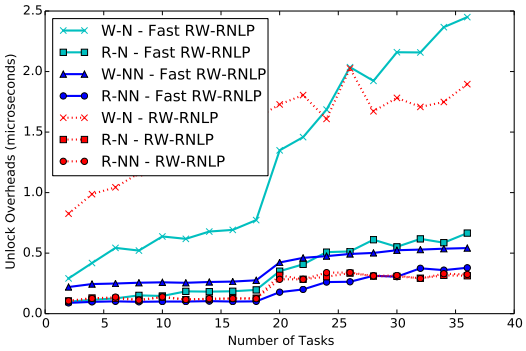

(b) Unlock overhead.

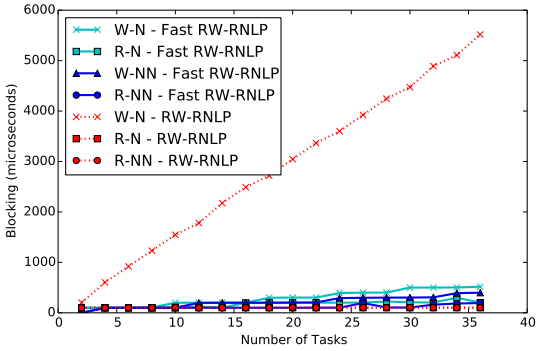

(c) Blocking.

Figure 107: (a) Lock and (b) unlock overheads and (c) blocking for nested and non-nested read and write requests under the RW-RNLP and the fast RW-RNLP. Here, for each request $\mathcal{R}_i$, $L_i = 100\mu$s, $n_r = 64$, $|D_i| = 1$ for non-nested requests, and $|D_i| = 2$ for nested requests. Each request was randomly chosen to be a read (as opposed to a write) with probability 0.2 and to be a nested request with probability 0.2. Due to write expansion, $|D_i|$ was inflated to 64 for all write requests under the RW-RNLP, as read requests can access any resource.

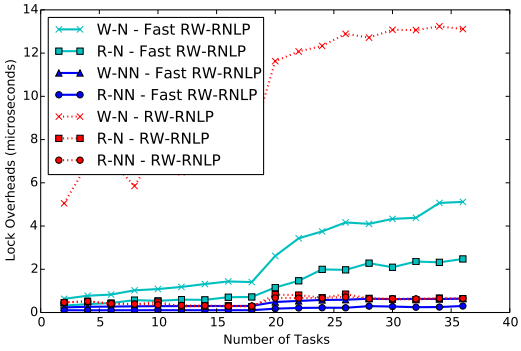

(a) Lock overhead.

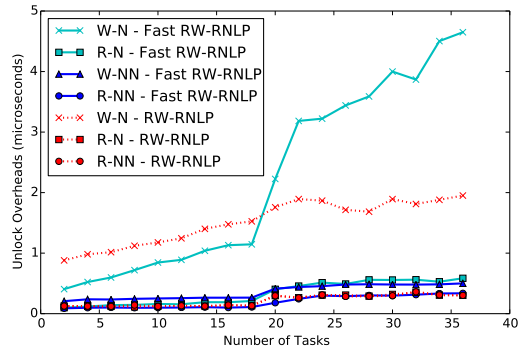

(b) Unlock overhead.

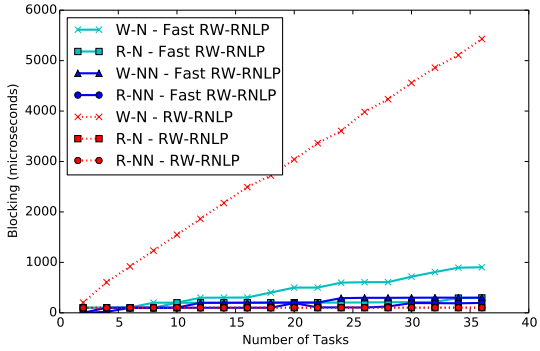

(c) Blocking.

Figure 108: (a) Lock and (b) unlock overheads and (c) blocking for nested and non-nested read and write requests under the RW-RNLP and the fast RW-RNLP. Here, for each request $\mathcal{R}_i$, $L_i = 100\mu$s, $n_r = 64$, $|D_i| = 1$ for non-nested requests, and $|D_i| = 2$ for nested requests. Each request was randomly chosen to be a read (as opposed to a write) with probability 0.2 and to be a nested request with probability 0.5. Due to write expansion, $|D_i|$ was inflated to 64 for all write requests under the RW-RNLP, as read requests can access any resource.

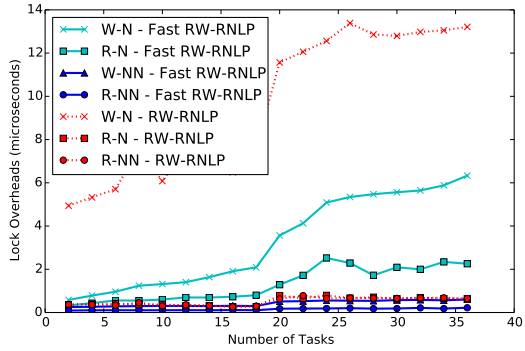

(a) Lock overhead.

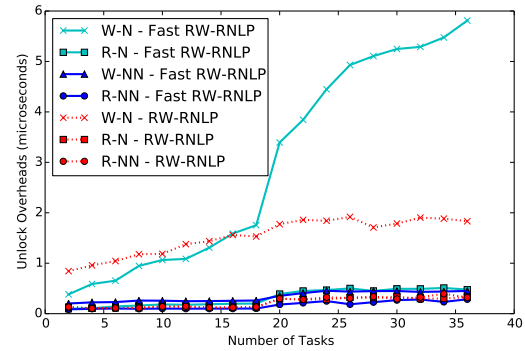

(b) Unlock overhead.

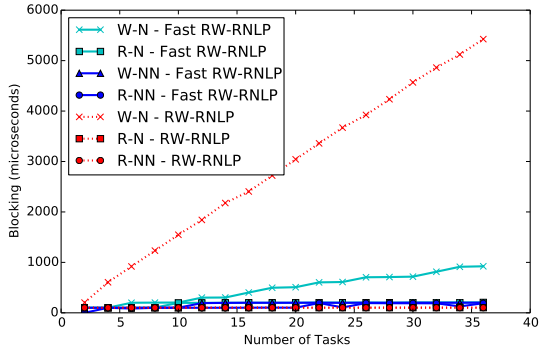

(c) Blocking.

Figure 109: (a) Lock and (b) unlock overheads and (c) blocking for nested and non-nested read and write requests under the RW-RNLP and the fast RW-RNLP. Here, for each request $\mathcal{R}_i$, $L_i = 100\mu$s, $n_r = 64$, $|D_i| = 1$ for non-nested requests, and $|D_i| = 2$ for nested requests. Each request was randomly chosen to be a read (as opposed to a write) with probability 0.2 and to be a nested request with probability 0.8. Due to write expansion, $|D_i|$ was inflated to 64 for all write requests under the RW-RNLP, as read requests can access any resource.

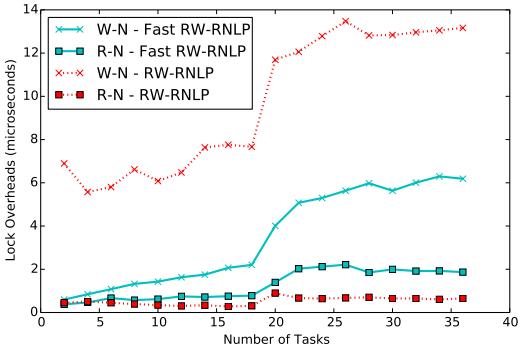

(a) Lock overhead.

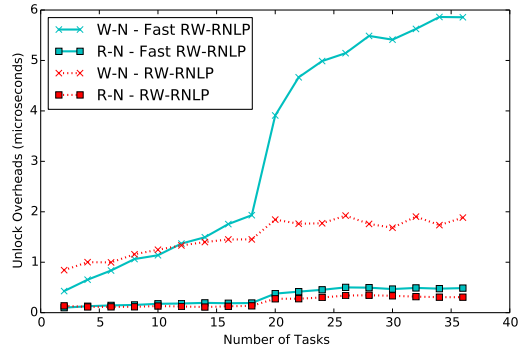

(b) Unlock overhead.

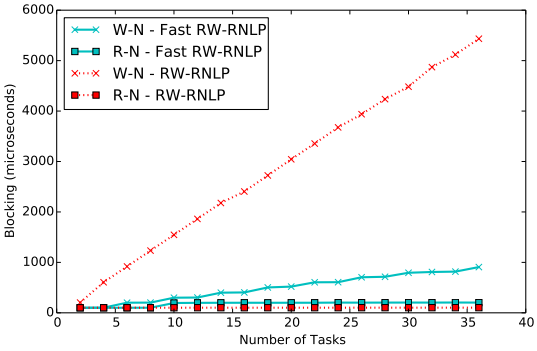

(c) Blocking.

Figure 110: (a) Lock and (b) unlock overheads and (c) blocking for nested read and write requests under the RW-RNLP and the fast RW-RNLP. Here, for each request $\mathcal{R}_i$, $L_i = 100\mu$s, $n_r = 64$, and $|D_i| = 2$. Each request was randomly chosen to be a read (as opposed to a write) with probability 0.2 and to be a nested request with probability 1. Due to write expansion, $|D_i|$ was inflated to 64 for all write requests under the RW-RNLP, as read requests can access any resource.

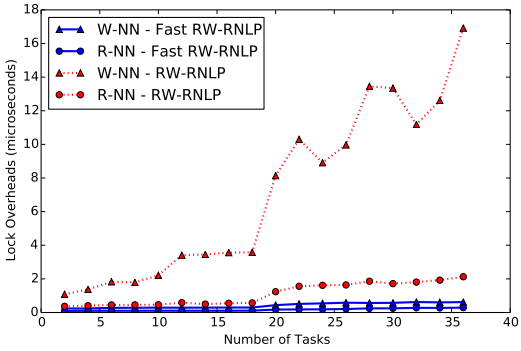

(a) Lock overhead.

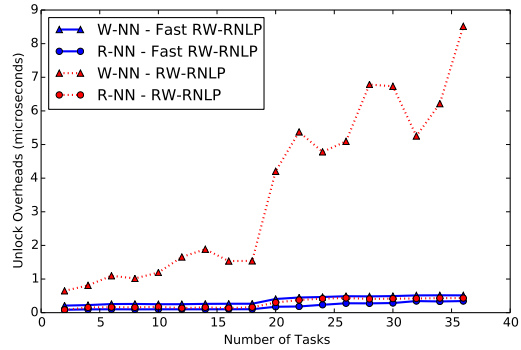

(b) Unlock overhead.

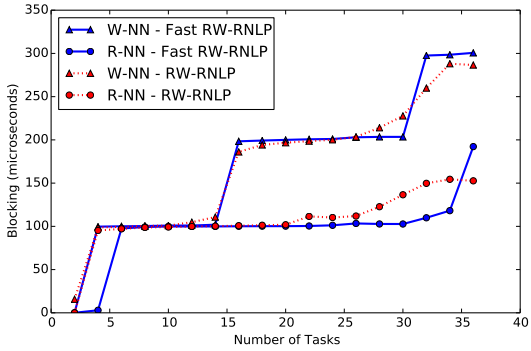

(c) Blocking.

Figure 111: (a) Lock and (b) unlock overheads and (c) blocking for non-nested read and write requests under the RW-RNLP and the fast RW-RNLP. Here, for each request $\mathcal{R}_i$, $L_i = 100\mu$s, $n_r = 64$, and $|D_i| = 1$. Each request was randomly chosen to be a read (as opposed to a write) with probability 0.5 and to be a nested request with probability 0.

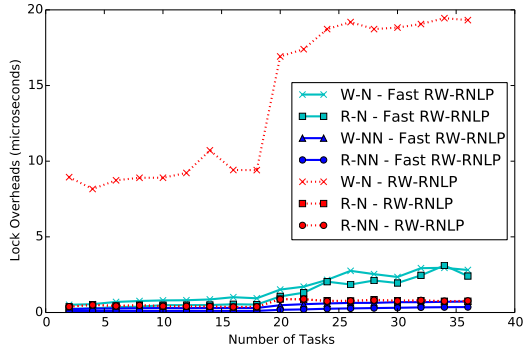

(a) Lock overhead.

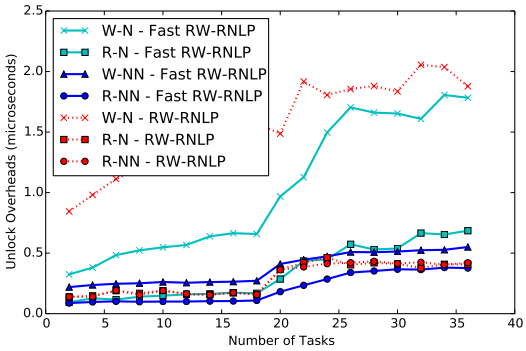

(b) Unlock overhead.

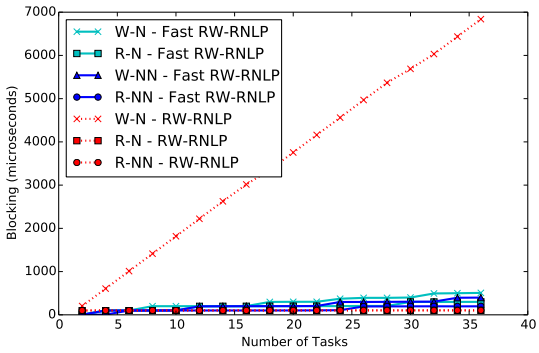

(c) Blocking.

Figure 112: (a) Lock and (b) unlock overheads and (c) blocking for nested and non-nested read and write requests under the RW-RNLP and the fast RW-RNLP. Here, for each request $\mathcal{R}_i$, $L_i = 100\mu$s, $n_r = 64$, $|D_i| = 1$ for non-nested requests, and $|D_i| = 2$ for nested requests. Each request was randomly chosen to be a read (as opposed to a write) with probability 0.5 and to be a nested request with probability 0.2. Due to write expansion, $|D_i|$ was inflated to 64 for all write requests under the RW-RNLP, as read requests can access any resource.

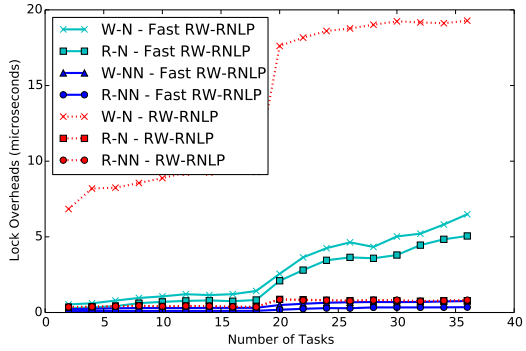

(a) Lock overhead.

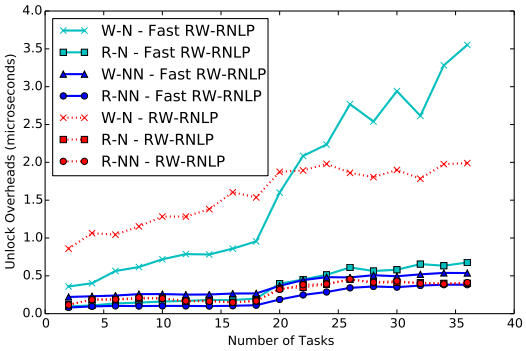

(b) Unlock overhead.

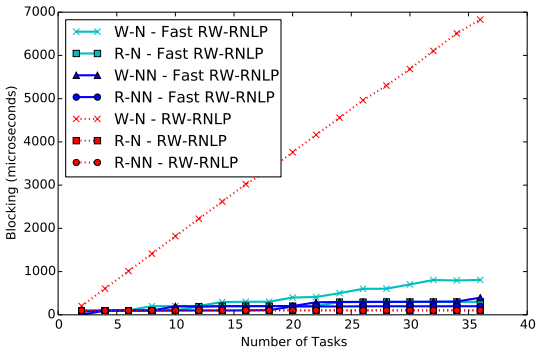

(c) Blocking.

Figure 113: (a) Lock and (b) unlock overheads and (c) blocking for nested and non-nested read and write requests under the RW-RNLP and the fast RW-RNLP. Here, for each request $\mathcal{R}_i$, $L_i = 100\mu$s, $n_r = 64$, $|D_i| = 1$ for non-nested requests, and $|D_i| = 2$ for nested requests. Each request was randomly chosen to be a read (as opposed to a write) with probability 0.5 and to be a nested request with probability 0.5. Due to write expansion, $|D_i|$ was inflated to 64 for all write requests under the RW-RNLP, as read requests can access any resource.

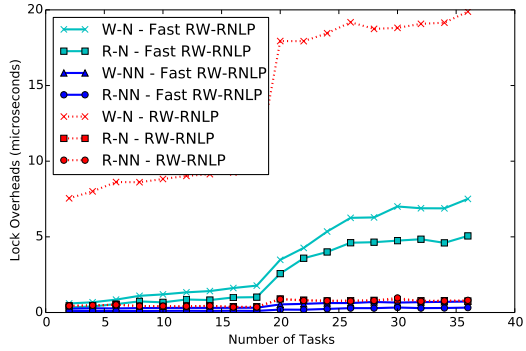

(a) Lock overhead.

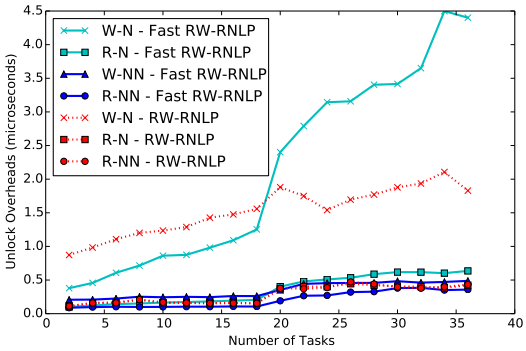

(b) Unlock overhead.

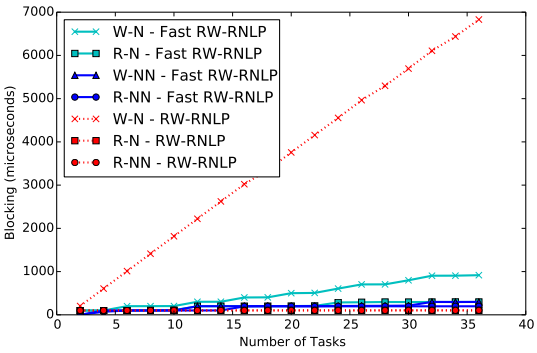

(c) Blocking.

Figure 114: (a) Lock and (b) unlock overheads and (c) blocking for nested and non-nested read and write requests under the RW-RNLP and the fast RW-RNLP. Here, for each request $\mathcal{R}_i$, $L_i = 100\mu$s, $n_r = 64$, $|D_i| = 1$ for non-nested requests, and $|D_i| = 2$ for nested requests. Each request was randomly chosen to be a read (as opposed to a write) with probability 0.5 and to be a nested request with probability 0.8. Due to write expansion, $|D_i|$ was inflated to 64 for all write requests under the RW-RNLP, as read requests can access any resource.

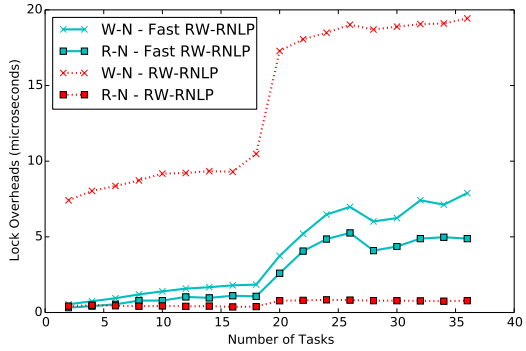

(a) Lock overhead.

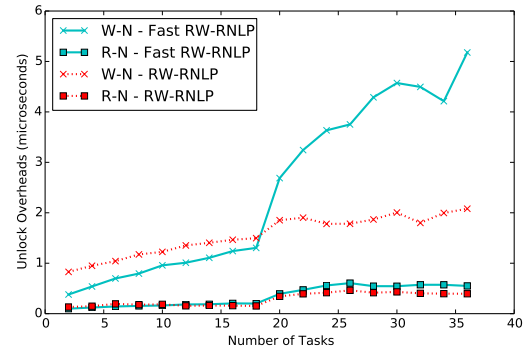

(b) Unlock overhead.

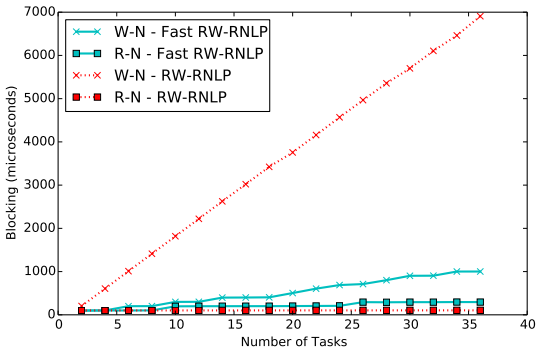

(c) Blocking.

Figure 115: (a) Lock and (b) unlock overheads and (c) blocking for nested read and write requests under the RW-RNLP and the fast RW-RNLP. Here, for each request $\mathcal{R}_i$, $L_i = 100\mu$s, $n_r = 64$, and $|D_i| = 2$. Each request was randomly chosen to be a read (as opposed to a write) with probability 0.5 and to be a nested request with probability 1. Due to write expansion, $|D_i|$ was inflated to 64 for all write requests under the RW-RNLP, as read requests can access any resource.

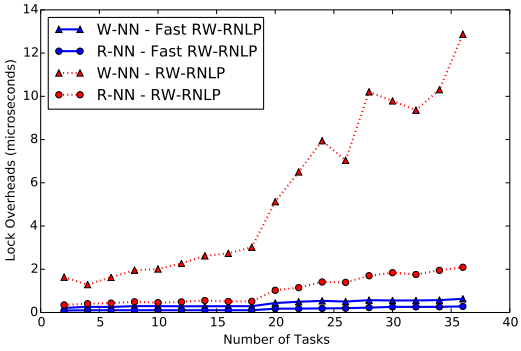

(a) Lock overhead.

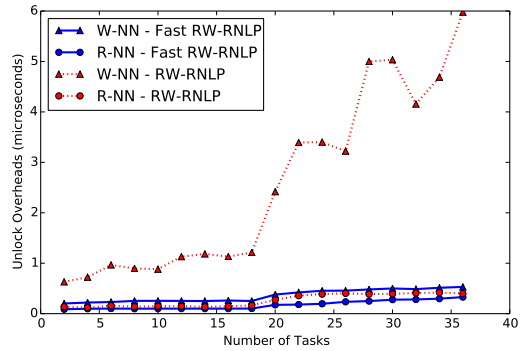

(b) Unlock overhead.

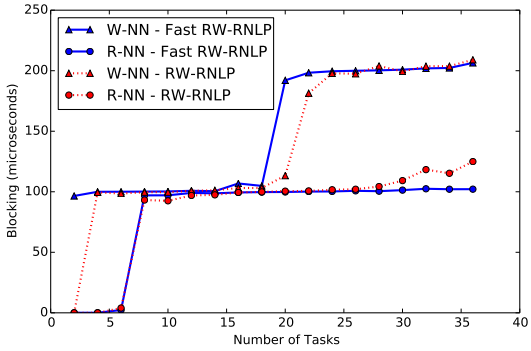

(c) Blocking.

Figure 116: (a) Lock and (b) unlock overheads and (c) blocking for non-nested read and write requests under the RW-RNLP and the fast RW-RNLP. Here, for each request $\mathcal{R}_i$, $L_i = 100\mu$s, $n_r = 64$, and $|D_i| = 1$. Each request was randomly chosen to be a read (as opposed to a write) with probability 0.8 and to be a nested request with probability 0.

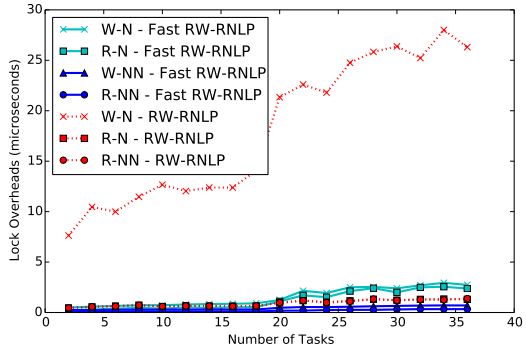

(a) Lock overhead.

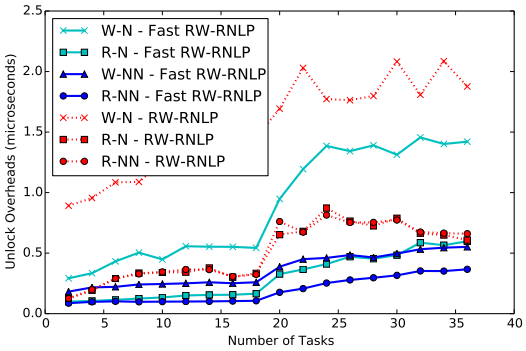

(b) Unlock overhead.

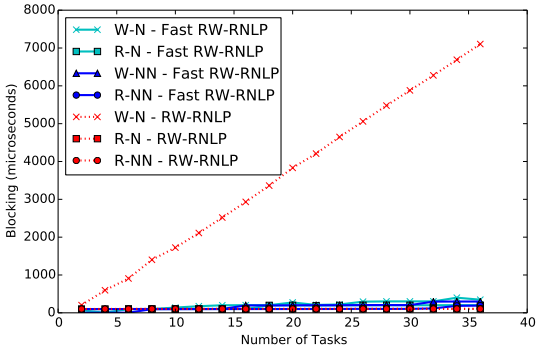

(c) Blocking.

Figure 117: (a) Lock and (b) unlock overheads and (c) blocking for nested and non-nested read and write requests under the RW-RNLP and the fast RW-RNLP. Here, for each request $\mathcal{R}_i$, $L_i = 100\mu$s, $n_r = 64$, $|D_i| = 1$ for non-nested requests, and $|D_i| = 2$ for nested requests. Each request was randomly chosen to be a read (as opposed to a write) with probability 0.8 and to be a nested request with probability 0.2. Due to write expansion, $|D_i|$ was inflated to 64 for all write requests under the RW-RNLP, as read requests can access any resource.

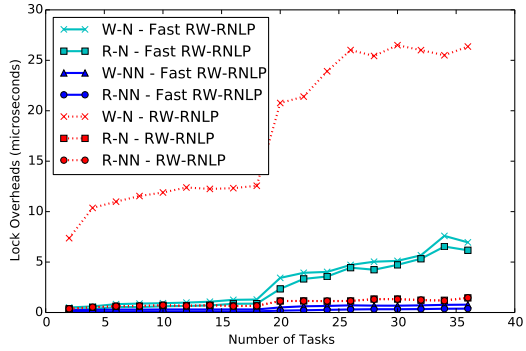

(a) Lock overhead.

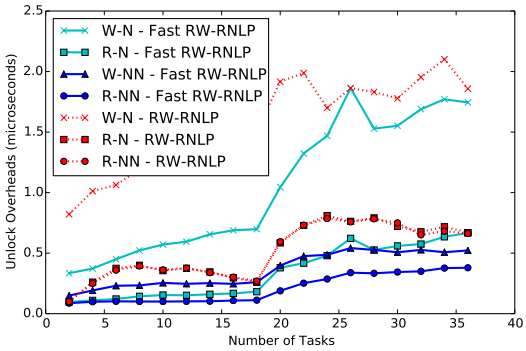

(b) Unlock overhead.

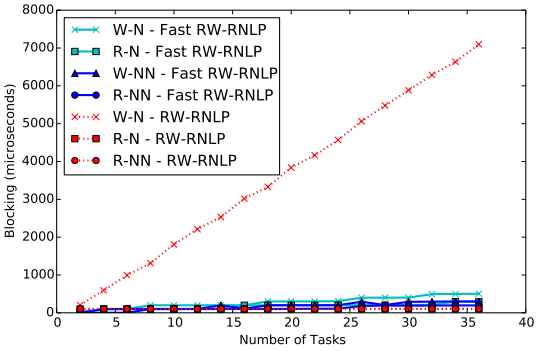

(c) Blocking.

Figure 118: (a) Lock and (b) unlock overheads and (c) blocking for nested and non-nested read and write requests under the RW-RNLP and the fast RW-RNLP. Here, for each request $\mathcal{R}_i$, $L_i = 100\mu$s, $n_r = 64$, $|D_i| = 1$ for non-nested requests, and $|D_i| = 2$ for nested requests. Each request was randomly chosen to be a read (as opposed to a write) with probability 0.8 and to be a nested request with probability 0.5. Due to write expansion, $|D_i|$ was inflated to 64 for all write requests under the RW-RNLP, as read requests can access any resource.

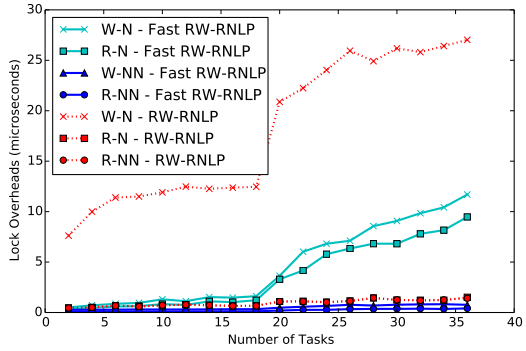

(a) Lock overhead.

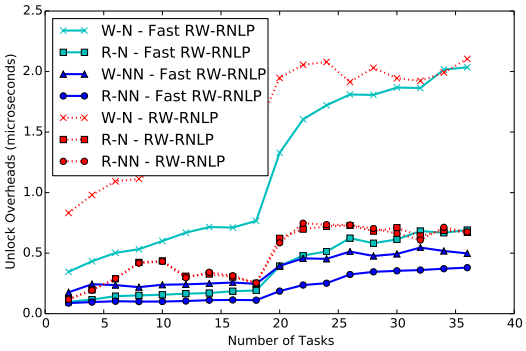

(b) Unlock overhead.

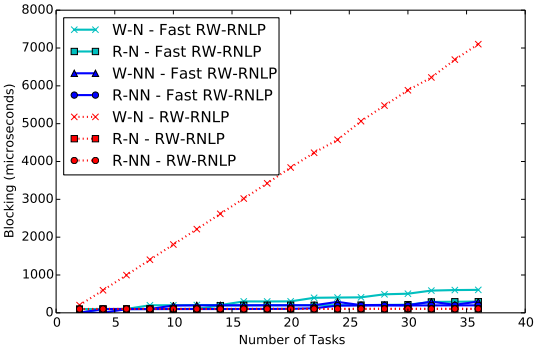

(c) Blocking.

Figure 119: (a) Lock and (b) unlock overheads and (c) blocking for nested and non-nested read and write requests under the RW-RNLP and the fast RW-RNLP. Here, for each request $\mathcal{R}_i$, $L_i = 100\mu$s, $n_r = 64$, $|D_i| = 1$ for non-nested requests, and $|D_i| = 2$ for nested requests. Each request was randomly chosen to be a read (as opposed to a write) with probability 0.8 and to be a nested request with probability 0.8. Due to write expansion, $|D_i|$ was inflated to 64 for all write requests under the RW-RNLP, as read requests can access any resource.

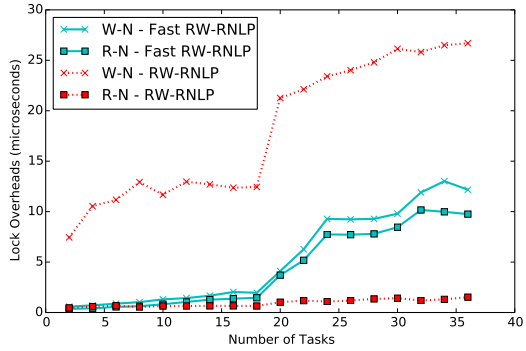

(a) Lock overhead.

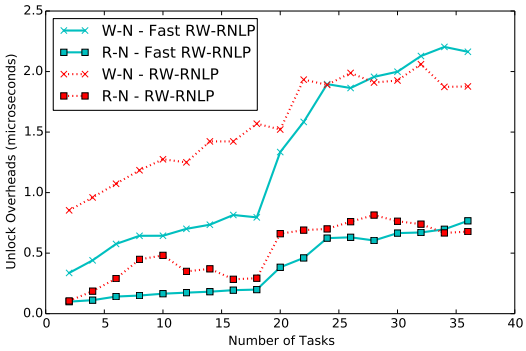

(b) Unlock overhead.

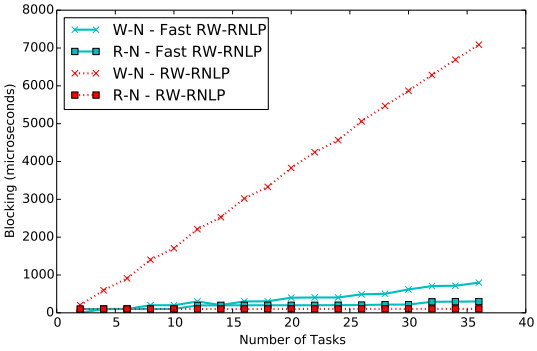

(c) Blocking.

Figure 120: (a) Lock and (b) unlock overheads and (c) blocking for nested read and write requests under the RW-RNLP and the fast RW-RNLP. Here, for each request $\mathcal{R}_i$, $L_i = 100\mu$s, $n_r = 64$, and $|D_i| = 2$. Each request was randomly chosen to be a read (as opposed to a write) with probability 0.8 and to be a nested request with probability 1. Due to write expansion, $|D_i|$ was inflated to 64 for all write requests under the RW-RNLP, as read requests can access any resource.

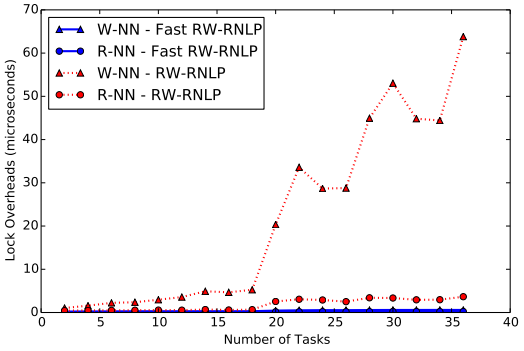

(a) Lock overhead.

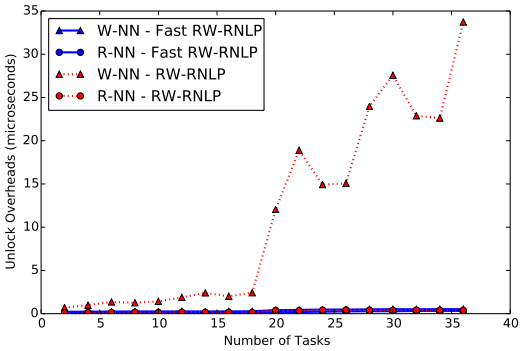

(b) Unlock overhead.

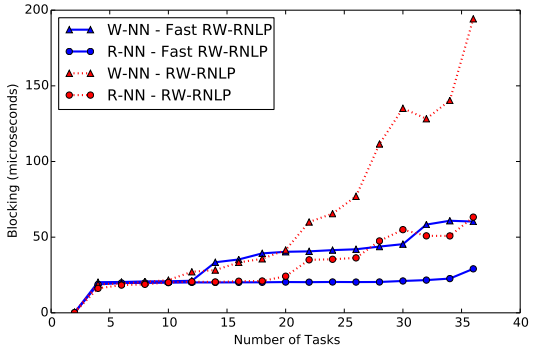

(c) Blocking.

Figure 121: (a) Lock and (b) unlock overheads and (c) blocking for non-nested read and write requests under the RW-RNLP and the fast RW-RNLP. Here, for each request $\mathcal{R}_i$, $L_i = 20\mu$s, $n_r = 64$, and $|D_i| = 1$. Each request was randomly chosen to be a read (as opposed to a write) with probability 0.2 and to be a nested request with probability 0.

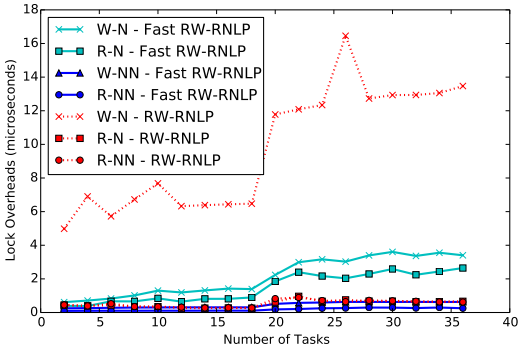

(a) Lock overhead.

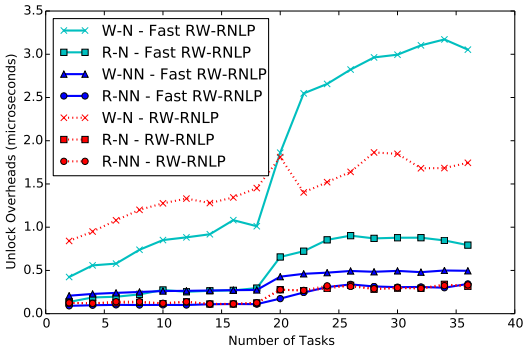

(b) Unlock overhead.

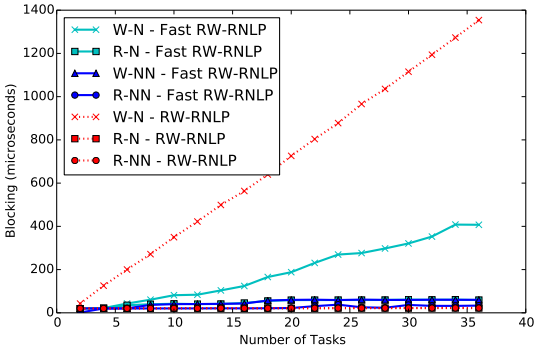

(c) Blocking.

Figure 122: (a) Lock and (b) unlock overheads and (c) blocking for nested and non-nested read and write requests under the RW-RNLP and the fast RW-RNLP. Here, for each request $\mathcal{R}_i$, $L_i = 20\mu$s, $n_r = 64$, $|D_i| = 1$ for non-nested requests, and $|D_i| = 4$ for nested requests. Each request was randomly chosen to be a read (as opposed to a write) with probability 0.2 and to be a nested request with probability 0.2. Due to write expansion, $|D_i|$ was inflated to 64 for all write requests under the RW-RNLP, as read requests can access any resource.

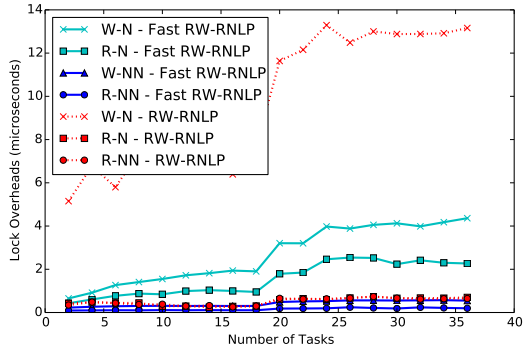

(a) Lock overhead.

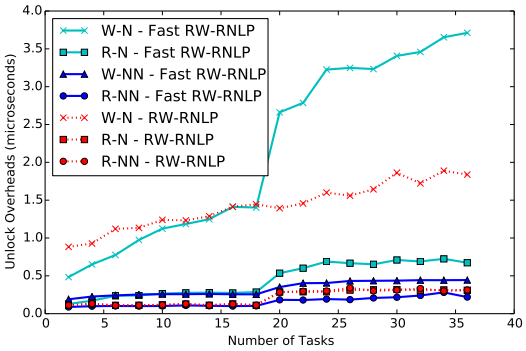

(b) Unlock overhead.

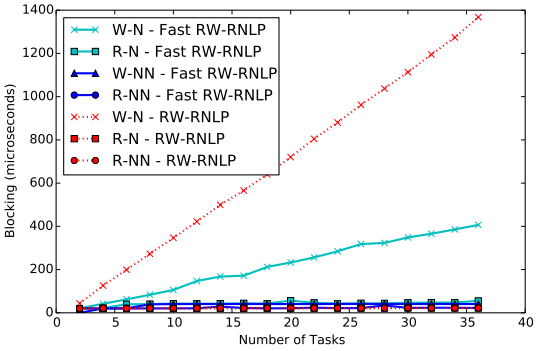

(c) Blocking.

Figure 123: (a) Lock and (b) unlock overheads and (c) blocking for nested and non-nested read and write requests under the RW-RNLP and the fast RW-RNLP. Here, for each request $\mathcal{R}_i$, $L_i = 20\mu$s, $n_r = 64$, $|D_i| = 1$ for non-nested requests, and $|D_i| = 4$ for nested requests. Each request was randomly chosen to be a read (as opposed to a write) with probability 0.2 and to be a nested request with probability 0.5. Due to write expansion, $|D_i|$ was inflated to 64 for all write requests under the RW-RNLP, as read requests can access any resource.

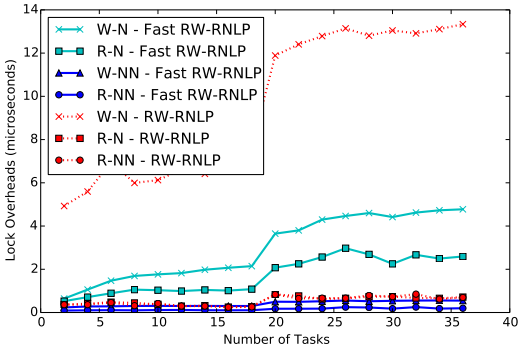

(a) Lock overhead.

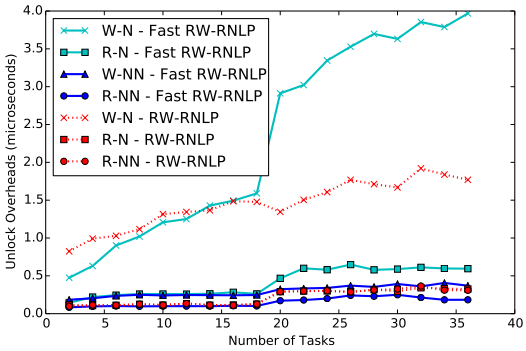

(b) Unlock overhead.

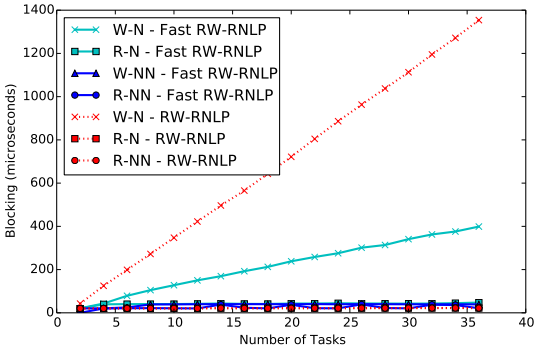

(c) Blocking.

Figure 124: (a) Lock and (b) unlock overheads and (c) blocking for nested and non-nested read and write requests under the RW-RNLP and the fast RW-RNLP. Here, for each request $\mathcal{R}_i$, $L_i = 20\mu$s, $n_r = 64$, $|D_i| = 1$ for non-nested requests, and $|D_i| = 4$ for nested requests. Each request was randomly chosen to be a read (as opposed to a write) with probability 0.2 and to be a nested request with probability 0.8. Due to write expansion, $|D_i|$ was inflated to 64 for all write requests under the RW-RNLP, as read requests can access any resource.

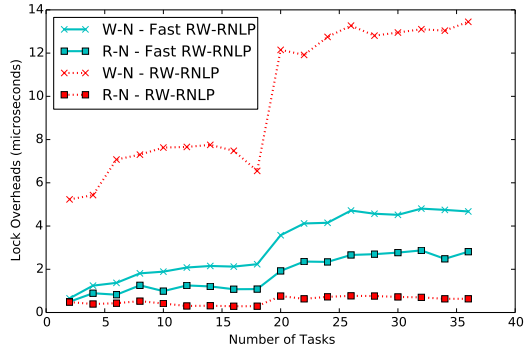

(a) Lock overhead.

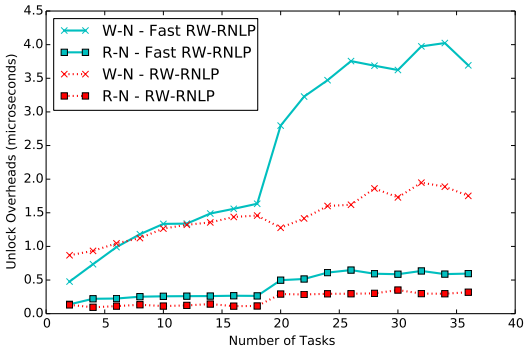

(b) Unlock overhead.

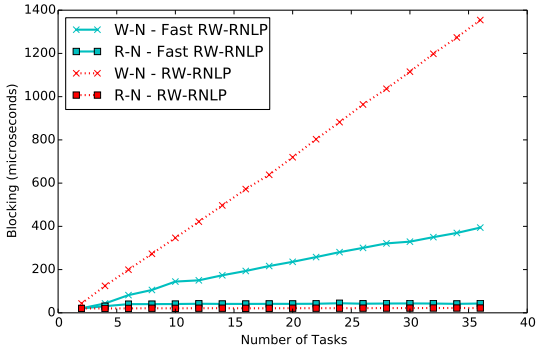

(c) Blocking.

Figure 125: (a) Lock and (b) unlock overheads and (c) blocking for nested read and write requests under the RW-RNLP and the fast RW-RNLP. Here, for each request $\mathcal{R}_i$, $L_i = 20\mu$s, $n_r = 64$, and $|D_i| = 4$. Each request was randomly chosen to be a read (as opposed to a write) with probability 0.2 and to be a nested request with probability 1. Due to write expansion, $|D_i|$ was inflated to 64 for all write requests under the RW-RNLP, as read requests can access any resource.

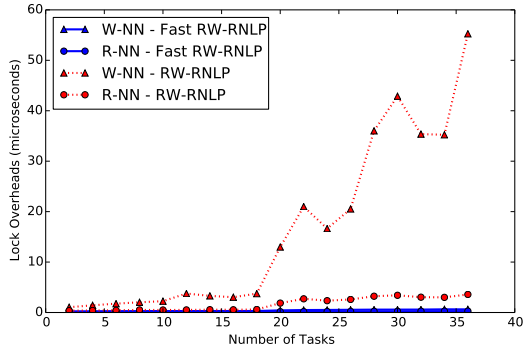

(a) Lock overhead.

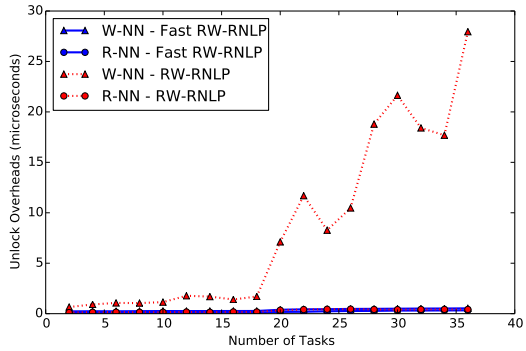

(b) Unlock overhead.

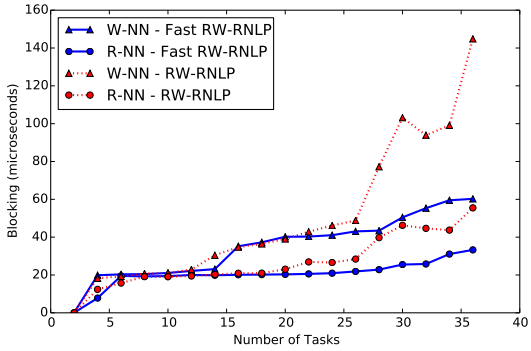

(c) Blocking.

Figure 126: (a) Lock and (b) unlock overheads and (c) blocking for non-nested read and write requests under the RW-RNLP and the fast RW-RNLP. Here, for each request $\mathcal{R}_i$, $L_i = 20\mu$s, $n_r = 64$, and $|D_i| = 1$. Each request was randomly chosen to be a read (as opposed to a write) with probability 0.5 and to be a nested request with probability 0.

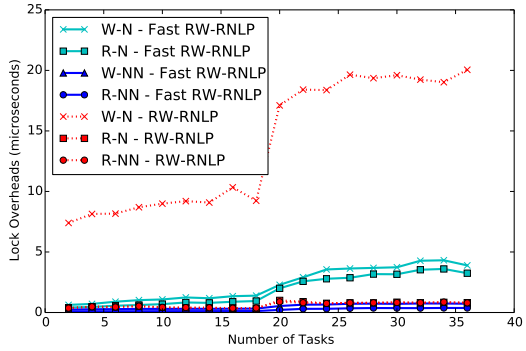

(a) Lock overhead.

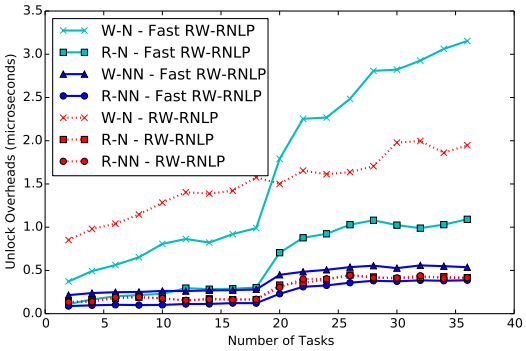

(b) Unlock overhead.

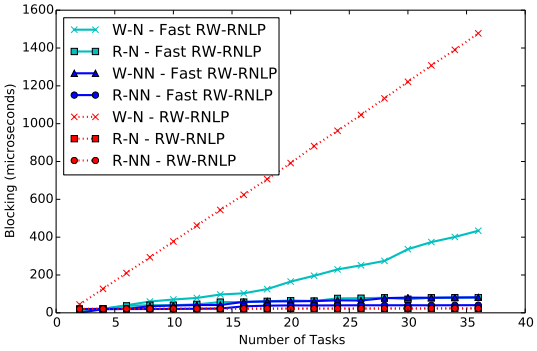

(c) Blocking.

Figure 127: (a) Lock and (b) unlock overheads and (c) blocking for nested and non-nested read and write requests under the RW-RNLP and the fast RW-RNLP. Here, for each request $\mathcal{R}_i$, $L_i = 20\mu$s, $n_r = 64$, $|D_i| = 1$ for non-nested requests, and $|D_i| = 4$ for nested requests. Each request was randomly chosen to be a read (as opposed to a write) with probability 0.5 and to be a nested request with probability 0.2. Due to write expansion, $|D_i|$ was inflated to 64 for all write requests under the RW-RNLP, as read requests can access any resource.

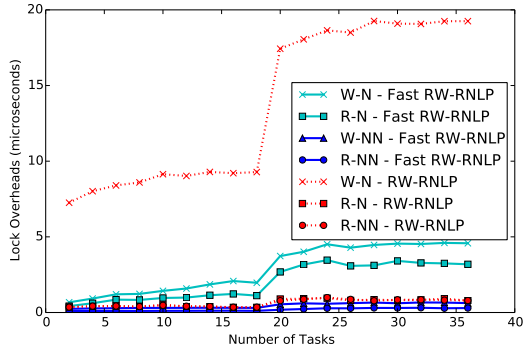

(a) Lock overhead.

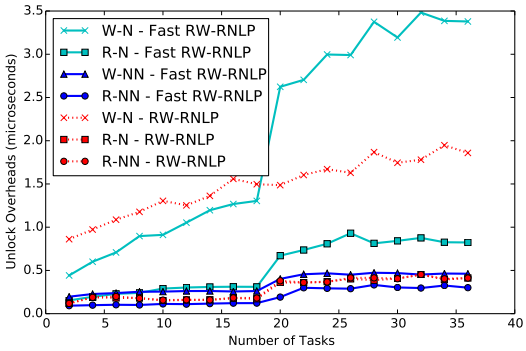

(b) Unlock overhead.

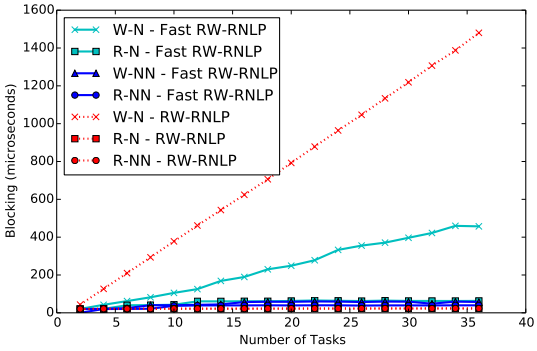

(c) Blocking.

Figure 128: (a) Lock and (b) unlock overheads and (c) blocking for nested and non-nested read and write requests under the RW-RNLP and the fast RW-RNLP. Here, for each request $\mathcal{R}_i$, $L_i = 20\mu$s, $n_r = 64$, $|D_i| = 1$ for non-nested requests, and $|D_i| = 4$ for nested requests. Each request was randomly chosen to be a read (as opposed to a write) with probability 0.5 and to be a nested request with probability 0.5. Due to write expansion, $|D_i|$ was inflated to 64 for all write requests under the RW-RNLP, as read requests can access any resource.

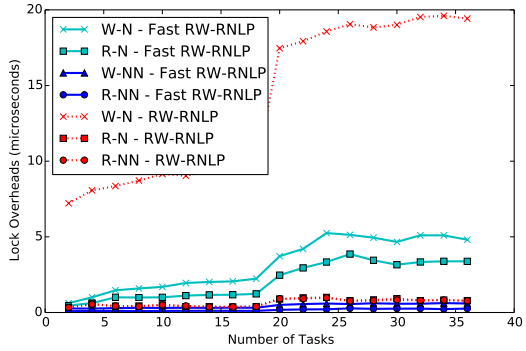

(a) Lock overhead.

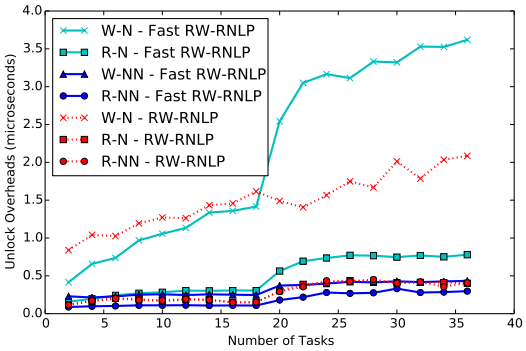

(b) Unlock overhead.

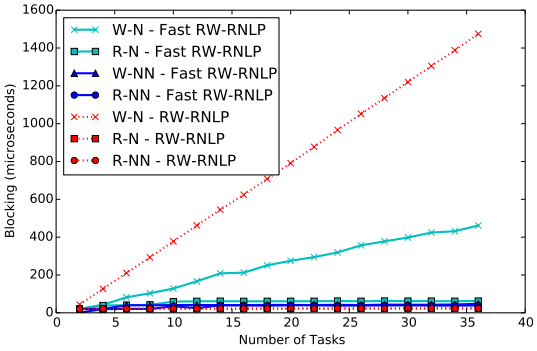

(c) Blocking.

Figure 129: (a) Lock and (b) unlock overheads and (c) blocking for nested and non-nested read and write requests under the RW-RNLP and the fast RW-RNLP. Here, for each request $\mathcal{R}_i$, $L_i = 20\mu$s, $n_r = 64$, $|D_i| = 1$ for non-nested requests, and $|D_i| = 4$ for nested requests. Each request was randomly chosen to be a read (as opposed to a write) with probability 0.5 and to be a nested request with probability 0.8. Due to write expansion, $|D_i|$ was inflated to 64 for all write requests under the RW-RNLP, as read requests can access any resource.

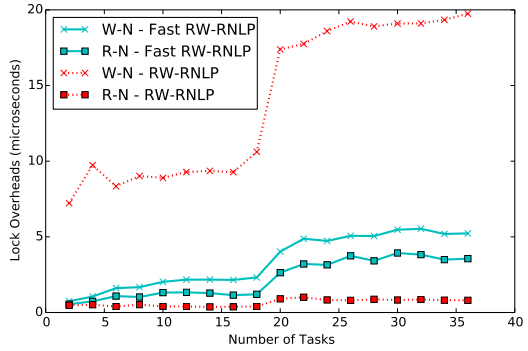

(a) Lock overhead.

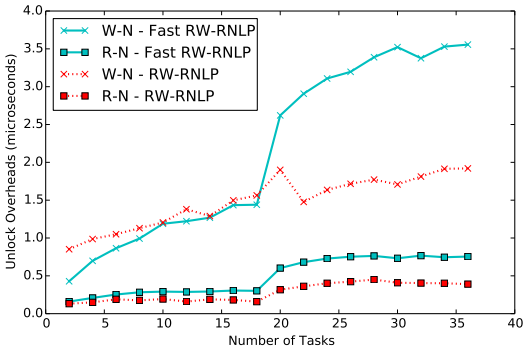

(b) Unlock overhead.

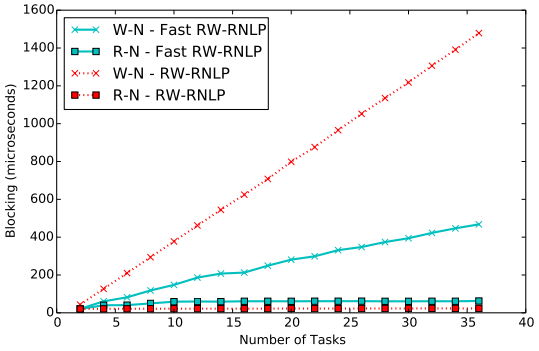

(c) Blocking.

Figure 130: (a) Lock and (b) unlock overheads and (c) blocking for nested read and write requests under the RW-RNLP and the fast RW-RNLP. Here, for each request $\mathcal{R}_i$, $L_i = 20\mu$s, $n_r = 64$, and $|D_i| = 4$. Each request was randomly chosen to be a read (as opposed to a write) with probability 0.5 and to be a nested request with probability 1. Due to write expansion, $|D_i|$ was inflated to 64 for all write requests under the RW-RNLP, as read requests can access any resource.

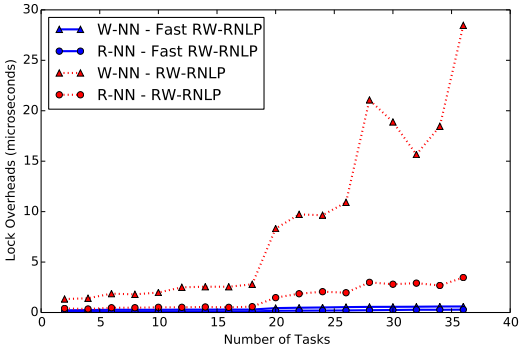

(a) Lock overhead.

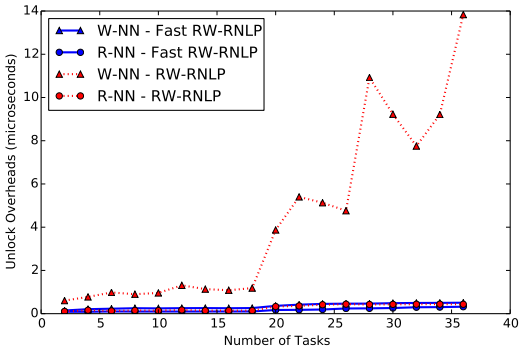

(b) Unlock overhead.

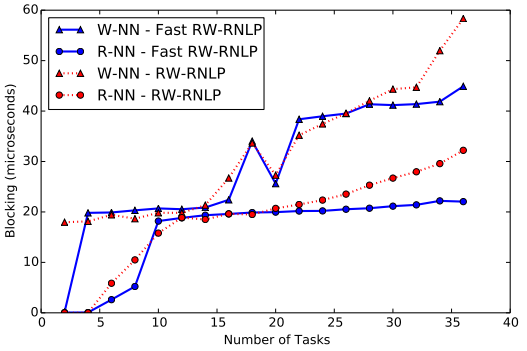

(c) Blocking.

Figure 131: (a) Lock and (b) unlock overheads and (c) blocking for non-nested read and write requests under the RW-RNLP and the fast RW-RNLP. Here, for each request $\mathcal{R}_i$, $L_i = 20\mu$s, $n_r = 64$, and $|D_i| = 1$. Each request was randomly chosen to be a read (as opposed to a write) with probability 0.8 and to be a nested request with probability 0.

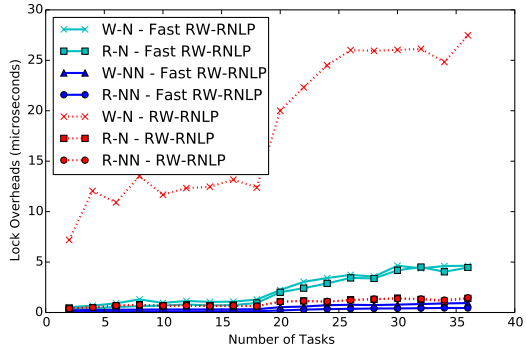

(a) Lock overhead.

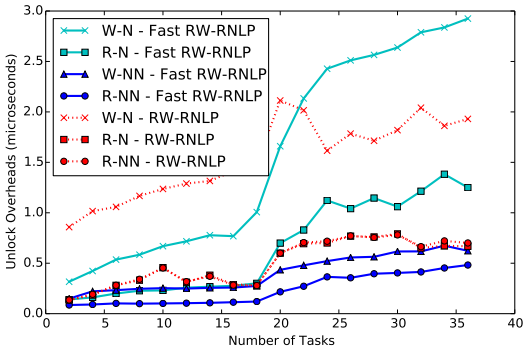

(b) Unlock overhead.

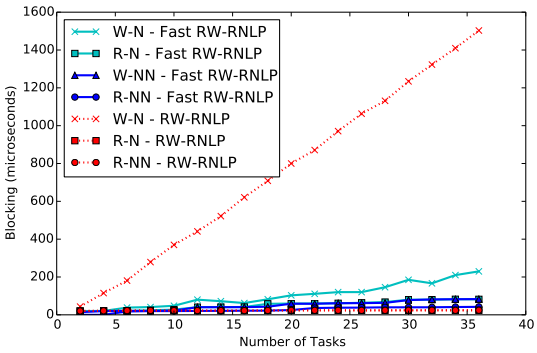

(c) Blocking.

Figure 132: (a) Lock and (b) unlock overheads and (c) blocking for nested and non-nested read and write requests under the RW-RNLP and the fast RW-RNLP. Here, for each request $\mathcal{R}_i$, $L_i = 20\mu$s, $n_r = 64$, $|D_i| = 1$ for non-nested requests, and $|D_i| = 4$ for nested requests. Each request was randomly chosen to be a read (as opposed to a write) with probability 0.8 and to be a nested request with probability 0.2. Due to write expansion, $|D_i|$ was inflated to 64 for all write requests under the RW-RNLP, as read requests can access any resource.

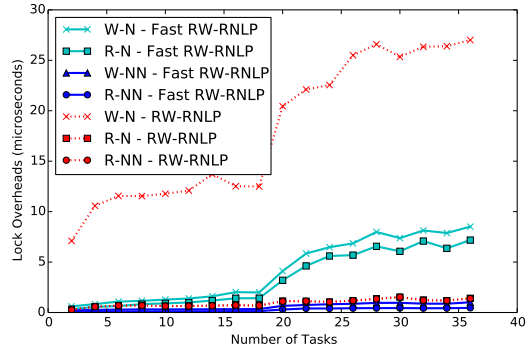

(a) Lock overhead.

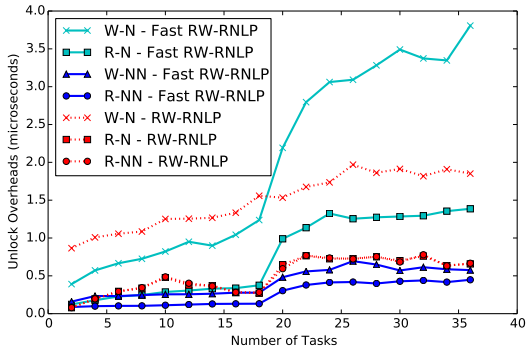

(b) Unlock overhead.

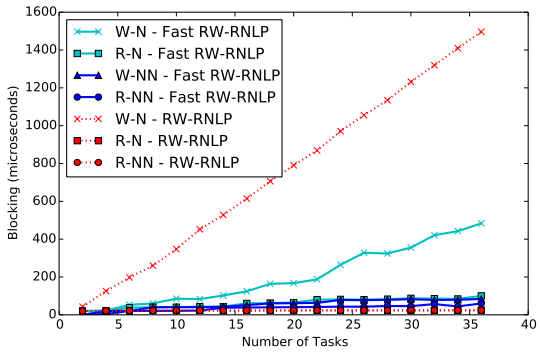

(c) Blocking.

Figure 133: (a) Lock and (b) unlock overheads and (c) blocking for nested and non-nested read and write requests under the RW-RNLP and the fast RW-RNLP. Here, for each request $\mathcal{R}_i$, $L_i = 20\mu$s, $n_r = 64$, $|D_i| = 1$ for non-nested requests, and $|D_i| = 4$ for nested requests. Each request was randomly chosen to be a read (as opposed to a write) with probability 0.8 and to be a nested request with probability 0.5. Due to write expansion, $|D_i|$ was inflated to 64 for all write requests under the RW-RNLP, as read requests can access any resource.

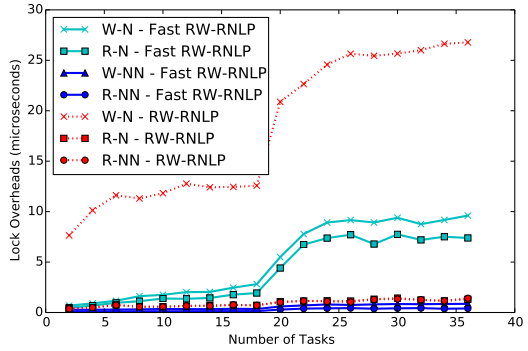

(a) Lock overhead.

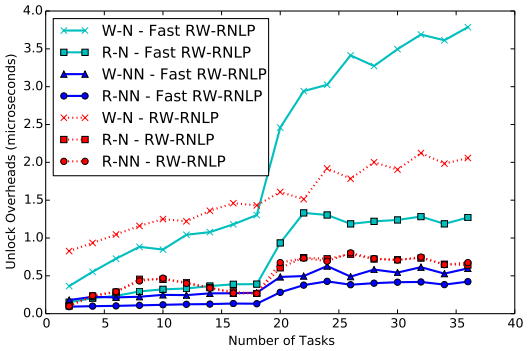

(b) Unlock overhead.

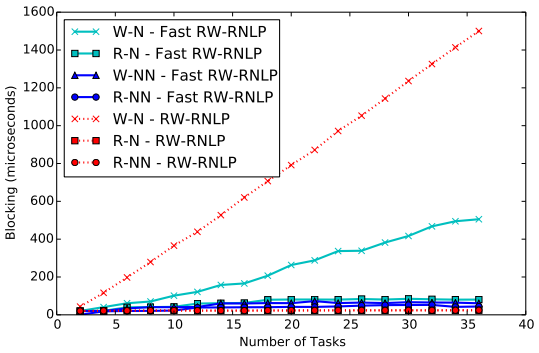

(c) Blocking.

Figure 134: (a) Lock and (b) unlock overheads and (c) blocking for nested and non-nested read and write requests under the RW-RNLP and the fast RW-RNLP. Here, for each request $\mathcal{R}_i$, $L_i = 20\mu$s, $n_r = 64$, $|D_i| = 1$ for non-nested requests, and $|D_i| = 4$ for nested requests. Each request was randomly chosen to be a read (as opposed to a write) with probability 0.8 and to be a nested request with probability 0.8. Due to write expansion, $|D_i|$ was inflated to 64 for all write requests under the RW-RNLP, as read requests can access any resource.

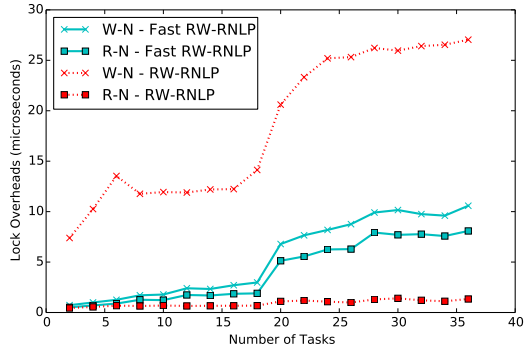

(a) Lock overhead.

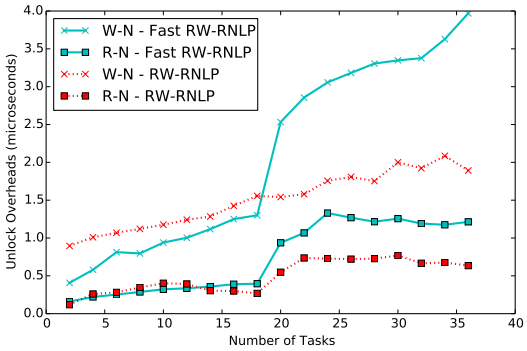

(b) Unlock overhead.

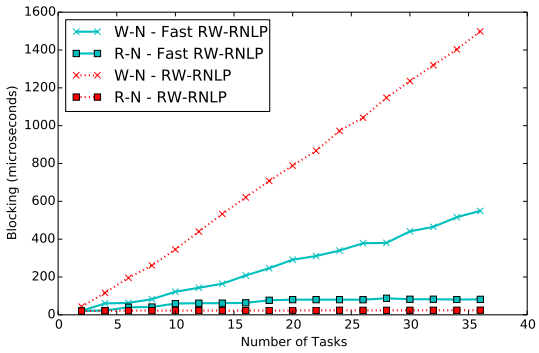

(c) Blocking.

Figure 135: (a) Lock and (b) unlock overheads and (c) blocking for nested read and write requests under the RW-RNLP and the fast RW-RNLP. Here, for each request $\mathcal{R}_i$, $L_i = 20\mu$s, $n_r = 64$, and $|D_i| = 4$. Each request was randomly chosen to be a read (as opposed to a write) with probability 0.8 and to be a nested request with probability 1. Due to write expansion, $|D_i|$ was inflated to 64 for all write requests under the RW-RNLP, as read requests can access any resource.

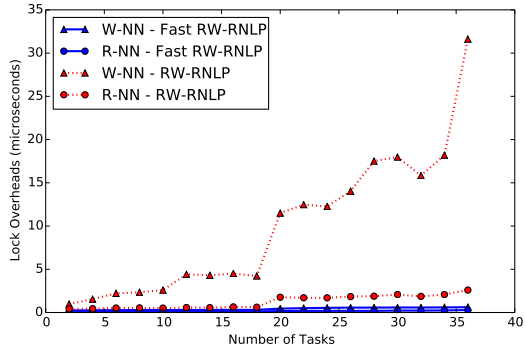

(a) Lock overhead.

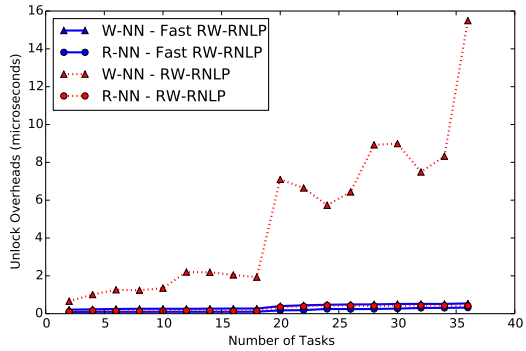

(b) Unlock overhead.

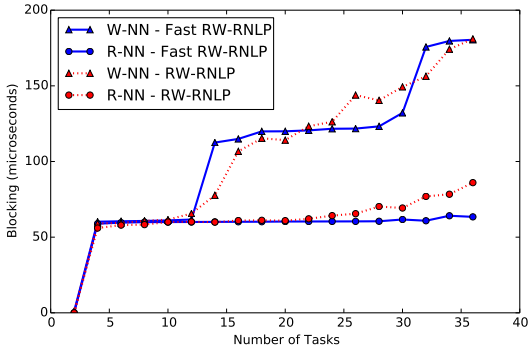

(c) Blocking.

Figure 136: (a) Lock and (b) unlock overheads and (c) blocking for non-nested read and write requests under the RW-RNLP and the fast RW-RNLP. Here, for each request $\mathcal{R}_i$, $L_i = 60\mu$s, $n_r = 64$, and $|D_i| = 1$. Each request was randomly chosen to be a read (as opposed to a write) with probability 0.2 and to be a nested request with probability 0.

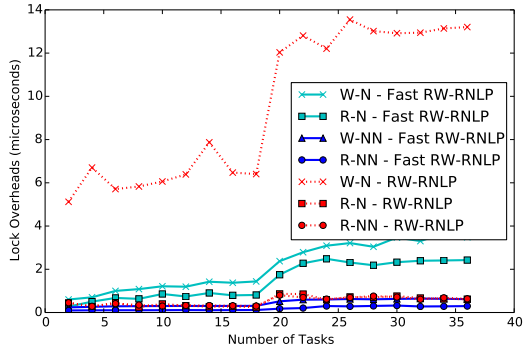

(a) Lock overhead.

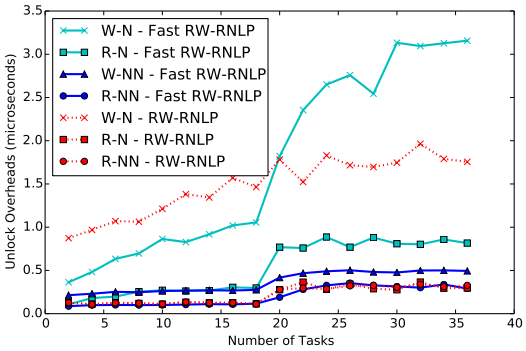

(b) Unlock overhead.

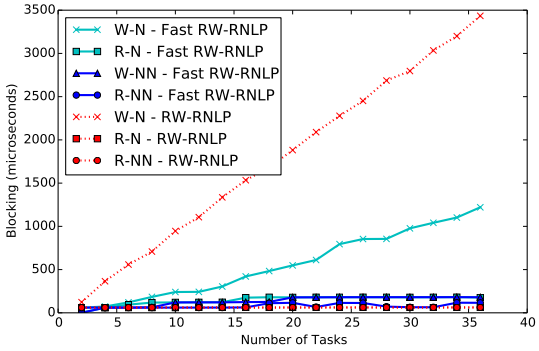

(c) Blocking.

Figure 137: (a) Lock and (b) unlock overheads and (c) blocking for nested and non-nested read and write requests under the RW-RNLP and the fast RW-RNLP. Here, for each request $\mathcal{R}_i$, $L_i = 60\mu$s, $n_r = 64$, $|D_i| = 1$ for non-nested requests, and $|D_i| = 4$ for nested requests. Each request was randomly chosen to be a read (as opposed to a write) with probability 0.2 and to be a nested request with probability 0.2. Due to write expansion, $|D_i|$ was inflated to 64 for all write requests under the RW-RNLP, as read requests can access any resource.

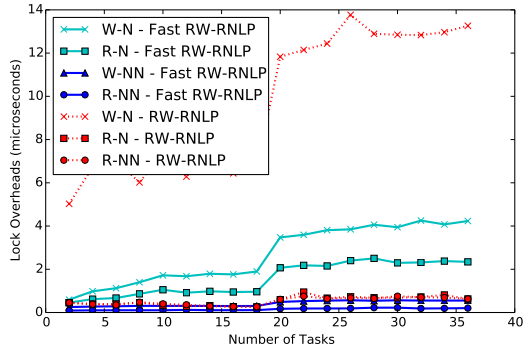

(a) Lock overhead.

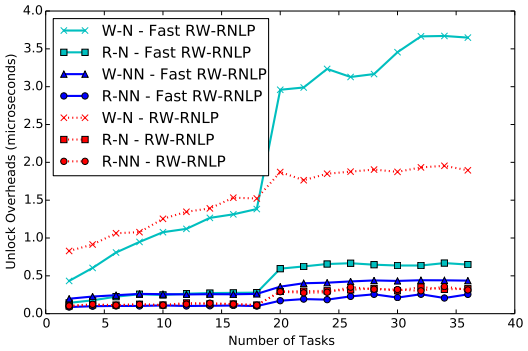

(b) Unlock overhead.

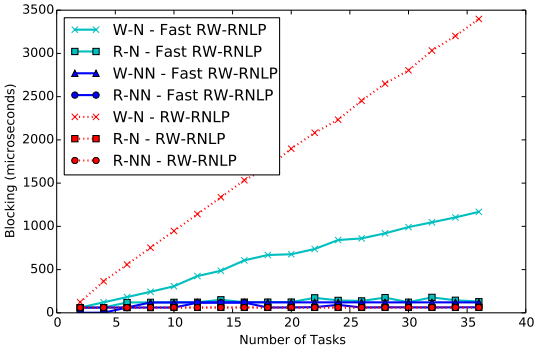

(c) Blocking.

Figure 138: (a) Lock and (b) unlock overheads and (c) blocking for nested and non-nested read and write requests under the RW-RNLP and the fast RW-RNLP. Here, for each request $\mathcal{R}_i$, $L_i = 60\mu$s, $n_r = 64$, $|D_i| = 1$ for non-nested requests, and $|D_i| = 4$ for nested requests. Each request was randomly chosen to be a read (as opposed to a write) with probability 0.2 and to be a nested request with probability 0.5. Due to write expansion, $|D_i|$ was inflated to 64 for all write requests under the RW-RNLP, as read requests can access any resource.

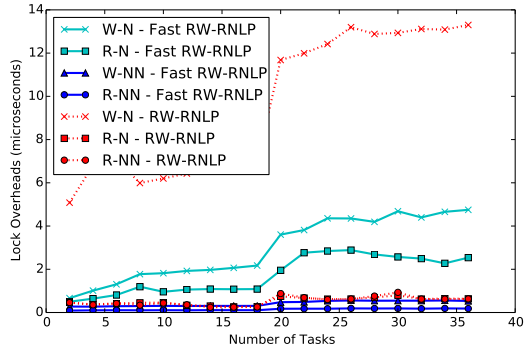

(a) Lock overhead.

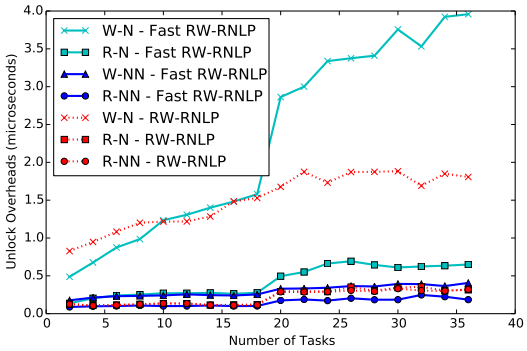

(b) Unlock overhead.

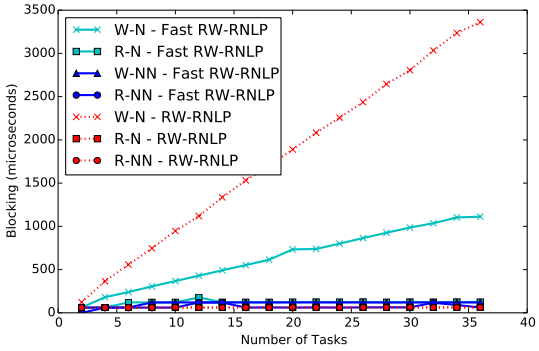

(c) Blocking.

Figure 139: (a) Lock and (b) unlock overheads and (c) blocking for nested and non-nested read and write requests under the RW-RNLP and the fast RW-RNLP. Here, for each request $\mathcal{R}_i$, $L_i = 60\mu$s, $n_r = 64$, $|D_i| = 1$ for non-nested requests, and $|D_i| = 4$ for nested requests. Each request was randomly chosen to be a read (as opposed to a write) with probability 0.2 and to be a nested request with probability 0.8. Due to write expansion, $|D_i|$ was inflated to 64 for all write requests under the RW-RNLP, as read requests can access any resource.

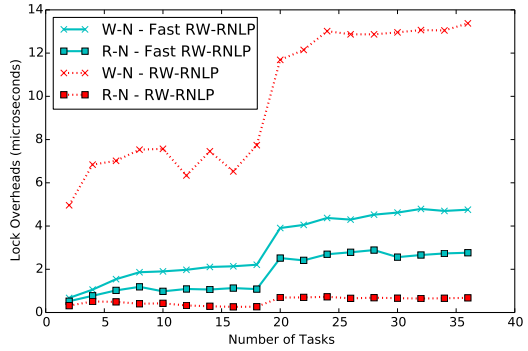

(a) Lock overhead.

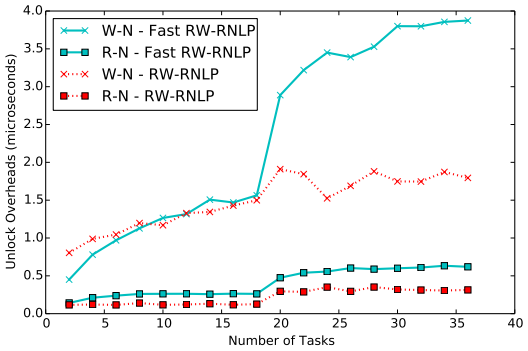

(b) Unlock overhead.

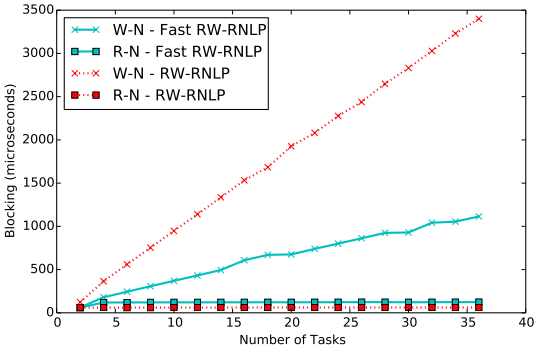

(c) Blocking.

Figure 140: (a) Lock and (b) unlock overheads and (c) blocking for nested read and write requests under the RW-RNLP and the fast RW-RNLP. Here, for each request $\mathcal{R}_i$, $L_i = 60\mu$s, $n_r = 64$, and $|D_i| = 4$. Each request was randomly chosen to be a read (as opposed to a write) with probability 0.2 and to be a nested request with probability 1. Due to write expansion, $|D_i|$ was inflated to 64 for all write requests under the RW-RNLP, as read requests can access any resource.

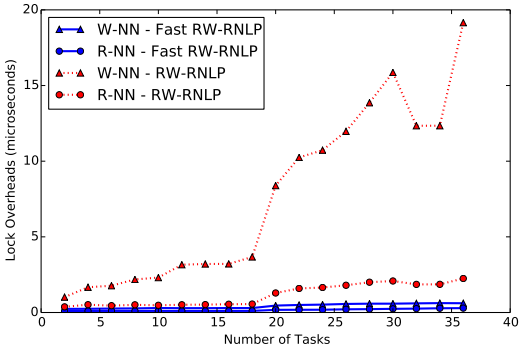

(a) Lock overhead.

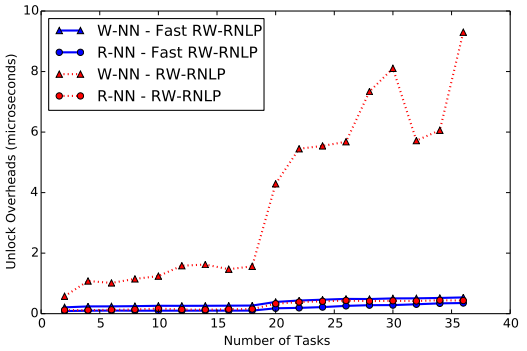

(b) Unlock overhead.

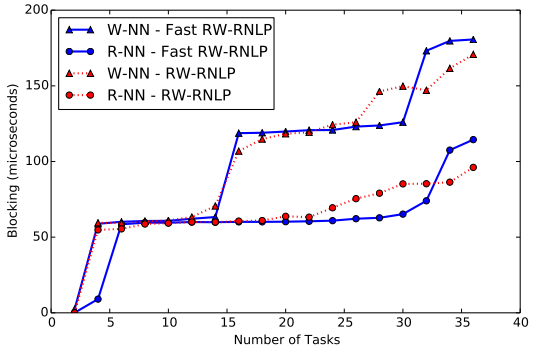

(c) Blocking.

Figure 141: (a) Lock and (b) unlock overheads and (c) blocking for non-nested read and write requests under the RW-RNLP and the fast RW-RNLP. Here, for each request $\mathcal{R}_i$, $L_i = 60\mu$s, $n_r = 64$, and $|D_i| = 1$. Each request was randomly chosen to be a read (as opposed to a write) with probability 0.5 and to be a nested request with probability 0.

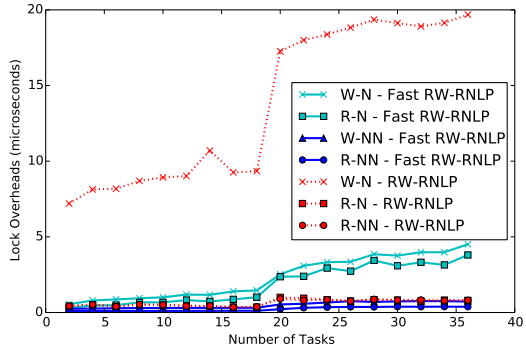

(a) Lock overhead.

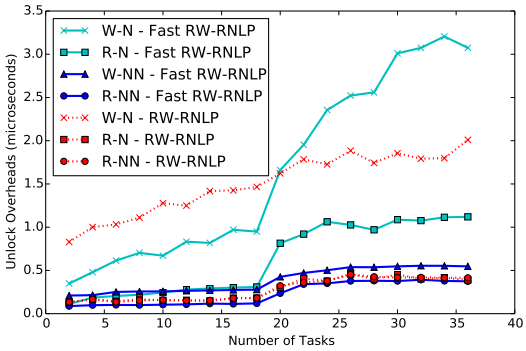

(b) Unlock overhead.

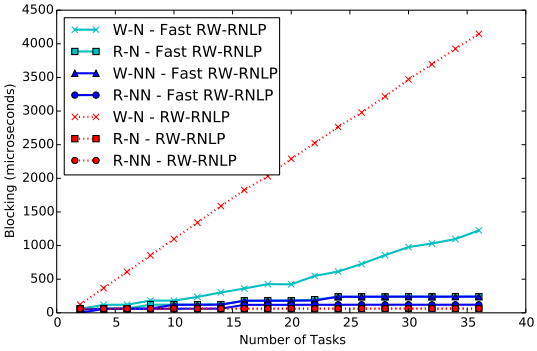

(c) Blocking.

Figure 142: (a) Lock and (b) unlock overheads and (c) blocking for nested and non-nested read and write requests under the RW-RNLP and the fast RW-RNLP. Here, for each request $\mathcal{R}_i$, $L_i = 60\mu$s, $n_r = 64$, $|D_i| = 1$ for non-nested requests, and $|D_i| = 4$ for nested requests. Each request was randomly chosen to be a read (as opposed to a write) with probability 0.5 and to be a nested request with probability 0.2. Due to write expansion, $|D_i|$ was inflated to 64 for all write requests under the RW-RNLP, as read requests can access any resource.

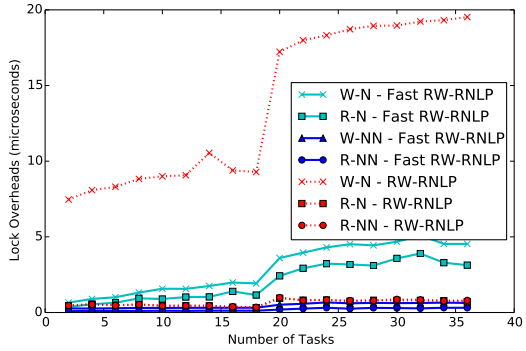

(a) Lock overhead.

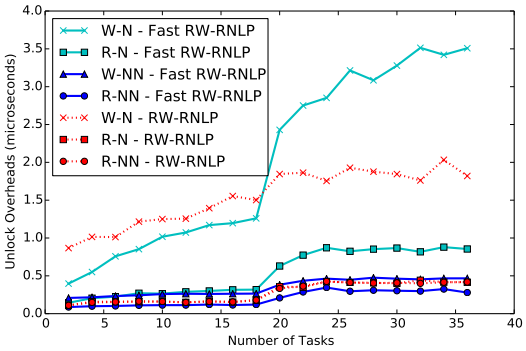

(b) Unlock overhead.

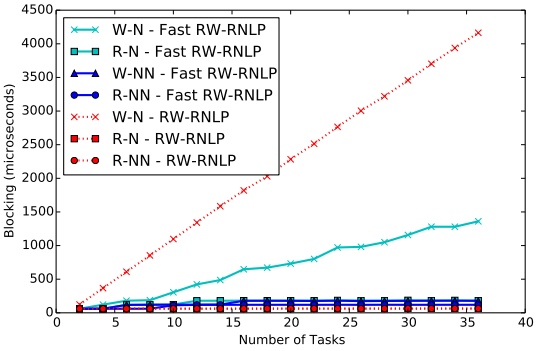

(c) Blocking.

Figure 143: (a) Lock and (b) unlock overheads and (c) blocking for nested and non-nested read and write requests under the RW-RNLP and the fast RW-RNLP. Here, for each request $\mathcal{R}_i$, $L_i = 60\mu$s, $n_r = 64$, $|D_i| = 1$ for non-nested requests, and $|D_i| = 4$ for nested requests. Each request was randomly chosen to be a read (as opposed to a write) with probability 0.5 and to be a nested request with probability 0.5. Due to write expansion, $|D_i|$ was inflated to 64 for all write requests under the RW-RNLP, as read requests can access any resource.

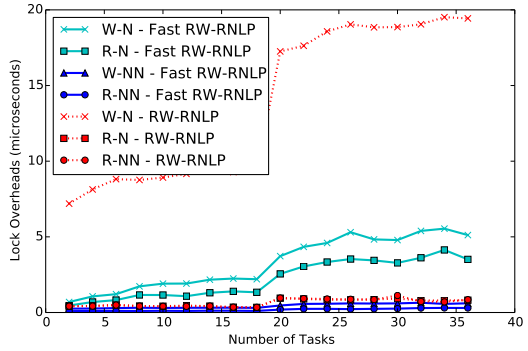

(a) Lock overhead.

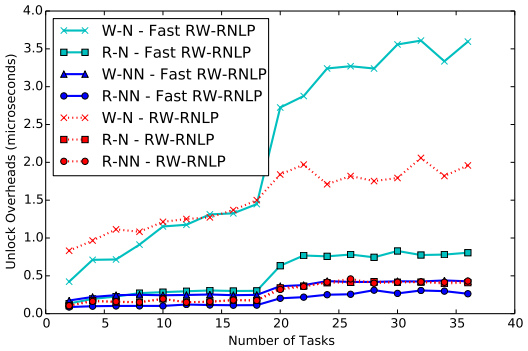

(b) Unlock overhead.

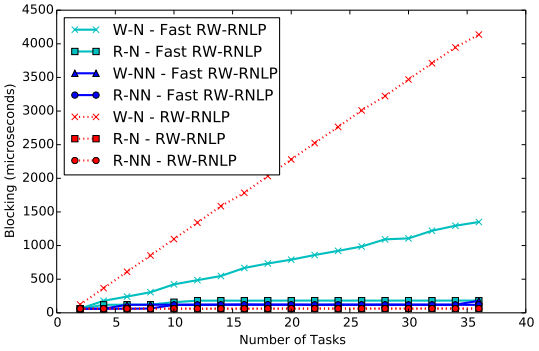

(c) Blocking.

Figure 144: (a) Lock and (b) unlock overheads and (c) blocking for nested and non-nested read and write requests under the RW-RNLP and the fast RW-RNLP. Here, for each request $\mathcal{R}_i$, $L_i = 60\mu$s, $n_r = 64$, $|D_i| = 1$ for non-nested requests, and $|D_i| = 4$ for nested requests. Each request was randomly chosen to be a read (as opposed to a write) with probability 0.5 and to be a nested request with probability 0.8. Due to write expansion, $|D_i|$ was inflated to 64 for all write requests under the RW-RNLP, as read requests can access any resource.

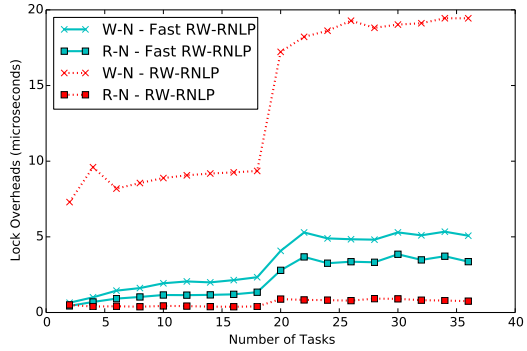

(a) Lock overhead.

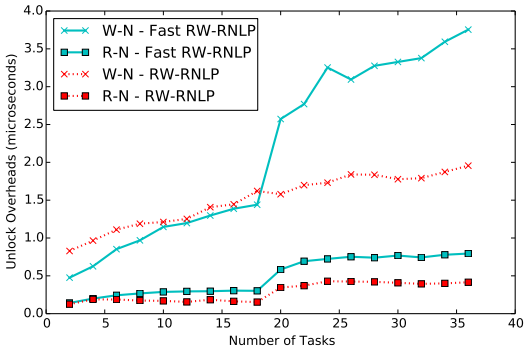

(b) Unlock overhead.

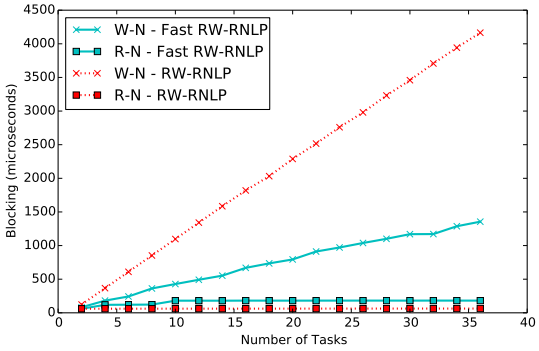

(c) Blocking.

Figure 145: (a) Lock and (b) unlock overheads and (c) blocking for nested read and write requests under the RW-RNLP and the fast RW-RNLP. Here, for each request $\mathcal{R}_i$, $L_i = 60\mu$s, $n_r = 64$, and $|D_i| = 4$. Each request was randomly chosen to be a read (as opposed to a write) with probability 0.5 and to be a nested request with probability 1. Due to write expansion, $|D_i|$ was inflated to 64 for all write requests under the RW-RNLP, as read requests can access any resource.

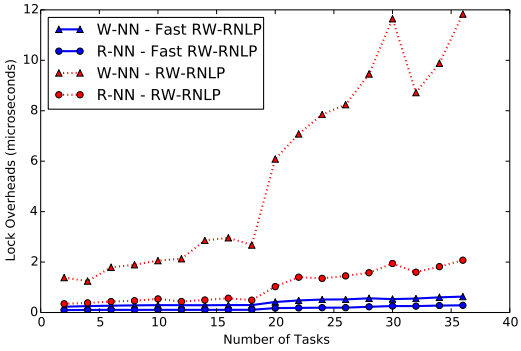

(a) Lock overhead.

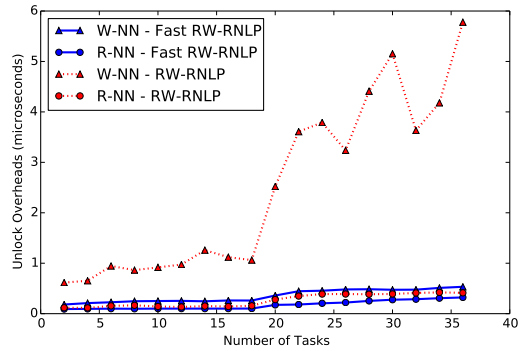

(b) Unlock overhead.

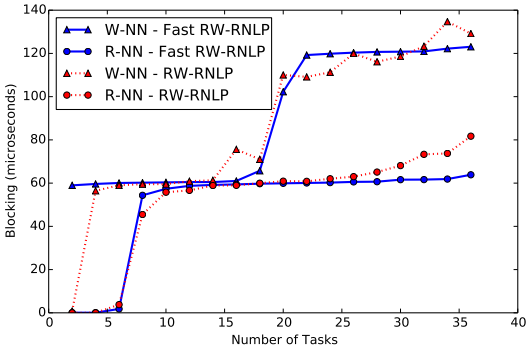

(c) Blocking.

Figure 146: (a) Lock and (b) unlock overheads and (c) blocking for non-nested read and write requests under the RW-RNLP and the fast RW-RNLP. Here, for each request $\mathcal{R}_i$, $L_i = 60\mu$s, $n_r = 64$, and $|D_i| = 1$. Each request was randomly chosen to be a read (as opposed to a write) with probability 0.8 and to be a nested request with probability 0.

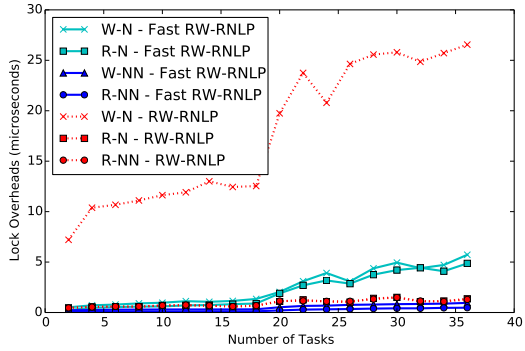

(a) Lock overhead.

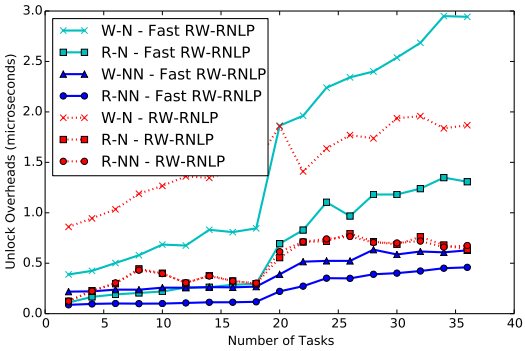

(b) Unlock overhead.

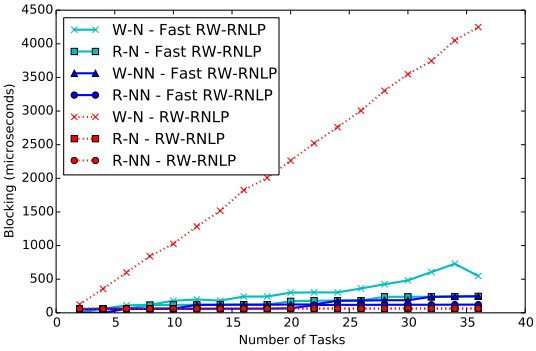

(c) Blocking.

Figure 147: (a) Lock and (b) unlock overheads and (c) blocking for nested and non-nested read and write requests under the RW-RNLP and the fast RW-RNLP. Here, for each request $\mathcal{R}_i$, $L_i = 60\mu$s, $n_r = 64$, $|D_i| = 1$ for non-nested requests, and $|D_i| = 4$ for nested requests. Each request was randomly chosen to be a read (as opposed to a write) with probability 0.8 and to be a nested request with probability 0.2. Due to write expansion, $|D_i|$ was inflated to 64 for all write requests under the RW-RNLP, as read requests can access any resource.

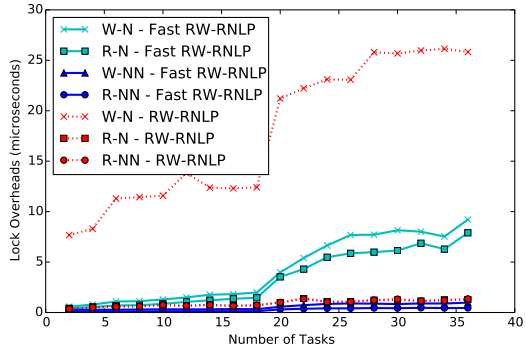

(a) Lock overhead.

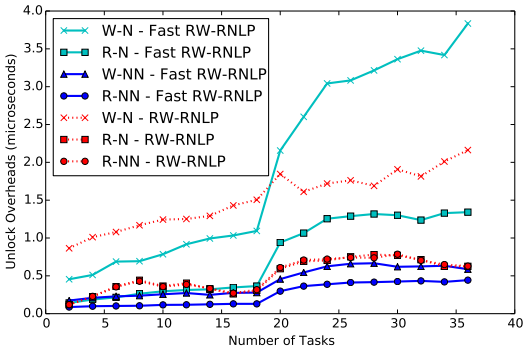

(b) Unlock overhead.

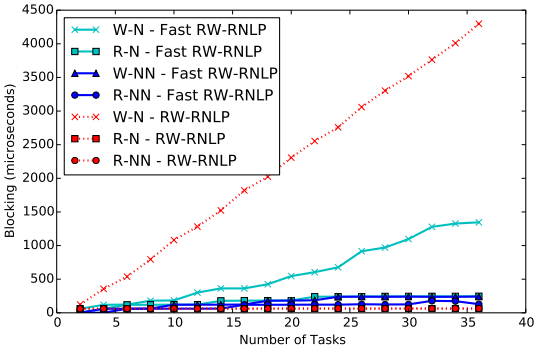

(c) Blocking.

Figure 148: (a) Lock and (b) unlock overheads and (c) blocking for nested and non-nested read and write requests under the RW-RNLP and the fast RW-RNLP. Here, for each request $\mathcal{R}_i$, $L_i = 60\mu$s, $n_r = 64$, $|D_i| = 1$ for non-nested requests, and $|D_i| = 4$ for nested requests. Each request was randomly chosen to be a read (as opposed to a write) with probability 0.8 and to be a nested request with probability 0.5. Due to write expansion, $|D_i|$ was inflated to 64 for all write requests under the RW-RNLP, as read requests can access any resource.

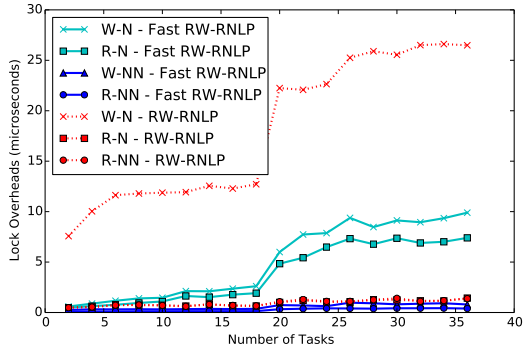

(a) Lock overhead.

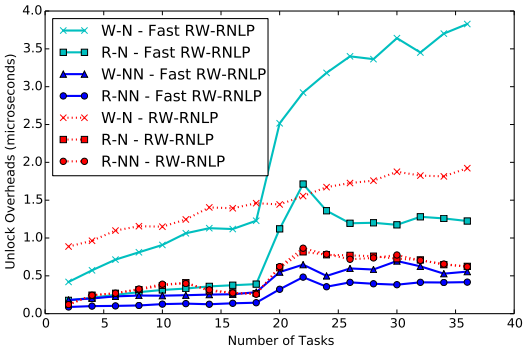

(b) Unlock overhead.

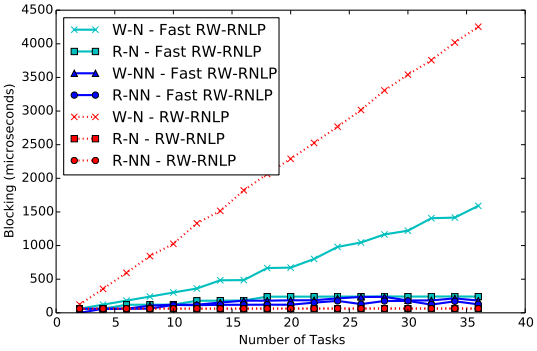

(c) Blocking.

Figure 149: (a) Lock and (b) unlock overheads and (c) blocking for nested and non-nested read and write requests under the RW-RNLP and the fast RW-RNLP. Here, for each request $\mathcal{R}_i$, $L_i = 60\mu$s, $n_r = 64$, $|D_i| = 1$ for non-nested requests, and $|D_i| = 4$ for nested requests. Each request was randomly chosen to be a read (as opposed to a write) with probability 0.8 and to be a nested request with probability 0.8. Due to write expansion, $|D_i|$ was inflated to 64 for all write requests under the RW-RNLP, as read requests can access any resource.

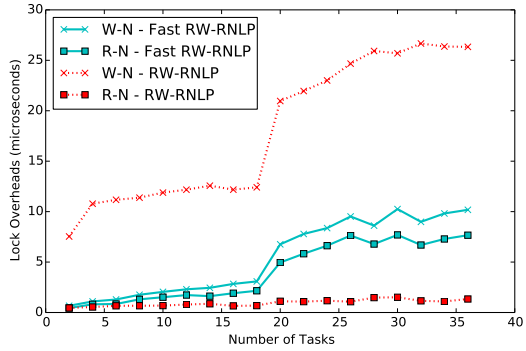

(a) Lock overhead.

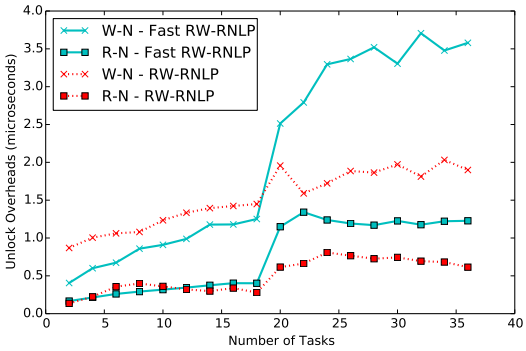

(b) Unlock overhead.

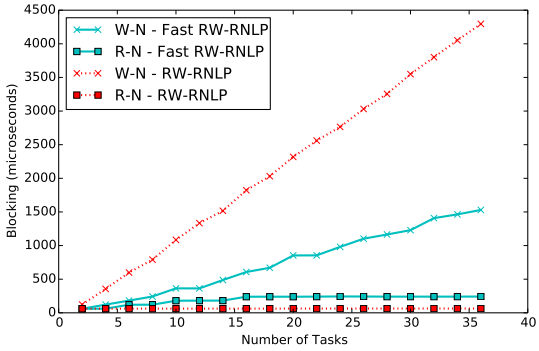

(c) Blocking.

Figure 150: (a) Lock and (b) unlock overheads and (c) blocking for nested read and write requests under the RW-RNLP and the fast RW-RNLP. Here, for each request $\mathcal{R}_i$, $L_i = 60\mu$s, $n_r = 64$, and $|D_i| = 4$. Each request was randomly chosen to be a read (as opposed to a write) with probability 0.8 and to be a nested request with probability 1. Due to write expansion, $|D_i|$ was inflated to 64 for all write requests under the RW-RNLP, as read requests can access any resource.

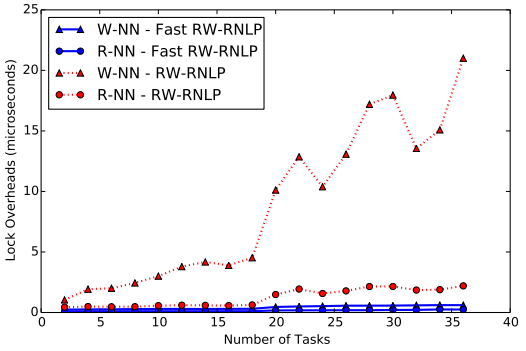

(a) Lock overhead.

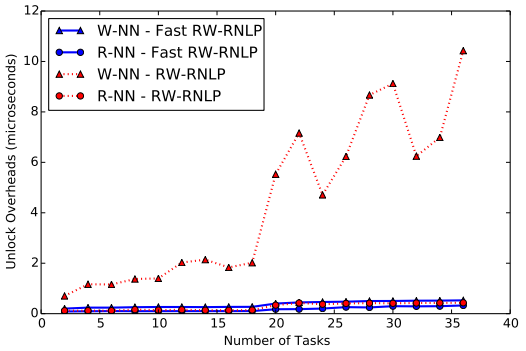

(b) Unlock overhead.

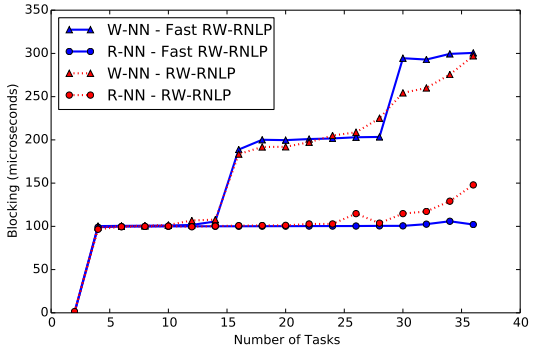

(c) Blocking.

Figure 151: (a) Lock and (b) unlock overheads and (c) blocking for non-nested read and write requests under the RW-RNLP and the fast RW-RNLP. Here, for each request $\mathcal{R}_i$, $L_i = 100\mu$s, $n_r = 64$, and $|D_i| = 1$. Each request was randomly chosen to be a read (as opposed to a write) with probability 0.2 and to be a nested request with probability 0.

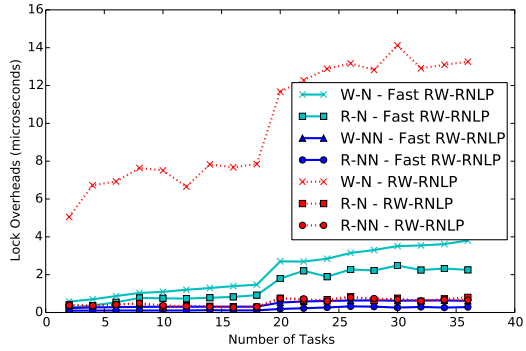

(a) Lock overhead.

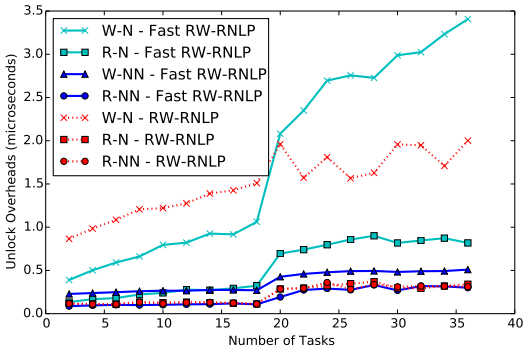

(b) Unlock overhead.

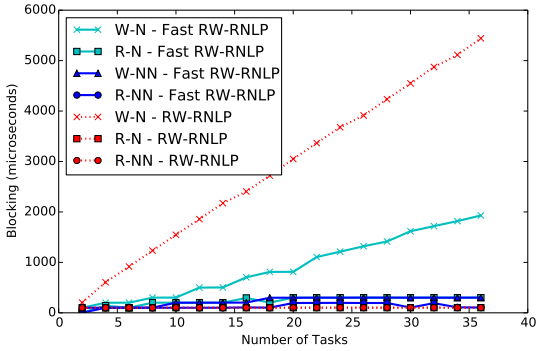

(c) Blocking.

Figure 152: (a) Lock and (b) unlock overheads and (c) blocking for nested and non-nested read and write requests under the RW-RNLP and the fast RW-RNLP. Here, for each request $\mathcal{R}_i$, $L_i = 100\mu$s, $n_r = 64$, $|D_i| = 1$ for non-nested requests, and $|D_i| = 4$ for nested requests. Each request was randomly chosen to be a read (as opposed to a write) with probability 0.2 and to be a nested request with probability 0.2. Due to write expansion, $|D_i|$ was inflated to 64 for all write requests under the RW-RNLP, as read requests can access any resource.

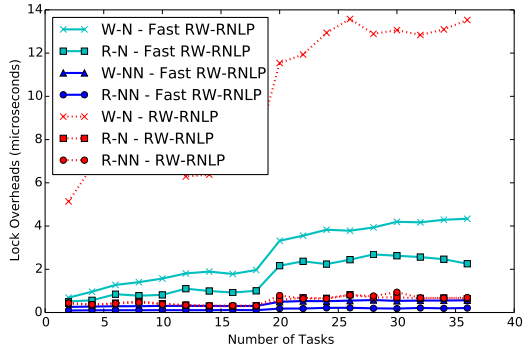

(a) Lock overhead.

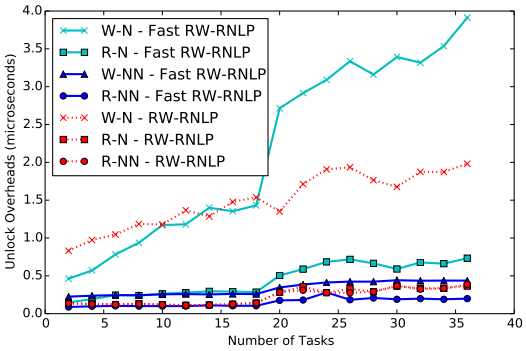

(b) Unlock overhead.

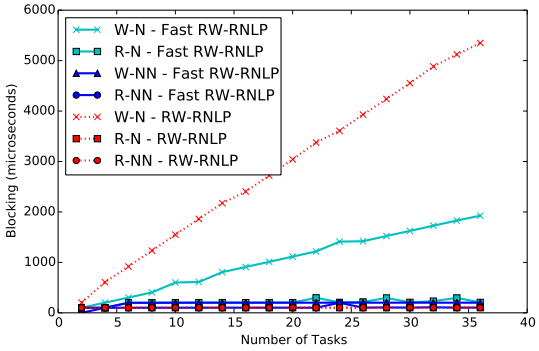

(c) Blocking.

Figure 153: (a) Lock and (b) unlock overheads and (c) blocking for nested and non-nested read and write requests under the RW-RNLP and the fast RW-RNLP. Here, for each request $\mathcal{R}_i$, $L_i = 100\mu$s, $n_r = 64$, $|D_i| = 1$ for non-nested requests, and $|D_i| = 4$ for nested requests. Each request was randomly chosen to be a read (as opposed to a write) with probability 0.2 and to be a nested request with probability 0.5. Due to write expansion, $|D_i|$ was inflated to 64 for all write requests under the RW-RNLP, as read requests can access any resource.

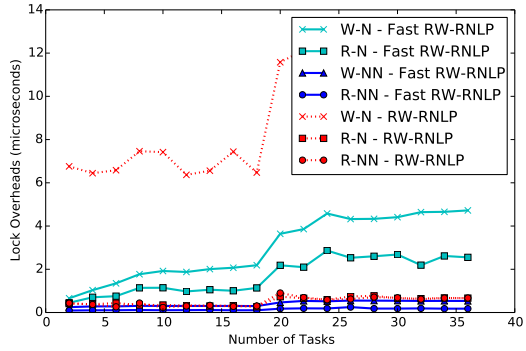

(a) Lock overhead.

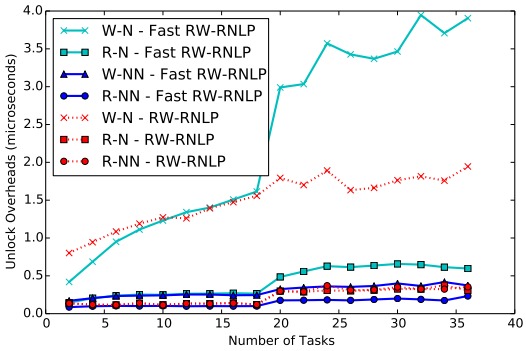

(b) Unlock overhead.

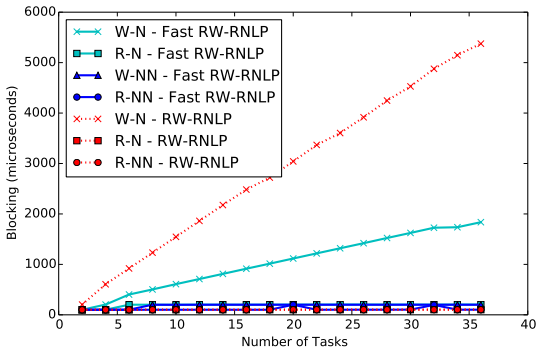

(c) Blocking.

Figure 154: (a) Lock and (b) unlock overheads and (c) blocking for nested and non-nested read and write requests under the RW-RNLP and the fast RW-RNLP. Here, for each request $\mathcal{R}_i$, $L_i = 100\mu$s, $n_r = 64$, $|D_i| = 1$ for non-nested requests, and $|D_i| = 4$ for nested requests. Each request was randomly chosen to be a read (as opposed to a write) with probability 0.2 and to be a nested request with probability 0.8. Due to write expansion, $|D_i|$ was inflated to 64 for all write requests under the RW-RNLP, as read requests can access any resource.

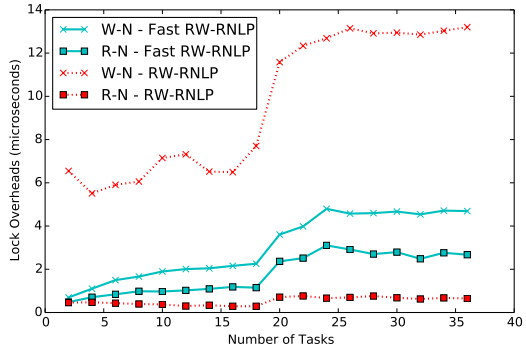

(a) Lock overhead.

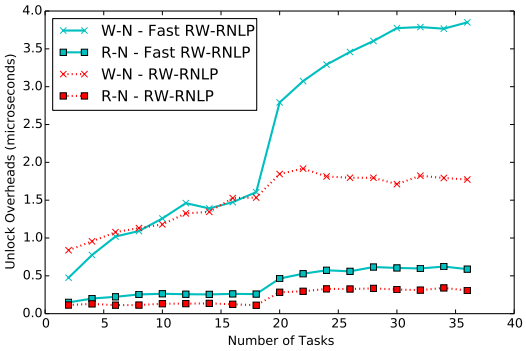

(b) Unlock overhead.

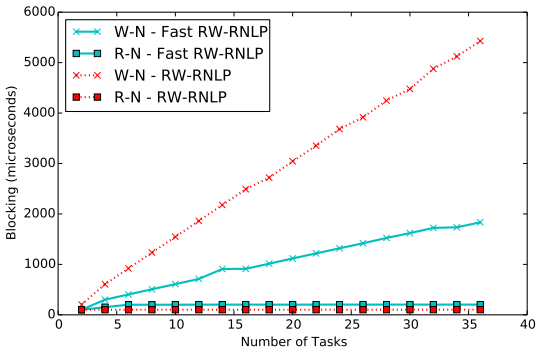

(c) Blocking.

Figure 155: (a) Lock and (b) unlock overheads and (c) blocking for nested read and write requests under the RW-RNLP and the fast RW-RNLP. Here, for each request $\mathcal{R}_i$, $L_i = 100\mu$s, $n_r = 64$, and $|D_i| = 4$. Each request was randomly chosen to be a read (as opposed to a write) with probability 0.2 and to be a nested request with probability 1. Due to write expansion, $|D_i|$ was inflated to 64 for all write requests under the RW-RNLP, as read requests can access any resource.

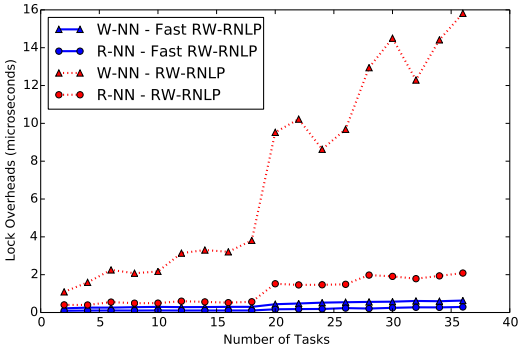

(a) Lock overhead.

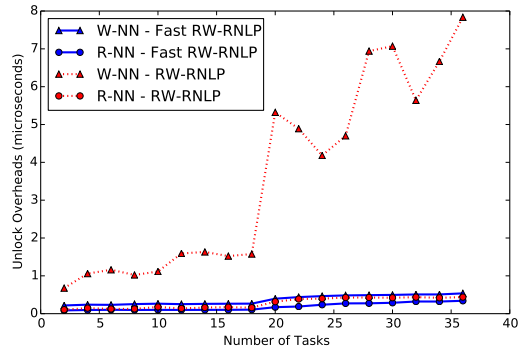

(b) Unlock overhead.

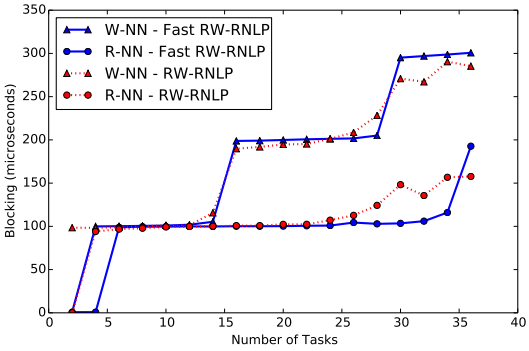

(c) Blocking.

Figure 156: (a) Lock and (b) unlock overheads and (c) blocking for non-nested read and write requests under the RW-RNLP and the fast RW-RNLP. Here, for each request $\mathcal{R}_i$, $L_i = 100\mu$s, $n_r = 64$, and $|D_i| = 1$. Each request was randomly chosen to be a read (as opposed to a write) with probability 0.5 and to be a nested request with probability 0.

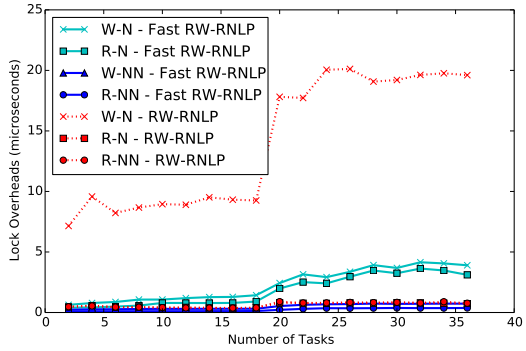

(a) Lock overhead.

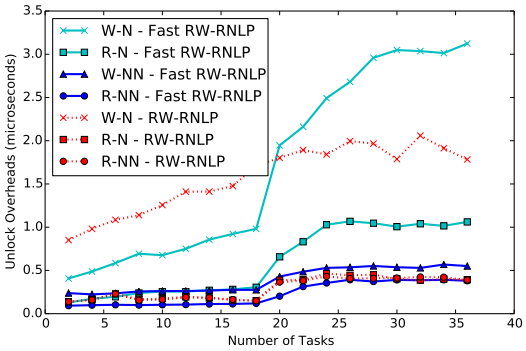

(b) Unlock overhead.

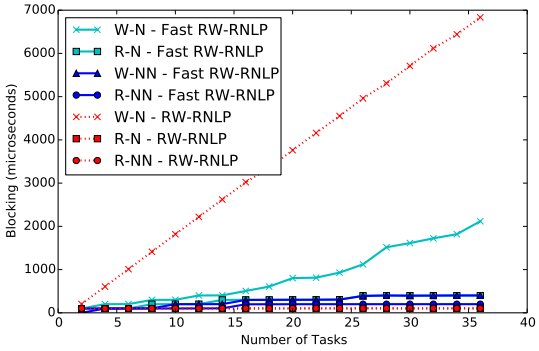

(c) Blocking.

Figure 157: (a) Lock and (b) unlock overheads and (c) blocking for nested and non-nested read and write requests under the RW-RNLP and the fast RW-RNLP. Here, for each request $\mathcal{R}_i$, $L_i = 100\mu$s, $n_r = 64$, $|D_i| = 1$ for non-nested requests, and $|D_i| = 4$ for nested requests. Each request was randomly chosen to be a read (as opposed to a write) with probability 0.5 and to be a nested request with probability 0.2. Due to write expansion, $|D_i|$ was inflated to 64 for all write requests under the RW-RNLP, as read requests can access any resource.

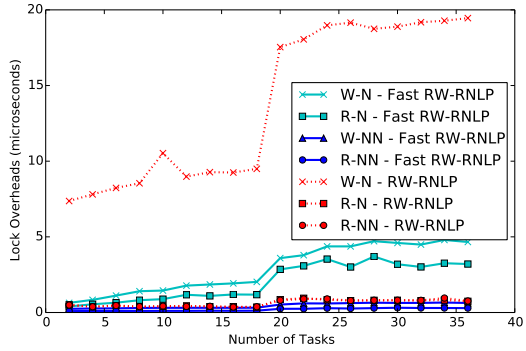

(a) Lock overhead.

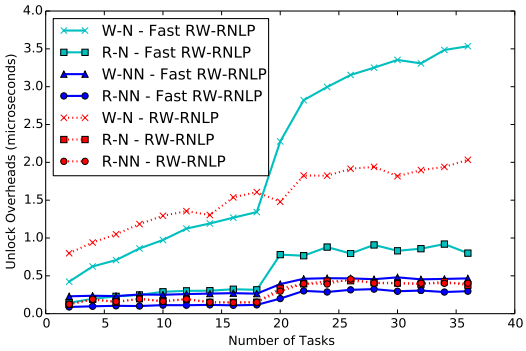

(b) Unlock overhead.

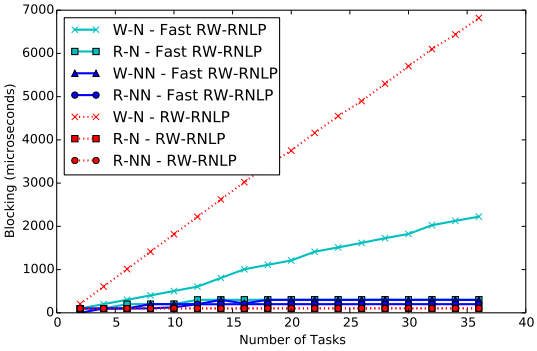

(c) Blocking.

Figure 158: (a) Lock and (b) unlock overheads and (c) blocking for nested and non-nested read and write requests under the RW-RNLP and the fast RW-RNLP. Here, for each request $\mathcal{R}_i$, $L_i = 100\mu$s, $n_r = 64$, $|D_i| = 1$ for non-nested requests, and $|D_i| = 4$ for nested requests. Each request was randomly chosen to be a read (as opposed to a write) with probability 0.5 and to be a nested request with probability 0.5. Due to write expansion, $|D_i|$ was inflated to 64 for all write requests under the RW-RNLP, as read requests can access any resource.

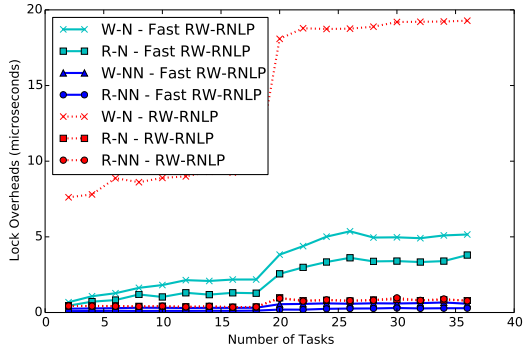

(a) Lock overhead.

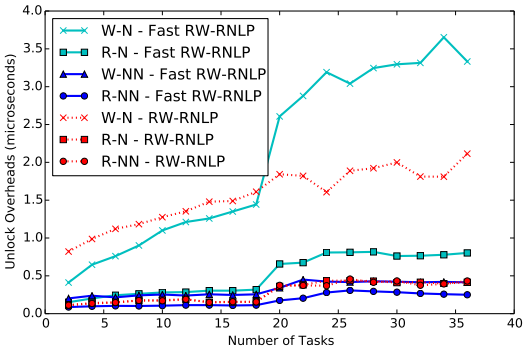

(b) Unlock overhead.

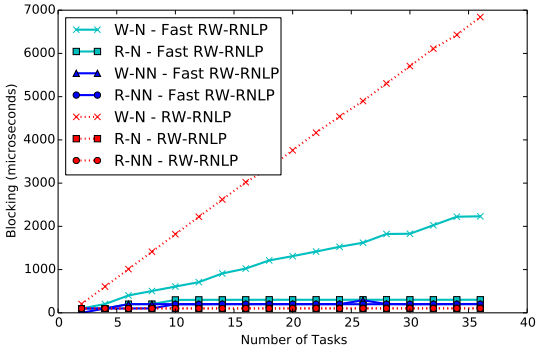

(c) Blocking.

Figure 159: (a) Lock and (b) unlock overheads and (c) blocking for nested and non-nested read and write requests under the RW-RNLP and the fast RW-RNLP. Here, for each request $\mathcal{R}_i$, $L_i = 100\mu$s, $n_r = 64$, $|D_i| = 1$ for non-nested requests, and $|D_i| = 4$ for nested requests. Each request was randomly chosen to be a read (as opposed to a write) with probability 0.5 and to be a nested request with probability 0.8. Due to write expansion, $|D_i|$ was inflated to 64 for all write requests under the RW-RNLP, as read requests can access any resource.

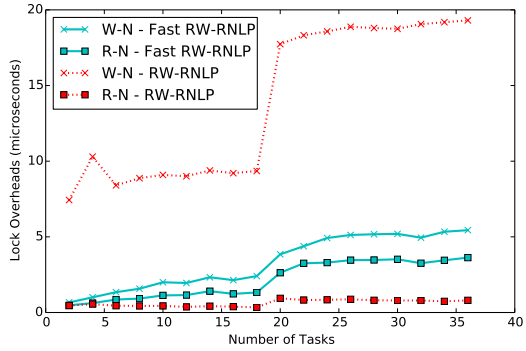

(a) Lock overhead.

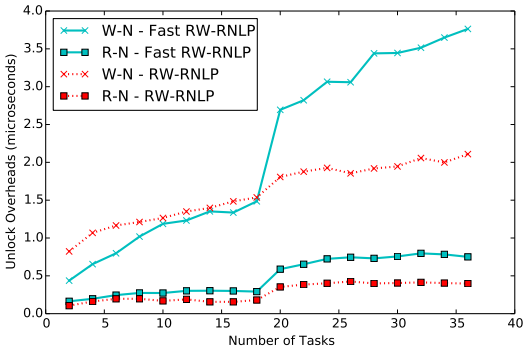

(b) Unlock overhead.

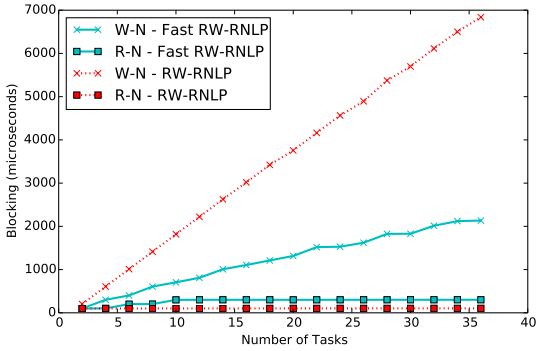

(c) Blocking.

Figure 160: (a) Lock and (b) unlock overheads and (c) blocking for nested read and write requests under the RW-RNLP and the fast RW-RNLP. Here, for each request $\mathcal{R}_i$, $L_i = 100\mu$s, $n_r = 64$, and $|D_i| = 4$. Each request was randomly chosen to be a read (as opposed to a write) with probability 0.5 and to be a nested request with probability 1. Due to write expansion, $|D_i|$ was inflated to 64 for all write requests under the RW-RNLP, as read requests can access any resource.

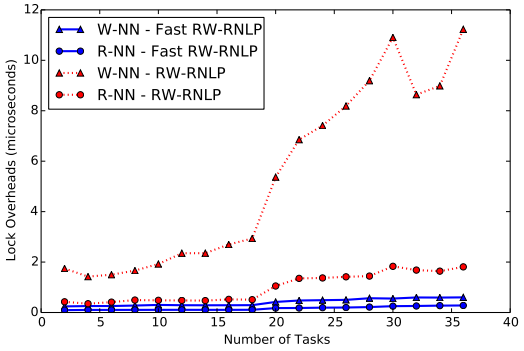

(a) Lock overhead.

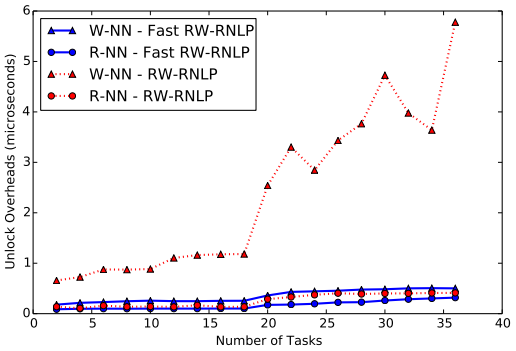

(b) Unlock overhead.

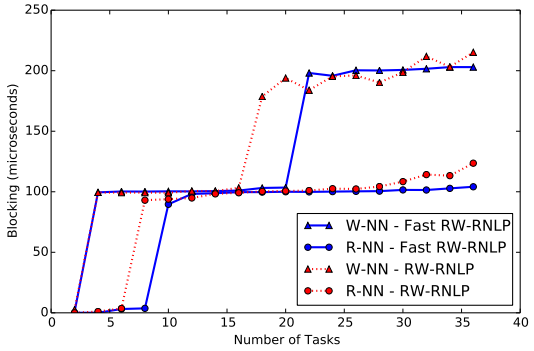

(c) Blocking.

Figure 161: (a) Lock and (b) unlock overheads and (c) blocking for non-nested read and write requests under the RW-RNLP and the fast RW-RNLP. Here, for each request $\mathcal{R}_i$, $L_i = 100\mu$s, $n_r = 64$, and $|D_i| = 1$. Each request was randomly chosen to be a read (as opposed to a write) with probability 0.8 and to be a nested request with probability 0.

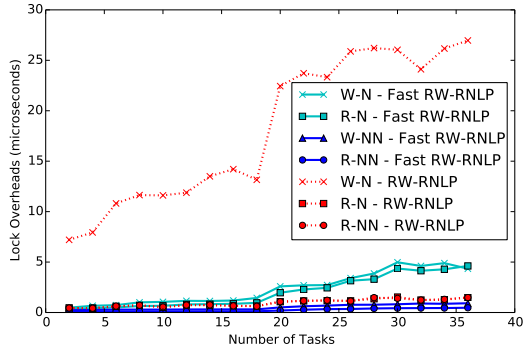

(a) Lock overhead.

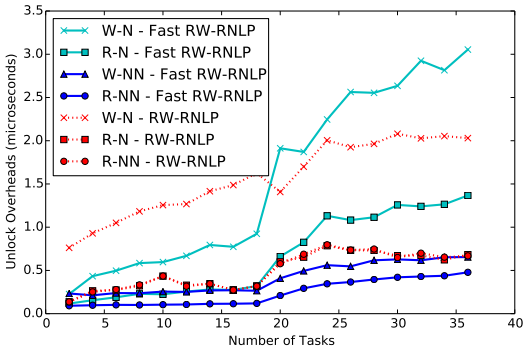

(b) Unlock overhead.

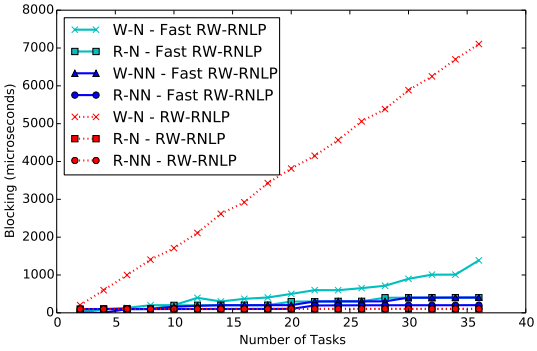

(c) Blocking.

Figure 162: (a) Lock and (b) unlock overheads and (c) blocking for nested and non-nested read and write requests under the RW-RNLP and the fast RW-RNLP. Here, for each request $\mathcal{R}_i$, $L_i = 100\mu$s, $n_r = 64$, $|D_i| = 1$ for non-nested requests, and $|D_i| = 4$ for nested requests. Each request was randomly chosen to be a read (as opposed to a write) with probability 0.8 and to be a nested request with probability 0.2. Due to write expansion, $|D_i|$ was inflated to 64 for all write requests under the RW-RNLP, as read requests can access any resource.

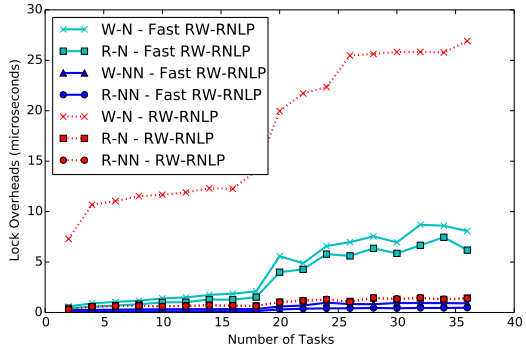

(a) Lock overhead.

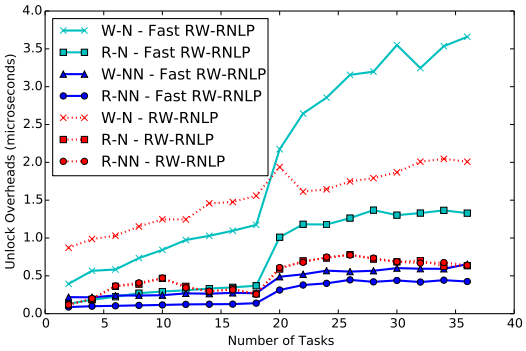

(b) Unlock overhead.

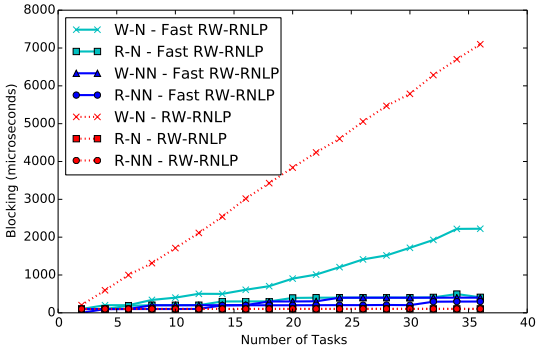

(c) Blocking.

Figure 163: (a) Lock and (b) unlock overheads and (c) blocking for nested and non-nested read and write requests under the RW-RNLP and the fast RW-RNLP. Here, for each request $\mathcal{R}_i$, $L_i = 100\mu$s, $n_r = 64$, $|D_i| = 1$ for non-nested requests, and $|D_i| = 4$ for nested requests. Each request was randomly chosen to be a read (as opposed to a write) with probability 0.8 and to be a nested request with probability 0.5. Due to write expansion, $|D_i|$ was inflated to 64 for all write requests under the RW-RNLP, as read requests can access any resource.

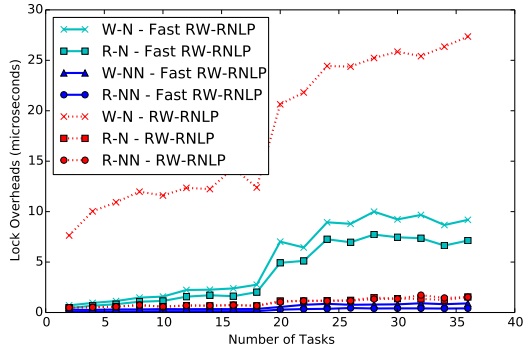

(a) Lock overhead.

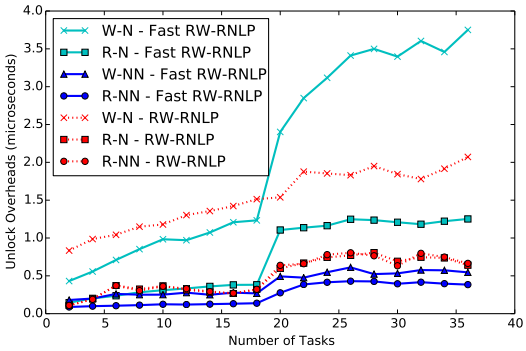

(b) Unlock overhead.

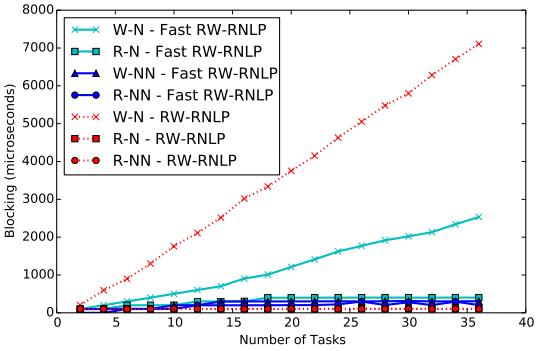

(c) Blocking.

Figure 164: (a) Lock and (b) unlock overheads and (c) blocking for nested and non-nested read and write requests under the RW-RNLP and the fast RW-RNLP. Here, for each request $\mathcal{R}_i$, $L_i = 100\mu$s, $n_r = 64$, $|D_i| = 1$ for non-nested requests, and $|D_i| = 4$ for nested requests. Each request was randomly chosen to be a read (as opposed to a write) with probability 0.8 and to be a nested request with probability 0.8. Due to write expansion, $|D_i|$ was inflated to 64 for all write requests under the RW-RNLP, as read requests can access any resource.

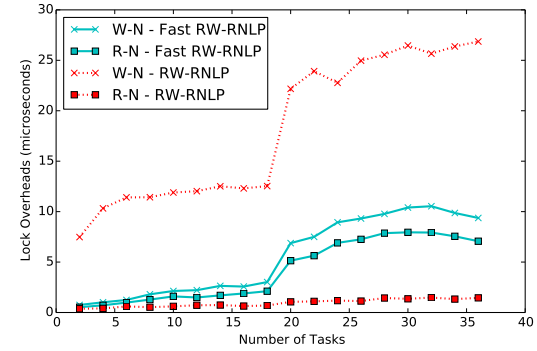

(a) Lock overhead.

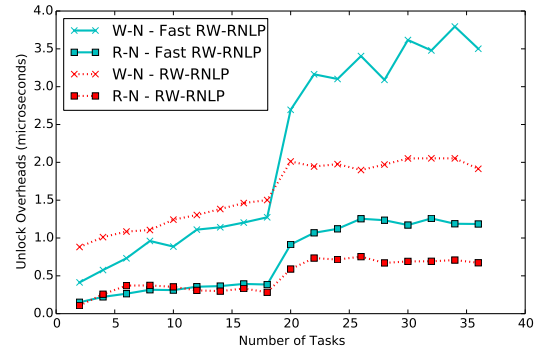

(b) Unlock overhead.

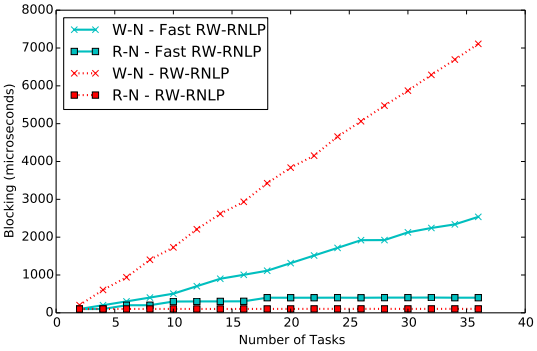

(c) Blocking.

Figure 165: (a) Lock and (b) unlock overheads and (c) blocking for nested read and write requests under the RW-RNLP and the fast RW-RNLP. Here, for each request $\mathcal{R}_i$, $L_i = 100\mu$s, $n_r = 64$, and $|D_i| = 4$. Each request was randomly chosen to be a read (as opposed to a write) with probability 0.8 and to be a nested request with probability 1. Due to write expansion, $|D_i|$ was inflated to 64 for all write requests under the RW-RNLP, as read requests can access any resource.

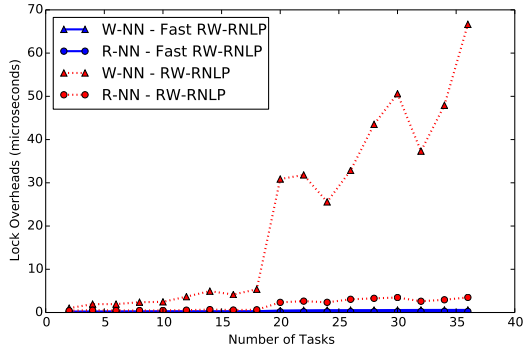

(a) Lock overhead.

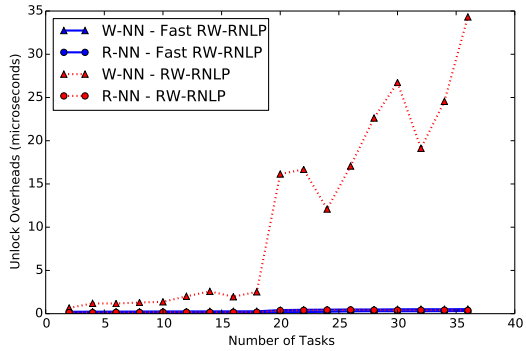

(b) Unlock overhead.

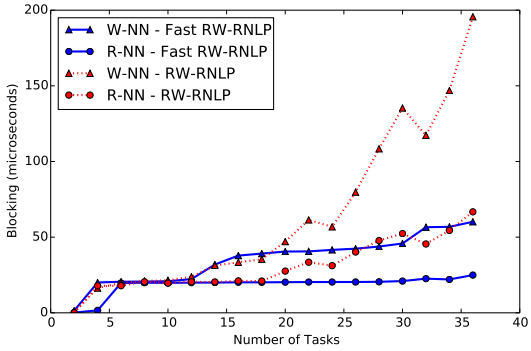

(c) Blocking.

Figure 166: (a) Lock and (b) unlock overheads and (c) blocking for non-nested read and write requests under the RW-RNLP and the fast RW-RNLP. Here, for each request $\mathcal{R}_i$, $L_i = 20\mu$s, $n_r = 64$, and $|D_i| = 1$. Each request was randomly chosen to be a read (as opposed to a write) with probability 0.2 and to be a nested request with probability 0.

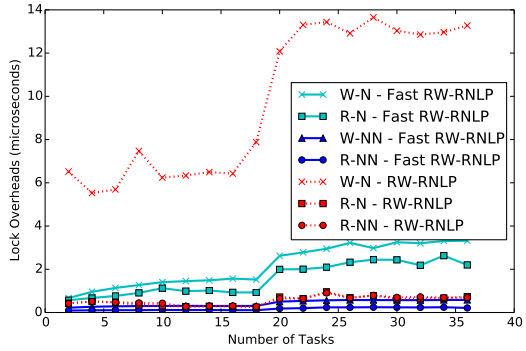

(a) Lock overhead.

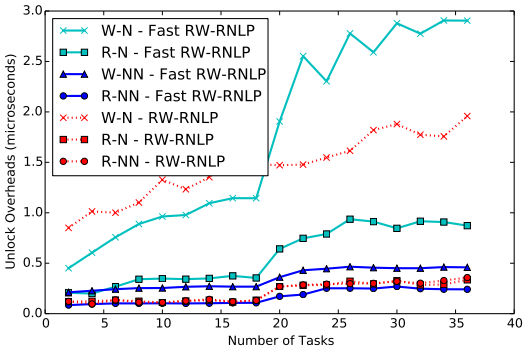

(b) Unlock overhead.

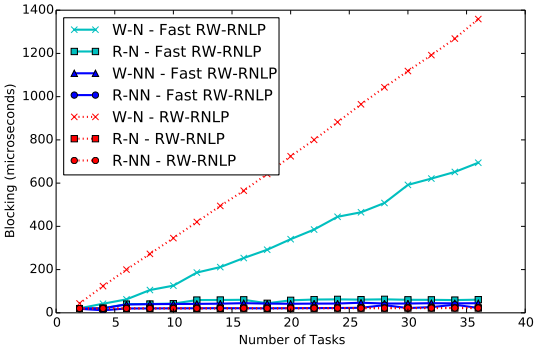

(c) Blocking.

Figure 167: (a) Lock and (b) unlock overheads and (c) blocking for nested and non-nested read and write requests under the RW-RNLP and the fast RW-RNLP. Here, for each request $\mathcal{R}_i$, $L_i = 20\mu$s, $n_r = 64$, $|D_i| = 1$ for non-nested requests, and $|D_i| = 6$ for nested requests. Each request was randomly chosen to be a read (as opposed to a write) with probability 0.2 and to be a nested request with probability 0.2. Due to write expansion, $|D_i|$ was inflated to 64 for all write requests under the RW-RNLP, as read requests can access any resource.

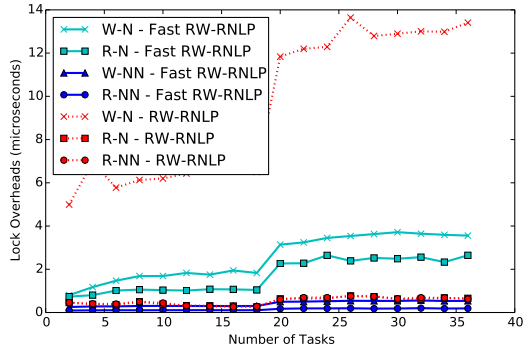

(a) Lock overhead.

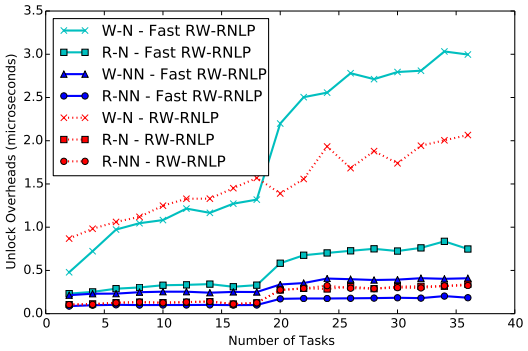

(b) Unlock overhead.

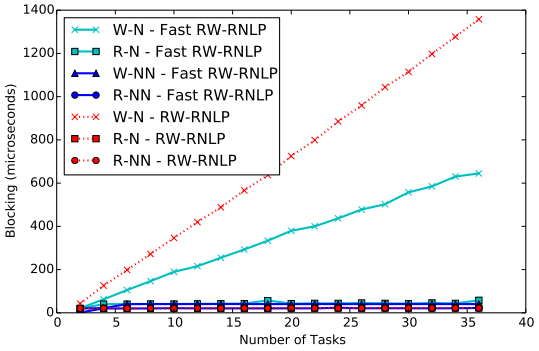

(c) Blocking.

Figure 168: (a) Lock and (b) unlock overheads and (c) blocking for nested and non-nested read and write requests under the RW-RNLP and the fast RW-RNLP. Here, for each request $\mathcal{R}_i$, $L_i = 20\mu$s, $n_r = 64$, $|D_i| = 1$ for non-nested requests, and $|D_i| = 6$ for nested requests. Each request was randomly chosen to be a read (as opposed to a write) with probability 0.2 and to be a nested request with probability 0.5. Due to write expansion, $|D_i|$ was inflated to 64 for all write requests under the RW-RNLP, as read requests can access any resource.

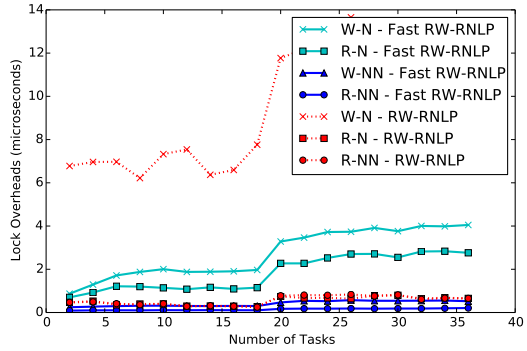

(a) Lock overhead.

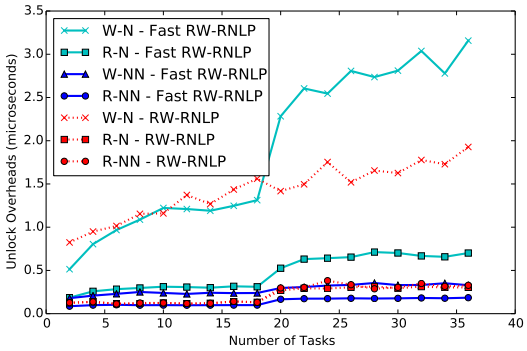

(b) Unlock overhead.

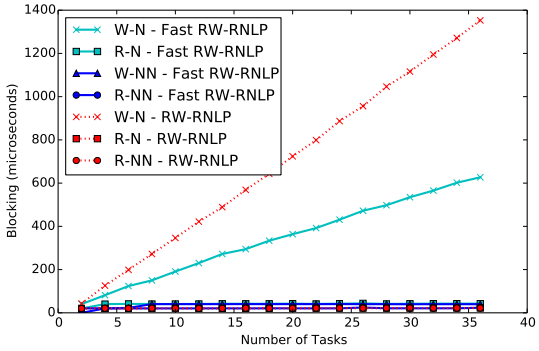

(c) Blocking.

Figure 169: (a) Lock and (b) unlock overheads and (c) blocking for nested and non-nested read and write requests under the RW-RNLP and the fast RW-RNLP. Here, for each request $\mathcal{R}_i$, $L_i = 20\mu$s, $n_r = 64$, $|D_i| = 1$ for non-nested requests, and $|D_i| = 6$ for nested requests. Each request was randomly chosen to be a read (as opposed to a write) with probability 0.2 and to be a nested request with probability 0.8. Due to write expansion, $|D_i|$ was inflated to 64 for all write requests under the RW-RNLP, as read requests can access any resource.

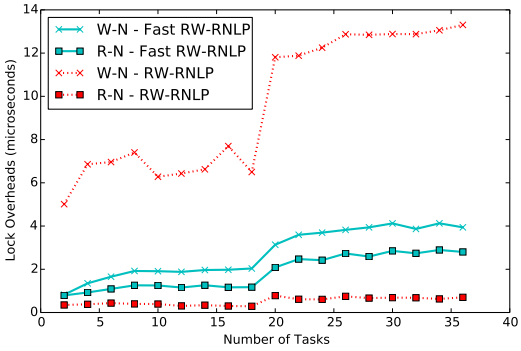

(a) Lock overhead.

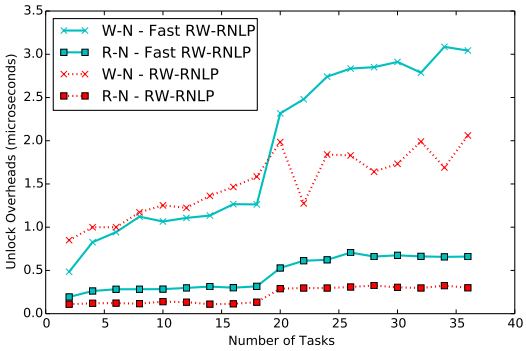

(b) Unlock overhead.

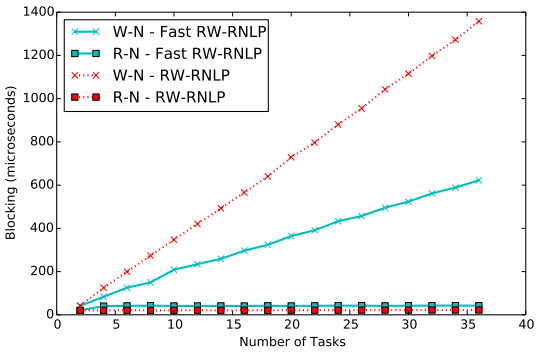

(c) Blocking.

Figure 170: (a) Lock and (b) unlock overheads and (c) blocking for nested read and write requests under the RW-RNLP and the fast RW-RNLP. Here, for each request $\mathcal{R}_i$, $L_i = 20\mu$s, $n_r = 64$, and $|D_i| = 6$. Each request was randomly chosen to be a read (as opposed to a write) with probability 0.2 and to be a nested request with probability 1. Due to write expansion, $|D_i|$ was inflated to 64 for all write requests under the RW-RNLP, as read requests can access any resource.

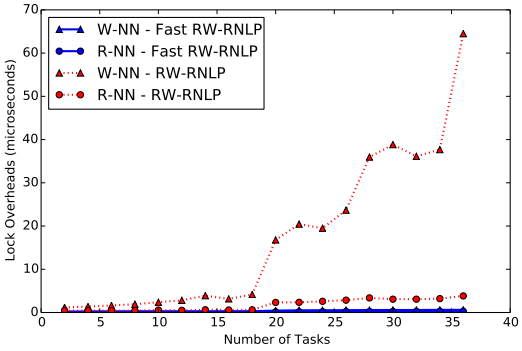

(a) Lock overhead.

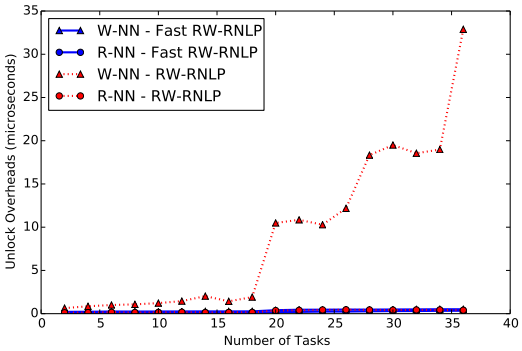

(b) Unlock overhead.

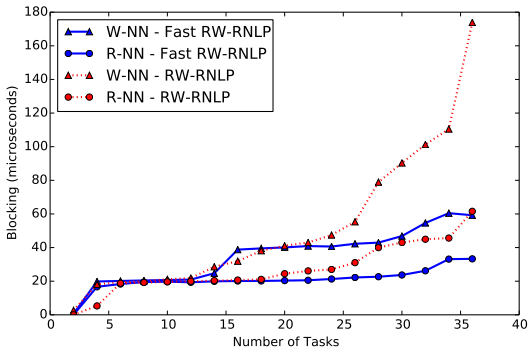

(c) Blocking.

Figure 171: (a) Lock and (b) unlock overheads and (c) blocking for non-nested read and write requests under the RW-RNLP and the fast RW-RNLP. Here, for each request $\mathcal{R}_i$, $L_i = 20\mu$s, $n_r = 64$, and $|D_i| = 1$. Each request was randomly chosen to be a read (as opposed to a write) with probability 0.5 and to be a nested request with probability 0.

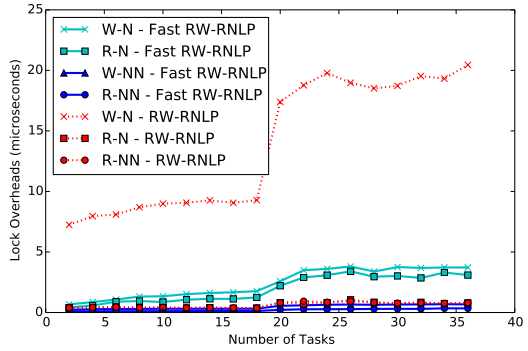

(a) Lock overhead.

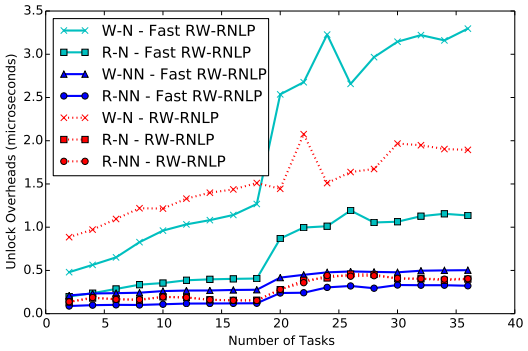

(b) Unlock overhead.

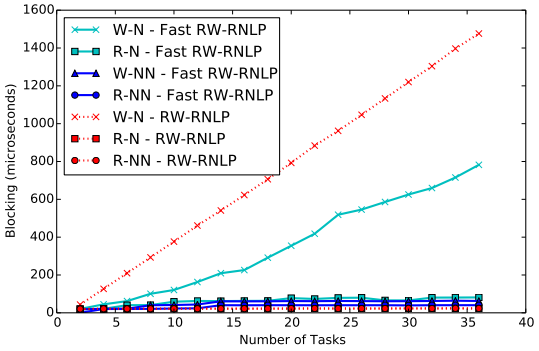

(c) Blocking.

Figure 172: (a) Lock and (b) unlock overheads and (c) blocking for nested and non-nested read and write requests under the RW-RNLP and the fast RW-RNLP. Here, for each request $\mathcal{R}_i$, $L_i = 20\mu$s, $n_r = 64$, $|D_i| = 1$ for non-nested requests, and $|D_i| = 6$ for nested requests. Each request was randomly chosen to be a read (as opposed to a write) with probability 0.5 and to be a nested request with probability 0.2. Due to write expansion, $|D_i|$ was inflated to 64 for all write requests under the RW-RNLP, as read requests can access any resource.

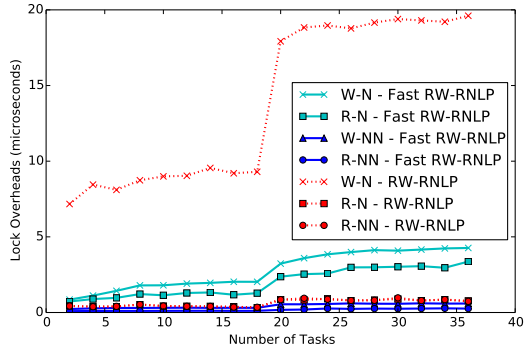

(a) Lock overhead.

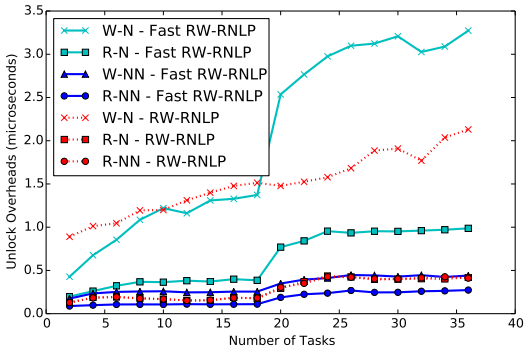

(b) Unlock overhead.

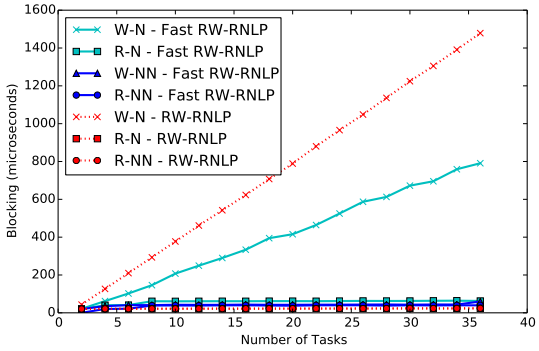

(c) Blocking.

Figure 173: (a) Lock and (b) unlock overheads and (c) blocking for nested and non-nested read and write requests under the RW-RNLP and the fast RW-RNLP. Here, for each request $\mathcal{R}_i$, $L_i = 20\mu$s, $n_r = 64$, $|D_i| = 1$ for non-nested requests, and $|D_i| = 6$ for nested requests. Each request was randomly chosen to be a read (as opposed to a write) with probability 0.5 and to be a nested request with probability 0.5. Due to write expansion, $|D_i|$ was inflated to 64 for all write requests under the RW-RNLP, as read requests can access any resource.

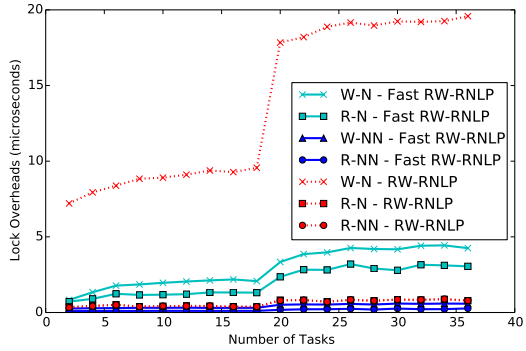

(a) Lock overhead.

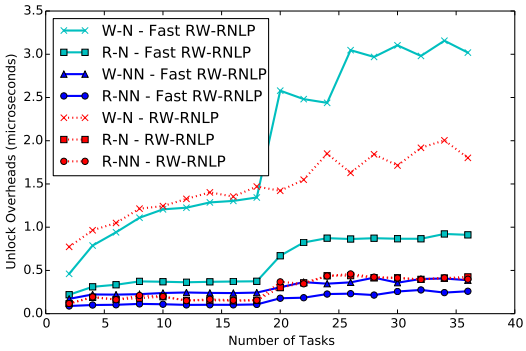

(b) Unlock overhead.

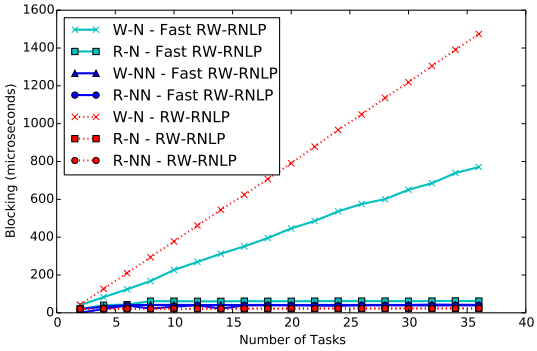

(c) Blocking.

Figure 174: (a) Lock and (b) unlock overheads and (c) blocking for nested and non-nested read and write requests under the RW-RNLP and the fast RW-RNLP. Here, for each request $\mathcal{R}_i$, $L_i = 20\mu$s, $n_r = 64$, $|D_i| = 1$ for non-nested requests, and $|D_i| = 6$ for nested requests. Each request was randomly chosen to be a read (as opposed to a write) with probability 0.5 and to be a nested request with probability 0.8. Due to write expansion, $|D_i|$ was inflated to 64 for all write requests under the RW-RNLP, as read requests can access any resource.

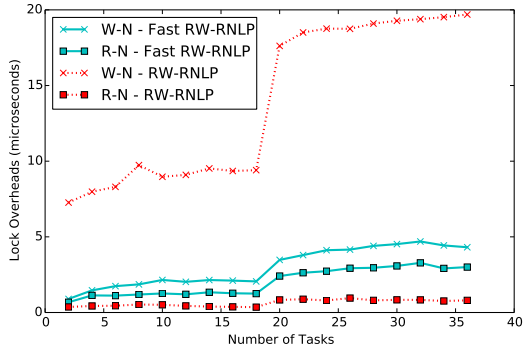

(a) Lock overhead.

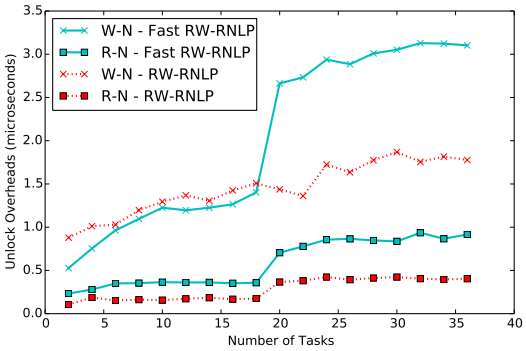

(b) Unlock overhead.

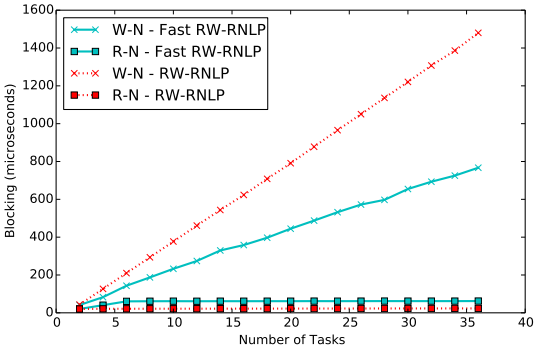

(c) Blocking.

Figure 175: (a) Lock and (b) unlock overheads and (c) blocking for nested read and write requests under the RW-RNLP and the fast RW-RNLP. Here, for each request $\mathcal{R}_i$, $L_i = 20\mu$s, $n_r = 64$, and $|D_i| = 6$. Each request was randomly chosen to be a read (as opposed to a write) with probability 0.5 and to be a nested request with probability 1. Due to write expansion, $|D_i|$ was inflated to 64 for all write requests under the RW-RNLP, as read requests can access any resource.

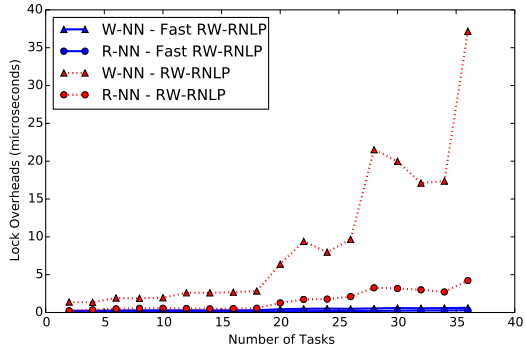

(a) Lock overhead.

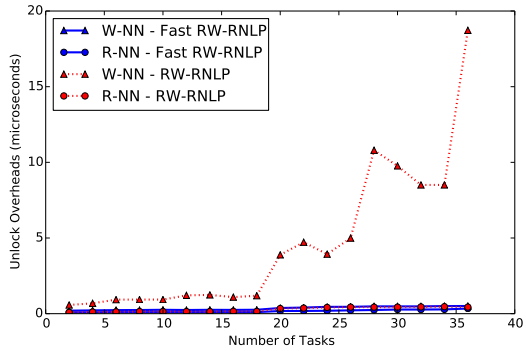

(b) Unlock overhead.

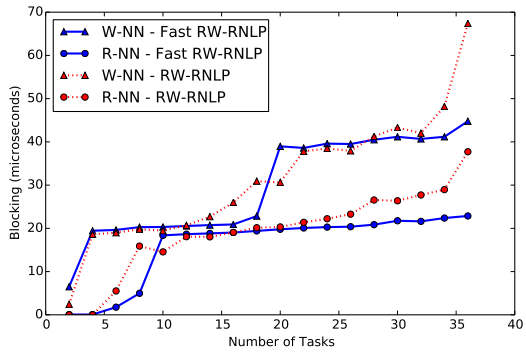

(c) Blocking.

Figure 176: (a) Lock and (b) unlock overheads and (c) blocking for non-nested read and write requests under the RW-RNLP and the fast RW-RNLP. Here, for each request $\mathcal{R}_i$, $L_i = 20\mu$s, $n_r = 64$, and $|D_i| = 1$. Each request was randomly chosen to be a read (as opposed to a write) with probability 0.8 and to be a nested request with probability 0.

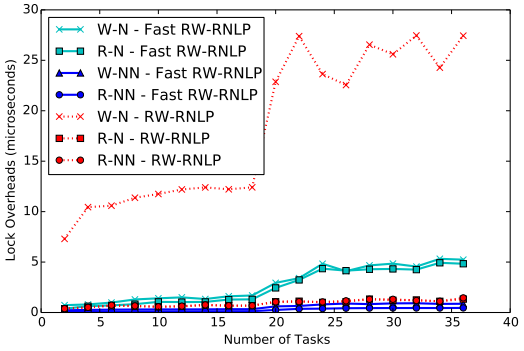

(a) Lock overhead.

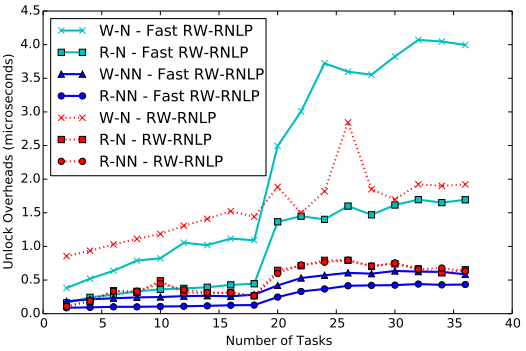

(b) Unlock overhead.

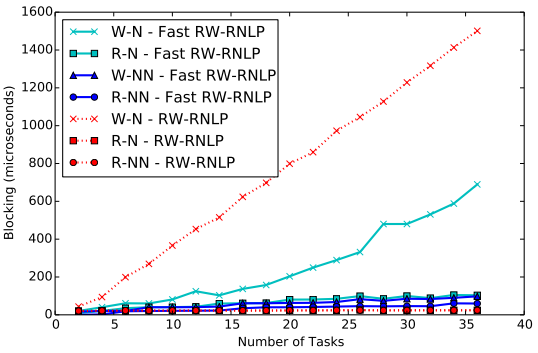

(c) Blocking.

Figure 177: (a) Lock and (b) unlock overheads and (c) blocking for nested and non-nested read and write requests under the RW-RNLP and the fast RW-RNLP. Here, for each request $\mathcal{R}_i$, $L_i = 20\mu$s, $n_r = 64$, $|D_i| = 1$ for non-nested requests, and $|D_i| = 6$ for nested requests. Each request was randomly chosen to be a read (as opposed to a write) with probability 0.8 and to be a nested request with probability 0.2. Due to write expansion, $|D_i|$ was inflated to 64 for all write requests under the RW-RNLP, as read requests can access any resource.

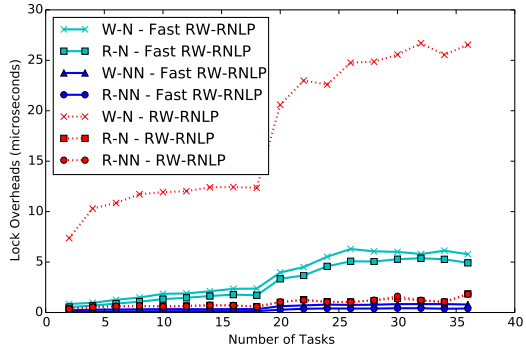

(a) Lock overhead.

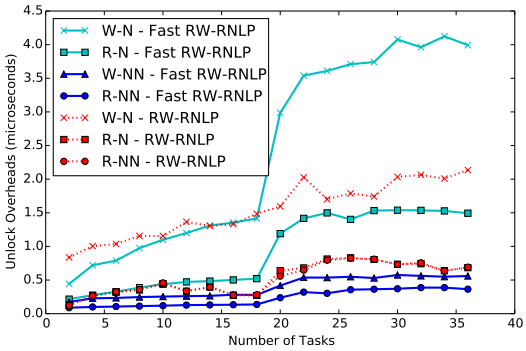

(b) Unlock overhead.

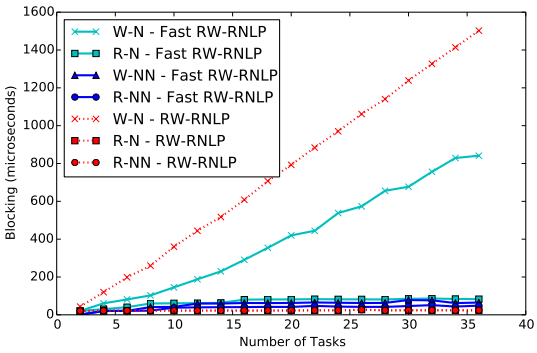

(c) Blocking.

Figure 178: (a) Lock and (b) unlock overheads and (c) blocking for nested and non-nested read and write requests under the RW-RNLP and the fast RW-RNLP. Here, for each request $\mathcal{R}_i$, $L_i = 20\mu$s, $n_r = 64$, $|D_i| = 1$ for non-nested requests, and $|D_i| = 6$ for nested requests. Each request was randomly chosen to be a read (as opposed to a write) with probability 0.8 and to be a nested request with probability 0.5. Due to write expansion, $|D_i|$ was inflated to 64 for all write requests under the RW-RNLP, as read requests can access any resource.

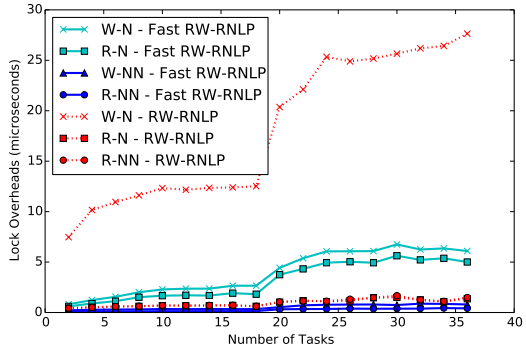

(a) Lock overhead.

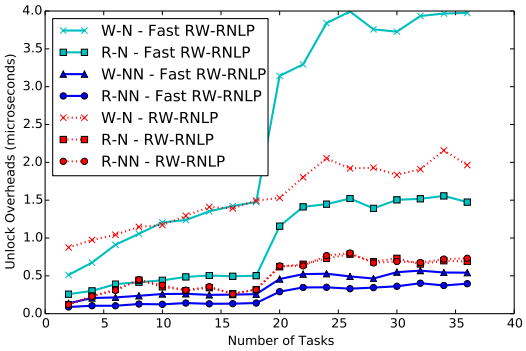

(b) Unlock overhead.

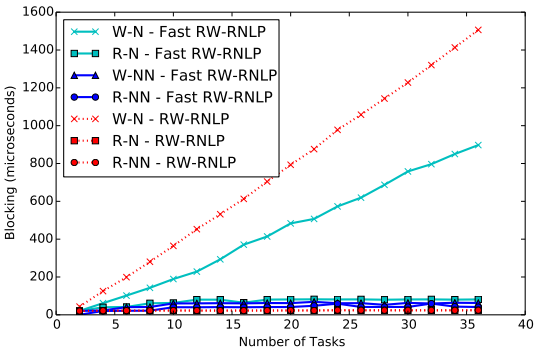

(c) Blocking.

Figure 179: (a) Lock and (b) unlock overheads and (c) blocking for nested and non-nested read and write requests under the RW-RNLP and the fast RW-RNLP. Here, for each request $\mathcal{R}_i$, $L_i = 20\mu$s, $n_r = 64$, $|D_i| = 1$ for non-nested requests, and $|D_i| = 6$ for nested requests. Each request was randomly chosen to be a read (as opposed to a write) with probability 0.8 and to be a nested request with probability 0.8. Due to write expansion, $|D_i|$ was inflated to 64 for all write requests under the RW-RNLP, as read requests can access any resource.

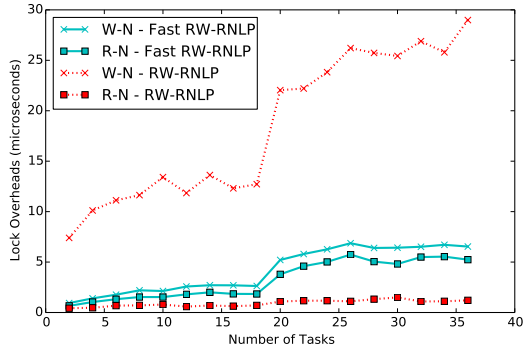

(a) Lock overhead.

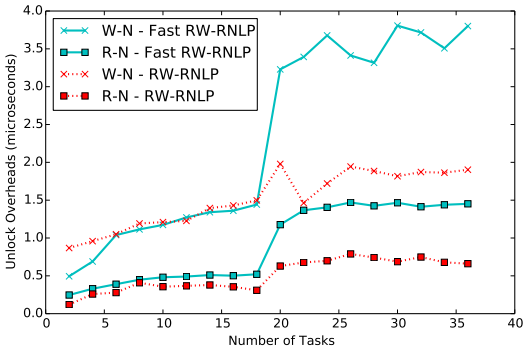

(b) Unlock overhead.

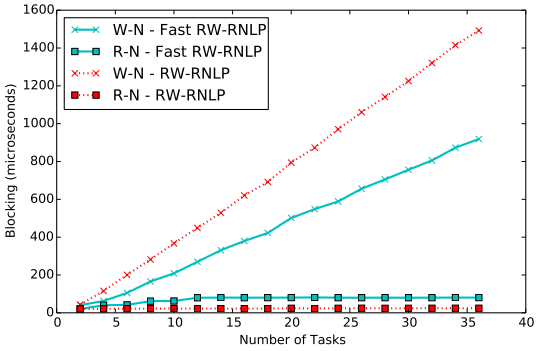

(c) Blocking.

Figure 180: (a) Lock and (b) unlock overheads and (c) blocking for nested read and write requests under the RW-RNLP and the fast RW-RNLP. Here, for each request $\mathcal{R}_i$, $L_i = 20\mu$s, $n_r = 64$, and $|D_i| = 6$. Each request was randomly chosen to be a read (as opposed to a write) with probability 0.8 and to be a nested request with probability 1. Due to write expansion, $|D_i|$ was inflated to 64 for all write requests under the RW-RNLP, as read requests can access any resource.

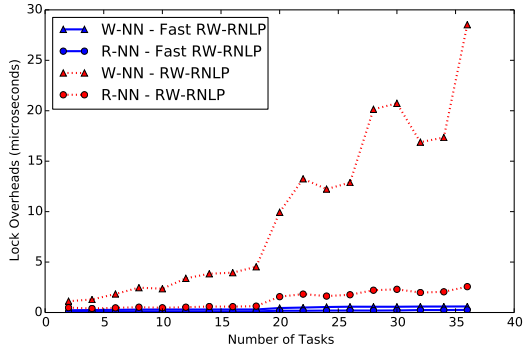

(a) Lock overhead.

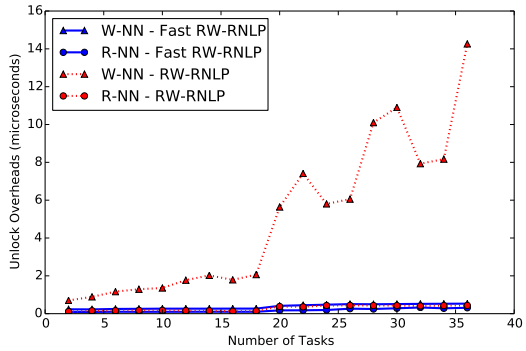

(b) Unlock overhead.

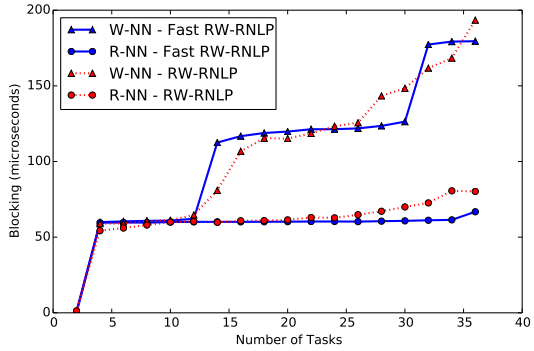

(c) Blocking.

Figure 181: (a) Lock and (b) unlock overheads and (c) blocking for non-nested read and write requests under the RW-RNLP and the fast RW-RNLP. Here, for each request $\mathcal{R}_i$, $L_i = 60\mu$s, $n_r = 64$, and $|D_i| = 1$. Each request was randomly chosen to be a read (as opposed to a write) with probability 0.2 and to be a nested request with probability 0.

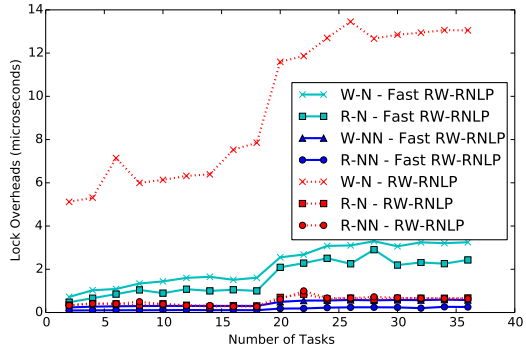

(a) Lock overhead.

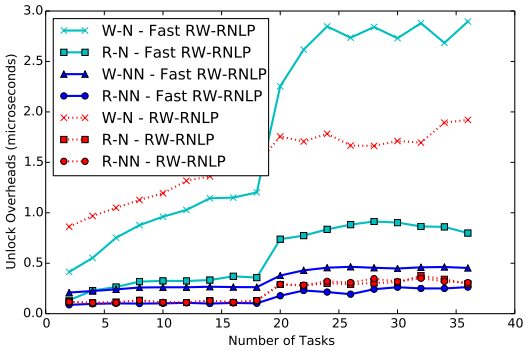

(b) Unlock overhead.

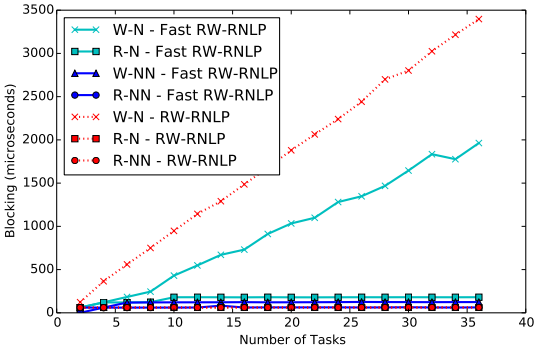

(c) Blocking.

Figure 182: (a) Lock and (b) unlock overheads and (c) blocking for nested and non-nested read and write requests under the RW-RNLP and the fast RW-RNLP. Here, for each request $\mathcal{R}_i$, $L_i = 60\mu$s, $n_r = 64$, $|D_i| = 1$ for non-nested requests, and $|D_i| = 6$ for nested requests. Each request was randomly chosen to be a read (as opposed to a write) with probability 0.2 and to be a nested request with probability 0.2. Due to write expansion, $|D_i|$ was inflated to 64 for all write requests under the RW-RNLP, as read requests can access any resource.

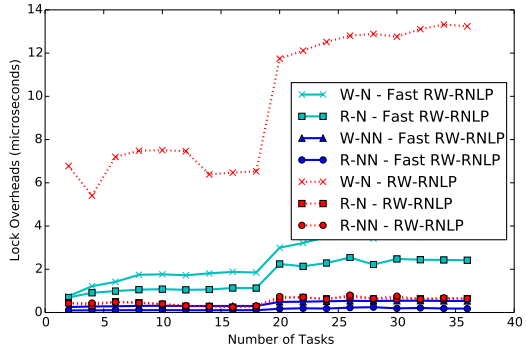

(a) Lock overhead.

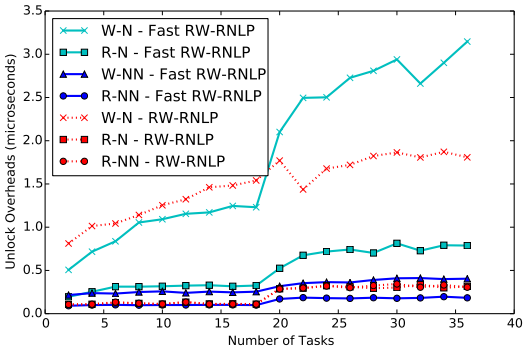

(b) Unlock overhead.

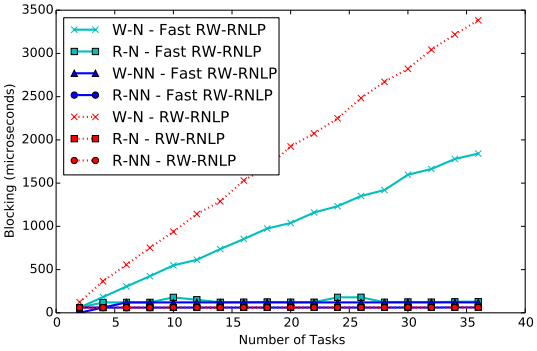

(c) Blocking.

Figure 183: (a) Lock and (b) unlock overheads and (c) blocking for nested and non-nested read and write requests under the RW-RNLP and the fast RW-RNLP. Here, for each request $\mathcal{R}_i$, $L_i = 60\mu$s, $n_r = 64$, $|D_i| = 1$ for non-nested requests, and $|D_i| = 6$ for nested requests. Each request was randomly chosen to be a read (as opposed to a write) with probability 0.2 and to be a nested request with probability 0.5. Due to write expansion, $|D_i|$ was inflated to 64 for all write requests under the RW-RNLP, as read requests can access any resource.

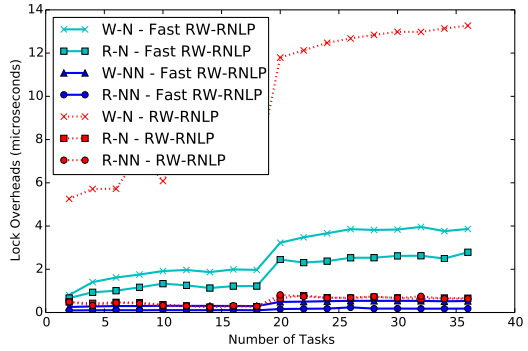

(a) Lock overhead.

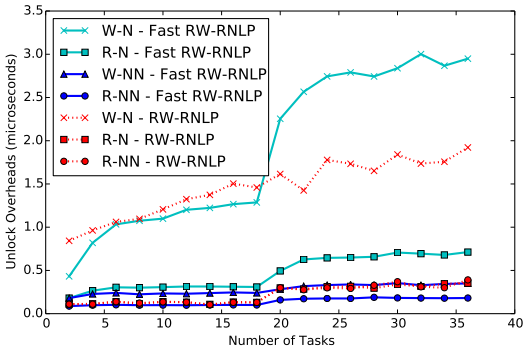

(b) Unlock overhead.

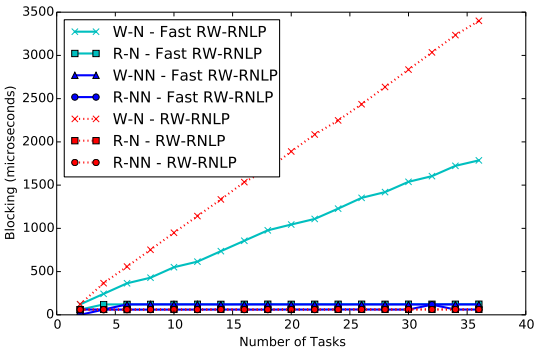

(c) Blocking.

Figure 184: (a) Lock and (b) unlock overheads and (c) blocking for nested and non-nested read and write requests under the RW-RNLP and the fast RW-RNLP. Here, for each request $\mathcal{R}_i$, $L_i = 60\mu$s, $n_r = 64$, $|D_i| = 1$ for non-nested requests, and $|D_i| = 6$ for nested requests. Each request was randomly chosen to be a read (as opposed to a write) with probability 0.2 and to be a nested request with probability 0.8. Due to write expansion, $|D_i|$ was inflated to 64 for all write requests under the RW-RNLP, as read requests can access any resource.

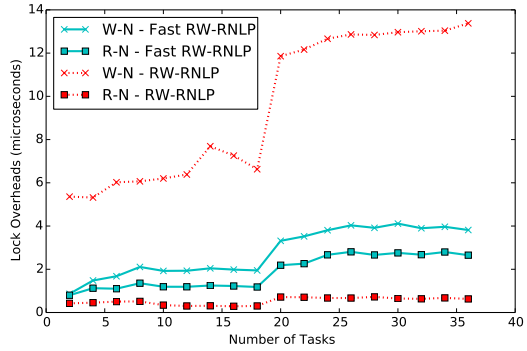

(a) Lock overhead.

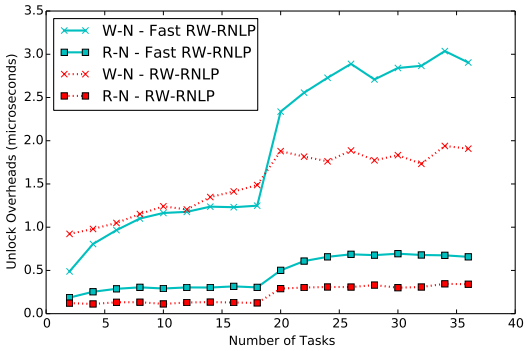

(b) Unlock overhead.

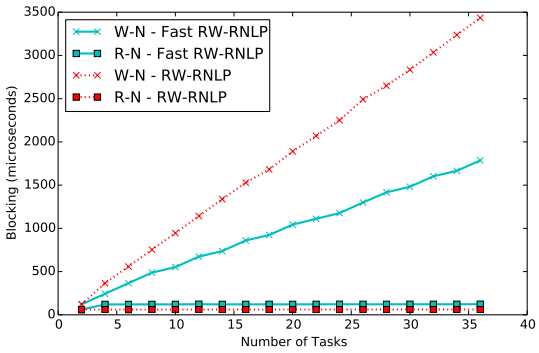

(c) Blocking.

Figure 185: (a) Lock and (b) unlock overheads and (c) blocking for nested read and write requests under the RW-RNLP and the fast RW-RNLP. Here, for each request $\mathcal{R}_i$, $L_i = 60\mu$s, $n_r = 64$, and $|D_i| = 6$. Each request was randomly chosen to be a read (as opposed to a write) with probability 0.2 and to be a nested request with probability 1. Due to write expansion, $|D_i|$ was inflated to 64 for all write requests under the RW-RNLP, as read requests can access any resource.

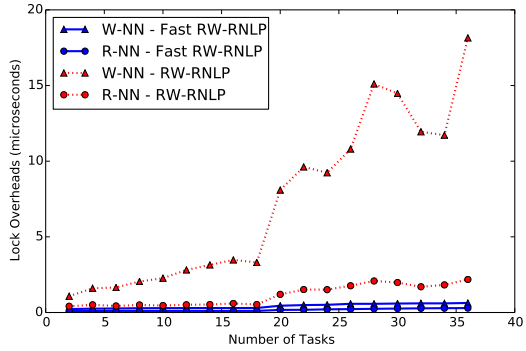

(a) Lock overhead.

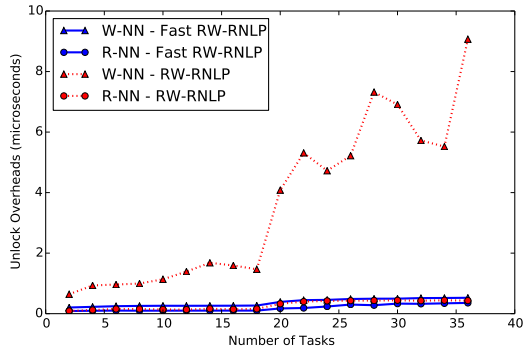

(b) Unlock overhead.

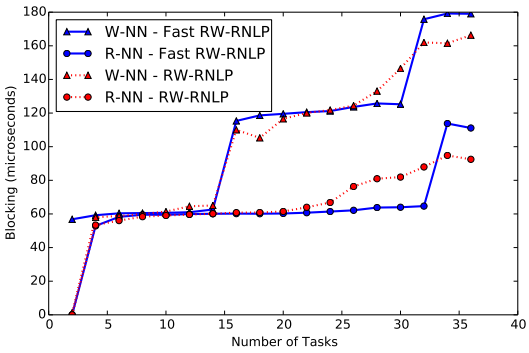

(c) Blocking.

Figure 186: (a) Lock and (b) unlock overheads and (c) blocking for non-nested read and write requests under the RW-RNLP and the fast RW-RNLP. Here, for each request $\mathcal{R}_i$, $L_i = 60\mu$s, $n_r = 64$, and $|D_i| = 1$. Each request was randomly chosen to be a read (as opposed to a write) with probability 0.5 and to be a nested request with probability 0.

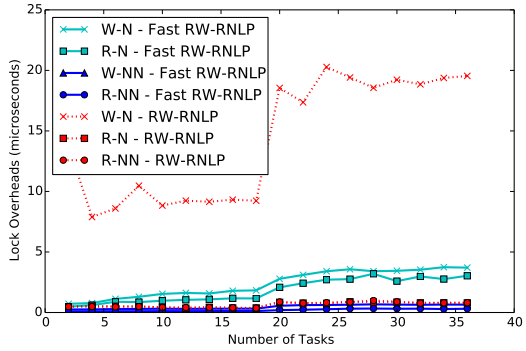

(a) Lock overhead.

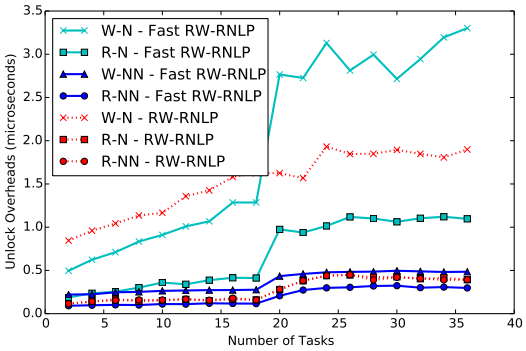

(b) Unlock overhead.

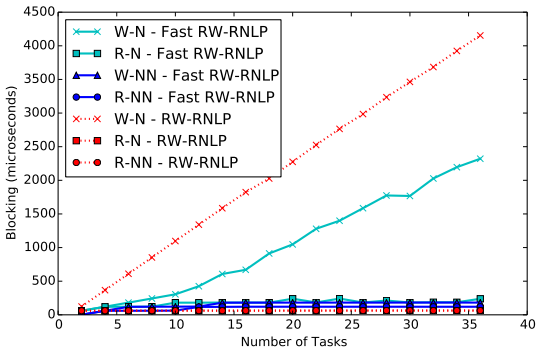

(c) Blocking.

Figure 187: (a) Lock and (b) unlock overheads and (c) blocking for nested and non-nested read and write requests under the RW-RNLP and the fast RW-RNLP. Here, for each request $\mathcal{R}_i$, $L_i = 60\mu$s, $n_r = 64$, $|D_i| = 1$ for non-nested requests, and $|D_i| = 6$ for nested requests. Each request was randomly chosen to be a read (as opposed to a write) with probability 0.5 and to be a nested request with probability 0.2. Due to write expansion, $|D_i|$ was inflated to 64 for all write requests under the RW-RNLP, as read requests can access any resource.

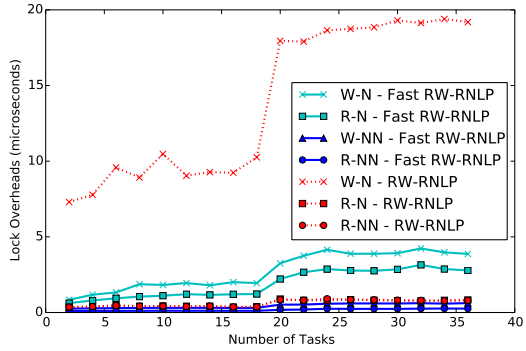

(a) Lock overhead.

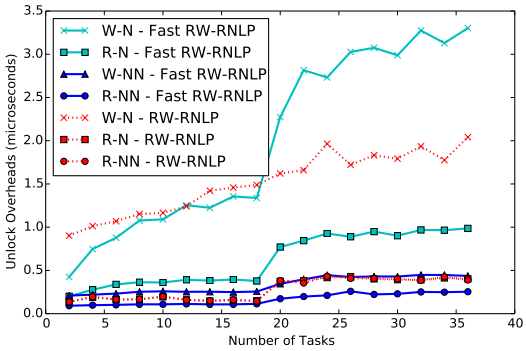

(b) Unlock overhead.

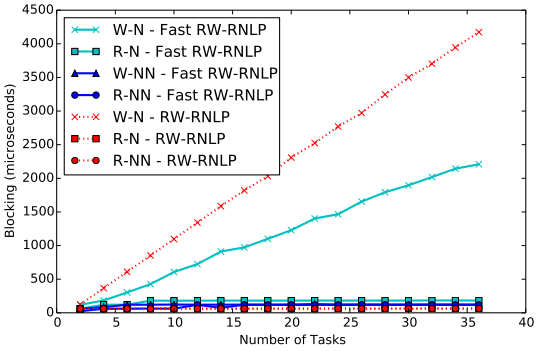

(c) Blocking.

Figure 188: (a) Lock and (b) unlock overheads and (c) blocking for nested and non-nested read and write requests under the RW-RNLP and the fast RW-RNLP. Here, for each request $\mathcal{R}_i$, $L_i = 60\mu$s, $n_r = 64$, $|D_i| = 1$ for non-nested requests, and $|D_i| = 6$ for nested requests. Each request was randomly chosen to be a read (as opposed to a write) with probability 0.5 and to be a nested request with probability 0.5. Due to write expansion, $|D_i|$ was inflated to 64 for all write requests under the RW-RNLP, as read requests can access any resource.

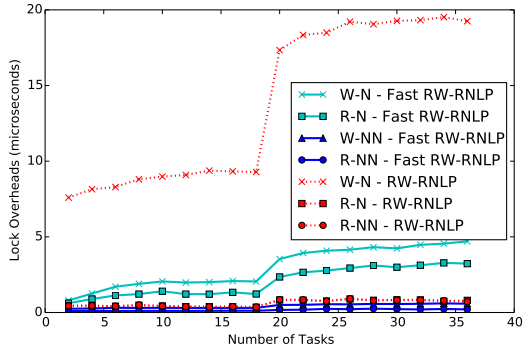

(a) Lock overhead.

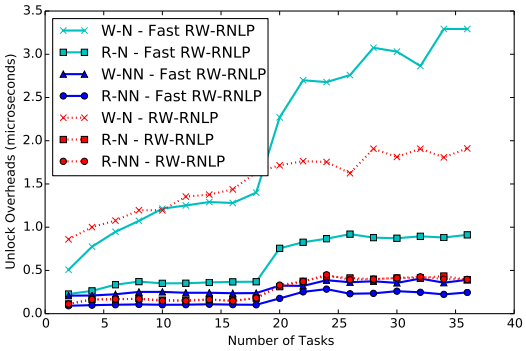

(b) Unlock overhead.

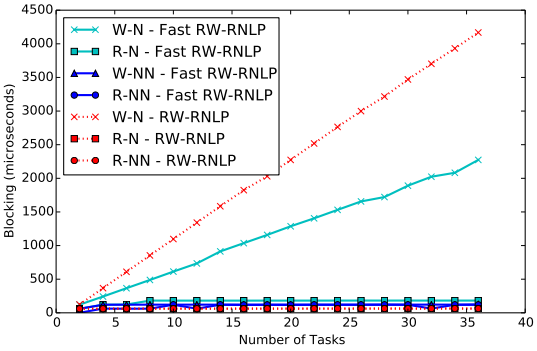

(c) Blocking.

Figure 189: (a) Lock and (b) unlock overheads and (c) blocking for nested and non-nested read and write requests under the RW-RNLP and the fast RW-RNLP. Here, for each request $\mathcal{R}_i$, $L_i = 60\mu$s, $n_r = 64$, $|D_i| = 1$ for non-nested requests, and $|D_i| = 6$ for nested requests. Each request was randomly chosen to be a read (as opposed to a write) with probability 0.5 and to be a nested request with probability 0.8. Due to write expansion, $|D_i|$ was inflated to 64 for all write requests under the RW-RNLP, as read requests can access any resource.

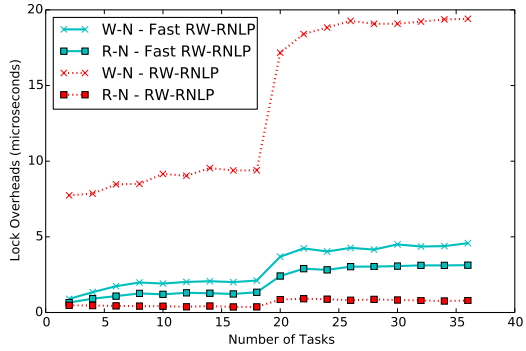

(a) Lock overhead.

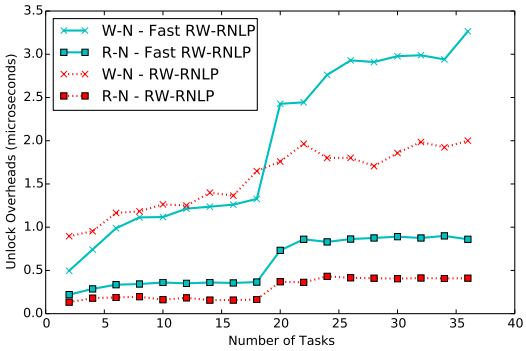

(b) Unlock overhead.

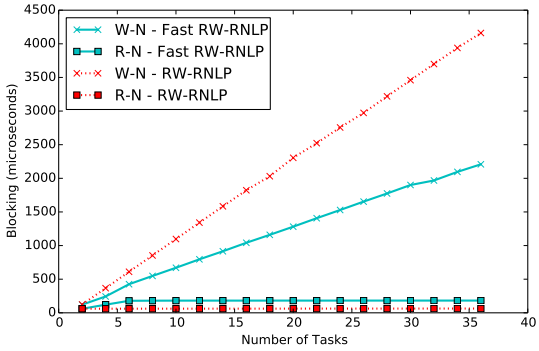

(c) Blocking.

Figure 190: (a) Lock and (b) unlock overheads and (c) blocking for nested read and write requests under the RW-RNLP and the fast RW-RNLP. Here, for each request $\mathcal{R}_i$, $L_i = 60\mu$s, $n_r = 64$, and $|D_i| = 6$. Each request was randomly chosen to be a read (as opposed to a write) with probability 0.5 and to be a nested request with probability 1. Due to write expansion, $|D_i|$ was inflated to 64 for all write requests under the RW-RNLP, as read requests can access any resource.

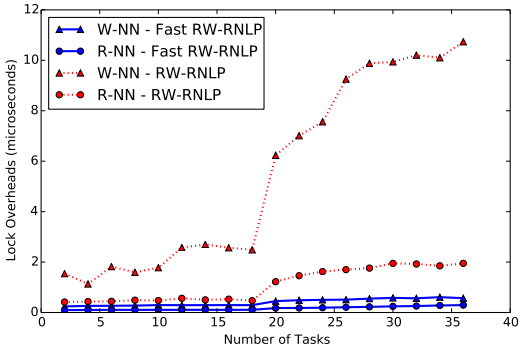

(a) Lock overhead.

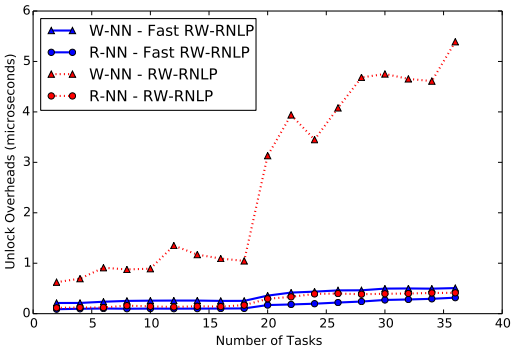

(b) Unlock overhead.

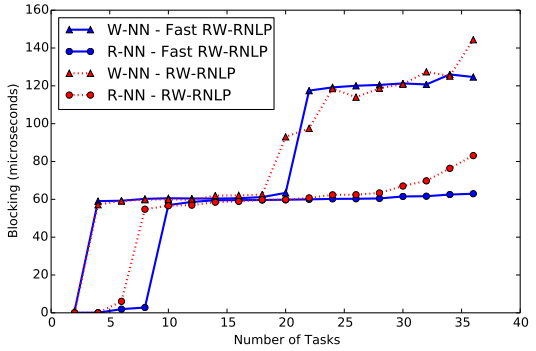

(c) Blocking.

Figure 191: (a) Lock and (b) unlock overheads and (c) blocking for non-nested read and write requests under the RW-RNLP and the fast RW-RNLP. Here, for each request $\mathcal{R}_i$, $L_i = 60\mu$s, $n_r = 64$, and $|D_i| = 1$. Each request was randomly chosen to be a read (as opposed to a write) with probability 0.8 and to be a nested request with probability 0.

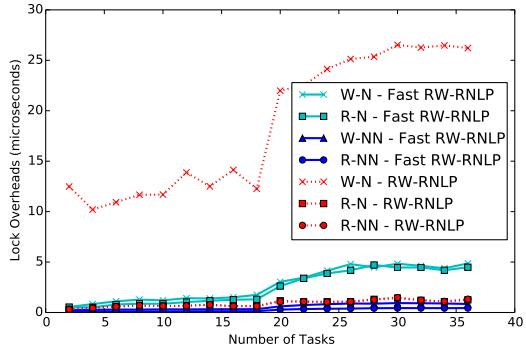

(a) Lock overhead.

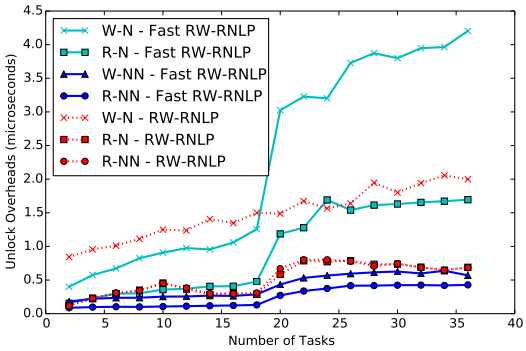

(b) Unlock overhead.

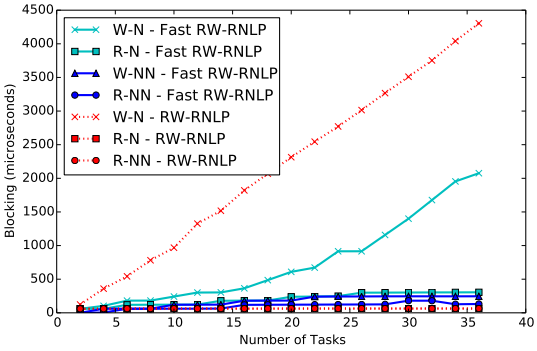

(c) Blocking.

Figure 192: (a) Lock and (b) unlock overheads and (c) blocking for nested and non-nested read and write requests under the RW-RNLP and the fast RW-RNLP. Here, for each request $\mathcal{R}_i$, $L_i = 60\mu$s, $n_r = 64$, $|D_i| = 1$ for non-nested requests, and $|D_i| = 6$ for nested requests. Each request was randomly chosen to be a read (as opposed to a write) with probability 0.8 and to be a nested request with probability 0.2. Due to write expansion, $|D_i|$ was inflated to 64 for all write requests under the RW-RNLP, as read requests can access any resource.

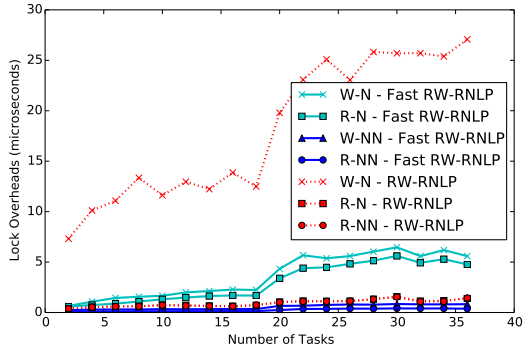

(a) Lock overhead.

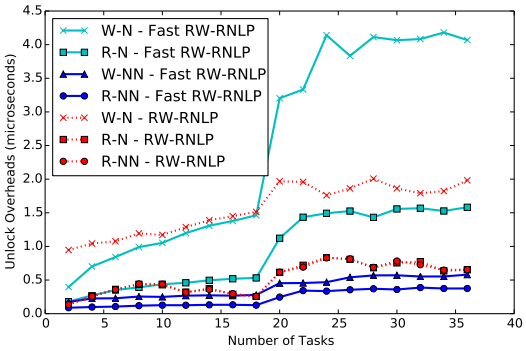

(b) Unlock overhead.

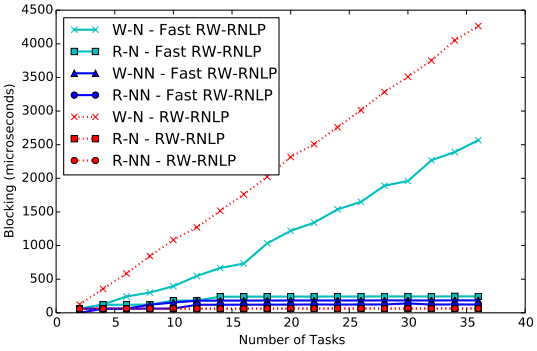

(c) Blocking.

Figure 193: (a) Lock and (b) unlock overheads and (c) blocking for nested and non-nested read and write requests under the RW-RNLP and the fast RW-RNLP. Here, for each request $\mathcal{R}_i$, $L_i = 60\mu$s, $n_r = 64$, $|D_i| = 1$ for non-nested requests, and $|D_i| = 6$ for nested requests. Each request was randomly chosen to be a read (as opposed to a write) with probability 0.8 and to be a nested request with probability 0.5. Due to write expansion, $|D_i|$ was inflated to 64 for all write requests under the RW-RNLP, as read requests can access any resource.

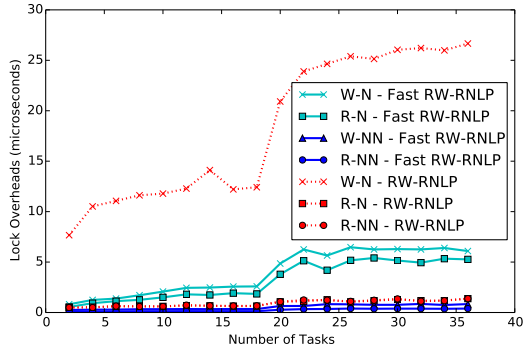

(a) Lock overhead.

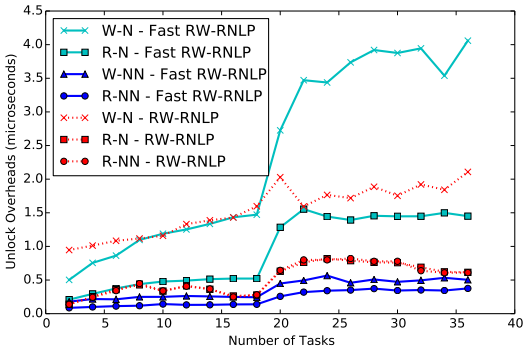

(b) Unlock overhead.

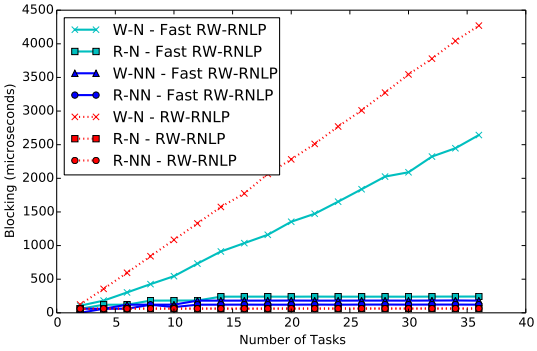

(c) Blocking.

Figure 194: (a) Lock and (b) unlock overheads and (c) blocking for nested and non-nested read and write requests under the RW-RNLP and the fast RW-RNLP. Here, for each request $\mathcal{R}_i$, $L_i = 60\mu$s, $n_r = 64$, $|D_i| = 1$ for non-nested requests, and $|D_i| = 6$ for nested requests. Each request was randomly chosen to be a read (as opposed to a write) with probability 0.8 and to be a nested request with probability 0.8. Due to write expansion, $|D_i|$ was inflated to 64 for all write requests under the RW-RNLP, as read requests can access any resource.

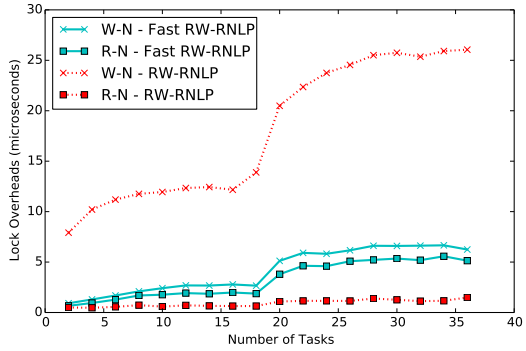

(a) Lock overhead.

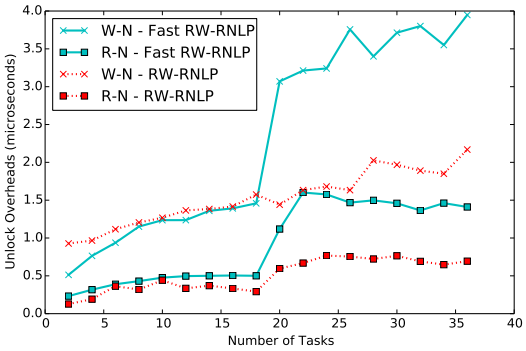

(b) Unlock overhead.

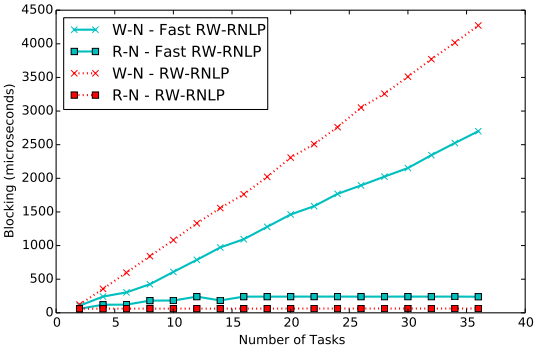

(c) Blocking.

Figure 195: (a) Lock and (b) unlock overheads and (c) blocking for nested read and write requests under the RW-RNLP and the fast RW-RNLP. Here, for each request $\mathcal{R}_i$, $L_i = 60\mu$s, $n_r = 64$, and $|D_i| = 6$. Each request was randomly chosen to be a read (as opposed to a write) with probability 0.8 and to be a nested request with probability 1. Due to write expansion, $|D_i|$ was inflated to 64 for all write requests under the RW-RNLP, as read requests can access any resource.

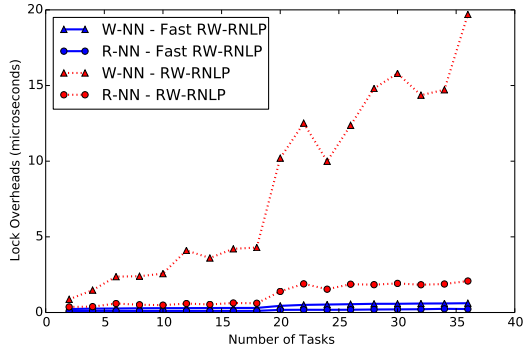

(a) Lock overhead.

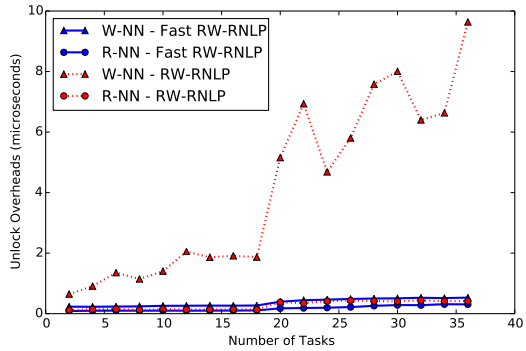

(b) Unlock overhead.

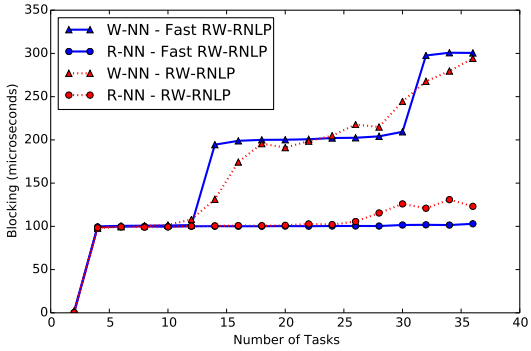

(c) Blocking.

Figure 196: (a) Lock and (b) unlock overheads and (c) blocking for non-nested read and write requests under the RW-RNLP and the fast RW-RNLP. Here, for each request $\mathcal{R}_i$, $L_i = 100\mu$s, $n_r = 64$, and $|D_i| = 1$. Each request was randomly chosen to be a read (as opposed to a write) with probability 0.2 and to be a nested request with probability 0.

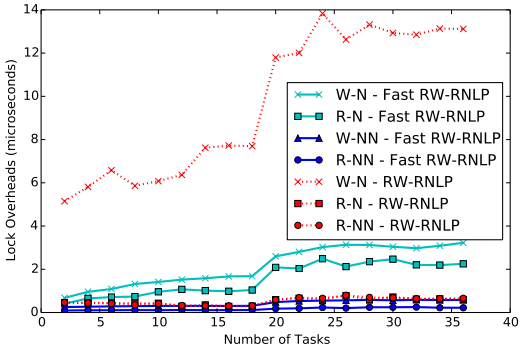

(a) Lock overhead.

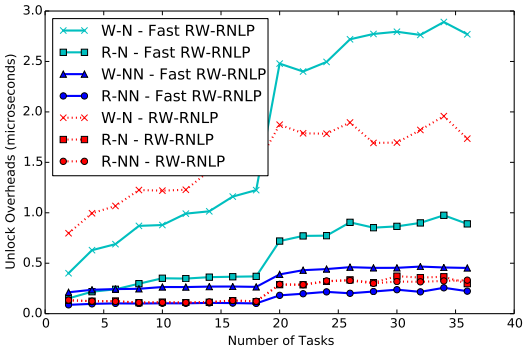

(b) Unlock overhead.

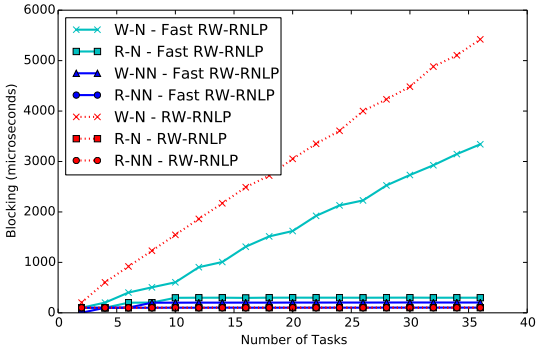

(c) Blocking.

Figure 197: (a) Lock and (b) unlock overheads and (c) blocking for nested and non-nested read and write requests under the RW-RNLP and the fast RW-RNLP. Here, for each request $\mathcal{R}_i$, $L_i = 100\mu$s, $n_r = 64$, $|D_i| = 1$ for non-nested requests, and $|D_i| = 6$ for nested requests. Each request was randomly chosen to be a read (as opposed to a write) with probability 0.2 and to be a nested request with probability 0.2. Due to write expansion, $|D_i|$ was inflated to 64 for all write requests under the RW-RNLP, as read requests can access any resource.

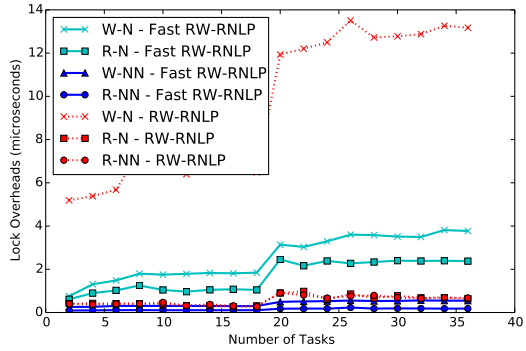

(a) Lock overhead.

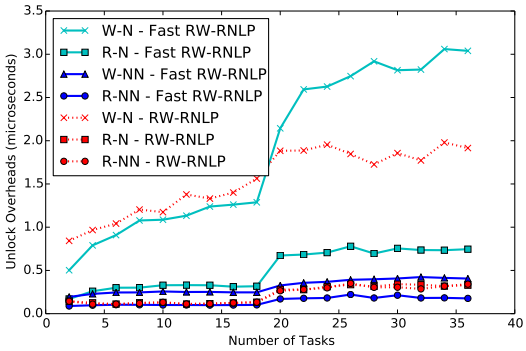

(b) Unlock overhead.

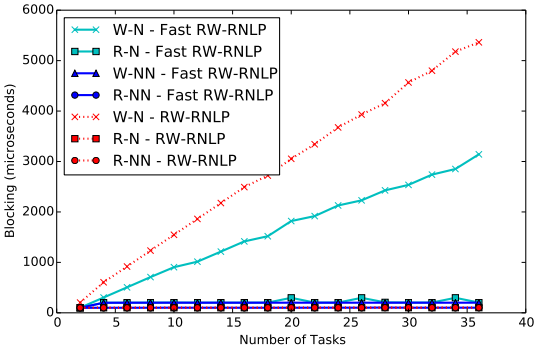

(c) Blocking.

Figure 198: (a) Lock and (b) unlock overheads and (c) blocking for nested and non-nested read and write requests under the RW-RNLP and the fast RW-RNLP. Here, for each request $\mathcal{R}_i$, $L_i = 100\mu$s, $n_r = 64$, $|D_i| = 1$ for non-nested requests, and $|D_i| = 6$ for nested requests. Each request was randomly chosen to be a read (as opposed to a write) with probability 0.2 and to be a nested request with probability 0.5. Due to write expansion, $|D_i|$ was inflated to 64 for all write requests under the RW-RNLP, as read requests can access any resource.

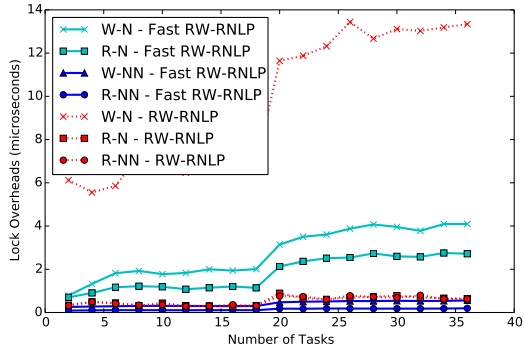

(a) Lock overhead.

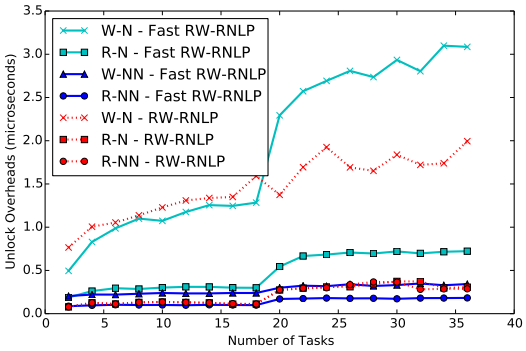

(b) Unlock overhead.

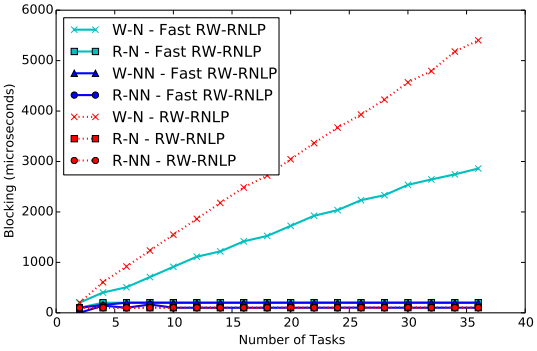

(c) Blocking.

Figure 199: (a) Lock and (b) unlock overheads and (c) blocking for nested and non-nested read and write requests under the RW-RNLP and the fast RW-RNLP. Here, for each request $\mathcal{R}_i$, $L_i = 100\mu$s, $n_r = 64$, $|D_i| = 1$ for non-nested requests, and $|D_i| = 6$ for nested requests. Each request was randomly chosen to be a read (as opposed to a write) with probability 0.2 and to be a nested request with probability 0.8. Due to write expansion, $|D_i|$ was inflated to 64 for all write requests under the RW-RNLP, as read requests can access any resource.

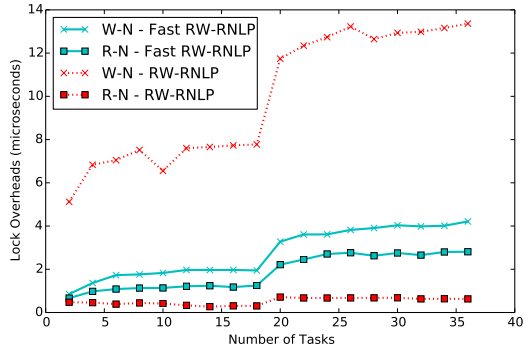

(a) Lock overhead.

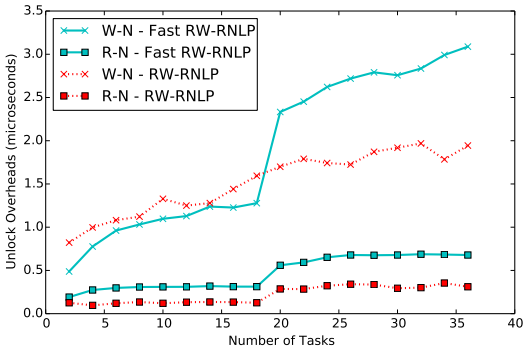

(b) Unlock overhead.

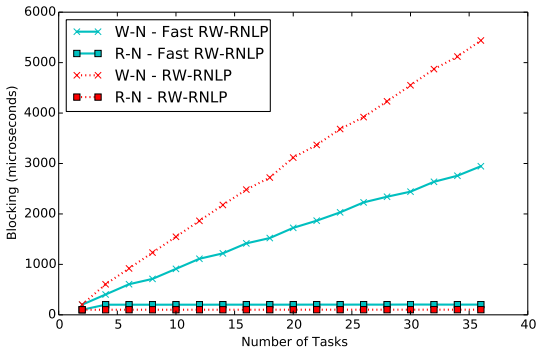

(c) Blocking.

Figure 200: (a) Lock and (b) unlock overheads and (c) blocking for nested read and write requests under the RW-RNLP and the fast RW-RNLP. Here, for each request $\mathcal{R}_i$, $L_i = 100\mu$s, $n_r = 64$, and $|D_i| = 6$. Each request was randomly chosen to be a read (as opposed to a write) with probability 0.2 and to be a nested request with probability 1. Due to write expansion, $|D_i|$ was inflated to 64 for all write requests under the RW-RNLP, as read requests can access any resource.

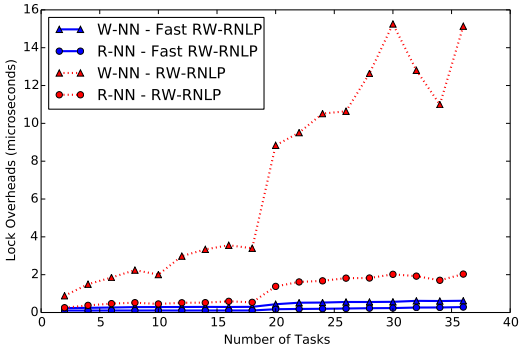

(a) Lock overhead.

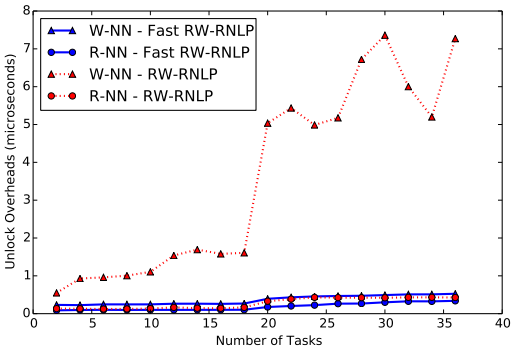

(b) Unlock overhead.

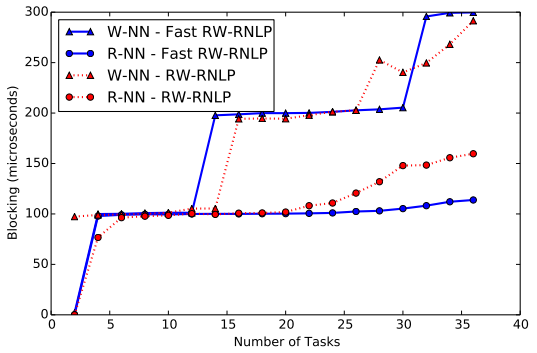

(c) Blocking.

Figure 201: (a) Lock and (b) unlock overheads and (c) blocking for non-nested read and write requests under the RW-RNLP and the fast RW-RNLP. Here, for each request $\mathcal{R}_i$, $L_i = 100\mu$s, $n_r = 64$, and $|D_i| = 1$. Each request was randomly chosen to be a read (as opposed to a write) with probability 0.5 and to be a nested request with probability 0.

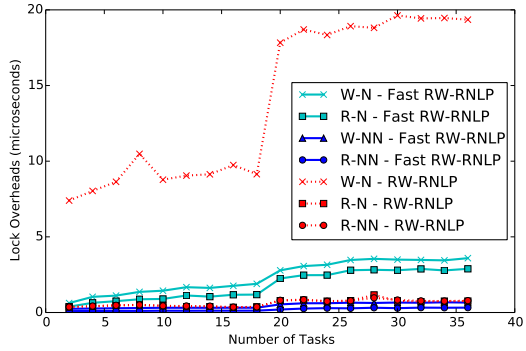

(a) Lock overhead.

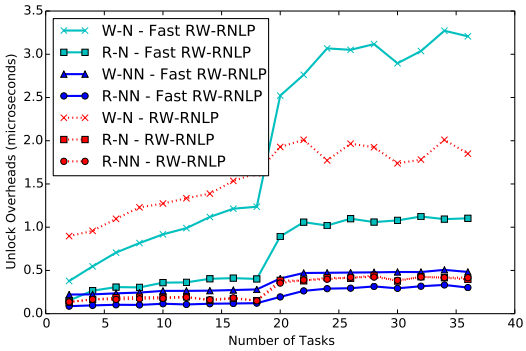

(b) Unlock overhead.

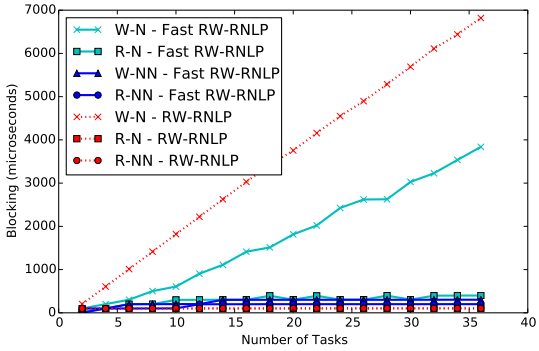

(c) Blocking.

Figure 202: (a) Lock and (b) unlock overheads and (c) blocking for nested and non-nested read and write requests under the RW-RNLP and the fast RW-RNLP. Here, for each request $\mathcal{R}_i$, $L_i = 100\mu$s, $n_r = 64$, $|D_i| = 1$ for non-nested requests, and $|D_i| = 6$ for nested requests. Each request was randomly chosen to be a read (as opposed to a write) with probability 0.5 and to be a nested request with probability 0.2. Due to write expansion, $|D_i|$ was inflated to 64 for all write requests under the RW-RNLP, as read requests can access any resource.

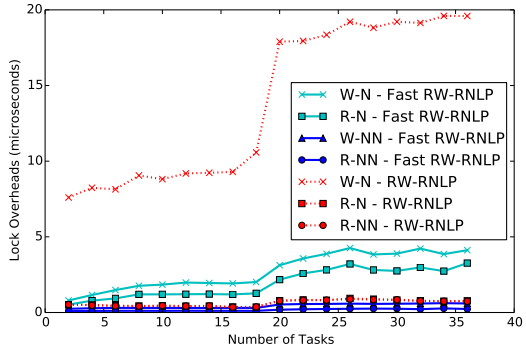

(a) Lock overhead.

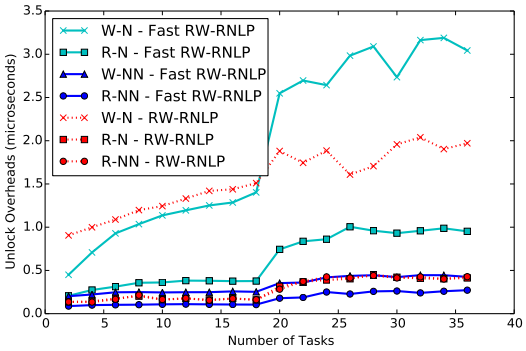

(b) Unlock overhead.

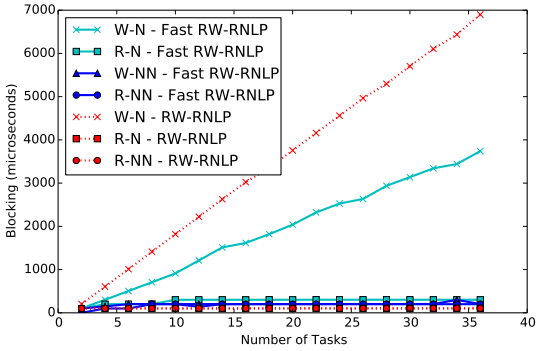

(c) Blocking.

Figure 203: (a) Lock and (b) unlock overheads and (c) blocking for nested and non-nested read and write requests under the RW-RNLP and the fast RW-RNLP. Here, for each request $\mathcal{R}_i$, $L_i = 100\mu$s, $n_r = 64$, $|D_i| = 1$ for non-nested requests, and $|D_i| = 6$ for nested requests. Each request was randomly chosen to be a read (as opposed to a write) with probability 0.5 and to be a nested request with probability 0.5. Due to write expansion, $|D_i|$ was inflated to 64 for all write requests under the RW-RNLP, as read requests can access any resource.

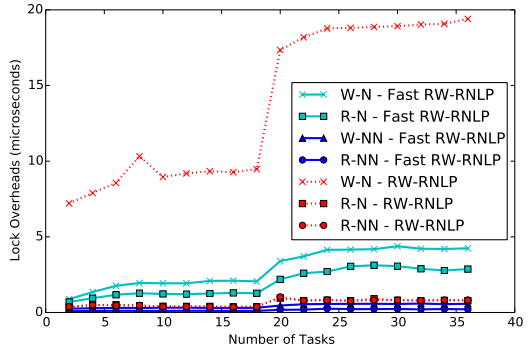

(a) Lock overhead.

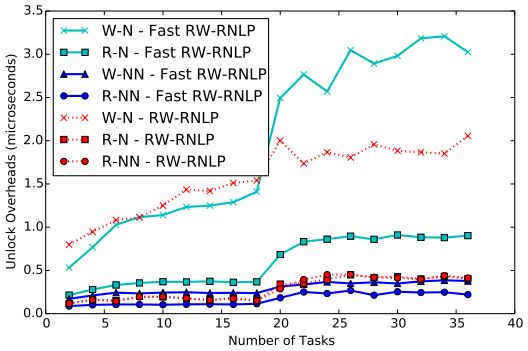

(b) Unlock overhead.

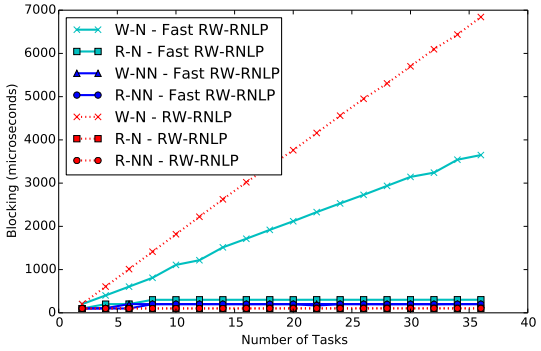

(c) Blocking.

Figure 204: (a) Lock and (b) unlock overheads and (c) blocking for nested and non-nested read and write requests under the RW-RNLP and the fast RW-RNLP. Here, for each request $\mathcal{R}_i$, $L_i = 100\mu$s, $n_r = 64$, $|D_i| = 1$ for non-nested requests, and $|D_i| = 6$ for nested requests. Each request was randomly chosen to be a read (as opposed to a write) with probability 0.5 and to be a nested request with probability 0.8. Due to write expansion, $|D_i|$ was inflated to 64 for all write requests under the RW-RNLP, as read requests can access any resource.

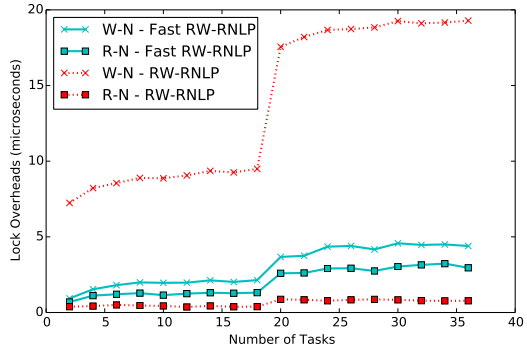

(a) Lock overhead.

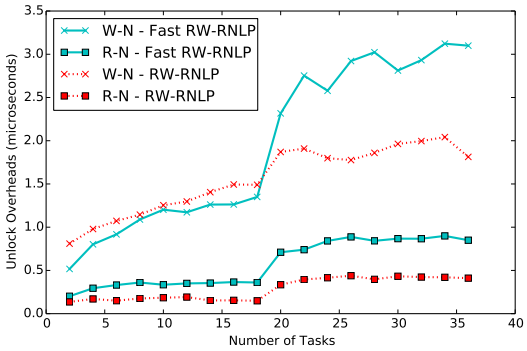

(b) Unlock overhead.

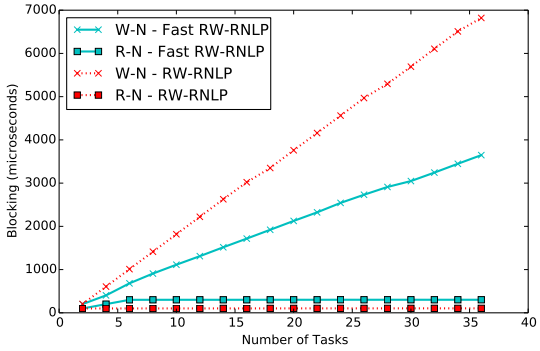

(c) Blocking.

Figure 205: (a) Lock and (b) unlock overheads and (c) blocking for nested read and write requests under the RW-RNLP and the fast RW-RNLP. Here, for each request $\mathcal{R}_i$, $L_i = 100\mu$s, $n_r = 64$, and $|D_i| = 6$. Each request was randomly chosen to be a read (as opposed to a write) with probability 0.5 and to be a nested request with probability 1. Due to write expansion, $|D_i|$ was inflated to 64 for all write requests under the RW-RNLP, as read requests can access any resource.

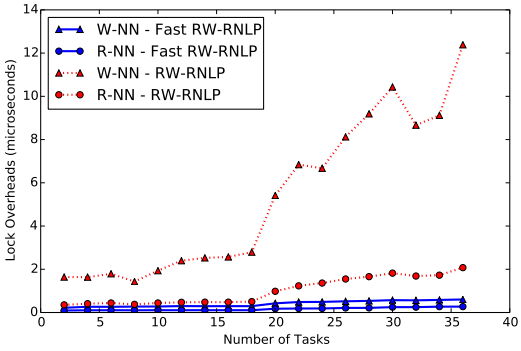

(a) Lock overhead.

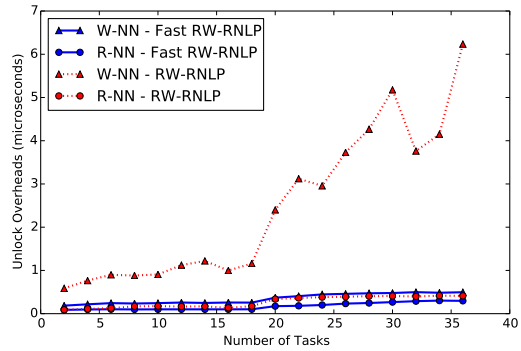

(b) Unlock overhead.

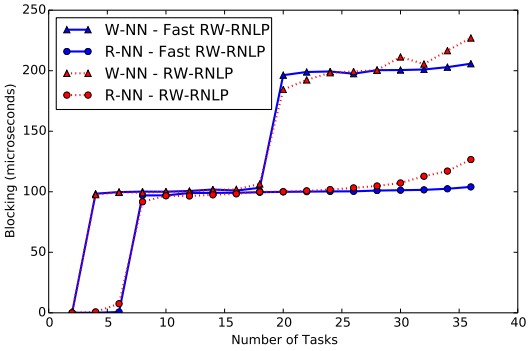

(c) Blocking.

Figure 206: (a) Lock and (b) unlock overheads and (c) blocking for non-nested read and write requests under the RW-RNLP and the fast RW-RNLP. Here, for each request $\mathcal{R}_i$, $L_i = 100\mu$s, $n_r = 64$, and $|D_i| = 1$. Each request was randomly chosen to be a read (as opposed to a write) with probability 0.8 and to be a nested request with probability 0.

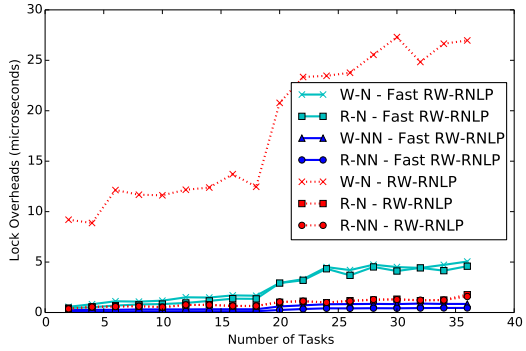

(a) Lock overhead.

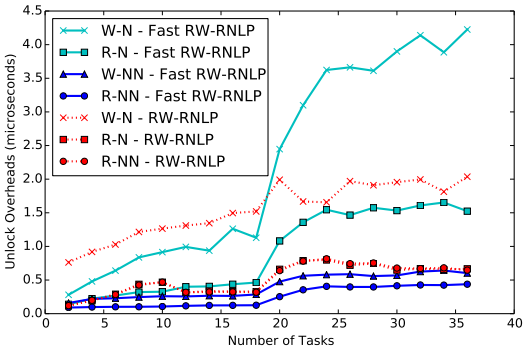

(b) Unlock overhead.

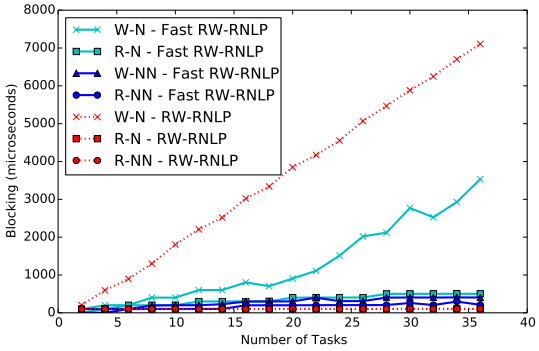

(c) Blocking.

Figure 207: (a) Lock and (b) unlock overheads and (c) blocking for nested and non-nested read and write requests under the RW-RNLP and the fast RW-RNLP. Here, for each request $\mathcal{R}_i$, $L_i = 100\mu$s, $n_r = 64$, $|D_i| = 1$ for non-nested requests, and $|D_i| = 6$ for nested requests. Each request was randomly chosen to be a read (as opposed to a write) with probability 0.8 and to be a nested request with probability 0.2. Due to write expansion, $|D_i|$ was inflated to 64 for all write requests under the RW-RNLP, as read requests can access any resource.

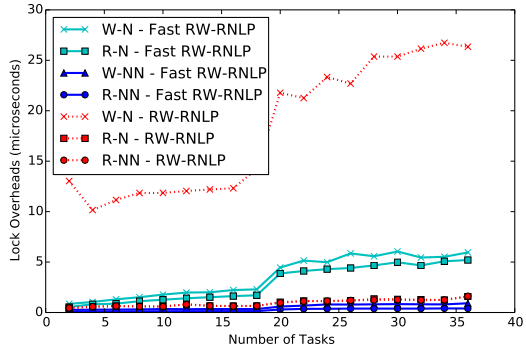

(a) Lock overhead.

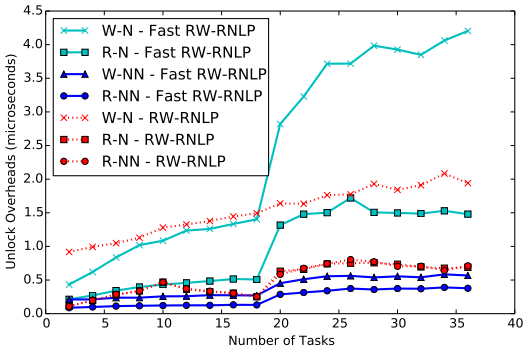

(b) Unlock overhead.

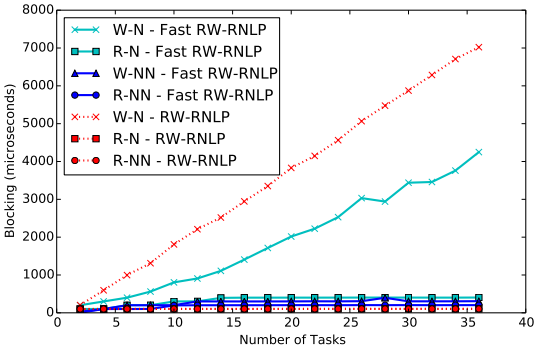

(c) Blocking.

Figure 208: (a) Lock and (b) unlock overheads and (c) blocking for nested and non-nested read and write requests under the RW-RNLP and the fast RW-RNLP. Here, for each request $\mathcal{R}_i$, $L_i = 100\mu$s, $n_r = 64$, $|D_i| = 1$ for non-nested requests, and $|D_i| = 6$ for nested requests. Each request was randomly chosen to be a read (as opposed to a write) with probability 0.8 and to be a nested request with probability 0.5. Due to write expansion, $|D_i|$ was inflated to 64 for all write requests under the RW-RNLP, as read requests can access any resource.

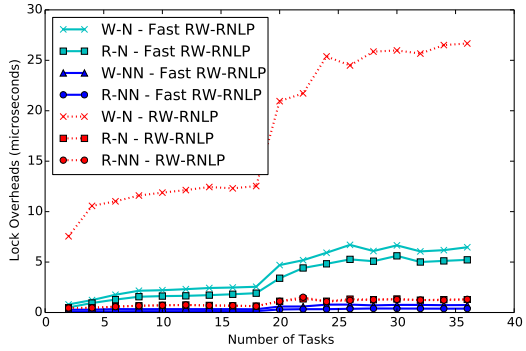

(a) Lock overhead.

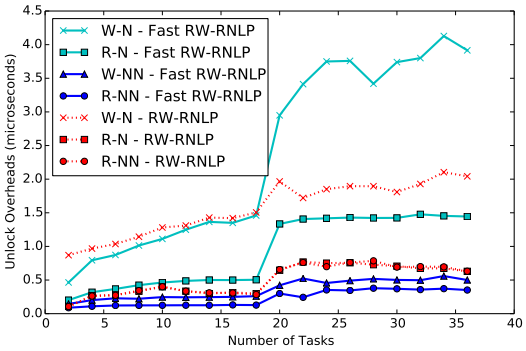

(b) Unlock overhead.

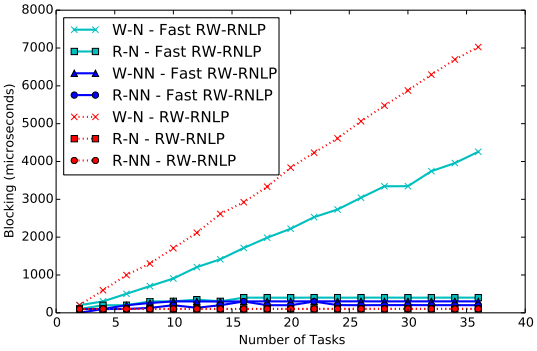

(c) Blocking.

Figure 209: (a) Lock and (b) unlock overheads and (c) blocking for nested and non-nested read and write requests under the RW-RNLP and the fast RW-RNLP. Here, for each request $\mathcal{R}_i$, $L_i = 100\mu$s, $n_r = 64$, $|D_i| = 1$ for non-nested requests, and $|D_i| = 6$ for nested requests. Each request was randomly chosen to be a read (as opposed to a write) with probability 0.8 and to be a nested request with probability 0.8. Due to write expansion, $|D_i|$ was inflated to 64 for all write requests under the RW-RNLP, as read requests can access any resource.

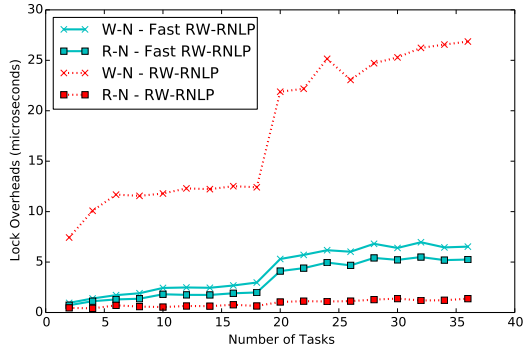

(a) Lock overhead.

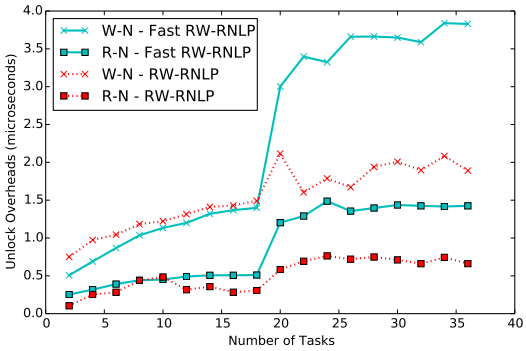

(b) Unlock overhead.

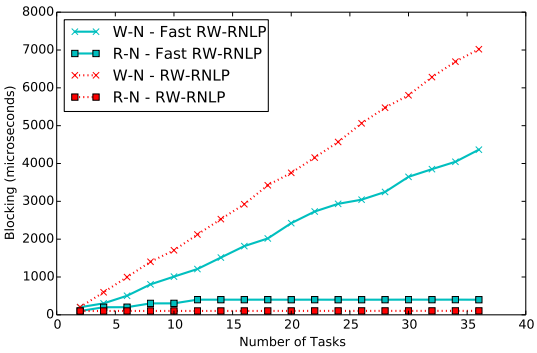

(c) Blocking.

Figure 210: (a) Lock and (b) unlock overheads and (c) blocking for nested read and write requests under the RW-RNLP and the fast RW-RNLP. Here, for each request $\mathcal{R}_i$, $L_i = 100\mu$s, $n_r = 64$, and $|D_i| = 6$. Each request was randomly chosen to be a read (as opposed to a write) with probability 0.8 and to be a nested request with probability 1. Due to write expansion, $|D_i|$ was inflated to 64 for all write requests under the RW-RNLP, as read requests can access any resource.

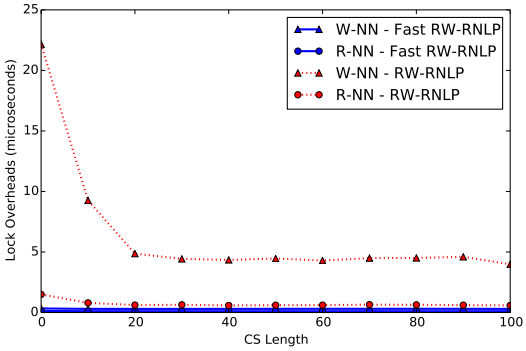

(a) Lock overhead.

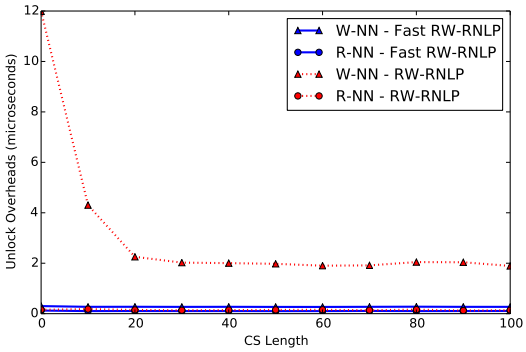

(b) Unlock overhead.

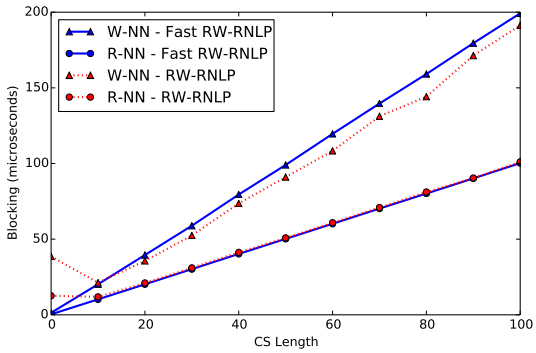

(c) Blocking.

Figure 211: (a) Lock and (b) unlock overheads and (c) blocking for non-nested read and write requests under the RW-RNLP and the fast RW-RNLP. Here, for each request $\mathcal{R}_i$, $m = 18$, $n_r = 64$, and $|D_i| = 1$. Each request was randomly chosen to be a read (as opposed to a write) with probability 0.2 and to be a nested request with probability 0.

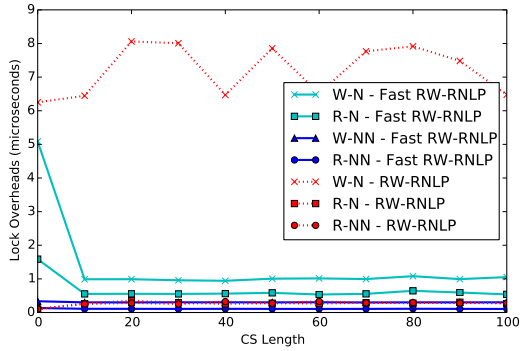

(a) Lock overhead.

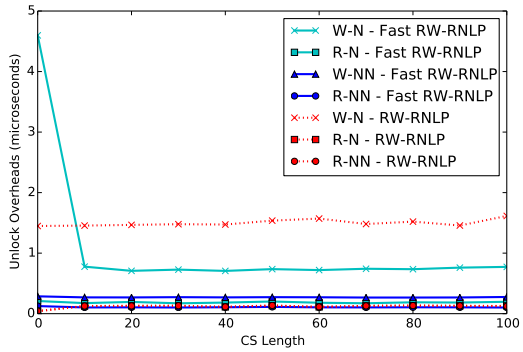

(b) Unlock overhead.

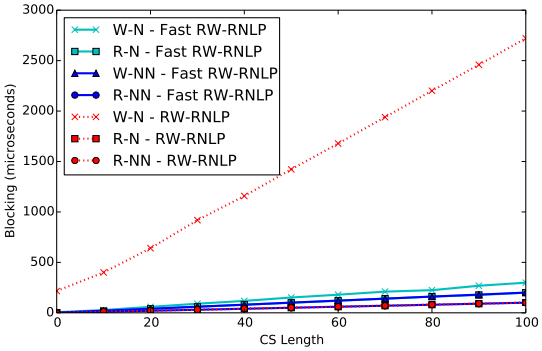

(c) Blocking.

Figure 212: (a) Lock and (b) unlock overheads and (c) blocking for nested and non-nested read and write requests under the RW-RNLP and the fast RW-RNLP. Here, for each request $\mathcal{R}_i$, $m = 18$, $n_r = 64$, $|D_i| = 1$ for non-nested requests, and $|D_i| = 2$ for nested requests. Each request was randomly chosen to be a read (as opposed to a write) with probability 0.2 and to be a nested request with probability 0.2. Due to write expansion, $|D_i|$ was inflated to 64 for all write requests under the RW-RNLP, as read requests can access any resource.

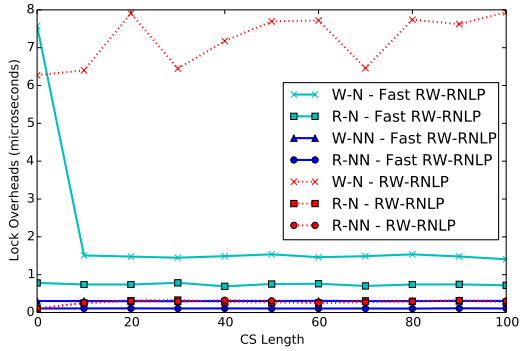

(a) Lock overhead.

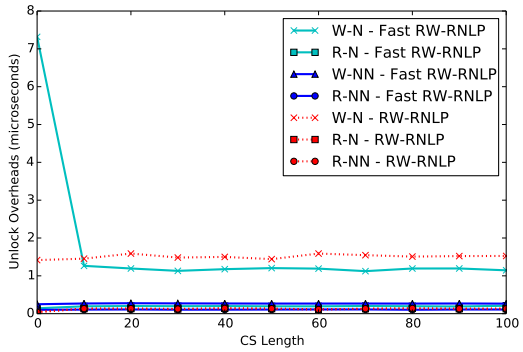

(b) Unlock overhead.

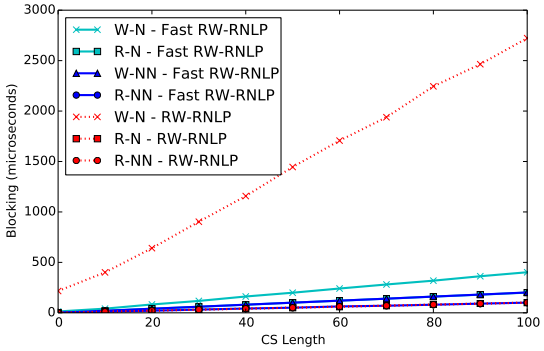

(c) Blocking.

Figure 213: (a) Lock and (b) unlock overheads and (c) blocking for nested and non-nested read and write requests under the RW-RNLP and the fast RW-RNLP. Here, for each request $\mathcal{R}_i$, $m = 18$, $n_r = 64$, $|D_i| = 1$ for non-nested requests, and $|D_i| = 2$ for nested requests. Each request was randomly chosen to be a read (as opposed to a write) with probability 0.2 and to be a nested request with probability 0.5. Due to write expansion, $|D_i|$ was inflated to 64 for all write requests under the RW-RNLP, as read requests can access any resource.

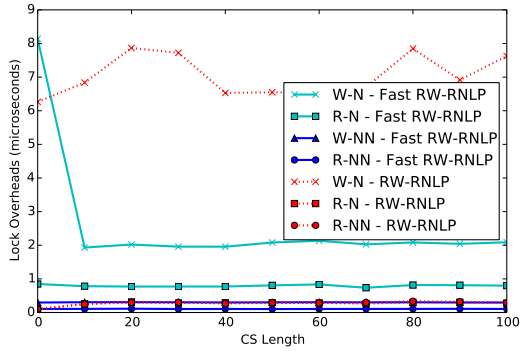

(a) Lock overhead.

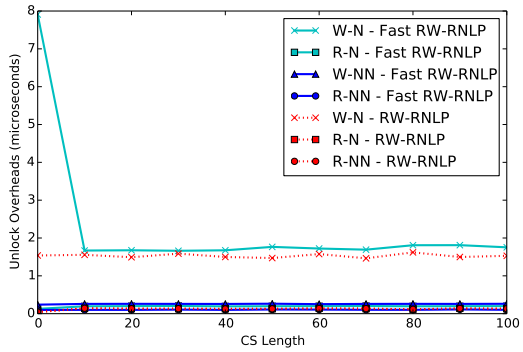

(b) Unlock overhead.

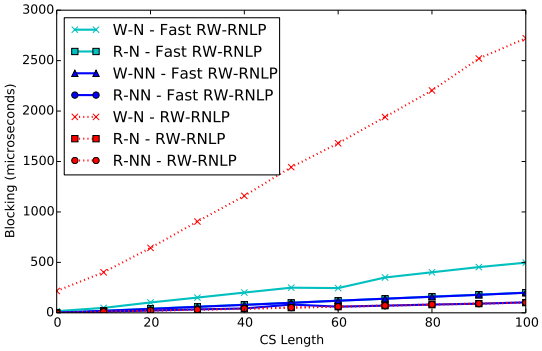

(c) Blocking.

Figure 214: (a) Lock and (b) unlock overheads and (c) blocking for nested and non-nested read and write requests under the RW-RNLP and the fast RW-RNLP. Here, for each request $\mathcal{R}_i$, $m = 18$, $n_r = 64$, $|D_i| = 1$ for non-nested requests, and $|D_i| = 2$ for nested requests. Each request was randomly chosen to be a read (as opposed to a write) with probability 0.2 and to be a nested request with probability 0.8. Due to write expansion, $|D_i|$ was inflated to 64 for all write requests under the RW-RNLP, as read requests can access any resource.

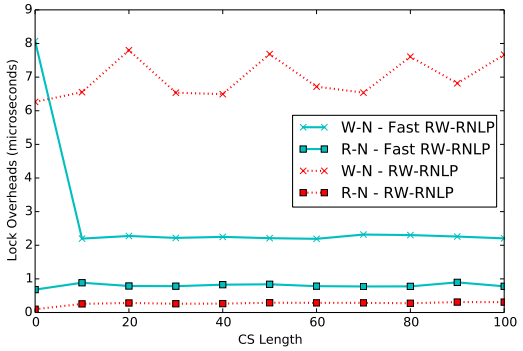

(a) Lock overhead.

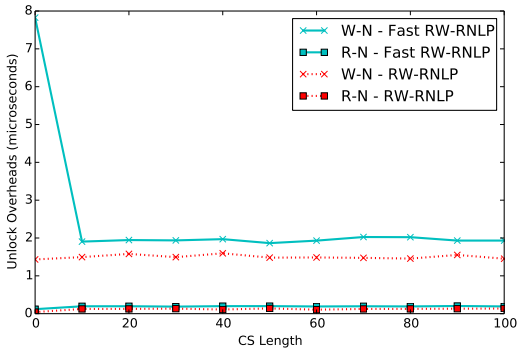

(b) Unlock overhead.

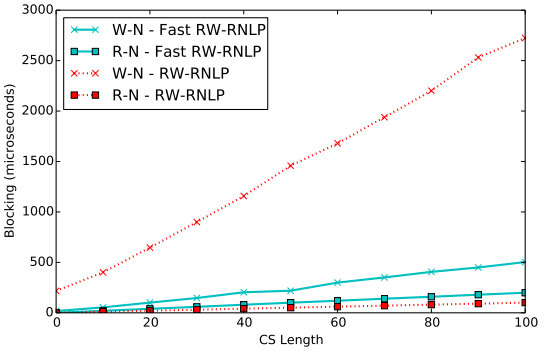

(c) Blocking.

Figure 215: (a) Lock and (b) unlock overheads and (c) blocking for nested read and write requests under the RW-RNLP and the fast RW-RNLP. Here, for each request $\mathcal{R}_i$, $m = 18$, $n_r = 64$, and $|D_i| = 2$. Each request was randomly chosen to be a read (as opposed to a write) with probability 0.2 and to be a nested request with probability 1. Due to write expansion, $|D_i|$ was inflated to 64 for all write requests under the RW-RNLP, as read requests can access any resource.

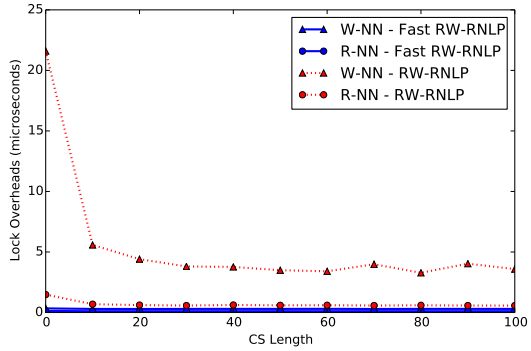

(a) Lock overhead.

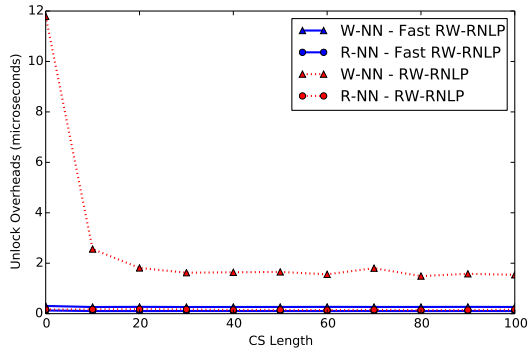

(b) Unlock overhead.

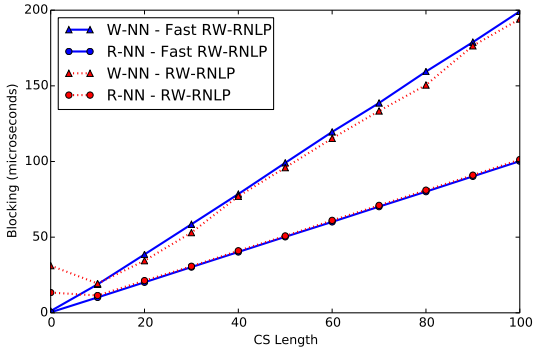

(c) Blocking.

Figure 216: (a) Lock and (b) unlock overheads and (c) blocking for non-nested read and write requests under the RW-RNLP and the fast RW-RNLP. Here, for each request $\mathcal{R}_i$, $m = 18$, $n_r = 64$, and $|D_i| = 1$. Each request was randomly chosen to be a read (as opposed to a write) with probability 0.5 and to be a nested request with probability 0.

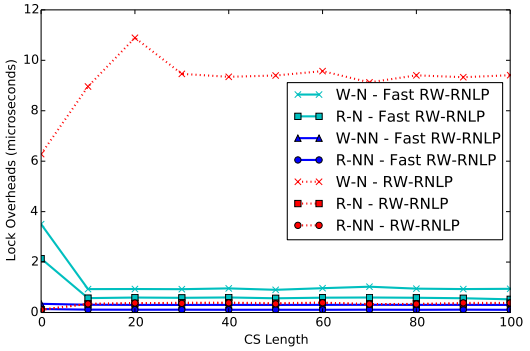

(a) Lock overhead.

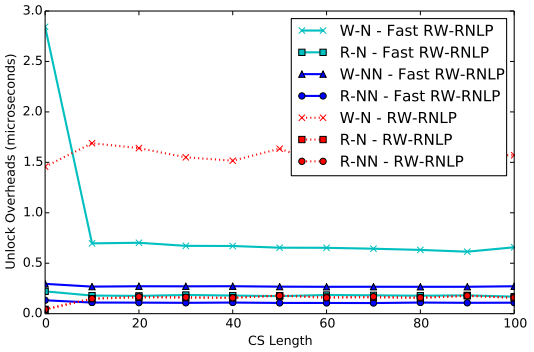

(b) Unlock overhead.

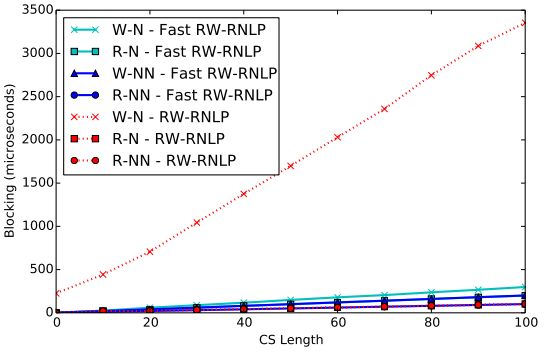

(c) Blocking.

Figure 217: (a) Lock and (b) unlock overheads and (c) blocking for nested and non-nested read and write requests under the RW-RNLP and the fast RW-RNLP. Here, for each request $\mathcal{R}_i$, $m = 18$, $n_r = 64$, $|D_i| = 1$ for non-nested requests, and $|D_i| = 2$ for nested requests. Each request was randomly chosen to be a read (as opposed to a write) with probability 0.5 and to be a nested request with probability 0.2. Due to write expansion, $|D_i|$ was inflated to 64 for all write requests under the RW-RNLP, as read requests can access any resource.

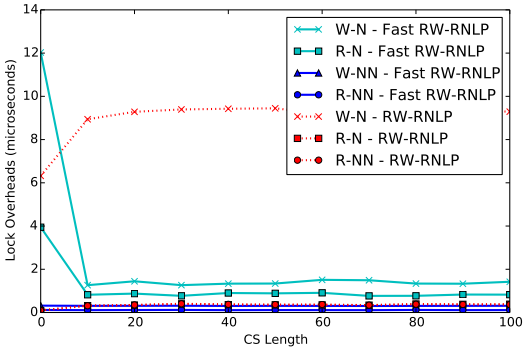

(a) Lock overhead.

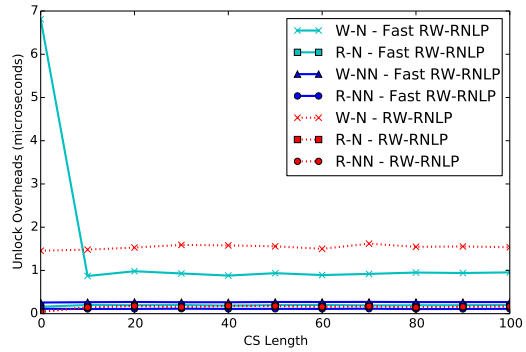

(b) Unlock overhead.

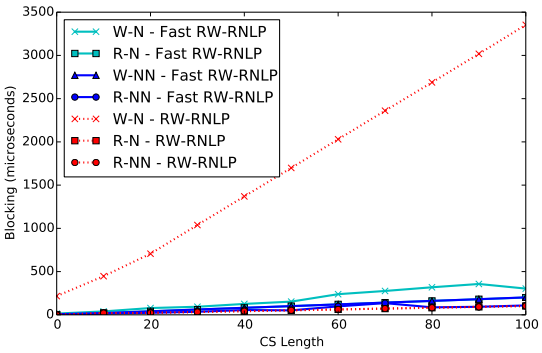

(c) Blocking.

Figure 218: (a) Lock and (b) unlock overheads and (c) blocking for nested and non-nested read and write requests under the RW-RNLP and the fast RW-RNLP. Here, for each request $\mathcal{R}_i$, $m = 18$, $n_r = 64$, $|D_i| = 1$ for non-nested requests, and $|D_i| = 2$ for nested requests. Each request was randomly chosen to be a read (as opposed to a write) with probability 0.5 and to be a nested request with probability 0.5. Due to write expansion, $|D_i|$ was inflated to 64 for all write requests under the RW-RNLP, as read requests can access any resource.

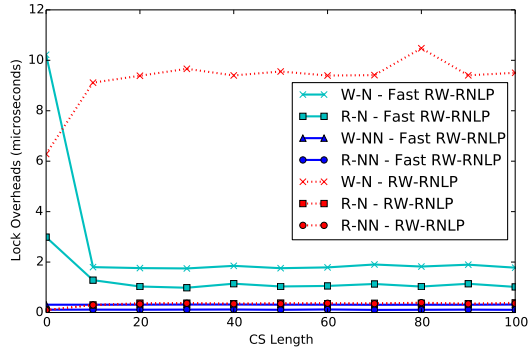

(a) Lock overhead.

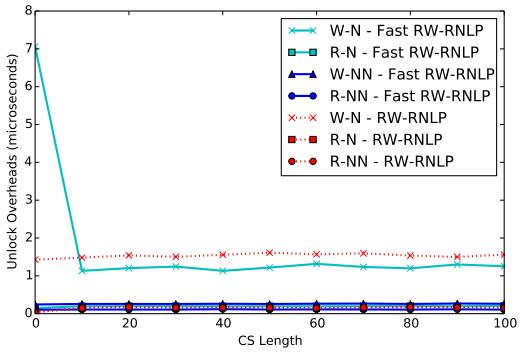

(b) Unlock overhead.

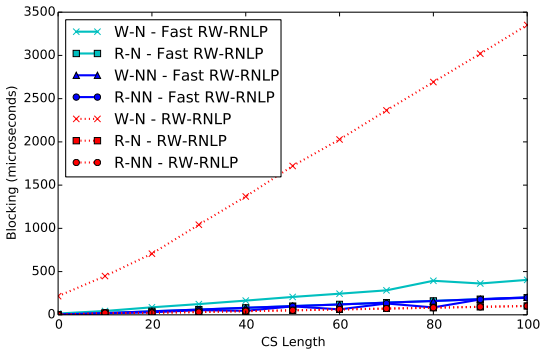

(c) Blocking.

Figure 219: (a) Lock and (b) unlock overheads and (c) blocking for nested and non-nested read and write requests under the RW-RNLP and the fast RW-RNLP. Here, for each request $\mathcal{R}_i$, $m = 18$, $n_r = 64$, $|D_i| = 1$ for non-nested requests, and $|D_i| = 2$ for nested requests. Each request was randomly chosen to be a read (as opposed to a write) with probability 0.5 and to be a nested request with probability 0.8. Due to write expansion, $|D_i|$ was inflated to 64 for all write requests under the RW-RNLP, as read requests can access any resource.

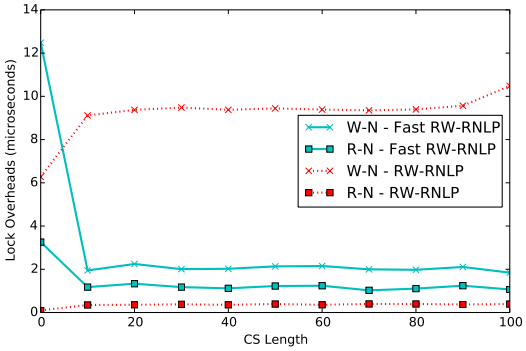

(a) Lock overhead.

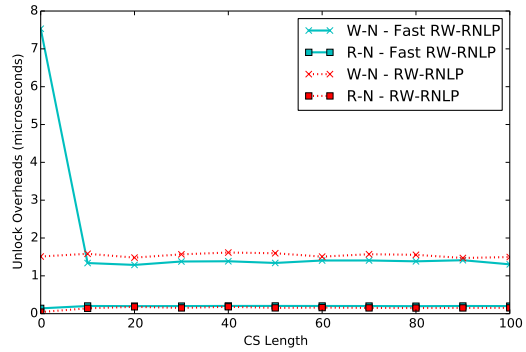

(b) Unlock overhead.

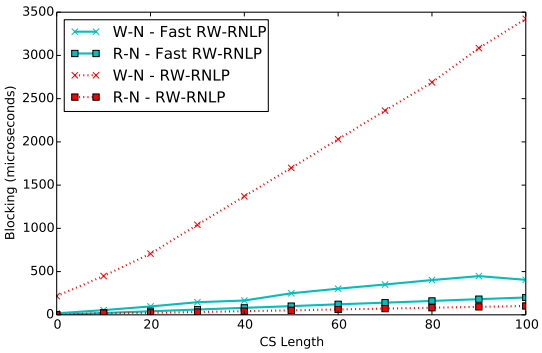

(c) Blocking.

Figure 220: (a) Lock and (b) unlock overheads and (c) blocking for nested read and write requests under the RW-RNLP and the fast RW-RNLP. Here, for each request $\mathcal{R}_i$, $m = 18$, $n_r = 64$, and $|D_i| = 2$. Each request was randomly chosen to be a read (as opposed to a write) with probability 0.5 and to be a nested request with probability 1. Due to write expansion, $|D_i|$ was inflated to 64 for all write requests under the RW-RNLP, as read requests can access any resource.

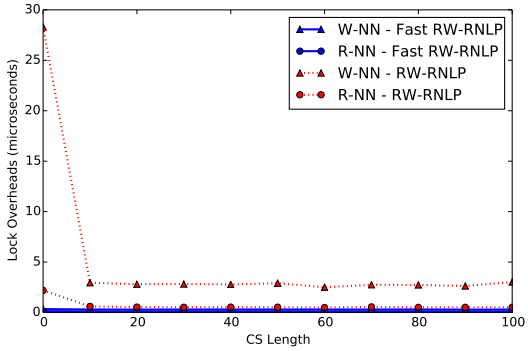

(a) Lock overhead.

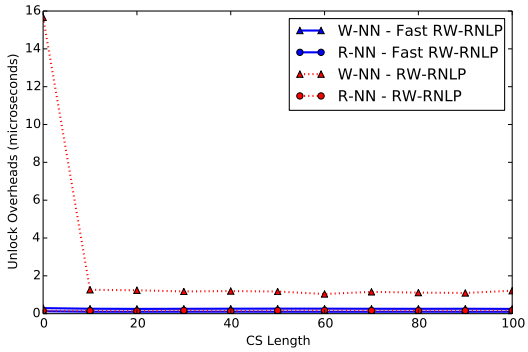

(b) Unlock overhead.

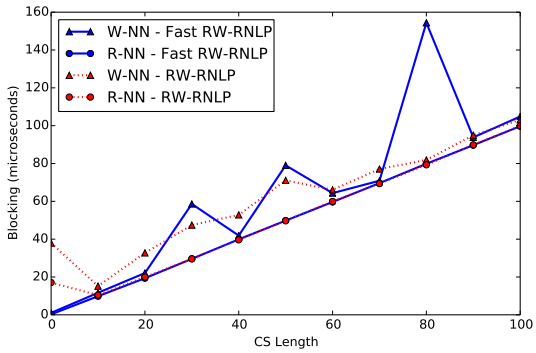

(c) Blocking.

Figure 221: (a) Lock and (b) unlock overheads and (c) blocking for non-nested read and write requests under the RW-RNLP and the fast RW-RNLP. Here, for each request $\mathcal{R}_i$, $m = 18$, $n_r = 64$, and $|D_i| = 1$. Each request was randomly chosen to be a read (as opposed to a write) with probability 0.8 and to be a nested request with probability 0.

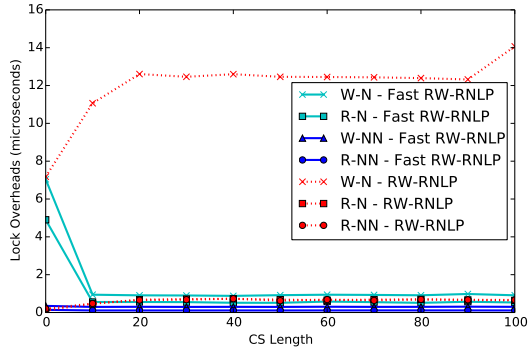

(a) Lock overhead.

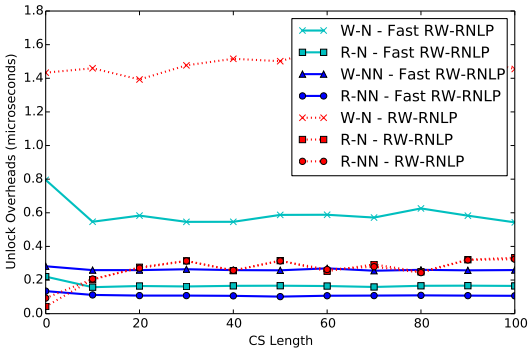

(b) Unlock overhead.

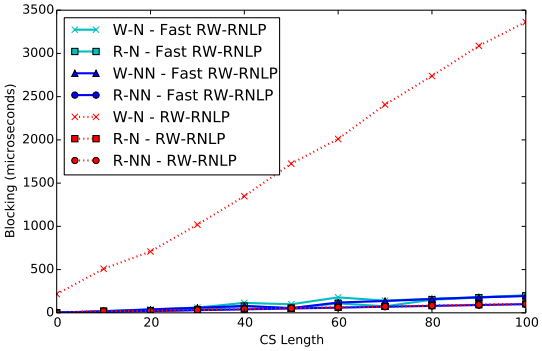

(c) Blocking.

Figure 222: (a) Lock and (b) unlock overheads and (c) blocking for nested and non-nested read and write requests under the RW-RNLP and the fast RW-RNLP. Here, for each request $\mathcal{R}_i$, $m = 18$, $n_r = 64$, $|D_i| = 1$ for non-nested requests, and $|D_i| = 2$ for nested requests. Each request was randomly chosen to be a read (as opposed to a write) with probability 0.8 and to be a nested request with probability 0.2. Due to write expansion, $|D_i|$ was inflated to 64 for all write requests under the RW-RNLP, as read requests can access any resource.

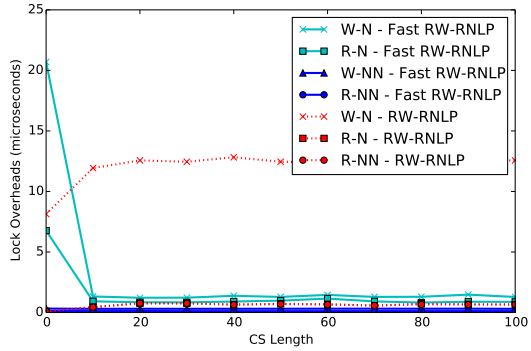

(a) Lock overhead.

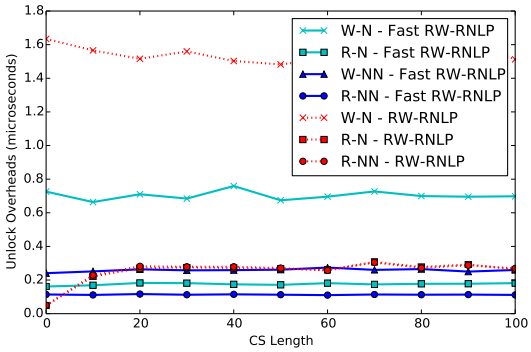

(b) Unlock overhead.

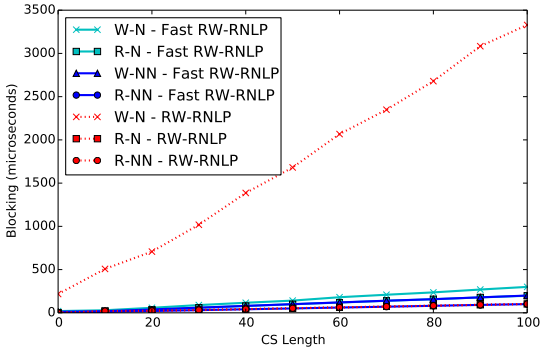

(c) Blocking.

Figure 223: (a) Lock and (b) unlock overheads and (c) blocking for nested and non-nested read and write requests under the RW-RNLP and the fast RW-RNLP. Here, for each request $\mathcal{R}_i$, $m = 18$, $n_r = 64$, $|D_i| = 1$ for non-nested requests, and $|D_i| = 2$ for nested requests. Each request was randomly chosen to be a read (as opposed to a write) with probability 0.8 and to be a nested request with probability 0.5. Due to write expansion, $|D_i|$ was inflated to 64 for all write requests under the RW-RNLP, as read requests can access any resource.

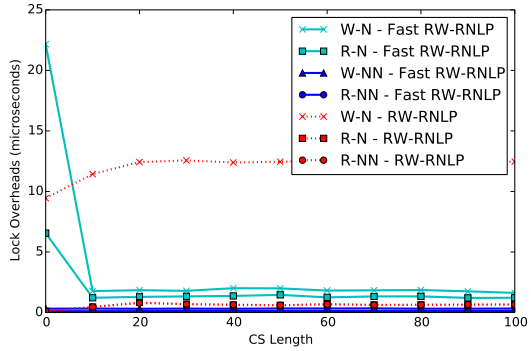

(a) Lock overhead.

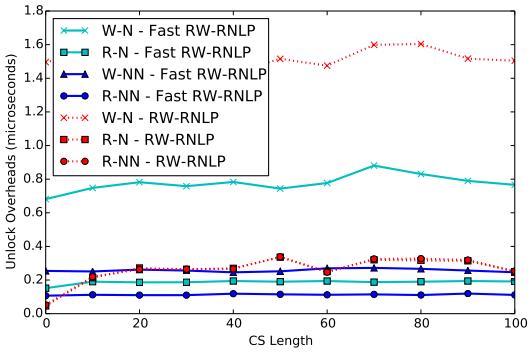

(b) Unlock overhead.

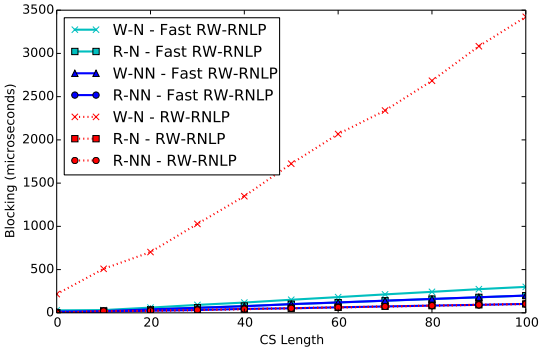

(c) Blocking.

Figure 224: (a) Lock and (b) unlock overheads and (c) blocking for nested and non-nested read and write requests under the RW-RNLP and the fast RW-RNLP. Here, for each request $\mathcal{R}_i$, $m = 18$, $n_r = 64$, $|D_i| = 1$ for non-nested requests, and $|D_i| = 2$ for nested requests. Each request was randomly chosen to be a read (as opposed to a write) with probability 0.8 and to be a nested request with probability 0.8. Due to write expansion, $|D_i|$ was inflated to 64 for all write requests under the RW-RNLP, as read requests can access any resource.

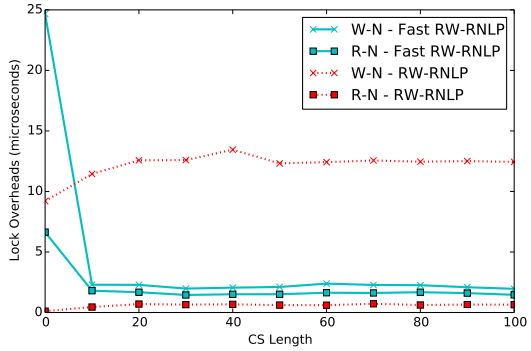

(a) Lock overhead.

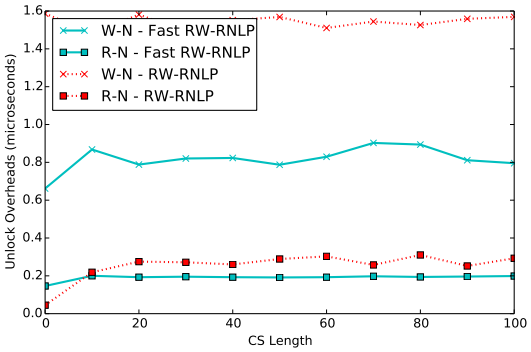

(b) Unlock overhead.

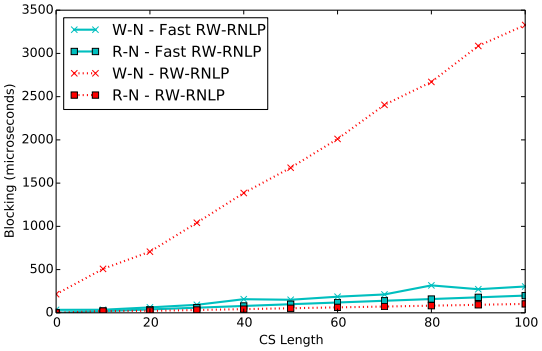

(c) Blocking.

Figure 225: (a) Lock and (b) unlock overheads and (c) blocking for nested read and write requests under the RW-RNLP and the fast RW-RNLP. Here, for each request $\mathcal{R}_i$, $m = 18$, $n_r = 64$, and $|D_i| = 2$. Each request was randomly chosen to be a read (as opposed to a write) with probability 0.8 and to be a nested request with probability 1. Due to write expansion, $|D_i|$ was inflated to 64 for all write requests under the RW-RNLP, as read requests can access any resource.

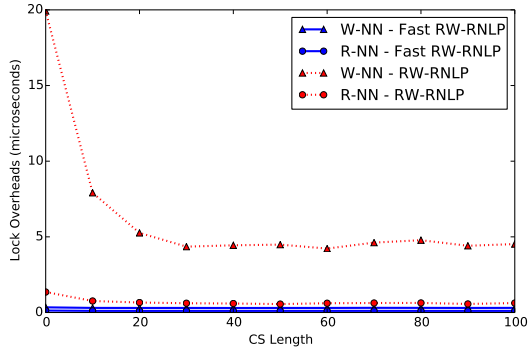

(a) Lock overhead.

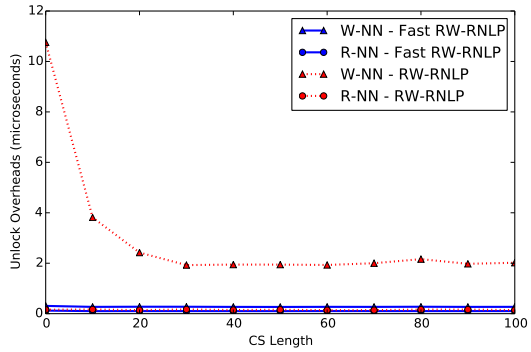

(b) Unlock overhead.

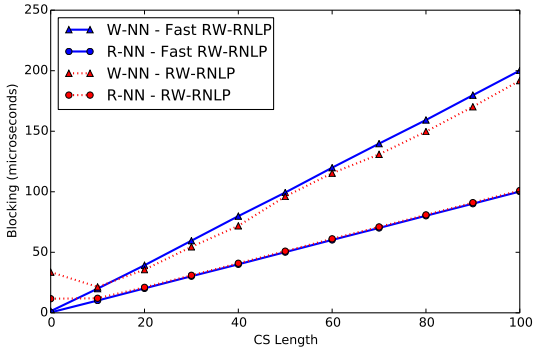

(c) Blocking.

Figure 226: (a) Lock and (b) unlock overheads and (c) blocking for non-nested read and write requests under the RW-RNLP and the fast RW-RNLP. Here, for each request $\mathcal{R}_i$, $m = 18$, $n_r = 64$, and $|D_i| = 1$. Each request was randomly chosen to be a read (as opposed to a write) with probability 0.2 and to be a nested request with probability 0.

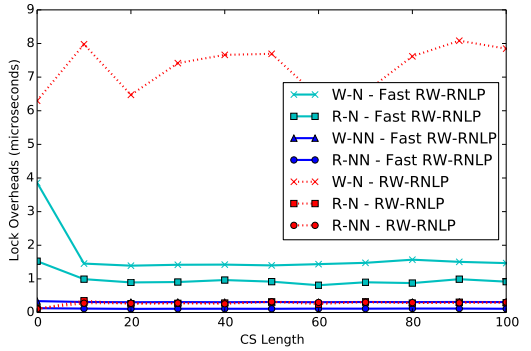

(a) Lock overhead.

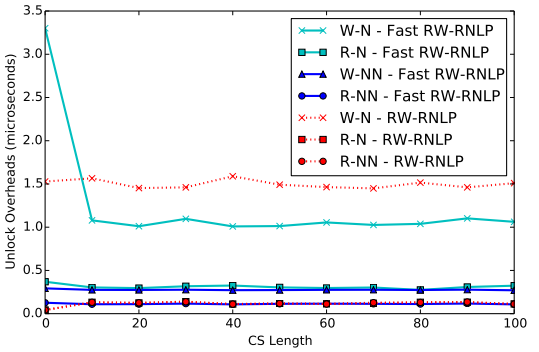

(b) Unlock overhead.

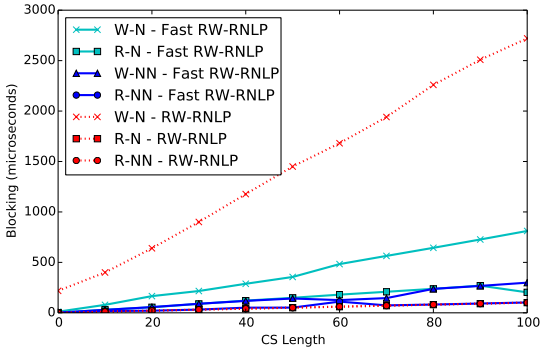

(c) Blocking.

Figure 227: (a) Lock and (b) unlock overheads and (c) blocking for nested and non-nested read and write requests under the RW-RNLP and the fast RW-RNLP. Here, for each request $\mathcal{R}_i$, $m = 18$, $n_r = 64$, $|D_i| = 1$ for non-nested requests, and $|D_i| = 4$ for nested requests. Each request was randomly chosen to be a read (as opposed to a write) with probability 0.2 and to be a nested request with probability 0.2. Due to write expansion, $|D_i|$ was inflated to 64 for all write requests under the RW-RNLP, as read requests can access any resource.

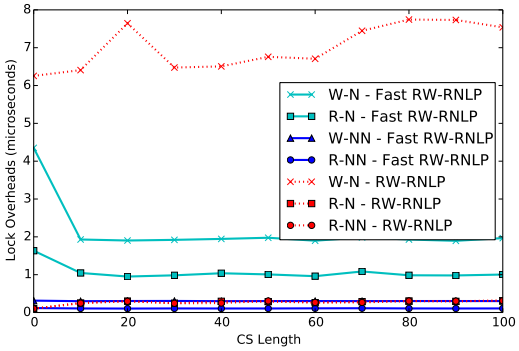

(a) Lock overhead.

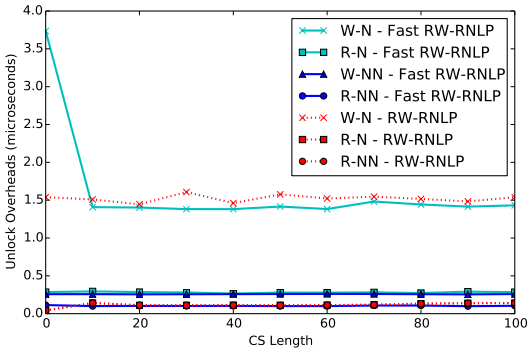

(b) Unlock overhead.

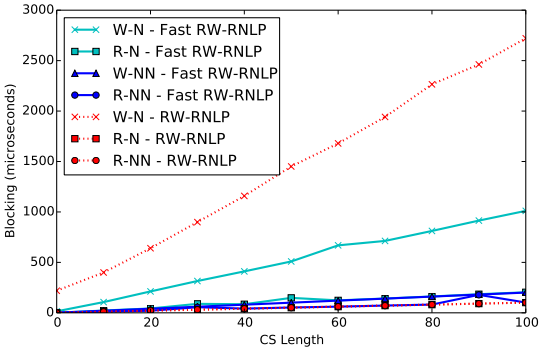

(c) Blocking.

Figure 228: (a) Lock and (b) unlock overheads and (c) blocking for nested and non-nested read and write requests under the RW-RNLP and the fast RW-RNLP. Here, for each request $\mathcal{R}_i$, $m = 18$, $n_r = 64$, $|D_i| = 1$ for non-nested requests, and $|D_i| = 4$ for nested requests. Each request was randomly chosen to be a read (as opposed to a write) with probability 0.2 and to be a nested request with probability 0.5. Due to write expansion, $|D_i|$ was inflated to 64 for all write requests under the RW-RNLP, as read requests can access any resource.

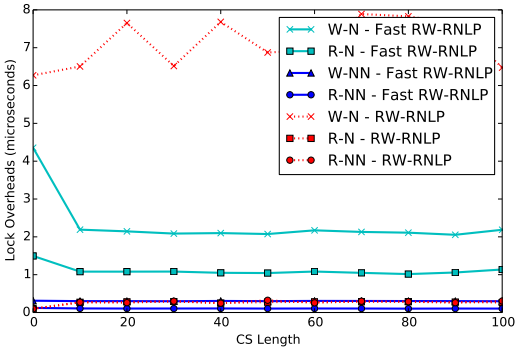

(a) Lock overhead.

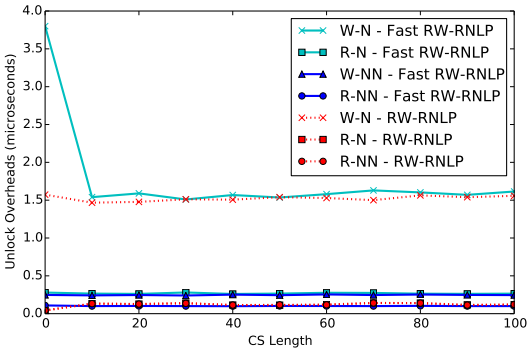

(b) Unlock overhead.

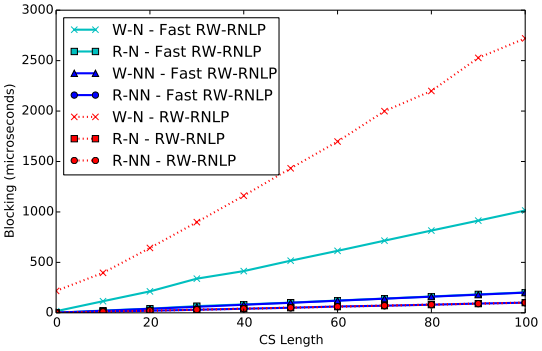

(c) Blocking.

Figure 229: (a) Lock and (b) unlock overheads and (c) blocking for nested and non-nested read and write requests under the RW-RNLP and the fast RW-RNLP. Here, for each request $\mathcal{R}_i$, $m = 18$, $n_r = 64$, $|D_i| = 1$ for non-nested requests, and $|D_i| = 4$ for nested requests. Each request was randomly chosen to be a read (as opposed to a write) with probability 0.2 and to be a nested request with probability 0.8. Due to write expansion, $|D_i|$ was inflated to 64 for all write requests under the RW-RNLP, as read requests can access any resource.

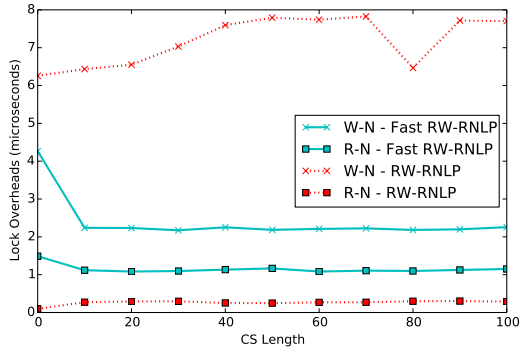

(a) Lock overhead.

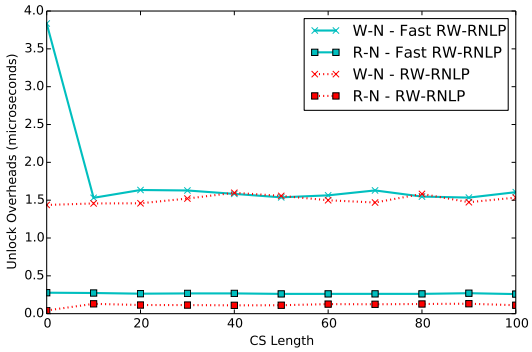

(b) Unlock overhead.

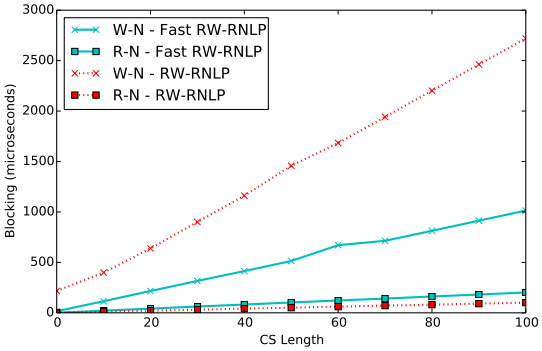

(c) Blocking.

Figure 230: (a) Lock and (b) unlock overheads and (c) blocking for nested read and write requests under the RW-RNLP and the fast RW-RNLP. Here, for each request $\mathcal{R}_i$, $m = 18$, $n_r = 64$, and $|D_i| = 4$. Each request was randomly chosen to be a read (as opposed to a write) with probability 0.2 and to be a nested request with probability 1. Due to write expansion, $|D_i|$ was inflated to 64 for all write requests under the RW-RNLP, as read requests can access any resource.

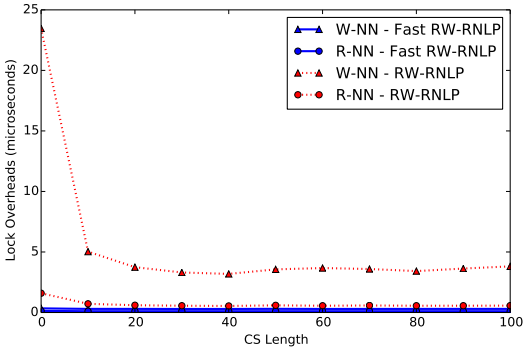

(a) Lock overhead.

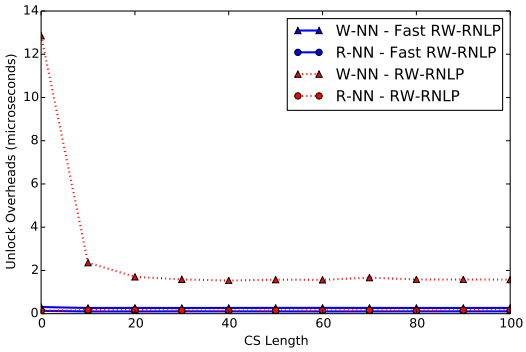

(b) Unlock overhead.

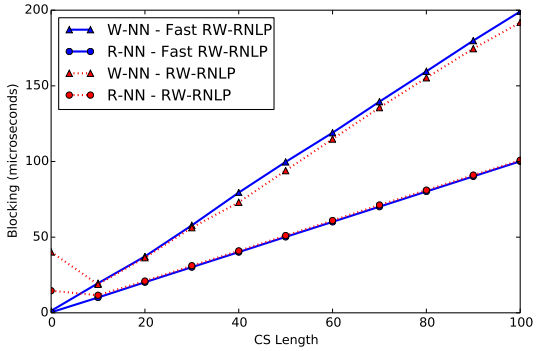

(c) Blocking.

Figure 231: (a) Lock and (b) unlock overheads and (c) blocking for non-nested read and write requests under the RW-RNLP and the fast RW-RNLP. Here, for each request $\mathcal{R}_i$, $m = 18$, $n_r = 64$, and $|D_i| = 1$. Each request was randomly chosen to be a read (as opposed to a write) with probability 0.5 and to be a nested request with probability 0.

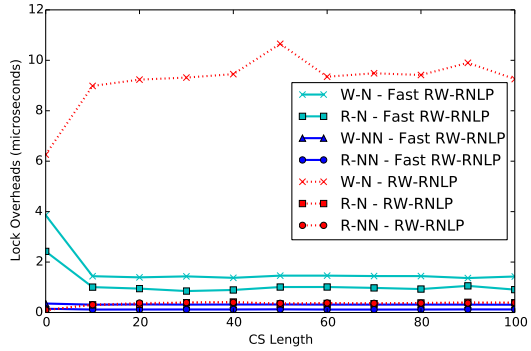

(a) Lock overhead.

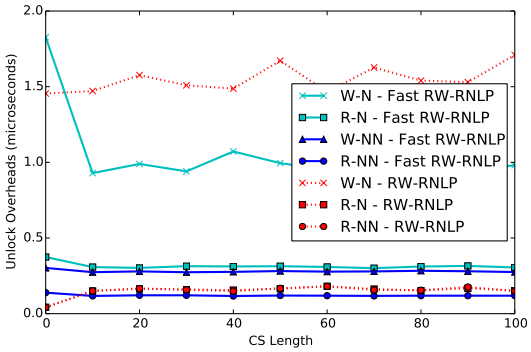

(b) Unlock overhead.

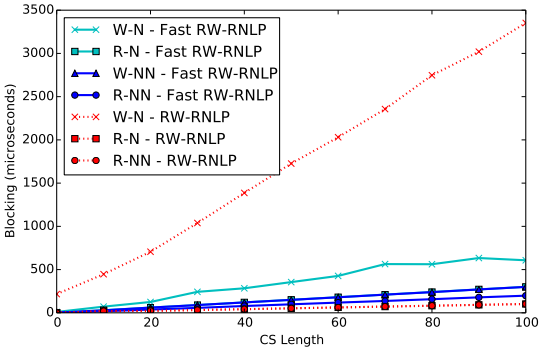

(c) Blocking.

Figure 232: (a) Lock and (b) unlock overheads and (c) blocking for nested and non-nested read and write requests under the RW-RNLP and the fast RW-RNLP. Here, for each request $\mathcal{R}_i$, $m = 18$, $n_r = 64$, $|D_i| = 1$ for non-nested requests, and $|D_i| = 4$ for nested requests. Each request was randomly chosen to be a read (as opposed to a write) with probability 0.5 and to be a nested request with probability 0.2. Due to write expansion, $|D_i|$ was inflated to 64 for all write requests under the RW-RNLP, as read requests can access any resource.

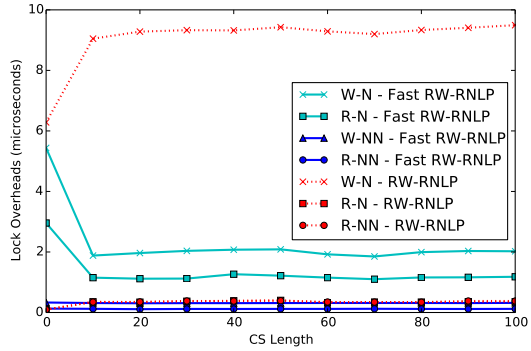

(a) Lock overhead.

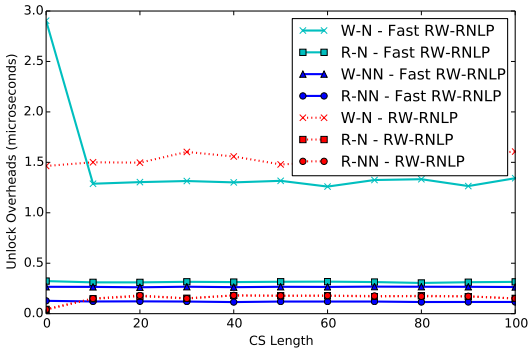

(b) Unlock overhead.

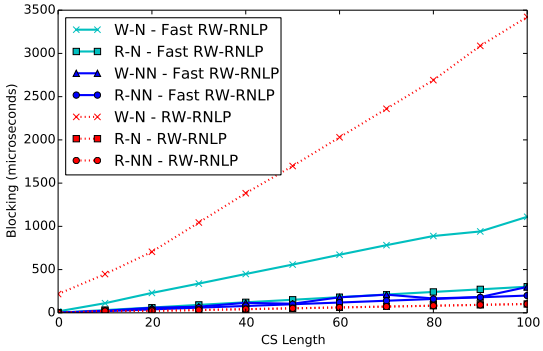

(c) Blocking.

Figure 233: (a) Lock and (b) unlock overheads and (c) blocking for nested and non-nested read and write requests under the RW-RNLP and the fast RW-RNLP. Here, for each request $\mathcal{R}_i$, $m = 18$, $n_r = 64$, $|D_i| = 1$ for non-nested requests, and $|D_i| = 4$ for nested requests. Each request was randomly chosen to be a read (as opposed to a write) with probability 0.5 and to be a nested request with probability 0.5. Due to write expansion, $|D_i|$ was inflated to 64 for all write requests under the RW-RNLP, as read requests can access any resource.

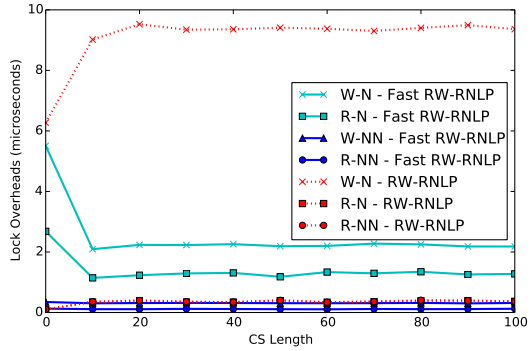

(a) Lock overhead.

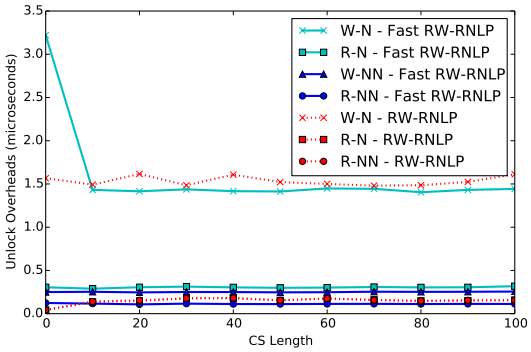

(b) Unlock overhead.

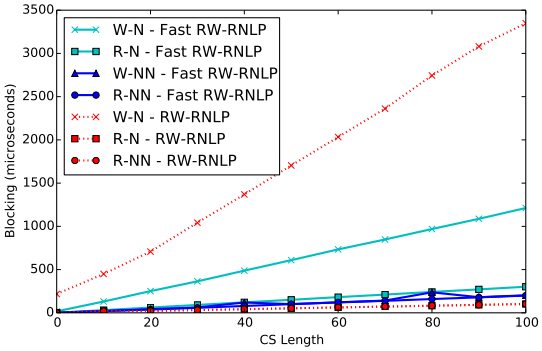

(c) Blocking.

Figure 234: (a) Lock and (b) unlock overheads and (c) blocking for nested and non-nested read and write requests under the RW-RNLP and the fast RW-RNLP. Here, for each request $\mathcal{R}_i$, $m = 18$, $n_r = 64$, $|D_i| = 1$ for non-nested requests, and $|D_i| = 4$ for nested requests. Each request was randomly chosen to be a read (as opposed to a write) with probability 0.5 and to be a nested request with probability 0.8. Due to write expansion, $|D_i|$ was inflated to 64 for all write requests under the RW-RNLP, as read requests can access any resource.

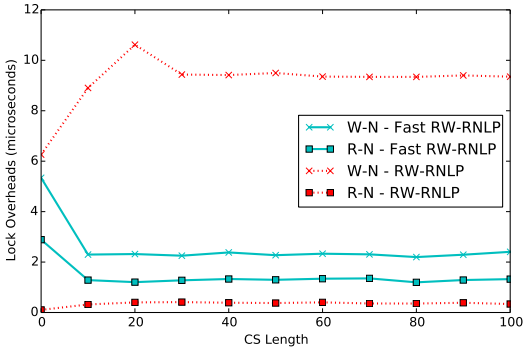

(a) Lock overhead.

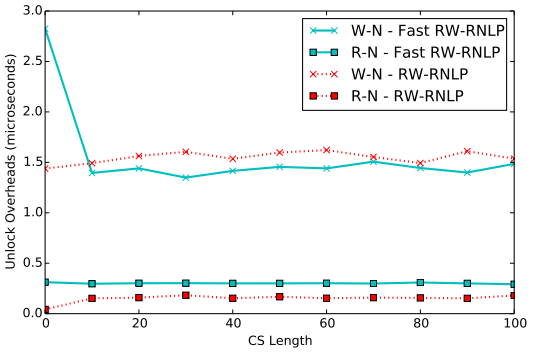

(b) Unlock overhead.

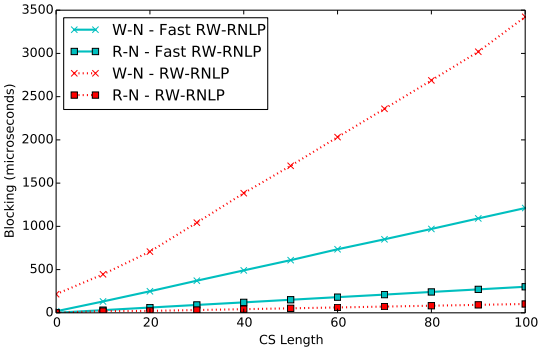

(c) Blocking.

Figure 235: (a) Lock and (b) unlock overheads and (c) blocking for nested read and write requests under the RW-RNLP and the fast RW-RNLP. Here, for each request $\mathcal{R}_i$, $m = 18$, $n_r = 64$, and $|D_i| = 4$. Each request was randomly chosen to be a read (as opposed to a write) with probability 0.5 and to be a nested request with probability 1. Due to write expansion, $|D_i|$ was inflated to 64 for all write requests under the RW-RNLP, as read requests can access any resource.

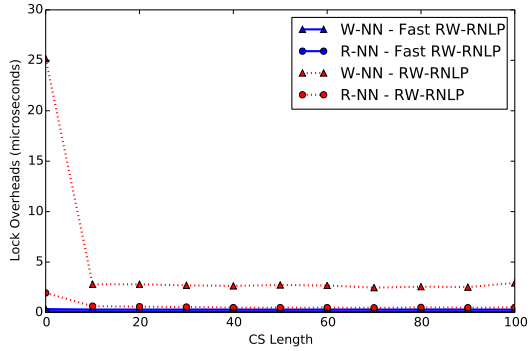

(a) Lock overhead.

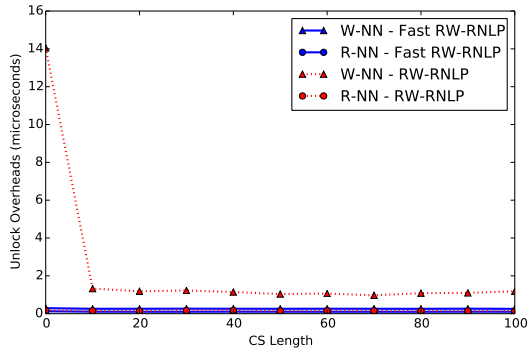

(b) Unlock overhead.

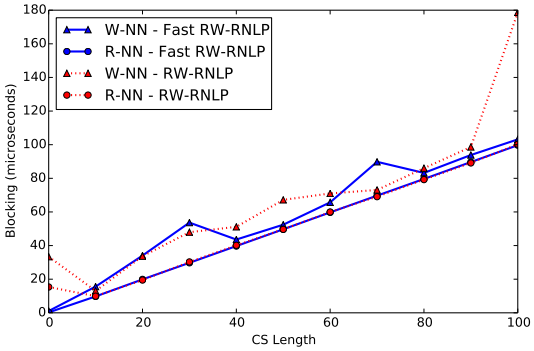

(c) Blocking.

Figure 236: (a) Lock and (b) unlock overheads and (c) blocking for non-nested read and write requests under the RW-RNLP and the fast RW-RNLP. Here, for each request $\mathcal{R}_i$, $m = 18$, $n_r = 64$, and $|D_i| = 1$. Each request was randomly chosen to be a read (as opposed to a write) with probability 0.8 and to be a nested request with probability 0.

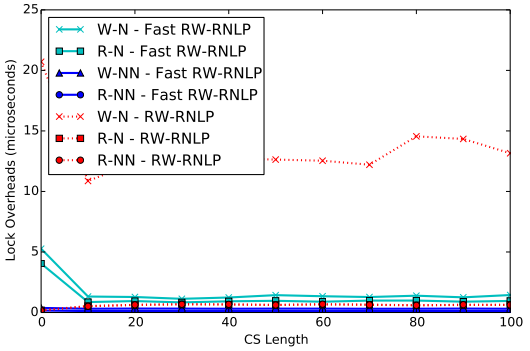

(a) Lock overhead.

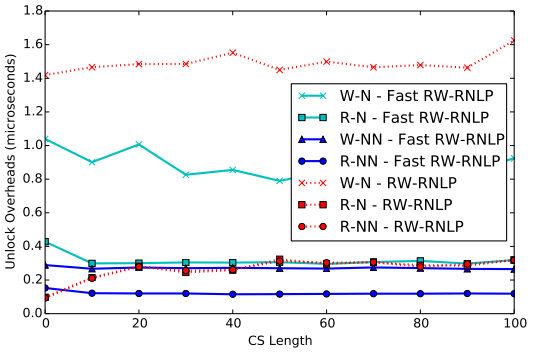

(b) Unlock overhead.

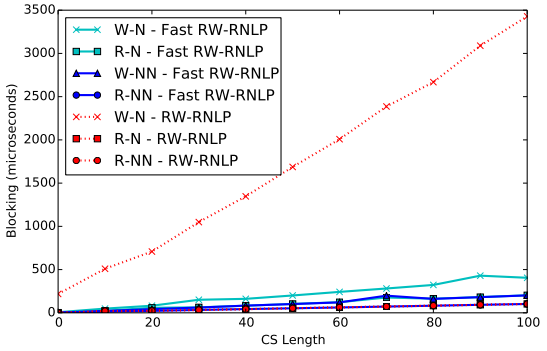

(c) Blocking.

Figure 237: (a) Lock and (b) unlock overheads and (c) blocking for nested and non-nested read and write requests under the RW-RNLP and the fast RW-RNLP. Here, for each request $\mathcal{R}_i$, $m = 18$, $n_r = 64$, $|D_i| = 1$ for non-nested requests, and $|D_i| = 4$ for nested requests. Each request was randomly chosen to be a read (as opposed to a write) with probability 0.8 and to be a nested request with probability 0.2. Due to write expansion, $|D_i|$ was inflated to 64 for all write requests under the RW-RNLP, as read requests can access any resource.

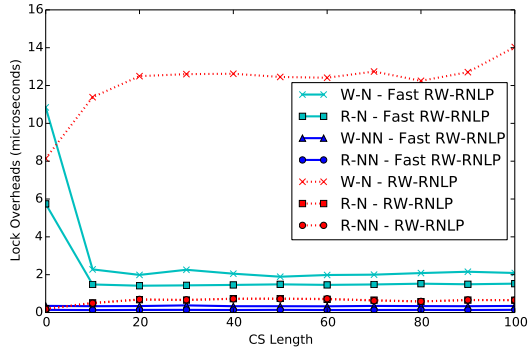

(a) Lock overhead.

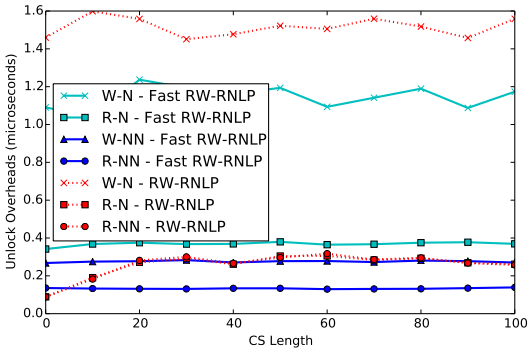

(b) Unlock overhead.

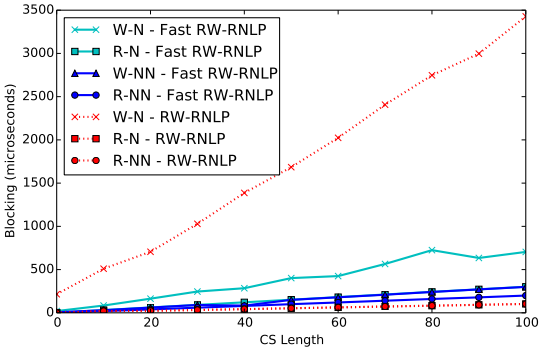

(c) Blocking.

Figure 238: (a) Lock and (b) unlock overheads and (c) blocking for nested and non-nested read and write requests under the RW-RNLP and the fast RW-RNLP. Here, for each request $\mathcal{R}_i$, $m = 18$, $n_r = 64$, $|D_i| = 1$ for non-nested requests, and $|D_i| = 4$ for nested requests. Each request was randomly chosen to be a read (as opposed to a write) with probability 0.8 and to be a nested request with probability 0.5. Due to write expansion, $|D_i|$ was inflated to 64 for all write requests under the RW-RNLP, as read requests can access any resource.

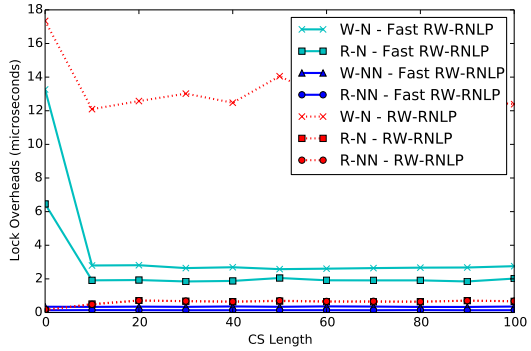

(a) Lock overhead.

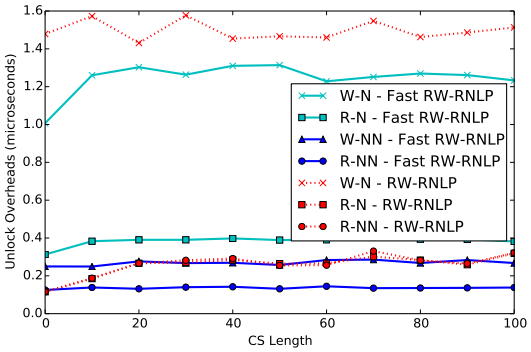

(b) Unlock overhead.

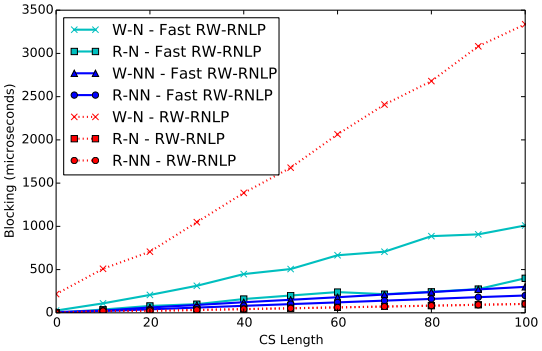

(c) Blocking.

Figure 239: (a) Lock and (b) unlock overheads and (c) blocking for nested and non-nested read and write requests under the RW-RNLP and the fast RW-RNLP. Here, for each request $\mathcal{R}_i$, $m = 18$, $n_r = 64$, $|D_i| = 1$ for non-nested requests, and $|D_i| = 4$ for nested requests. Each request was randomly chosen to be a read (as opposed to a write) with probability 0.8 and to be a nested request with probability 0.8. Due to write expansion, $|D_i|$ was inflated to 64 for all write requests under the RW-RNLP, as read requests can access any resource.

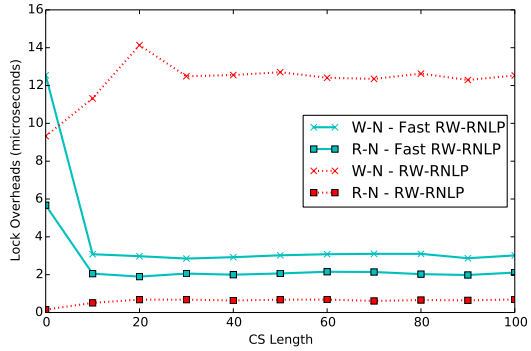

(a) Lock overhead.

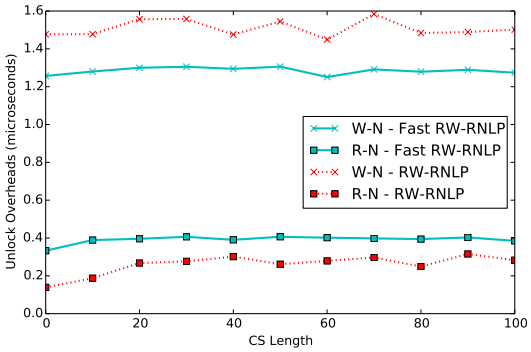

(b) Unlock overhead.

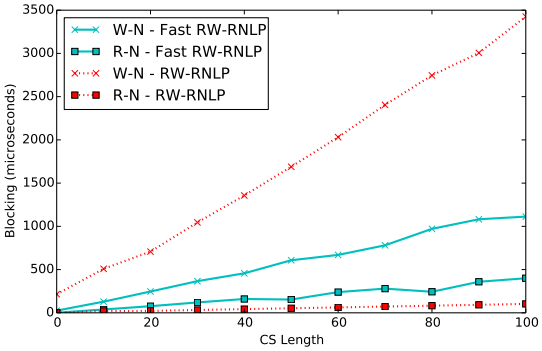

(c) Blocking.

Figure 240: (a) Lock and (b) unlock overheads and (c) blocking for nested read and write requests under the RW-RNLP and the fast RW-RNLP. Here, for each request $\mathcal{R}_i$, $m = 18$, $n_r = 64$, and $|D_i| = 4$. Each request was randomly chosen to be a read (as opposed to a write) with probability 0.8 and to be a nested request with probability 1. Due to write expansion, $|D_i|$ was inflated to 64 for all write requests under the RW-RNLP, as read requests can access any resource.

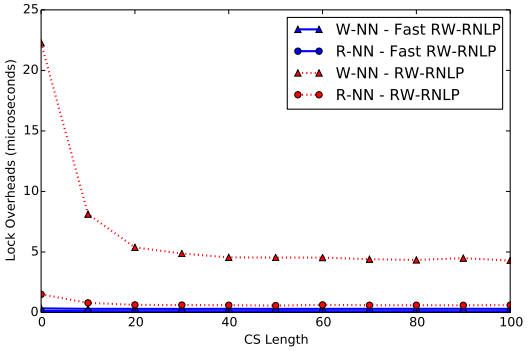

(a) Lock overhead.

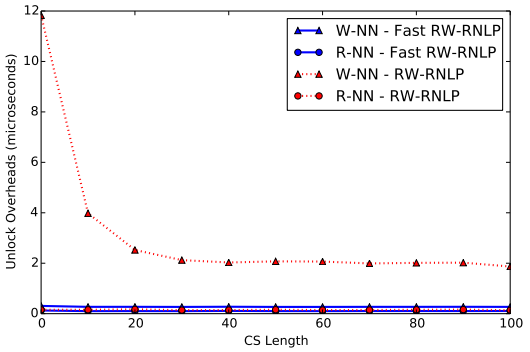

(b) Unlock overhead.

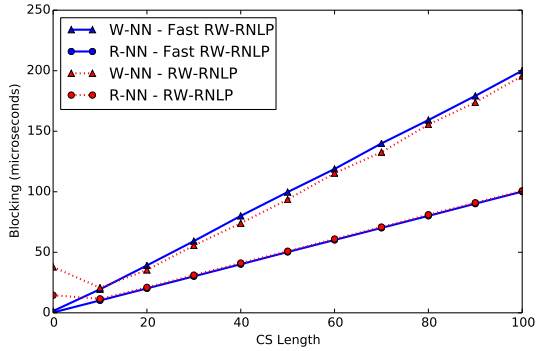

(c) Blocking.

Figure 241: (a) Lock and (b) unlock overheads and (c) blocking for non-nested read and write requests under the RW-RNLP and the fast RW-RNLP. Here, for each request $\mathcal{R}_i$, $m = 18$, $n_r = 64$, and $|D_i| = 1$. Each request was randomly chosen to be a read (as opposed to a write) with probability 0.2 and to be a nested request with probability 0.

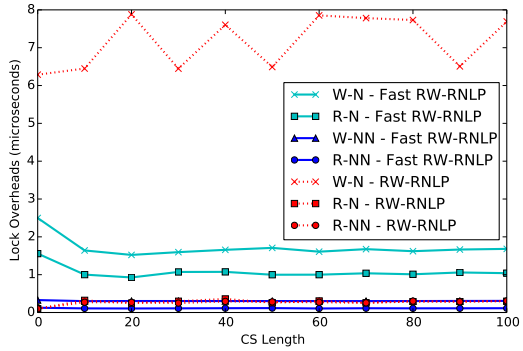

(a) Lock overhead.

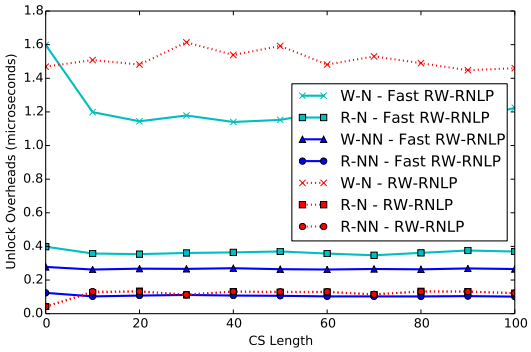

(b) Unlock overhead.

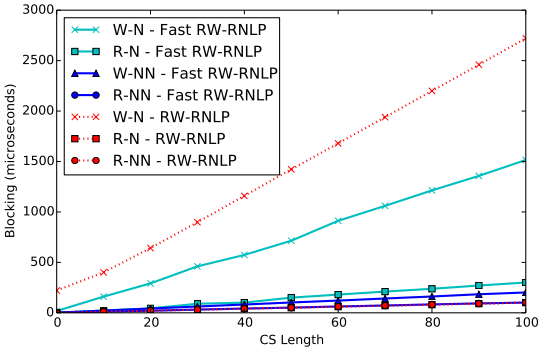

(c) Blocking.

Figure 242: (a) Lock and (b) unlock overheads and (c) blocking for nested and non-nested read and write requests under the RW-RNLP and the fast RW-RNLP. Here, for each request $\mathcal{R}_i$, $m = 18$, $n_r = 64$, $|D_i| = 1$ for non-nested requests, and $|D_i| = 6$ for nested requests. Each request was randomly chosen to be a read (as opposed to a write) with probability 0.2 and to be a nested request with probability 0.2. Due to write expansion, $|D_i|$ was inflated to 64 for all write requests under the RW-RNLP, as read requests can access any resource.

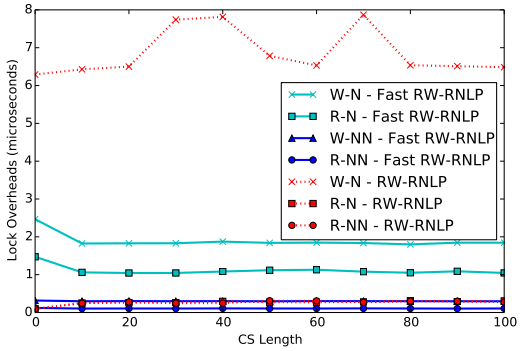

(a) Lock overhead.

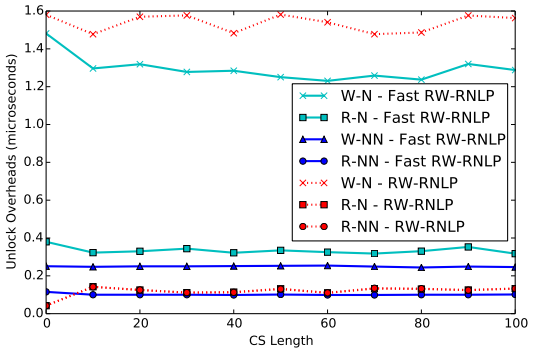

(b) Unlock overhead.

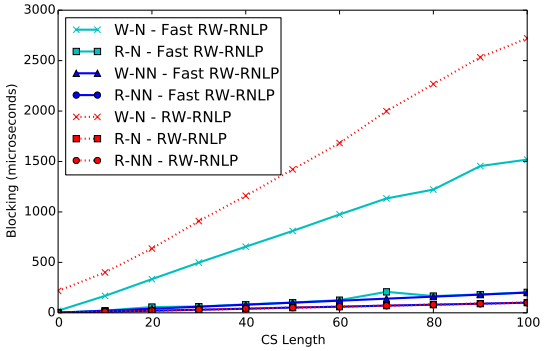

(c) Blocking.

Figure 243: (a) Lock and (b) unlock overheads and (c) blocking for nested and non-nested read and write requests under the RW-RNLP and the fast RW-RNLP. Here, for each request $\mathcal{R}_i$, $m = 18$, $n_r = 64$, $|D_i| = 1$ for non-nested requests, and $|D_i| = 6$ for nested requests. Each request was randomly chosen to be a read (as opposed to a write) with probability 0.2 and to be a nested request with probability 0.5. Due to write expansion, $|D_i|$ was inflated to 64 for all write requests under the RW-RNLP, as read requests can access any resource.

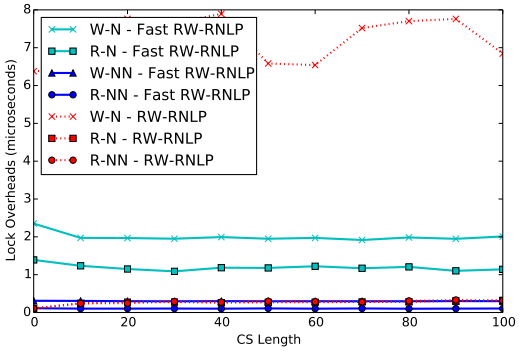

(a) Lock overhead.

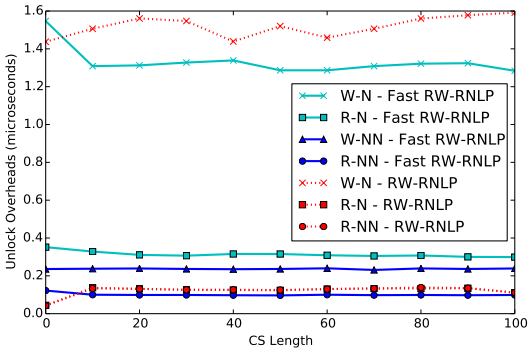

(b) Unlock overhead.

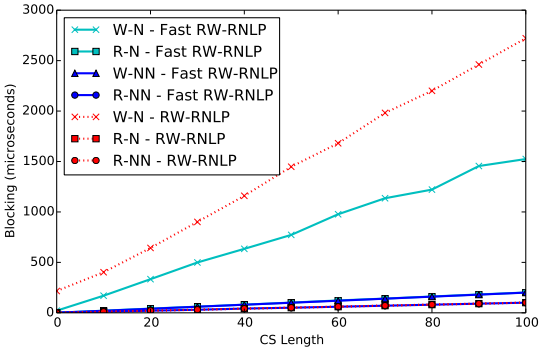

(c) Blocking.

Figure 244: (a) Lock and (b) unlock overheads and (c) blocking for nested and non-nested read and write requests under the RW-RNLP and the fast RW-RNLP. Here, for each request $\mathcal{R}_i$, $m = 18$, $n_r = 64$, $|D_i| = 1$ for non-nested requests, and $|D_i| = 6$ for nested requests. Each request was randomly chosen to be a read (as opposed to a write) with probability 0.2 and to be a nested request with probability 0.8. Due to write expansion, $|D_i|$ was inflated to 64 for all write requests under the RW-RNLP, as read requests can access any resource.

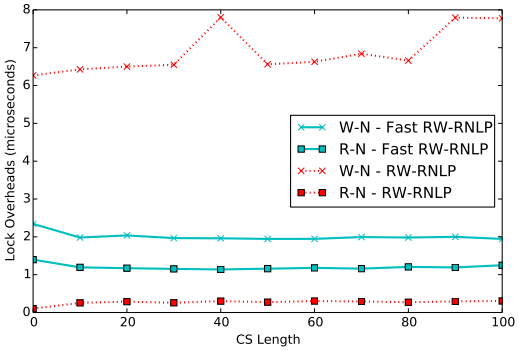

(a) Lock overhead.

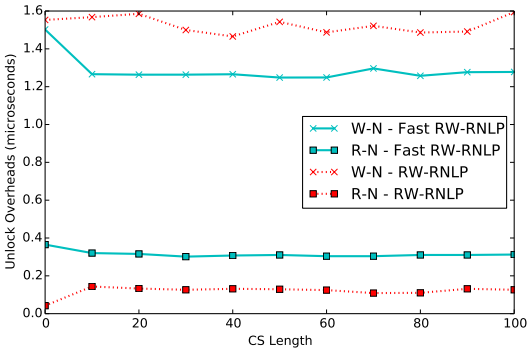

(b) Unlock overhead.

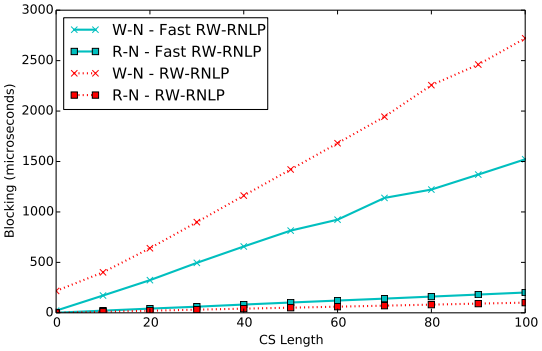

(c) Blocking.

Figure 245: (a) Lock and (b) unlock overheads and (c) blocking for nested read and write requests under the RW-RNLP and the fast RW-RNLP. Here, for each request $\mathcal{R}_i$, $m = 18$, $n_r = 64$, and $|D_i| = 6$. Each request was randomly chosen to be a read (as opposed to a write) with probability 0.2 and to be a nested request with probability 1. Due to write expansion, $|D_i|$ was inflated to 64 for all write requests under the RW-RNLP, as read requests can access any resource.

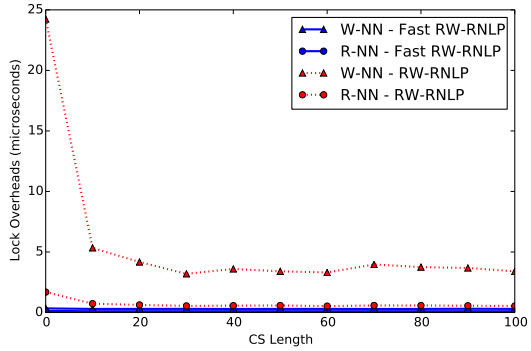

(a) Lock overhead.

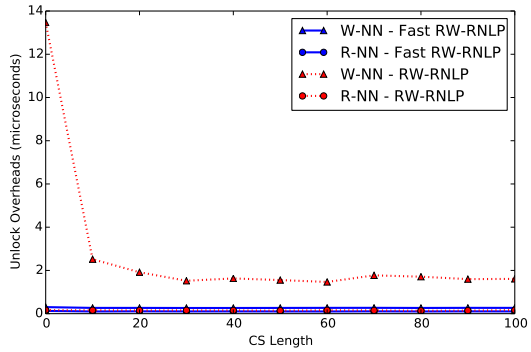

(b) Unlock overhead.

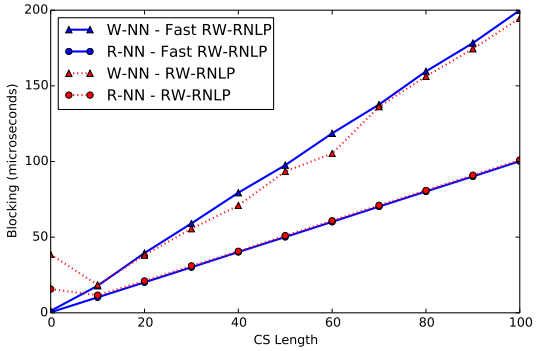

(c) Blocking.

Figure 246: (a) Lock and (b) unlock overheads and (c) blocking for non-nested read and write requests under the RW-RNLP and the fast RW-RNLP. Here, for each request $\mathcal{R}_i$, $m = 18$, $n_r = 64$, and $|D_i| = 1$. Each request was randomly chosen to be a read (as opposed to a write) with probability 0.5 and to be a nested request with probability 0.

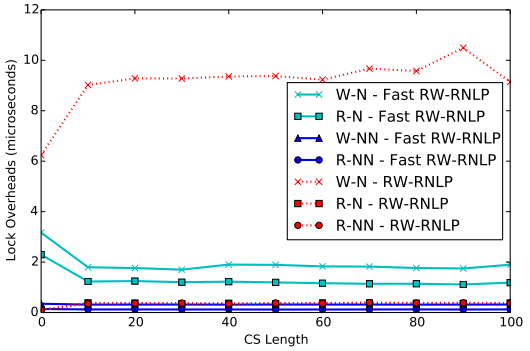

(a) Lock overhead.

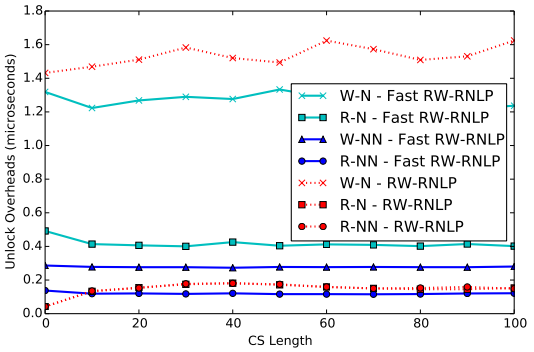

(b) Unlock overhead.

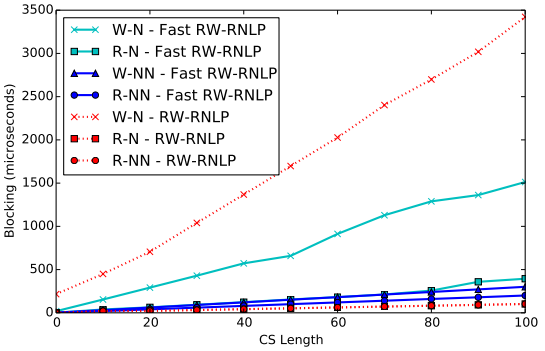

(c) Blocking.

Figure 247: (a) Lock and (b) unlock overheads and (c) blocking for nested and non-nested read and write requests under the RW-RNLP and the fast RW-RNLP. Here, for each request $\mathcal{R}_i$, $m = 18$, $n_r = 64$, $|D_i| = 1$ for non-nested requests, and $|D_i| = 6$ for nested requests. Each request was randomly chosen to be a read (as opposed to a write) with probability 0.5 and to be a nested request with probability 0.2. Due to write expansion, $|D_i|$ was inflated to 64 for all write requests under the RW-RNLP, as read requests can access any resource.

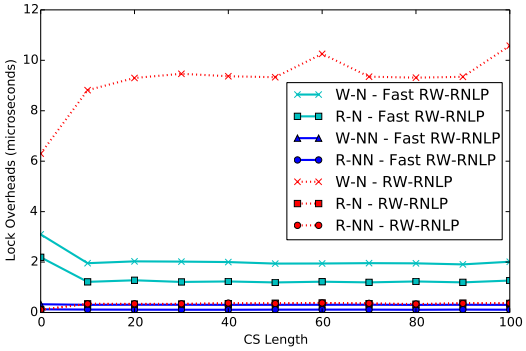

(a) Lock overhead.

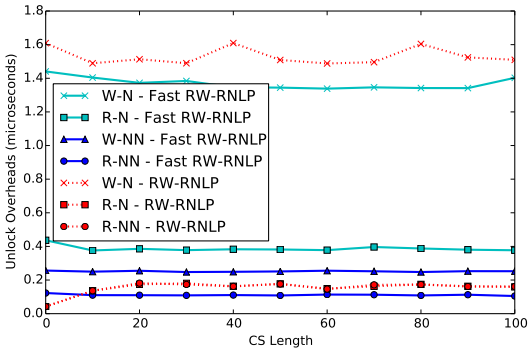

(b) Unlock overhead.

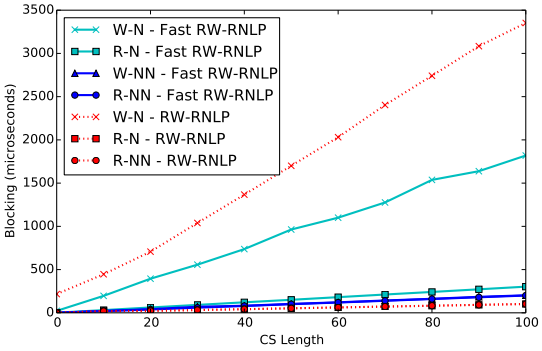

(c) Blocking.

Figure 248: (a) Lock and (b) unlock overheads and (c) blocking for nested and non-nested read and write requests under the RW-RNLP and the fast RW-RNLP. Here, for each request $\mathcal{R}_i$, $m = 18$, $n_r = 64$, $|D_i| = 1$ for non-nested requests, and $|D_i| = 6$ for nested requests. Each request was randomly chosen to be a read (as opposed to a write) with probability 0.5 and to be a nested request with probability 0.5. Due to write expansion, $|D_i|$ was inflated to 64 for all write requests under the RW-RNLP, as read requests can access any resource.

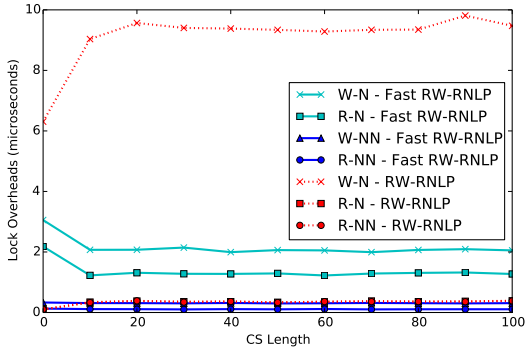

(a) Lock overhead.

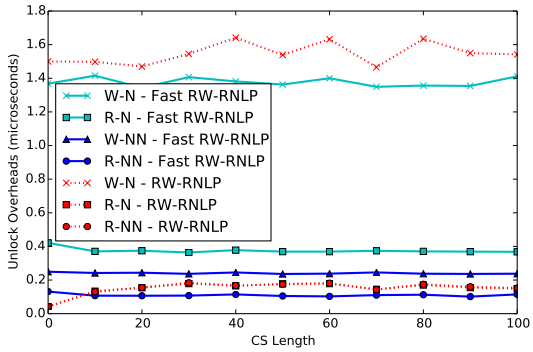

(b) Unlock overhead.

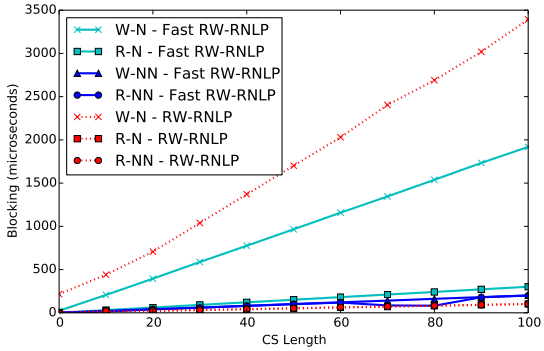

(c) Blocking.

Figure 249: (a) Lock and (b) unlock overheads and (c) blocking for nested and non-nested read and write requests under the RW-RNLP and the fast RW-RNLP. Here, for each request $\mathcal{R}_i$, $m = 18$, $n_r = 64$, $|D_i| = 1$ for non-nested requests, and $|D_i| = 6$ for nested requests. Each request was randomly chosen to be a read (as opposed to a write) with probability 0.5 and to be a nested request with probability 0.8. Due to write expansion, $|D_i|$ was inflated to 64 for all write requests under the RW-RNLP, as read requests can access any resource.

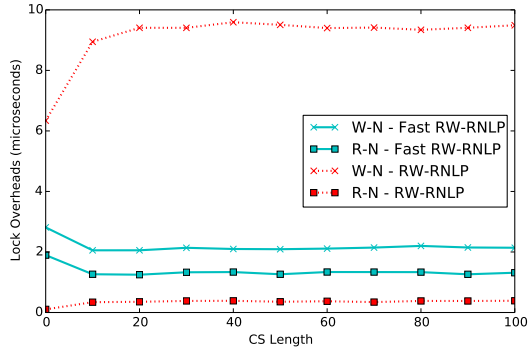

(a) Lock overhead.

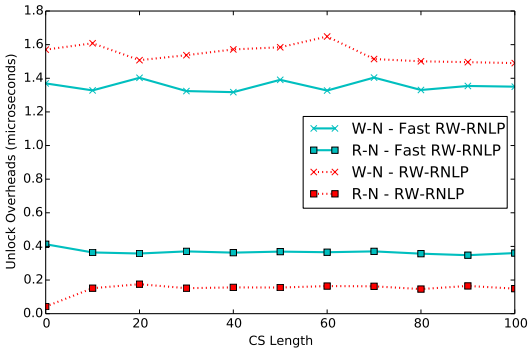

(b) Unlock overhead.

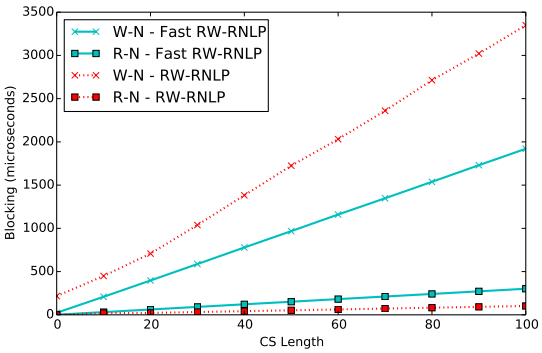

(c) Blocking.

Figure 250: (a) Lock and (b) unlock overheads and (c) blocking for nested read and write requests under the RW-RNLP and the fast RW-RNLP. Here, for each request $\mathcal{R}_i$, $m = 18$, $n_r = 64$, and $|D_i| = 6$. Each request was randomly chosen to be a read (as opposed to a write) with probability 0.5 and to be a nested request with probability 1. Due to write expansion, $|D_i|$ was inflated to 64 for all write requests under the RW-RNLP, as read requests can access any resource.

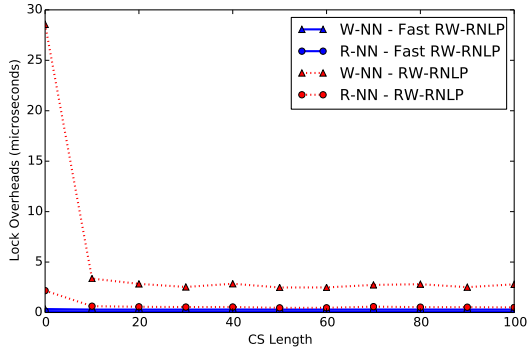

(a) Lock overhead.

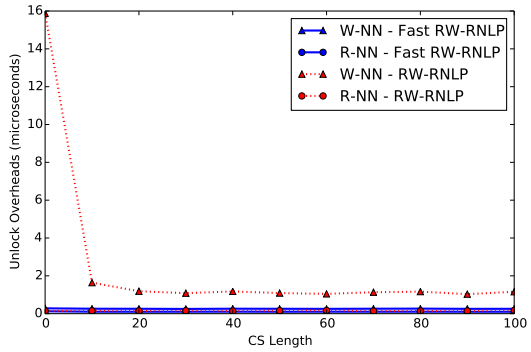

(b) Unlock overhead.

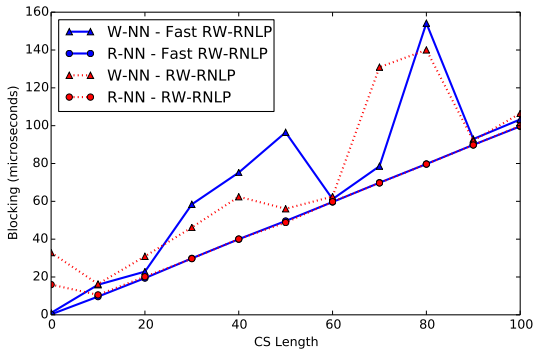

(c) Blocking.

Figure 251: (a) Lock and (b) unlock overheads and (c) blocking for non-nested read and write requests under the RW-RNLP and the fast RW-RNLP. Here, for each request $\mathcal{R}_i$, $m = 18$, $n_r = 64$, and $|D_i| = 1$. Each request was randomly chosen to be a read (as opposed to a write) with probability 0.8 and to be a nested request with probability 0.

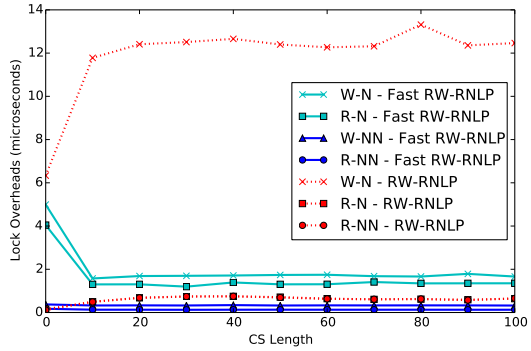

(a) Lock overhead.

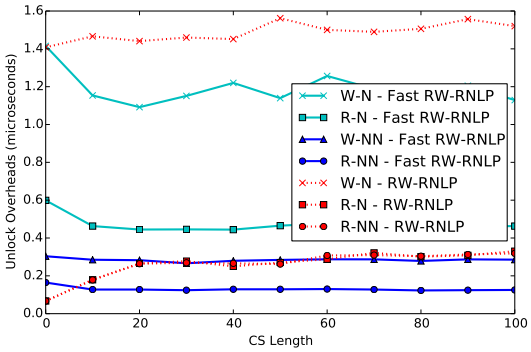

(b) Unlock overhead.

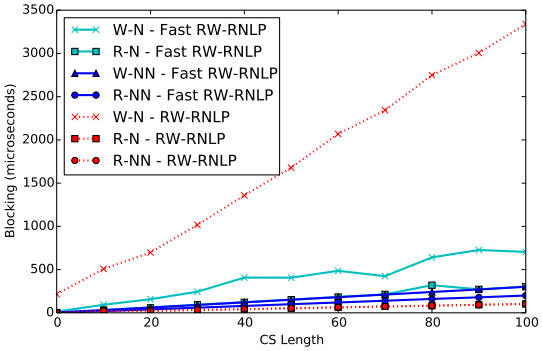

(c) Blocking.

Figure 252: (a) Lock and (b) unlock overheads and (c) blocking for nested and non-nested read and write requests under the RW-RNLP and the fast RW-RNLP. Here, for each request $\mathcal{R}_i$, $m = 18$, $n_r = 64$, $|D_i| = 1$ for non-nested requests, and $|D_i| = 6$ for nested requests. Each request was randomly chosen to be a read (as opposed to a write) with probability 0.8 and to be a nested request with probability 0.2. Due to write expansion, $|D_i|$ was inflated to 64 for all write requests under the RW-RNLP, as read requests can access any resource.

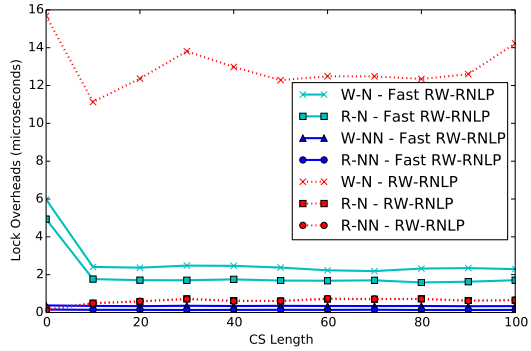

(a) Lock overhead.

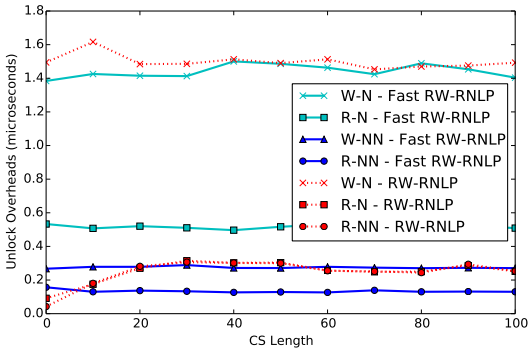

(b) Unlock overhead.

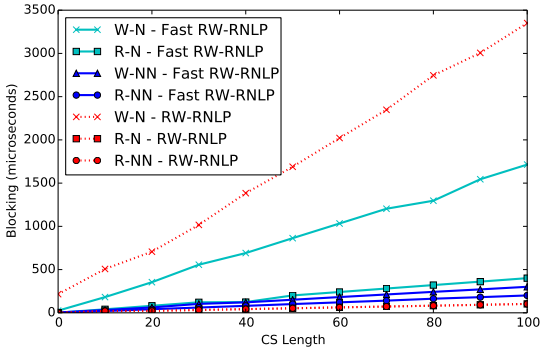

(c) Blocking.

Figure 253: (a) Lock and (b) unlock overheads and (c) blocking for nested and non-nested read and write requests under the RW-RNLP and the fast RW-RNLP. Here, for each request $\mathcal{R}_i$, $m = 18$, $n_r = 64$, $|D_i| = 1$ for non-nested requests, and $|D_i| = 6$ for nested requests. Each request was randomly chosen to be a read (as opposed to a write) with probability 0.8 and to be a nested request with probability 0.5. Due to write expansion, $|D_i|$ was inflated to 64 for all write requests under the RW-RNLP, as read requests can access any resource.

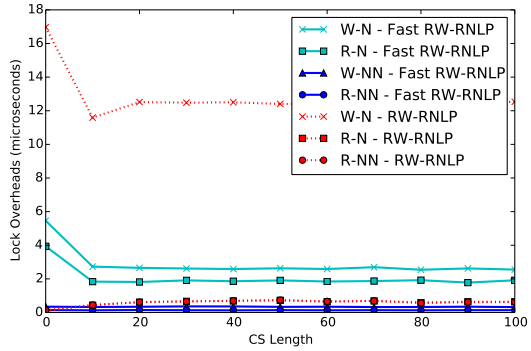

(a) Lock overhead.

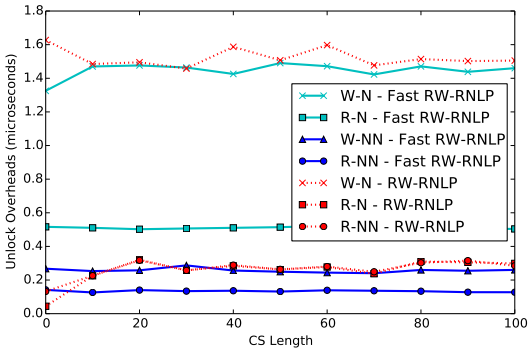

(b) Unlock overhead.

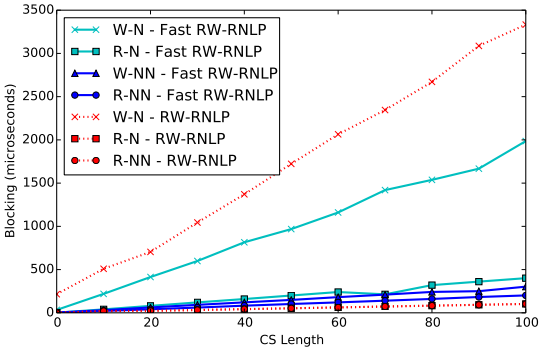

(c) Blocking.

Figure 254: (a) Lock and (b) unlock overheads and (c) blocking for nested and non-nested read and write requests under the RW-RNLP and the fast RW-RNLP. Here, for each request $\mathcal{R}_i$, $m = 18$, $n_r = 64$, $|D_i| = 1$ for non-nested requests, and $|D_i| = 6$ for nested requests. Each request was randomly chosen to be a read (as opposed to a write) with probability 0.8 and to be a nested request with probability 0.8. Due to write expansion, $|D_i|$ was inflated to 64 for all write requests under the RW-RNLP, as read requests can access any resource.

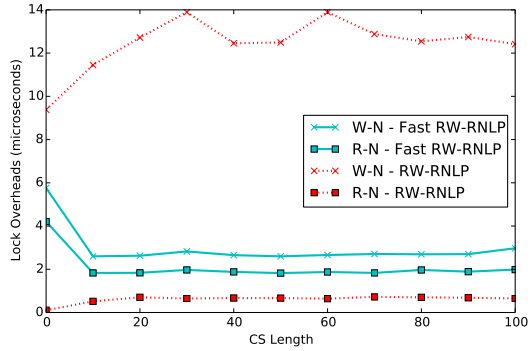

(a) Lock overhead.

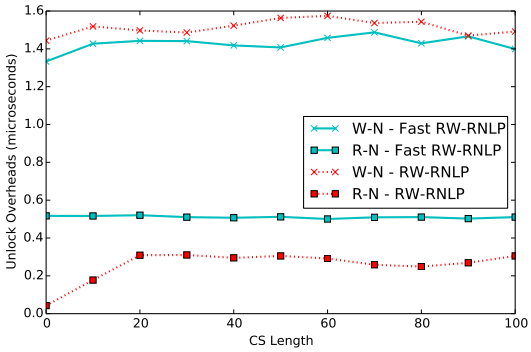

(b) Unlock overhead.

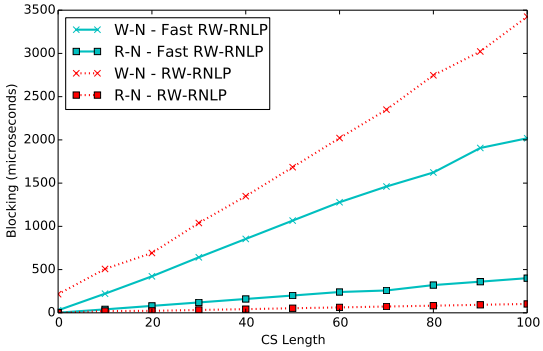

(c) Blocking.

Figure 255: (a) Lock and (b) unlock overheads and (c) blocking for nested read and write requests under the RW-RNLP and the fast RW-RNLP. Here, for each request $\mathcal{R}_i$, $m = 18$, $n_r = 64$, and $|D_i| = 6$. Each request was randomly chosen to be a read (as opposed to a write) with probability 0.8 and to be a nested request with probability 1. Due to write expansion, $|D_i|$ was inflated to 64 for all write requests under the RW-RNLP, as read requests can access any resource.

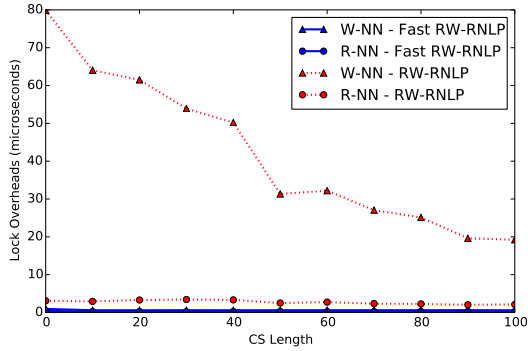

(a) Lock overhead.

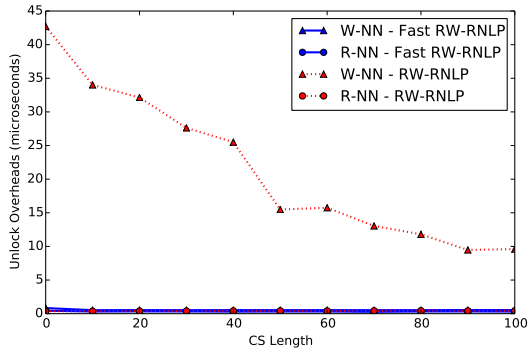

(b) Unlock overhead.

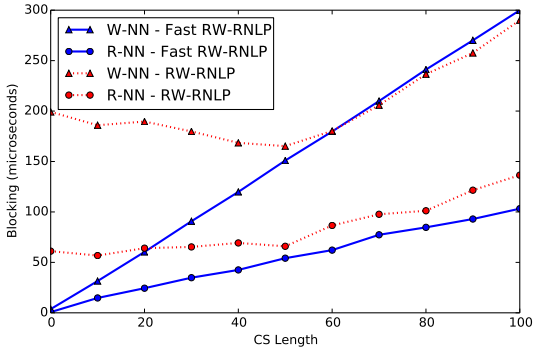

(c) Blocking.

Figure 256: (a) Lock and (b) unlock overheads and (c) blocking for non-nested read and write requests under the RW-RNLP and the fast RW-RNLP. Here, for each request $\mathcal{R}_i$, $m = 36$, $n_r = 64$, and $|D_i| = 1$. Each request was randomly chosen to be a read (as opposed to a write) with probability 0.2 and to be a nested request with probability 0.

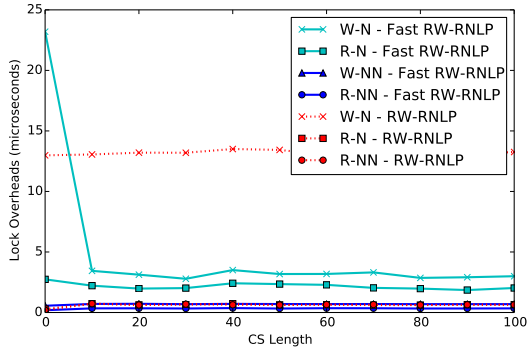

(a) Lock overhead.

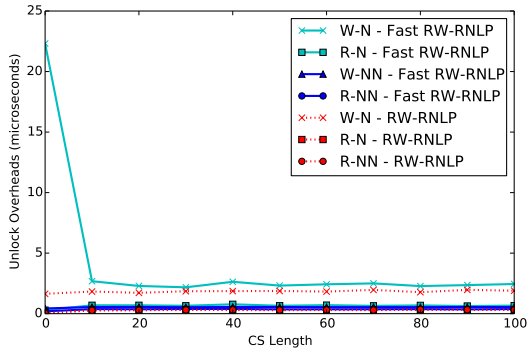

(b) Unlock overhead.

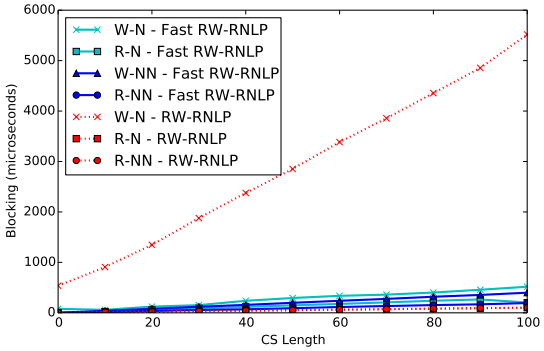

(c) Blocking.

Figure 257: (a) Lock and (b) unlock overheads and (c) blocking for nested and non-nested read and write requests under the RW-RNLP and the fast RW-RNLP. Here, for each request $\mathcal{R}_i$, $m = 36$, $n_r = 64$, $|D_i| = 1$ for non-nested requests, and $|D_i| = 2$ for nested requests. Each request was randomly chosen to be a read (as opposed to a write) with probability 0.2 and to be a nested request with probability 0.2. Due to write expansion, $|D_i|$ was inflated to 64 for all write requests under the RW-RNLP, as read requests can access any resource.

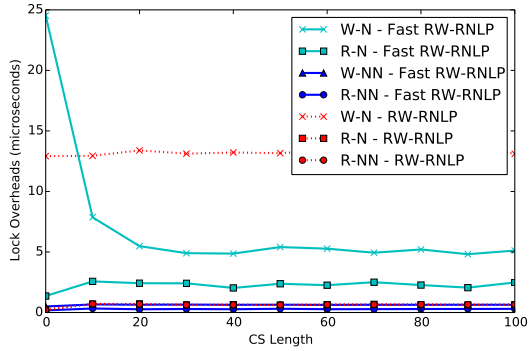

(a) Lock overhead.

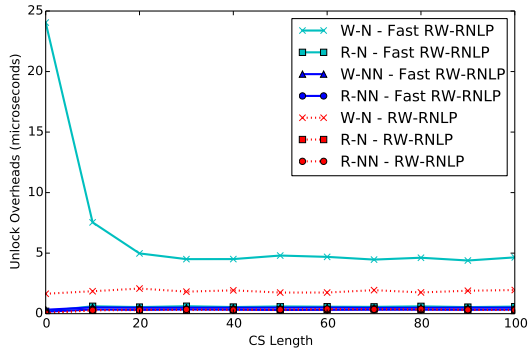

(b) Unlock overhead.

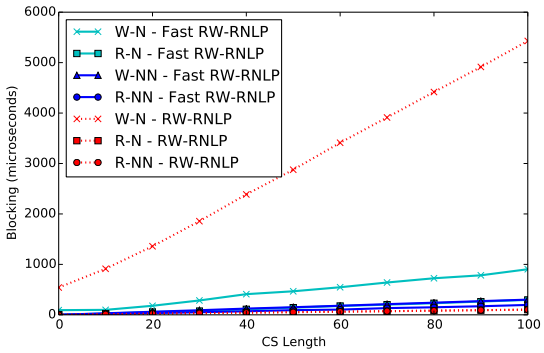

(c) Blocking.

Figure 258: (a) Lock and (b) unlock overheads and (c) blocking for nested and non-nested read and write requests under the RW-RNLP and the fast RW-RNLP. Here, for each request $\mathcal{R}_i$, $m = 36$, $n_r = 64$, $|D_i| = 1$ for non-nested requests, and $|D_i| = 2$ for nested requests. Each request was randomly chosen to be a read (as opposed to a write) with probability 0.2 and to be a nested request with probability 0.5. Due to write expansion, $|D_i|$ was inflated to 64 for all write requests under the RW-RNLP, as read requests can access any resource.

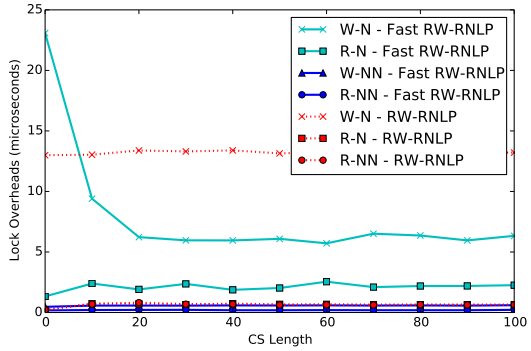

(a) Lock overhead.

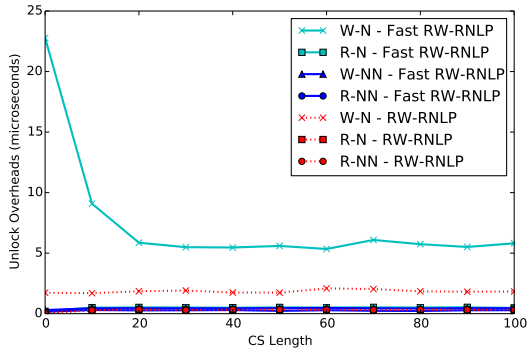

(b) Unlock overhead.

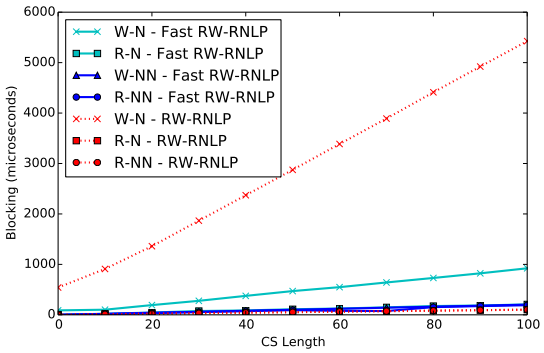

(c) Blocking.

Figure 259: (a) Lock and (b) unlock overheads and (c) blocking for nested and non-nested read and write requests under the RW-RNLP and the fast RW-RNLP. Here, for each request $\mathcal{R}_i$, $m = 36$, $n_r = 64$, $|D_i| = 1$ for non-nested requests, and $|D_i| = 2$ for nested requests. Each request was randomly chosen to be a read (as opposed to a write) with probability 0.2 and to be a nested request with probability 0.8. Due to write expansion, $|D_i|$ was inflated to 64 for all write requests under the RW-RNLP, as read requests can access any resource.

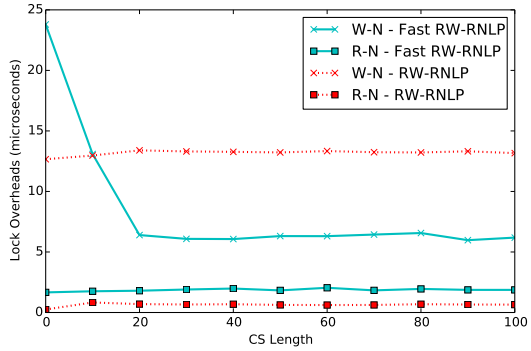

(a) Lock overhead.

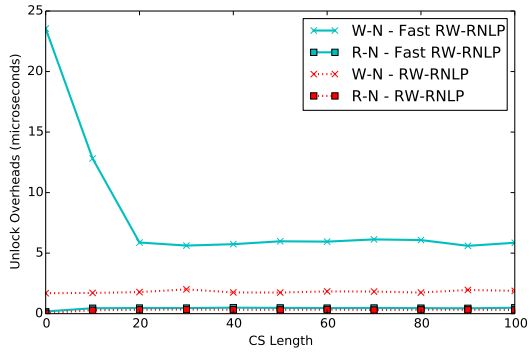

(b) Unlock overhead.

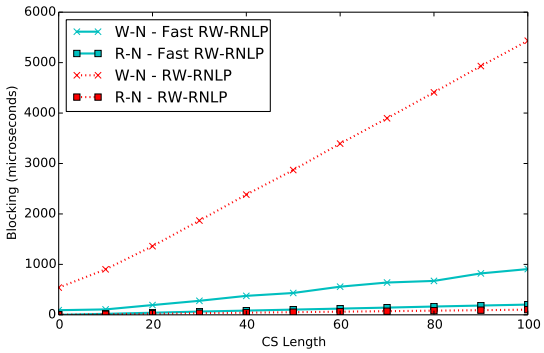

(c) Blocking.

Figure 260: (a) Lock and (b) unlock overheads and (c) blocking for nested read and write requests under the RW-RNLP and the fast RW-RNLP. Here, for each request $\mathcal{R}_i$, $m = 36$, $n_r = 64$, and $|D_i| = 2$. Each request was randomly chosen to be a read (as opposed to a write) with probability 0.2 and to be a nested request with probability 1. Due to write expansion, $|D_i|$ was inflated to 64 for all write requests under the RW-RNLP, as read requests can access any resource.

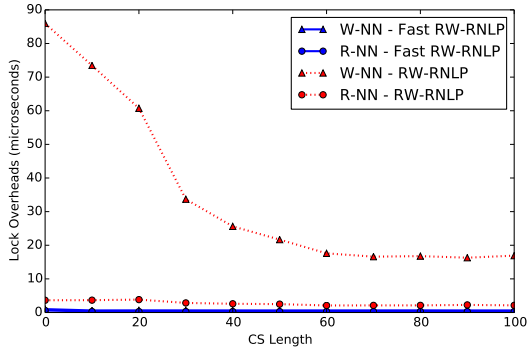

(a) Lock overhead.

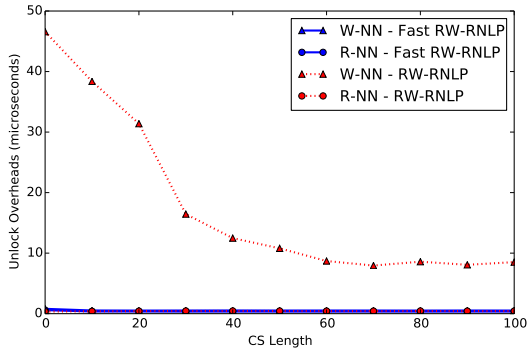

(b) Unlock overhead.

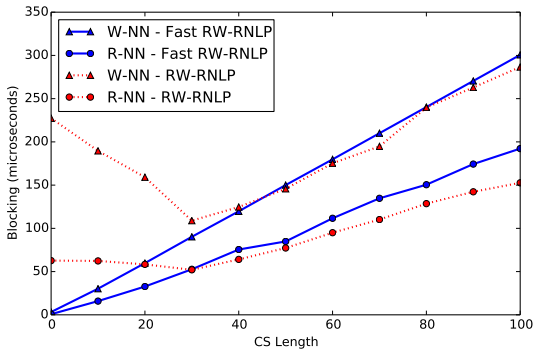

(c) Blocking.

Figure 261: (a) Lock and (b) unlock overheads and (c) blocking for non-nested read and write requests under the RW-RNLP and the fast RW-RNLP. Here, for each request $\mathcal{R}_i$, $m = 36$, $n_r = 64$, and $|D_i| = 1$. Each request was randomly chosen to be a read (as opposed to a write) with probability 0.5 and to be a nested request with probability 0.

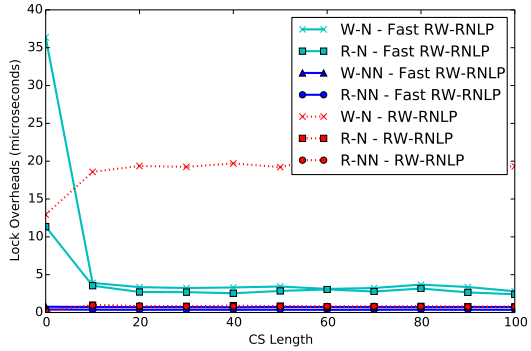

(a) Lock overhead.

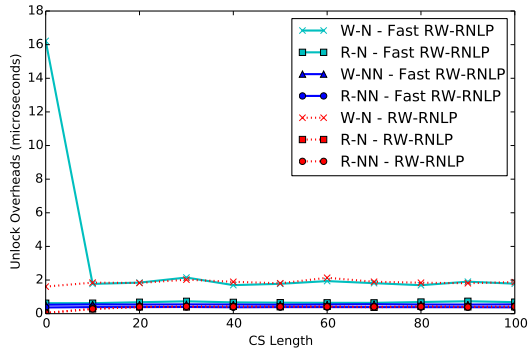

(b) Unlock overhead.

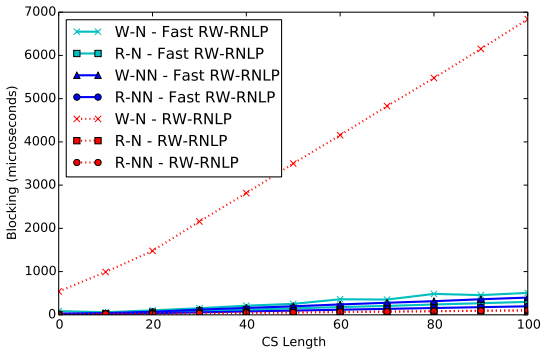

(c) Blocking.

Figure 262: (a) Lock and (b) unlock overheads and (c) blocking for nested and non-nested read and write requests under the RW-RNLP and the fast RW-RNLP. Here, for each request $\mathcal{R}_i$, $m = 36$, $n_r = 64$, $|D_i| = 1$ for non-nested requests, and $|D_i| = 2$ for nested requests. Each request was randomly chosen to be a read (as opposed to a write) with probability 0.5 and to be a nested request with probability 0.2. Due to write expansion, $|D_i|$ was inflated to 64 for all write requests under the RW-RNLP, as read requests can access any resource.

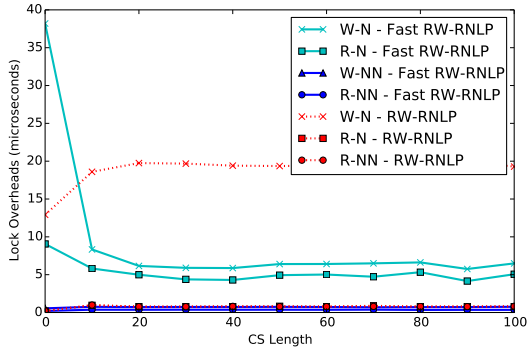

(a) Lock overhead.

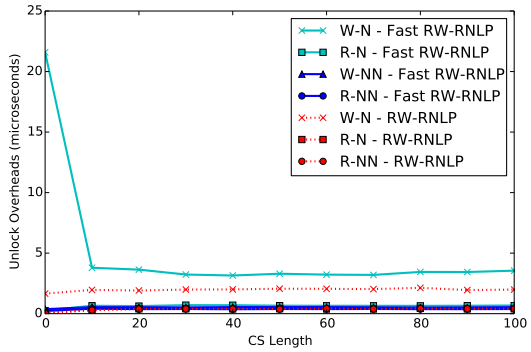

(b) Unlock overhead.

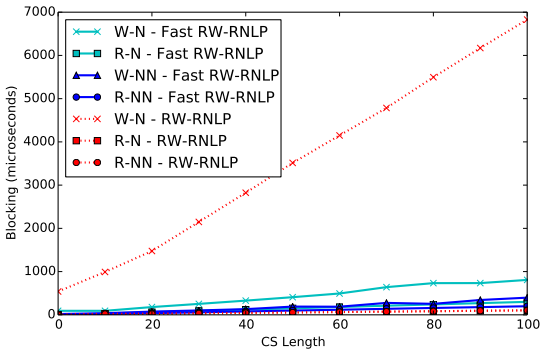

(c) Blocking.

Figure 263: (a) Lock and (b) unlock overheads and (c) blocking for nested and non-nested read and write requests under the RW-RNLP and the fast RW-RNLP. Here, for each request $\mathcal{R}_i$, $m = 36$, $n_r = 64$, $|D_i| = 1$ for non-nested requests, and $|D_i| = 2$ for nested requests. Each request was randomly chosen to be a read (as opposed to a write) with probability 0.5 and to be a nested request with probability 0.5. Due to write expansion, $|D_i|$ was inflated to 64 for all write requests under the RW-RNLP, as read requests can access any resource.

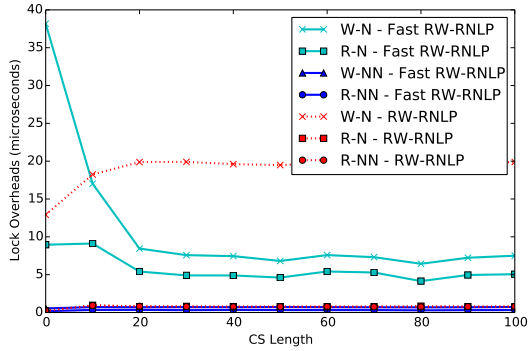

(a) Lock overhead.

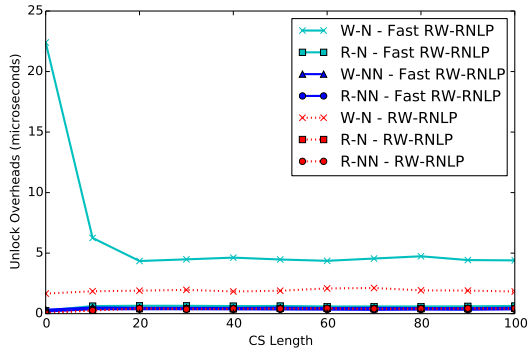

(b) Unlock overhead.

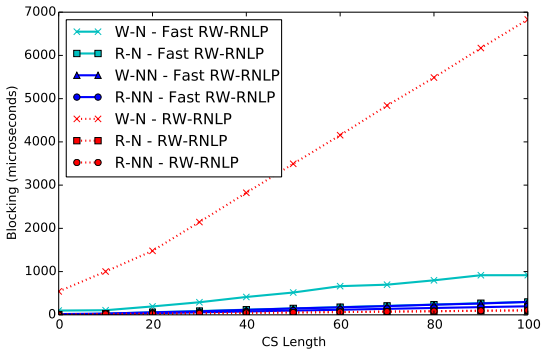

(c) Blocking.

Figure 264: (a) Lock and (b) unlock overheads and (c) blocking for nested and non-nested read and write requests under the RW-RNLP and the fast RW-RNLP. Here, for each request $\mathcal{R}_i$, $m = 36$, $n_r = 64$, $|D_i| = 1$ for non-nested requests, and $|D_i| = 2$ for nested requests. Each request was randomly chosen to be a read (as opposed to a write) with probability 0.5 and to be a nested request with probability 0.8. Due to write expansion, $|D_i|$ was inflated to 64 for all write requests under the RW-RNLP, as read requests can access any resource.

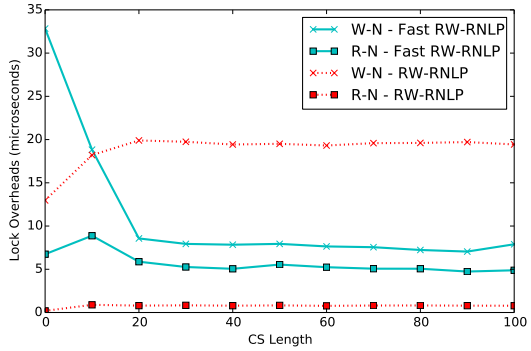

(a) Lock overhead.

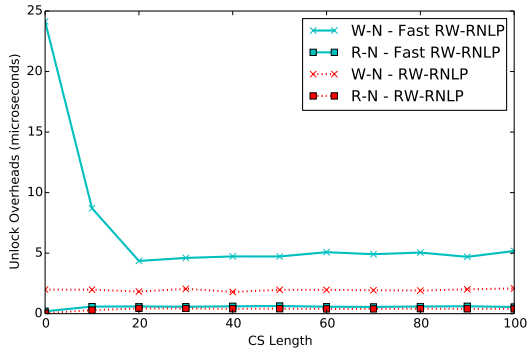

(b) Unlock overhead.

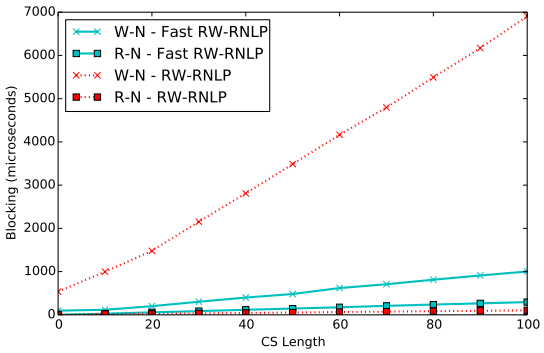

(c) Blocking.

Figure 265: (a) Lock and (b) unlock overheads and (c) blocking for nested read and write requests under the RW-RNLP and the fast RW-RNLP. Here, for each request $\mathcal{R}_i$, $m = 36$, $n_r = 64$, and $|D_i| = 2$. Each request was randomly chosen to be a read (as opposed to a write) with probability 0.5 and to be a nested request with probability 1. Due to write expansion, $|D_i|$ was inflated to 64 for all write requests under the RW-RNLP, as read requests can access any resource.

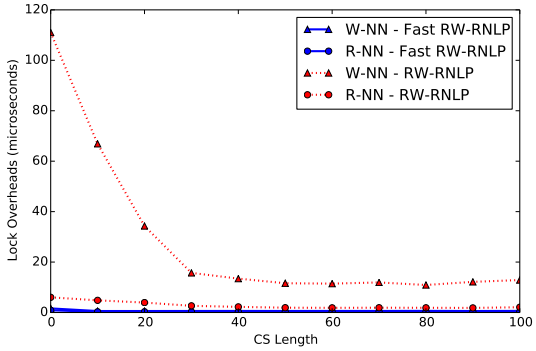

(a) Lock overhead.

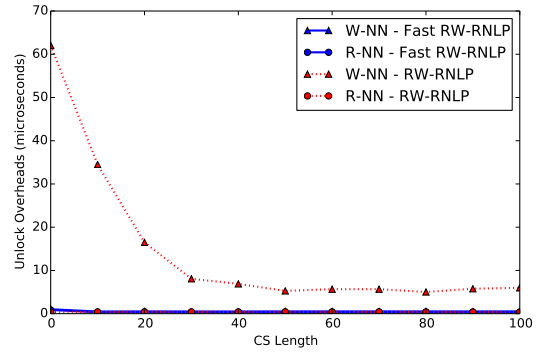

(b) Unlock overhead.

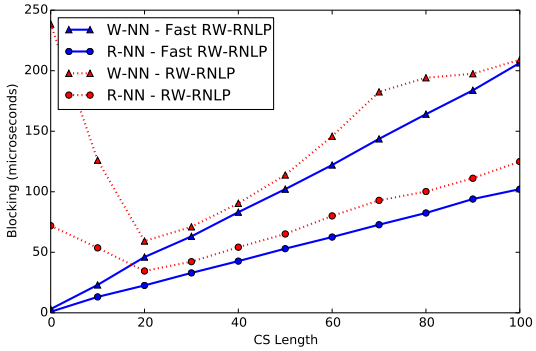

(c) Blocking.

Figure 266: (a) Lock and (b) unlock overheads and (c) blocking for non-nested read and write requests under the RW-RNLP and the fast RW-RNLP. Here, for each request $\mathcal{R}_i$, $m = 36$, $n_r = 64$, and $|D_i| = 1$. Each request was randomly chosen to be a read (as opposed to a write) with probability 0.8 and to be a nested request with probability 0.

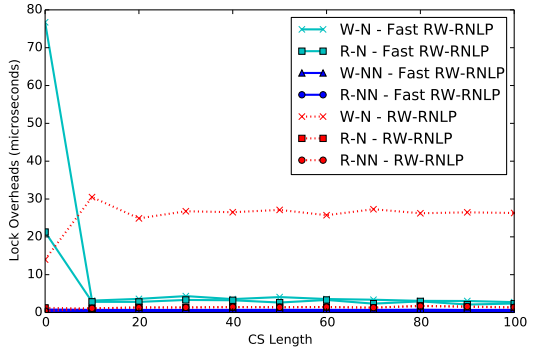

(a) Lock overhead.

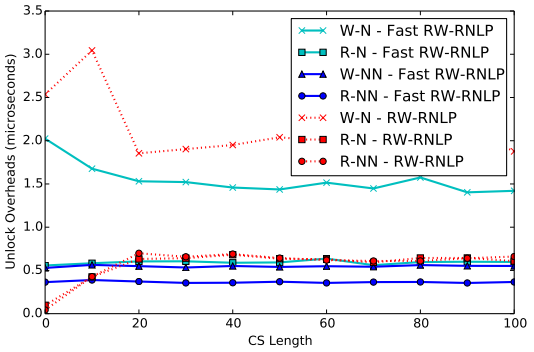

(b) Unlock overhead.

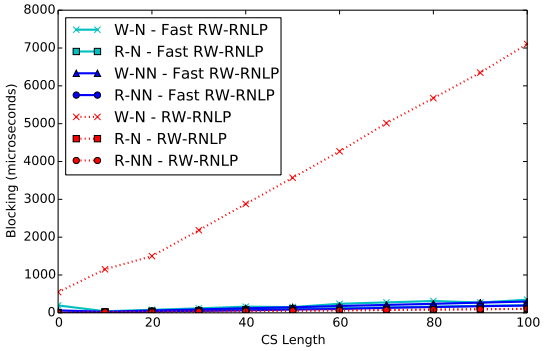

(c) Blocking.

Figure 267: (a) Lock and (b) unlock overheads and (c) blocking for nested and non-nested read and write requests under the RW-RNLP and the fast RW-RNLP. Here, for each request $\mathcal{R}_i$, $m = 36$, $n_r = 64$, $|D_i| = 1$ for non-nested requests, and $|D_i| = 2$ for nested requests. Each request was randomly chosen to be a read (as opposed to a write) with probability 0.8 and to be a nested request with probability 0.2. Due to write expansion, $|D_i|$ was inflated to 64 for all write requests under the RW-RNLP, as read requests can access any resource.

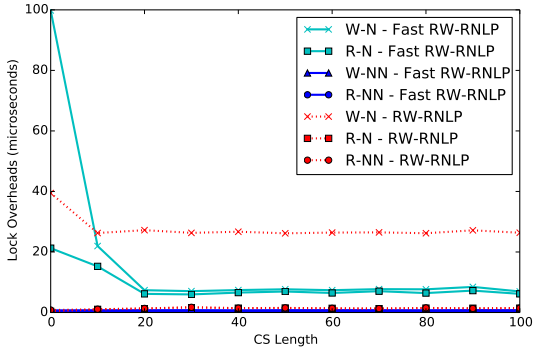

(a) Lock overhead.

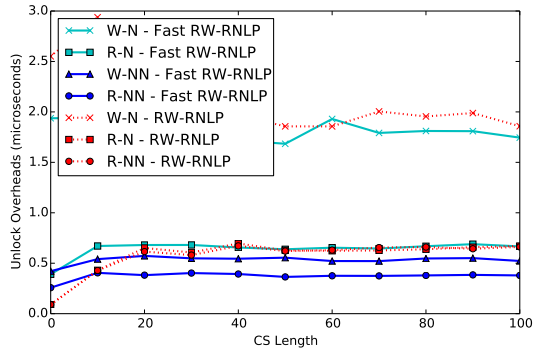

(b) Unlock overhead.

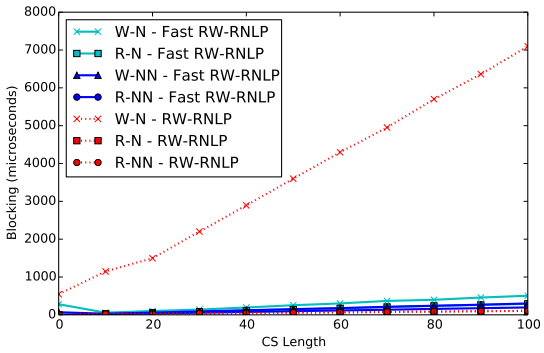

(c) Blocking.

Figure 268: (a) Lock and (b) unlock overheads and (c) blocking for nested and non-nested read and write requests under the RW-RNLP and the fast RW-RNLP. Here, for each request $\mathcal{R}_i$, $m = 36$, $n_r = 64$, $|D_i| = 1$ for non-nested requests, and $|D_i| = 2$ for nested requests. Each request was randomly chosen to be a read (as opposed to a write) with probability 0.8 and to be a nested request with probability 0.5. Due to write expansion, $|D_i|$ was inflated to 64 for all write requests under the RW-RNLP, as read requests can access any resource.

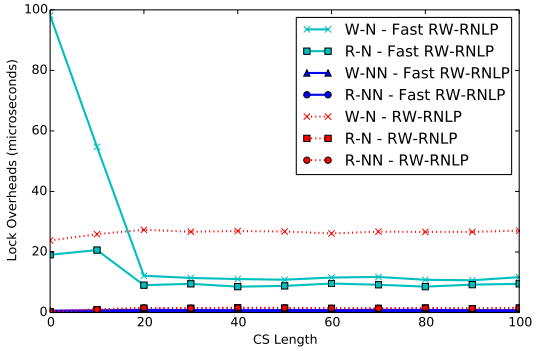

(a) Lock overhead.

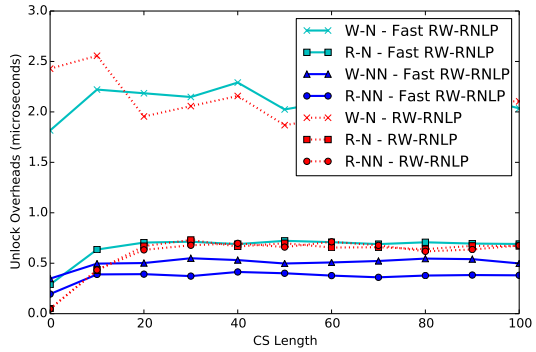

(b) Unlock overhead.

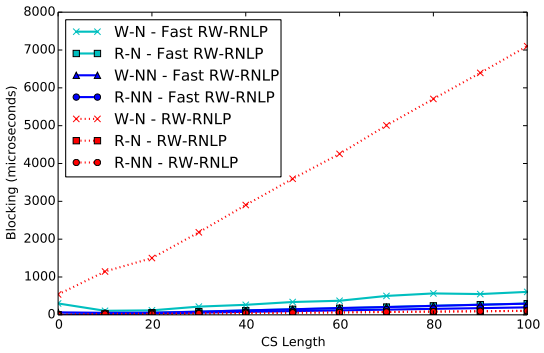

(c) Blocking.

Figure 269: (a) Lock and (b) unlock overheads and (c) blocking for nested and non-nested read and write requests under the RW-RNLP and the fast RW-RNLP. Here, for each request $\mathcal{R}_i$, $m = 36$, $n_r = 64$, $|D_i| = 1$ for non-nested requests, and $|D_i| = 2$ for nested requests. Each request was randomly chosen to be a read (as opposed to a write) with probability 0.8 and to be a nested request with probability 0.8. Due to write expansion, $|D_i|$ was inflated to 64 for all write requests under the RW-RNLP, as read requests can access any resource.

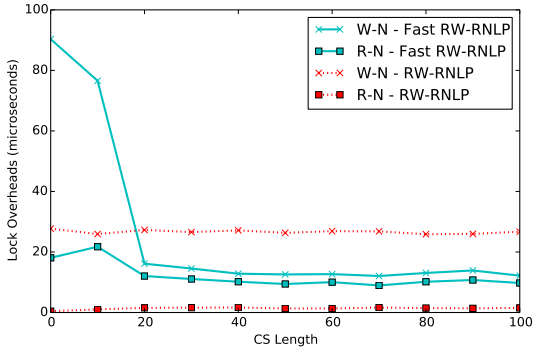

(a) Lock overhead.

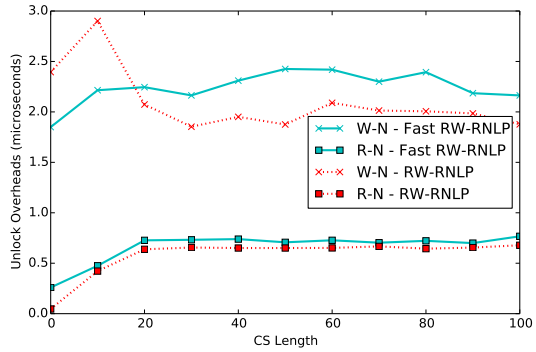

(b) Unlock overhead.

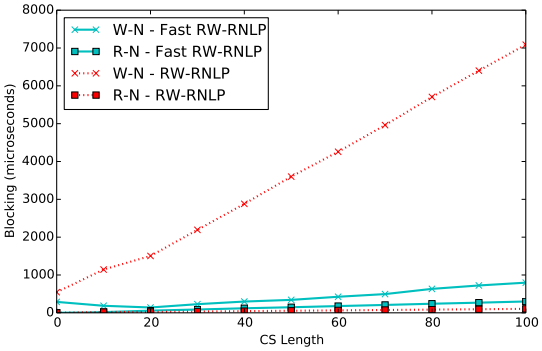

(c) Blocking.

Figure 270: (a) Lock and (b) unlock overheads and (c) blocking for nested read and write requests under the RW-RNLP and the fast RW-RNLP. Here, for each request $\mathcal{R}_i$, $m = 36$, $n_r = 64$, and $|D_i| = 2$. Each request was randomly chosen to be a read (as opposed to a write) with probability 0.8 and to be a nested request with probability 1. Due to write expansion, $|D_i|$ was inflated to 64 for all write requests under the RW-RNLP, as read requests can access any resource.

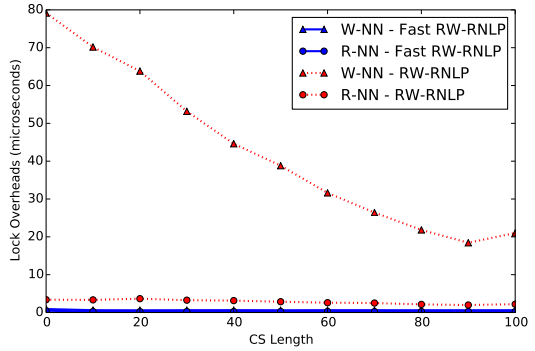

(a) Lock overhead.

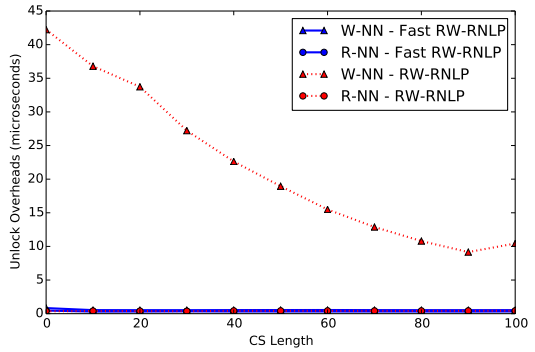

(b) Unlock overhead.

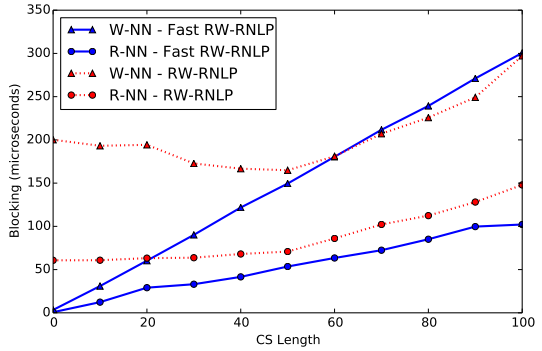

(c) Blocking.

Figure 271: (a) Lock and (b) unlock overheads and (c) blocking for non-nested read and write requests under the RW-RNLP and the fast RW-RNLP. Here, for each request $\mathcal{R}_i$, $m = 36$, $n_r = 64$, and $|D_i| = 1$. Each request was randomly chosen to be a read (as opposed to a write) with probability 0.2 and to be a nested request with probability 0.

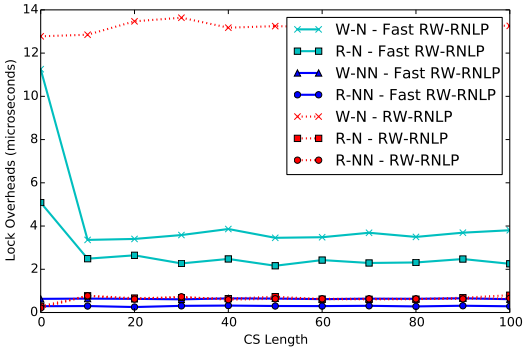

(a) Lock overhead.

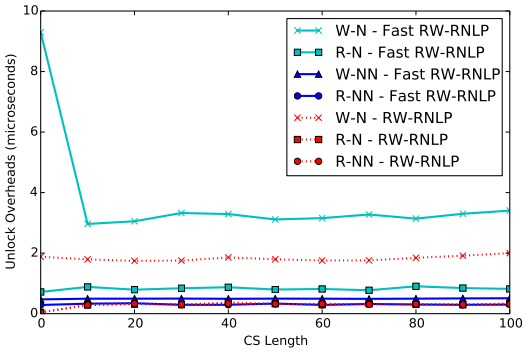

(b) Unlock overhead.

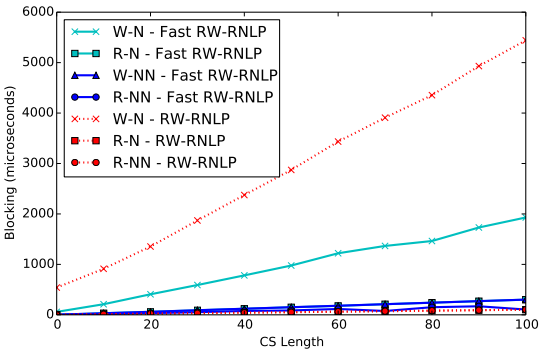

(c) Blocking.

Figure 272: (a) Lock and (b) unlock overheads and (c) blocking for nested and non-nested read and write requests under the RW-RNLP and the fast RW-RNLP. Here, for each request $\mathcal{R}_i$, $m = 36$, $n_r = 64$, $|D_i| = 1$ for non-nested requests, and $|D_i| = 4$ for nested requests. Each request was randomly chosen to be a read (as opposed to a write) with probability 0.2 and to be a nested request with probability 0.2. Due to write expansion, $|D_i|$ was inflated to 64 for all write requests under the RW-RNLP, as read requests can access any resource.

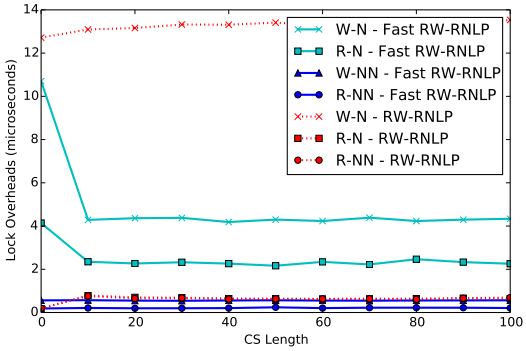

(a) Lock overhead.

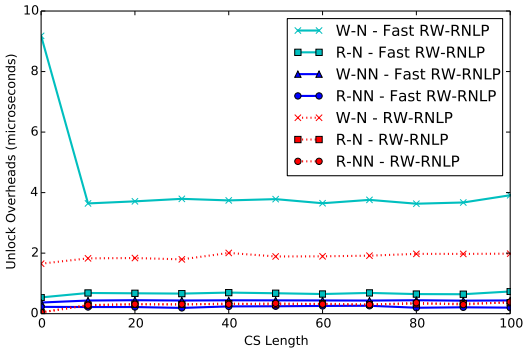

(b) Unlock overhead.

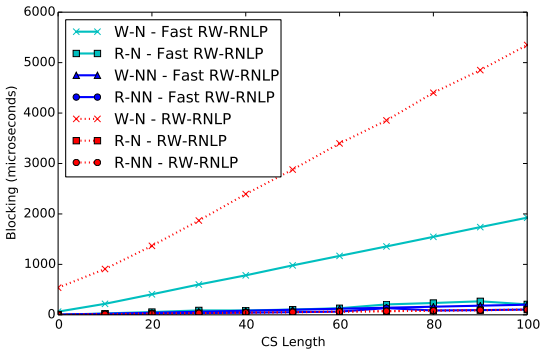

(c) Blocking.

Figure 273: (a) Lock and (b) unlock overheads and (c) blocking for nested and non-nested read and write requests under the RW-RNLP and the fast RW-RNLP. Here, for each request $\mathcal{R}_i$, $m = 36$, $n_r = 64$, $|D_i| = 1$ for non-nested requests, and $|D_i| = 4$ for nested requests. Each request was randomly chosen to be a read (as opposed to a write) with probability 0.2 and to be a nested request with probability 0.5. Due to write expansion, $|D_i|$ was inflated to 64 for all write requests under the RW-RNLP, as read requests can access any resource.

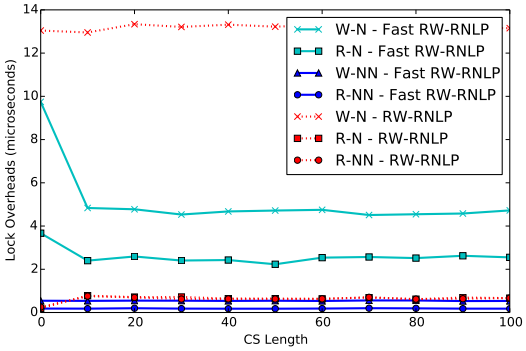

(a) Lock overhead.

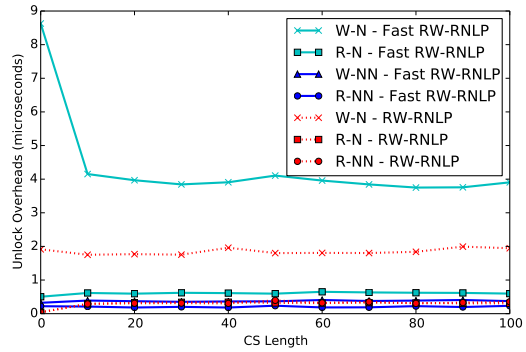

(b) Unlock overhead.

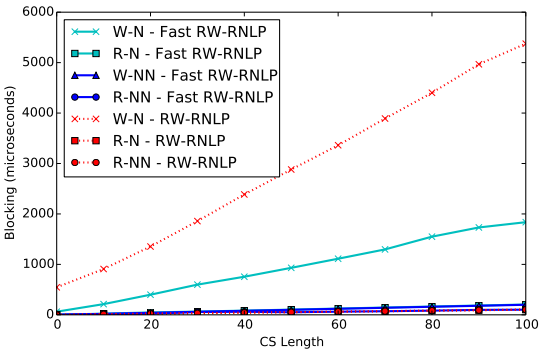

(c) Blocking.

Figure 274: (a) Lock and (b) unlock overheads and (c) blocking for nested and non-nested read and write requests under the RW-RNLP and the fast RW-RNLP. Here, for each request $\mathcal{R}_i$, $m = 36$, $n_r = 64$, $|D_i| = 1$ for non-nested requests, and $|D_i| = 4$ for nested requests. Each request was randomly chosen to be a read (as opposed to a write) with probability 0.2 and to be a nested request with probability 0.8. Due to write expansion, $|D_i|$ was inflated to 64 for all write requests under the RW-RNLP, as read requests can access any resource.

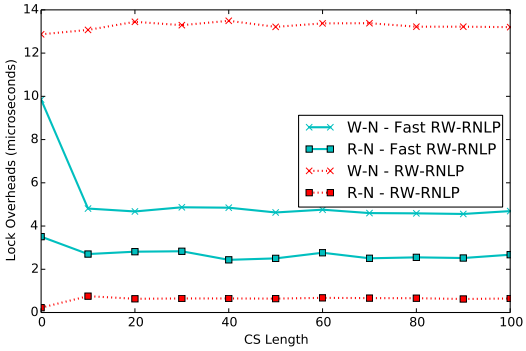

(a) Lock overhead.

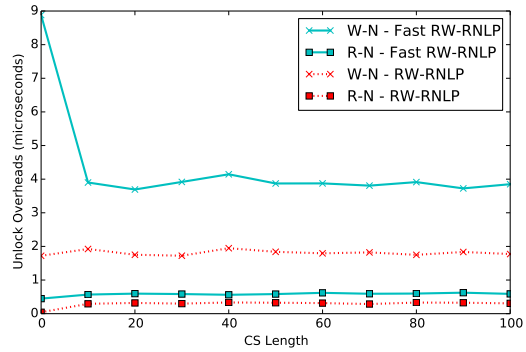

(b) Unlock overhead.

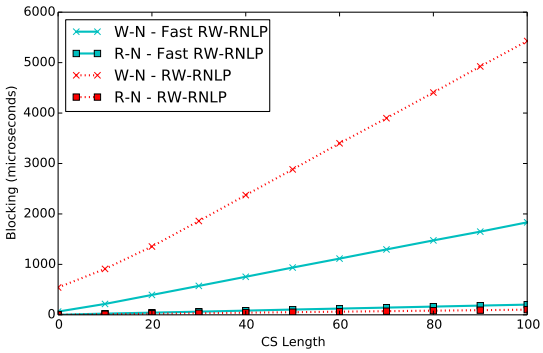

(c) Blocking.

Figure 275: (a) Lock and (b) unlock overheads and (c) blocking for nested read and write requests under the RW-RNLP and the fast RW-RNLP. Here, for each request $\mathcal{R}_i$, $m = 36$, $n_r = 64$, and $|D_i| = 4$. Each request was randomly chosen to be a read (as opposed to a write) with probability 0.2 and to be a nested request with probability 1. Due to write expansion, $|D_i|$ was inflated to 64 for all write requests under the RW-RNLP, as read requests can access any resource.

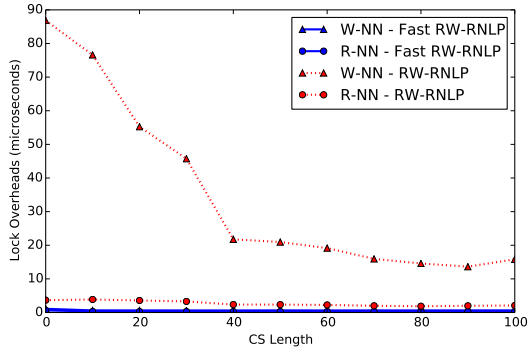

(a) Lock overhead.

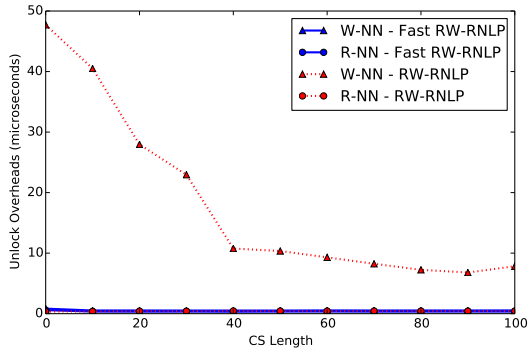

(b) Unlock overhead.

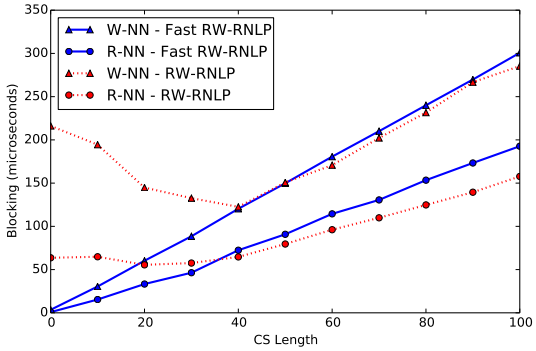

(c) Blocking.

Figure 276: (a) Lock and (b) unlock overheads and (c) blocking for non-nested read and write requests under the RW-RNLP and the fast RW-RNLP. Here, for each request $\mathcal{R}_i$, $m = 36$, $n_r = 64$, and $|D_i| = 1$. Each request was randomly chosen to be a read (as opposed to a write) with probability 0.5 and to be a nested request with probability 0.

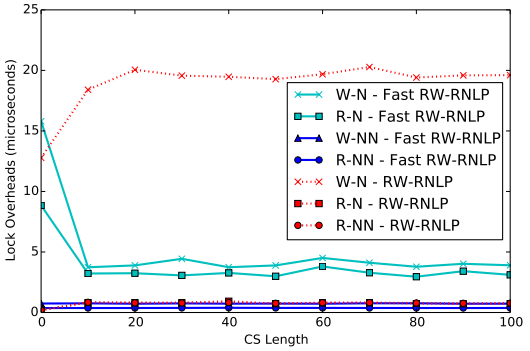

(a) Lock overhead.

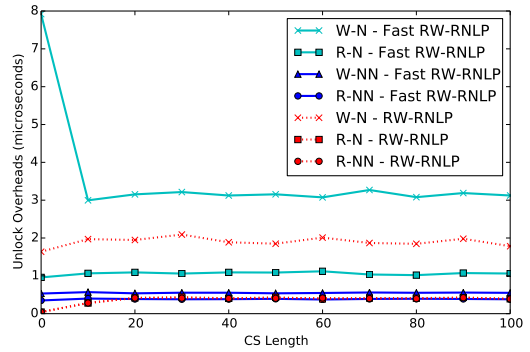

(b) Unlock overhead.

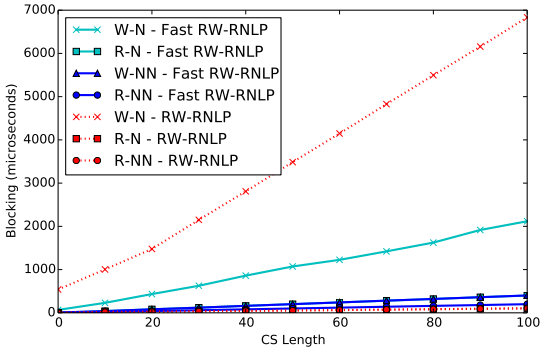

(c) Blocking.

Figure 277: (a) Lock and (b) unlock overheads and (c) blocking for nested and non-nested read and write requests under the RW-RNLP and the fast RW-RNLP. Here, for each request $\mathcal{R}_i$, $m = 36$, $n_r = 64$, $|D_i| = 1$ for non-nested requests, and $|D_i| = 4$ for nested requests. Each request was randomly chosen to be a read (as opposed to a write) with probability 0.5 and to be a nested request with probability 0.2. Due to write expansion, $|D_i|$ was inflated to 64 for all write requests under the RW-RNLP, as read requests can access any resource.

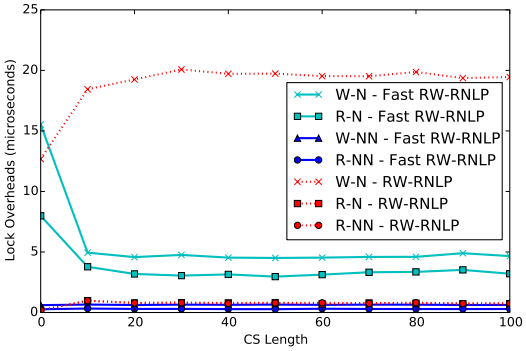

(a) Lock overhead.

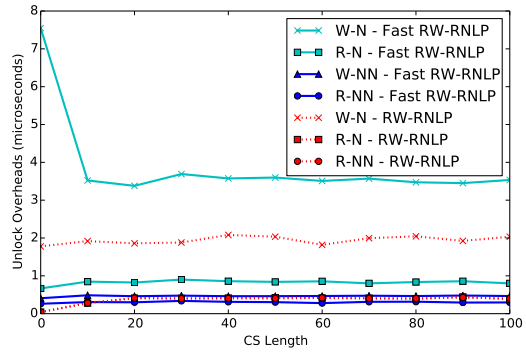

(b) Unlock overhead.

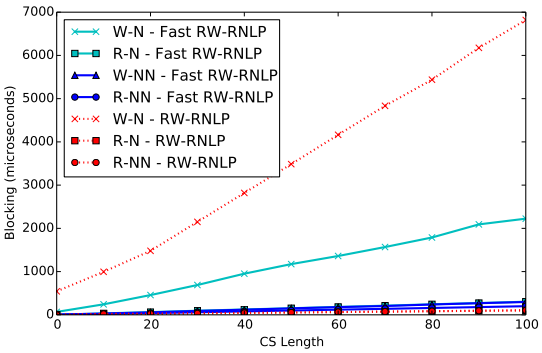

(c) Blocking.

Figure 278: (a) Lock and (b) unlock overheads and (c) blocking for nested and non-nested read and write requests under the RW-RNLP and the fast RW-RNLP. Here, for each request $\mathcal{R}_i$, $m = 36$, $n_r = 64$, $|D_i| = 1$ for non-nested requests, and $|D_i| = 4$ for nested requests. Each request was randomly chosen to be a read (as opposed to a write) with probability 0.5 and to be a nested request with probability 0.5. Due to write expansion, $|D_i|$ was inflated to 64 for all write requests under the RW-RNLP, as read requests can access any resource.

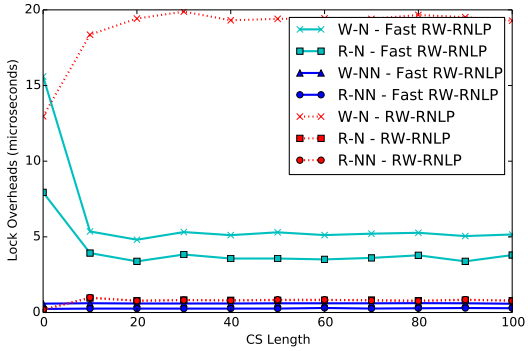

(a) Lock overhead.

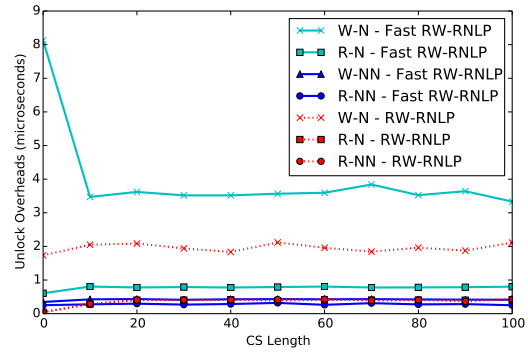

(b) Unlock overhead.

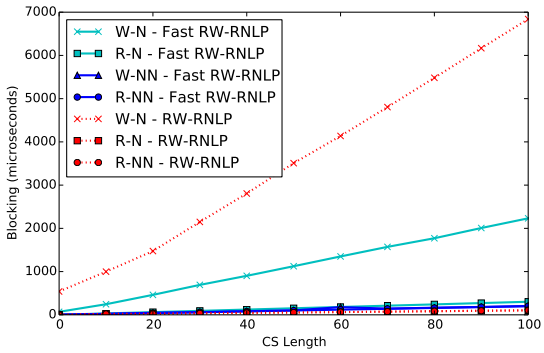

(c) Blocking.

Figure 279: (a) Lock and (b) unlock overheads and (c) blocking for nested and non-nested read and write requests under the RW-RNLP and the fast RW-RNLP. Here, for each request $\mathcal{R}_i$, $m = 36$, $n_r = 64$, $|D_i| = 1$ for non-nested requests, and $|D_i| = 4$ for nested requests. Each request was randomly chosen to be a read (as opposed to a write) with probability 0.5 and to be a nested request with probability 0.8. Due to write expansion, $|D_i|$ was inflated to 64 for all write requests under the RW-RNLP, as read requests can access any resource.

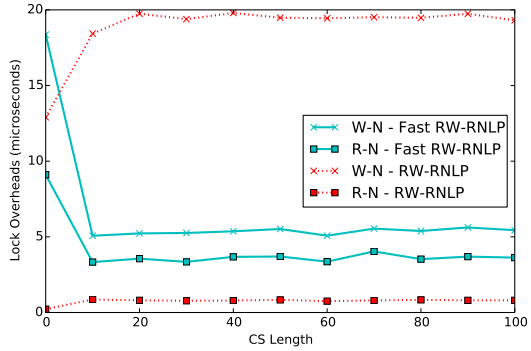

(a) Lock overhead.

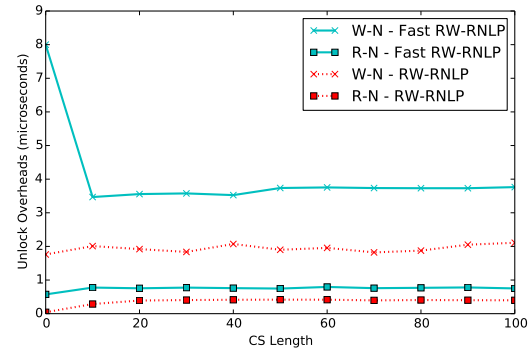

(b) Unlock overhead.

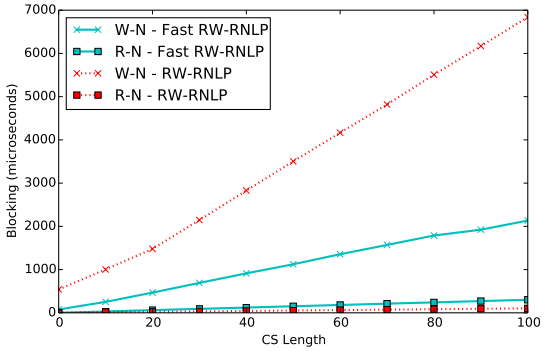

(c) Blocking.

Figure 280: (a) Lock and (b) unlock overheads and (c) blocking for nested read and write requests under the RW-RNLP and the fast RW-RNLP. Here, for each request $\mathcal{R}_i$, $m = 36$, $n_r = 64$, and $|D_i| = 4$. Each request was randomly chosen to be a read (as opposed to a write) with probability 0.5 and to be a nested request with probability 1. Due to write expansion, $|D_i|$ was inflated to 64 for all write requests under the RW-RNLP, as read requests can access any resource.

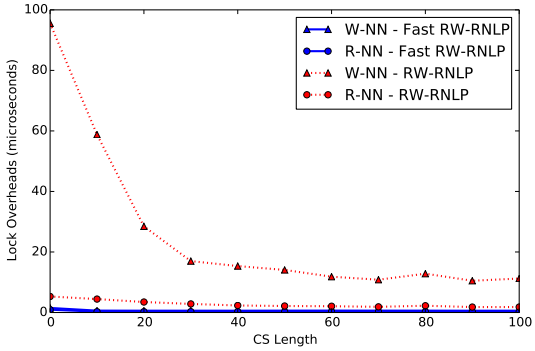

(a) Lock overhead.

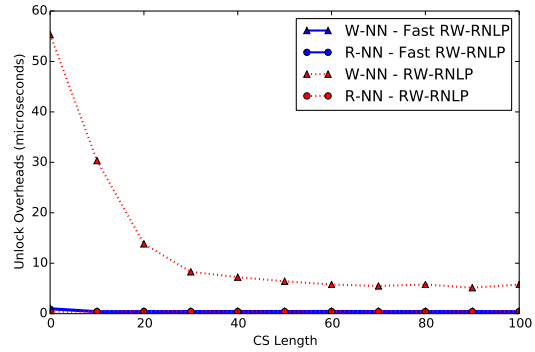

(b) Unlock overhead.

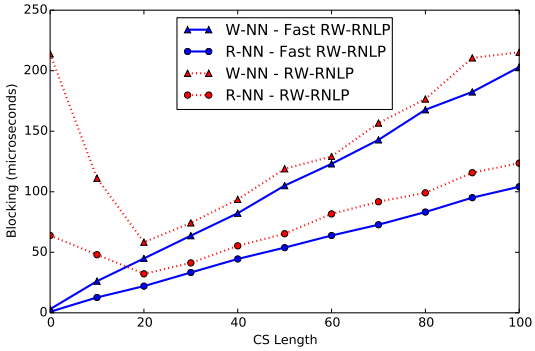

(c) Blocking.

Figure 281: (a) Lock and (b) unlock overheads and (c) blocking for non-nested read and write requests under the RW-RNLP and the fast RW-RNLP. Here, for each request $\mathcal{R}_i$, $m = 36$, $n_r = 64$, and $|D_i| = 1$. Each request was randomly chosen to be a read (as opposed to a write) with probability 0.8 and to be a nested request with probability 0.

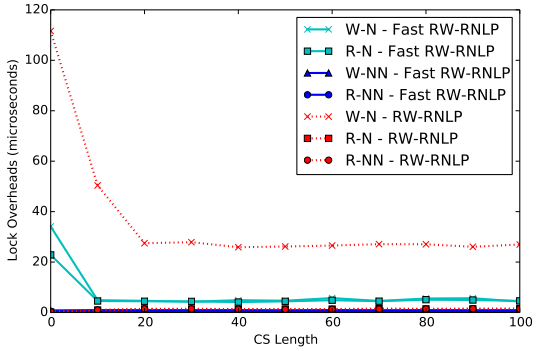

(a) Lock overhead.

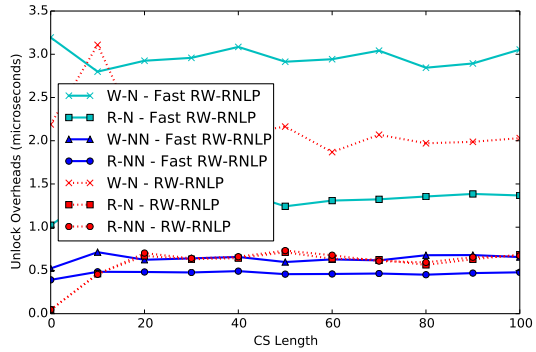

(b) Unlock overhead.

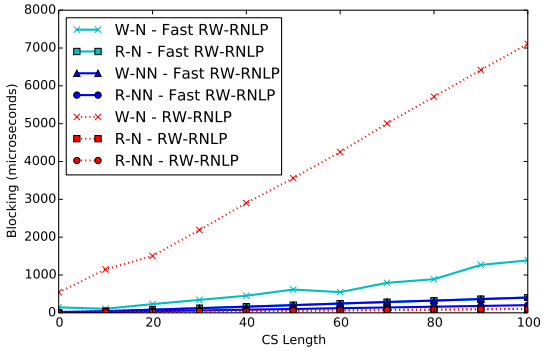

(c) Blocking.

Figure 282: (a) Lock and (b) unlock overheads and (c) blocking for nested and non-nested read and write requests under the RW-RNLP and the fast RW-RNLP. Here, for each request $\mathcal{R}_i$, $m = 36$, $n_r = 64$, $|D_i| = 1$ for non-nested requests, and $|D_i| = 4$ for nested requests. Each request was randomly chosen to be a read (as opposed to a write) with probability 0.8 and to be a nested request with probability 0.2. Due to write expansion, $|D_i|$ was inflated to 64 for all write requests under the RW-RNLP, as read requests can access any resource.

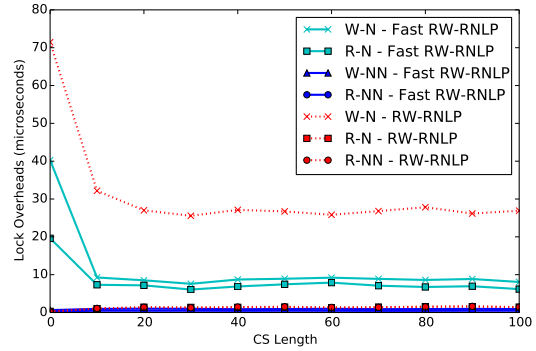

(a) Lock overhead.

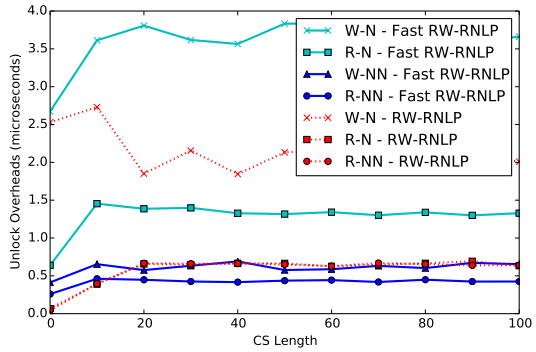

(b) Unlock overhead.

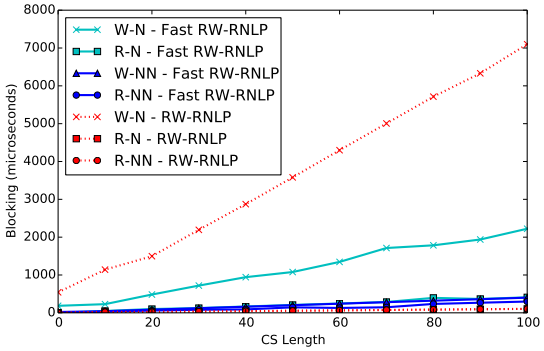

(c) Blocking.

Figure 283: (a) Lock and (b) unlock overheads and (c) blocking for nested and non-nested read and write requests under the RW-RNLP and the fast RW-RNLP. Here, for each request $\mathcal{R}_i$, $m = 36$, $n_r = 64$, $|D_i| = 1$ for non-nested requests, and $|D_i| = 4$ for nested requests. Each request was randomly chosen to be a read (as opposed to a write) with probability 0.8 and to be a nested request with probability 0.5. Due to write expansion, $|D_i|$ was inflated to 64 for all write requests under the RW-RNLP, as read requests can access any resource.

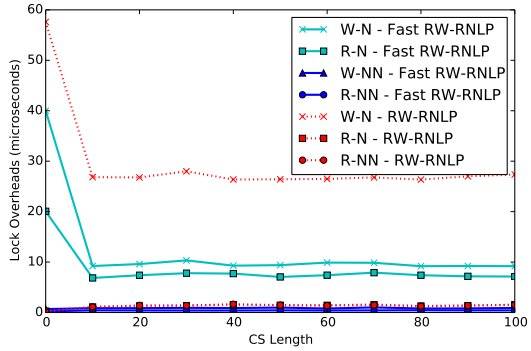

(a) Lock overhead.

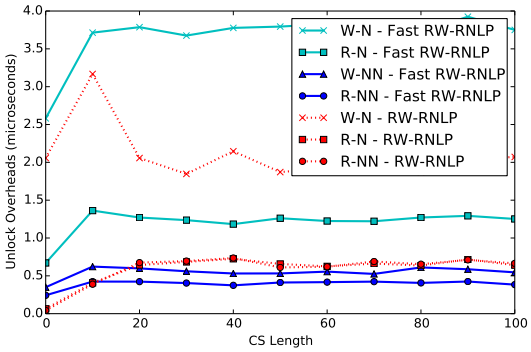

(b) Unlock overhead.

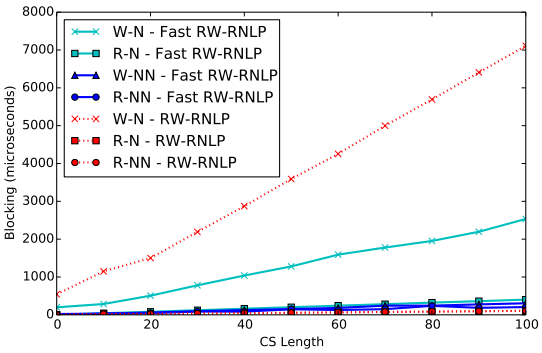

(c) Blocking.

Figure 284: (a) Lock and (b) unlock overheads and (c) blocking for nested and non-nested read and write requests under the RW-RNLP and the fast RW-RNLP. Here, for each request $\mathcal{R}_i$, $m = 36$, $n_r = 64$, $|D_i| = 1$ for non-nested requests, and $|D_i| = 4$ for nested requests. Each request was randomly chosen to be a read (as opposed to a write) with probability 0.8 and to be a nested request with probability 0.8. Due to write expansion, $|D_i|$ was inflated to 64 for all write requests under the RW-RNLP, as read requests can access any resource.

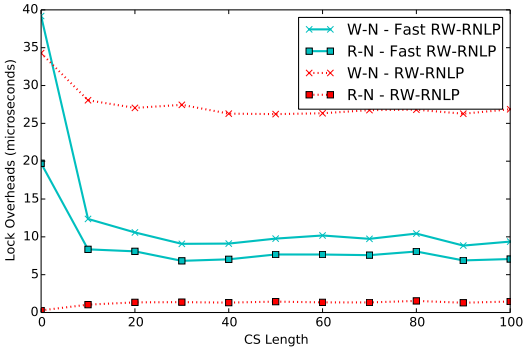

(a) Lock overhead.

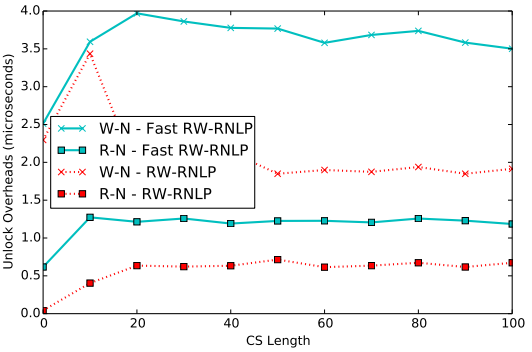

(b) Unlock overhead.

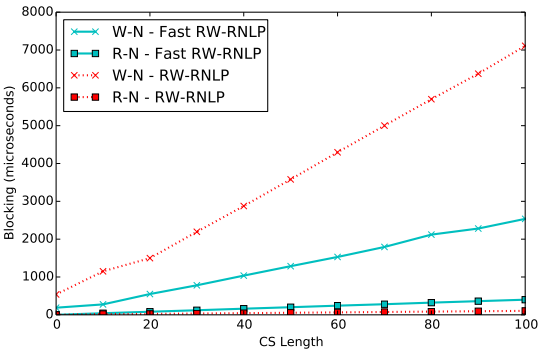

(c) Blocking.

Figure 285: (a) Lock and (b) unlock overheads and (c) blocking for nested read and write requests under the RW-RNLP and the fast RW-RNLP. Here, for each request $\mathcal{R}_i$, $m = 36$, $n_r = 64$, and $|D_i| = 4$. Each request was randomly chosen to be a read (as opposed to a write) with probability 0.8 and to be a nested request with probability 1. Due to write expansion, $|D_i|$ was inflated to 64 for all write requests under the RW-RNLP, as read requests can access any resource.

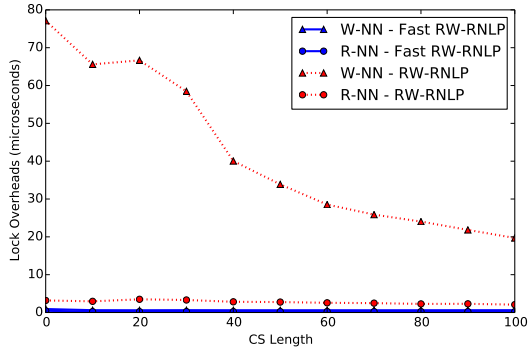

(a) Lock overhead.

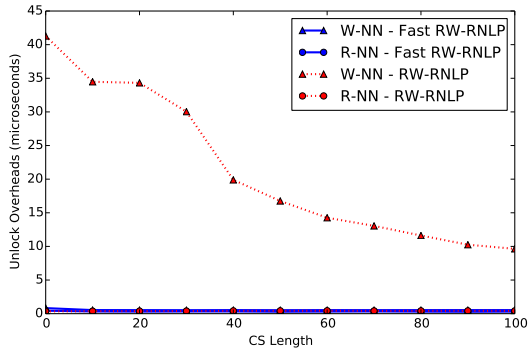

(b) Unlock overhead.

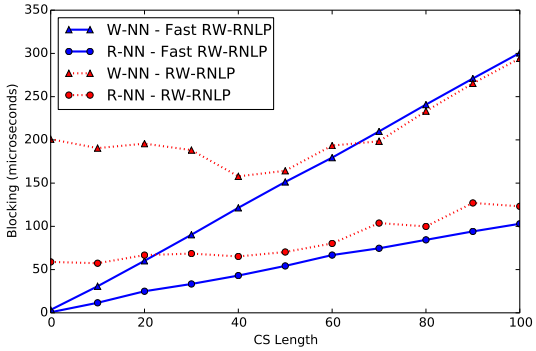

(c) Blocking.

Figure 286: (a) Lock and (b) unlock overheads and (c) blocking for non-nested read and write requests under the RW-RNLP and the fast RW-RNLP. Here, for each request $\mathcal{R}_i$, $m = 36$, $n_r = 64$, and $|D_i| = 1$. Each request was randomly chosen to be a read (as opposed to a write) with probability 0.2 and to be a nested request with probability 0.

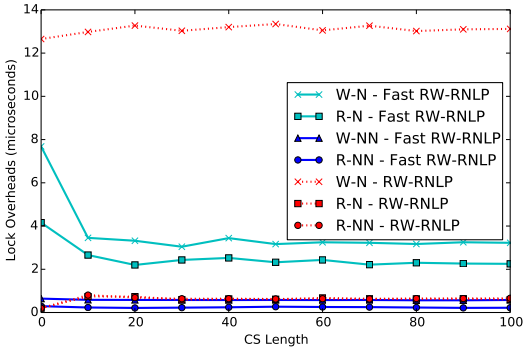

(a) Lock overhead.

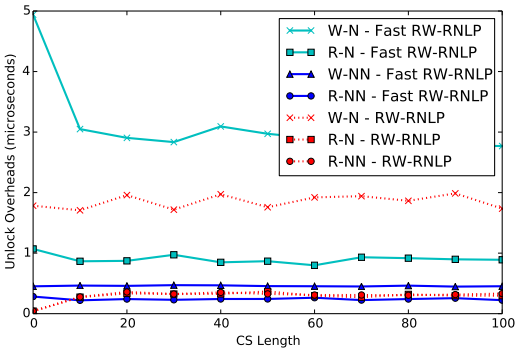

(b) Unlock overhead.

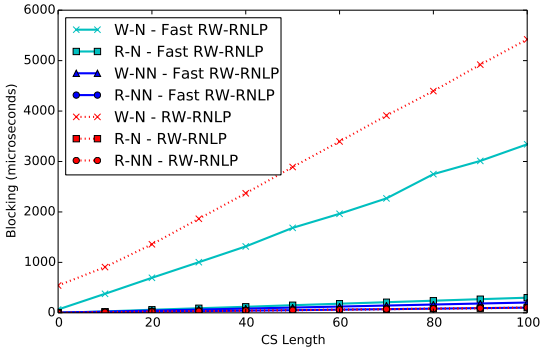

(c) Blocking.

Figure 287: (a) Lock and (b) unlock overheads and (c) blocking for nested and non-nested read and write requests under the RW-RNLP and the fast RW-RNLP. Here, for each request $\mathcal{R}_i$, $m = 36$, $n_r = 64$, $|D_i| = 1$ for non-nested requests, and $|D_i| = 6$ for nested requests. Each request was randomly chosen to be a read (as opposed to a write) with probability 0.2 and to be a nested request with probability 0.2. Due to write expansion, $|D_i|$ was inflated to 64 for all write requests under the RW-RNLP, as read requests can access any resource.

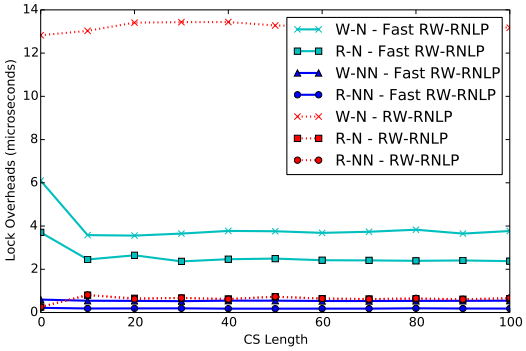

(a) Lock overhead.

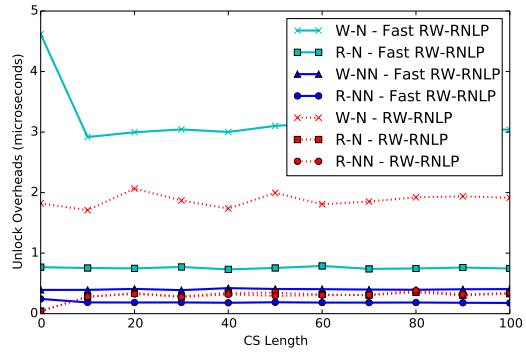

(b) Unlock overhead.

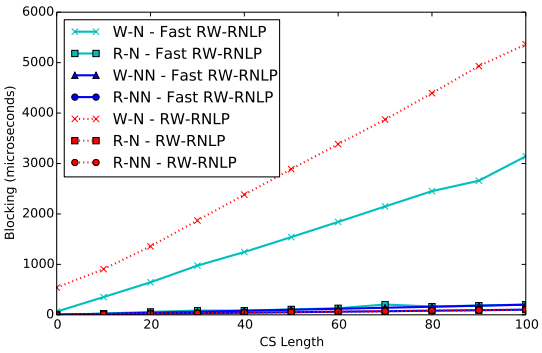

(c) Blocking.

Figure 288: (a) Lock and (b) unlock overheads and (c) blocking for nested and non-nested read and write requests under the RW-RNLP and the fast RW-RNLP. Here, for each request $\mathcal{R}_i$, $m = 36$, $n_r = 64$, $|D_i| = 1$ for non-nested requests, and $|D_i| = 6$ for nested requests. Each request was randomly chosen to be a read (as opposed to a write) with probability 0.2 and to be a nested request with probability 0.5. Due to write expansion, $|D_i|$ was inflated to 64 for all write requests under the RW-RNLP, as read requests can access any resource.

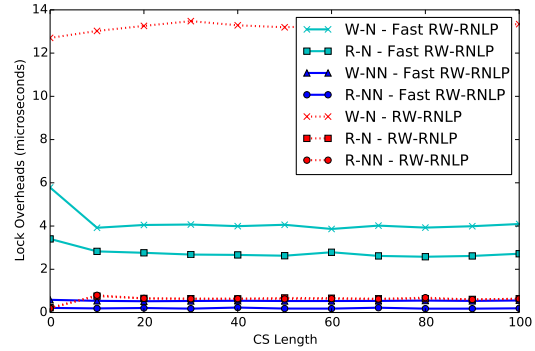

(a) Lock overhead.

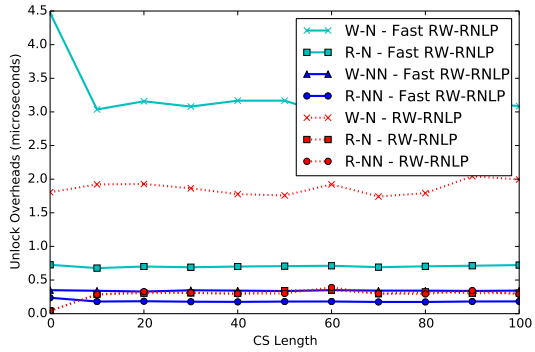

(b) Unlock overhead.

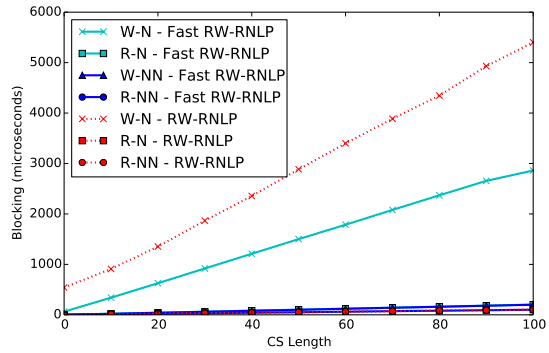

(c) Blocking.

Figure 289: (a) Lock and (b) unlock overheads and (c) blocking for nested and non-nested read and write requests under the RW-RNLP and the fast RW-RNLP. Here, for each request $\mathcal{R}_i$, $m = 36$, $n_r = 64$, $|D_i| = 1$ for non-nested requests, and $|D_i| = 6$ for nested requests. Each request was randomly chosen to be a read (as opposed to a write) with probability 0.2 and to be a nested request with probability 0.8. Due to write expansion, $|D_i|$ was inflated to 64 for all write requests under the RW-RNLP, as read requests can access any resource.

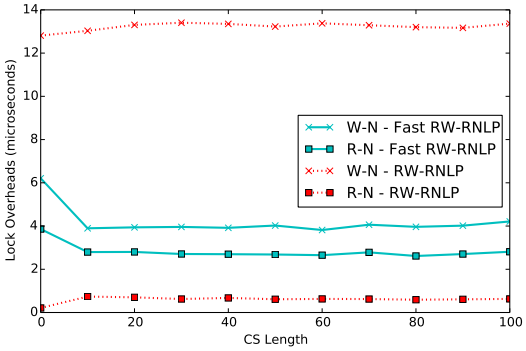

(a) Lock overhead.

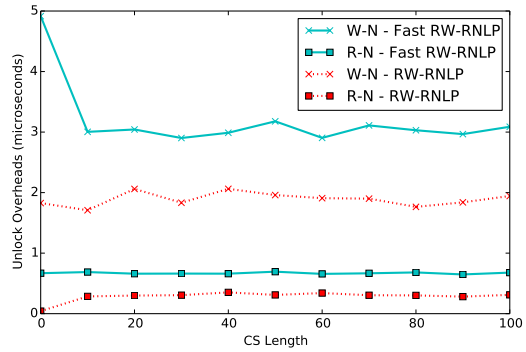

(b) Unlock overhead.

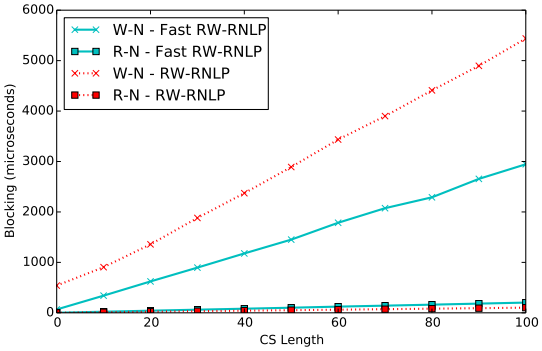

(c) Blocking.

Figure 290: (a) Lock and (b) unlock overheads and (c) blocking for nested read and write requests under the RW-RNLP and the fast RW-RNLP. Here, for each request $\mathcal{R}_i$, $m = 36$, $n_r = 64$, and $|D_i| = 6$. Each request was randomly chosen to be a read (as opposed to a write) with probability 0.2 and to be a nested request with probability 1. Due to write expansion, $|D_i|$ was inflated to 64 for all write requests under the RW-RNLP, as read requests can access any resource.

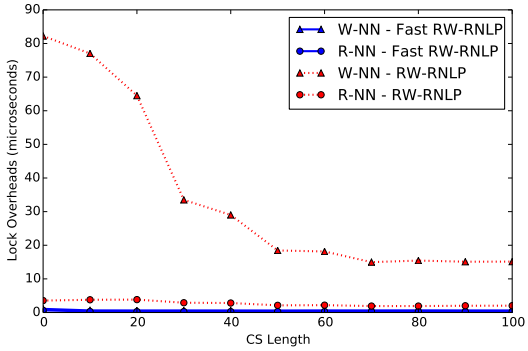

(a) Lock overhead.

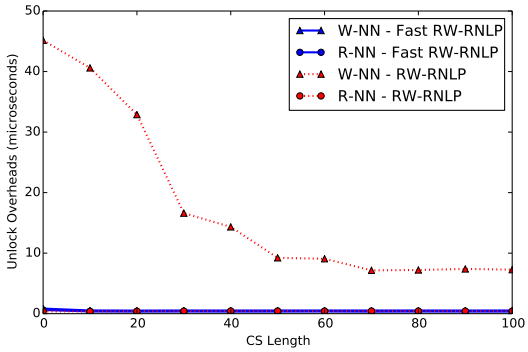

(b) Unlock overhead.

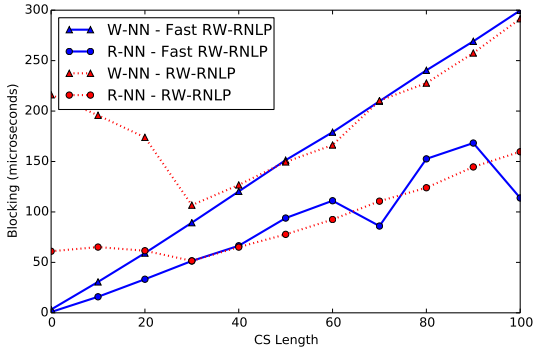

(c) Blocking.

Figure 291: (a) Lock and (b) unlock overheads and (c) blocking for non-nested read and write requests under the RW-RNLP and the fast RW-RNLP. Here, for each request $\mathcal{R}_i$, $m = 36$, $n_r = 64$, and $|D_i| = 1$. Each request was randomly chosen to be a read (as opposed to a write) with probability 0.5 and to be a nested request with probability 0.

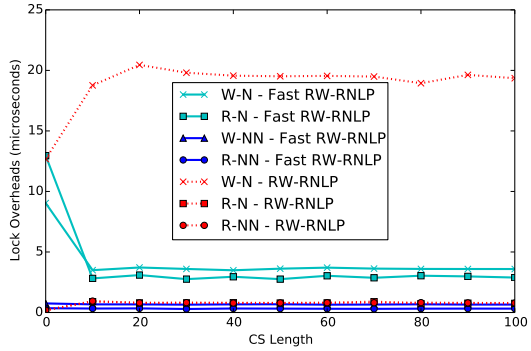

(a) Lock overhead.

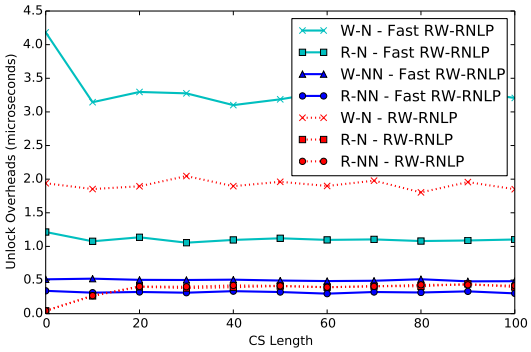

(b) Unlock overhead.

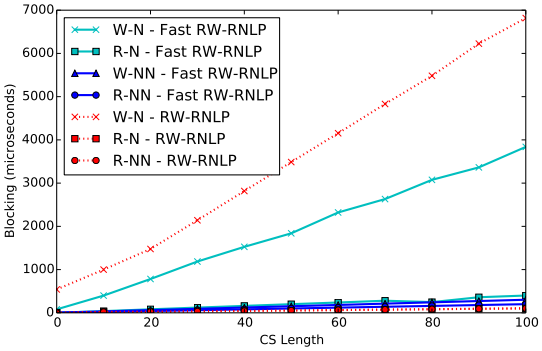

(c) Blocking.

Figure 292: (a) Lock and (b) unlock overheads and (c) blocking for nested and non-nested read and write requests under the RW-RNLP and the fast RW-RNLP. Here, for each request $\mathcal{R}_i$, $m = 36$, $n_r = 64$, $|D_i| = 1$ for non-nested requests, and $|D_i| = 6$ for nested requests. Each request was randomly chosen to be a read (as opposed to a write) with probability 0.5 and to be a nested request with probability 0.2. Due to write expansion, $|D_i|$ was inflated to 64 for all write requests under the RW-RNLP, as read requests can access any resource.

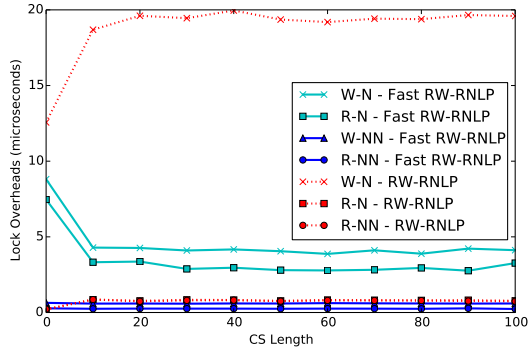

(a) Lock overhead.

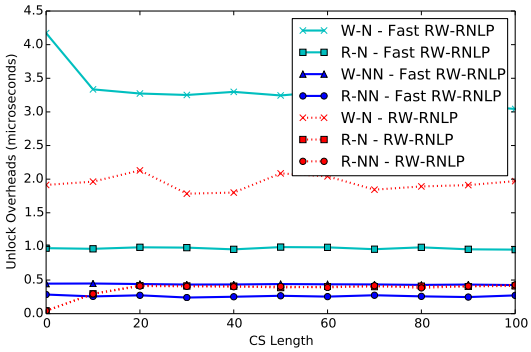

(b) Unlock overhead.

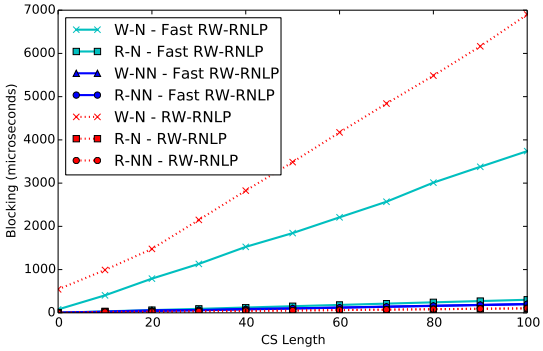

(c) Blocking.

Figure 293: (a) Lock and (b) unlock overheads and (c) blocking for nested and non-nested read and write requests under the RW-RNLP and the fast RW-RNLP. Here, for each request $\mathcal{R}_i$, $m = 36$, $n_r = 64$, $|D_i| = 1$ for non-nested requests, and $|D_i| = 6$ for nested requests. Each request was randomly chosen to be a read (as opposed to a write) with probability 0.5 and to be a nested request with probability 0.5. Due to write expansion, $|D_i|$ was inflated to 64 for all write requests under the RW-RNLP, as read requests can access any resource.

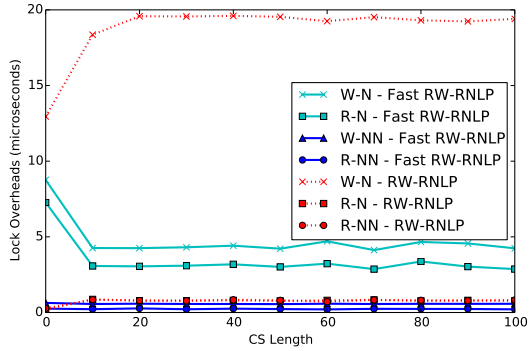

(a) Lock overhead.

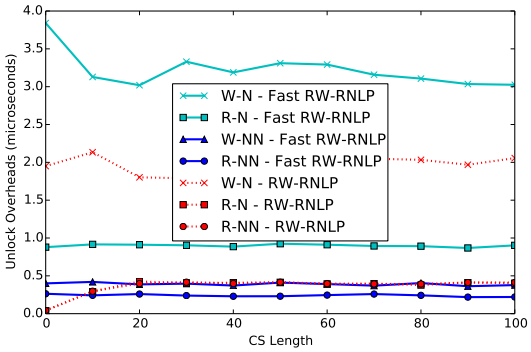

(b) Unlock overhead.

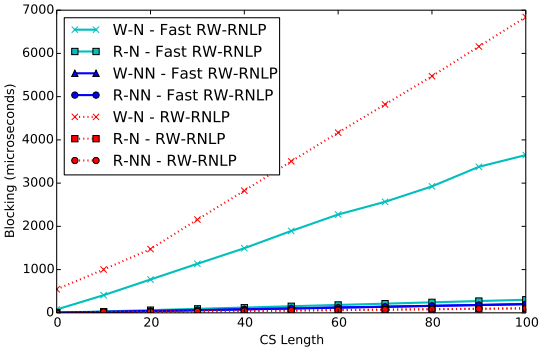

(c) Blocking.

Figure 294: (a) Lock and (b) unlock overheads and (c) blocking for nested and non-nested read and write requests under the RW-RNLP and the fast RW-RNLP. Here, for each request $\mathcal{R}_i$, $m = 36$, $n_r = 64$, $|D_i| = 1$ for non-nested requests, and $|D_i| = 6$ for nested requests. Each request was randomly chosen to be a read (as opposed to a write) with probability 0.5 and to be a nested request with probability 0.8. Due to write expansion, $|D_i|$ was inflated to 64 for all write requests under the RW-RNLP, as read requests can access any resource.

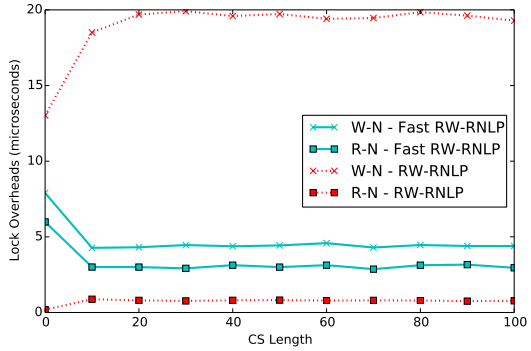

(a) Lock overhead.

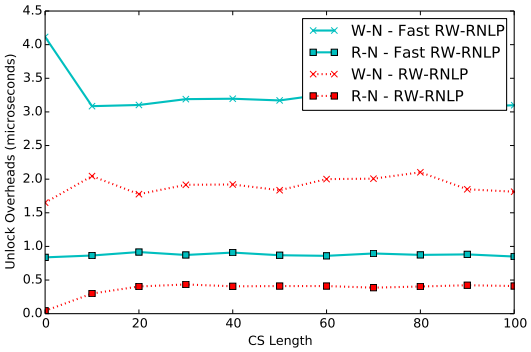

(b) Unlock overhead.

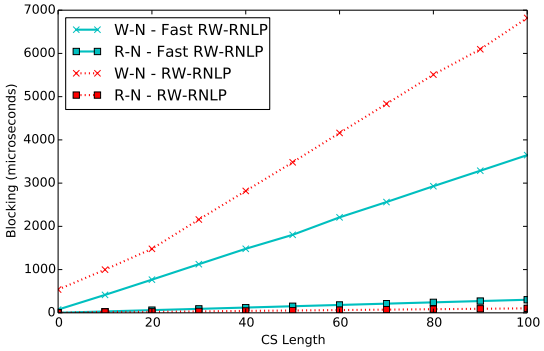

(c) Blocking.

Figure 295: (a) Lock and (b) unlock overheads and (c) blocking for nested read and write requests under the RW-RNLP and the fast RW-RNLP. Here, for each request $\mathcal{R}_i$, $m = 36$, $n_r = 64$, and $|D_i| = 6$. Each request was randomly chosen to be a read (as opposed to a write) with probability 0.5 and to be a nested request with probability 1. Due to write expansion, $|D_i|$ was inflated to 64 for all write requests under the RW-RNLP, as read requests can access any resource.

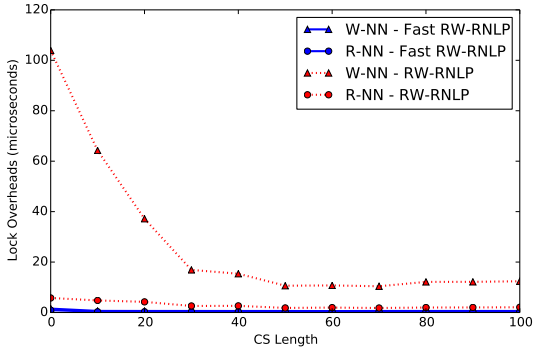

(a) Lock overhead.

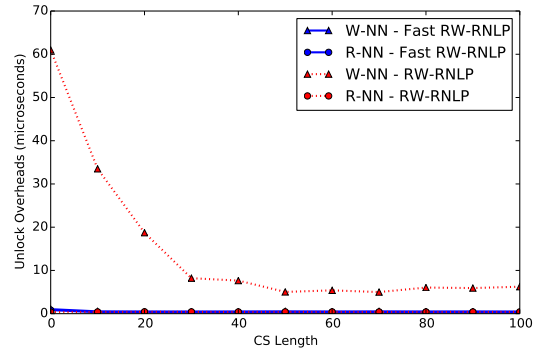

(b) Unlock overhead.

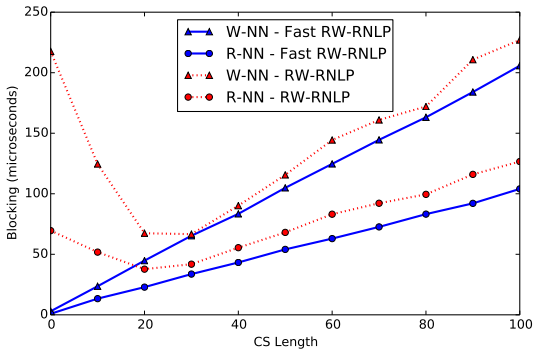

(c) Blocking.

Figure 296: (a) Lock and (b) unlock overheads and (c) blocking for non-nested read and write requests under the RW-RNLP and the fast RW-RNLP. Here, for each request $\mathcal{R}_i$, $m = 36$, $n_r = 64$, and $|D_i| = 1$. Each request was randomly chosen to be a read (as opposed to a write) with probability 0.8 and to be a nested request with probability 0.

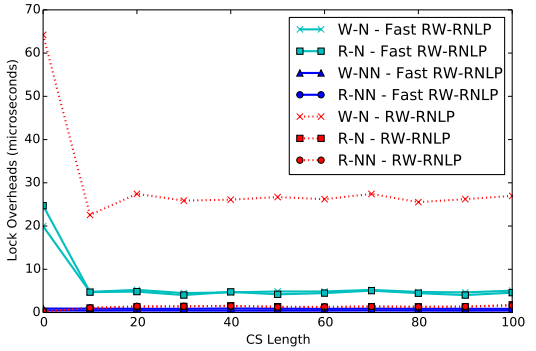

(a) Lock overhead.

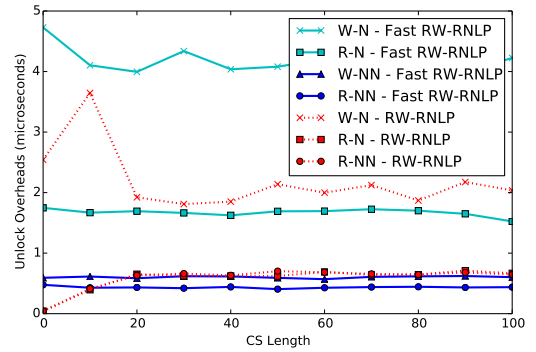

(b) Unlock overhead.

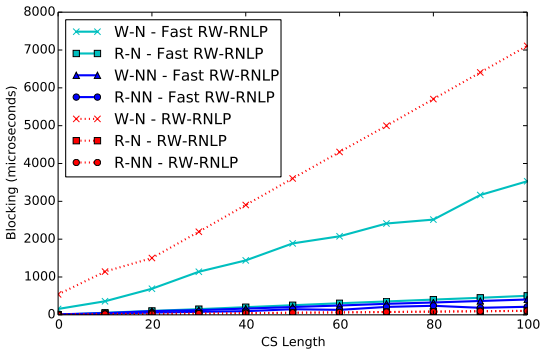

(c) Blocking.

Figure 297: (a) Lock and (b) unlock overheads and (c) blocking for nested and non-nested read and write requests under the RW-RNLP and the fast RW-RNLP. Here, for each request $\mathcal{R}_i$, $m = 36$, $n_r = 64$, $|D_i| = 1$ for non-nested requests, and $|D_i| = 6$ for nested requests. Each request was randomly chosen to be a read (as opposed to a write) with probability 0.8 and to be a nested request with probability 0.2. Due to write expansion, $|D_i|$ was inflated to 64 for all write requests under the RW-RNLP, as read requests can access any resource.

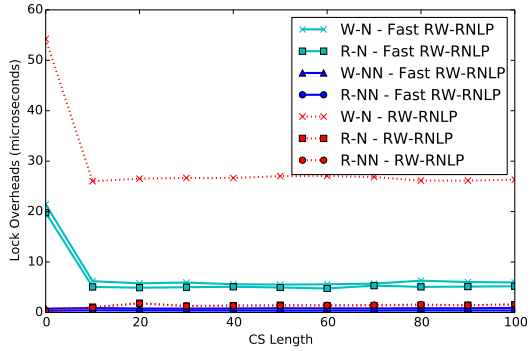

(a) Lock overhead.

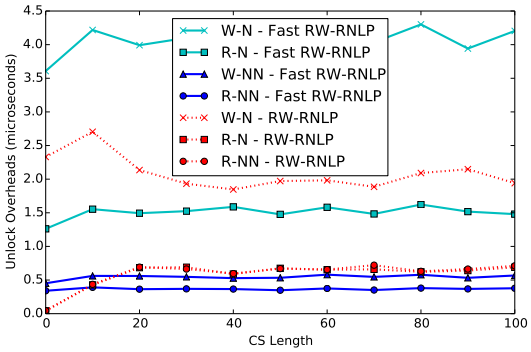

(b) Unlock overhead.

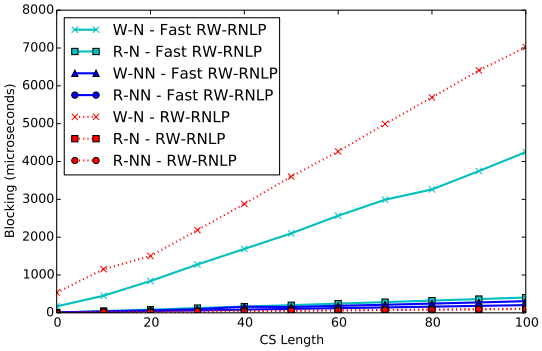

(c) Blocking.

Figure 298: (a) Lock and (b) unlock overheads and (c) blocking for nested and non-nested read and write requests under the RW-RNLP and the fast RW-RNLP. Here, for each request $\mathcal{R}_i$, $m = 36$, $n_r = 64$, $|D_i| = 1$ for non-nested requests, and $|D_i| = 6$ for nested requests. Each request was randomly chosen to be a read (as opposed to a write) with probability 0.8 and to be a nested request with probability 0.5. Due to write expansion, $|D_i|$ was inflated to 64 for all write requests under the RW-RNLP, as read requests can access any resource.

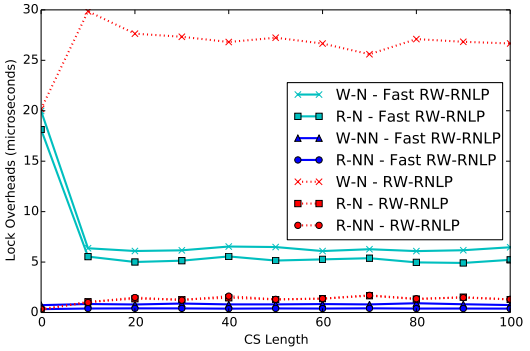

(a) Lock overhead.

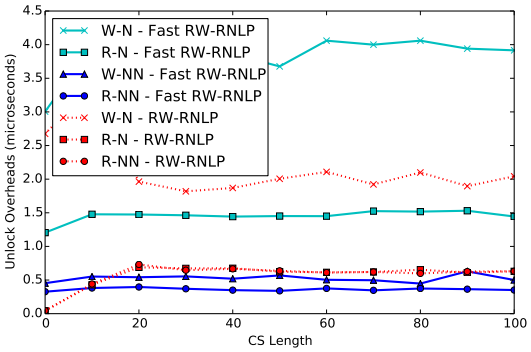

(b) Unlock overhead.

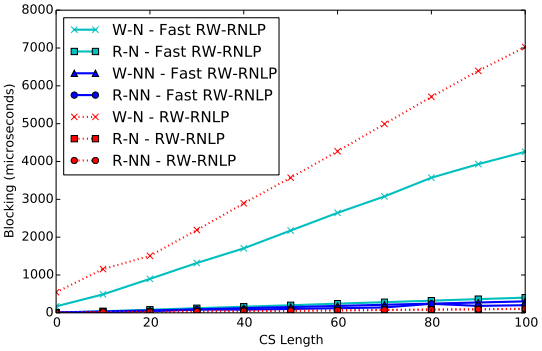

(c) Blocking.

Figure 299: (a) Lock and (b) unlock overheads and (c) blocking for nested and non-nested read and write requests under the RW-RNLP and the fast RW-RNLP. Here, for each request $\mathcal{R}_i$, $m = 36$, $n_r = 64$, $|D_i| = 1$ for non-nested requests, and $|D_i| = 6$ for nested requests. Each request was randomly chosen to be a read (as opposed to a write) with probability 0.8 and to be a nested request with probability 0.8. Due to write expansion, $|D_i|$ was inflated to 64 for all write requests under the RW-RNLP, as read requests can access any resource.

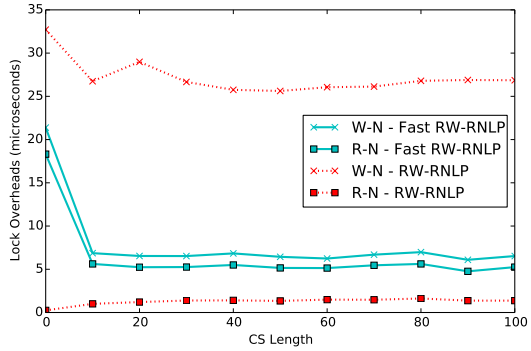

(a) Lock overhead.

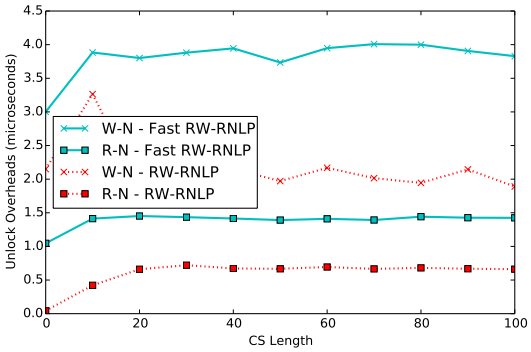

(b) Unlock overhead.

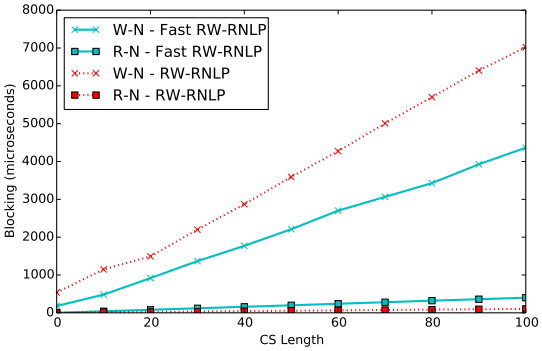

(c) Blocking.

Figure 300: (a) Lock and (b) unlock overheads and (c) blocking for nested read and write requests under the RW-RNLP and the fast RW-RNLP. Here, for each request $\mathcal{R}_i$, $m = 36$, $n_r = 64$, and $|D_i| = 6$. Each request was randomly chosen to be a read (as opposed to a write) with probability 0.8 and to be a nested request with probability 1. Due to write expansion, $|D_i|$ was inflated to 64 for all write requests under the RW-RNLP, as read requests can access any resource.

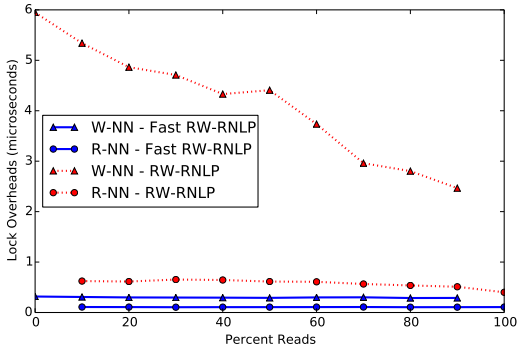

(a) Lock overhead.

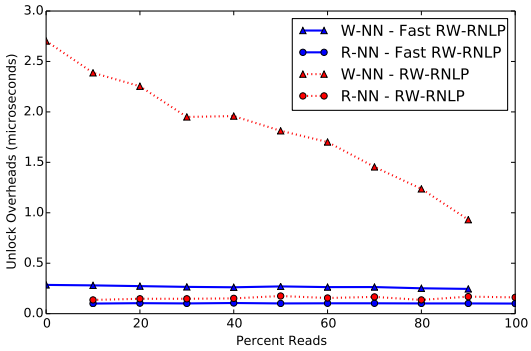

(b) Unlock overhead.

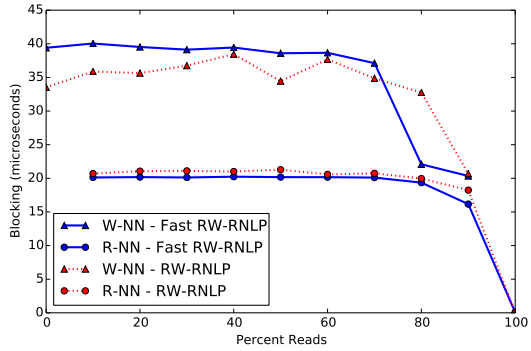

(c) Blocking.

Figure 301: (a) Lock and (b) unlock overheads and (c) blocking for non-nested read and write requests under the RW-RNLP and the fast RW-RNLP. Here, for each request $\mathcal{R}_i$, $m = 18$, $L_i = 20\mu$s, $n_r = 64$, and $|D_i| = 1$. Each request was randomly chosen to be a read (as opposed to a write) with probability as shown and to be a nested request with probability 0.

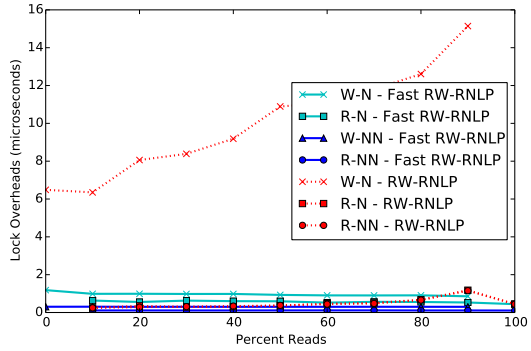

(a) Lock overhead.

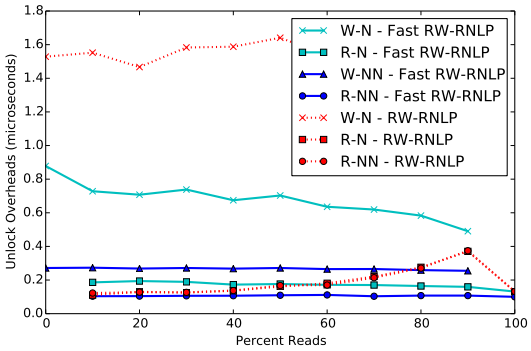

(b) Unlock overhead.

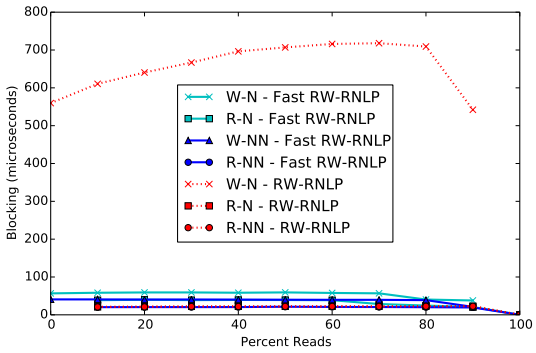

(c) Blocking.

Figure 302: (a) Lock and (b) unlock overheads and (c) blocking for nested and non-nested read and write requests under the RW-RNLP and the fast RW-RNLP. Here, for each request $\mathcal{R}_i$, $m = 18$, $L_i = 20\mu$s, $n_r = 64$, $|D_i| = 1$ for non-nested requests, and $|D_i| = 2$ for nested requests. Each request was randomly chosen to be a read (as opposed to a write) with probability as shown and to be a nested request with probability 0.2. Due to write expansion, $|D_i|$ was inflated to 64 for all write requests under the RW-RNLP, as read requests can access any resource.

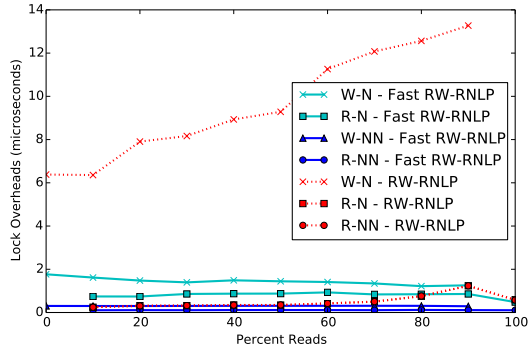

(a) Lock overhead.

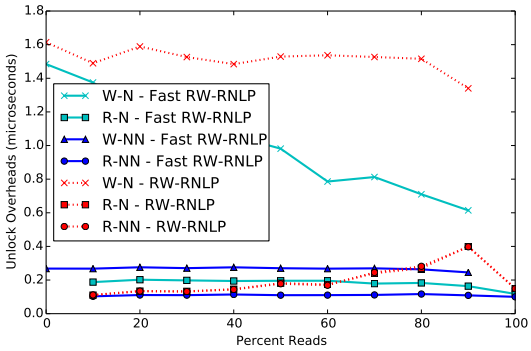

(b) Unlock overhead.

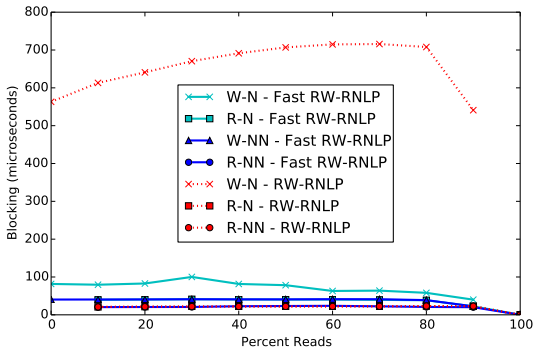

(c) Blocking.

Figure 303: (a) Lock and (b) unlock overheads and (c) blocking for nested and non-nested read and write requests under the RW-RNLP and the fast RW-RNLP. Here, for each request $\mathcal{R}_i$, $m = 18$, $L_i = 20\mu$s, $n_r = 64$, $|D_i| = 1$ for non-nested requests, and $|D_i| = 2$ for nested requests. Each request was randomly chosen to be a read (as opposed to a write) with probability as shown and to be a nested request with probability 0.5. Due to write expansion, $|D_i|$ was inflated to 64 for all write requests under the RW-RNLP, as read requests can access any resource.

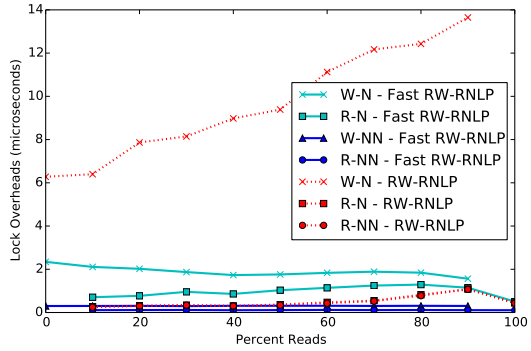

(a) Lock overhead.

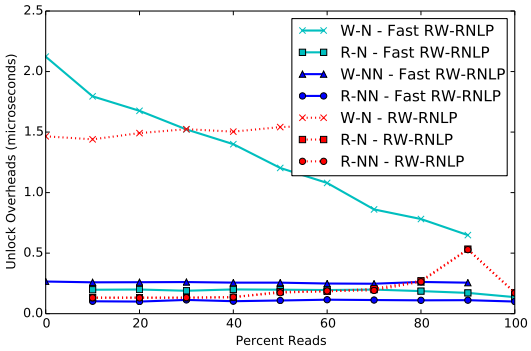

(b) Unlock overhead.

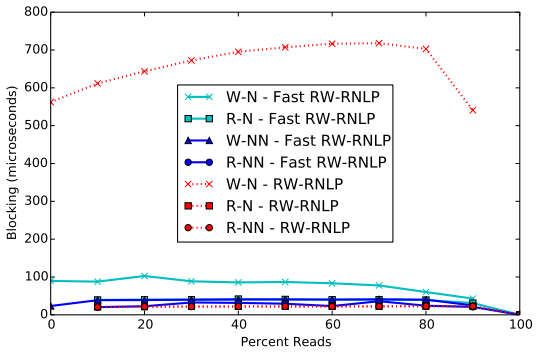

(c) Blocking.

Figure 304: (a) Lock and (b) unlock overheads and (c) blocking for nested and non-nested read and write requests under the RW-RNLP and the fast RW-RNLP. Here, for each request $\mathcal{R}_i$, $m = 18$, $L_i = 20\mu$s, $n_r = 64$, $|D_i| = 1$ for non-nested requests, and $|D_i| = 2$ for nested requests. Each request was randomly chosen to be a read (as opposed to a write) with probability as shown and to be a nested request with probability 0.8. Due to write expansion, $|D_i|$ was inflated to 64 for all write requests under the RW-RNLP, as read requests can access any resource.

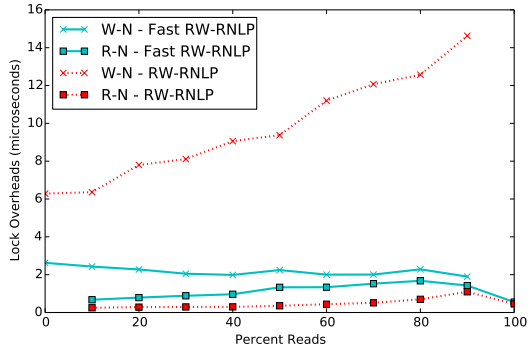

(a) Lock overhead.

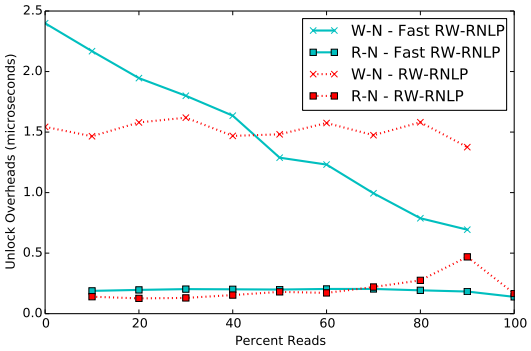

(b) Unlock overhead.

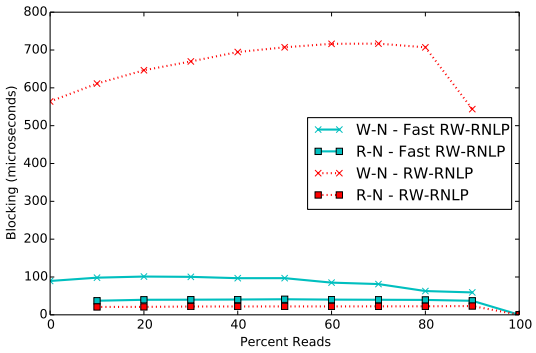

(c) Blocking.

Figure 305: (a) Lock and (b) unlock overheads and (c) blocking for nested read and write requests under the RW-RNLP and the fast RW-RNLP. Here, for each request $\mathcal{R}_i$, $m = 18$, $L_i = 20\mu$s, $n_r = 64$, and $|D_i| = 2$. Each request was randomly chosen to be a read (as opposed to a write) with probability as shown and to be a nested request with probability 1. Due to write expansion, $|D_i|$ was inflated to 64 for all write requests under the RW-RNLP, as read requests can access any resource.

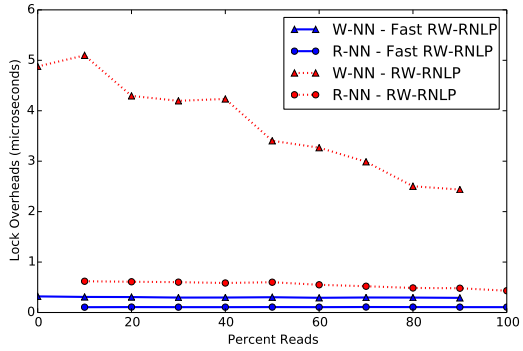

(a) Lock overhead.

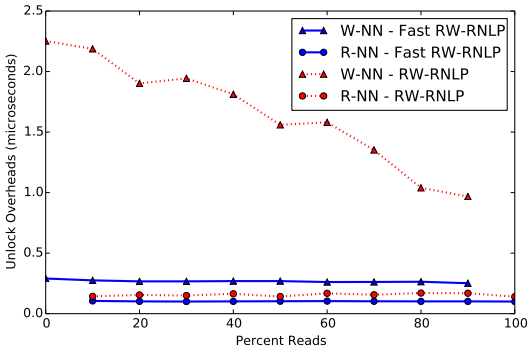

(b) Unlock overhead.

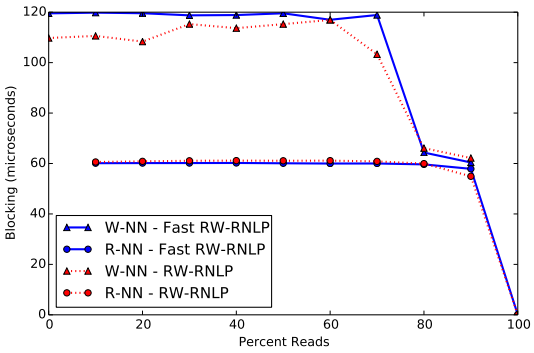

(c) Blocking.

Figure 306: (a) Lock and (b) unlock overheads and (c) blocking for non-nested read and write requests under the RW-RNLP and the fast RW-RNLP. Here, for each request $\mathcal{R}_i$, $m = 18$, $L_i = 60\mu$s, $n_r = 64$, and $|D_i| = 1$. Each request was randomly chosen to be a read (as opposed to a write) with probability as shown and to be a nested request with probability 0.

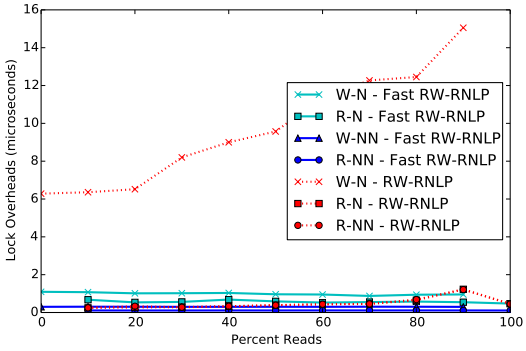

(a) Lock overhead.

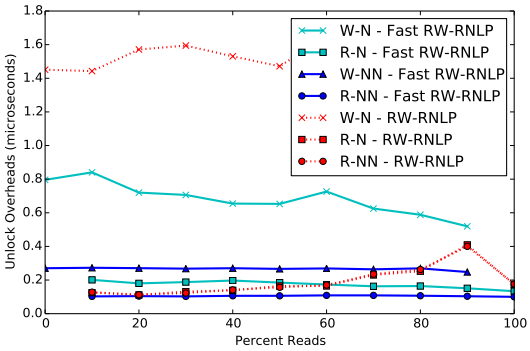

(b) Unlock overhead.

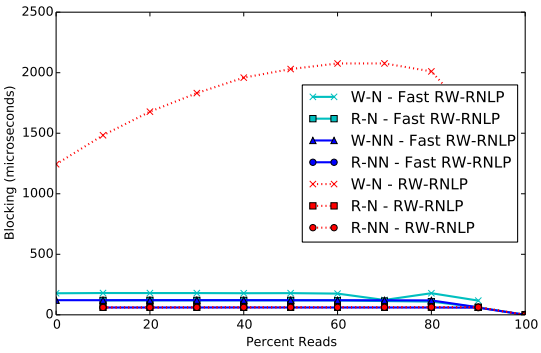

(c) Blocking.

Figure 307: (a) Lock and (b) unlock overheads and (c) blocking for nested and non-nested read and write requests under the RW-RNLP and the fast RW-RNLP. Here, for each request $\mathcal{R}_i$, $m = 18$, $L_i = 60\mu$s, $n_r = 64$, $|D_i| = 1$ for non-nested requests, and $|D_i| = 2$ for nested requests. Each request was randomly chosen to be a read (as opposed to a write) with probability as shown and to be a nested request with probability 0.2. Due to write expansion, $|D_i|$ was inflated to 64 for all write requests under the RW-RNLP, as read requests can access any resource.

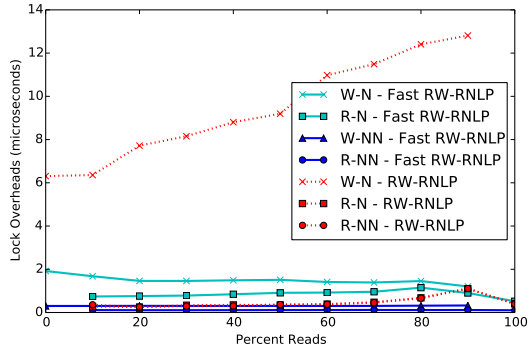

(a) Lock overhead.

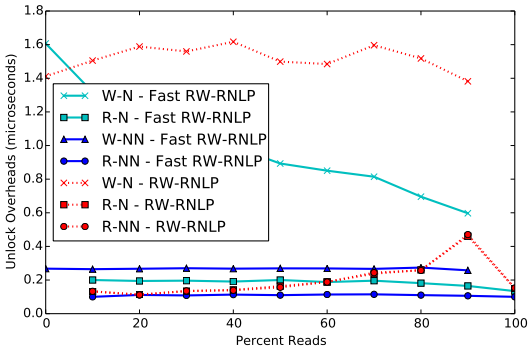

(b) Unlock overhead.

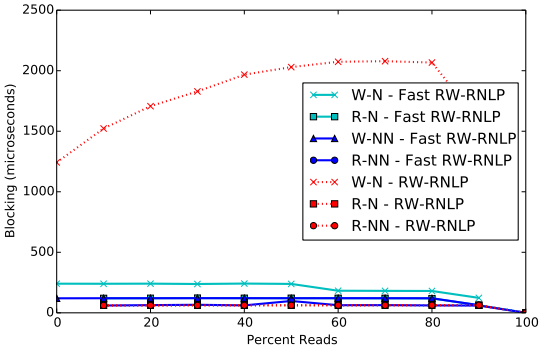

(c) Blocking.

Figure 308: (a) Lock and (b) unlock overheads and (c) blocking for nested and non-nested read and write requests under the RW-RNLP and the fast RW-RNLP. Here, for each request $\mathcal{R}_i$, $m = 18$, $L_i = 60\mu$s, $n_r = 64$, $|D_i| = 1$ for non-nested requests, and $|D_i| = 2$ for nested requests. Each request was randomly chosen to be a read (as opposed to a write) with probability as shown and to be a nested request with probability 0.5. Due to write expansion, $|D_i|$ was inflated to 64 for all write requests under the RW-RNLP, as read requests can access any resource.

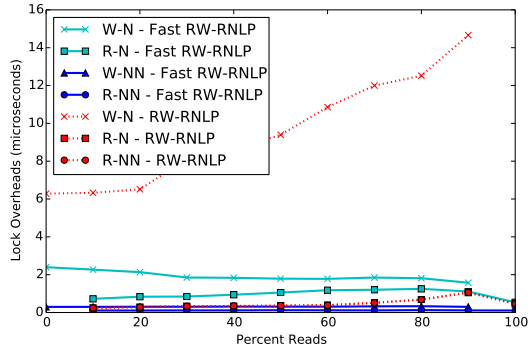

(a) Lock overhead.

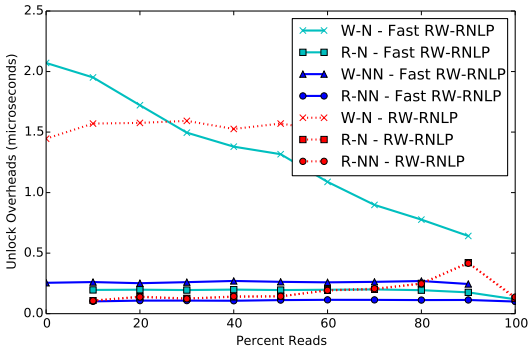

(b) Unlock overhead.

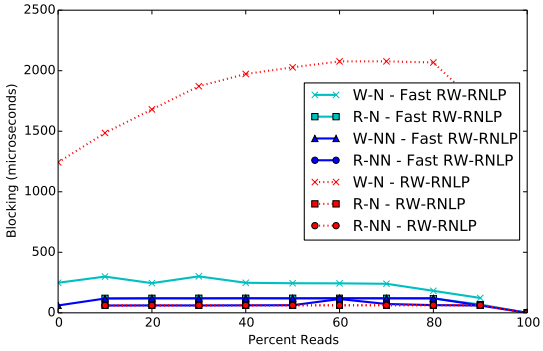

(c) Blocking.

Figure 309: (a) Lock and (b) unlock overheads and (c) blocking for nested and non-nested read and write requests under the RW-RNLP and the fast RW-RNLP. Here, for each request $\mathcal{R}_i$, $m = 18$, $L_i = 60\mu$s, $n_r = 64$, $|D_i| = 1$ for non-nested requests, and $|D_i| = 2$ for nested requests. Each request was randomly chosen to be a read (as opposed to a write) with probability as shown and to be a nested request with probability 0.8. Due to write expansion, $|D_i|$ was inflated to 64 for all write requests under the RW-RNLP, as read requests can access any resource.

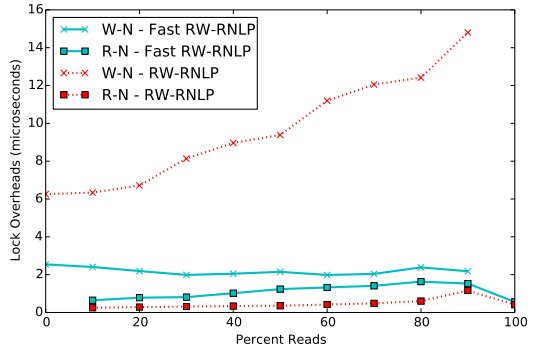

(a) Lock overhead.

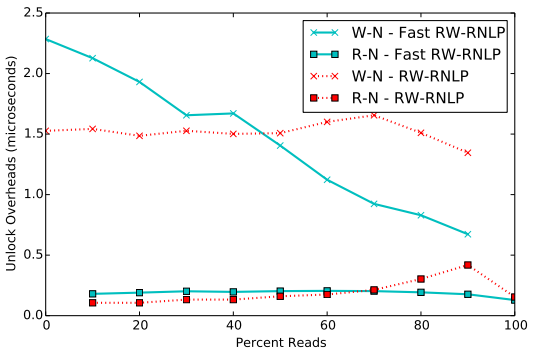

(b) Unlock overhead.

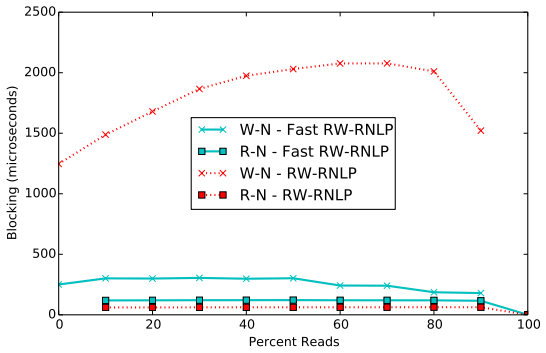

(c) Blocking.

Figure 310: (a) Lock and (b) unlock overheads and (c) blocking for nested read and write requests under the RW-RNLP and the fast RW-RNLP. Here, for each request $\mathcal{R}_i$, $m = 18$, $L_i = 60\mu$s, $n_r = 64$, and $|D_i| = 2$. Each request was randomly chosen to be a read (as opposed to a write) with probability as shown and to be a nested request with probability 1. Due to write expansion, $|D_i|$ was inflated to 64 for all write requests under the RW-RNLP, as read requests can access any resource.

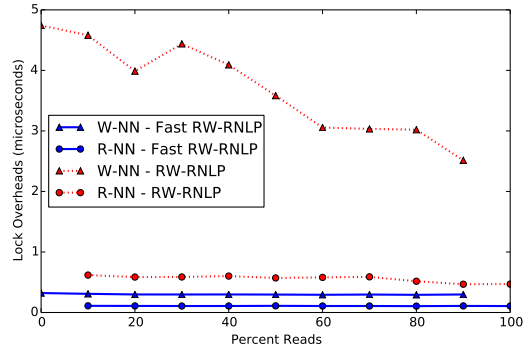

(a) Lock overhead.

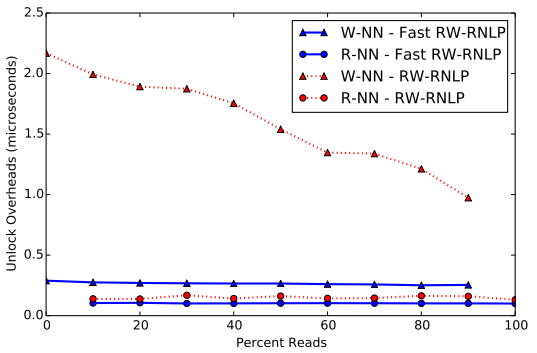

(b) Unlock overhead.

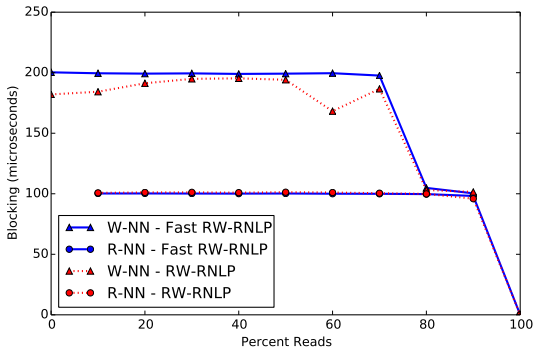

(c) Blocking.

Figure 311: (a) Lock and (b) unlock overheads and (c) blocking for non-nested read and write requests under the RW-RNLP and the fast RW-RNLP. Here, for each request $\mathcal{R}_i$, $m = 18$, $L_i = 100\mu$s, $n_r = 64$, and $|D_i| = 1$. Each request was randomly chosen to be a read (as opposed to a write) with probability as shown and to be a nested request with probability 0.

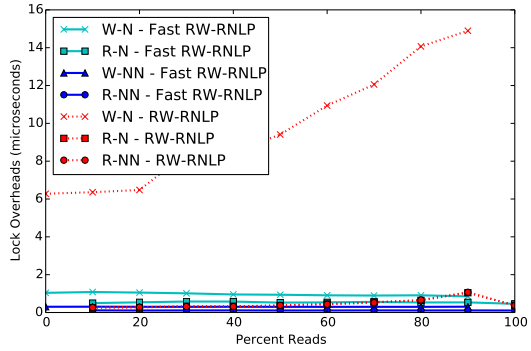

(a) Lock overhead.

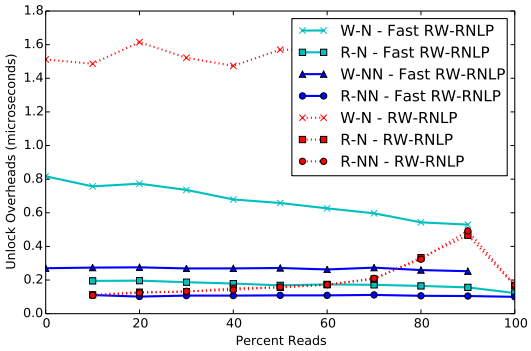

(b) Unlock overhead.

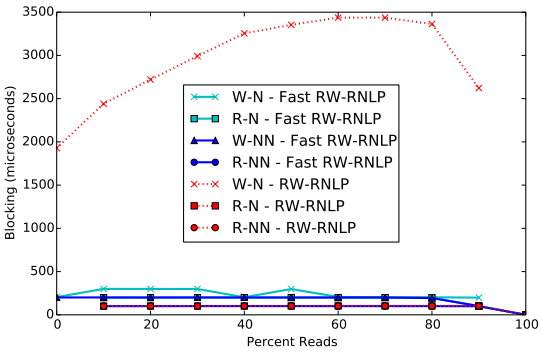

(c) Blocking.

Figure 312: (a) Lock and (b) unlock overheads and (c) blocking for nested and non-nested read and write requests under the RW-RNLP and the fast RW-RNLP. Here, for each request $\mathcal{R}_i$, $m = 18$, $L_i = 100\mu$s, $n_r = 64$, $|D_i| = 1$ for non-nested requests, and $|D_i| = 2$ for nested requests. Each request was randomly chosen to be a read (as opposed to a write) with probability as shown and to be a nested request with probability 0.2. Due to write expansion, $|D_i|$ was inflated to 64 for all write requests under the RW-RNLP, as read requests can access any resource.

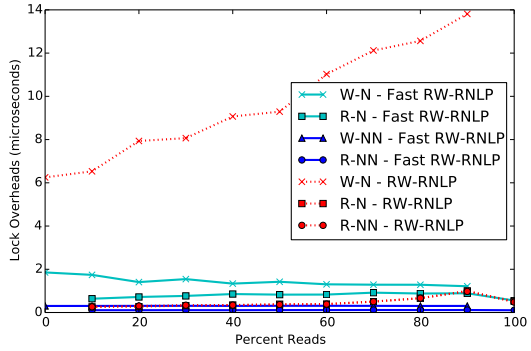

(a) Lock overhead.

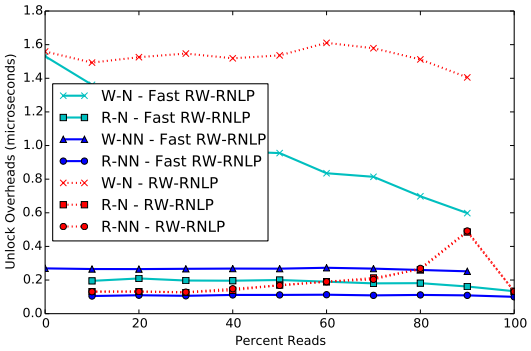

(b) Unlock overhead.

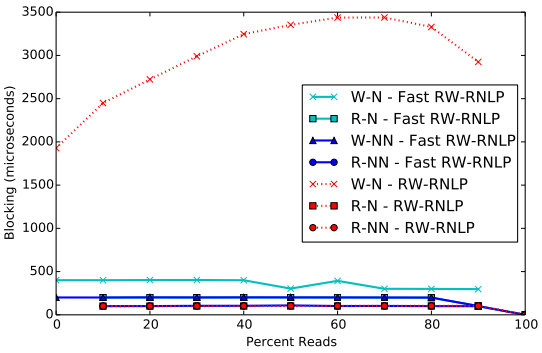

(c) Blocking.

Figure 313: (a) Lock and (b) unlock overheads and (c) blocking for nested and non-nested read and write requests under the RW-RNLP and the fast RW-RNLP. Here, for each request $\mathcal{R}_i$, $m = 18$, $L_i = 100\mu$s, $n_r = 64$, $|D_i| = 1$ for non-nested requests, and $|D_i| = 2$ for nested requests. Each request was randomly chosen to be a read (as opposed to a write) with probability as shown and to be a nested request with probability 0.5. Due to write expansion, $|D_i|$ was inflated to 64 for all write requests under the RW-RNLP, as read requests can access any resource.

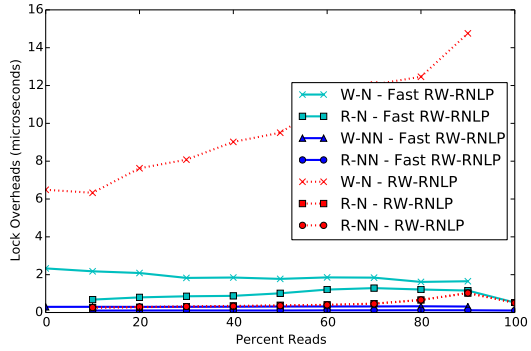

(a) Lock overhead.

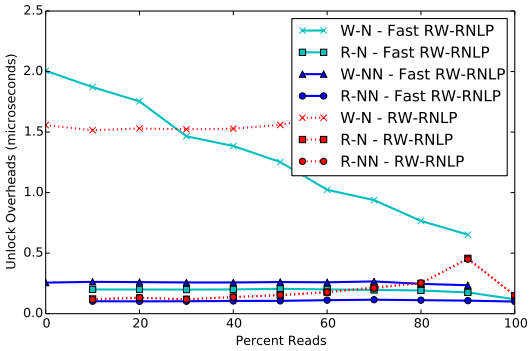

(b) Unlock overhead.

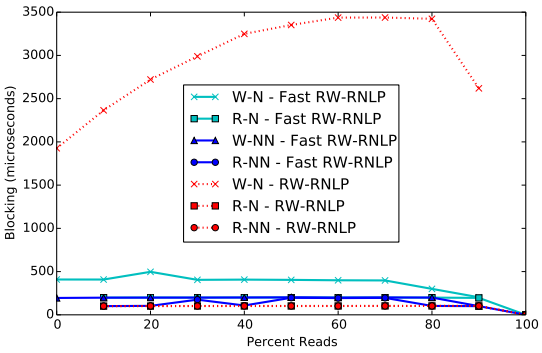

(c) Blocking.

Figure 314: (a) Lock and (b) unlock overheads and (c) blocking for nested and non-nested read and write requests under the RW-RNLP and the fast RW-RNLP. Here, for each request $\mathcal{R}_i$, $m = 18$, $L_i = 100\mu$s, $n_r = 64$, $|D_i| = 1$ for non-nested requests, and $|D_i| = 2$ for nested requests. Each request was randomly chosen to be a read (as opposed to a write) with probability as shown and to be a nested request with probability 0.8. Due to write expansion, $|D_i|$ was inflated to 64 for all write requests under the RW-RNLP, as read requests can access any resource.

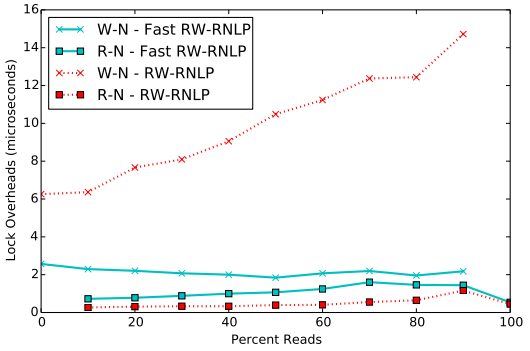

(a) Lock overhead.

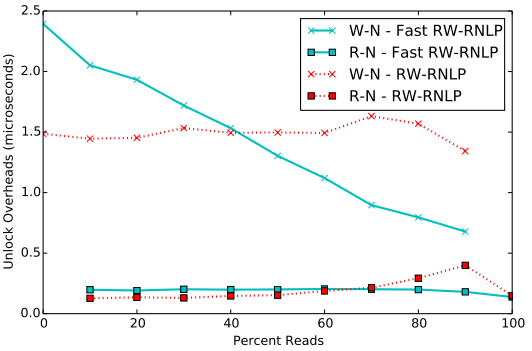

(b) Unlock overhead.

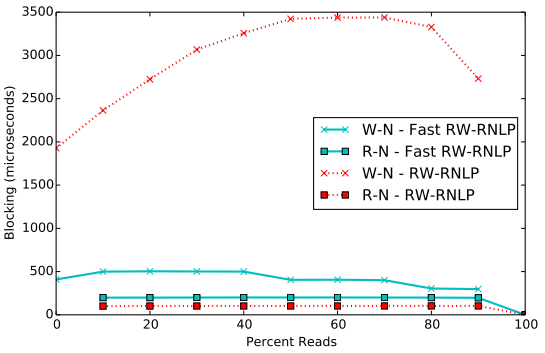

(c) Blocking.

Figure 315: (a) Lock and (b) unlock overheads and (c) blocking for nested read and write requests under the RW-RNLP and the fast RW-RNLP. Here, for each request $\mathcal{R}_i$, $m = 18$, $L_i = 100\mu$s, $n_r = 64$, and $|D_i| = 2$. Each request was randomly chosen to be a read (as opposed to a write) with probability as shown and to be a nested request with probability 1. Due to write expansion, $|D_i|$ was inflated to 64 for all write requests under the RW-RNLP, as read requests can access any resource.

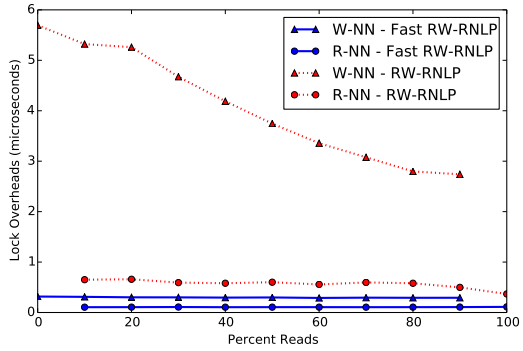

(a) Lock overhead.

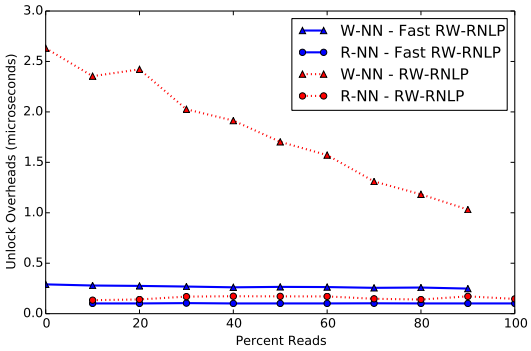

(b) Unlock overhead.

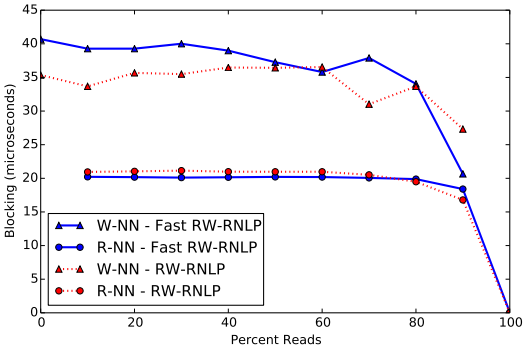

(c) Blocking.

Figure 316: (a) Lock and (b) unlock overheads and (c) blocking for non-nested read and write requests under the RW-RNLP and the fast RW-RNLP. Here, for each request $\mathcal{R}_i$, $m = 18$, $L_i = 20\mu$s, $n_r = 64$, and $|D_i| = 1$. Each request was randomly chosen to be a read (as opposed to a write) with probability as shown and to be a nested request with probability 0.

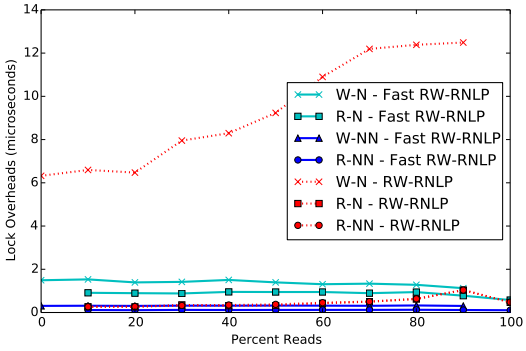

(a) Lock overhead.

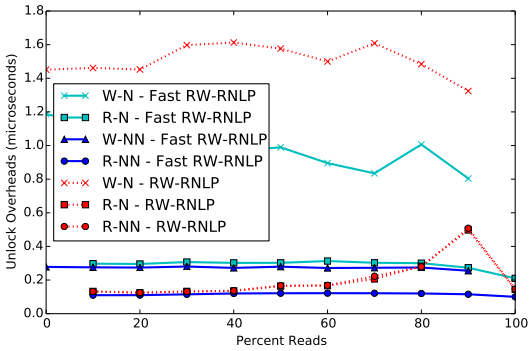

(b) Unlock overhead.

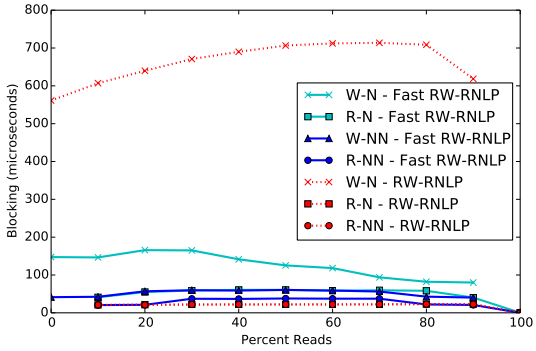

(c) Blocking.

Figure 317: (a) Lock and (b) unlock overheads and (c) blocking for nested and non-nested read and write requests under the RW-RNLP and the fast RW-RNLP. Here, for each request $\mathcal{R}_i$, $m = 18$, $L_i = 20\mu$s, $n_r = 64$, $|D_i| = 1$ for non-nested requests, and $|D_i| = 4$ for nested requests. Each request was randomly chosen to be a read (as opposed to a write) with probability as shown and to be a nested request with probability 0.2. Due to write expansion, $|D_i|$ was inflated to 64 for all write requests under the RW-RNLP, as read requests can access any resource.

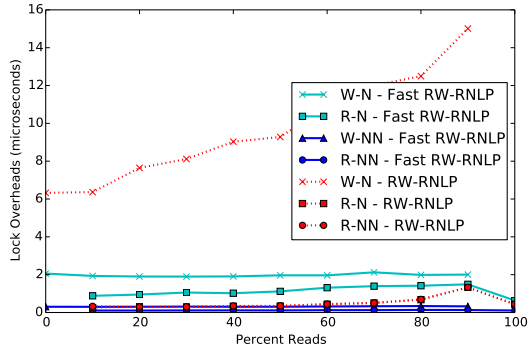

(a) Lock overhead.

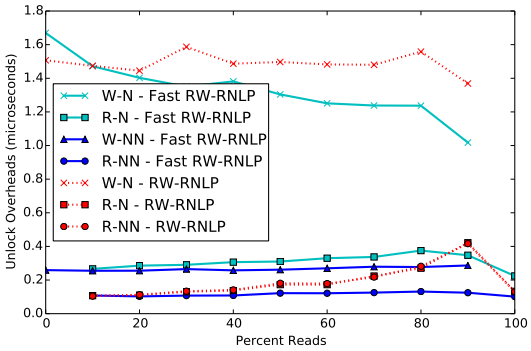

(b) Unlock overhead.

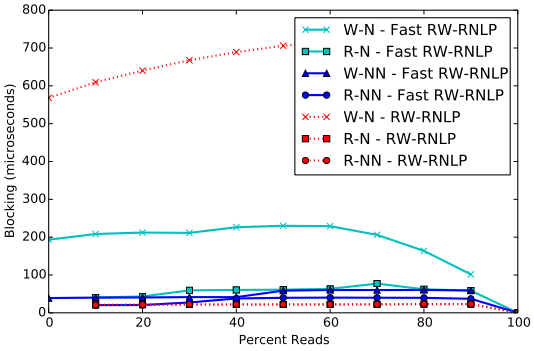

(c) Blocking.

Figure 318: (a) Lock and (b) unlock overheads and (c) blocking for nested and non-nested read and write requests under the RW-RNLP and the fast RW-RNLP. Here, for each request $\mathcal{R}_i$, $m = 18$, $L_i = 20\mu$s, $n_r = 64$, $|D_i| = 1$ for non-nested requests, and $|D_i| = 4$ for nested requests. Each request was randomly chosen to be a read (as opposed to a write) with probability as shown and to be a nested request with probability 0.5. Due to write expansion, $|D_i|$ was inflated to 64 for all write requests under the RW-RNLP, as read requests can access any resource.

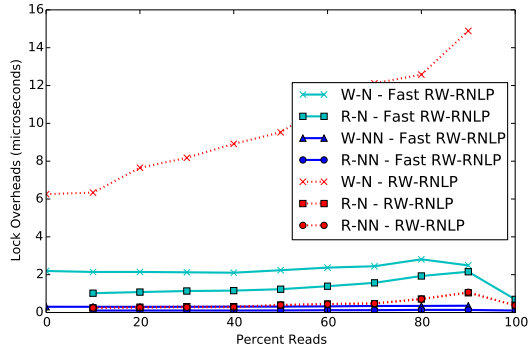

(a) Lock overhead.

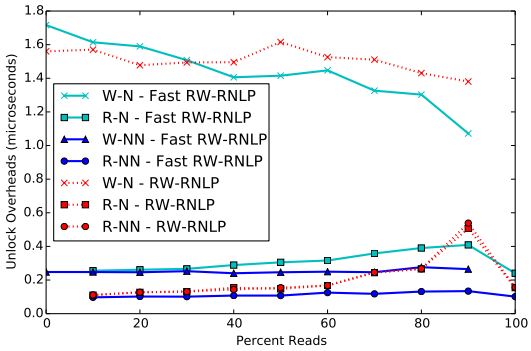

(b) Unlock overhead.

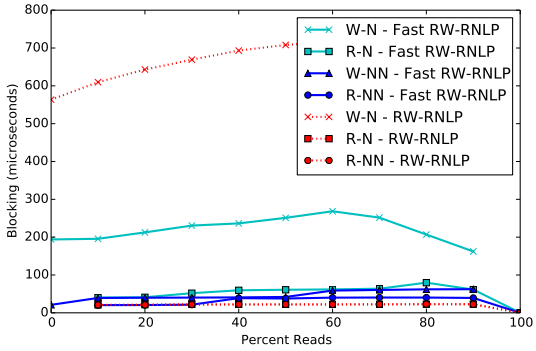

(c) Blocking.

Figure 319: (a) Lock and (b) unlock overheads and (c) blocking for nested and non-nested read and write requests under the RW-RNLP and the fast RW-RNLP. Here, for each request $\mathcal{R}_i$, $m = 18$, $L_i = 20\mu$s, $n_r = 64$, $|D_i| = 1$ for non-nested requests, and $|D_i| = 4$ for nested requests. Each request was randomly chosen to be a read (as opposed to a write) with probability as shown and to be a nested request with probability 0.8. Due to write expansion, $|D_i|$ was inflated to 64 for all write requests under the RW-RNLP, as read requests can access any resource.

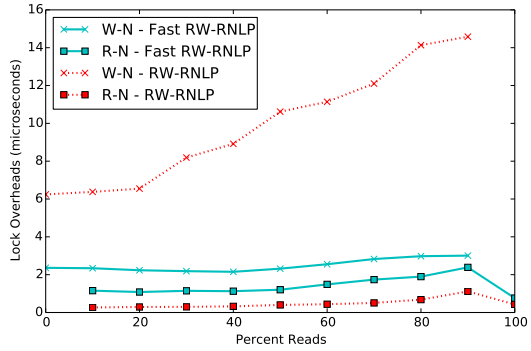

(a) Lock overhead.

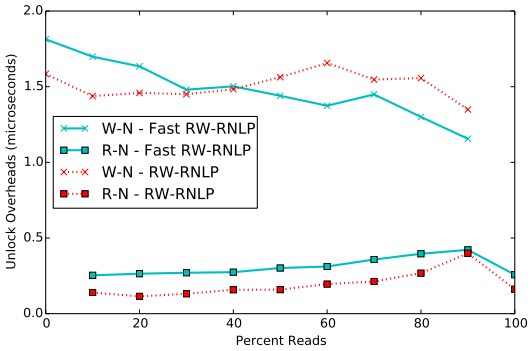

(b) Unlock overhead.

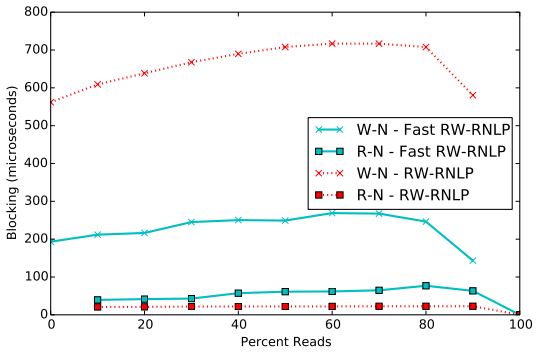

(c) Blocking.

Figure 320: (a) Lock and (b) unlock overheads and (c) blocking for nested read and write requests under the RW-RNLP and the fast RW-RNLP. Here, for each request $\mathcal{R}_i$, $m = 18$, $L_i = 20\mu$s, $n_r = 64$, and $|D_i| = 4$. Each request was randomly chosen to be a read (as opposed to a write) with probability as shown and to be a nested request with probability 1. Due to write expansion, $|D_i|$ was inflated to 64 for all write requests under the RW-RNLP, as read requests can access any resource.

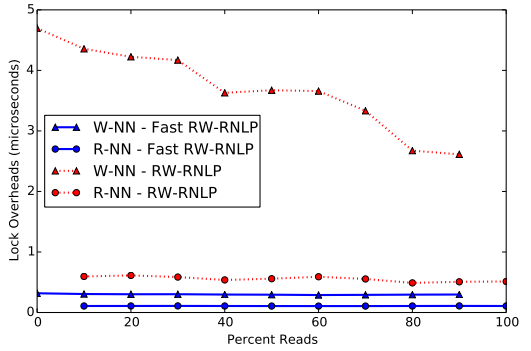

(a) Lock overhead.

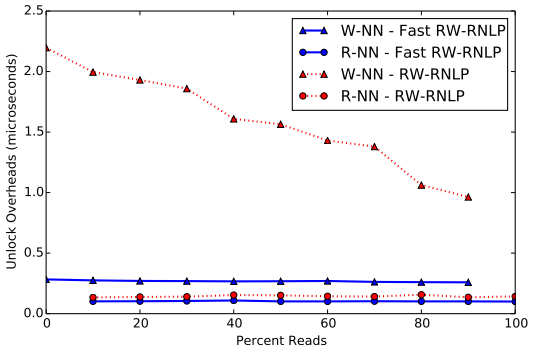

(b) Unlock overhead.

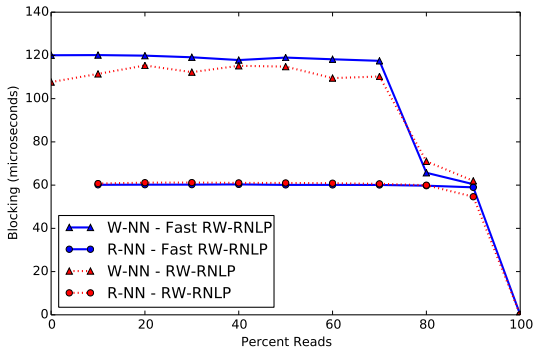

(c) Blocking.

Figure 321: (a) Lock and (b) unlock overheads and (c) blocking for non-nested read and write requests under the RW-RNLP and the fast RW-RNLP. Here, for each request $\mathcal{R}_i$, $m = 18$, $L_i = 60\mu$s, $n_r = 64$, and $|D_i| = 1$. Each request was randomly chosen to be a read (as opposed to a write) with probability as shown and to be a nested request with probability 0.

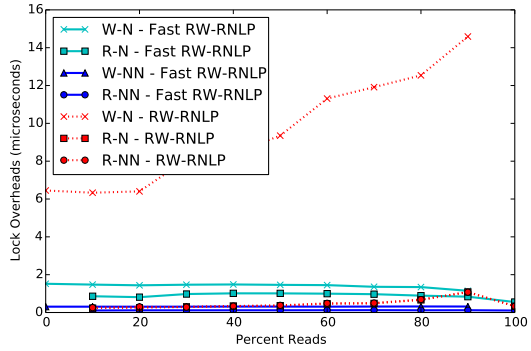

(a) Lock overhead.

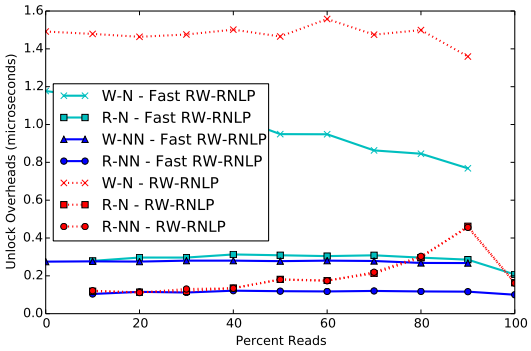

(b) Unlock overhead.

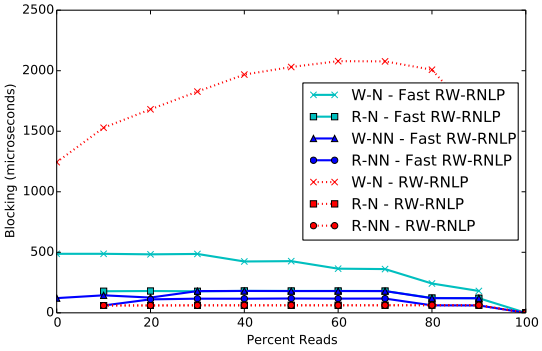

(c) Blocking.

Figure 322: (a) Lock and (b) unlock overheads and (c) blocking for nested and non-nested read and write requests under the RW-RNLP and the fast RW-RNLP. Here, for each request $\mathcal{R}_i$, $m = 18$, $L_i = 60\mu$s, $n_r = 64$, $|D_i| = 1$ for non-nested requests, and $|D_i| = 4$ for nested requests. Each request was randomly chosen to be a read (as opposed to a write) with probability as shown and to be a nested request with probability 0.2. Due to write expansion, $|D_i|$ was inflated to 64 for all write requests under the RW-RNLP, as read requests can access any resource.

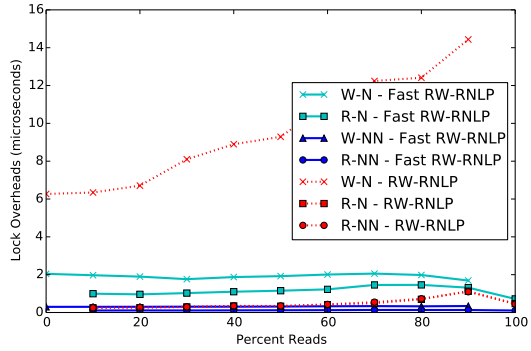

(a) Lock overhead.

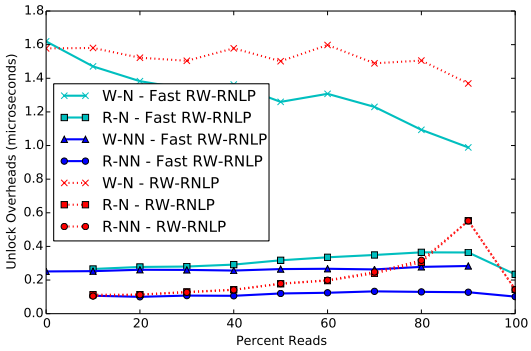

(b) Unlock overhead.

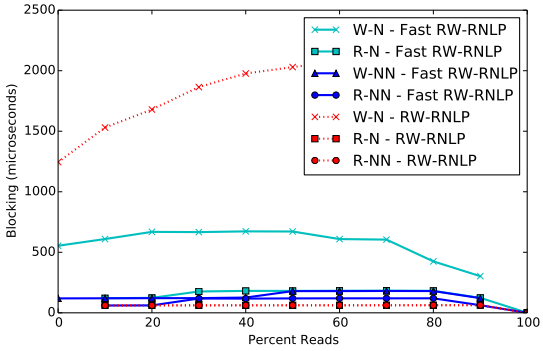

(c) Blocking.

Figure 323: (a) Lock and (b) unlock overheads and (c) blocking for nested and non-nested read and write requests under the RW-RNLP and the fast RW-RNLP. Here, for each request $\mathcal{R}_i$, $m = 18$, $L_i = 60\mu$s, $n_r = 64$, $|D_i| = 1$ for non-nested requests, and $|D_i| = 4$ for nested requests. Each request was randomly chosen to be a read (as opposed to a write) with probability as shown and to be a nested request with probability 0.5. Due to write expansion, $|D_i|$ was inflated to 64 for all write requests under the RW-RNLP, as read requests can access any resource.

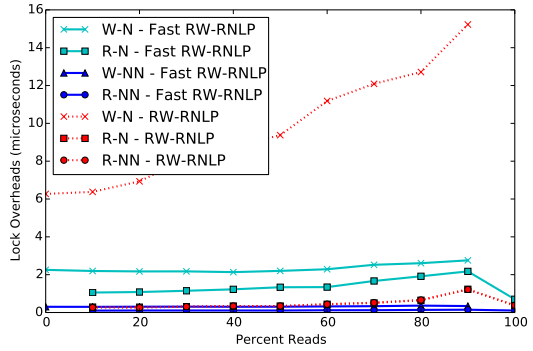

(a) Lock overhead.

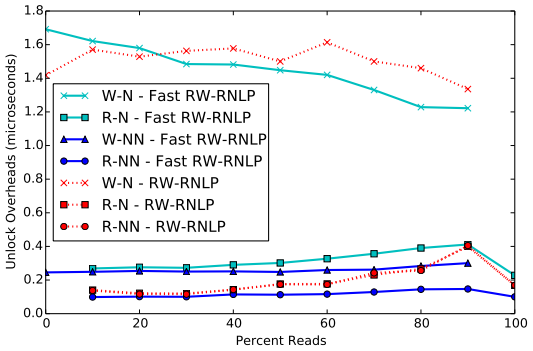

(b) Unlock overhead.

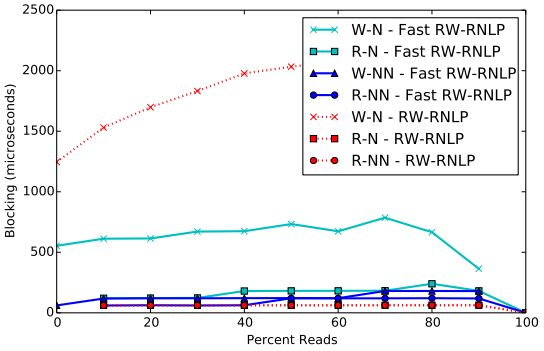

(c) Blocking.

Figure 324: (a) Lock and (b) unlock overheads and (c) blocking for nested and non-nested read and write requests under the RW-RNLP and the fast RW-RNLP. Here, for each request $\mathcal{R}_i$, $m = 18$, $L_i = 60\mu$s, $n_r = 64$, $|D_i| = 1$ for non-nested requests, and $|D_i| = 4$ for nested requests. Each request was randomly chosen to be a read (as opposed to a write) with probability as shown and to be a nested request with probability 0.8. Due to write expansion, $|D_i|$ was inflated to 64 for all write requests under the RW-RNLP, as read requests can access any resource.

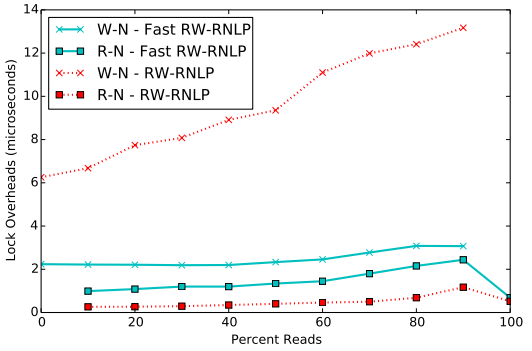

(a) Lock overhead.

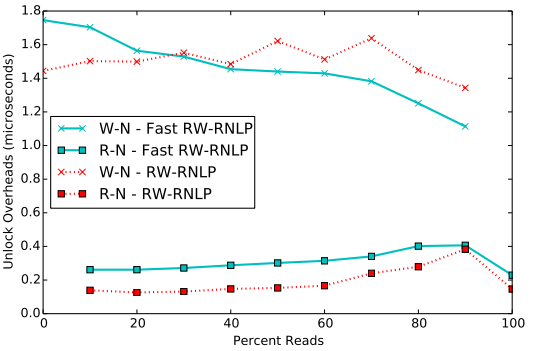

(b) Unlock overhead.

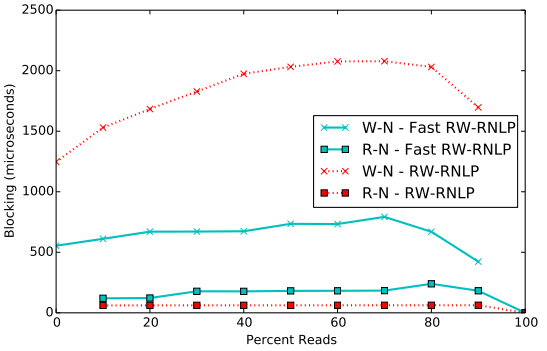

(c) Blocking.

Figure 325: (a) Lock and (b) unlock overheads and (c) blocking for nested read and write requests under the RW-RNLP and the fast RW-RNLP. Here, for each request $\mathcal{R}_i$, $m = 18$, $L_i = 60\mu$s, $n_r = 64$, and $|D_i| = 4$. Each request was randomly chosen to be a read (as opposed to a write) with probability as shown and to be a nested request with probability 1. Due to write expansion, $|D_i|$ was inflated to 64 for all write requests under the RW-RNLP, as read requests can access any resource.

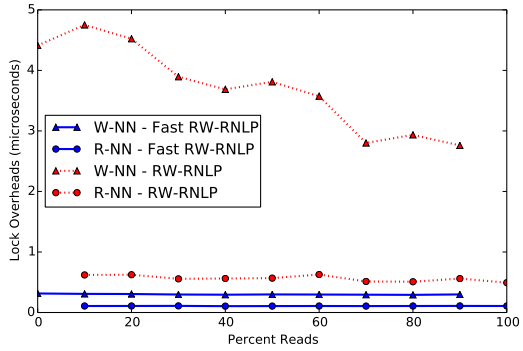

(a) Lock overhead.

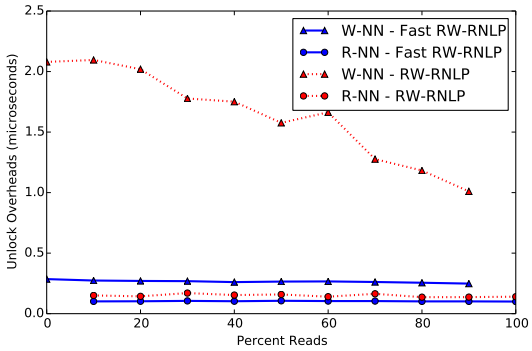

(b) Unlock overhead.

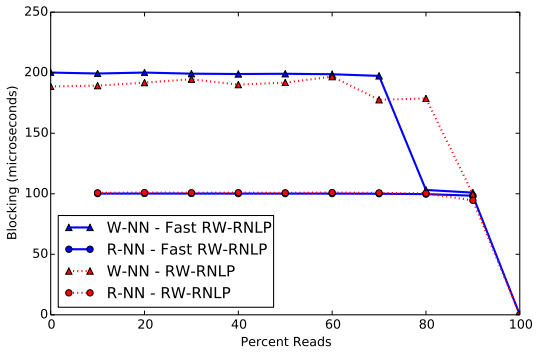

(c) Blocking.

Figure 326: (a) Lock and (b) unlock overheads and (c) blocking for non-nested read and write requests under the RW-RNLP and the fast RW-RNLP. Here, for each request $\mathcal{R}_i$, $m = 18$, $L_i = 100\mu$s, $n_r = 64$, and $|D_i| = 1$. Each request was randomly chosen to be a read (as opposed to a write) with probability as shown and to be a nested request with probability 0.

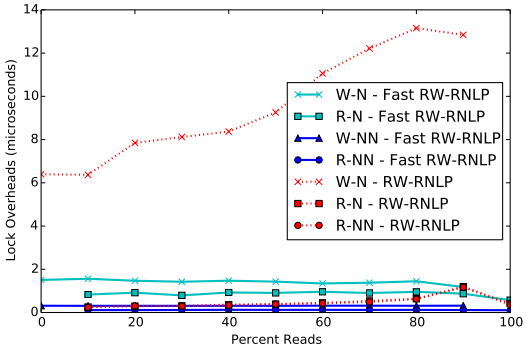

(a) Lock overhead.

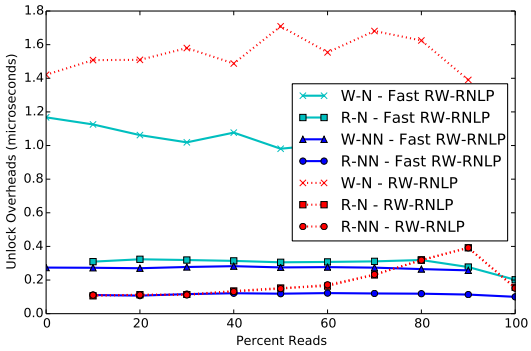

(b) Unlock overhead.

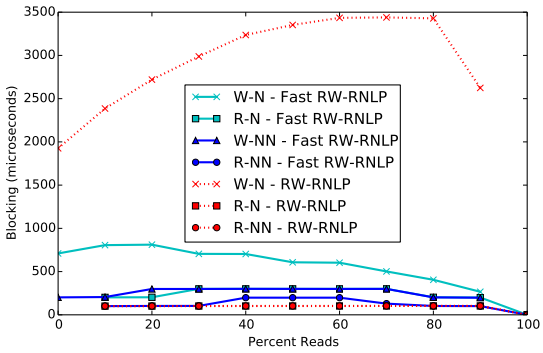

(c) Blocking.

Figure 327: (a) Lock and (b) unlock overheads and (c) blocking for nested and non-nested read and write requests under the RW-RNLP and the fast RW-RNLP. Here, for each request $\mathcal{R}_i$, $m = 18$, $L_i = 100\mu$s, $n_r = 64$, $|D_i| = 1$ for non-nested requests, and $|D_i| = 4$ for nested requests. Each request was randomly chosen to be a read (as opposed to a write) with probability as shown and to be a nested request with probability 0.2. Due to write expansion, $|D_i|$ was inflated to 64 for all write requests under the RW-RNLP, as read requests can access any resource.

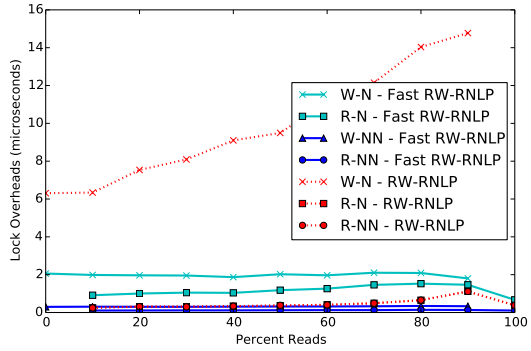

(a) Lock overhead.

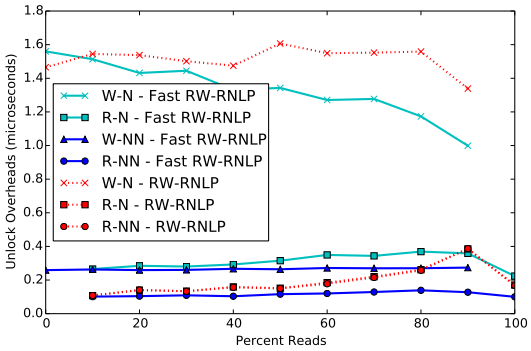

(b) Unlock overhead.

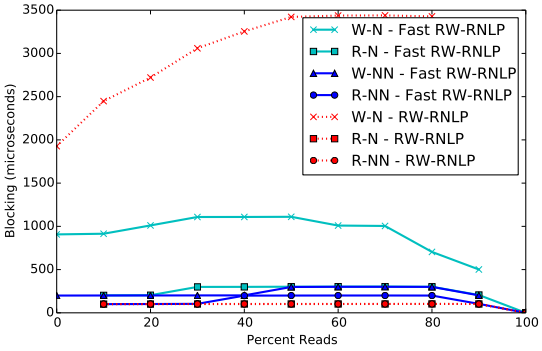

(c) Blocking.

Figure 328: (a) Lock and (b) unlock overheads and (c) blocking for nested and non-nested read and write requests under the RW-RNLP and the fast RW-RNLP. Here, for each request $\mathcal{R}_i$, $m = 18$, $L_i = 100\mu$s, $n_r = 64$, $|D_i| = 1$ for non-nested requests, and $|D_i| = 4$ for nested requests. Each request was randomly chosen to be a read (as opposed to a write) with probability as shown and to be a nested request with probability 0.5. Due to write expansion, $|D_i|$ was inflated to 64 for all write requests under the RW-RNLP, as read requests can access any resource.

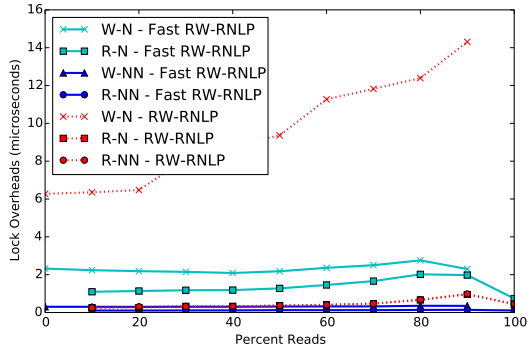

(a) Lock overhead.

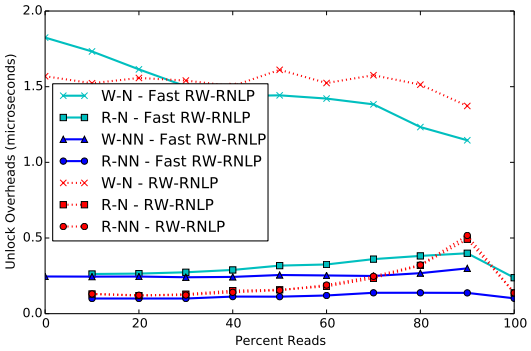

(b) Unlock overhead.

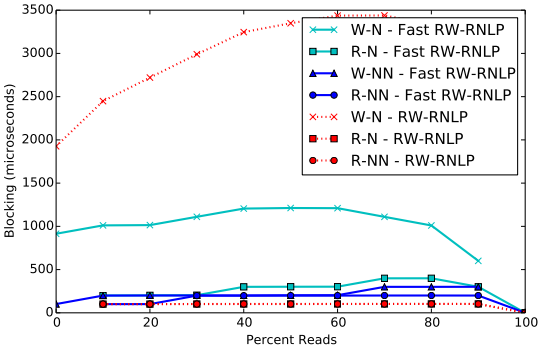

(c) Blocking.

Figure 329: (a) Lock and (b) unlock overheads and (c) blocking for nested and non-nested read and write requests under the RW-RNLP and the fast RW-RNLP. Here, for each request $\mathcal{R}_i$, $m = 18$, $L_i = 100\mu$s, $n_r = 64$, $|D_i| = 1$ for non-nested requests, and $|D_i| = 4$ for nested requests. Each request was randomly chosen to be a read (as opposed to a write) with probability as shown and to be a nested request with probability 0.8. Due to write expansion, $|D_i|$ was inflated to 64 for all write requests under the RW-RNLP, as read requests can access any resource.

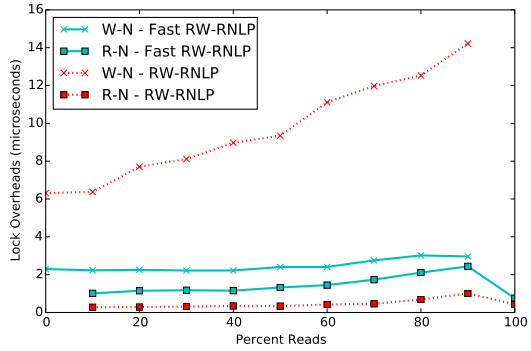

(a) Lock overhead.

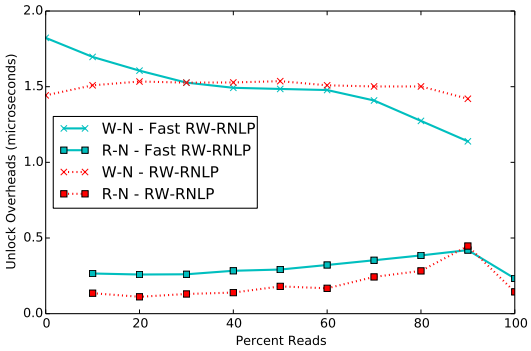

(b) Unlock overhead.

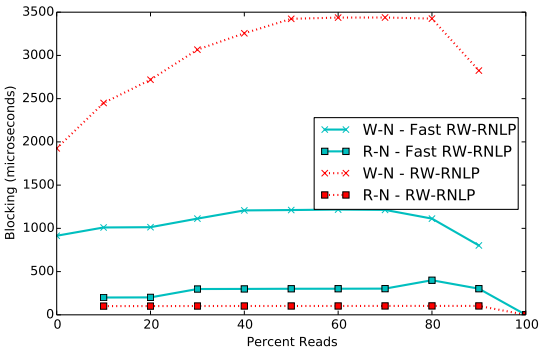

(c) Blocking.

Figure 330: (a) Lock and (b) unlock overheads and (c) blocking for nested read and write requests under the RW-RNLP and the fast RW-RNLP. Here, for each request $\mathcal{R}_i$, $m = 18$, $L_i = 100\mu$s, $n_r = 64$, and $|D_i| = 4$. Each request was randomly chosen to be a read (as opposed to a write) with probability as shown and to be a nested request with probability 1. Due to write expansion, $|D_i|$ was inflated to 64 for all write requests under the RW-RNLP, as read requests can access any resource.

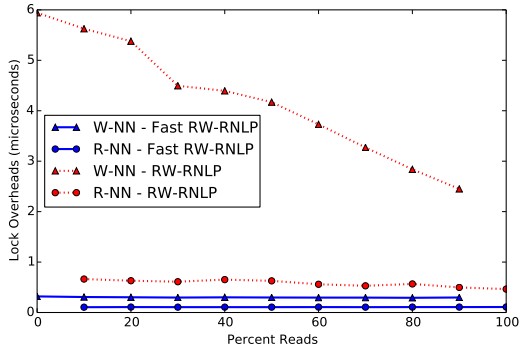

(a) Lock overhead.

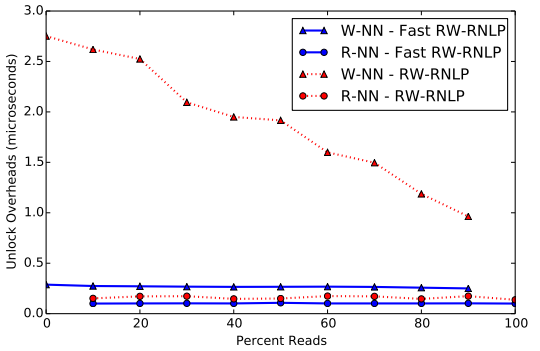

(b) Unlock overhead.

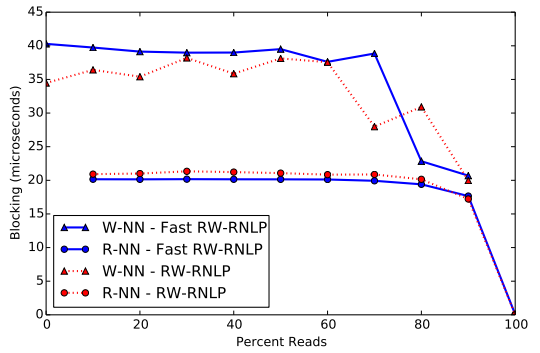

(c) Blocking.

Figure 331: (a) Lock and (b) unlock overheads and (c) blocking for non-nested read and write requests under the RW-RNLP and the fast RW-RNLP. Here, for each request $\mathcal{R}_i$, $m = 18$, $L_i = 20\mu$s, $n_r = 64$, and $|D_i| = 1$. Each request was randomly chosen to be a read (as opposed to a write) with probability as shown and to be a nested request with probability 0.

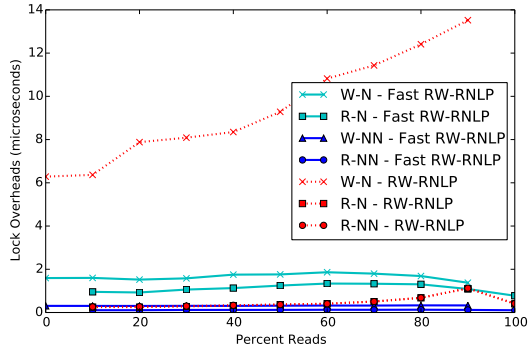

(a) Lock overhead.

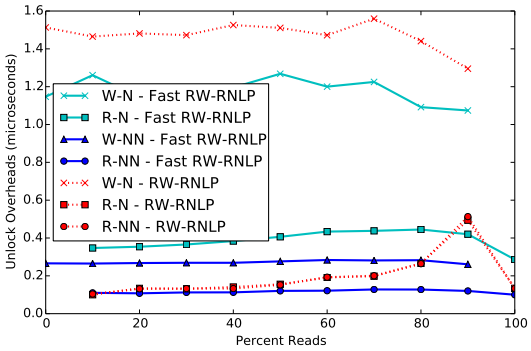

(b) Unlock overhead.

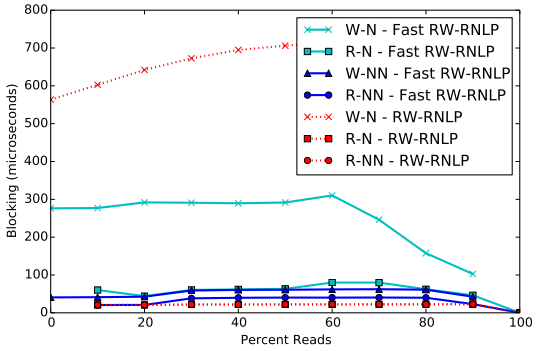

(c) Blocking.

Figure 332: (a) Lock and (b) unlock overheads and (c) blocking for nested and non-nested read and write requests under the RW-RNLP and the fast RW-RNLP. Here, for each request $\mathcal{R}_i$, $m = 18$, $L_i = 20\mu$s, $n_r = 64$, $|D_i| = 1$ for non-nested requests, and $|D_i| = 6$ for nested requests. Each request was randomly chosen to be a read (as opposed to a write) with probability as shown and to be a nested request with probability 0.2. Due to write expansion, $|D_i|$ was inflated to 64 for all write requests under the RW-RNLP, as read requests can access any resource.

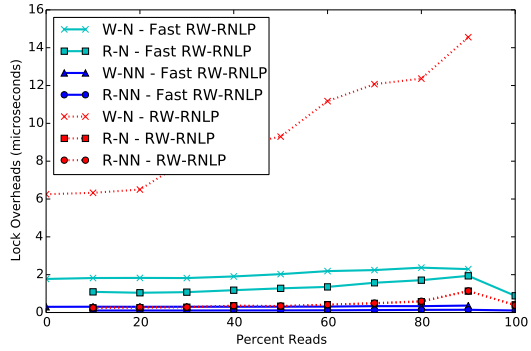

(a) Lock overhead.

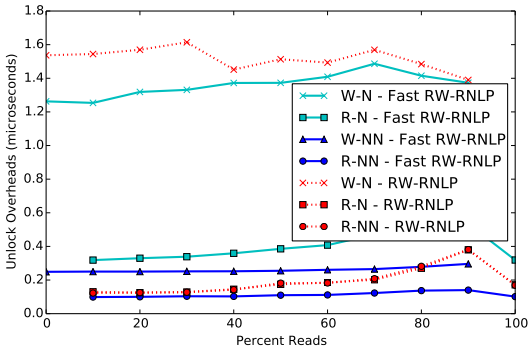

(b) Unlock overhead.

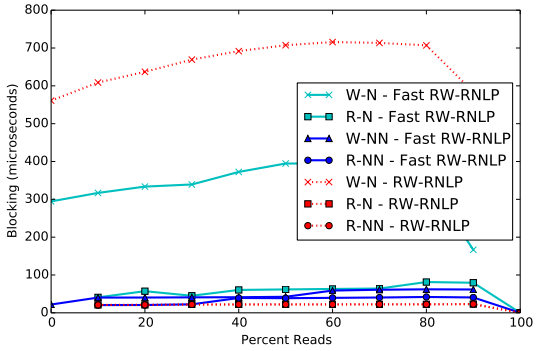

(c) Blocking.

Figure 333: (a) Lock and (b) unlock overheads and (c) blocking for nested and non-nested read and write requests under the RW-RNLP and the fast RW-RNLP. Here, for each request $\mathcal{R}_i$, $m = 18$, $L_i = 20\mu$s, $n_r = 64$, $|D_i| = 1$ for non-nested requests, and $|D_i| = 6$ for nested requests. Each request was randomly chosen to be a read (as opposed to a write) with probability as shown and to be a nested request with probability 0.5. Due to write expansion, $|D_i|$ was inflated to 64 for all write requests under the RW-RNLP, as read requests can access any resource.

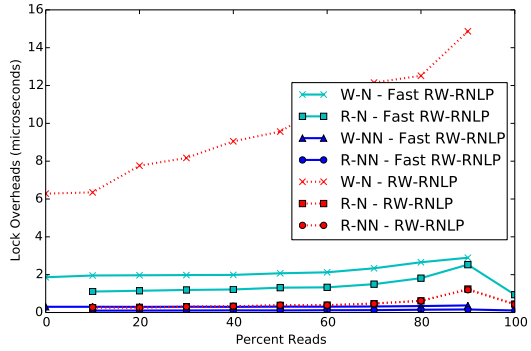

(a) Lock overhead.

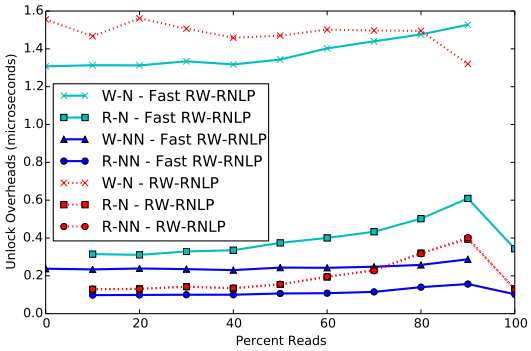

(b) Unlock overhead.

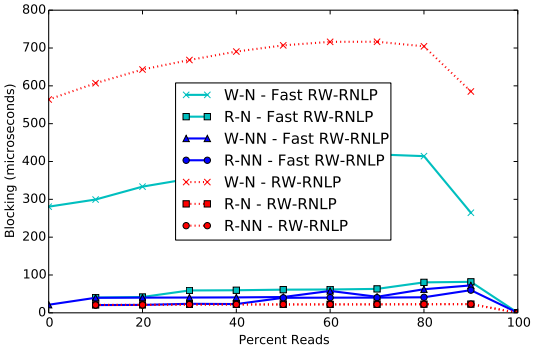

(c) Blocking.

Figure 334: (a) Lock and (b) unlock overheads and (c) blocking for nested and non-nested read and write requests under the RW-RNLP and the fast RW-RNLP. Here, for each request $\mathcal{R}_i$, $m = 18$, $L_i = 20\mu$s, $n_r = 64$, $|D_i| = 1$ for non-nested requests, and $|D_i| = 6$ for nested requests. Each request was randomly chosen to be a read (as opposed to a write) with probability as shown and to be a nested request with probability 0.8. Due to write expansion, $|D_i|$ was inflated to 64 for all write requests under the RW-RNLP, as read requests can access any resource.

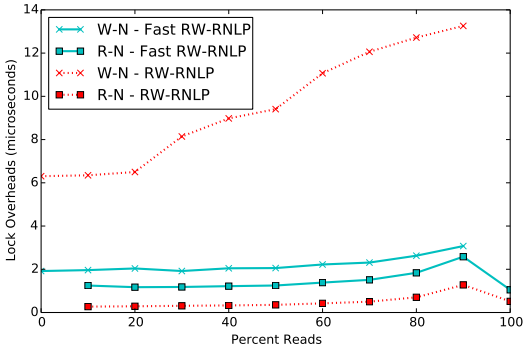

(a) Lock overhead.

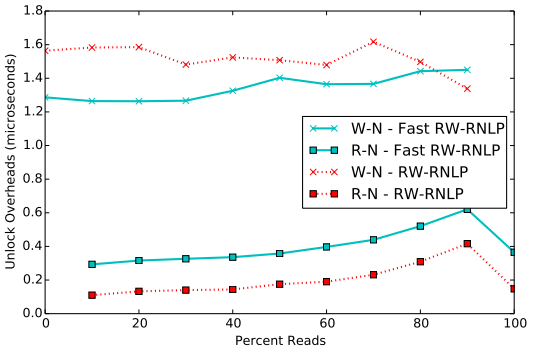

(b) Unlock overhead.

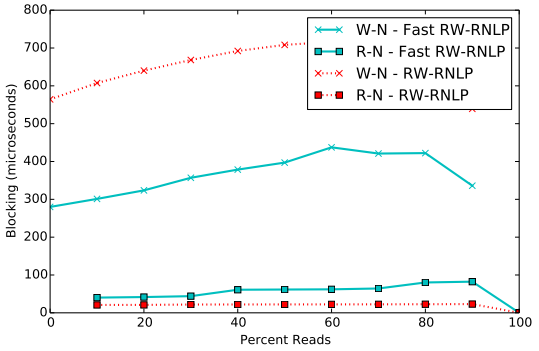

(c) Blocking.

Figure 335: (a) Lock and (b) unlock overheads and (c) blocking for nested read and write requests under the RW-RNLP and the fast RW-RNLP. Here, for each request $\mathcal{R}_i$, $m = 18$, $L_i = 20\mu$s, $n_r = 64$, and $|D_i| = 6$. Each request was randomly chosen to be a read (as opposed to a write) with probability as shown and to be a nested request with probability 1. Due to write expansion, $|D_i|$ was inflated to 64 for all write requests under the RW-RNLP, as read requests can access any resource.

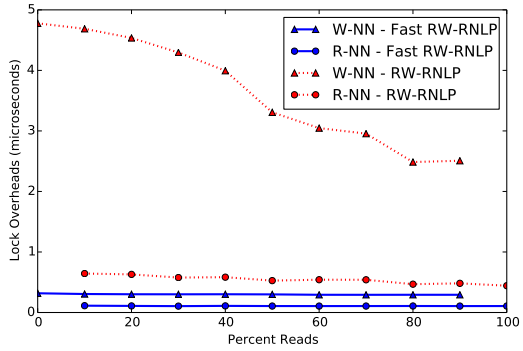

(a) Lock overhead.

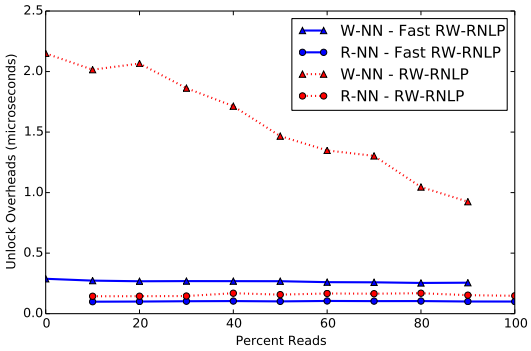

(b) Unlock overhead.

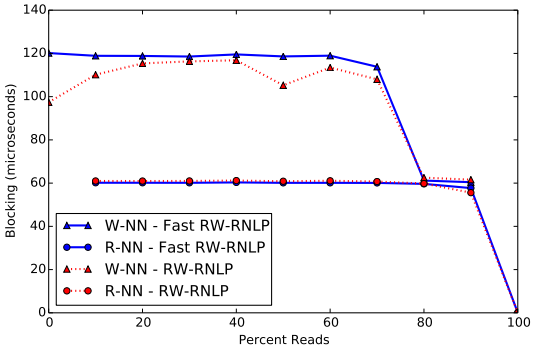

(c) Blocking.

Figure 336: (a) Lock and (b) unlock overheads and (c) blocking for non-nested read and write requests under the RW-RNLP and the fast RW-RNLP. Here, for each request $\mathcal{R}_i$, $m = 18$, $L_i = 60\mu$s, $n_r = 64$, and $|D_i| = 1$. Each request was randomly chosen to be a read (as opposed to a write) with probability as shown and to be a nested request with probability 0.

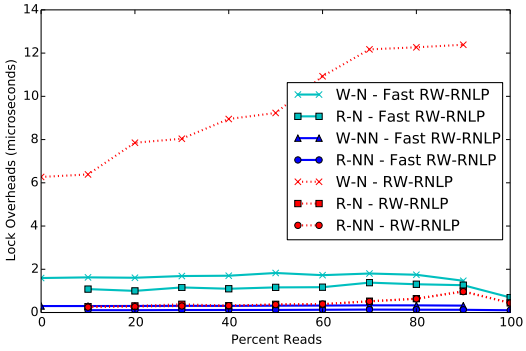

(a) Lock overhead.

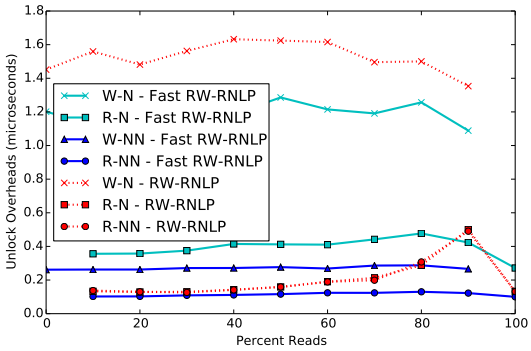

(b) Unlock overhead.

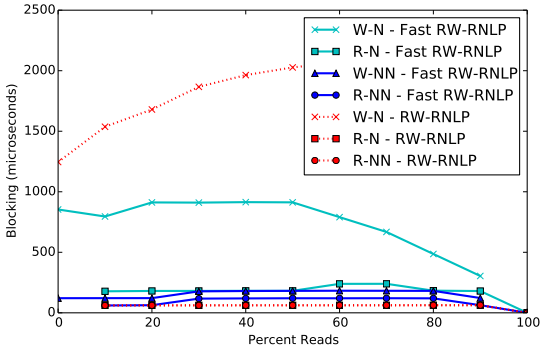

(c) Blocking.

Figure 337: (a) Lock and (b) unlock overheads and (c) blocking for nested and non-nested read and write requests under the RW-RNLP and the fast RW-RNLP. Here, for each request $\mathcal{R}_i$, $m = 18$, $L_i = 60\mu$s, $n_r = 64$, $|D_i| = 1$ for non-nested requests, and $|D_i| = 6$ for nested requests. Each request was randomly chosen to be a read (as opposed to a write) with probability as shown and to be a nested request with probability 0.2. Due to write expansion, $|D_i|$ was inflated to 64 for all write requests under the RW-RNLP, as read requests can access any resource.

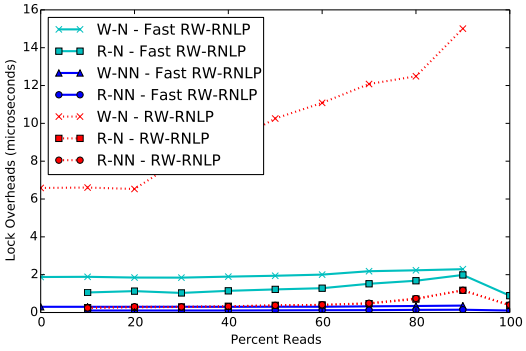

(a) Lock overhead.

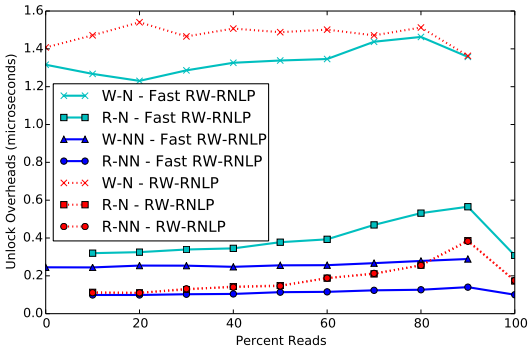

(b) Unlock overhead.

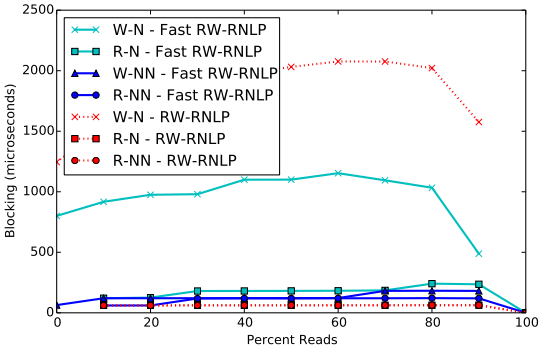

(c) Blocking.

Figure 338: (a) Lock and (b) unlock overheads and (c) blocking for nested and non-nested read and write requests under the RW-RNLP and the fast RW-RNLP. Here, for each request $\mathcal{R}_i$, $m = 18$, $L_i = 60\mu$s, $n_r = 64$, $|D_i| = 1$ for non-nested requests, and $|D_i| = 6$ for nested requests. Each request was randomly chosen to be a read (as opposed to a write) with probability as shown and to be a nested request with probability 0.5. Due to write expansion, $|D_i|$ was inflated to 64 for all write requests under the RW-RNLP, as read requests can access any resource.

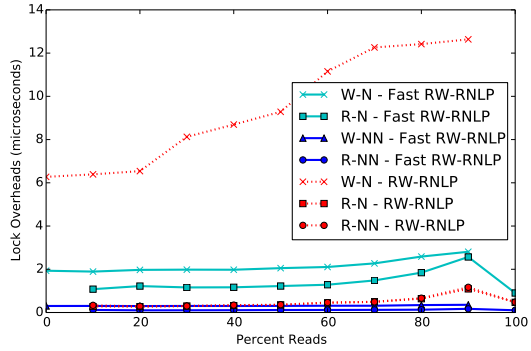

(a) Lock overhead.

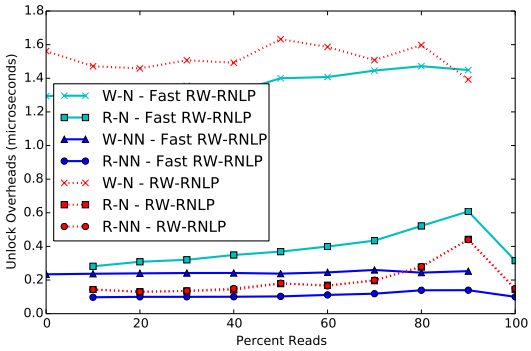

(b) Unlock overhead.

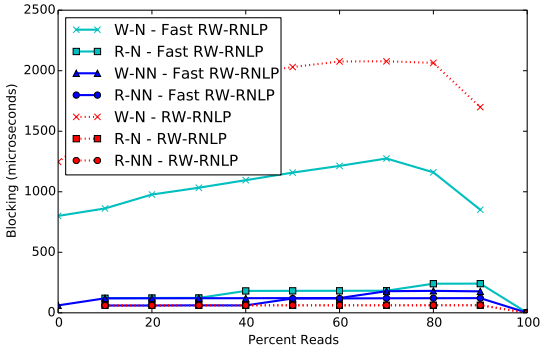

(c) Blocking.

Figure 339: (a) Lock and (b) unlock overheads and (c) blocking for nested and non-nested read and write requests under the RW-RNLP and the fast RW-RNLP. Here, for each request $\mathcal{R}_i$, $m = 18$, $L_i = 60\mu$s, $n_r = 64$, $|D_i| = 1$ for non-nested requests, and $|D_i| = 6$ for nested requests. Each request was randomly chosen to be a read (as opposed to a write) with probability as shown and to be a nested request with probability 0.8. Due to write expansion, $|D_i|$ was inflated to 64 for all write requests under the RW-RNLP, as read requests can access any resource.

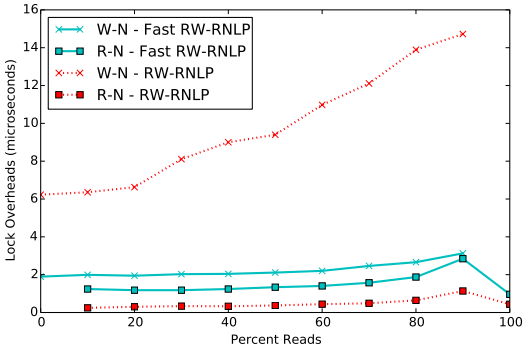

(a) Lock overhead.

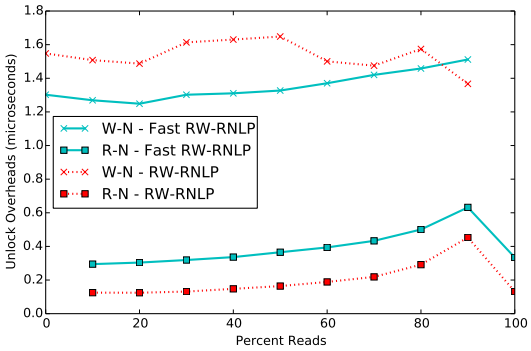

(b) Unlock overhead.

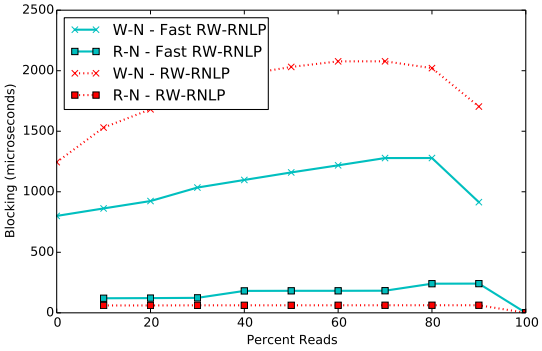

(c) Blocking.

Figure 340: (a) Lock and (b) unlock overheads and (c) blocking for nested read and write requests under the RW-RNLP and the fast RW-RNLP. Here, for each request $\mathcal{R}_i$, $m = 18$, $L_i = 60\mu$s, $n_r = 64$, and $|D_i| = 6$. Each request was randomly chosen to be a read (as opposed to a write) with probability as shown and to be a nested request with probability 1. Due to write expansion, $|D_i|$ was inflated to 64 for all write requests under the RW-RNLP, as read requests can access any resource.

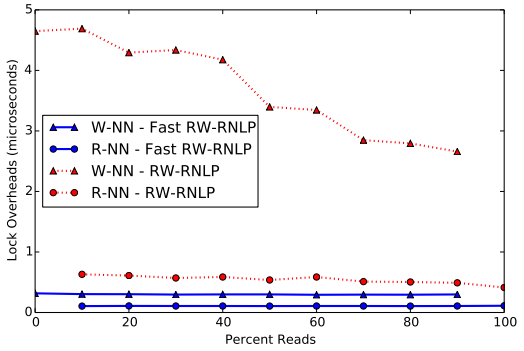

(a) Lock overhead.

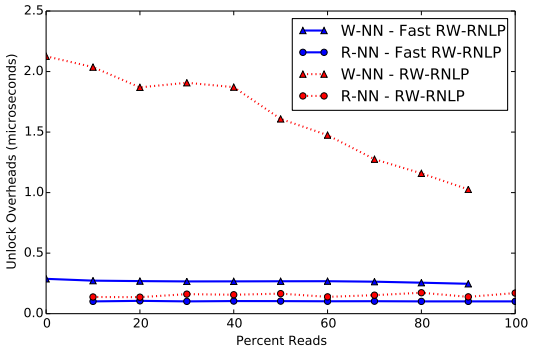

(b) Unlock overhead.

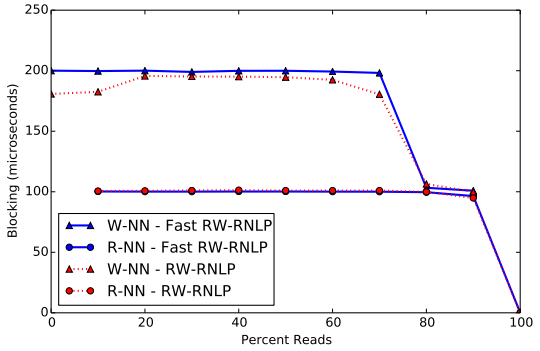

(c) Blocking.

Figure 341: (a) Lock and (b) unlock overheads and (c) blocking for non-nested read and write requests under the RW-RNLP and the fast RW-RNLP. Here, for each request $\mathcal{R}_i$, $m = 18$, $L_i = 100\mu$s, $n_r = 64$, and $|D_i| = 1$. Each request was randomly chosen to be a read (as opposed to a write) with probability as shown and to be a nested request with probability 0.

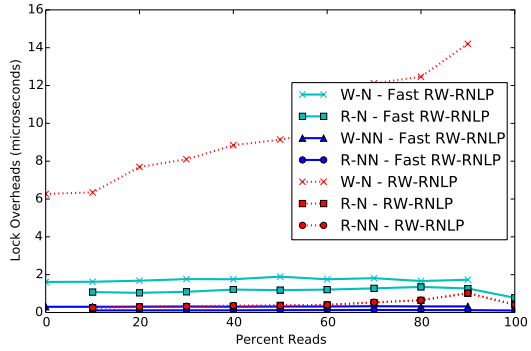

(a) Lock overhead.

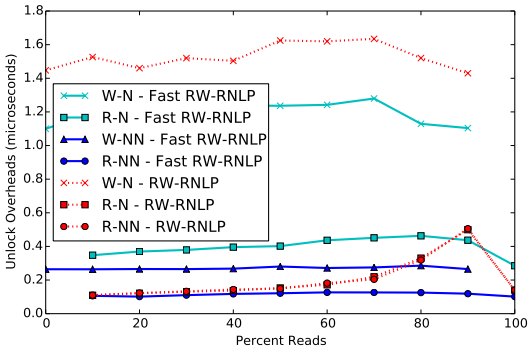

(b) Unlock overhead.

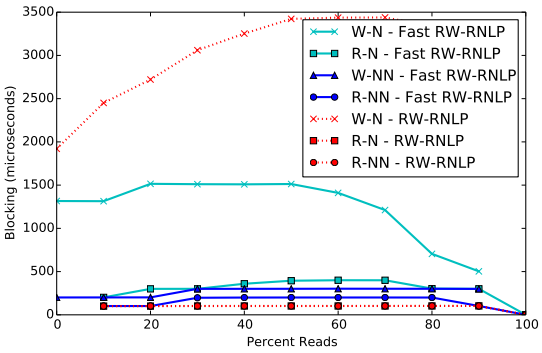

(c) Blocking.

Figure 342: (a) Lock and (b) unlock overheads and (c) blocking for nested and non-nested read and write requests under the RW-RNLP and the fast RW-RNLP. Here, for each request $\mathcal{R}_i$, $m = 18$, $L_i = 100\mu$s, $n_r = 64$, $|D_i| = 1$ for non-nested requests, and $|D_i| = 6$ for nested requests. Each request was randomly chosen to be a read (as opposed to a write) with probability as shown and to be a nested request with probability 0.2. Due to write expansion, $|D_i|$ was inflated to 64 for all write requests under the RW-RNLP, as read requests can access any resource.

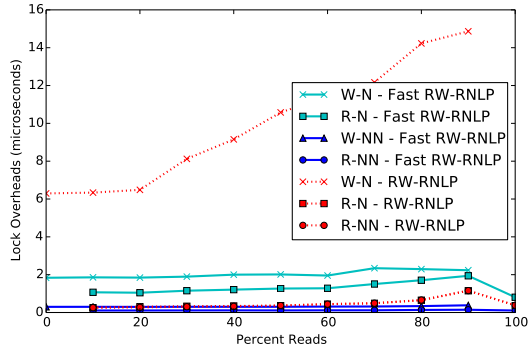

(a) Lock overhead.

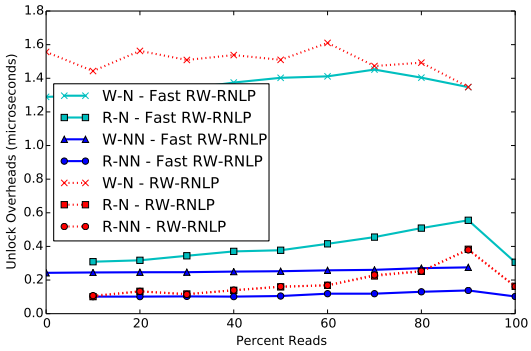

(b) Unlock overhead.

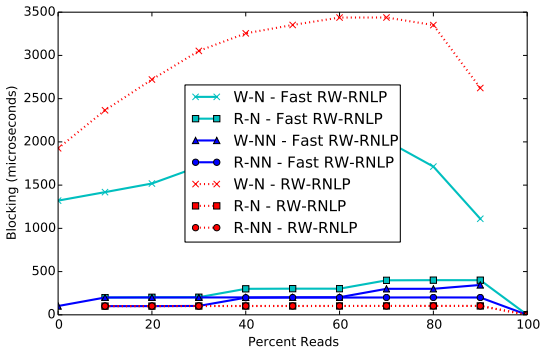

(c) Blocking.

Figure 343: (a) Lock and (b) unlock overheads and (c) blocking for nested and non-nested read and write requests under the RW-RNLP and the fast RW-RNLP. Here, for each request $\mathcal{R}_i$, $m = 18$, $L_i = 100\mu$s, $n_r = 64$, $|D_i| = 1$ for non-nested requests, and $|D_i| = 6$ for nested requests. Each request was randomly chosen to be a read (as opposed to a write) with probability as shown and to be a nested request with probability 0.5. Due to write expansion, $|D_i|$ was inflated to 64 for all write requests under the RW-RNLP, as read requests can access any resource.

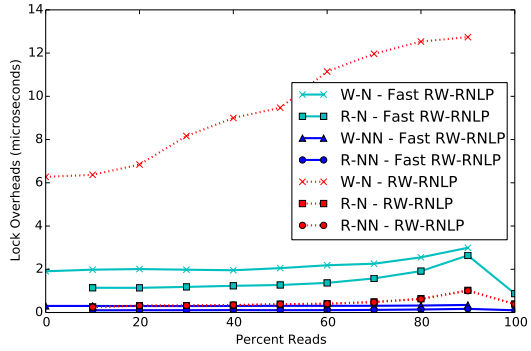

(a) Lock overhead.

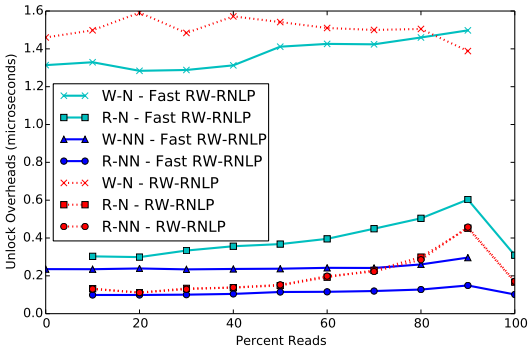

(b) Unlock overhead.

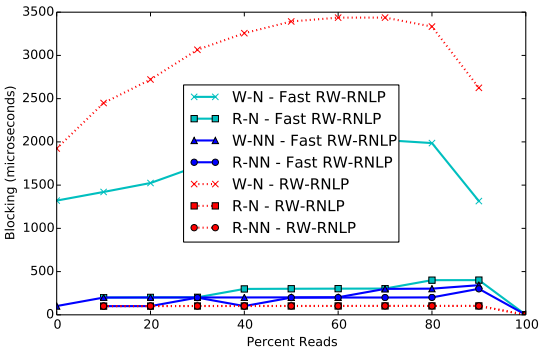

(c) Blocking.

Figure 344: (a) Lock and (b) unlock overheads and (c) blocking for nested and non-nested read and write requests under the RW-RNLP and the fast RW-RNLP. Here, for each request $\mathcal{R}_i$, $m = 18$, $L_i = 100\mu$s, $n_r = 64$, $|D_i| = 1$ for non-nested requests, and $|D_i| = 6$ for nested requests. Each request was randomly chosen to be a read (as opposed to a write) with probability as shown and to be a nested request with probability 0.8. Due to write expansion, $|D_i|$ was inflated to 64 for all write requests under the RW-RNLP, as read requests can access any resource.

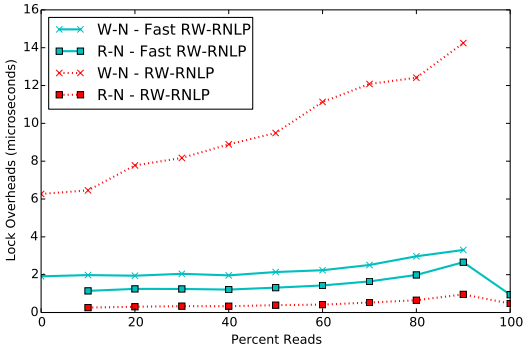

(a) Lock overhead.

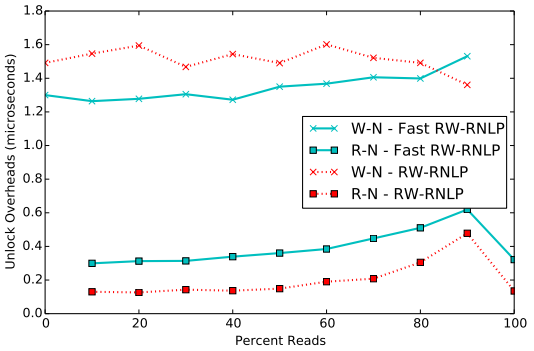

(b) Unlock overhead.

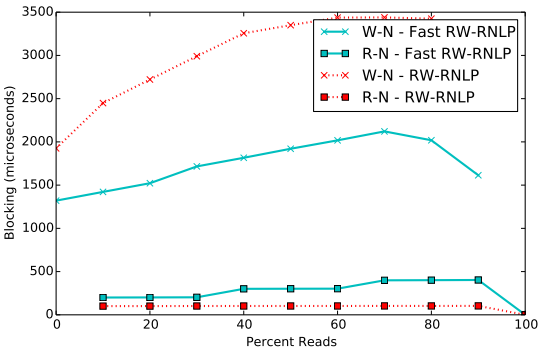

(c) Blocking.

Figure 345: (a) Lock and (b) unlock overheads and (c) blocking for nested read and write requests under the RW-RNLP and the fast RW-RNLP. Here, for each request $\mathcal{R}_i$, $m = 18$, $L_i = 100\mu$s, $n_r = 64$, and $|D_i| = 6$. Each request was randomly chosen to be a read (as opposed to a write) with probability as shown and to be a nested request with probability 1. Due to write expansion, $|D_i|$ was inflated to 64 for all write requests under the RW-RNLP, as read requests can access any resource.

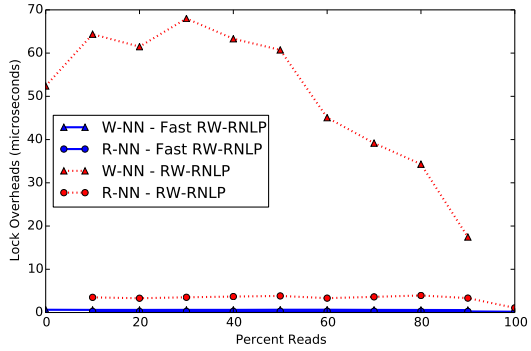

(a) Lock overhead.

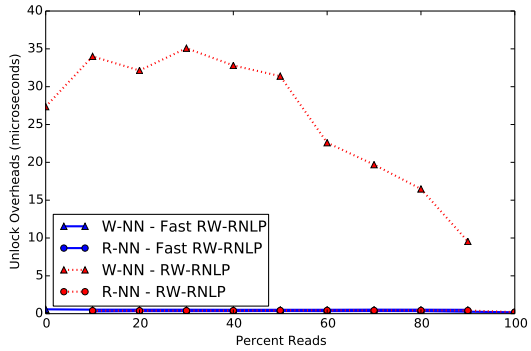

(b) Unlock overhead.

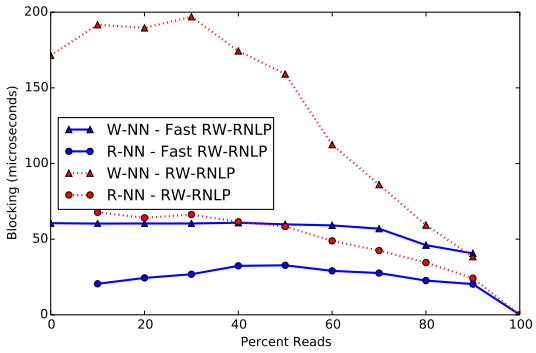

(c) Blocking.

Figure 346: (a) Lock and (b) unlock overheads and (c) blocking for non-nested read and write requests under the RW-RNLP and the fast RW-RNLP. Here, for each request $\mathcal{R}_i$, $m = 36$, $L_i = 20\mu$s, $n_r = 64$, and $|D_i| = 1$. Each request was randomly chosen to be a read (as opposed to a write) with probability as shown and to be a nested request with probability 0.

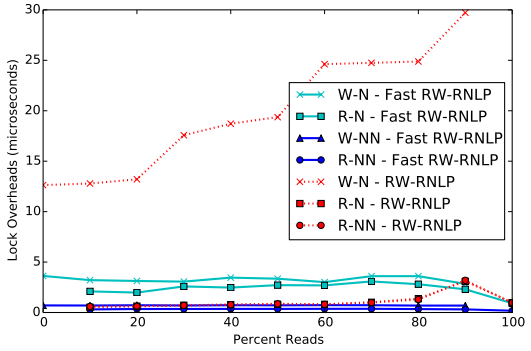

(a) Lock overhead.

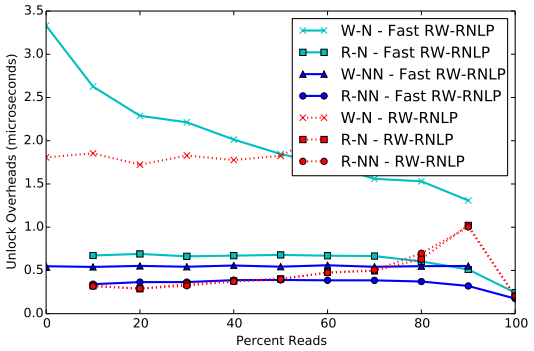

(b) Unlock overhead.

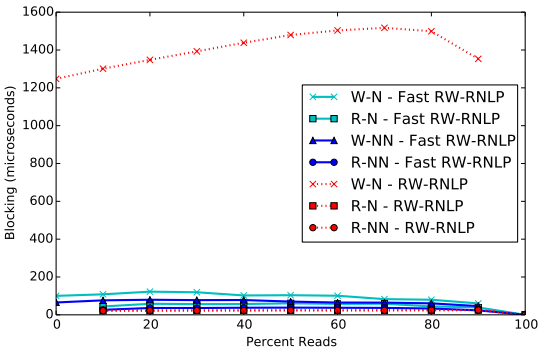

(c) Blocking.

Figure 347: (a) Lock and (b) unlock overheads and (c) blocking for nested and non-nested read and write requests under the RW-RNLP and the fast RW-RNLP. Here, for each request $\mathcal{R}_i$, $m = 36$, $L_i = 20\mu$s, $n_r = 64$, $|D_i| = 1$ for non-nested requests, and $|D_i| = 2$ for nested requests. Each request was randomly chosen to be a read (as opposed to a write) with probability as shown and to be a nested request with probability 0.2. Due to write expansion, $|D_i|$ was inflated to 64 for all write requests under the RW-RNLP, as read requests can access any resource.

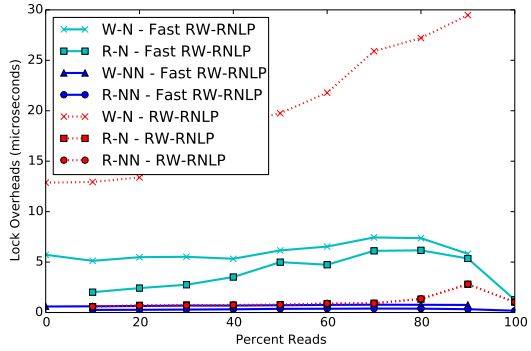

(a) Lock overhead.

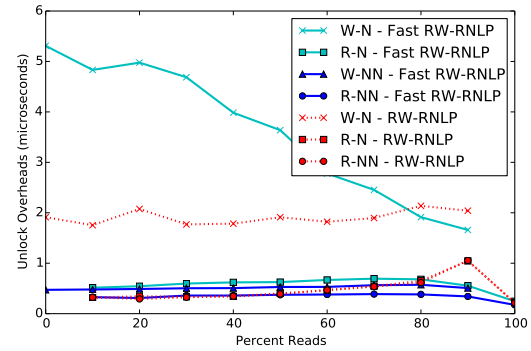

(b) Unlock overhead.

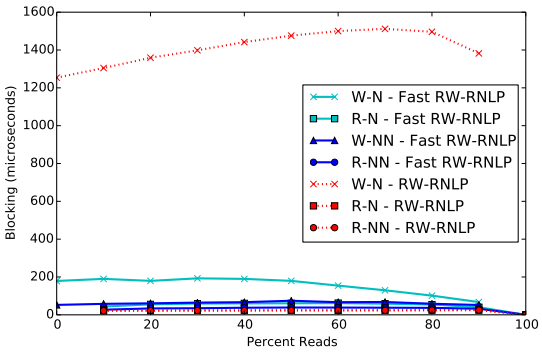

(c) Blocking.

Figure 348: (a) Lock and (b) unlock overheads and (c) blocking for nested and non-nested read and write requests under the RW-RNLP and the fast RW-RNLP. Here, for each request $\mathcal{R}_i$, $m = 36$, $L_i = 20\mu$s, $n_r = 64$, $|D_i| = 1$ for non-nested requests, and $|D_i| = 2$ for nested requests. Each request was randomly chosen to be a read (as opposed to a write) with probability as shown and to be a nested request with probability 0.5. Due to write expansion, $|D_i|$ was inflated to 64 for all write requests under the RW-RNLP, as read requests can access any resource.

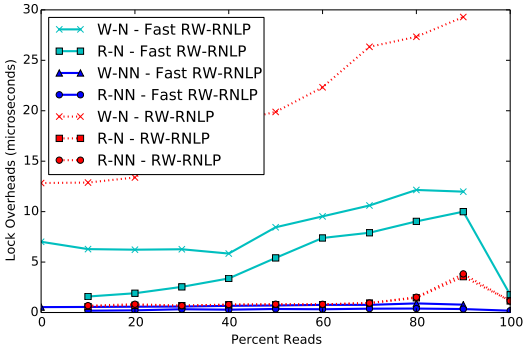

(a) Lock overhead.

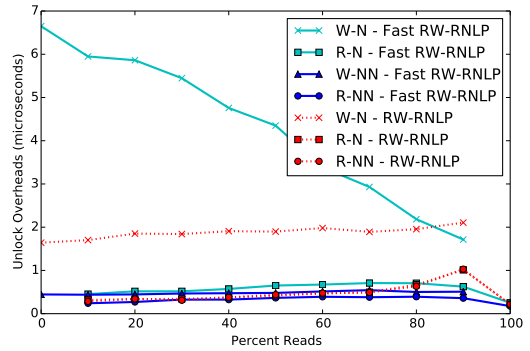

(b) Unlock overhead.

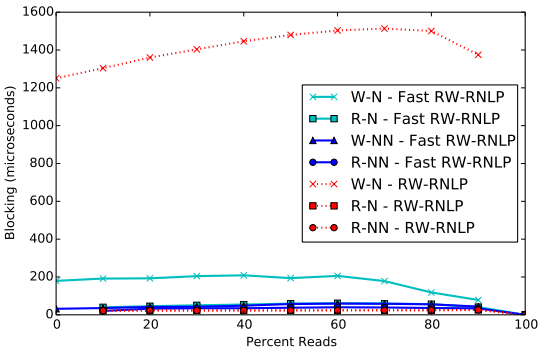

(c) Blocking.

Figure 349: (a) Lock and (b) unlock overheads and (c) blocking for nested and non-nested read and write requests under the RW-RNLP and the fast RW-RNLP. Here, for each request $\mathcal{R}_i$, $m = 36$, $L_i = 20\mu$s, $n_r = 64$, $|D_i| = 1$ for non-nested requests, and $|D_i| = 2$ for nested requests. Each request was randomly chosen to be a read (as opposed to a write) with probability as shown and to be a nested request with probability 0.8. Due to write expansion, $|D_i|$ was inflated to 64 for all write requests under the RW-RNLP, as read requests can access any resource.

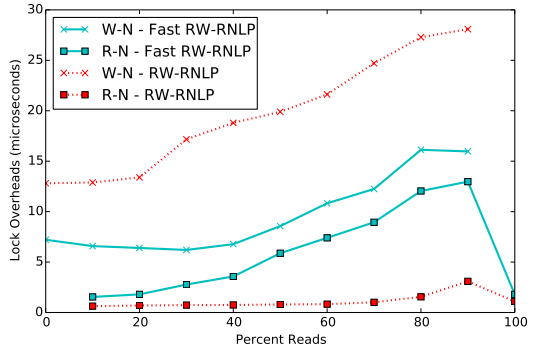

(a) Lock overhead.

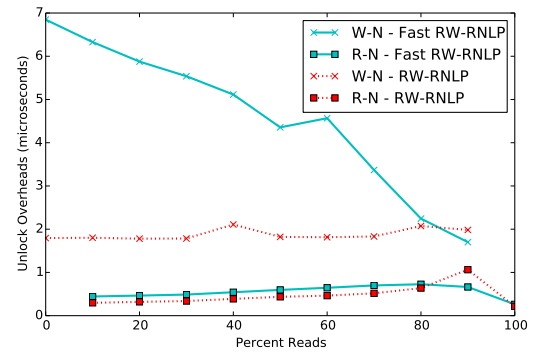

(b) Unlock overhead.

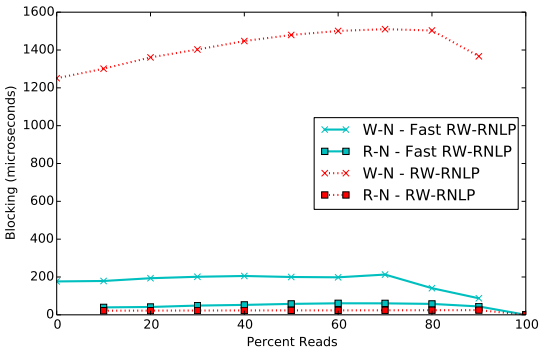

(c) Blocking.

Figure 350: (a) Lock and (b) unlock overheads and (c) blocking for nested read and write requests under the RW-RNLP and the fast RW-RNLP. Here, for each request $\mathcal{R}_i$, $m = 36$, $L_i = 20\mu$s, $n_r = 64$, and $|D_i| = 2$. Each request was randomly chosen to be a read (as opposed to a write) with probability as shown and to be a nested request with probability 1. Due to write expansion, $|D_i|$ was inflated to 64 for all write requests under the RW-RNLP, as read requests can access any resource.

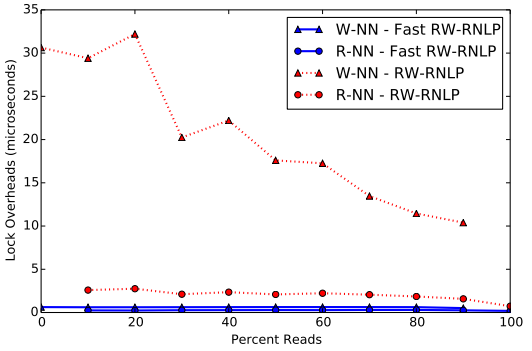

(a) Lock overhead.

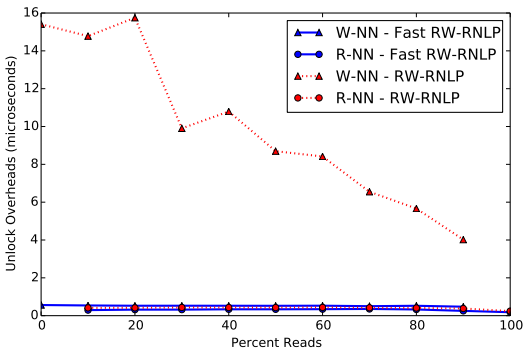

(b) Unlock overhead.

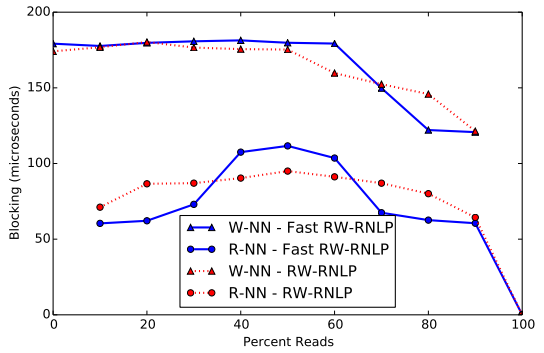

(c) Blocking.

Figure 351: (a) Lock and (b) unlock overheads and (c) blocking for non-nested read and write requests under the RW-RNLP and the fast RW-RNLP. Here, for each request $\mathcal{R}_i$, $m = 36$, $L_i = 60\mu$s, $n_r = 64$, and $|D_i| = 1$. Each request was randomly chosen to be a read (as opposed to a write) with probability as shown and to be a nested request with probability 0.

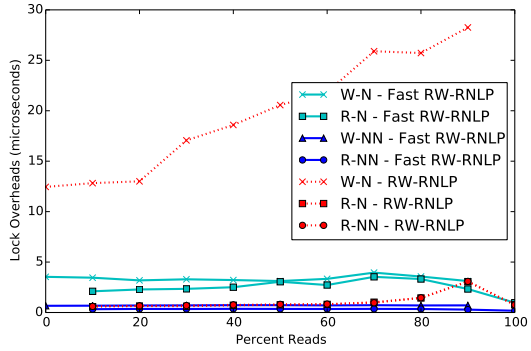

(a) Lock overhead.

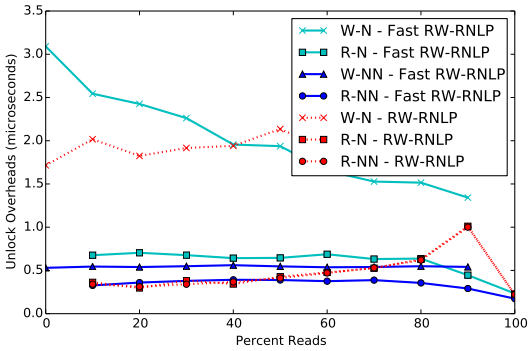

(b) Unlock overhead.

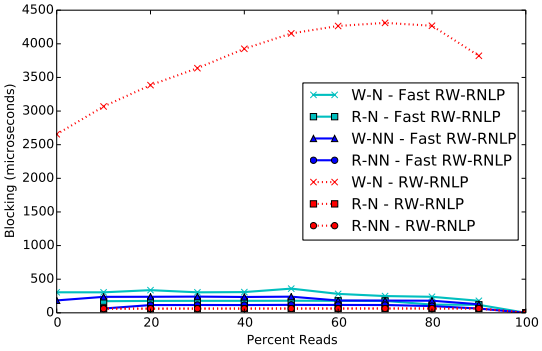

(c) Blocking.

Figure 352: (a) Lock and (b) unlock overheads and (c) blocking for nested and non-nested read and write requests under the RW-RNLP and the fast RW-RNLP. Here, for each request $\mathcal{R}_i$, $m = 36$, $L_i = 60\mu$s, $n_r = 64$, $|D_i| = 1$ for non-nested requests, and $|D_i| = 2$ for nested requests. Each request was randomly chosen to be a read (as opposed to a write) with probability as shown and to be a nested request with probability 0.2. Due to write expansion, $|D_i|$ was inflated to 64 for all write requests under the RW-RNLP, as read requests can access any resource.

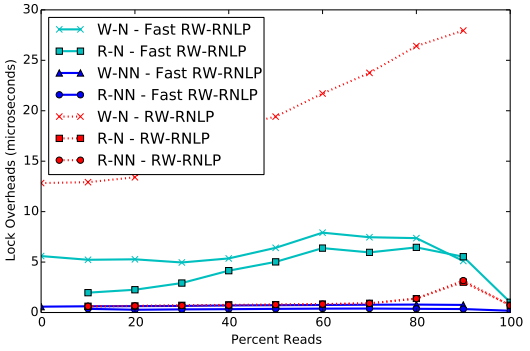

(a) Lock overhead.

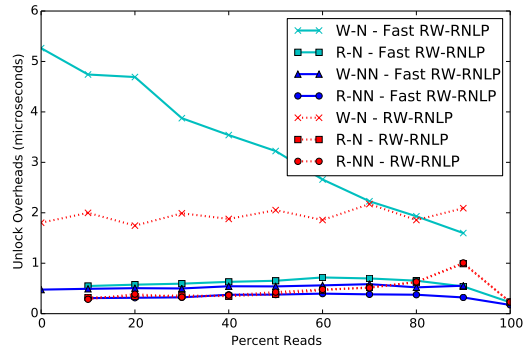

(b) Unlock overhead.

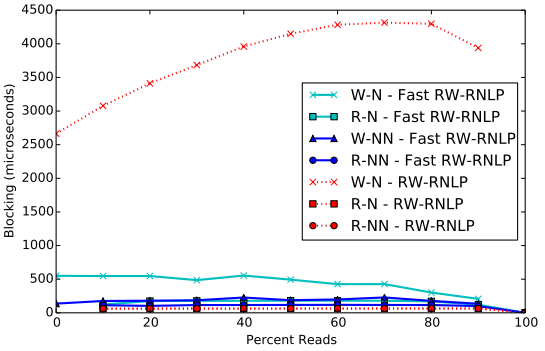

(c) Blocking.

Figure 353: (a) Lock and (b) unlock overheads and (c) blocking for nested and non-nested read and write requests under the RW-RNLP and the fast RW-RNLP. Here, for each request $\mathcal{R}_i$, $m = 36$, $L_i = 60\mu$s, $n_r = 64$, $|D_i| = 1$ for non-nested requests, and $|D_i| = 2$ for nested requests. Each request was randomly chosen to be a read (as opposed to a write) with probability as shown and to be a nested request with probability 0.5. Due to write expansion, $|D_i|$ was inflated to 64 for all write requests under the RW-RNLP, as read requests can access any resource.

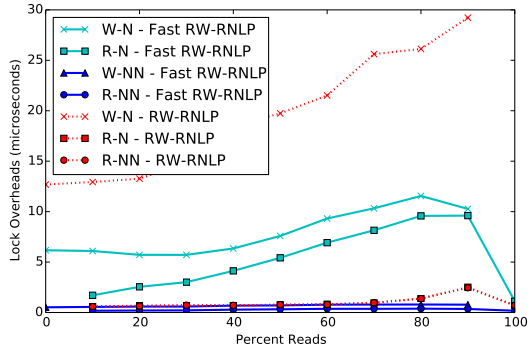

(a) Lock overhead.

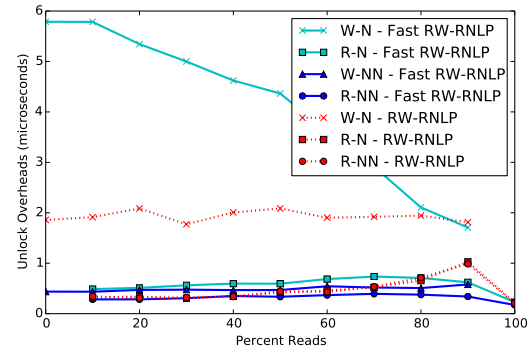

(b) Unlock overhead.

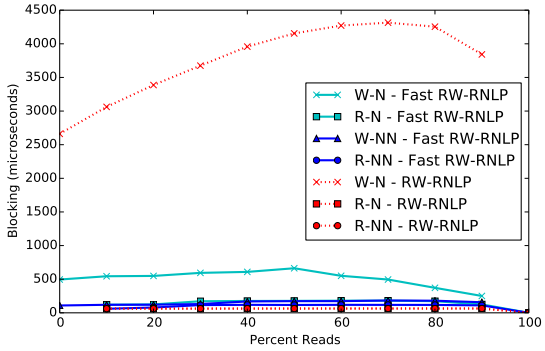

(c) Blocking.

Figure 354: (a) Lock and (b) unlock overheads and (c) blocking for nested and non-nested read and write requests under the RW-RNLP and the fast RW-RNLP. Here, for each request $\mathcal{R}_i$, $m = 36$, $L_i = 60\mu$s, $n_r = 64$, $|D_i| = 1$ for non-nested requests, and $|D_i| = 2$ for nested requests. Each request was randomly chosen to be a read (as opposed to a write) with probability as shown and to be a nested request with probability 0.8. Due to write expansion, $|D_i|$ was inflated to 64 for all write requests under the RW-RNLP, as read requests can access any resource.

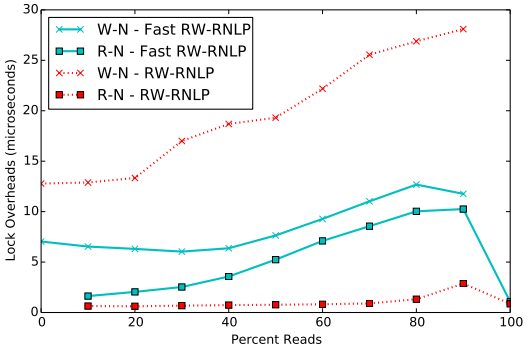

(a) Lock overhead.

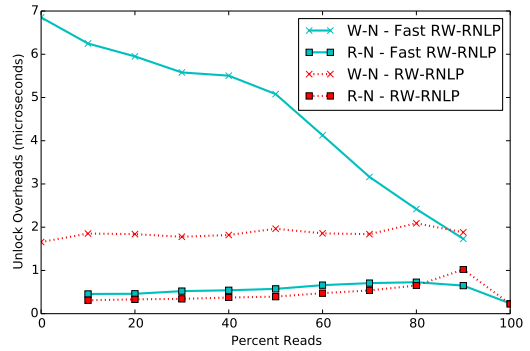

(b) Unlock overhead.

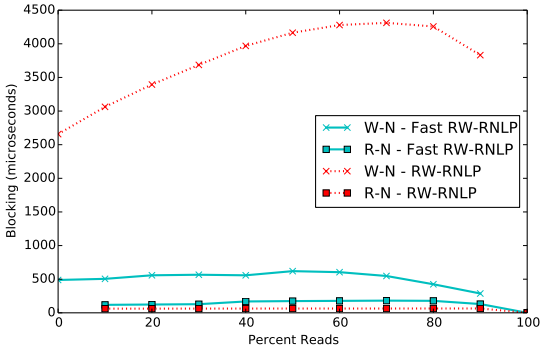

(c) Blocking.

Figure 355: (a) Lock and (b) unlock overheads and (c) blocking for nested read and write requests under the RW-RNLP and the fast RW-RNLP. Here, for each request $\mathcal{R}_i$, $m = 36$, $L_i = 60\mu$s, $n_r = 64$, and $|D_i| = 2$. Each request was randomly chosen to be a read (as opposed to a write) with probability as shown and to be a nested request with probability 1. Due to write expansion, $|D_i|$ was inflated to 64 for all write requests under the RW-RNLP, as read requests can access any resource.

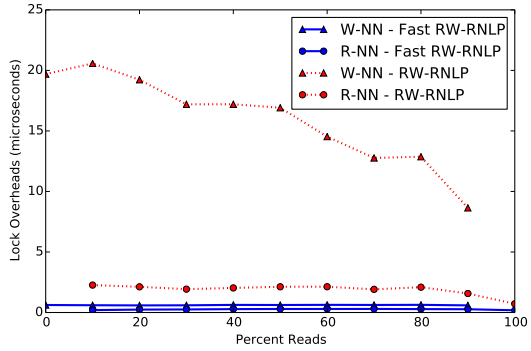

(a) Lock overhead.

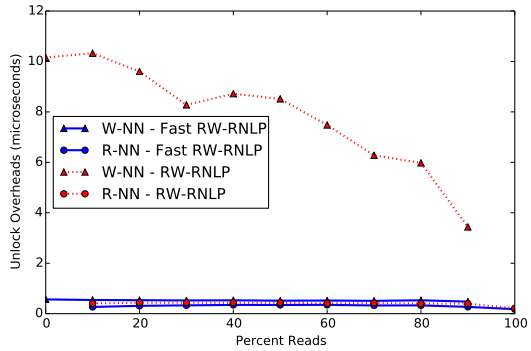

(b) Unlock overhead.

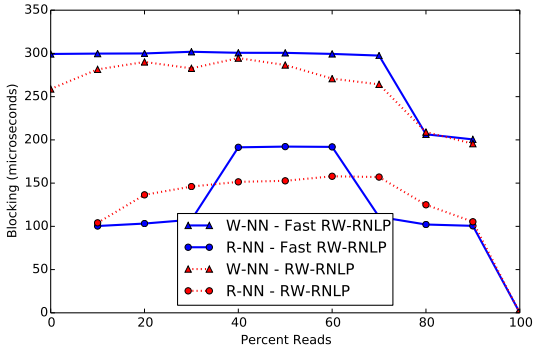

(c) Blocking.

Figure 356: (a) Lock and (b) unlock overheads and (c) blocking for non-nested read and write requests under the RW-RNLP and the fast RW-RNLP. Here, for each request $\mathcal{R}_i$, $m = 36$, $L_i = 100\mu$s, $n_r = 64$, and $|D_i| = 1$. Each request was randomly chosen to be a read (as opposed to a write) with probability as shown and to be a nested request with probability 0.

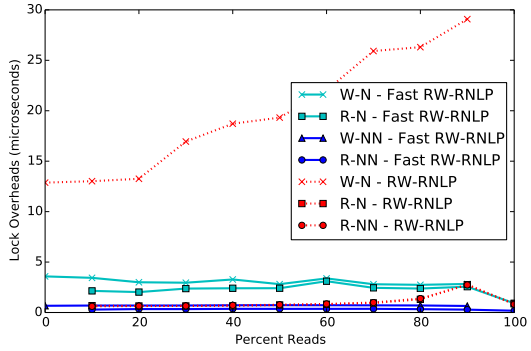

(a) Lock overhead.

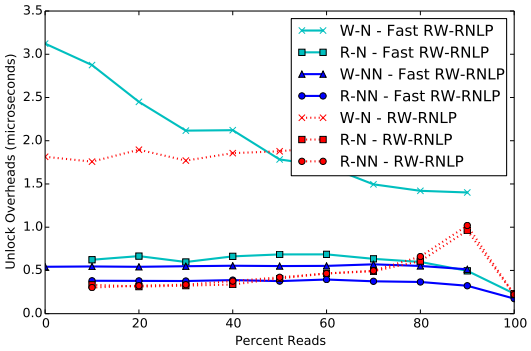

(b) Unlock overhead.

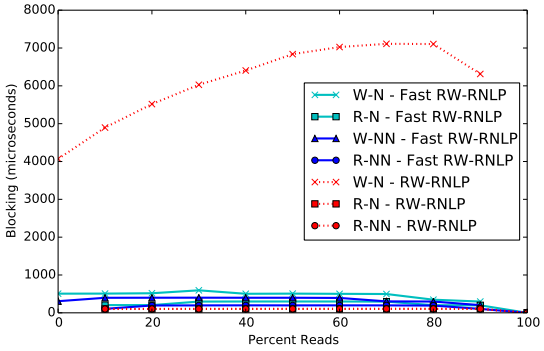

(c) Blocking.

Figure 357: (a) Lock and (b) unlock overheads and (c) blocking for nested and non-nested read and write requests under the RW-RNLP and the fast RW-RNLP. Here, for each request $\mathcal{R}_i$, $m = 36$, $L_i = 100\mu$s, $n_r = 64$, $|D_i| = 1$ for non-nested requests, and $|D_i| = 2$ for nested requests. Each request was randomly chosen to be a read (as opposed to a write) with probability as shown and to be a nested request with probability 0.2. Due to write expansion, $|D_i|$ was inflated to 64 for all write requests under the RW-RNLP, as read requests can access any resource.

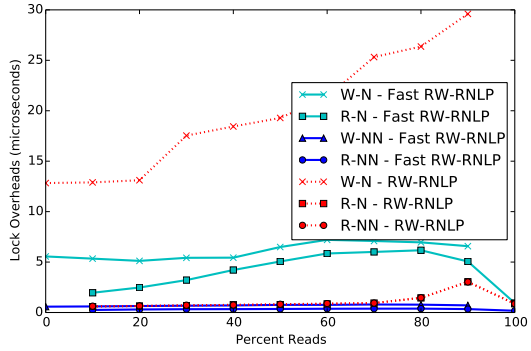

(a) Lock overhead.

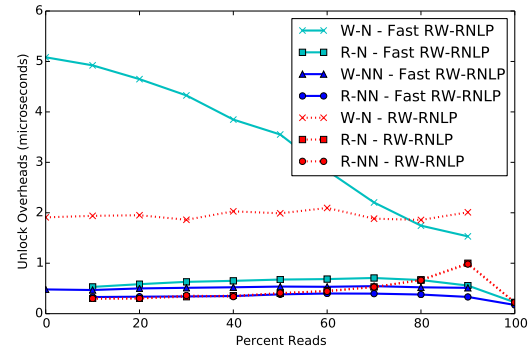

(b) Unlock overhead.

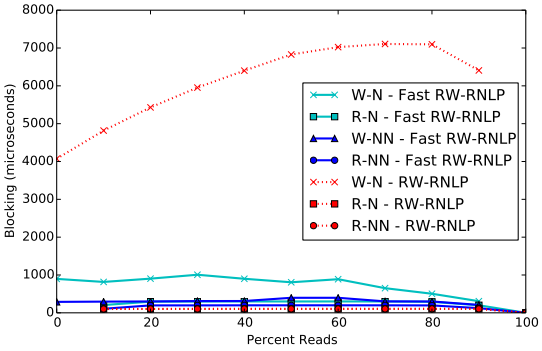

(c) Blocking.

Figure 358: (a) Lock and (b) unlock overheads and (c) blocking for nested and non-nested read and write requests under the RW-RNLP and the fast RW-RNLP. Here, for each request $\mathcal{R}_i$, $m = 36$, $L_i = 100\mu$s, $n_r = 64$, $|D_i| = 1$ for non-nested requests, and $|D_i| = 2$ for nested requests. Each request was randomly chosen to be a read (as opposed to a write) with probability as shown and to be a nested request with probability 0.5. Due to write expansion, $|D_i|$ was inflated to 64 for all write requests under the RW-RNLP, as read requests can access any resource.

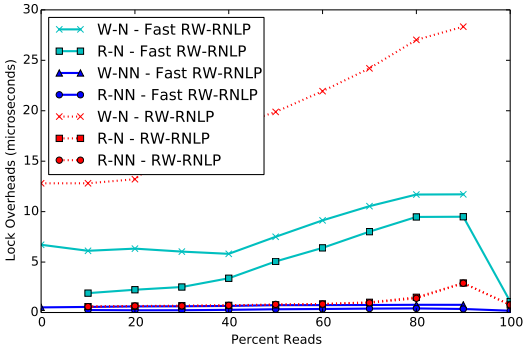

(a) Lock overhead.

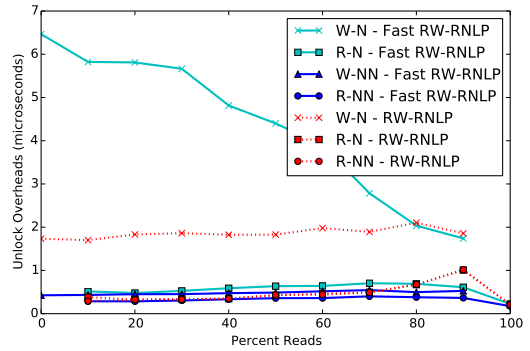

(b) Unlock overhead.

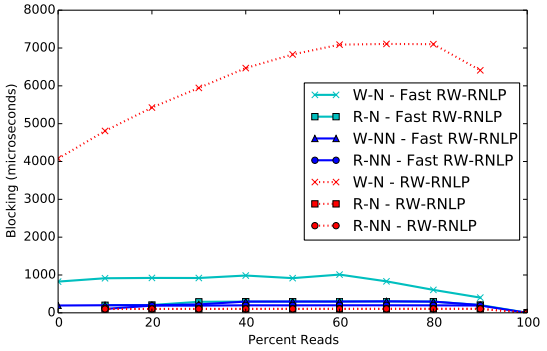

(c) Blocking.

Figure 359: (a) Lock and (b) unlock overheads and (c) blocking for nested and non-nested read and write requests under the RW-RNLP and the fast RW-RNLP. Here, for each request $\mathcal{R}_i$, $m = 36$, $L_i = 100\mu$s, $n_r = 64$, $|D_i| = 1$ for non-nested requests, and $|D_i| = 2$ for nested requests. Each request was randomly chosen to be a read (as opposed to a write) with probability as shown and to be a nested request with probability 0.8. Due to write expansion, $|D_i|$ was inflated to 64 for all write requests under the RW-RNLP, as read requests can access any resource.

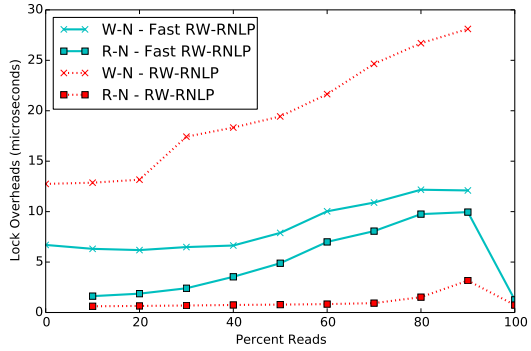

(a) Lock overhead.

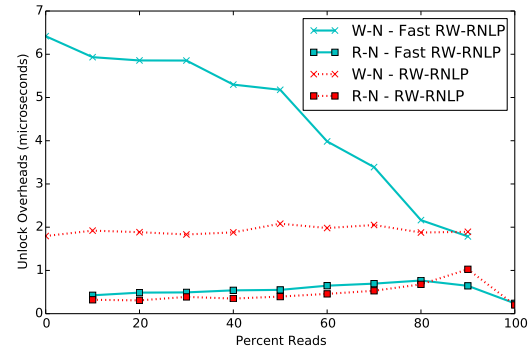

(b) Unlock overhead.

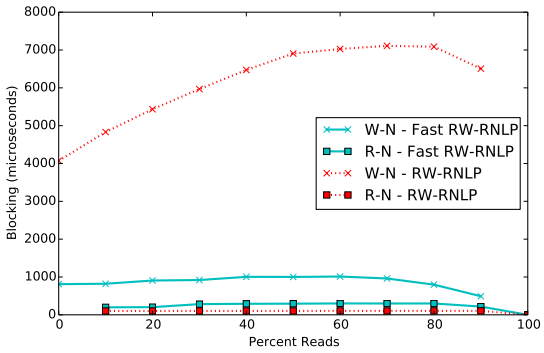

(c) Blocking.

Figure 360: (a) Lock and (b) unlock overheads and (c) blocking for nested read and write requests under the RW-RNLP and the fast RW-RNLP. Here, for each request $\mathcal{R}_i$, $m = 36$, $L_i = 100\mu$s, $n_r = 64$, and $|D_i| = 2$. Each request was randomly chosen to be a read (as opposed to a write) with probability as shown and to be a nested request with probability 1. Due to write expansion, $|D_i|$ was inflated to 64 for all write requests under the RW-RNLP, as read requests can access any resource.

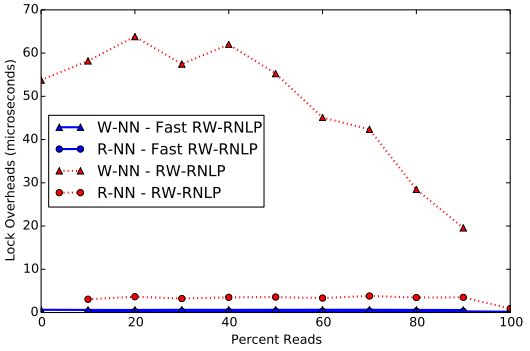

(a) Lock overhead.

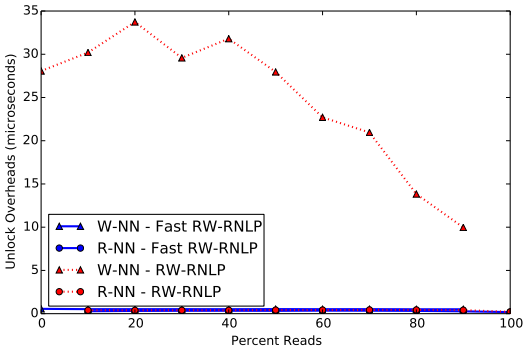

(b) Unlock overhead.

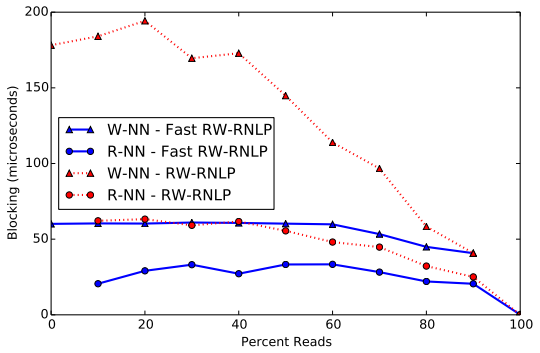

(c) Blocking.

Figure 361: (a) Lock and (b) unlock overheads and (c) blocking for non-nested read and write requests under the RW-RNLP and the fast RW-RNLP. Here, for each request $\mathcal{R}_i$, $m = 36$, $L_i = 20\mu$s, $n_r = 64$, and $|D_i| = 1$. Each request was randomly chosen to be a read (as opposed to a write) with probability as shown and to be a nested request with probability 0.

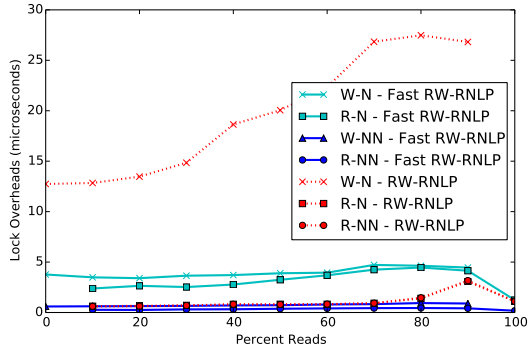

(a) Lock overhead.

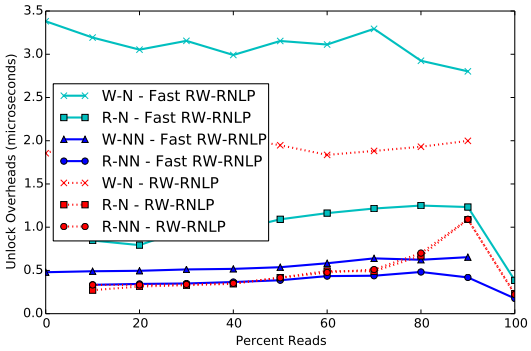

(b) Unlock overhead.

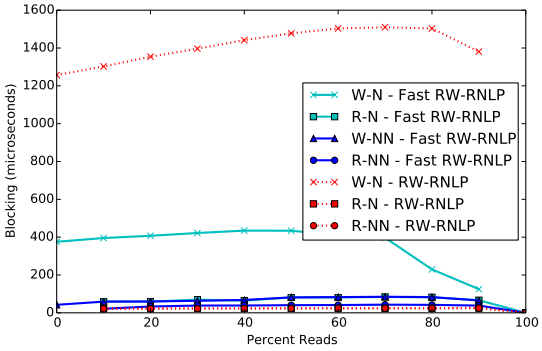

(c) Blocking.

Figure 362: (a) Lock and (b) unlock overheads and (c) blocking for nested and non-nested read and write requests under the RW-RNLP and the fast RW-RNLP. Here, for each request $\mathcal{R}_i$, $m = 36$, $L_i = 20\mu$s, $n_r = 64$, $|D_i| = 1$ for non-nested requests, and $|D_i| = 4$ for nested requests. Each request was randomly chosen to be a read (as opposed to a write) with probability as shown and to be a nested request with probability 0.2. Due to write expansion, $|D_i|$ was inflated to 64 for all write requests under the RW-RNLP, as read requests can access any resource.

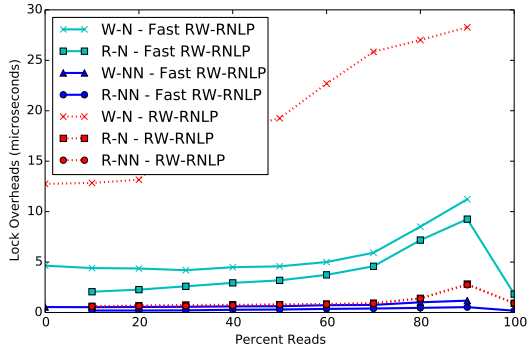

(a) Lock overhead.

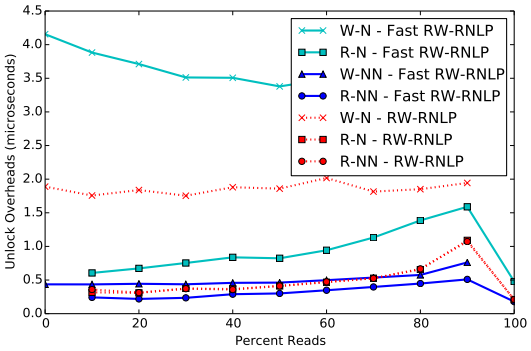

(b) Unlock overhead.

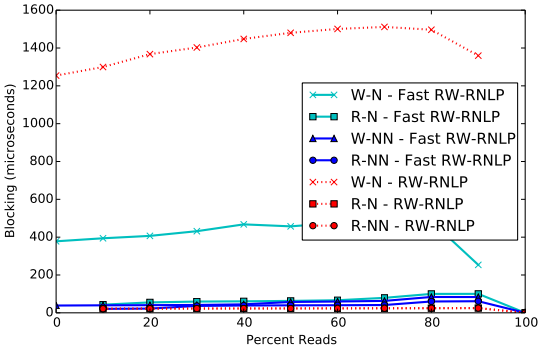

(c) Blocking.

Figure 363: (a) Lock and (b) unlock overheads and (c) blocking for nested and non-nested read and write requests under the RW-RNLP and the fast RW-RNLP. Here, for each request $\mathcal{R}_i$, $m = 36$, $L_i = 20\mu$s, $n_r = 64$, $|D_i| = 1$ for non-nested requests, and $|D_i| = 4$ for nested requests. Each request was randomly chosen to be a read (as opposed to a write) with probability as shown and to be a nested request with probability 0.5. Due to write expansion, $|D_i|$ was inflated to 64 for all write requests under the RW-RNLP, as read requests can access any resource.

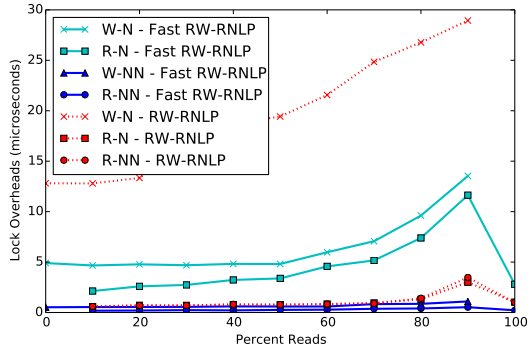

(a) Lock overhead.

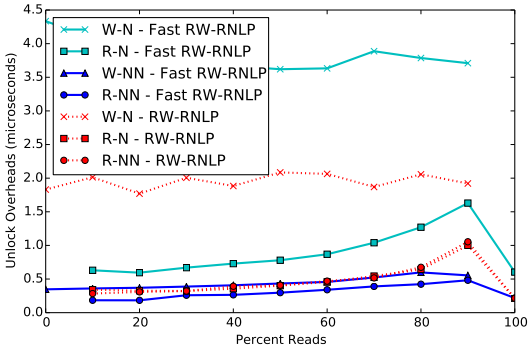

(b) Unlock overhead.

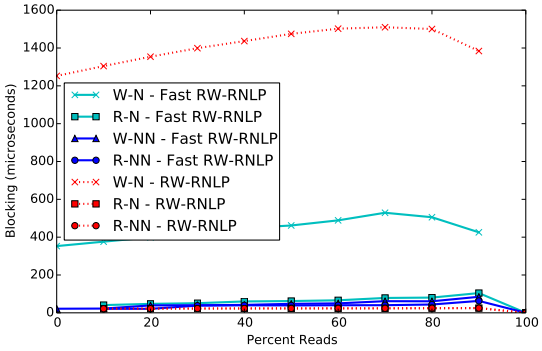

(c) Blocking.

Figure 364: (a) Lock and (b) unlock overheads and (c) blocking for nested and non-nested read and write requests under the RW-RNLP and the fast RW-RNLP. Here, for each request $\mathcal{R}_i$, $m = 36$, $L_i = 20\mu$s, $n_r = 64$, $|D_i| = 1$ for non-nested requests, and $|D_i| = 4$ for nested requests. Each request was randomly chosen to be a read (as opposed to a write) with probability as shown and to be a nested request with probability 0.8. Due to write expansion, $|D_i|$ was inflated to 64 for all write requests under the RW-RNLP, as read requests can access any resource.

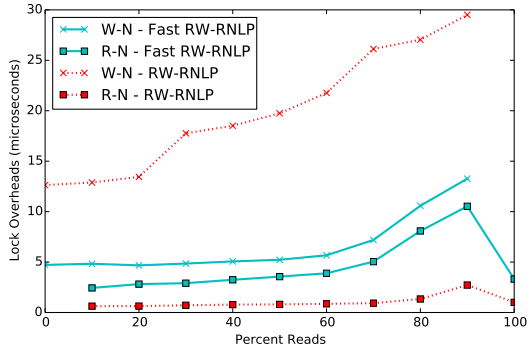

(a) Lock overhead.

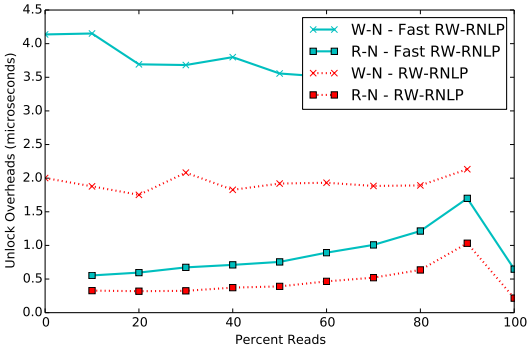

(b) Unlock overhead.

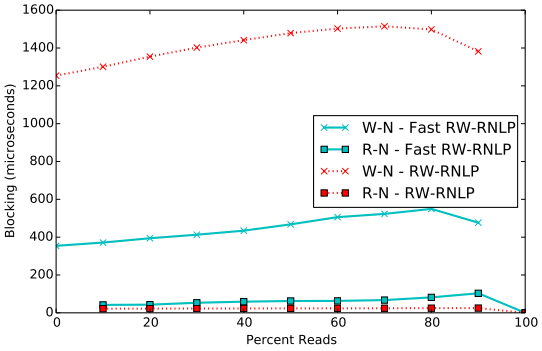

(c) Blocking.

Figure 365: (a) Lock and (b) unlock overheads and (c) blocking for nested read and write requests under the RW-RNLP and the fast RW-RNLP. Here, for each request $\mathcal{R}_i$, $m = 36$, $L_i = 20\mu$s, $n_r = 64$, and $|D_i| = 4$. Each request was randomly chosen to be a read (as opposed to a write) with probability as shown and to be a nested request with probability 1. Due to write expansion, $|D_i|$ was inflated to 64 for all write requests under the RW-RNLP, as read requests can access any resource.

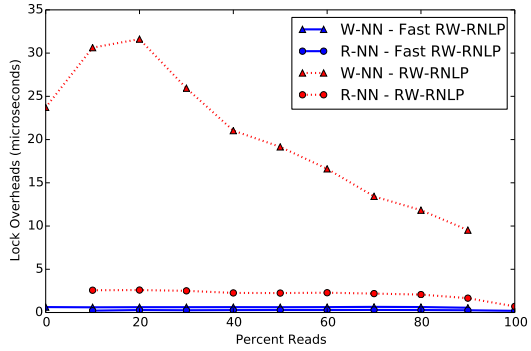

(a) Lock overhead.

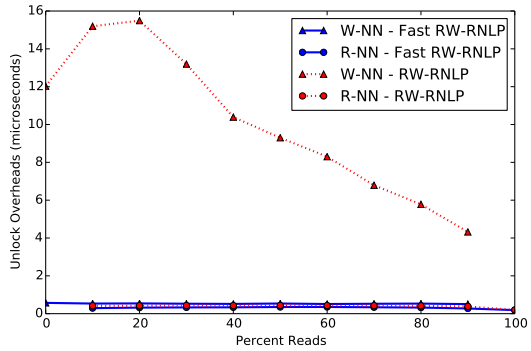

(b) Unlock overhead.

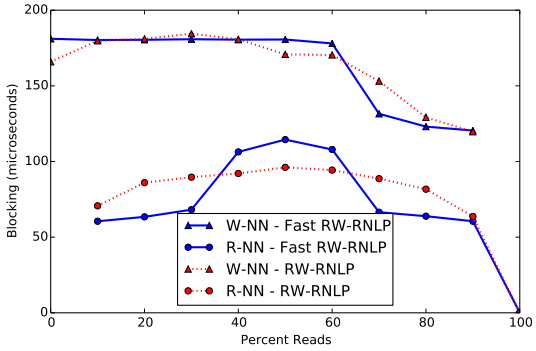

(c) Blocking.

Figure 366: (a) Lock and (b) unlock overheads and (c) blocking for non-nested read and write requests under the RW-RNLP and the fast RW-RNLP. Here, for each request $\mathcal{R}_i$, $m = 36$, $L_i = 60\mu$s, $n_r = 64$, and $|D_i| = 1$. Each request was randomly chosen to be a read (as opposed to a write) with probability as shown and to be a nested request with probability 0.

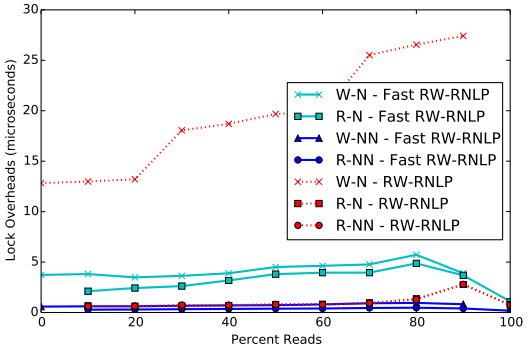

(a) Lock overhead.

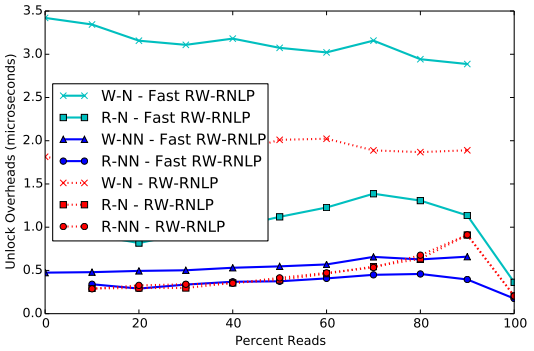

(b) Unlock overhead.

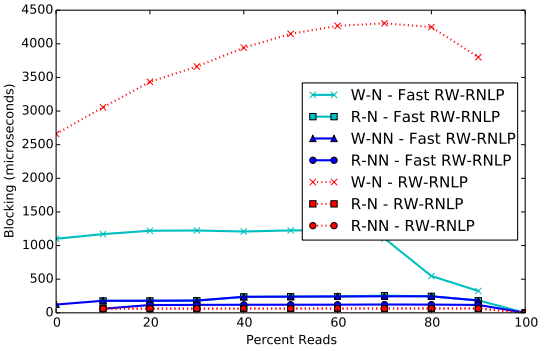

(c) Blocking.

Figure 367: (a) Lock and (b) unlock overheads and (c) blocking for nested and non-nested read and write requests under the RW-RNLP and the fast RW-RNLP. Here, for each request $\mathcal{R}_i$, $m = 36$, $L_i = 60\mu$s, $n_r = 64$, $|D_i| = 1$ for non-nested requests, and $|D_i| = 4$ for nested requests. Each request was randomly chosen to be a read (as opposed to a write) with probability as shown and to be a nested request with probability 0.2. Due to write expansion, $|D_i|$ was inflated to 64 for all write requests under the RW-RNLP, as read requests can access any resource.

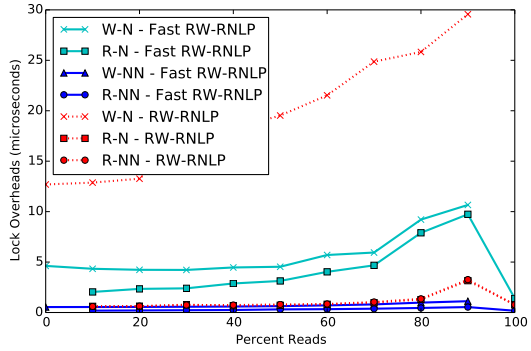

(a) Lock overhead.

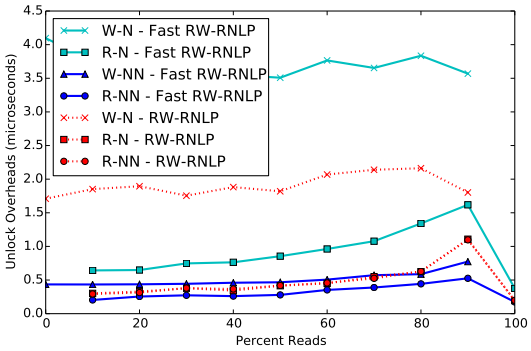

(b) Unlock overhead.

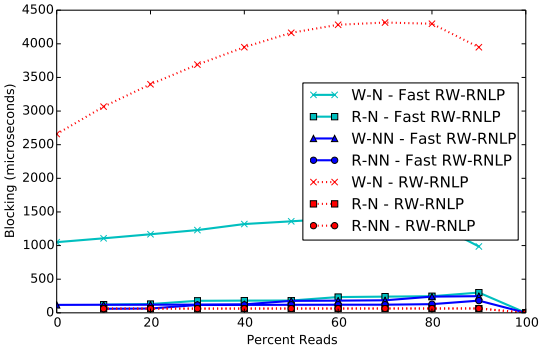

(c) Blocking.

Figure 368: (a) Lock and (b) unlock overheads and (c) blocking for nested and non-nested read and write requests under the RW-RNLP and the fast RW-RNLP. Here, for each request $\mathcal{R}_i$, $m = 36$, $L_i = 60\mu$s, $n_r = 64$, $|D_i| = 1$ for non-nested requests, and $|D_i| = 4$ for nested requests. Each request was randomly chosen to be a read (as opposed to a write) with probability as shown and to be a nested request with probability 0.5. Due to write expansion, $|D_i|$ was inflated to 64 for all write requests under the RW-RNLP, as read requests can access any resource.

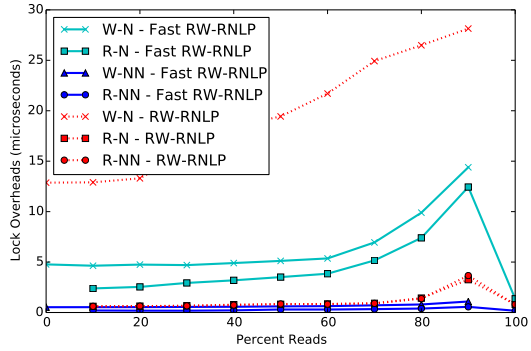

(a) Lock overhead.

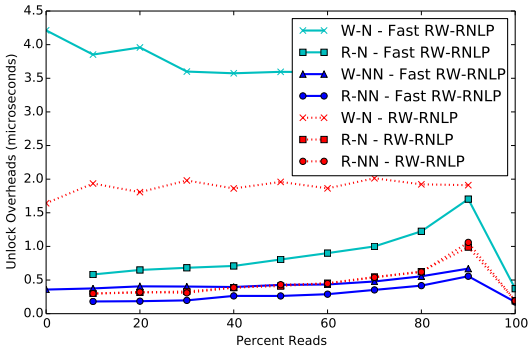

(b) Unlock overhead.

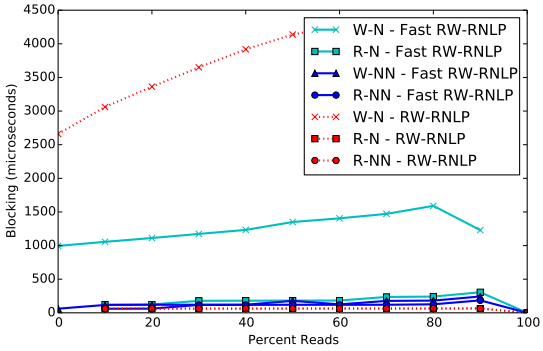

(c) Blocking.

Figure 369: (a) Lock and (b) unlock overheads and (c) blocking for nested and non-nested read and write requests under the RW-RNLP and the fast RW-RNLP. Here, for each request $\mathcal{R}_i$, $m = 36$, $L_i = 60\mu$s, $n_r = 64$, $|D_i| = 1$ for non-nested requests, and $|D_i| = 4$ for nested requests. Each request was randomly chosen to be a read (as opposed to a write) with probability as shown and to be a nested request with probability 0.8. Due to write expansion, $|D_i|$ was inflated to 64 for all write requests under the RW-RNLP, as read requests can access any resource.

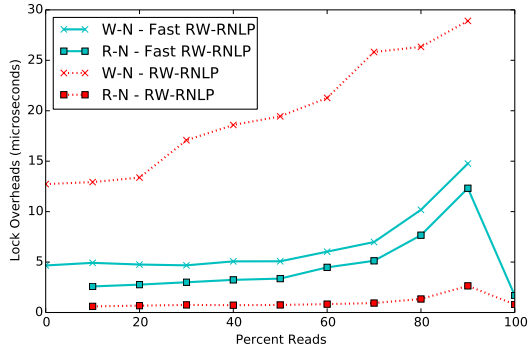

(a) Lock overhead.

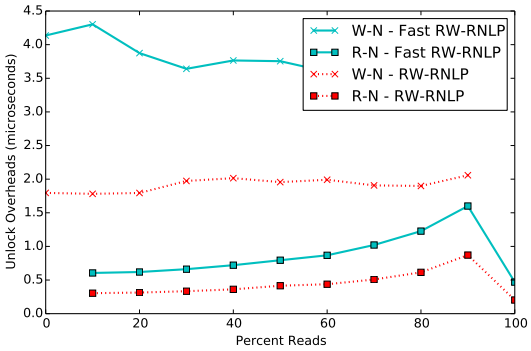

(b) Unlock overhead.

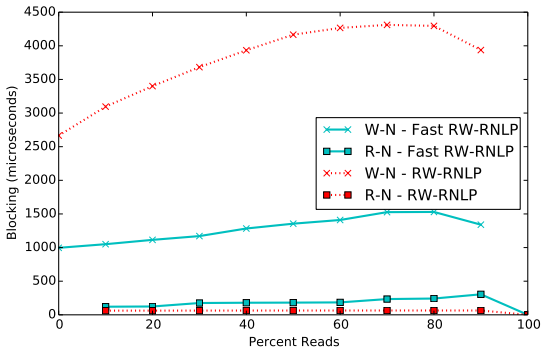

(c) Blocking.

Figure 370: (a) Lock and (b) unlock overheads and (c) blocking for nested read and write requests under the RW-RNLP and the fast RW-RNLP. Here, for each request $\mathcal{R}_i$, $m = 36$, $L_i = 60\mu$s, $n_r = 64$, and $|D_i| = 4$. Each request was randomly chosen to be a read (as opposed to a write) with probability as shown and to be a nested request with probability 1. Due to write expansion, $|D_i|$ was inflated to 64 for all write requests under the RW-RNLP, as read requests can access any resource.

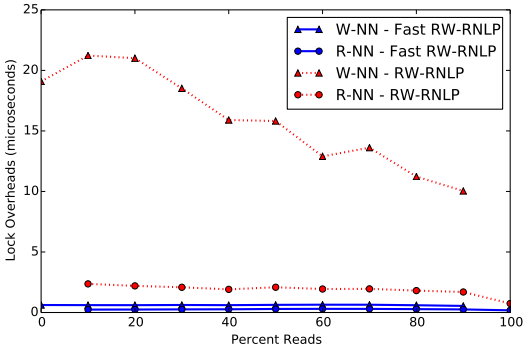

(a) Lock overhead.

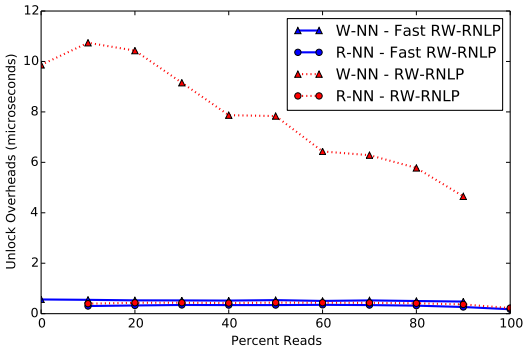

(b) Unlock overhead.

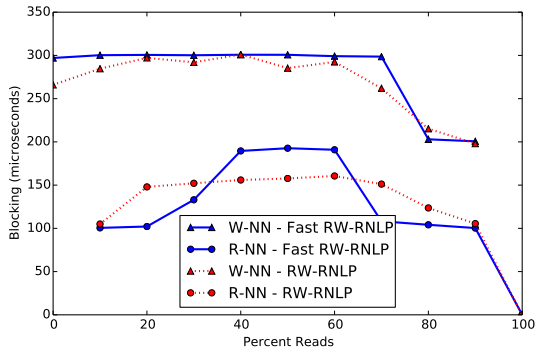

(c) Blocking.

Figure 371: (a) Lock and (b) unlock overheads and (c) blocking for non-nested read and write requests under the RW-RNLP and the fast RW-RNLP. Here, for each request $\mathcal{R}_i$, $m = 36$, $L_i = 100\mu$s, $n_r = 64$, and $|D_i| = 1$. Each request was randomly chosen to be a read (as opposed to a write) with probability as shown and to be a nested request with probability 0.

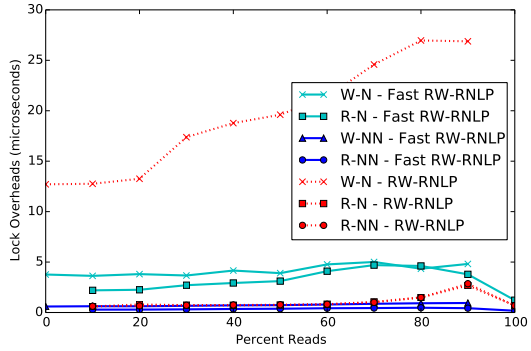

(a) Lock overhead.

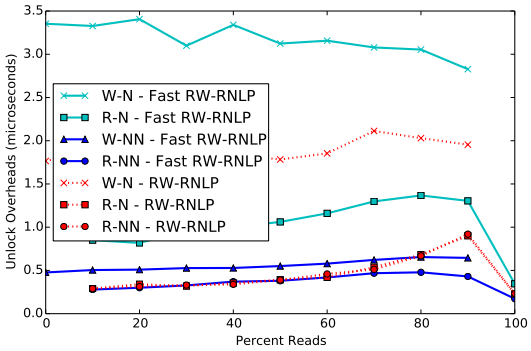

(b) Unlock overhead.

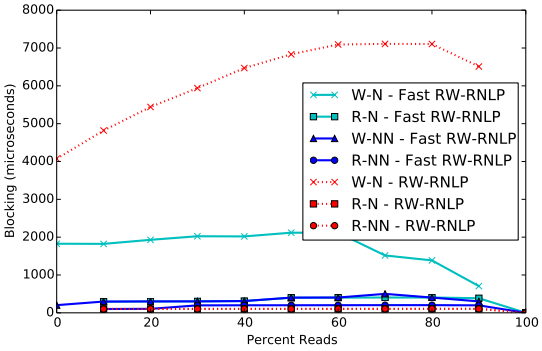

(c) Blocking.

Figure 372: (a) Lock and (b) unlock overheads and (c) blocking for nested and non-nested read and write requests under the RW-RNLP and the fast RW-RNLP. Here, for each request $\mathcal{R}_i$, $m = 36$, $L_i = 100\mu$s, $n_r = 64$, $|D_i| = 1$ for non-nested requests, and $|D_i| = 4$ for nested requests. Each request was randomly chosen to be a read (as opposed to a write) with probability as shown and to be a nested request with probability 0.2. Due to write expansion, $|D_i|$ was inflated to 64 for all write requests under the RW-RNLP, as read requests can access any resource.

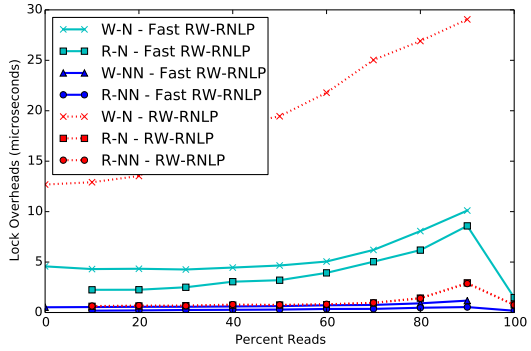

(a) Lock overhead.

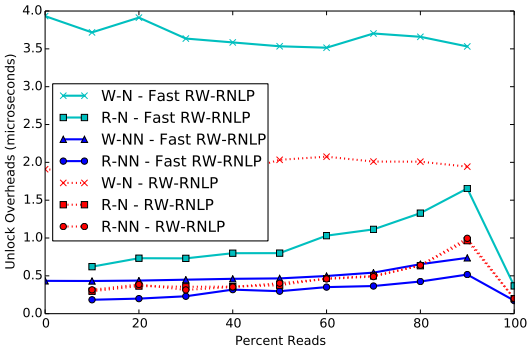

(b) Unlock overhead.

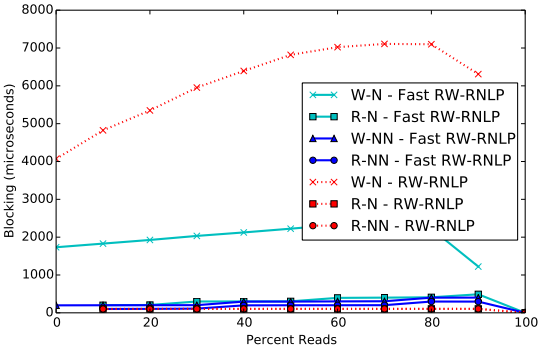

(c) Blocking.

Figure 373: (a) Lock and (b) unlock overheads and (c) blocking for nested and non-nested read and write requests under the RW-RNLP and the fast RW-RNLP. Here, for each request $\mathcal{R}_i$, $m = 36$, $L_i = 100\mu$s, $n_r = 64$, $|D_i| = 1$ for non-nested requests, and $|D_i| = 4$ for nested requests. Each request was randomly chosen to be a read (as opposed to a write) with probability as shown and to be a nested request with probability 0.5. Due to write expansion, $|D_i|$ was inflated to 64 for all write requests under the RW-RNLP, as read requests can access any resource.

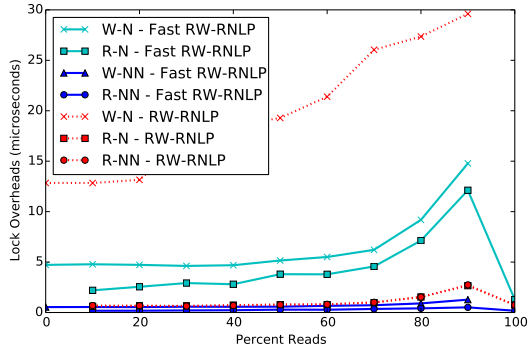

(a) Lock overhead.

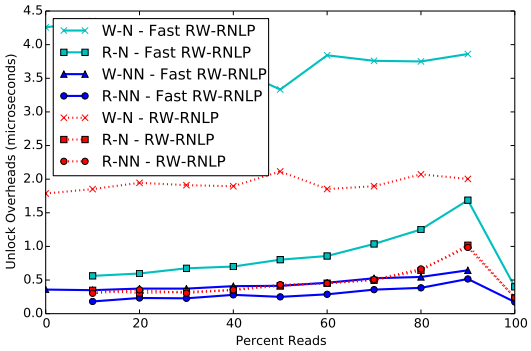

(b) Unlock overhead.

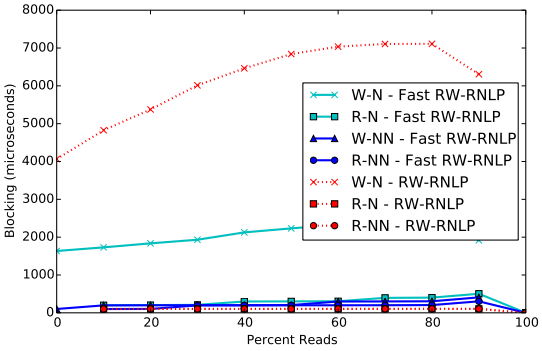

(c) Blocking.

Figure 374: (a) Lock and (b) unlock overheads and (c) blocking for nested and non-nested read and write requests under the RW-RNLP and the fast RW-RNLP. Here, for each request $\mathcal{R}_i$, $m = 36$, $L_i = 100\mu$s, $n_r = 64$, $|D_i| = 1$ for non-nested requests, and $|D_i| = 4$ for nested requests. Each request was randomly chosen to be a read (as opposed to a write) with probability as shown and to be a nested request with probability 0.8. Due to write expansion, $|D_i|$ was inflated to 64 for all write requests under the RW-RNLP, as read requests can access any resource.

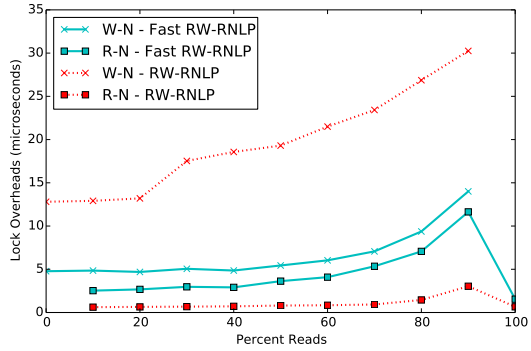

(a) Lock overhead.

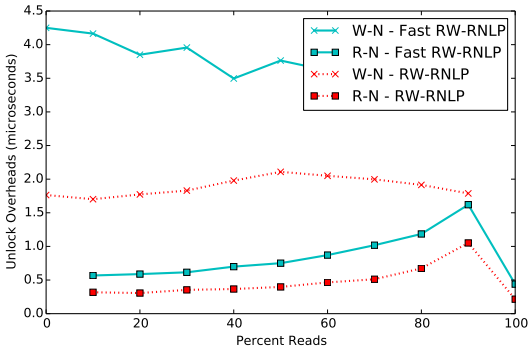

(b) Unlock overhead.

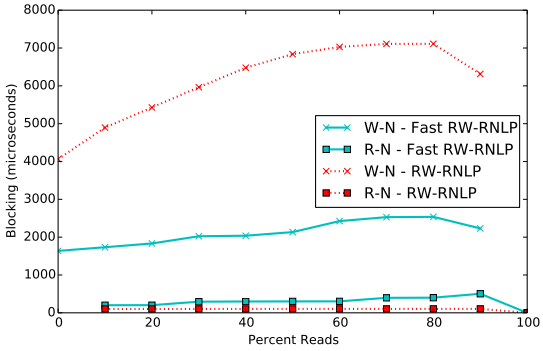

(c) Blocking.

Figure 375: (a) Lock and (b) unlock overheads and (c) blocking for nested read and write requests under the RW-RNLP and the fast RW-RNLP. Here, for each request $\mathcal{R}_i$, $m = 36$, $L_i = 100\mu$s, $n_r = 64$, and $|D_i| = 4$. Each request was randomly chosen to be a read (as opposed to a write) with probability as shown and to be a nested request with probability 1. Due to write expansion, $|D_i|$ was inflated to 64 for all write requests under the RW-RNLP, as read requests can access any resource.

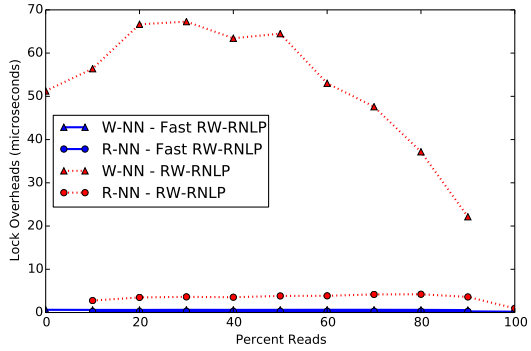

(a) Lock overhead.

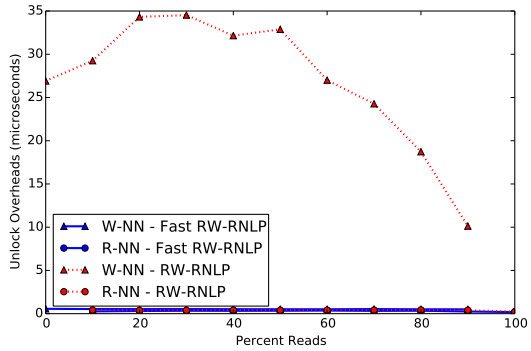

(b) Unlock overhead.

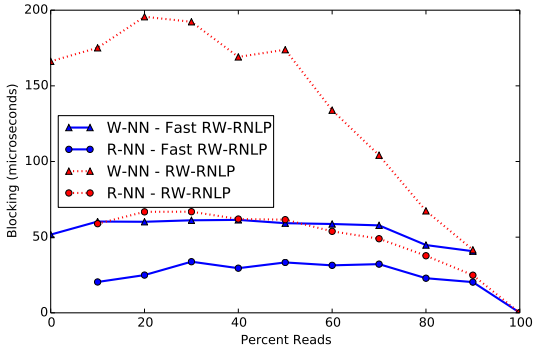

(c) Blocking.

Figure 376: (a) Lock and (b) unlock overheads and (c) blocking for non-nested read and write requests under the RW-RNLP and the fast RW-RNLP. Here, for each request $\mathcal{R}_i$, $m = 36$, $L_i = 20\mu$s, $n_r = 64$, and $|D_i| = 1$. Each request was randomly chosen to be a read (as opposed to a write) with probability as shown and to be a nested request with probability 0.

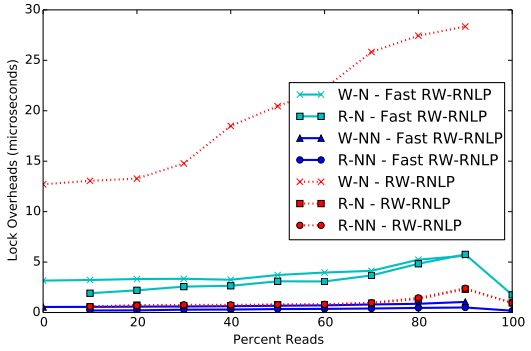

(a) Lock overhead.

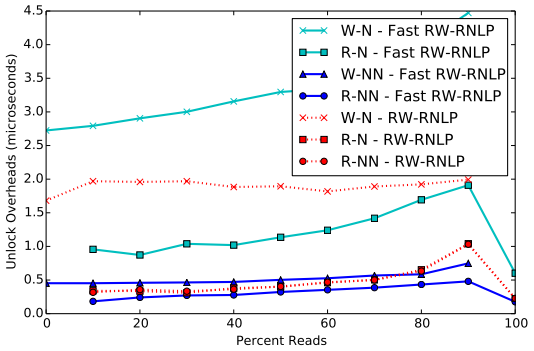

(b) Unlock overhead.

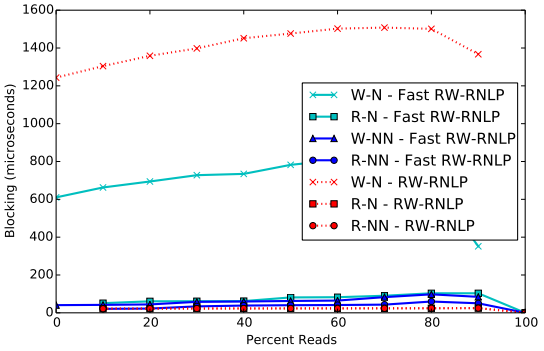

(c) Blocking.

Figure 377: (a) Lock and (b) unlock overheads and (c) blocking for nested and non-nested read and write requests under the RW-RNLP and the fast RW-RNLP. Here, for each request $\mathcal{R}_i$, $m = 36$, $L_i = 20\mu$s, $n_r = 64$, $|D_i| = 1$ for non-nested requests, and $|D_i| = 6$ for nested requests. Each request was randomly chosen to be a read (as opposed to a write) with probability as shown and to be a nested request with probability 0.2. Due to write expansion, $|D_i|$ was inflated to 64 for all write requests under the RW-RNLP, as read requests can access any resource.

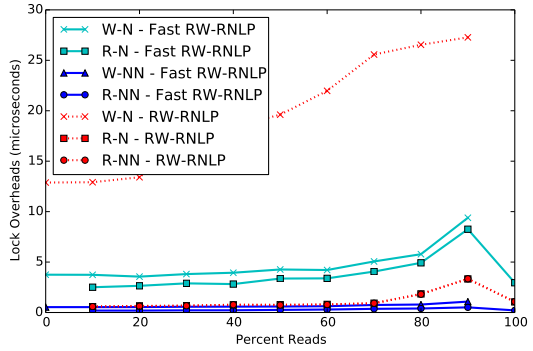

(a) Lock overhead.

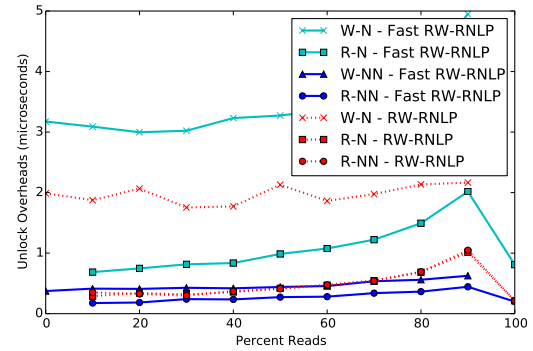

(b) Unlock overhead.

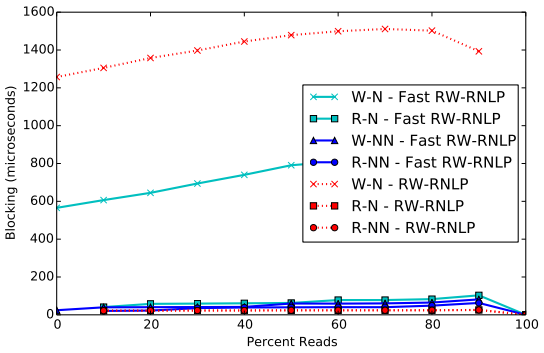

(c) Blocking.

Figure 378: (a) Lock and (b) unlock overheads and (c) blocking for nested and non-nested read and write requests under the RW-RNLP and the fast RW-RNLP. Here, for each request $\mathcal{R}_i$, $m = 36$, $L_i = 20\mu$s, $n_r = 64$, $|D_i| = 1$ for non-nested requests, and $|D_i| = 6$ for nested requests. Each request was randomly chosen to be a read (as opposed to a write) with probability as shown and to be a nested request with probability 0.5. Due to write expansion, $|D_i|$ was inflated to 64 for all write requests under the RW-RNLP, as read requests can access any resource.

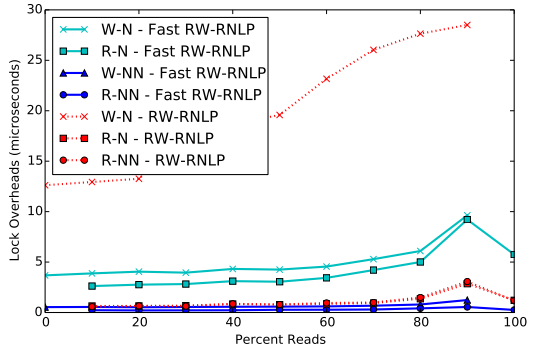

(a) Lock overhead.

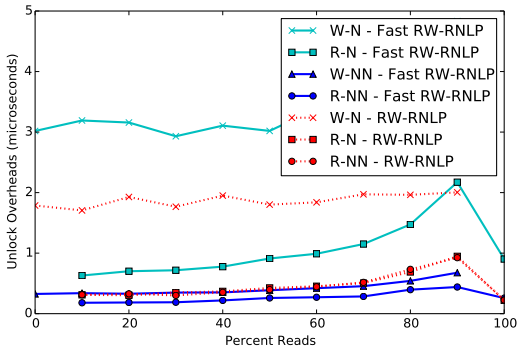

(b) Unlock overhead.

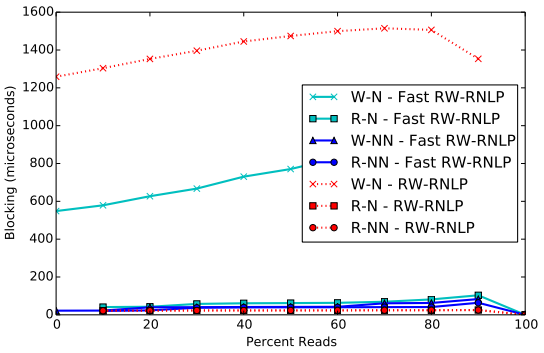

(c) Blocking.

Figure 379: (a) Lock and (b) unlock overheads and (c) blocking for nested and non-nested read and write requests under the RW-RNLP and the fast RW-RNLP. Here, for each request $\mathcal{R}_i$, $m = 36$, $L_i = 20\mu$s, $n_r = 64$, $|D_i| = 1$ for non-nested requests, and $|D_i| = 6$ for nested requests. Each request was randomly chosen to be a read (as opposed to a write) with probability as shown and to be a nested request with probability 0.8. Due to write expansion, $|D_i|$ was inflated to 64 for all write requests under the RW-RNLP, as read requests can access any resource.

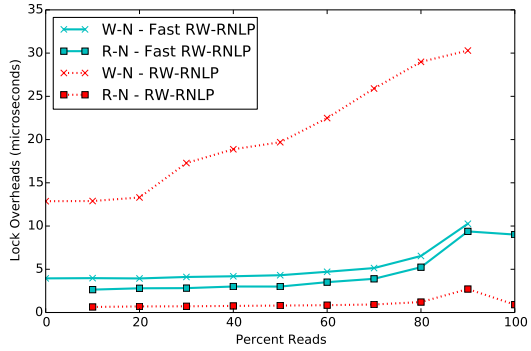

(a) Lock overhead.

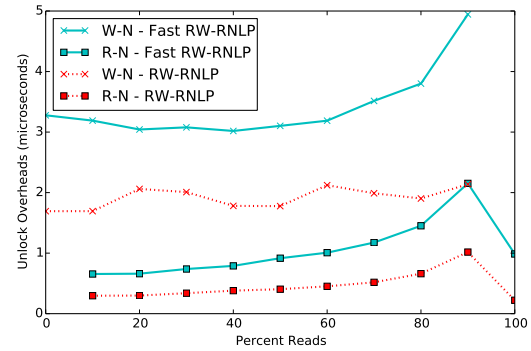

(b) Unlock overhead.

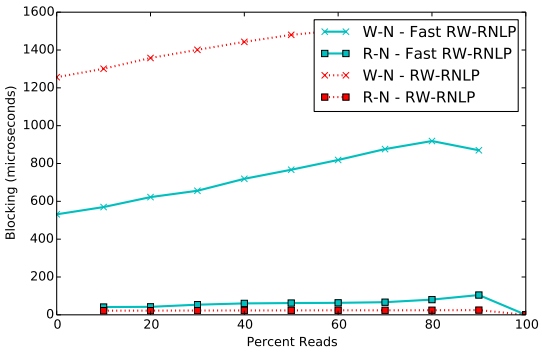

(c) Blocking.

Figure 380: (a) Lock and (b) unlock overheads and (c) blocking for nested read and write requests under the RW-RNLP and the fast RW-RNLP. Here, for each request $\mathcal{R}_i$, $m = 36$, $L_i = 20\mu$s, $n_r = 64$, and $|D_i| = 6$. Each request was randomly chosen to be a read (as opposed to a write) with probability as shown and to be a nested request with probability 1. Due to write expansion, $|D_i|$ was inflated to 64 for all write requests under the RW-RNLP, as read requests can access any resource.

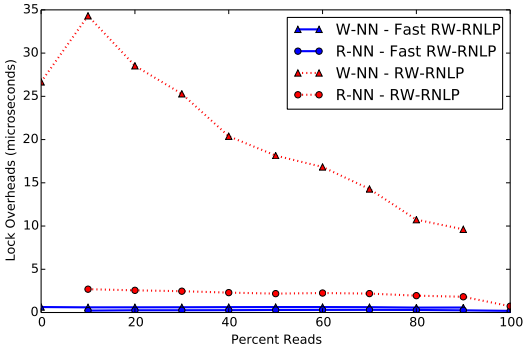

(a) Lock overhead.

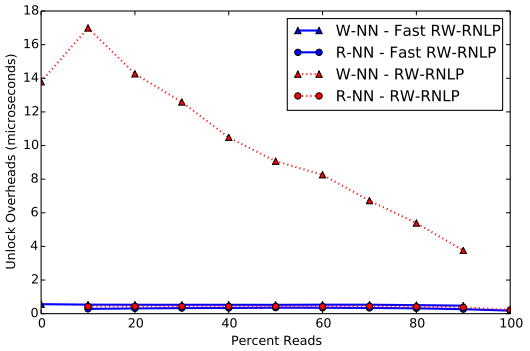

(b) Unlock overhead.

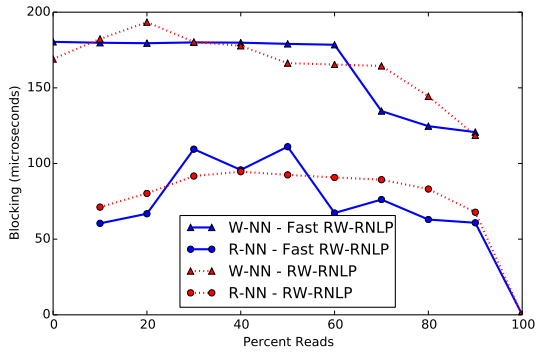

(c) Blocking.

Figure 381: (a) Lock and (b) unlock overheads and (c) blocking for non-nested read and write requests under the RW-RNLP and the fast RW-RNLP. Here, for each request $\mathcal{R}_i$, $m = 36$, $L_i = 60\mu$s, $n_r = 64$, and $|D_i| = 1$. Each request was randomly chosen to be a read (as opposed to a write) with probability as shown and to be a nested request with probability 0.

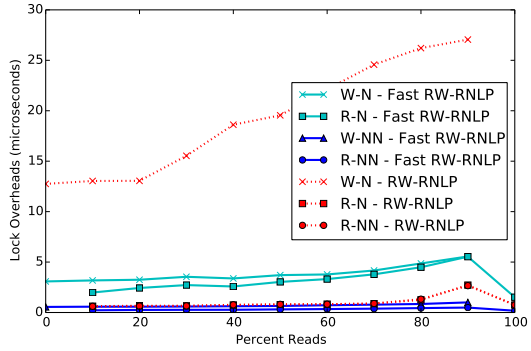

(a) Lock overhead.

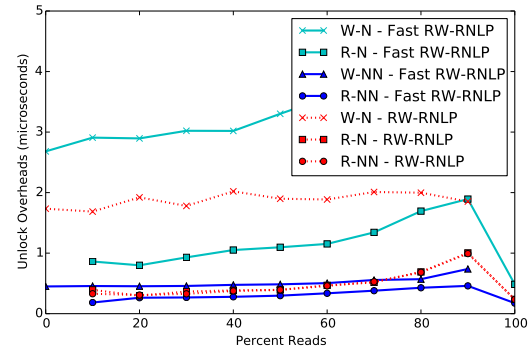

(b) Unlock overhead.

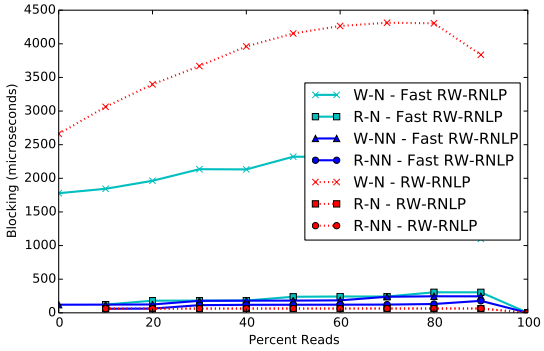

(c) Blocking.

Figure 382: (a) Lock and (b) unlock overheads and (c) blocking for nested and non-nested read and write requests under the RW-RNLP and the fast RW-RNLP. Here, for each request $\mathcal{R}_i$, $m = 36$, $L_i = 60\mu$s, $n_r = 64$, $|D_i| = 1$ for non-nested requests, and $|D_i| = 6$ for nested requests. Each request was randomly chosen to be a read (as opposed to a write) with probability as shown and to be a nested request with probability 0.2. Due to write expansion, $|D_i|$ was inflated to 64 for all write requests under the RW-RNLP, as read requests can access any resource.

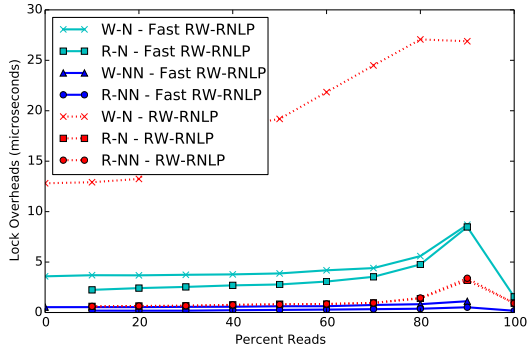

(a) Lock overhead.

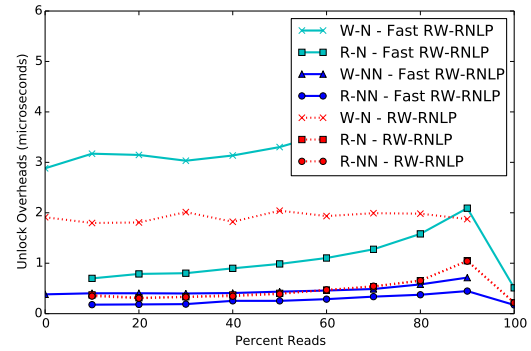

(b) Unlock overhead.

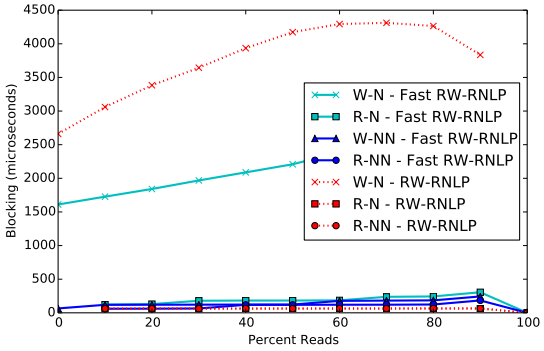

(c) Blocking.

Figure 383: (a) Lock and (b) unlock overheads and (c) blocking for nested and non-nested read and write requests under the RW-RNLP and the fast RW-RNLP. Here, for each request $\mathcal{R}_i$, $m = 36$, $L_i = 60\mu$s, $n_r = 64$, $|D_i| = 1$ for non-nested requests, and $|D_i| = 6$ for nested requests. Each request was randomly chosen to be a read (as opposed to a write) with probability as shown and to be a nested request with probability 0.5. Due to write expansion, $|D_i|$ was inflated to 64 for all write requests under the RW-RNLP, as read requests can access any resource.

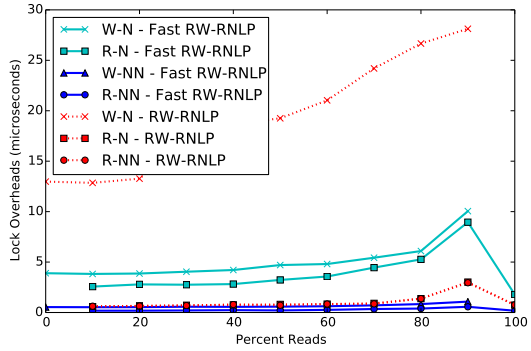

(a) Lock overhead.

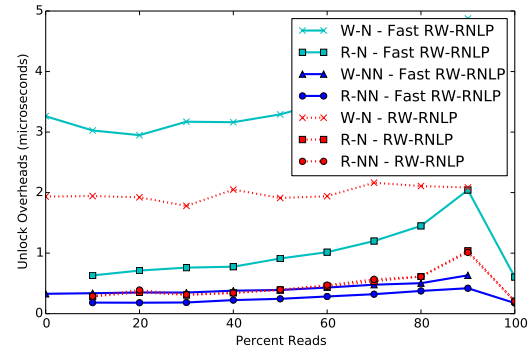

(b) Unlock overhead.

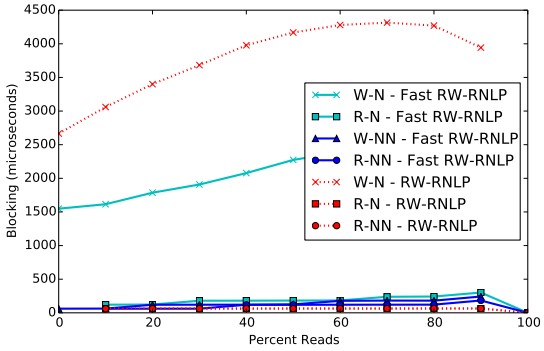

(c) Blocking.

Figure 384: (a) Lock and (b) unlock overheads and (c) blocking for nested and non-nested read and write requests under the RW-RNLP and the fast RW-RNLP. Here, for each request $\mathcal{R}_i$, $m = 36$, $L_i = 60\mu$s, $n_r = 64$, $|D_i| = 1$ for non-nested requests, and $|D_i| = 6$ for nested requests. Each request was randomly chosen to be a read (as opposed to a write) with probability as shown and to be a nested request with probability 0.8. Due to write expansion, $|D_i|$ was inflated to 64 for all write requests under the RW-RNLP, as read requests can access any resource.

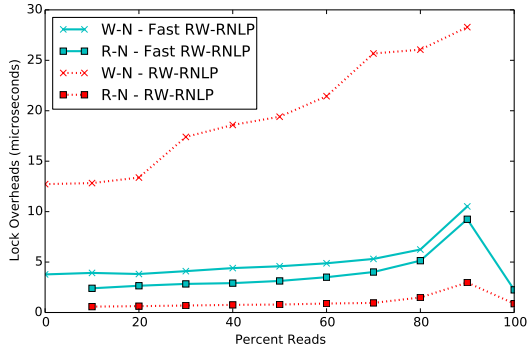

(a) Lock overhead.

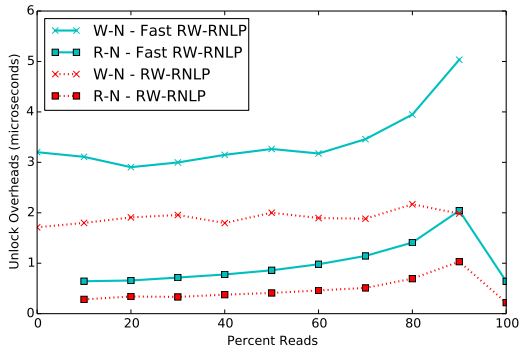

(b) Unlock overhead.

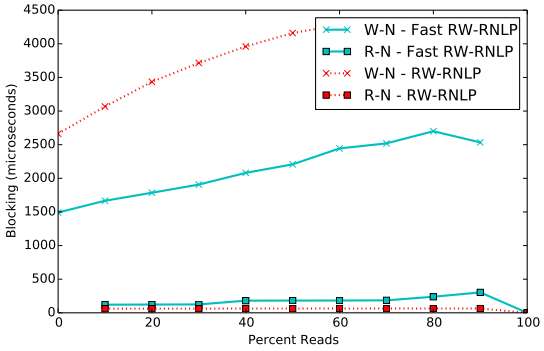

(c) Blocking.

Figure 385: (a) Lock and (b) unlock overheads and (c) blocking for nested read and write requests under the RW-RNLP and the fast RW-RNLP. Here, for each request $\mathcal{R}_i$, $m = 36$, $L_i = 60\mu$s, $n_r = 64$, and $|D_i| = 6$. Each request was randomly chosen to be a read (as opposed to a write) with probability as shown and to be a nested request with probability 1. Due to write expansion, $|D_i|$ was inflated to 64 for all write requests under the RW-RNLP, as read requests can access any resource.

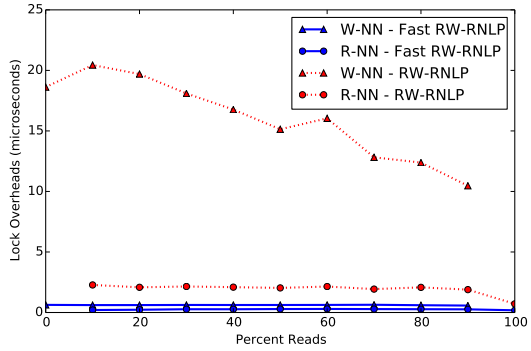

(a) Lock overhead.

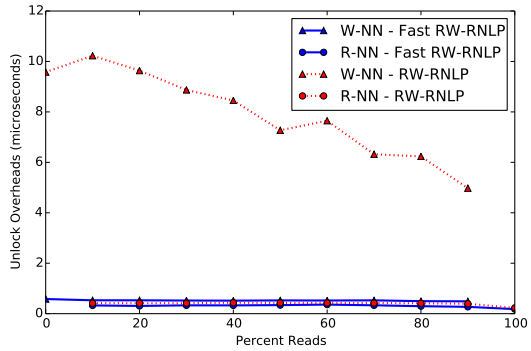

(b) Unlock overhead.

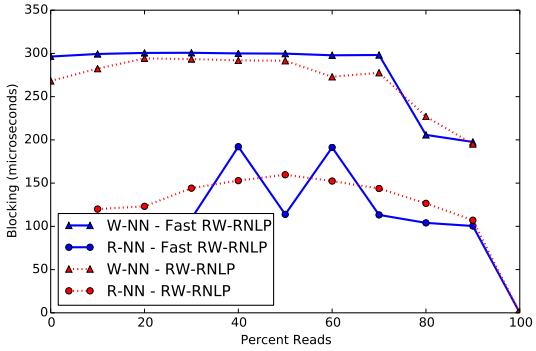

(c) Blocking.

Figure 386: (a) Lock and (b) unlock overheads and (c) blocking for non-nested read and write requests under the RW-RNLP and the fast RW-RNLP. Here, for each request $\mathcal{R}_i$, $m = 36$, $L_i = 100\mu$s, $n_r = 64$, and $|D_i| = 1$. Each request was randomly chosen to be a read (as opposed to a write) with probability as shown and to be a nested request with probability 0.

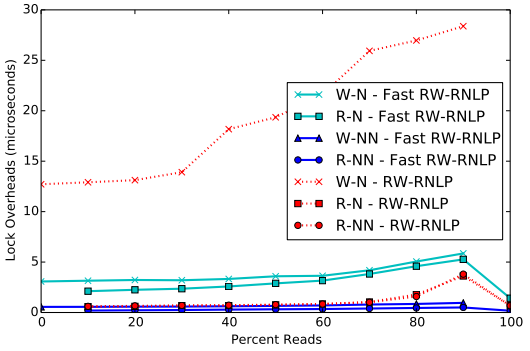

(a) Lock overhead.

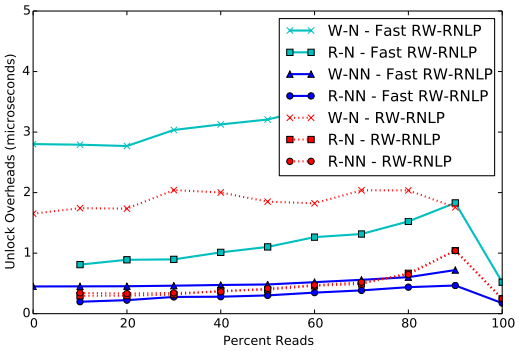

(b) Unlock overhead.

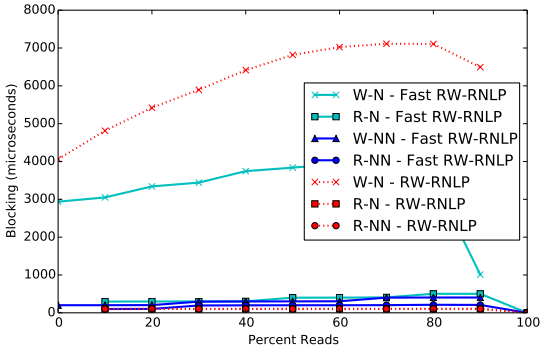

(c) Blocking.

Figure 387: (a) Lock and (b) unlock overheads and (c) blocking for nested and non-nested read and write requests under the RW-RNLP and the fast RW-RNLP. Here, for each request $\mathcal{R}_i$, $m = 36$, $L_i = 100\mu$s, $n_r = 64$, $|D_i| = 1$ for non-nested requests, and $|D_i| = 6$ for nested requests. Each request was randomly chosen to be a read (as opposed to a write) with probability as shown and to be a nested request with probability 0.2. Due to write expansion, $|D_i|$ was inflated to 64 for all write requests under the RW-RNLP, as read requests can access any resource.

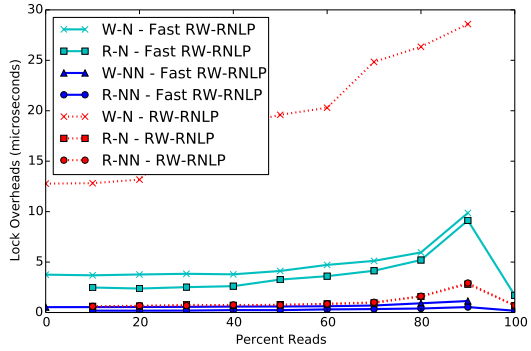

(a) Lock overhead.

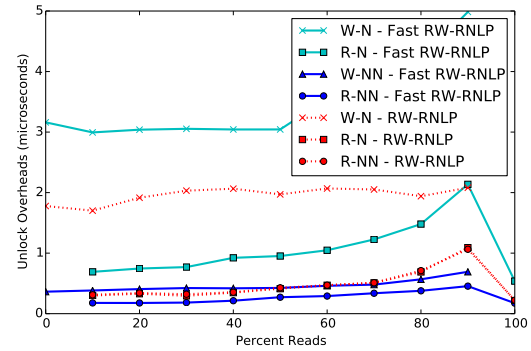

(b) Unlock overhead.

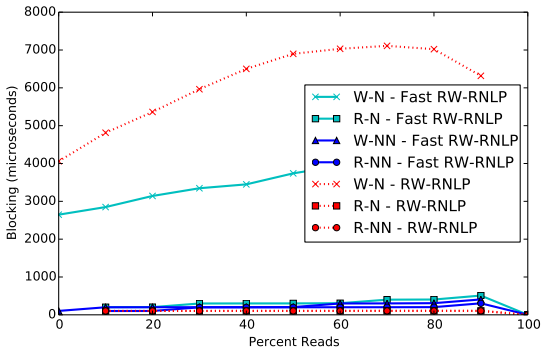

(c) Blocking.

Figure 388: (a) Lock and (b) unlock overheads and (c) blocking for nested and non-nested read and write requests under the RW-RNLP and the fast RW-RNLP. Here, for each request $\mathcal{R}_i$, $m = 36$, $L_i = 100\mu$s, $n_r = 64$, $|D_i| = 1$ for non-nested requests, and $|D_i| = 6$ for nested requests. Each request was randomly chosen to be a read (as opposed to a write) with probability as shown and to be a nested request with probability 0.5. Due to write expansion, $|D_i|$ was inflated to 64 for all write requests under the RW-RNLP, as read requests can access any resource.

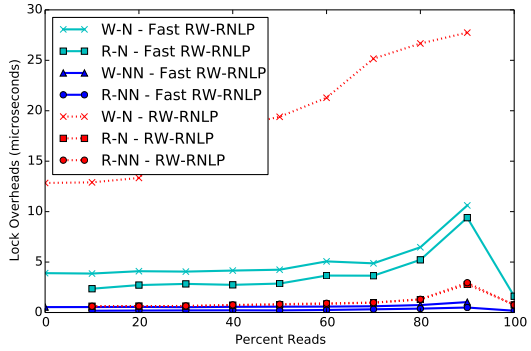

(a) Lock overhead.

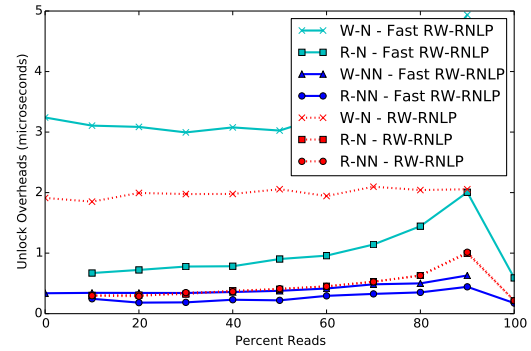

(b) Unlock overhead.

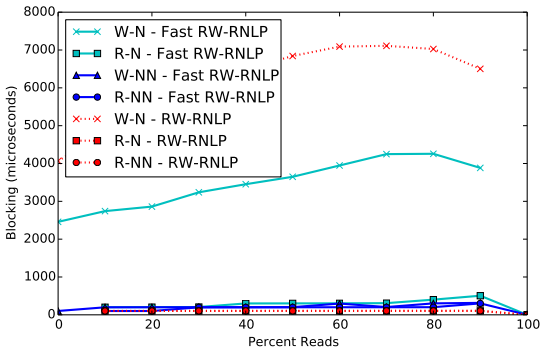

(c) Blocking.

Figure 389: (a) Lock and (b) unlock overheads and (c) blocking for nested and non-nested read and write requests under the RW-RNLP and the fast RW-RNLP. Here, for each request $\mathcal{R}_i$, $m = 36$, $L_i = 100\mu$s, $n_r = 64$, $|D_i| = 1$ for non-nested requests, and $|D_i| = 6$ for nested requests. Each request was randomly chosen to be a read (as opposed to a write) with probability as shown and to be a nested request with probability 0.8. Due to write expansion, $|D_i|$ was inflated to 64 for all write requests under the RW-RNLP, as read requests can access any resource.

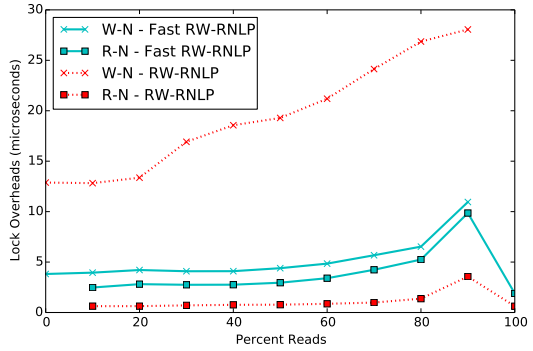

(a) Lock overhead.

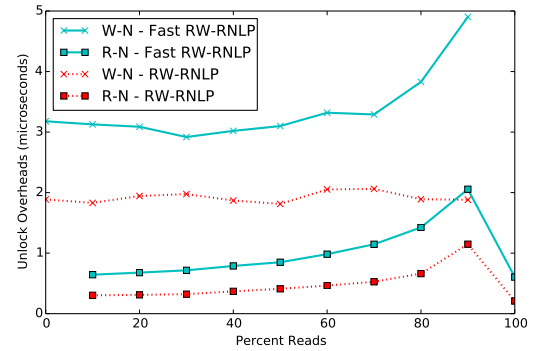

(b) Unlock overhead.

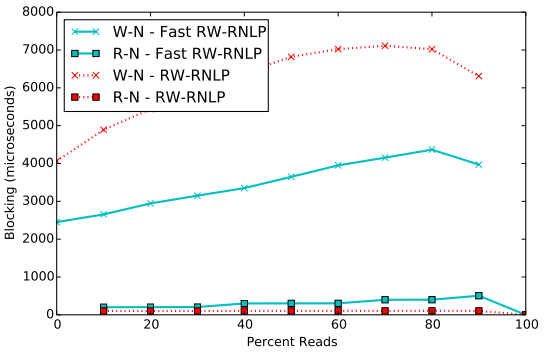

(c) Blocking.

Figure 390: (a) Lock and (b) unlock overheads and (c) blocking for nested read and write requests under the RW-RNLP and the fast RW-RNLP. Here, for each request $\mathcal{R}_i$, $m = 36$, $L_i = 100\mu$s, $n_r = 64$, and $|D_i| = 6$. Each request was randomly chosen to be a read (as opposed to a write) with probability as shown and to be a nested request with probability 1. Due to write expansion, $|D_i|$ was inflated to 64 for all write requests under the RW-RNLP, as read requests can access any resource.

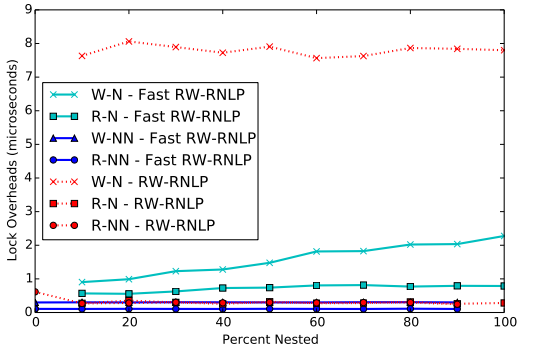

(a) Lock overhead.

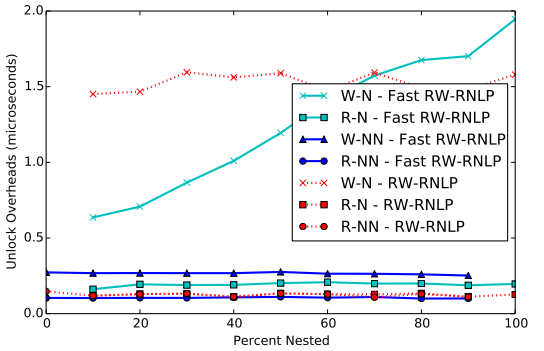

(b) Unlock overhead.

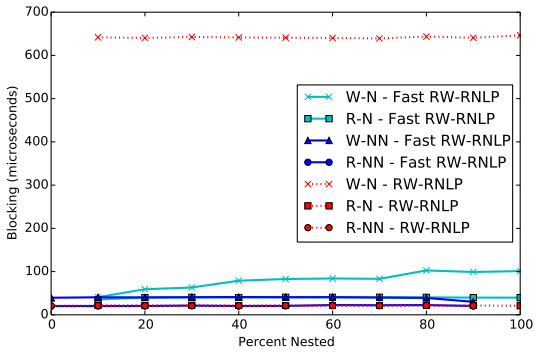

(c) Blocking.

Figure 391: (a) Lock and (b) unlock overheads and (c) blocking for nested and non-nested read and write requests under the RW-RNLP and the fast RW-RNLP. Here, for each request $\mathcal{R}_i$, $m = 18$, $L_i = 20\mu$s, $n_r = 64$, $|D_i| = 1$ for non-nested requests, and $|D_i| = 2$ for nested requests. Each request was randomly chosen to be a read (as opposed to a write) with probability 0.2 and to be a nested request with probability as shown. Due to write expansion, $|D_i|$ was inflated to 64 for all write requests under the RW-RNLP, as read requests can access any resource.

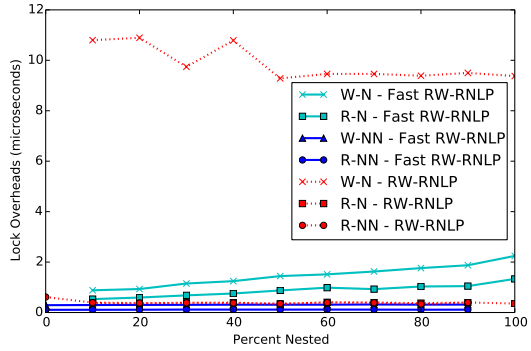

(a) Lock overhead.

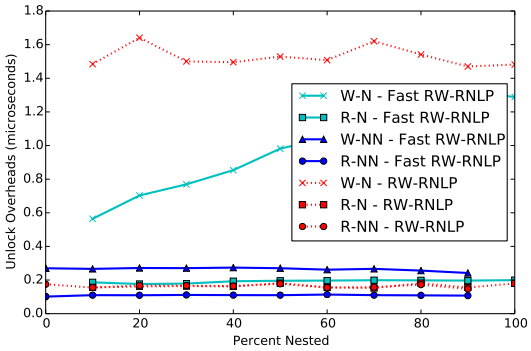

(b) Unlock overhead.

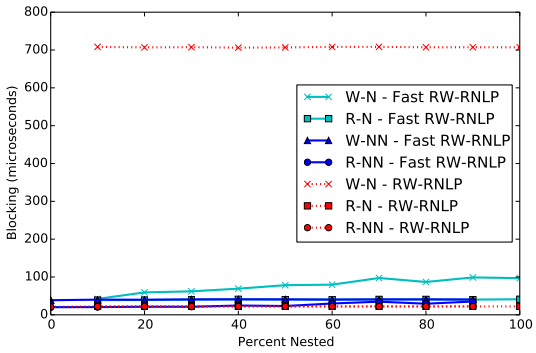

(c) Blocking.

Figure 392: (a) Lock and (b) unlock overheads and (c) blocking for nested and non-nested read and write requests under the RW-RNLP and the fast RW-RNLP. Here, for each request $\mathcal{R}_i$, $m = 18$, $L_i = 20\mu$s, $n_r = 64$, $|D_i| = 1$ for non-nested requests, and $|D_i| = 2$ for nested requests. Each request was randomly chosen to be a read (as opposed to a write) with probability 0.5 and to be a nested request with probability as shown. Due to write expansion, $|D_i|$ was inflated to 64 for all write requests under the RW-RNLP, as read requests can access any resource.

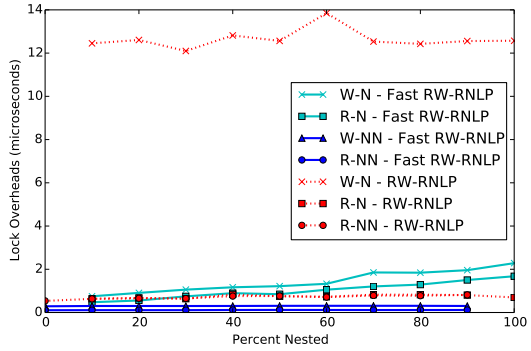

(a) Lock overhead.

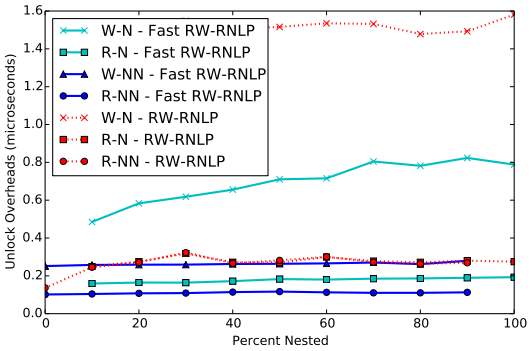

(b) Unlock overhead.

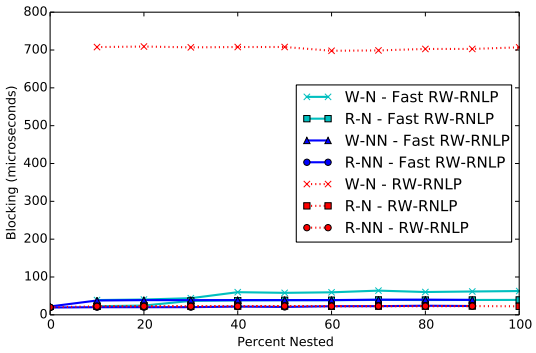

(c) Blocking.

Figure 393: (a) Lock and (b) unlock overheads and (c) blocking for nested and non-nested read and write requests under the RW-RNLP and the fast RW-RNLP. Here, for each request $\mathcal{R}_i$, $m = 18$, $L_i = 20\mu$s, $n_r = 64$, $|D_i| = 1$ for non-nested requests, and $|D_i| = 2$ for nested requests. Each request was randomly chosen to be a read (as opposed to a write) with probability 0.8 and to be a nested request with probability as shown. Due to write expansion, $|D_i|$ was inflated to 64 for all write requests under the RW-RNLP, as read requests can access any resource.

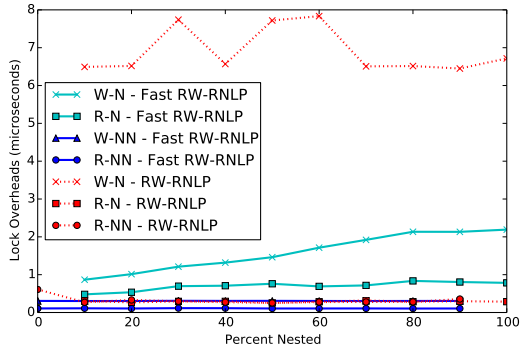

(a) Lock overhead.

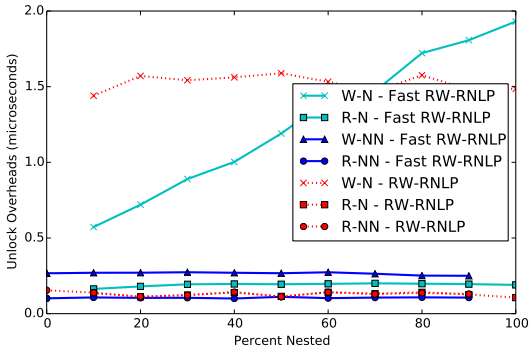

(b) Unlock overhead.

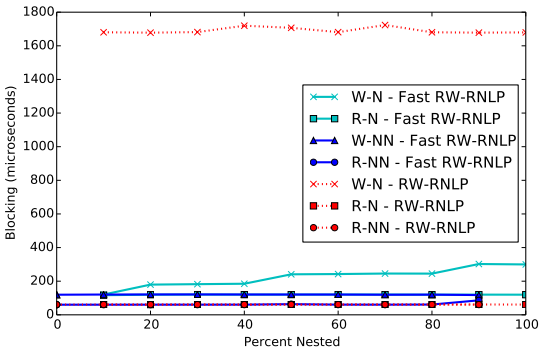

(c) Blocking.

Figure 394: (a) Lock and (b) unlock overheads and (c) blocking for nested and non-nested read and write requests under the RW-RNLP and the fast RW-RNLP. Here, for each request $\mathcal{R}_i$, $m = 18$, $L_i = 60\mu$s, $n_r = 64$, $|D_i| = 1$ for non-nested requests, and $|D_i| = 2$ for nested requests. Each request was randomly chosen to be a read (as opposed to a write) with probability 0.2 and to be a nested request with probability as shown. Due to write expansion, $|D_i|$ was inflated to 64 for all write requests under the RW-RNLP, as read requests can access any resource.

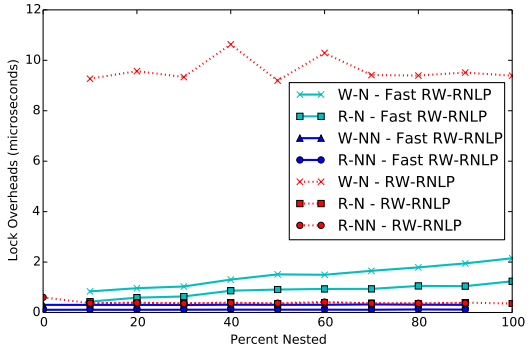

(a) Lock overhead.

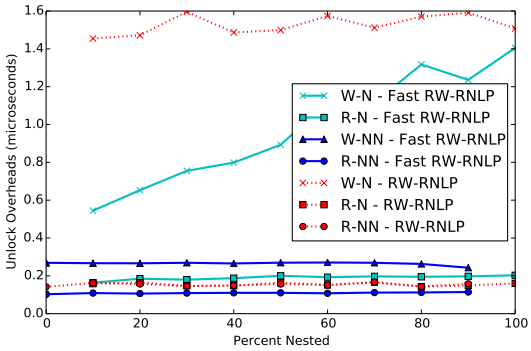

(b) Unlock overhead.

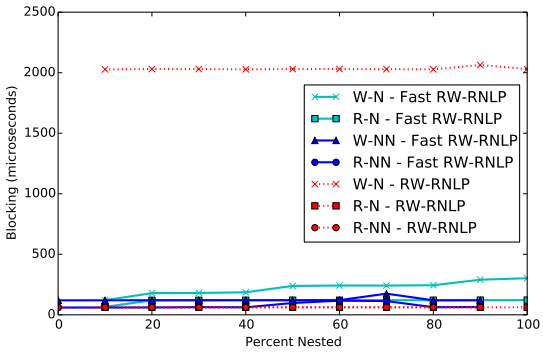

(c) Blocking.

Figure 395: (a) Lock and (b) unlock overheads and (c) blocking for nested and non-nested read and write requests under the RW-RNLP and the fast RW-RNLP. Here, for each request $\mathcal{R}_i$, $m = 18$, $L_i = 60\mu$s, $n_r = 64$, $|D_i| = 1$ for non-nested requests, and $|D_i| = 2$ for nested requests. Each request was randomly chosen to be a read (as opposed to a write) with probability 0.5 and to be a nested request with probability as shown. Due to write expansion, $|D_i|$ was inflated to 64 for all write requests under the RW-RNLP, as read requests can access any resource.

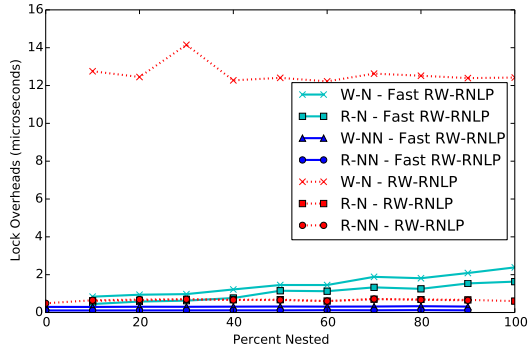

(a) Lock overhead.

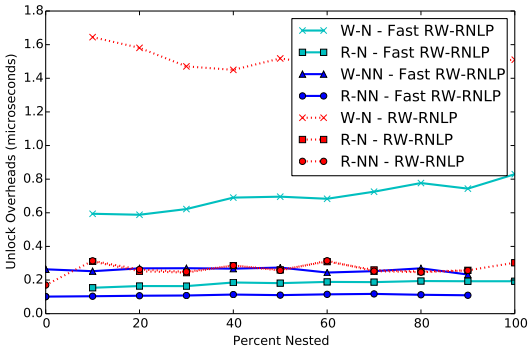

(b) Unlock overhead.

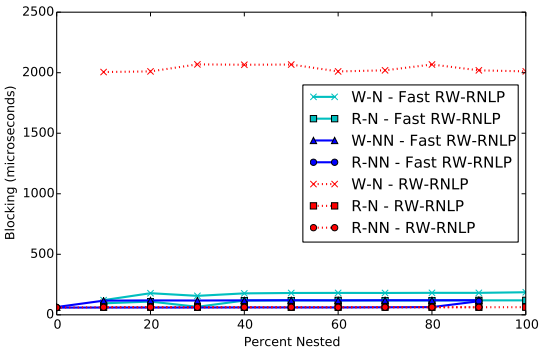

(c) Blocking.

Figure 396: (a) Lock and (b) unlock overheads and (c) blocking for nested and non-nested read and write requests under the RW-RNLP and the fast RW-RNLP. Here, for each request $\mathcal{R}_i$, $m = 18$, $L_i = 60\mu$s, $n_r = 64$, $|D_i| = 1$ for non-nested requests, and $|D_i| = 2$ for nested requests. Each request was randomly chosen to be a read (as opposed to a write) with probability 0.8 and to be a nested request with probability as shown. Due to write expansion, $|D_i|$ was inflated to 64 for all write requests under the RW-RNLP, as read requests can access any resource.

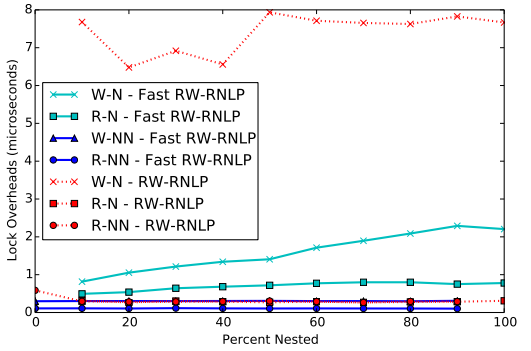

(a) Lock overhead.

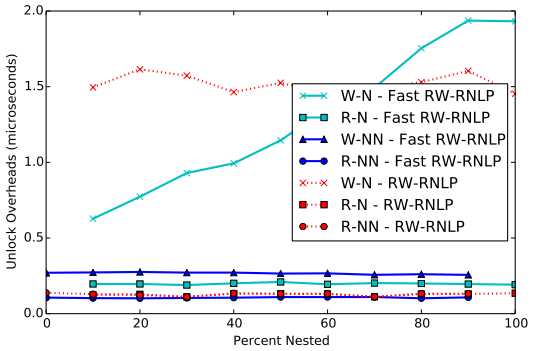

(b) Unlock overhead.

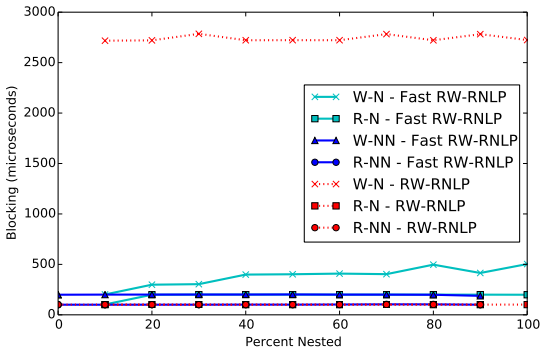

(c) Blocking.

Figure 397: (a) Lock and (b) unlock overheads and (c) blocking for nested and non-nested read and write requests under the RW-RNLP and the fast RW-RNLP. Here, for each request $\mathcal{R}_i$, $m = 18$, $L_i = 100\mu$s, $n_r = 64$, $|D_i| = 1$ for non-nested requests, and $|D_i| = 2$ for nested requests. Each request was randomly chosen to be a read (as opposed to a write) with probability 0.2 and to be a nested request with probability as shown. Due to write expansion, $|D_i|$ was inflated to 64 for all write requests under the RW-RNLP, as read requests can access any resource.

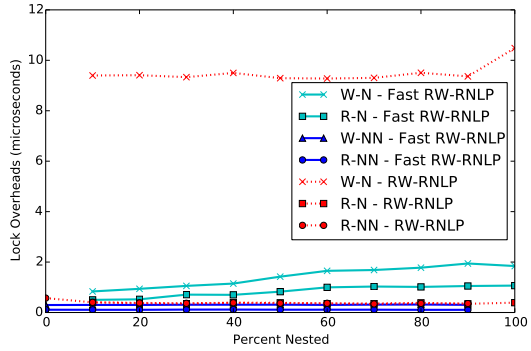

(a) Lock overhead.

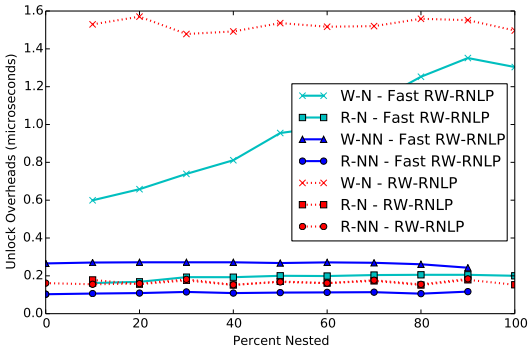

(b) Unlock overhead.

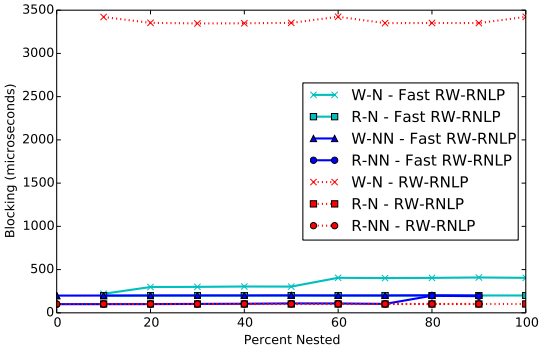

(c) Blocking.

Figure 398: (a) Lock and (b) unlock overheads and (c) blocking for nested and non-nested read and write requests under the RW-RNLP and the fast RW-RNLP. Here, for each request $\mathcal{R}_i$, $m = 18$, $L_i = 100\mu$s, $n_r = 64$, $|D_i| = 1$ for non-nested requests, and $|D_i| = 2$ for nested requests. Each request was randomly chosen to be a read (as opposed to a write) with probability 0.5 and to be a nested request with probability as shown. Due to write expansion, $|D_i|$ was inflated to 64 for all write requests under the RW-RNLP, as read requests can access any resource.

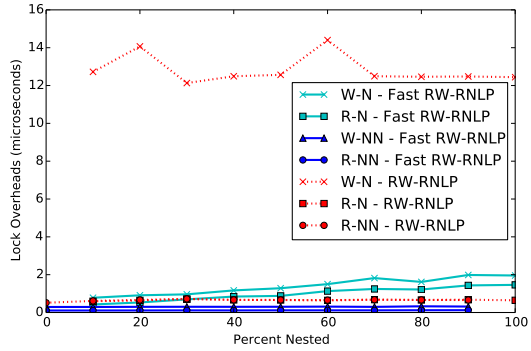

(a) Lock overhead.

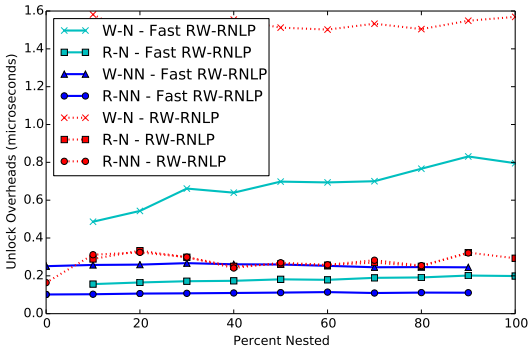

(b) Unlock overhead.

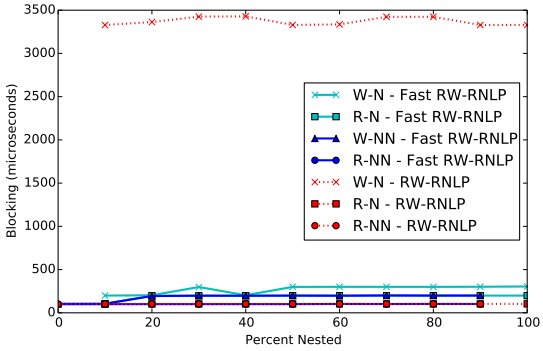

(c) Blocking.

Figure 399: (a) Lock and (b) unlock overheads and (c) blocking for nested and non-nested read and write requests under the RW-RNLP and the fast RW-RNLP. Here, for each request $\mathcal{R}_i$, $m = 18$, $L_i = 100\mu$s, $n_r = 64$, $|D_i| = 1$ for non-nested requests, and $|D_i| = 2$ for nested requests. Each request was randomly chosen to be a read (as opposed to a write) with probability 0.8 and to be a nested request with probability as shown. Due to write expansion, $|D_i|$ was inflated to 64 for all write requests under the RW-RNLP, as read requests can access any resource.

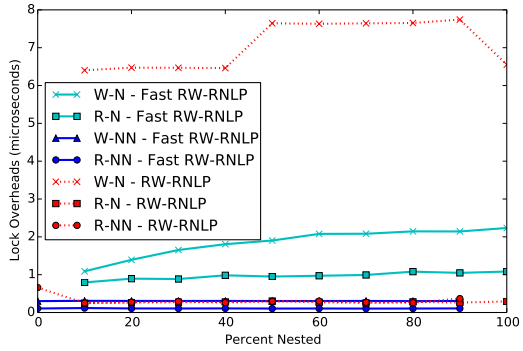

(a) Lock overhead.

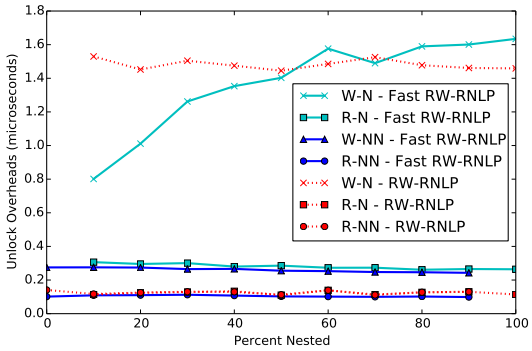

(b) Unlock overhead.

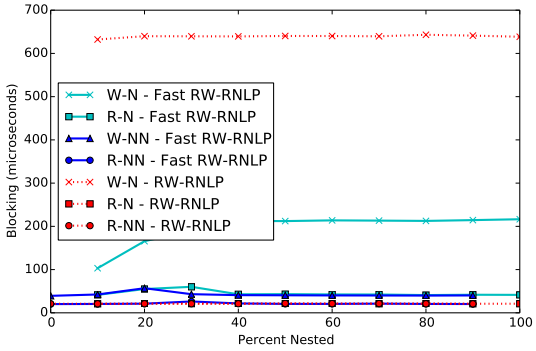

(c) Blocking.

Figure 400: (a) Lock and (b) unlock overheads and (c) blocking for nested and non-nested read and write requests under the RW-RNLP and the fast RW-RNLP. Here, for each request $\mathcal{R}_i$, $m = 18$, $L_i = 20\mu$s, $n_r = 64$, $|D_i| = 1$ for non-nested requests, and $|D_i| = 4$ for nested requests. Each request was randomly chosen to be a read (as opposed to a write) with probability 0.2 and to be a nested request with probability as shown. Due to write expansion, $|D_i|$ was inflated to 64 for all write requests under the RW-RNLP, as read requests can access any resource.

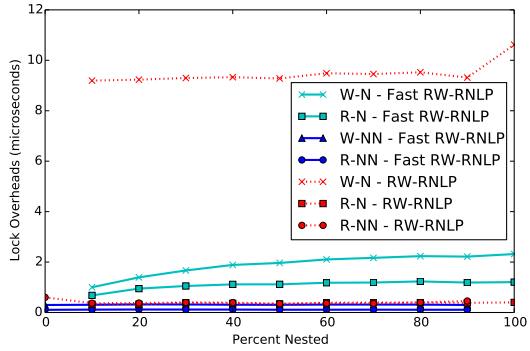

(a) Lock overhead.

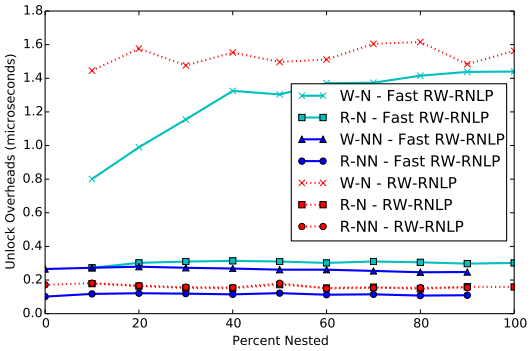

(b) Unlock overhead.

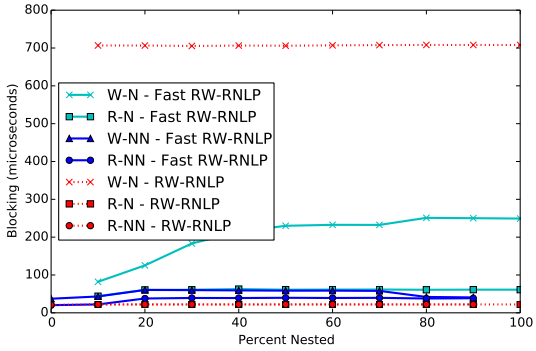

(c) Blocking.

Figure 401: (a) Lock and (b) unlock overheads and (c) blocking for nested and non-nested read and write requests under the RW-RNLP and the fast RW-RNLP. Here, for each request $\mathcal{R}_i$, $m = 18$, $L_i = 20\mu$s, $n_r = 64$, $|D_i| = 1$ for non-nested requests, and $|D_i| = 4$ for nested requests. Each request was randomly chosen to be a read (as opposed to a write) with probability 0.5 and to be a nested request with probability as shown. Due to write expansion, $|D_i|$ was inflated to 64 for all write requests under the RW-RNLP, as read requests can access any resource.

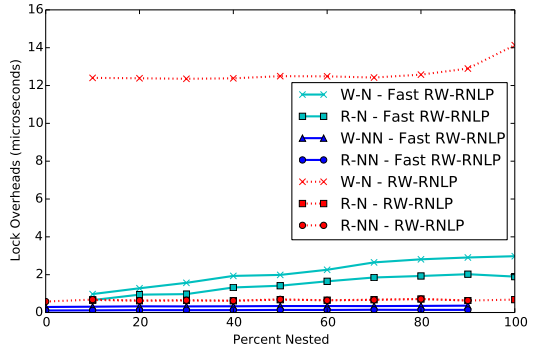

(a) Lock overhead.

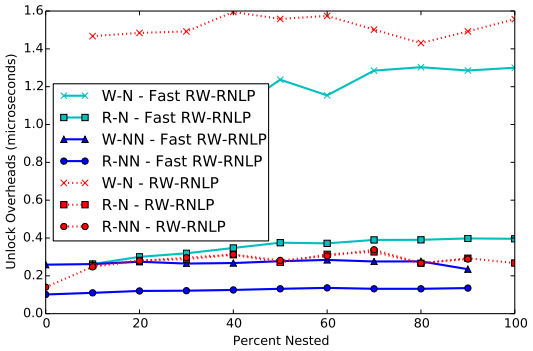

(b) Unlock overhead.

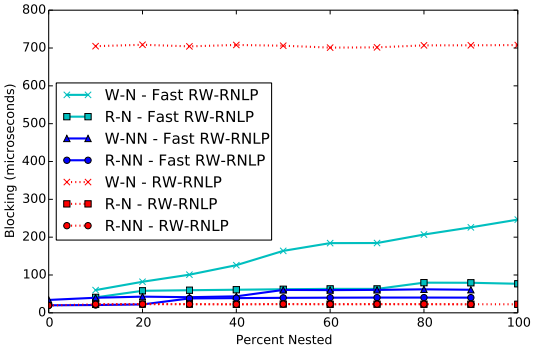

(c) Blocking.

Figure 402: (a) Lock and (b) unlock overheads and (c) blocking for nested and non-nested read and write requests under the RW-RNLP and the fast RW-RNLP. Here, for each request $\mathcal{R}_i$, $m = 18$, $L_i = 20\mu$s, $n_r = 64$, $|D_i| = 1$ for non-nested requests, and $|D_i| = 4$ for nested requests. Each request was randomly chosen to be a read (as opposed to a write) with probability 0.8 and to be a nested request with probability as shown. Due to write expansion, $|D_i|$ was inflated to 64 for all write requests under the RW-RNLP, as read requests can access any resource.

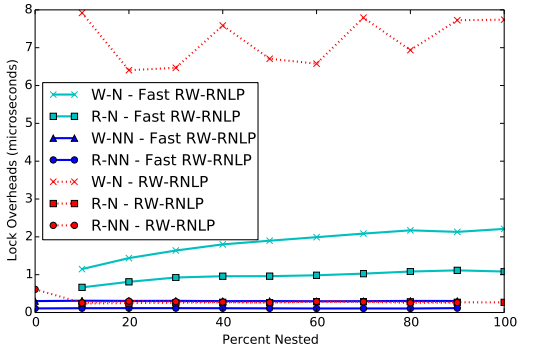

(a) Lock overhead.

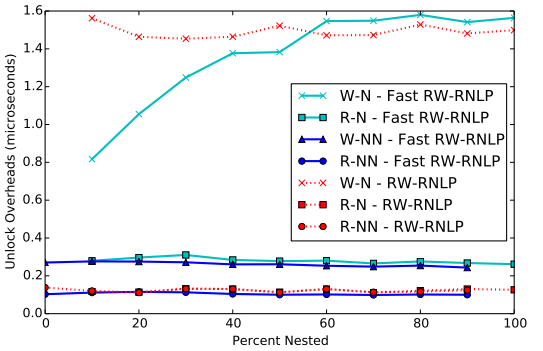

(b) Unlock overhead.

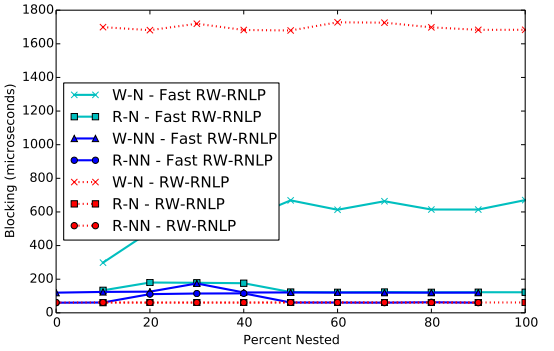

(c) Blocking.

Figure 403: (a) Lock and (b) unlock overheads and (c) blocking for nested and non-nested read and write requests under the RW-RNLP and the fast RW-RNLP. Here, for each request $\mathcal{R}_i$, $m = 18$, $L_i = 60\mu$s, $n_r = 64$, $|D_i| = 1$ for non-nested requests, and $|D_i| = 4$ for nested requests. Each request was randomly chosen to be a read (as opposed to a write) with probability 0.2 and to be a nested request with probability as shown. Due to write expansion, $|D_i|$ was inflated to 64 for all write requests under the RW-RNLP, as read requests can access any resource.

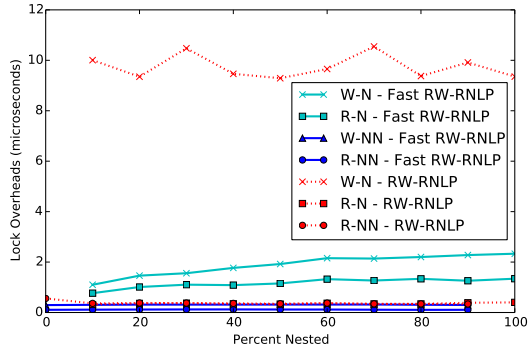

(a) Lock overhead.

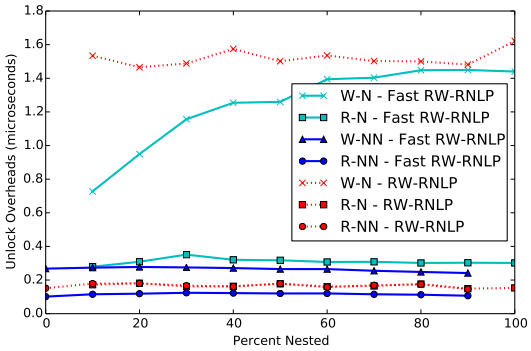

(b) Unlock overhead.

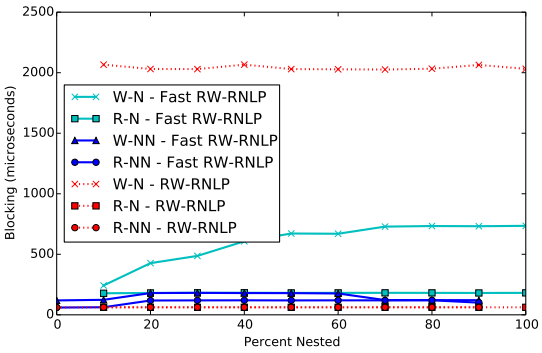

(c) Blocking.

Figure 404: (a) Lock and (b) unlock overheads and (c) blocking for nested and non-nested read and write requests under the RW-RNLP and the fast RW-RNLP. Here, for each request $\mathcal{R}_i$, $m = 18$, $L_i = 60\mu$s, $n_r = 64$, $|D_i| = 1$ for non-nested requests, and $|D_i| = 4$ for nested requests. Each request was randomly chosen to be a read (as opposed to a write) with probability 0.5 and to be a nested request with probability as shown. Due to write expansion, $|D_i|$ was inflated to 64 for all write requests under the RW-RNLP, as read requests can access any resource.

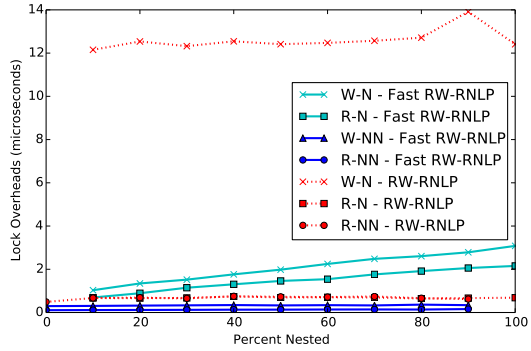

(a) Lock overhead.

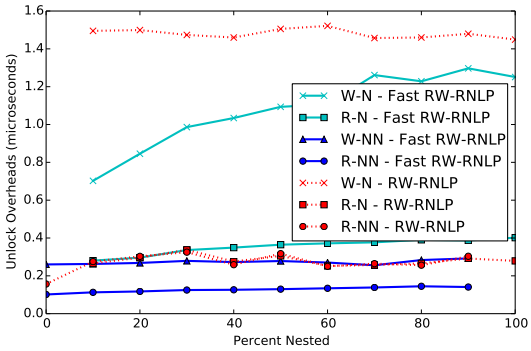

(b) Unlock overhead.

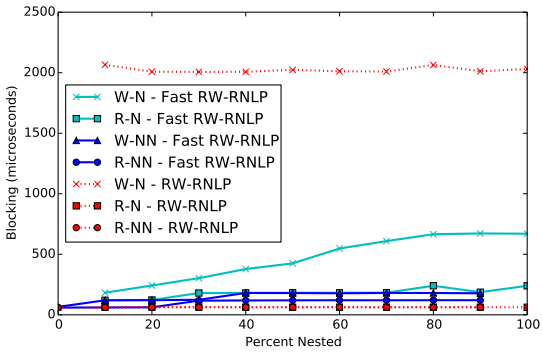

(c) Blocking.

Figure 405: (a) Lock and (b) unlock overheads and (c) blocking for nested and non-nested read and write requests under the RW-RNLP and the fast RW-RNLP. Here, for each request $\mathcal{R}_i$, $m = 18$, $L_i = 60\mu$s, $n_r = 64$, $|D_i| = 1$ for non-nested requests, and $|D_i| = 4$ for nested requests. Each request was randomly chosen to be a read (as opposed to a write) with probability 0.8 and to be a nested request with probability as shown. Due to write expansion, $|D_i|$ was inflated to 64 for all write requests under the RW-RNLP, as read requests can access any resource.

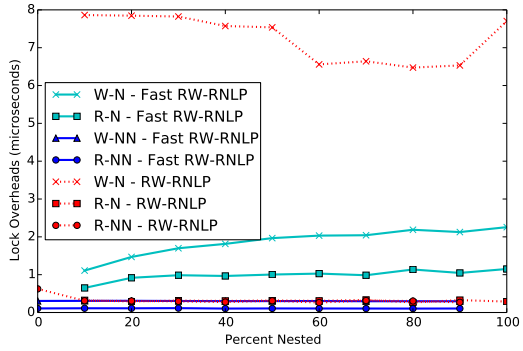

(a) Lock overhead.

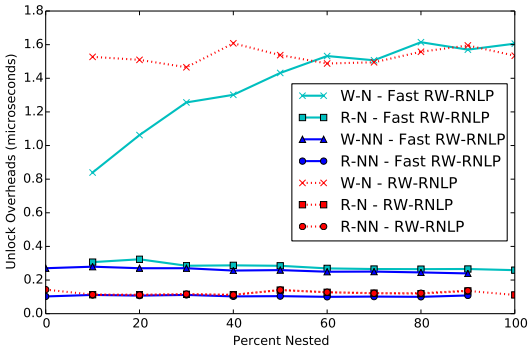

(b) Unlock overhead.

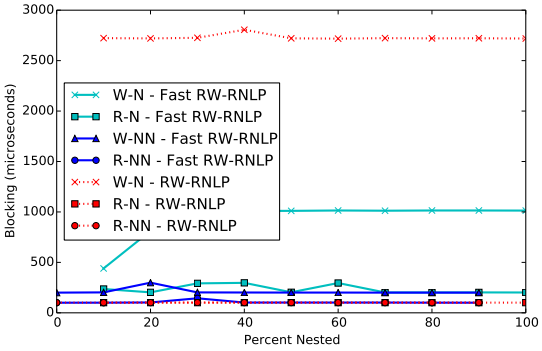

(c) Blocking.

Figure 406: (a) Lock and (b) unlock overheads and (c) blocking for nested and non-nested read and write requests under the RW-RNLP and the fast RW-RNLP. Here, for each request $\mathcal{R}_i$, $m = 18$, $L_i = 100\mu$s, $n_r = 64$, $|D_i| = 1$ for non-nested requests, and $|D_i| = 4$ for nested requests. Each request was randomly chosen to be a read (as opposed to a write) with probability 0.2 and to be a nested request with probability as shown. Due to write expansion, $|D_i|$ was inflated to 64 for all write requests under the RW-RNLP, as read requests can access any resource.

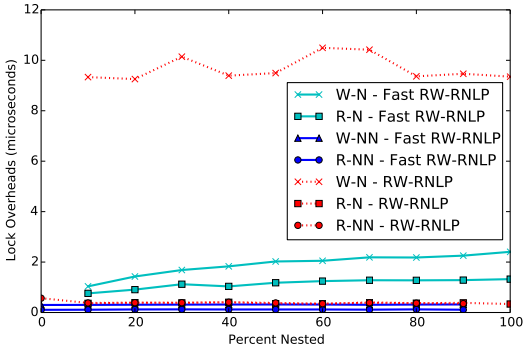

(a) Lock overhead.

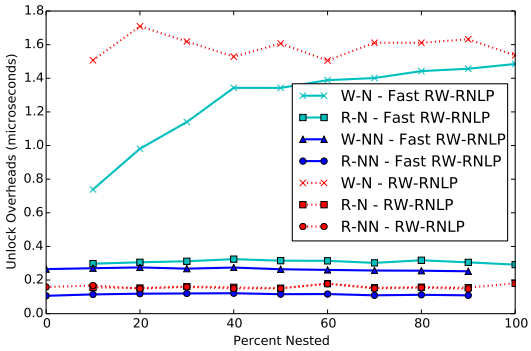

(b) Unlock overhead.

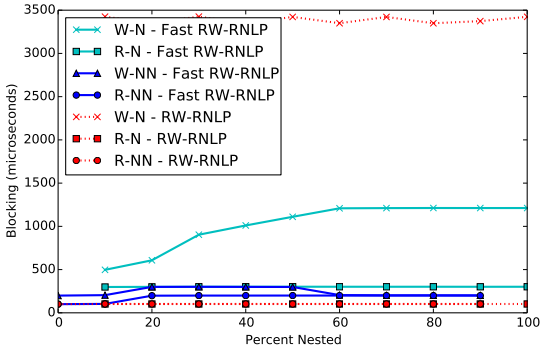

(c) Blocking.

Figure 407: (a) Lock and (b) unlock overheads and (c) blocking for nested and non-nested read and write requests under the RW-RNLP and the fast RW-RNLP. Here, for each request $\mathcal{R}_i$, $m = 18$, $L_i = 100\mu$s, $n_r = 64$, $|D_i| = 1$ for non-nested requests, and $|D_i| = 4$ for nested requests. Each request was randomly chosen to be a read (as opposed to a write) with probability 0.5 and to be a nested request with probability as shown. Due to write expansion, $|D_i|$ was inflated to 64 for all write requests under the RW-RNLP, as read requests can access any resource.

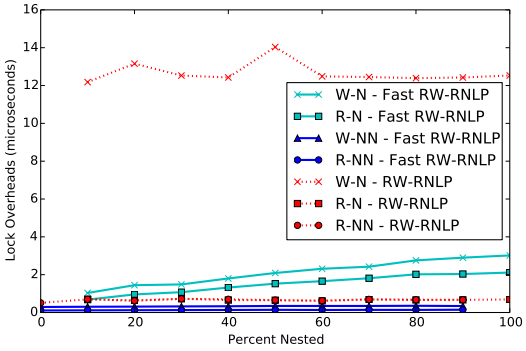

(a) Lock overhead.

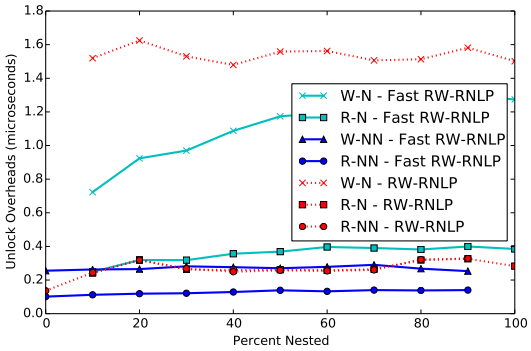

(b) Unlock overhead.

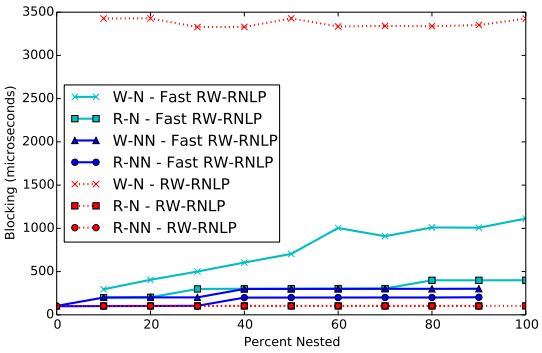

(c) Blocking.

Figure 408: (a) Lock and (b) unlock overheads and (c) blocking for nested and non-nested read and write requests under the RW-RNLP and the fast RW-RNLP. Here, for each request $\mathcal{R}_i$, $m = 18$, $L_i = 100\mu$s, $n_r = 64$, $|D_i| = 1$ for non-nested requests, and $|D_i| = 4$ for nested requests. Each request was randomly chosen to be a read (as opposed to a write) with probability 0.8 and to be a nested request with probability as shown. Due to write expansion, $|D_i|$ was inflated to 64 for all write requests under the RW-RNLP, as read requests can access any resource.

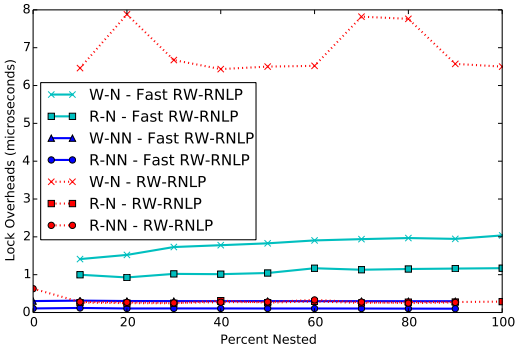

(a) Lock overhead.

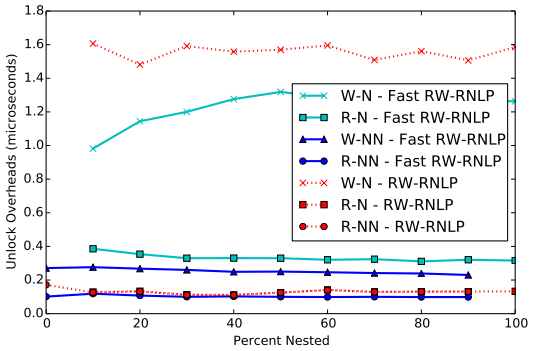

(b) Unlock overhead.

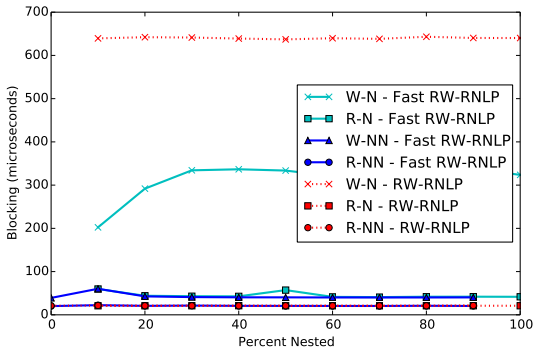

(c) Blocking.

Figure 409: (a) Lock and (b) unlock overheads and (c) blocking for nested and non-nested read and write requests under the RW-RNLP and the fast RW-RNLP. Here, for each request $\mathcal{R}_i$, $m = 18$, $L_i = 20\mu$s, $n_r = 64$, $|D_i| = 1$ for non-nested requests, and $|D_i| = 6$ for nested requests. Each request was randomly chosen to be a read (as opposed to a write) with probability 0.2 and to be a nested request with probability as shown. Due to write expansion, $|D_i|$ was inflated to 64 for all write requests under the RW-RNLP, as read requests can access any resource.

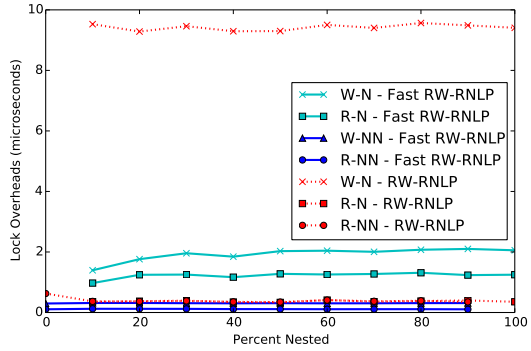

(a) Lock overhead.

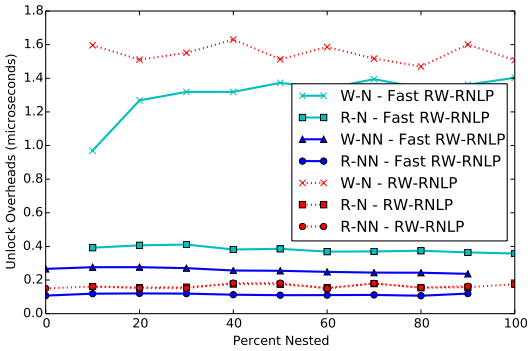

(b) Unlock overhead.

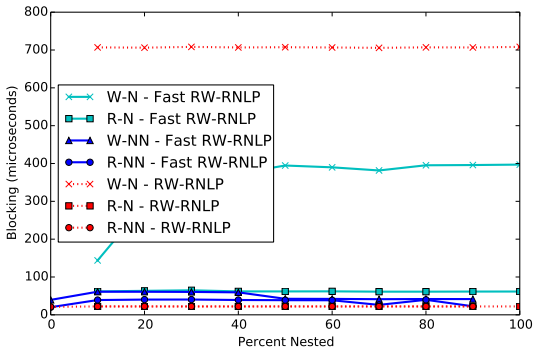

(c) Blocking.

Figure 410: (a) Lock and (b) unlock overheads and (c) blocking for nested and non-nested read and write requests under the RW-RNLP and the fast RW-RNLP. Here, for each request $\mathcal{R}_i$, $m = 18$, $L_i = 20\mu$s, $n_r = 64$, $|D_i| = 1$ for non-nested requests, and $|D_i| = 6$ for nested requests. Each request was randomly chosen to be a read (as opposed to a write) with probability 0.5 and to be a nested request with probability as shown. Due to write expansion, $|D_i|$ was inflated to 64 for all write requests under the RW-RNLP, as read requests can access any resource.

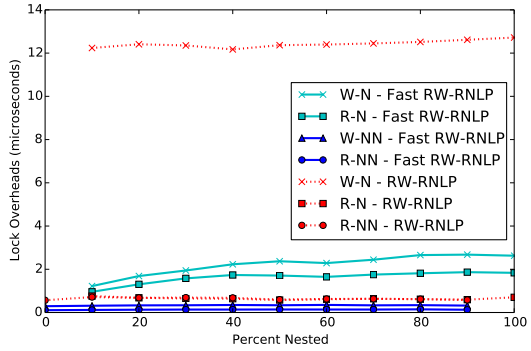

(a) Lock overhead.

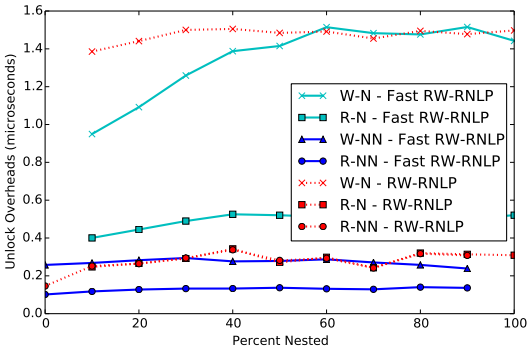

(b) Unlock overhead.

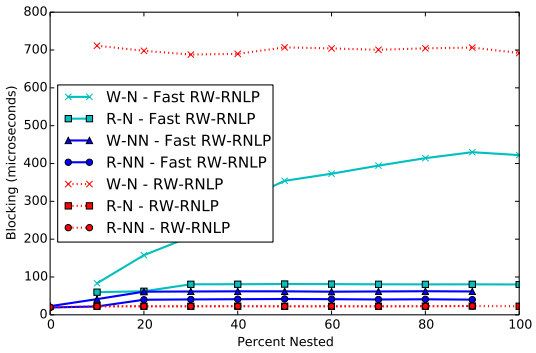

(c) Blocking.

Figure 411: (a) Lock and (b) unlock overheads and (c) blocking for nested and non-nested read and write requests under the RW-RNLP and the fast RW-RNLP. Here, for each request $\mathcal{R}_i$, $m = 18$, $L_i = 20\mu$s, $n_r = 64$, $|D_i| = 1$ for non-nested requests, and $|D_i| = 6$ for nested requests. Each request was randomly chosen to be a read (as opposed to a write) with probability 0.8 and to be a nested request with probability as shown. Due to write expansion, $|D_i|$ was inflated to 64 for all write requests under the RW-RNLP, as read requests can access any resource.

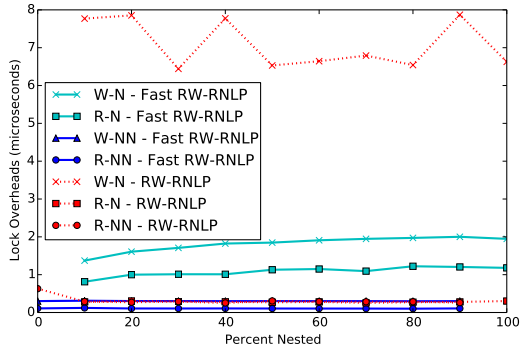

(a) Lock overhead.

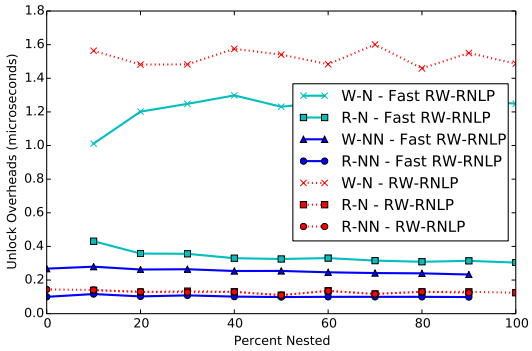

(b) Unlock overhead.

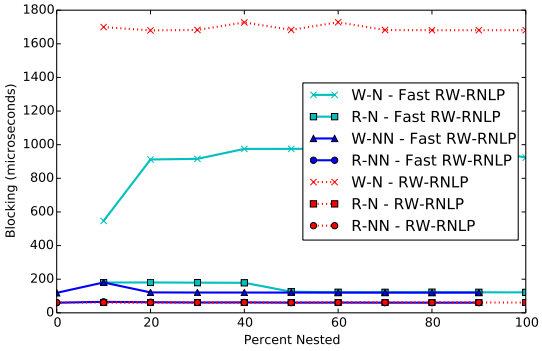

(c) Blocking.

Figure 412: (a) Lock and (b) unlock overheads and (c) blocking for nested and non-nested read and write requests under the RW-RNLP and the fast RW-RNLP. Here, for each request $\mathcal{R}_i$, $m = 18$, $L_i = 60\mu$s, $n_r = 64$, $|D_i| = 1$ for non-nested requests, and $|D_i| = 6$ for nested requests. Each request was randomly chosen to be a read (as opposed to a write) with probability 0.2 and to be a nested request with probability as shown. Due to write expansion, $|D_i|$ was inflated to 64 for all write requests under the RW-RNLP, as read requests can access any resource.

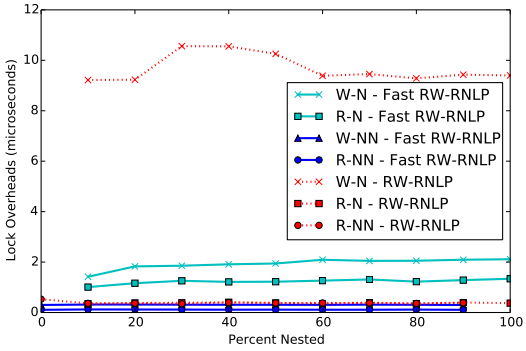

(a) Lock overhead.

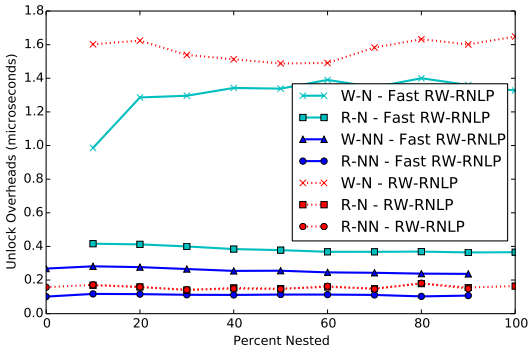

(b) Unlock overhead.

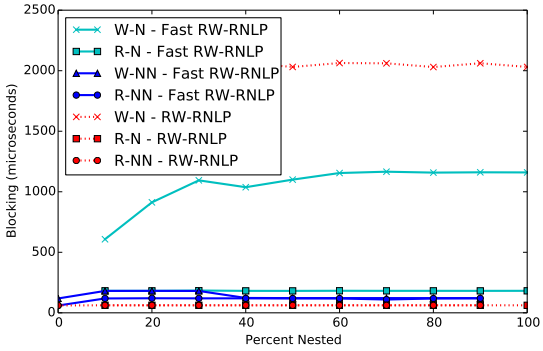

(c) Blocking.

Figure 413: (a) Lock and (b) unlock overheads and (c) blocking for nested and non-nested read and write requests under the RW-RNLP and the fast RW-RNLP. Here, for each request $\mathcal{R}_i$, $m = 18$, $L_i = 60\mu$s, $n_r = 64$, $|D_i| = 1$ for non-nested requests, and $|D_i| = 6$ for nested requests. Each request was randomly chosen to be a read (as opposed to a write) with probability 0.5 and to be a nested request with probability as shown. Due to write expansion, $|D_i|$ was inflated to 64 for all write requests under the RW-RNLP, as read requests can access any resource.

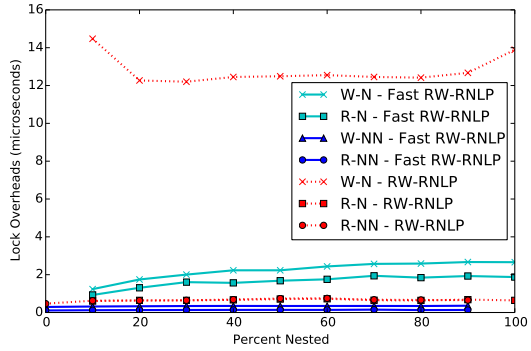

(a) Lock overhead.

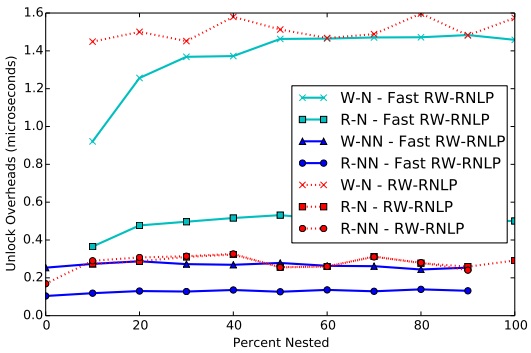

(b) Unlock overhead.

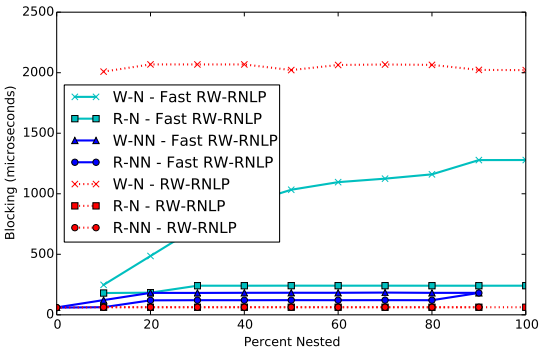

(c) Blocking.

Figure 414: (a) Lock and (b) unlock overheads and (c) blocking for nested and non-nested read and write requests under the RW-RNLP and the fast RW-RNLP. Here, for each request $\mathcal{R}_i$, $m = 18$, $L_i = 60\mu$s, $n_r = 64$, $|D_i| = 1$ for non-nested requests, and $|D_i| = 6$ for nested requests. Each request was randomly chosen to be a read (as opposed to a write) with probability 0.8 and to be a nested request with probability as shown. Due to write expansion, $|D_i|$ was inflated to 64 for all write requests under the RW-RNLP, as read requests can access any resource.

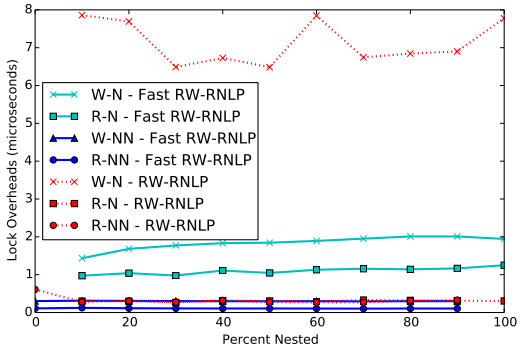

(a) Lock overhead.

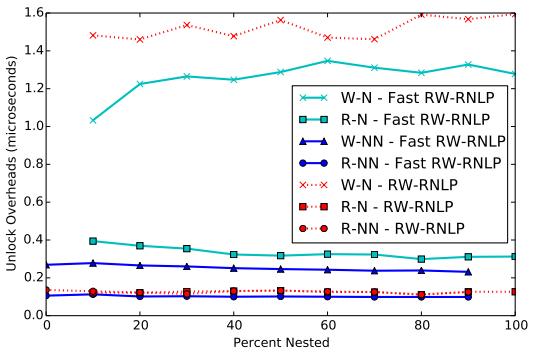

(b) Unlock overhead.

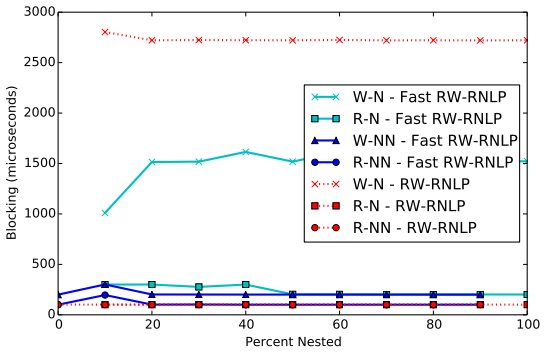

(c) Blocking.

Figure 415: (a) Lock and (b) unlock overheads and (c) blocking for nested and non-nested read and write requests under the RW-RNLP and the fast RW-RNLP. Here, for each request $\mathcal{R}_i$, $m = 18$, $L_i = 100\mu$s, $n_r = 64$, $|D_i| = 1$ for non-nested requests, and $|D_i| = 6$ for nested requests. Each request was randomly chosen to be a read (as opposed to a write) with probability 0.2 and to be a nested request with probability as shown. Due to write expansion, $|D_i|$ was inflated to 64 for all write requests under the RW-RNLP, as read requests can access any resource.

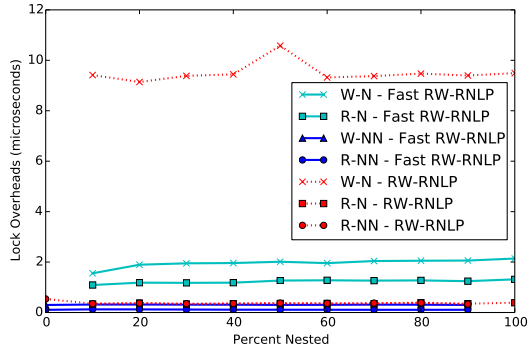

(a) Lock overhead.

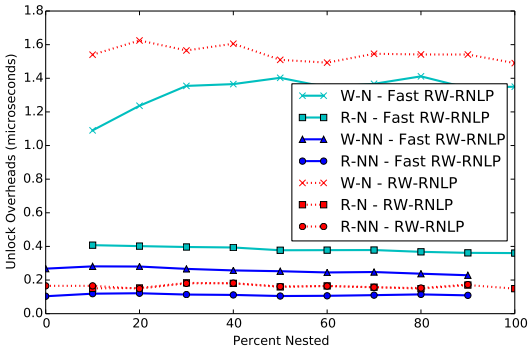

(b) Unlock overhead.

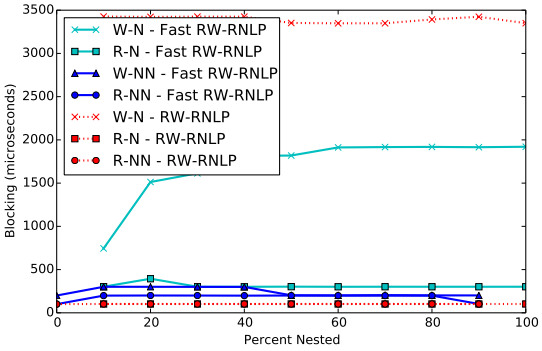

(c) Blocking.

Figure 416: (a) Lock and (b) unlock overheads and (c) blocking for nested and non-nested read and write requests under the RW-RNLP and the fast RW-RNLP. Here, for each request $\mathcal{R}_i$, $m = 18$, $L_i = 100\mu$s, $n_r = 64$, $|D_i| = 1$ for non-nested requests, and $|D_i| = 6$ for nested requests. Each request was randomly chosen to be a read (as opposed to a write) with probability 0.5 and to be a nested request with probability as shown. Due to write expansion, $|D_i|$ was inflated to 64 for all write requests under the RW-RNLP, as read requests can access any resource.

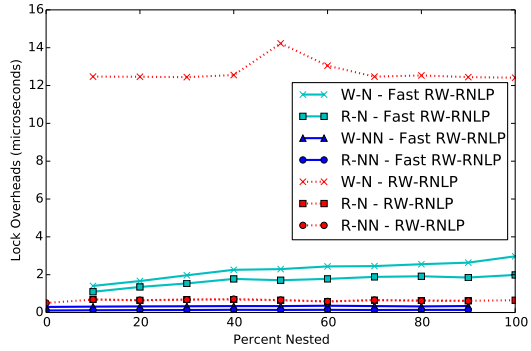

(a) Lock overhead.

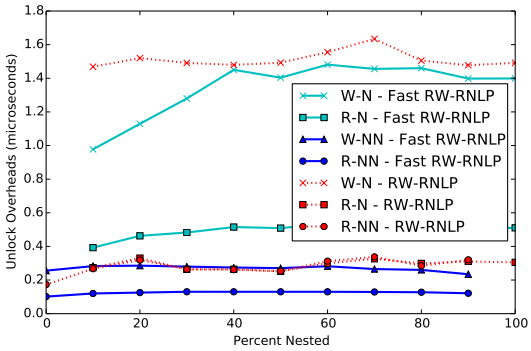

(b) Unlock overhead.

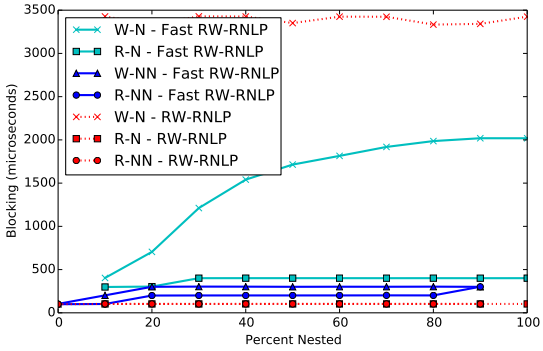

(c) Blocking.

Figure 417: (a) Lock and (b) unlock overheads and (c) blocking for nested and non-nested read and write requests under the RW-RNLP and the fast RW-RNLP. Here, for each request $\mathcal{R}_i$, $m = 18$, $L_i = 100\mu$s, $n_r = 64$, $|D_i| = 1$ for non-nested requests, and $|D_i| = 6$ for nested requests. Each request was randomly chosen to be a read (as opposed to a write) with probability 0.8 and to be a nested request with probability as shown. Due to write expansion, $|D_i|$ was inflated to 64 for all write requests under the RW-RNLP, as read requests can access any resource.

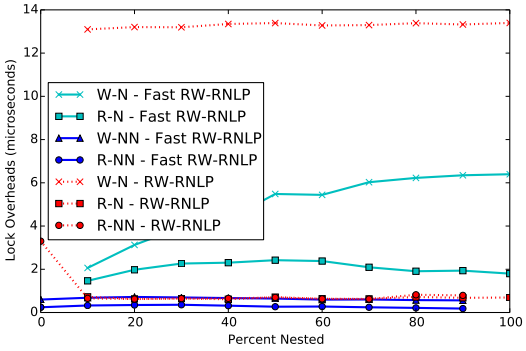

(a) Lock overhead.

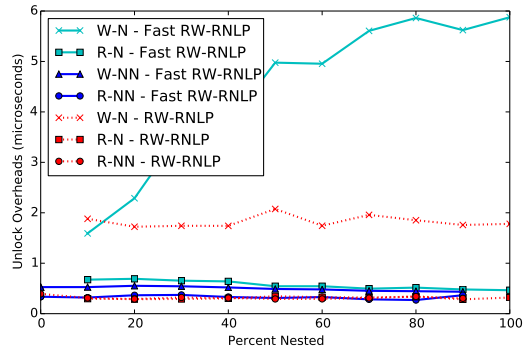

(b) Unlock overhead.

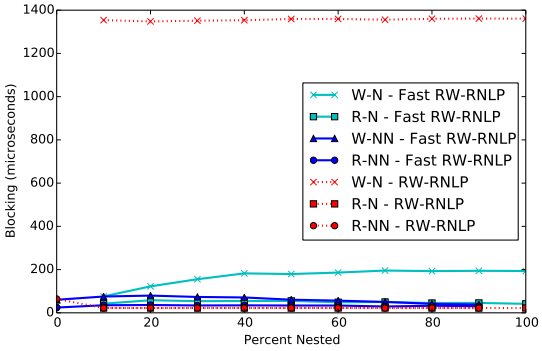

(c) Blocking.

Figure 418: (a) Lock and (b) unlock overheads and (c) blocking for nested and non-nested read and write requests under the RW-RNLP and the fast RW-RNLP. Here, for each request $\mathcal{R}_i$, $m = 36$, $L_i = 20\mu$s, $n_r = 64$, $|D_i| = 1$ for non-nested requests, and $|D_i| = 2$ for nested requests. Each request was randomly chosen to be a read (as opposed to a write) with probability 0.2 and to be a nested request with probability as shown. Due to write expansion, $|D_i|$ was inflated to 64 for all write requests under the RW-RNLP, as read requests can access any resource.

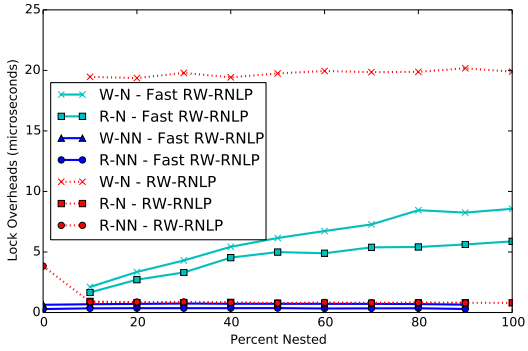

(a) Lock overhead.

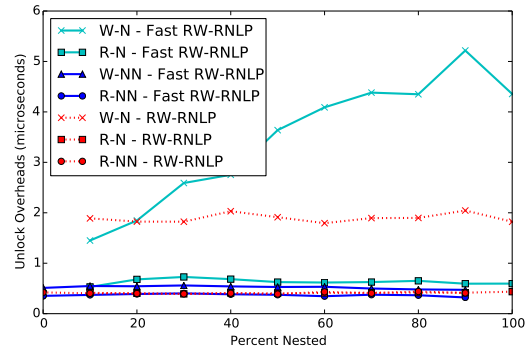

(b) Unlock overhead.

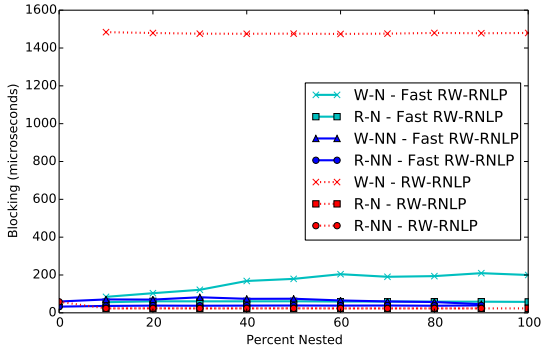

(c) Blocking.

Figure 419: (a) Lock and (b) unlock overheads and (c) blocking for nested and non-nested read and write requests under the RW-RNLP and the fast RW-RNLP. Here, for each request $\mathcal{R}_i$, $m = 36$, $L_i = 20\mu$s, $n_r = 64$, $|D_i| = 1$ for non-nested requests, and $|D_i| = 2$ for nested requests. Each request was randomly chosen to be a read (as opposed to a write) with probability 0.5 and to be a nested request with probability as shown. Due to write expansion, $|D_i|$ was inflated to 64 for all write requests under the RW-RNLP, as read requests can access any resource.

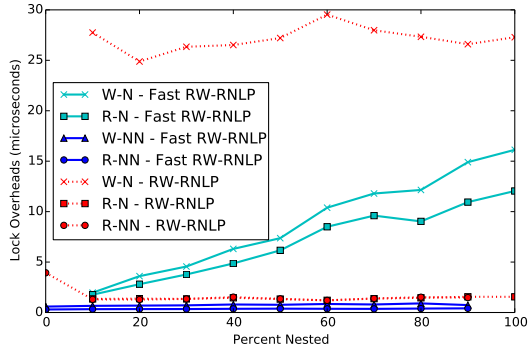

(a) Lock overhead.

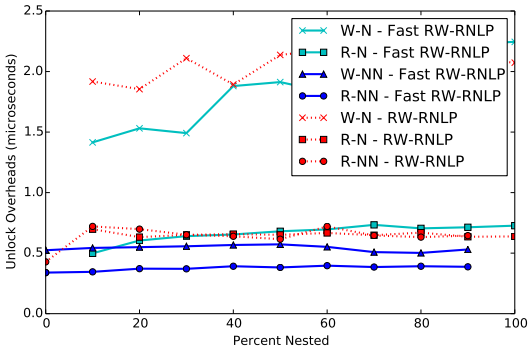

(b) Unlock overhead.

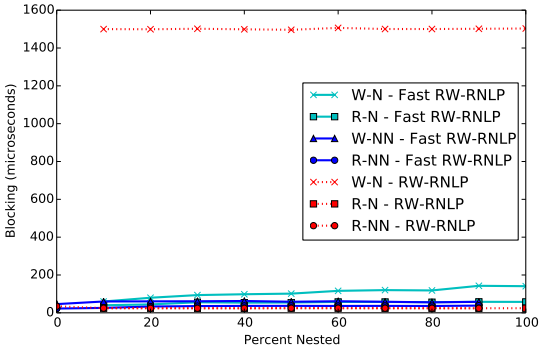

(c) Blocking.

Figure 420: (a) Lock and (b) unlock overheads and (c) blocking for nested and non-nested read and write requests under the RW-RNLP and the fast RW-RNLP. Here, for each request $\mathcal{R}_i$, $m = 36$, $L_i = 20\mu$s, $n_r = 64$, $|D_i| = 1$ for non-nested requests, and $|D_i| = 2$ for nested requests. Each request was randomly chosen to be a read (as opposed to a write) with probability 0.8 and to be a nested request with probability as shown. Due to write expansion, $|D_i|$ was inflated to 64 for all write requests under the RW-RNLP, as read requests can access any resource.

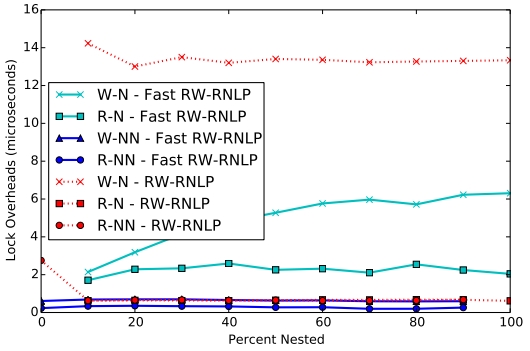

(a) Lock overhead.

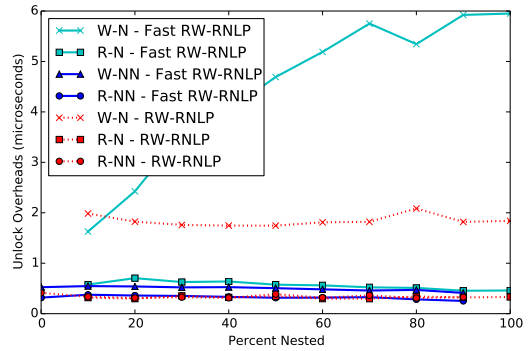

(b) Unlock overhead.

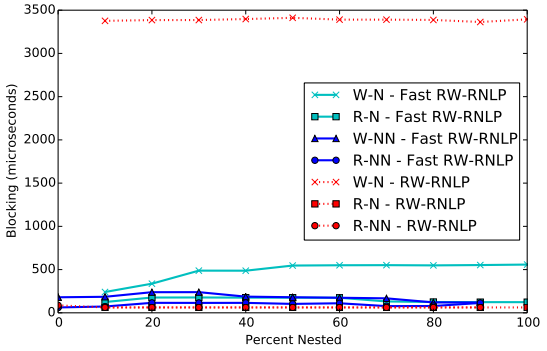

(c) Blocking.

Figure 421: (a) Lock and (b) unlock overheads and (c) blocking for nested and non-nested read and write requests under the RW-RNLP and the fast RW-RNLP. Here, for each request $\mathcal{R}_i$, $m = 36$, $L_i = 60\mu$s, $n_r = 64$, $|D_i| = 1$ for non-nested requests, and $|D_i| = 2$ for nested requests. Each request was randomly chosen to be a read (as opposed to a write) with probability 0.2 and to be a nested request with probability as shown. Due to write expansion, $|D_i|$ was inflated to 64 for all write requests under the RW-RNLP, as read requests can access any resource.

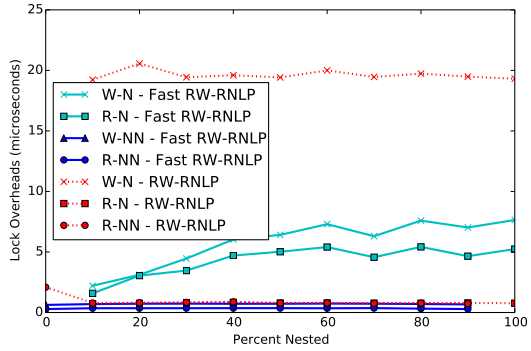

(a) Lock overhead.

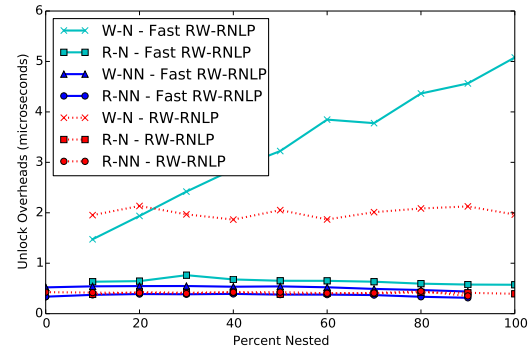

(b) Unlock overhead.

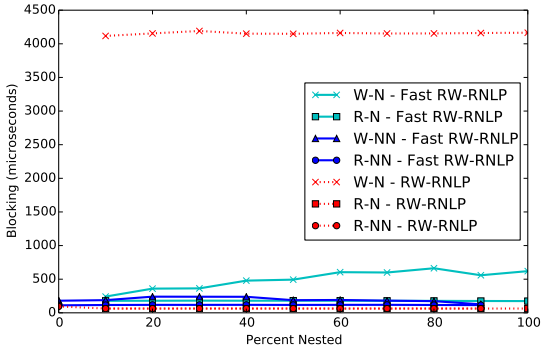

(c) Blocking.

Figure 422: (a) Lock and (b) unlock overheads and (c) blocking for nested and non-nested read and write requests under the RW-RNLP and the fast RW-RNLP. Here, for each request $\mathcal{R}_i$, $m = 36$, $L_i = 60\mu$s, $n_r = 64$, $|D_i| = 1$ for non-nested requests, and $|D_i| = 2$ for nested requests. Each request was randomly chosen to be a read (as opposed to a write) with probability 0.5 and to be a nested request with probability as shown. Due to write expansion, $|D_i|$ was inflated to 64 for all write requests under the RW-RNLP, as read requests can access any resource.

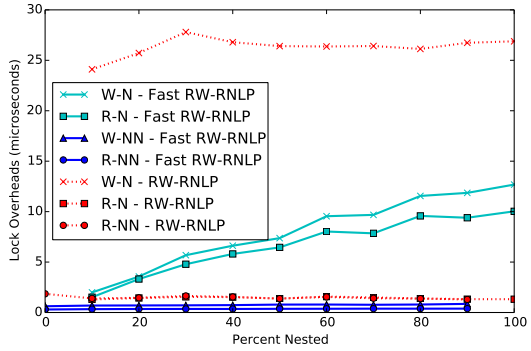

(a) Lock overhead.

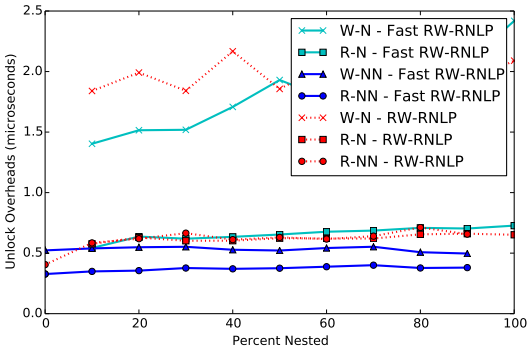

(b) Unlock overhead.

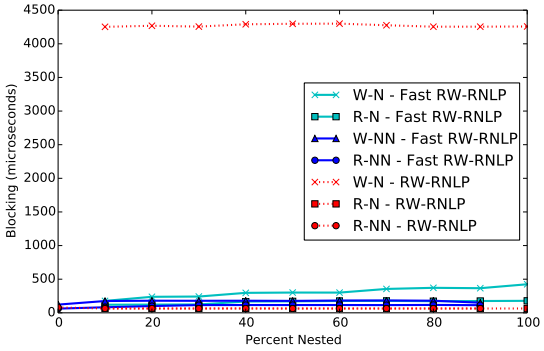

(c) Blocking.

Figure 423: (a) Lock and (b) unlock overheads and (c) blocking for nested and non-nested read and write requests under the RW-RNLP and the fast RW-RNLP. Here, for each request $\mathcal{R}_i$, $m = 36$, $L_i = 60\mu$s, $n_r = 64$, $|D_i| = 1$ for non-nested requests, and $|D_i| = 2$ for nested requests. Each request was randomly chosen to be a read (as opposed to a write) with probability 0.8 and to be a nested request with probability as shown. Due to write expansion, $|D_i|$ was inflated to 64 for all write requests under the RW-RNLP, as read requests can access any resource.

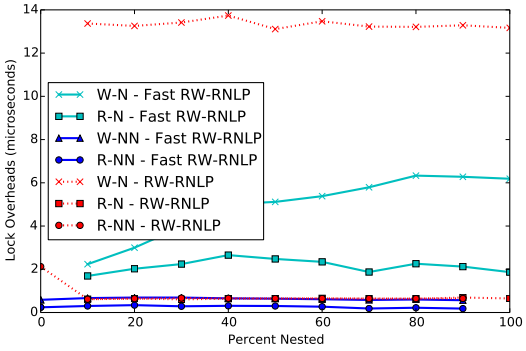

(a) Lock overhead.

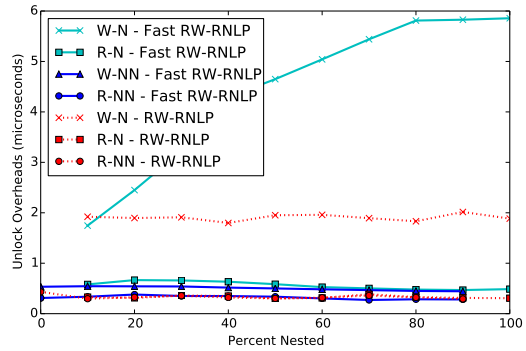

(b) Unlock overhead.

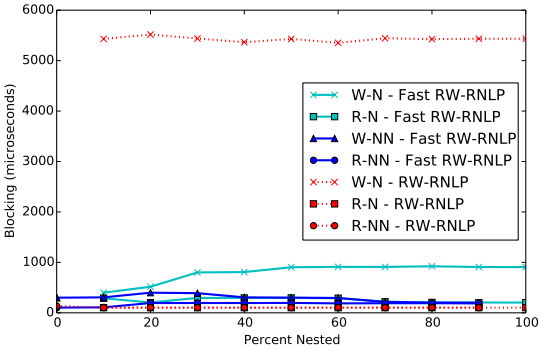

(c) Blocking.

Figure 424: (a) Lock and (b) unlock overheads and (c) blocking for nested and non-nested read and write requests under the RW-RNLP and the fast RW-RNLP. Here, for each request $\mathcal{R}_i$, $m = 36$, $L_i = 100\mu$s, $n_r = 64$, $|D_i| = 1$ for non-nested requests, and $|D_i| = 2$ for nested requests. Each request was randomly chosen to be a read (as opposed to a write) with probability 0.2 and to be a nested request with probability as shown. Due to write expansion, $|D_i|$ was inflated to 64 for all write requests under the RW-RNLP, as read requests can access any resource.

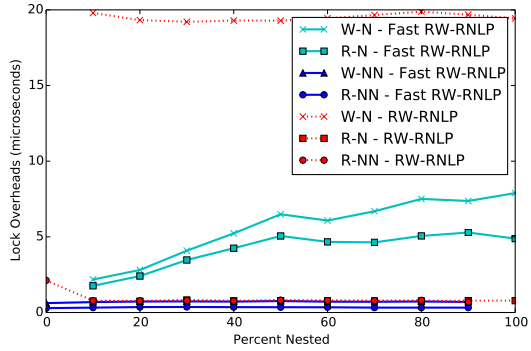

(a) Lock overhead.

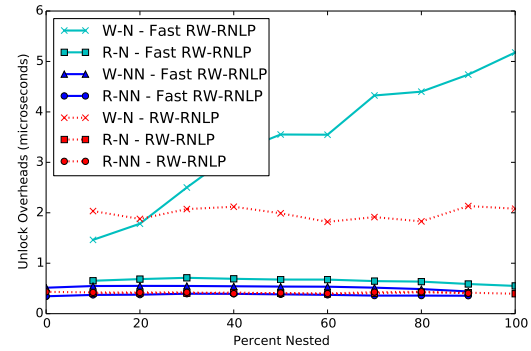

(b) Unlock overhead.

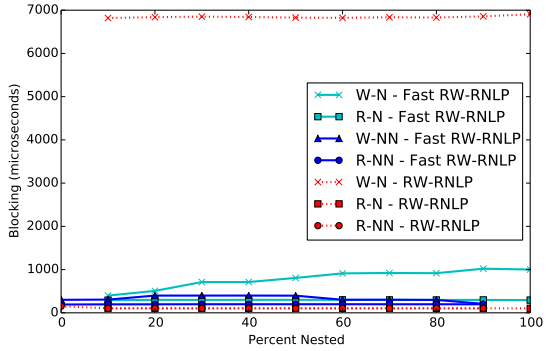

(c) Blocking.

Figure 425: (a) Lock and (b) unlock overheads and (c) blocking for nested and non-nested read and write requests under the RW-RNLP and the fast RW-RNLP. Here, for each request $\mathcal{R}_i$, $m = 36$, $L_i = 100\mu$s, $n_r = 64$, $|D_i| = 1$ for non-nested requests, and $|D_i| = 2$ for nested requests. Each request was randomly chosen to be a read (as opposed to a write) with probability 0.5 and to be a nested request with probability as shown. Due to write expansion, $|D_i|$ was inflated to 64 for all write requests under the RW-RNLP, as read requests can access any resource.

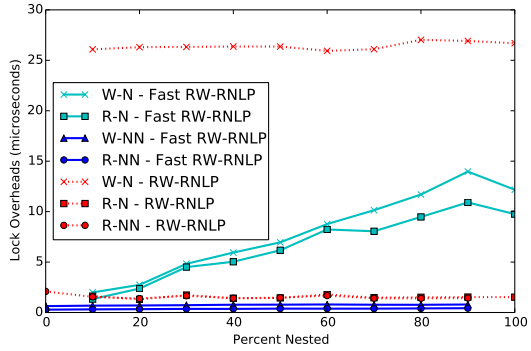

(a) Lock overhead.

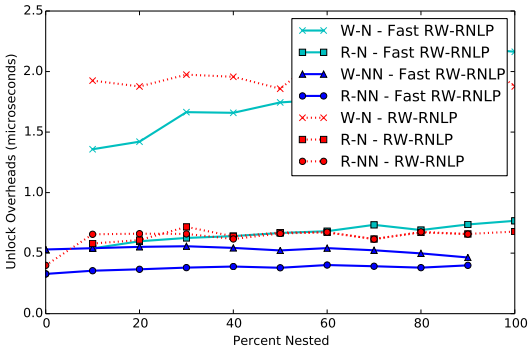

(b) Unlock overhead.

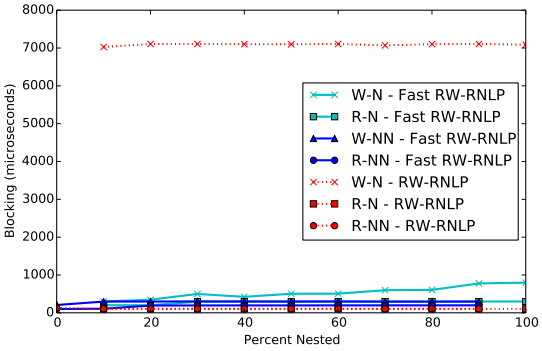

(c) Blocking.

Figure 426: (a) Lock and (b) unlock overheads and (c) blocking for nested and non-nested read and write requests under the RW-RNLP and the fast RW-RNLP. Here, for each request $\mathcal{R}_i$, $m = 36$, $L_i = 100\mu$s, $n_r = 64$, $|D_i| = 1$ for non-nested requests, and $|D_i| = 2$ for nested requests. Each request was randomly chosen to be a read (as opposed to a write) with probability 0.8 and to be a nested request with probability as shown. Due to write expansion, $|D_i|$ was inflated to 64 for all write requests under the RW-RNLP, as read requests can access any resource.

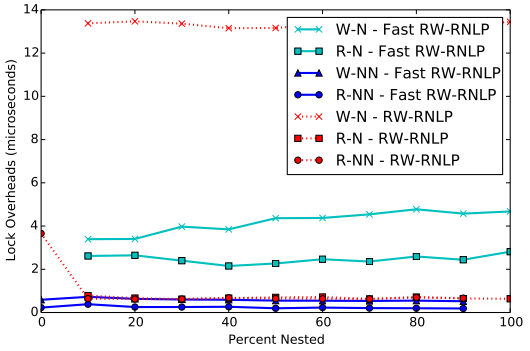

(a) Lock overhead.

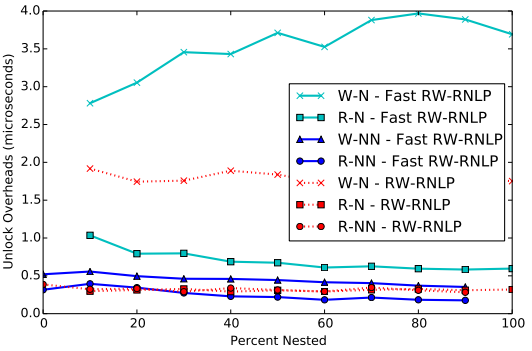

(b) Unlock overhead.

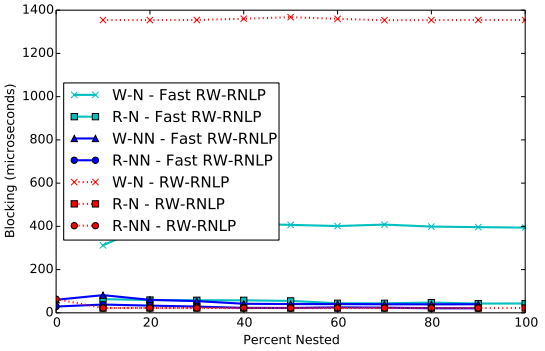

(c) Blocking.

Figure 427: (a) Lock and (b) unlock overheads and (c) blocking for nested and non-nested read and write requests under the RW-RNLP and the fast RW-RNLP. Here, for each request $\mathcal{R}_i$, $m = 36$, $L_i = 20\mu$s, $n_r = 64$, $|D_i| = 1$ for non-nested requests, and $|D_i| = 4$ for nested requests. Each request was randomly chosen to be a read (as opposed to a write) with probability 0.2 and to be a nested request with probability as shown. Due to write expansion, $|D_i|$ was inflated to 64 for all write requests under the RW-RNLP, as read requests can access any resource.

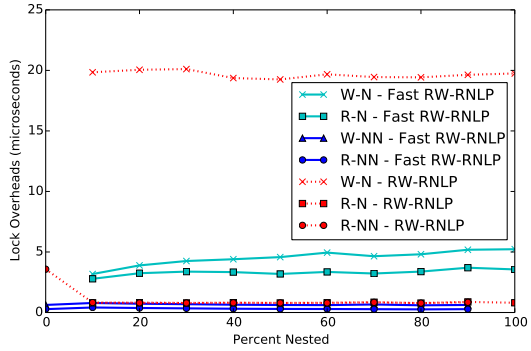

(a) Lock overhead.

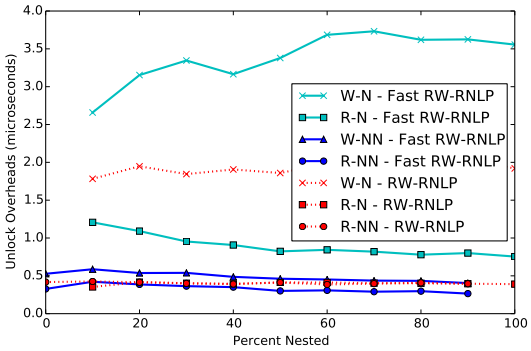

(b) Unlock overhead.

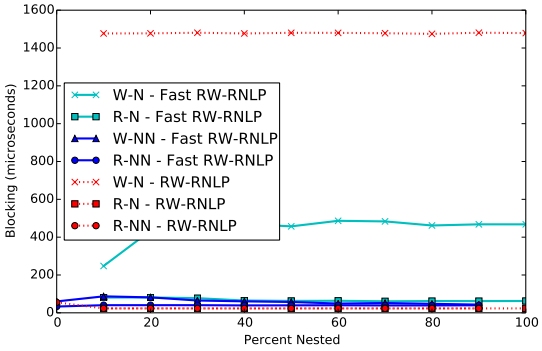

(c) Blocking.

Figure 428: (a) Lock and (b) unlock overheads and (c) blocking for nested and non-nested read and write requests under the RW-RNLP and the fast RW-RNLP. Here, for each request $\mathcal{R}_i$, $m = 36$, $L_i = 20\mu$s, $n_r = 64$, $|D_i| = 1$ for non-nested requests, and $|D_i| = 4$ for nested requests. Each request was randomly chosen to be a read (as opposed to a write) with probability 0.5 and to be a nested request with probability as shown. Due to write expansion, $|D_i|$ was inflated to 64 for all write requests under the RW-RNLP, as read requests can access any resource.

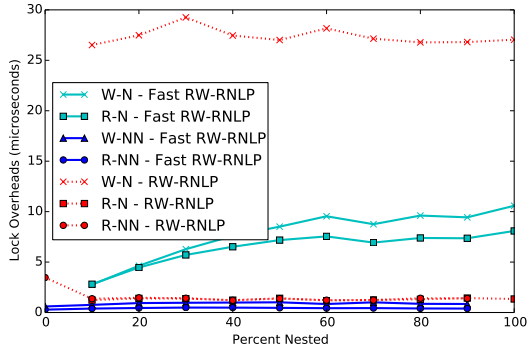

(a) Lock overhead.

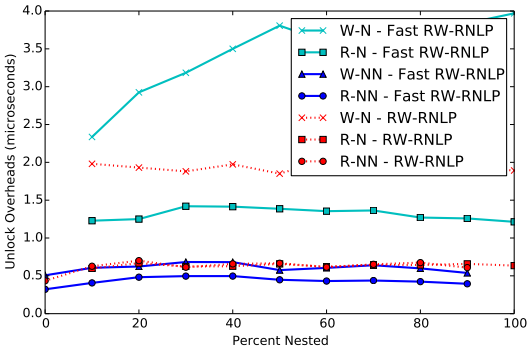

(b) Unlock overhead.

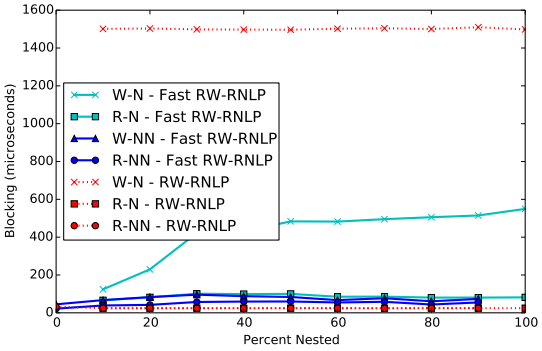

(c) Blocking.

Figure 429: (a) Lock and (b) unlock overheads and (c) blocking for nested and non-nested read and write requests under the RW-RNLP and the fast RW-RNLP. Here, for each request $\mathcal{R}_i$, $m = 36$, $L_i = 20\mu$s, $n_r = 64$, $|D_i| = 1$ for non-nested requests, and $|D_i| = 4$ for nested requests. Each request was randomly chosen to be a read (as opposed to a write) with probability 0.8 and to be a nested request with probability as shown. Due to write expansion, $|D_i|$ was inflated to 64 for all write requests under the RW-RNLP, as read requests can access any resource.

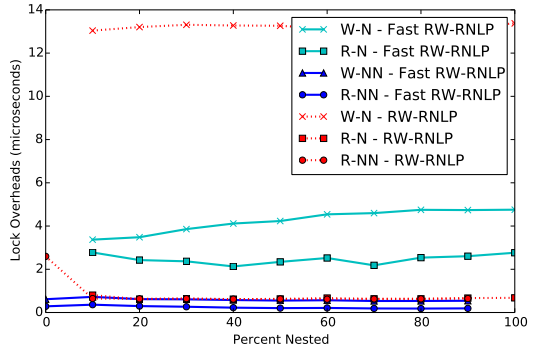

(a) Lock overhead.

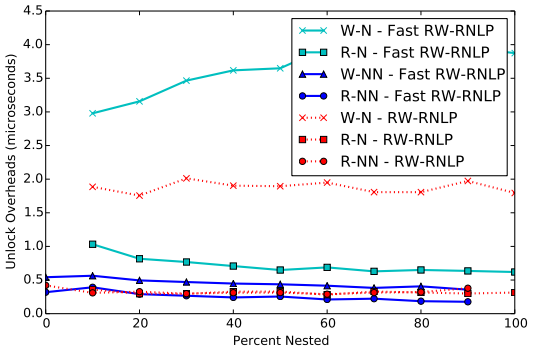

(b) Unlock overhead.

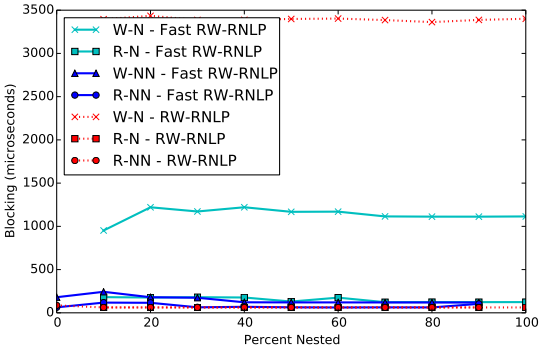

(c) Blocking.

Figure 430: (a) Lock and (b) unlock overheads and (c) blocking for nested and non-nested read and write requests under the RW-RNLP and the fast RW-RNLP. Here, for each request $\mathcal{R}_i$, $m = 36$, $L_i = 60\mu$s, $n_r = 64$, $|D_i| = 1$ for non-nested requests, and $|D_i| = 4$ for nested requests. Each request was randomly chosen to be a read (as opposed to a write) with probability 0.2 and to be a nested request with probability as shown. Due to write expansion, $|D_i|$ was inflated to 64 for all write requests under the RW-RNLP, as read requests can access any resource.

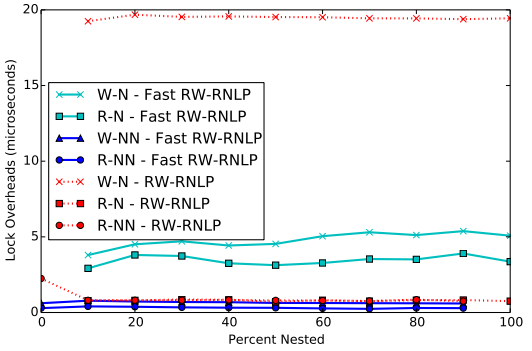

(a) Lock overhead.

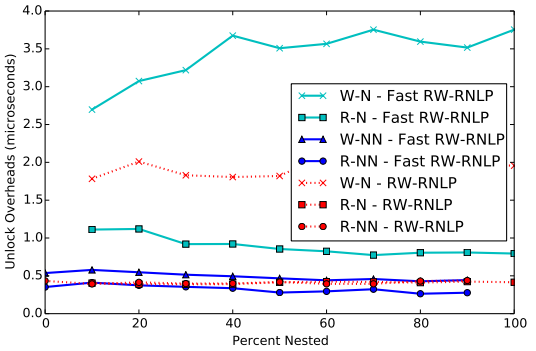

(b) Unlock overhead.

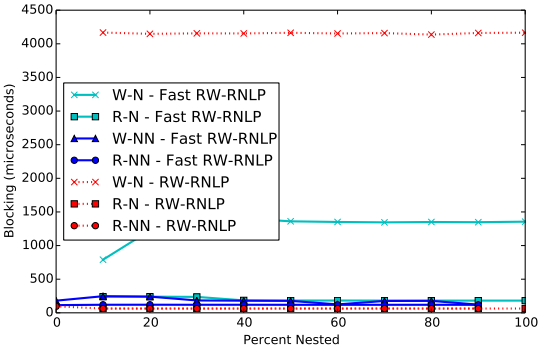

(c) Blocking.

Figure 431: (a) Lock and (b) unlock overheads and (c) blocking for nested and non-nested read and write requests under the RW-RNLP and the fast RW-RNLP. Here, for each request $\mathcal{R}_i$, $m = 36$, $L_i = 60\mu$s, $n_r = 64$, $|D_i| = 1$ for non-nested requests, and $|D_i| = 4$ for nested requests. Each request was randomly chosen to be a read (as opposed to a write) with probability 0.5 and to be a nested request with probability as shown. Due to write expansion, $|D_i|$ was inflated to 64 for all write requests under the RW-RNLP, as read requests can access any resource.

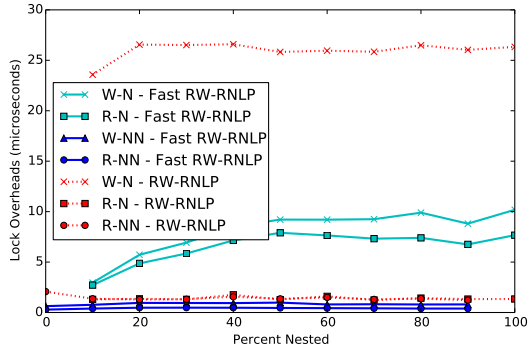

(a) Lock overhead.

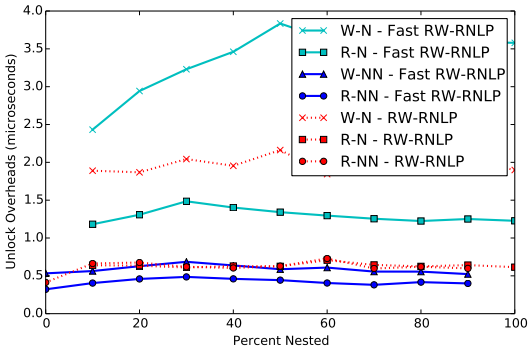

(b) Unlock overhead.

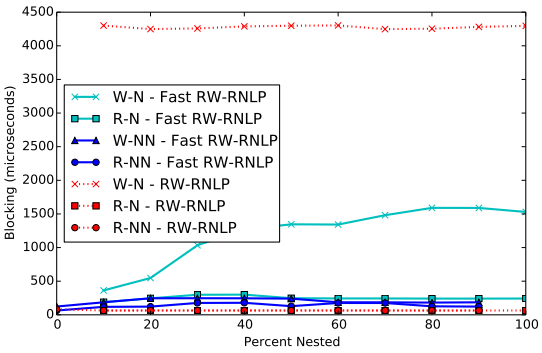

(c) Blocking.

Figure 432: (a) Lock and (b) unlock overheads and (c) blocking for nested and non-nested read and write requests under the RW-RNLP and the fast RW-RNLP. Here, for each request $\mathcal{R}_i$, $m = 36$, $L_i = 60\mu$s, $n_r = 64$, $|D_i| = 1$ for non-nested requests, and $|D_i| = 4$ for nested requests. Each request was randomly chosen to be a read (as opposed to a write) with probability 0.8 and to be a nested request with probability as shown. Due to write expansion, $|D_i|$ was inflated to 64 for all write requests under the RW-RNLP, as read requests can access any resource.

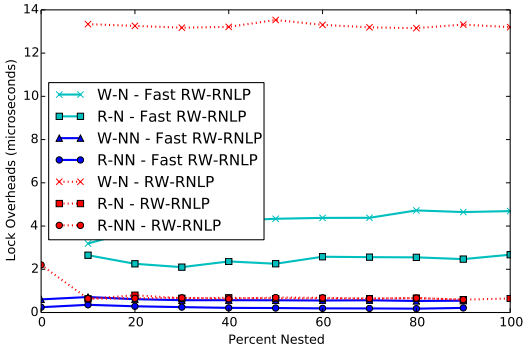

(a) Lock overhead.

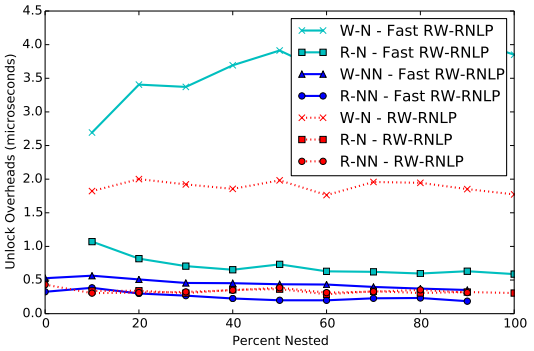

(b) Unlock overhead.

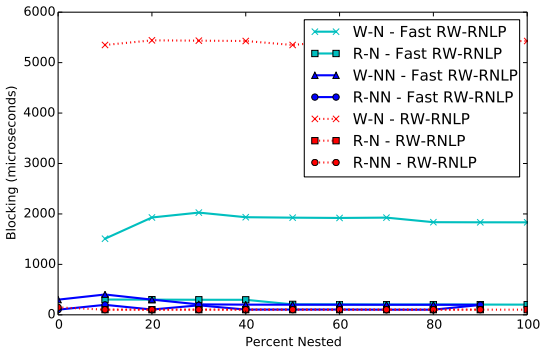

(c) Blocking.

Figure 433: (a) Lock and (b) unlock overheads and (c) blocking for nested and non-nested read and write requests under the RW-RNLP and the fast RW-RNLP. Here, for each request $\mathcal{R}_i$, $m = 36$, $L_i = 100\mu$s, $n_r = 64$, $|D_i| = 1$ for non-nested requests, and $|D_i| = 4$ for nested requests. Each request was randomly chosen to be a read (as opposed to a write) with probability 0.2 and to be a nested request with probability as shown. Due to write expansion, $|D_i|$ was inflated to 64 for all write requests under the RW-RNLP, as read requests can access any resource.

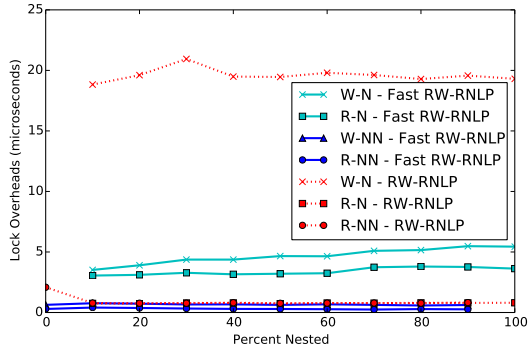

(a) Lock overhead.

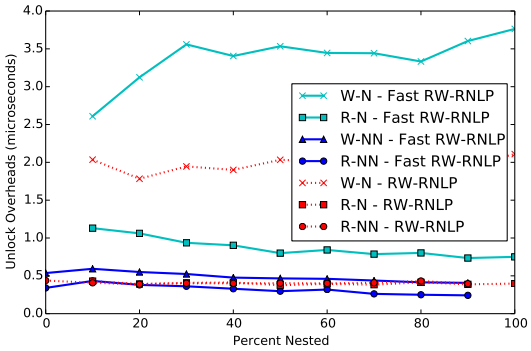

(b) Unlock overhead.

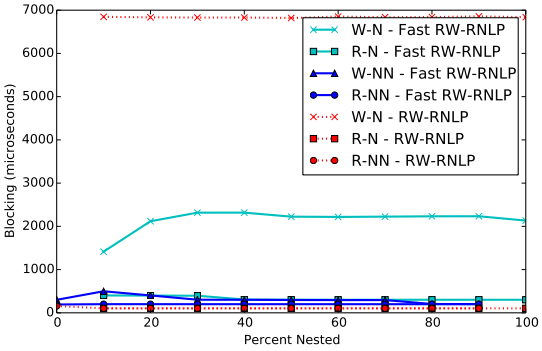

(c) Blocking.

Figure 434: (a) Lock and (b) unlock overheads and (c) blocking for nested and non-nested read and write requests under the RW-RNLP and the fast RW-RNLP. Here, for each request $\mathcal{R}_i$, $m = 36$, $L_i = 100\mu$s, $n_r = 64$, $|D_i| = 1$ for non-nested requests, and $|D_i| = 4$ for nested requests. Each request was randomly chosen to be a read (as opposed to a write) with probability 0.5 and to be a nested request with probability as shown. Due to write expansion, $|D_i|$ was inflated to 64 for all write requests under the RW-RNLP, as read requests can access any resource.

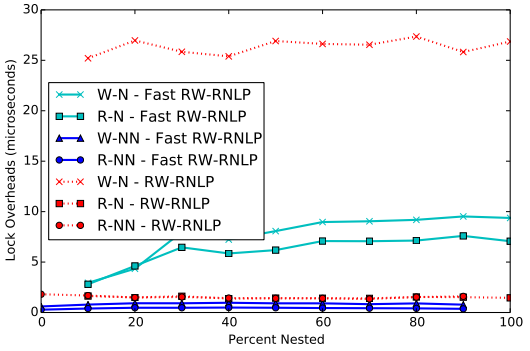

(a) Lock overhead.

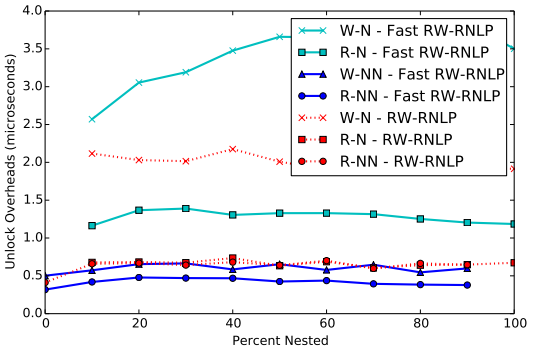

(b) Unlock overhead.

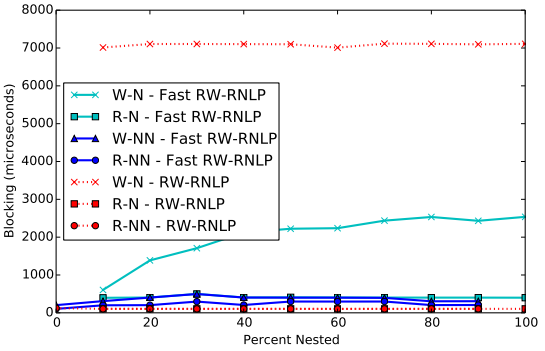

(c) Blocking.

Figure 435: (a) Lock and (b) unlock overheads and (c) blocking for nested and non-nested read and write requests under the RW-RNLP and the fast RW-RNLP. Here, for each request $\mathcal{R}_i$, $m = 36$, $L_i = 100\mu$s, $n_r = 64$, $|D_i| = 1$ for non-nested requests, and $|D_i| = 4$ for nested requests. Each request was randomly chosen to be a read (as opposed to a write) with probability 0.8 and to be a nested request with probability as shown. Due to write expansion, $|D_i|$ was inflated to 64 for all write requests under the RW-RNLP, as read requests can access any resource.

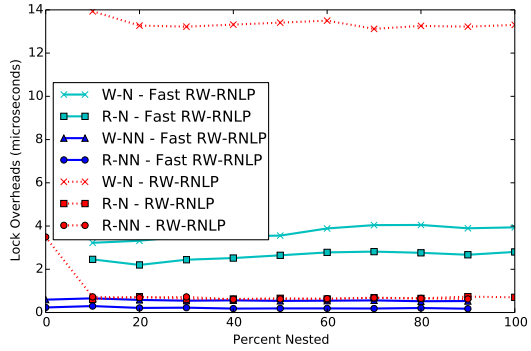

(a) Lock overhead.

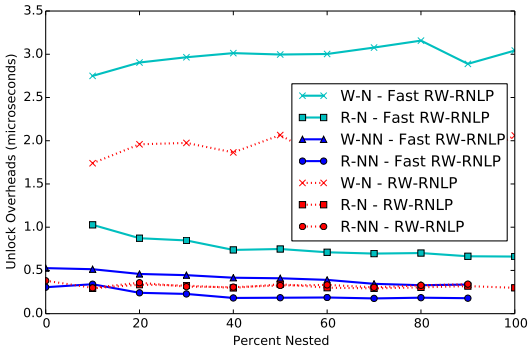

(b) Unlock overhead.

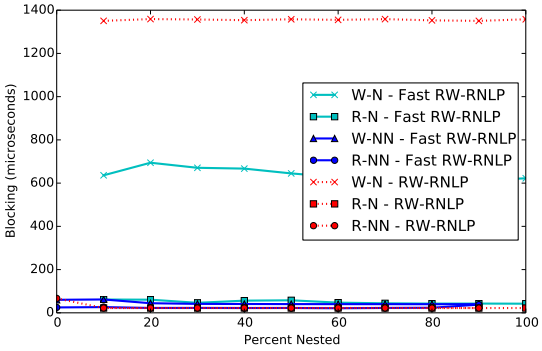

(c) Blocking.

Figure 436: (a) Lock and (b) unlock overheads and (c) blocking for nested and non-nested read and write requests under the RW-RNLP and the fast RW-RNLP. Here, for each request $\mathcal{R}_i$, $m = 36$, $L_i = 20\mu$s, $n_r = 64$, $|D_i| = 1$ for non-nested requests, and $|D_i| = 6$ for nested requests. Each request was randomly chosen to be a read (as opposed to a write) with probability 0.2 and to be a nested request with probability as shown. Due to write expansion, $|D_i|$ was inflated to 64 for all write requests under the RW-RNLP, as read requests can access any resource.

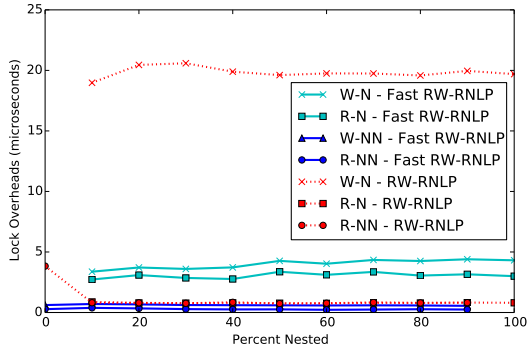

(a) Lock overhead.

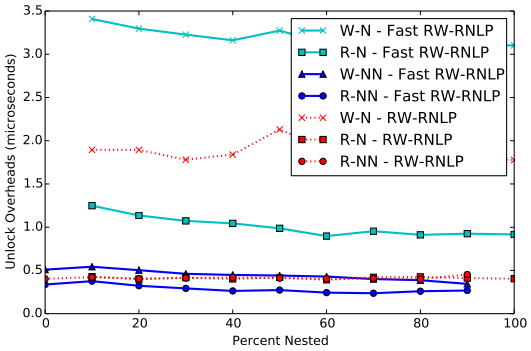

(b) Unlock overhead.

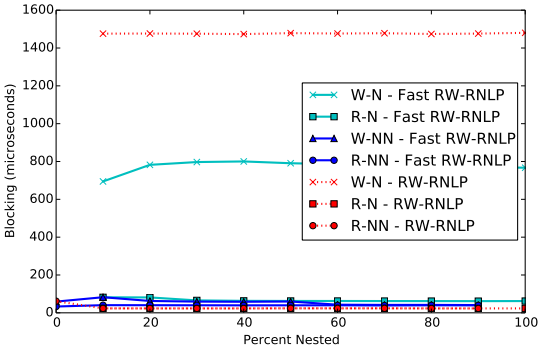

(c) Blocking.

Figure 437: (a) Lock and (b) unlock overheads and (c) blocking for nested and non-nested read and write requests under the RW-RNLP and the fast RW-RNLP. Here, for each request $\mathcal{R}_i$, $m = 36$, $L_i = 20\mu$s, $n_r = 64$, $|D_i| = 1$ for non-nested requests, and $|D_i| = 6$ for nested requests. Each request was randomly chosen to be a read (as opposed to a write) with probability 0.5 and to be a nested request with probability as shown. Due to write expansion, $|D_i|$ was inflated to 64 for all write requests under the RW-RNLP, as read requests can access any resource.

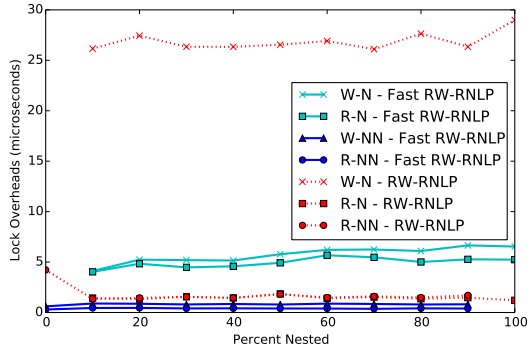

(a) Lock overhead.

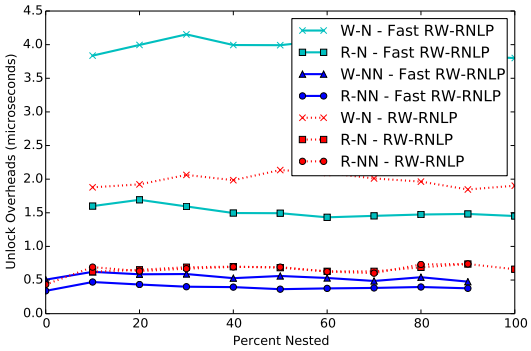

(b) Unlock overhead.

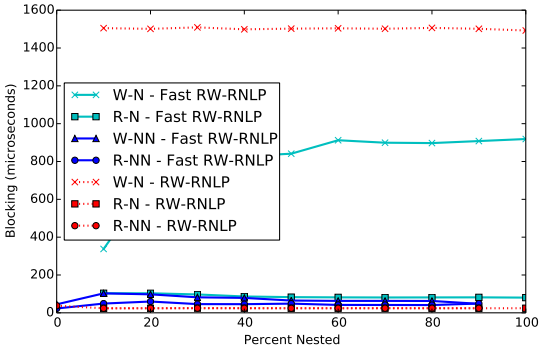

(c) Blocking.

Figure 438: (a) Lock and (b) unlock overheads and (c) blocking for nested and non-nested read and write requests under the RW-RNLP and the fast RW-RNLP. Here, for each request $\mathcal{R}_i$, $m = 36$, $L_i = 20\mu$s, $n_r = 64$, $|D_i| = 1$ for non-nested requests, and $|D_i| = 6$ for nested requests. Each request was randomly chosen to be a read (as opposed to a write) with probability 0.8 and to be a nested request with probability as shown. Due to write expansion, $|D_i|$ was inflated to 64 for all write requests under the RW-RNLP, as read requests can access any resource.

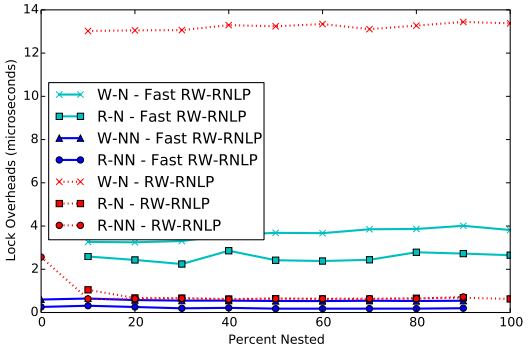

(a) Lock overhead.

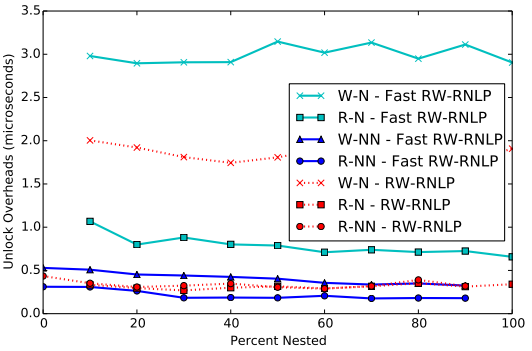

(b) Unlock overhead.

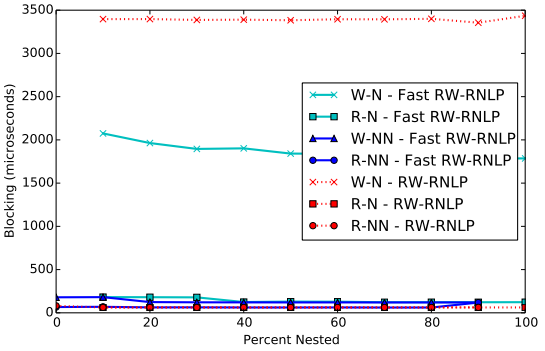

(c) Blocking.

Figure 439: (a) Lock and (b) unlock overheads and (c) blocking for nested and non-nested read and write requests under the RW-RNLP and the fast RW-RNLP. Here, for each request $\mathcal{R}_i$, $m = 36$, $L_i = 60\mu$s, $n_r = 64$, $|D_i| = 1$ for non-nested requests, and $|D_i| = 6$ for nested requests. Each request was randomly chosen to be a read (as opposed to a write) with probability 0.2 and to be a nested request with probability as shown. Due to write expansion, $|D_i|$ was inflated to 64 for all write requests under the RW-RNLP, as read requests can access any resource.

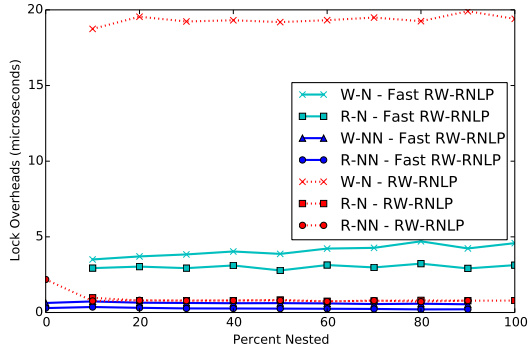

(a) Lock overhead.

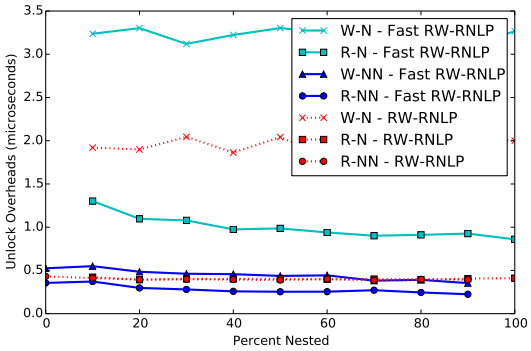

(b) Unlock overhead.

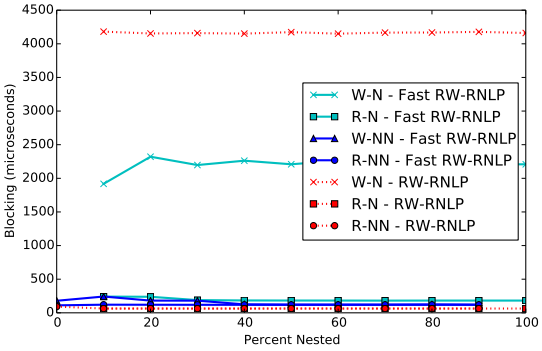

(c) Blocking.

Figure 440: (a) Lock and (b) unlock overheads and (c) blocking for nested and non-nested read and write requests under the RW-RNLP and the fast RW-RNLP. Here, for each request $\mathcal{R}_i$, $m = 36$, $L_i = 60\mu$s, $n_r = 64$, $|D_i| = 1$ for non-nested requests, and $|D_i| = 6$ for nested requests. Each request was randomly chosen to be a read (as opposed to a write) with probability 0.5 and to be a nested request with probability as shown. Due to write expansion, $|D_i|$ was inflated to 64 for all write requests under the RW-RNLP, as read requests can access any resource.

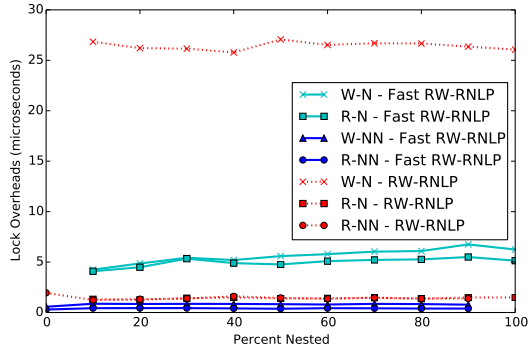

(a) Lock overhead.

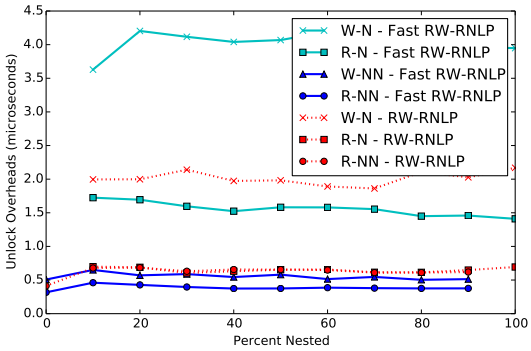

(b) Unlock overhead.

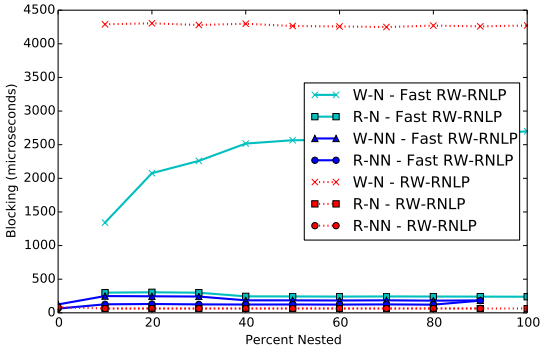

(c) Blocking.

Figure 441: (a) Lock and (b) unlock overheads and (c) blocking for nested and non-nested read and write requests under the RW-RNLP and the fast RW-RNLP. Here, for each request $\mathcal{R}_i$, $m = 36$, $L_i = 60\mu$s, $n_r = 64$, $|D_i| = 1$ for non-nested requests, and $|D_i| = 6$ for nested requests. Each request was randomly chosen to be a read (as opposed to a write) with probability 0.8 and to be a nested request with probability as shown. Due to write expansion, $|D_i|$ was inflated to 64 for all write requests under the RW-RNLP, as read requests can access any resource.

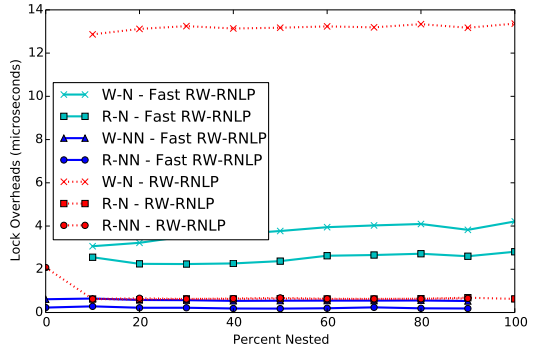

(a) Lock overhead.

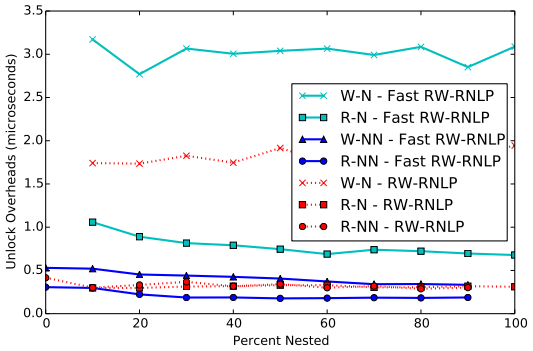

(b) Unlock overhead.

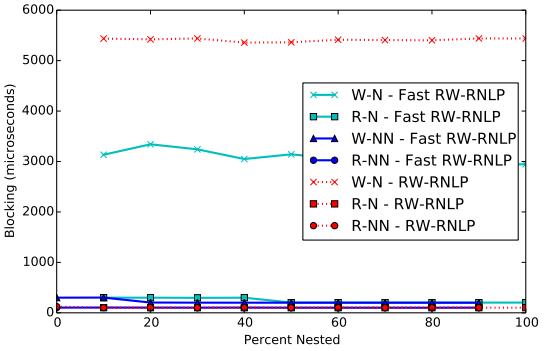

(c) Blocking.

Figure 442: (a) Lock and (b) unlock overheads and (c) blocking for nested and non-nested read and write requests under the RW-RNLP and the fast RW-RNLP. Here, for each request $\mathcal{R}_i$, $m = 36$, $L_i = 100\mu$s, $n_r = 64$, $|D_i| = 1$ for non-nested requests, and $|D_i| = 6$ for nested requests. Each request was randomly chosen to be a read (as opposed to a write) with probability 0.2 and to be a nested request with probability as shown. Due to write expansion, $|D_i|$ was inflated to 64 for all write requests under the RW-RNLP, as read requests can access any resource.

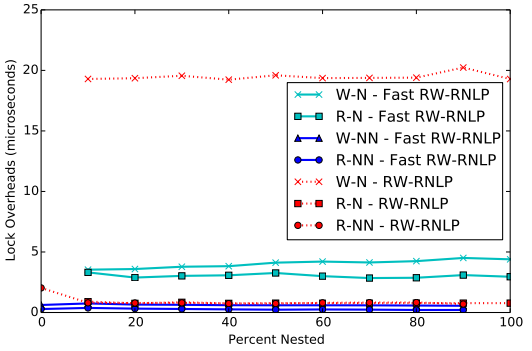

(a) Lock overhead.

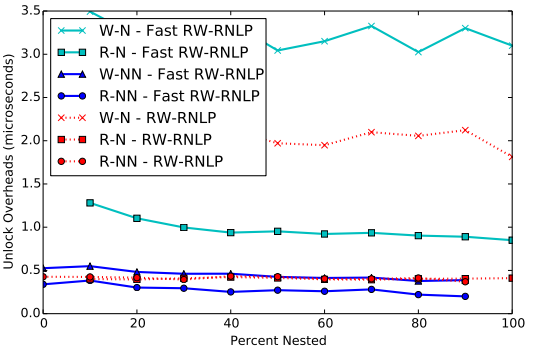

(b) Unlock overhead.

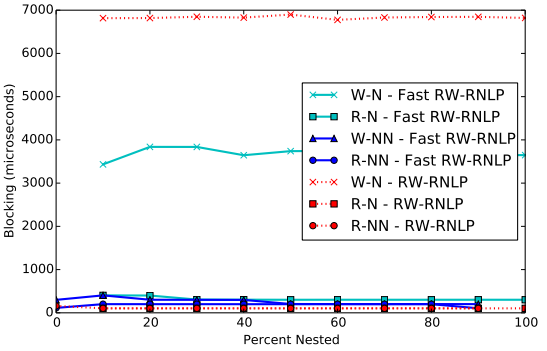

(c) Blocking.

Figure 443: (a) Lock and (b) unlock overheads and (c) blocking for nested and non-nested read and write requests under the RW-RNLP and the fast RW-RNLP. Here, for each request $\mathcal{R}_i$, $m = 36$, $L_i = 100\mu$s, $n_r = 64$, $|D_i| = 1$ for non-nested requests, and $|D_i| = 6$ for nested requests. Each request was randomly chosen to be a read (as opposed to a write) with probability 0.5 and to be a nested request with probability as shown. Due to write expansion, $|D_i|$ was inflated to 64 for all write requests under the RW-RNLP, as read requests can access any resource.

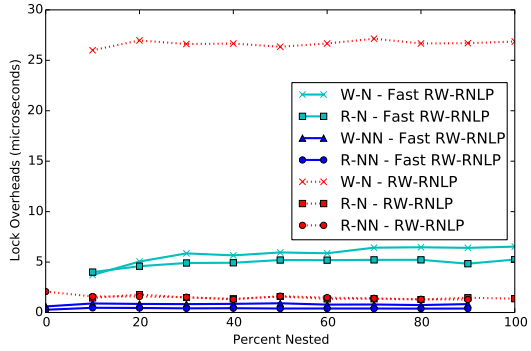

(a) Lock overhead.

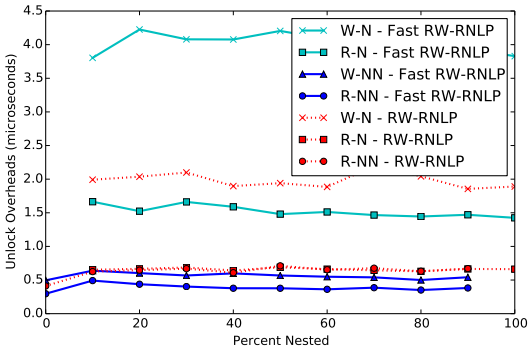

(b) Unlock overhead.

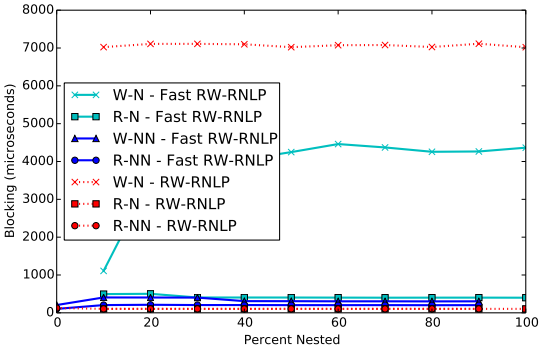

(c) Blocking.

Figure 444: (a) Lock and (b) unlock overheads and (c) blocking for nested and non-nested read and write requests under the RW-RNLP and the fast RW-RNLP. Here, for each request $\mathcal{R}_i$, $m = 36$, $L_i = 100\mu$s, $n_r = 64$, $|D_i| = 1$ for non-nested requests, and $|D_i| = 6$ for nested requests. Each request was randomly chosen to be a read (as opposed to a write) with probability 0.8 and to be a nested request with probability as shown. Due to write expansion, $|D_i|$ was inflated to 64 for all write requests under the RW-RNLP, as read requests can access any resource.

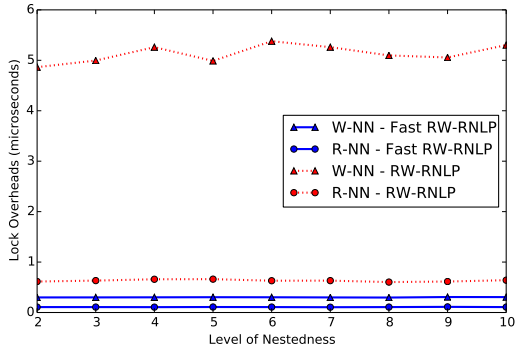

(a) Lock overhead.

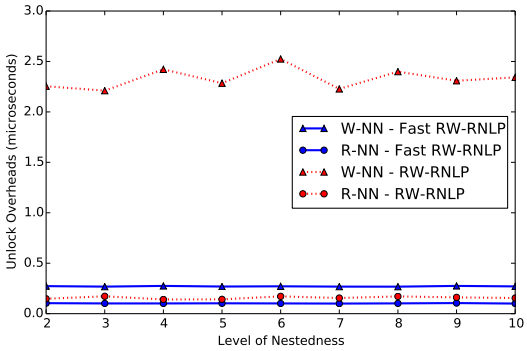

(b) Unlock overhead.

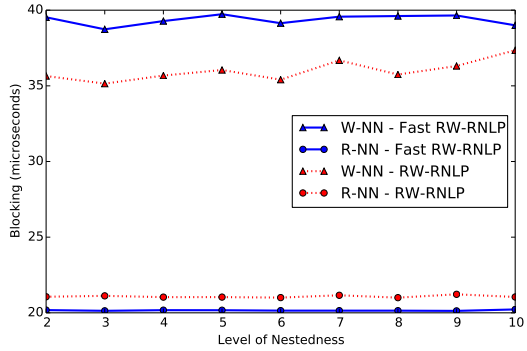

(c) Blocking.

Figure 445: (a) Lock and (b) unlock overheads and (c) blocking for non-nested read and write requests under the RW-RNLP and the fast RW-RNLP. Here, for each request $\mathcal{R}_i$, $m = 18$, $L_i = 20\mu$s, $n_r = 64$, and $|D_i|$ is as shown. Each request was randomly chosen to be a read (as opposed to a write) with probability 0.2 and to be a nested request with probability 0.

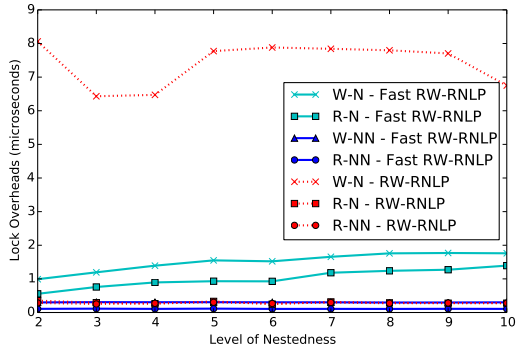

(a) Lock overhead.

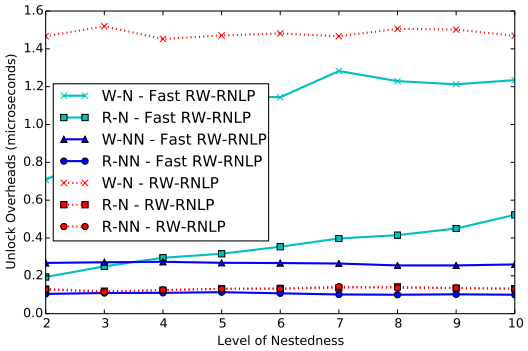

(b) Unlock overhead.

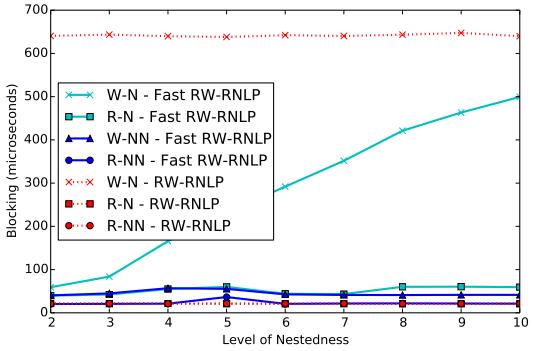

(c) Blocking.

Figure 446: (a) Lock and (b) unlock overheads and (c) blocking for nested and non-nested read and write requests under the RW-RNLP and the fast RW-RNLP. Here, for each request $\mathcal{R}_i$, $m = 18$, $L_i = 20\mu$s, $n_r = 64$, and $|D_i|$ is as shown. Each request was randomly chosen to be a read (as opposed to a write) with probability 0.2 and to be a nested request with probability 0.2. Due to write expansion, $|D_i|$ was inflated to 64 for all write requests under the RW-RNLP, as read requests can access any resource.

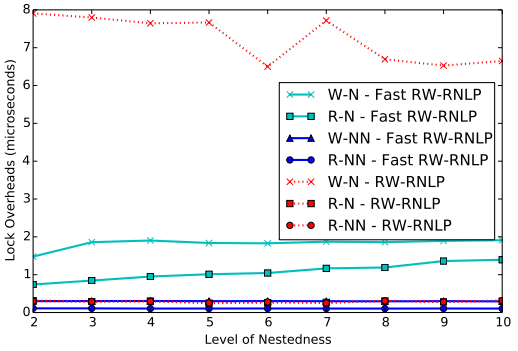

(a) Lock overhead.

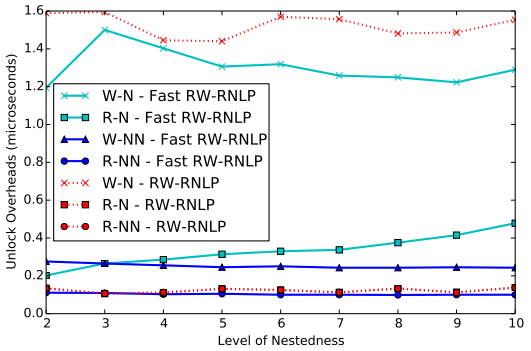

(b) Unlock overhead.

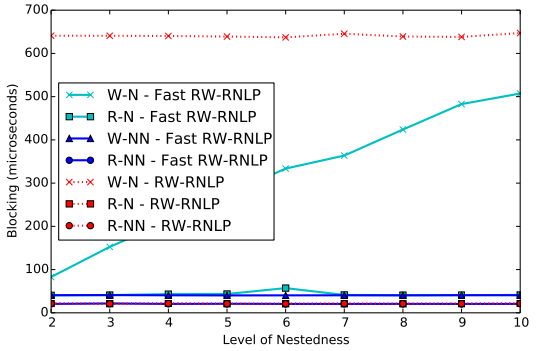

(c) Blocking.

Figure 447: (a) Lock and (b) unlock overheads and (c) blocking for nested and non-nested read and write requests under the RW-RNLP and the fast RW-RNLP. Here, for each request $\mathcal{R}_i$, $m = 18$, $L_i = 20\mu$s, $n_r = 64$, and $|D_i|$ is as shown. Each request was randomly chosen to be a read (as opposed to a write) with probability 0.2 and to be a nested request with probability 0.5. Due to write expansion, $|D_i|$ was inflated to 64 for all write requests under the RW-RNLP, as read requests can access any resource.

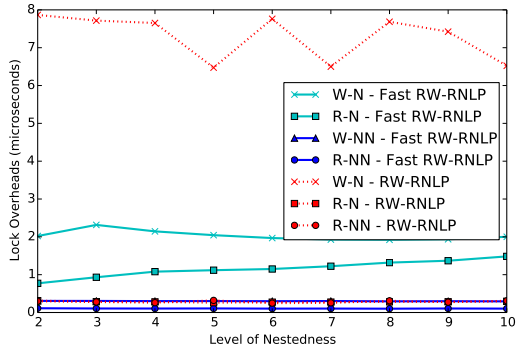

(a) Lock overhead.

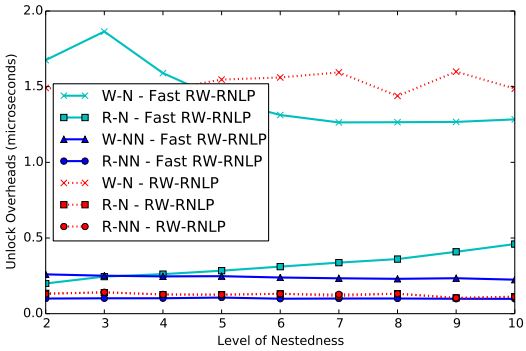

(b) Unlock overhead.

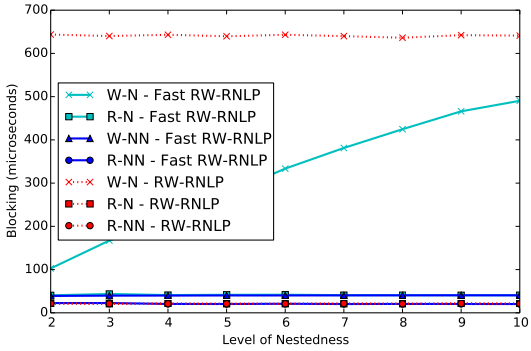

(c) Blocking.

Figure 448: (a) Lock and (b) unlock overheads and (c) blocking for nested and non-nested read and write requests under the RW-RNLP and the fast RW-RNLP. Here, for each request $\mathcal{R}_i$, $m = 18$, $L_i = 20\mu$s, $n_r = 64$, and $|D_i|$ is as shown. Each request was randomly chosen to be a read (as opposed to a write) with probability 0.2 and to be a nested request with probability 0.8. Due to write expansion, $|D_i|$ was inflated to 64 for all write requests under the RW-RNLP, as read requests can access any resource.

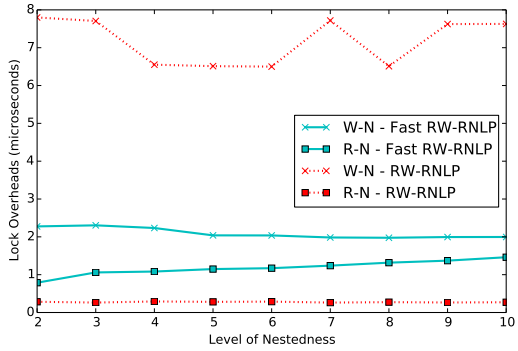

(a) Lock overhead.

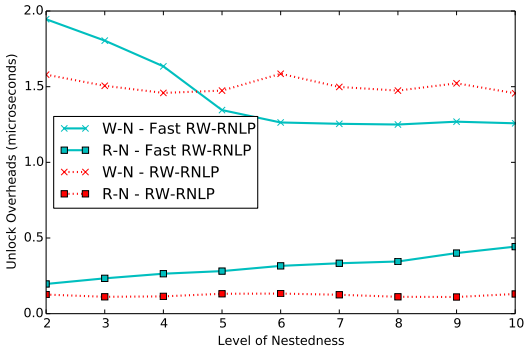

(b) Unlock overhead.

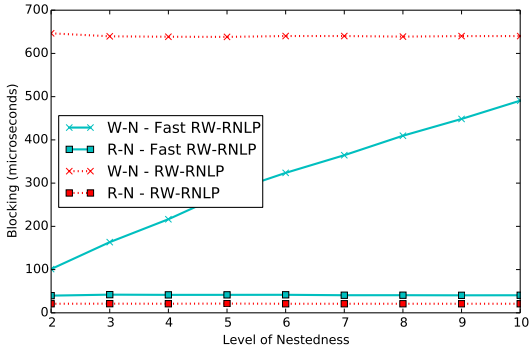

(c) Blocking.

Figure 449: (a) Lock and (b) unlock overheads and (c) blocking for nested read and write requests under the RW-RNLP and the fast RW-RNLP. Here, for each request $\mathcal{R}_i$, $m = 18$, $L_i = 20\mu$s, $n_r = 64$, and $|D_i|$ is as shown. Each request was randomly chosen to be a read (as opposed to a write) with probability 0.2 and to be a nested request with probability 1. Due to write expansion, $|D_i|$ was inflated to 64 for all write requests under the RW-RNLP, as read requests can access any resource.

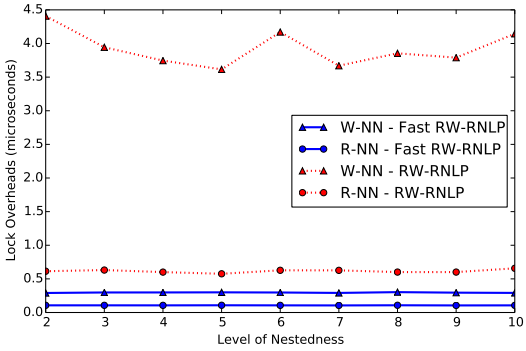

(a) Lock overhead.

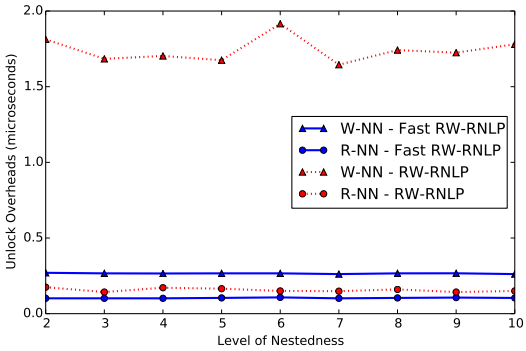

(b) Unlock overhead.

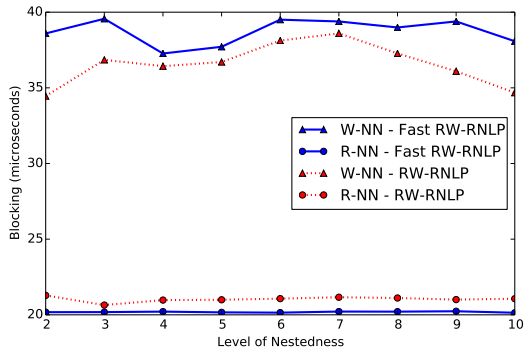

(c) Blocking.

Figure 450: (a) Lock and (b) unlock overheads and (c) blocking for non-nested read and write requests under the RW-RNLP and the fast RW-RNLP. Here, for each request $\mathcal{R}_i$, $m = 18$, $L_i = 20\mu$s, $n_r = 64$, and $|D_i|$ is as shown. Each request was randomly chosen to be a read (as opposed to a write) with probability 0.5 and to be a nested request with probability 0.

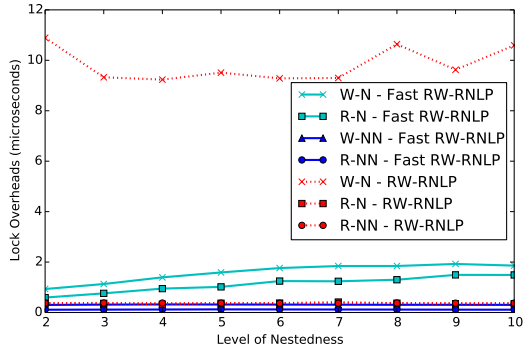

(a) Lock overhead.

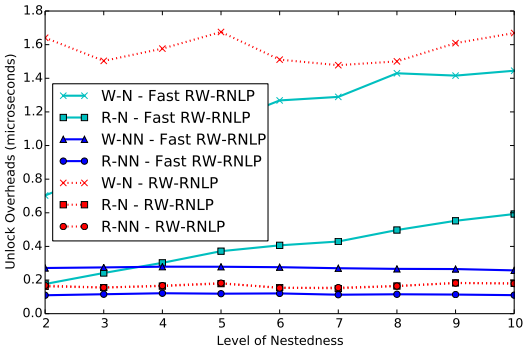

(b) Unlock overhead.

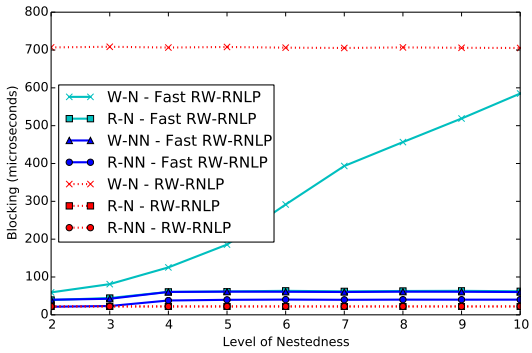

(c) Blocking.

Figure 451: (a) Lock and (b) unlock overheads and (c) blocking for nested and non-nested read and write requests under the RW-RNLP and the fast RW-RNLP. Here, for each request $\mathcal{R}_i$, $m = 18$, $L_i = 20\mu$s, $n_r = 64$, and $|D_i|$ is as shown. Each request was randomly chosen to be a read (as opposed to a write) with probability 0.5 and to be a nested request with probability 0.2. Due to write expansion, $|D_i|$ was inflated to 64 for all write requests under the RW-RNLP, as read requests can access any resource.

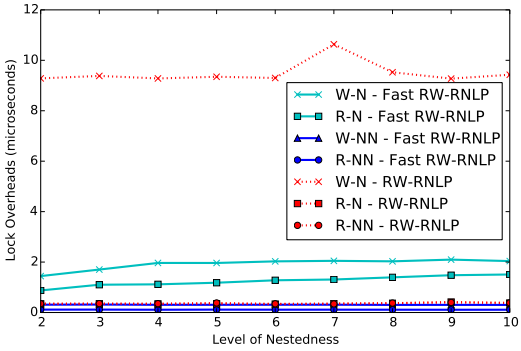

(a) Lock overhead.

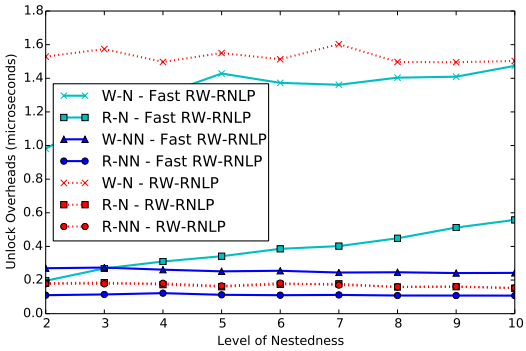

(b) Unlock overhead.

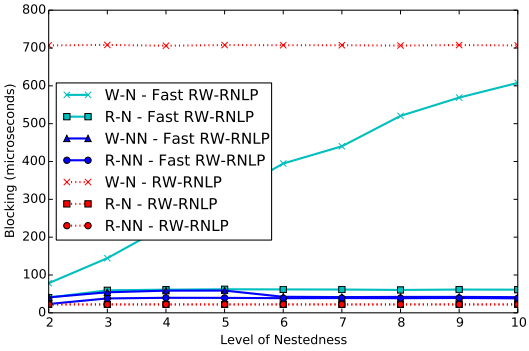

(c) Blocking.

Figure 452: (a) Lock and (b) unlock overheads and (c) blocking for nested and non-nested read and write requests under the RW-RNLP and the fast RW-RNLP. Here, for each request $\mathcal{R}_i$, $m = 18$, $L_i = 20\mu$s, $n_r = 64$, and $|D_i|$ is as shown. Each request was randomly chosen to be a read (as opposed to a write) with probability 0.5 and to be a nested request with probability 0.5. Due to write expansion, $|D_i|$ was inflated to 64 for all write requests under the RW-RNLP, as read requests can access any resource.

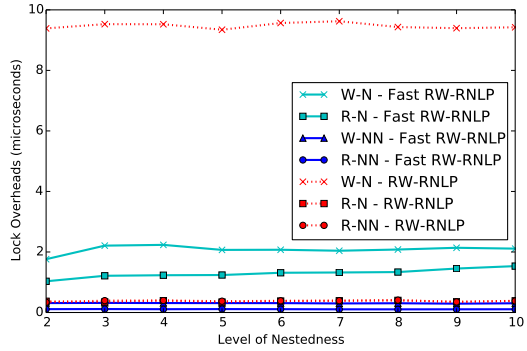

(a) Lock overhead.

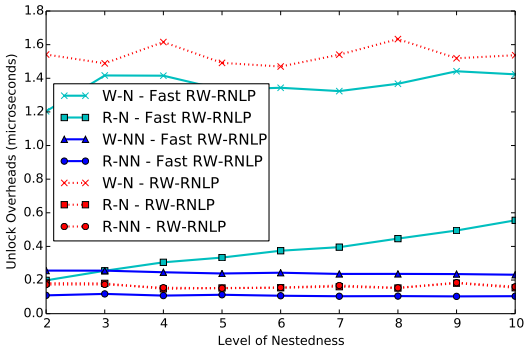

(b) Unlock overhead.

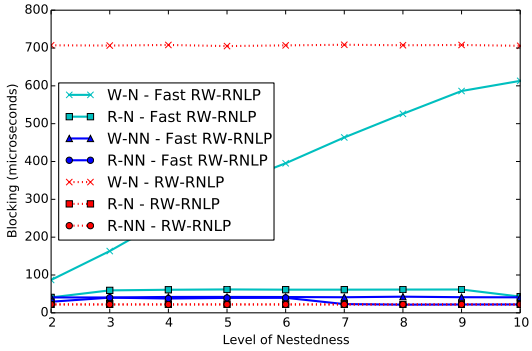

(c) Blocking.

Figure 453: (a) Lock and (b) unlock overheads and (c) blocking for nested and non-nested read and write requests under the RW-RNLP and the fast RW-RNLP. Here, for each request $\mathcal{R}_i$, $m = 18$, $L_i = 20\mu$s, $n_r = 64$, and $|D_i|$ is as shown. Each request was randomly chosen to be a read (as opposed to a write) with probability 0.5 and to be a nested request with probability 0.8. Due to write expansion, $|D_i|$ was inflated to 64 for all write requests under the RW-RNLP, as read requests can access any resource.

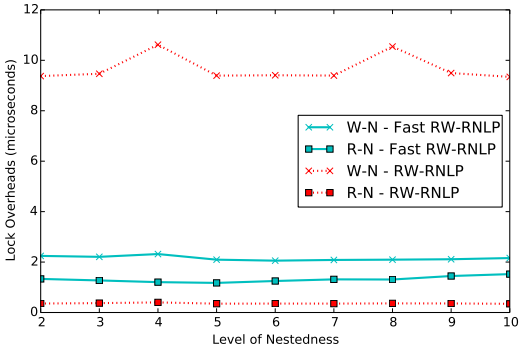

(a) Lock overhead.

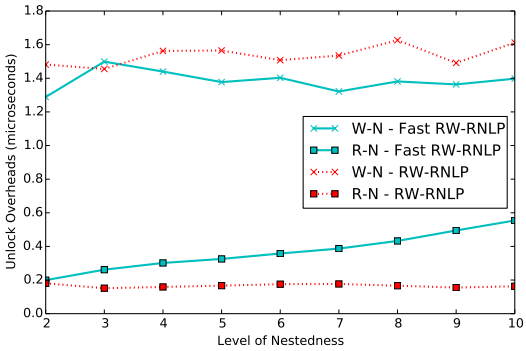

(b) Unlock overhead.

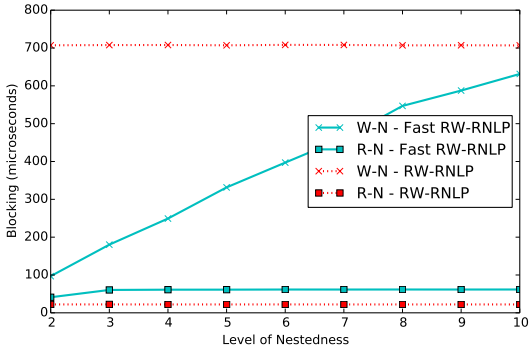

(c) Blocking.

Figure 454: (a) Lock and (b) unlock overheads and (c) blocking for nested read and write requests under the RW-RNLP and the fast RW-RNLP. Here, for each request $\mathcal{R}_i$, $m = 18$, $L_i = 20\mu$s, $n_r = 64$, and $|D_i|$ is as shown. Each request was randomly chosen to be a read (as opposed to a write) with probability 0.5 and to be a nested request with probability 1. Due to write expansion, $|D_i|$ was inflated to 64 for all write requests under the RW-RNLP, as read requests can access any resource.

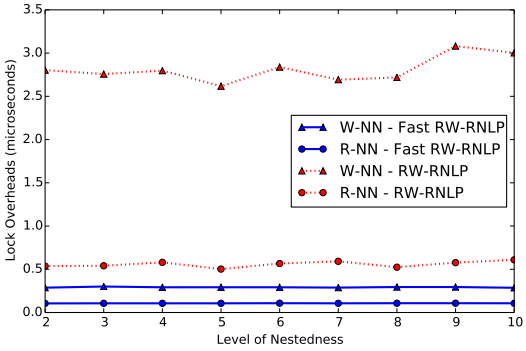

(a) Lock overhead.

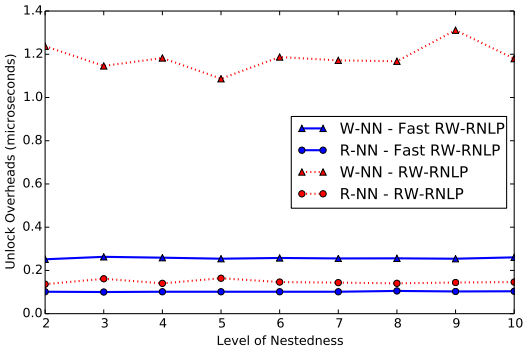

(b) Unlock overhead.

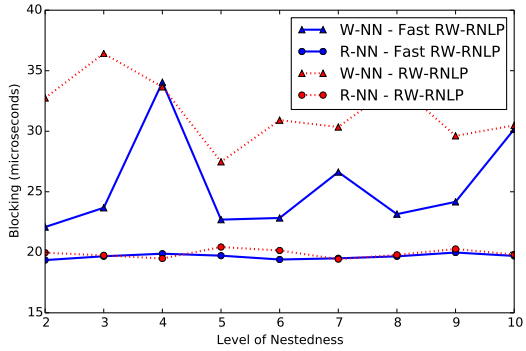

(c) Blocking.

Figure 455: (a) Lock and (b) unlock overheads and (c) blocking for non-nested read and write requests under the RW-RNLP and the fast RW-RNLP. Here, for each request $\mathcal{R}_i$, $m = 18$, $L_i = 20\mu$s, $n_r = 64$, and $|D_i|$ is as shown. Each request was randomly chosen to be a read (as opposed to a write) with probability 0.8 and to be a nested request with probability 0.

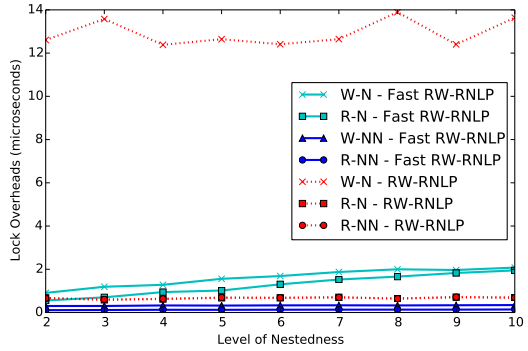

(a) Lock overhead.

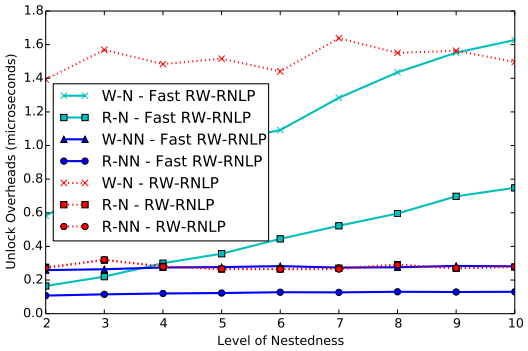

(b) Unlock overhead.

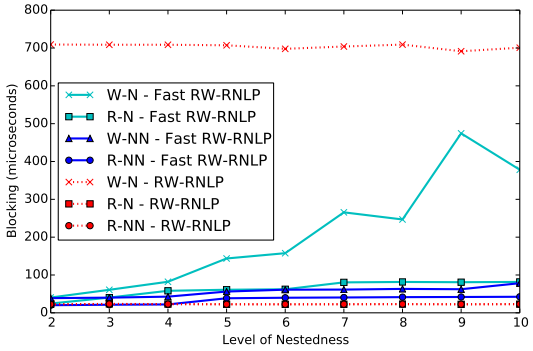

(c) Blocking.

Figure 456: (a) Lock and (b) unlock overheads and (c) blocking for nested and non-nested read and write requests under the RW-RNLP and the fast RW-RNLP. Here, for each request $\mathcal{R}_i$, $m = 18$, $L_i = 20\mu$s, $n_r = 64$, and $|D_i|$ is as shown. Each request was randomly chosen to be a read (as opposed to a write) with probability 0.8 and to be a nested request with probability 0.2. Due to write expansion, $|D_i|$ was inflated to 64 for all write requests under the RW-RNLP, as read requests can access any resource.

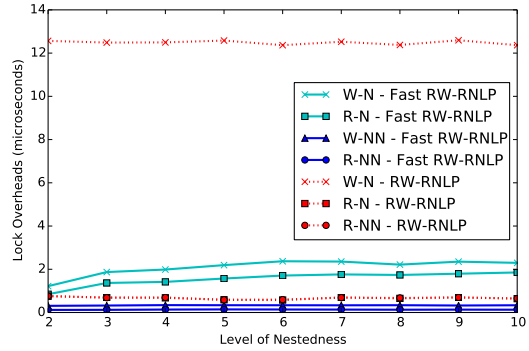

(a) Lock overhead.

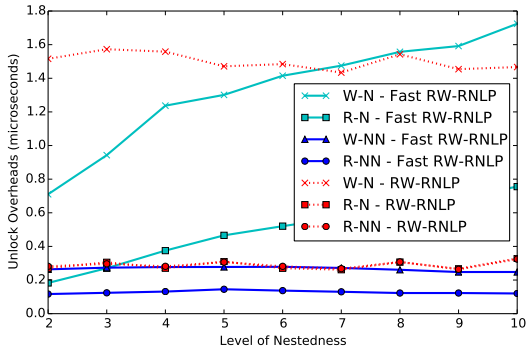

(b) Unlock overhead.

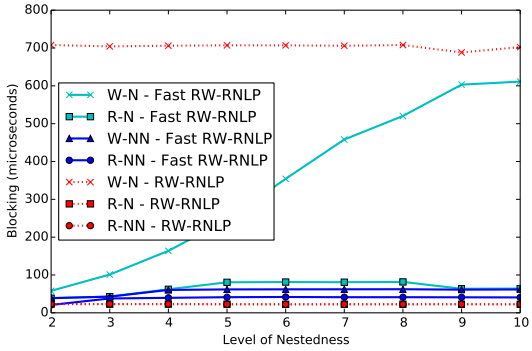

(c) Blocking.

Figure 457: (a) Lock and (b) unlock overheads and (c) blocking for nested and non-nested read and write requests under the RW-RNLP and the fast RW-RNLP. Here, for each request $\mathcal{R}_i$, $m = 18$, $L_i = 20\mu$s, $n_r = 64$, and $|D_i|$ is as shown. Each request was randomly chosen to be a read (as opposed to a write) with probability 0.8 and to be a nested request with probability 0.5. Due to write expansion, $|D_i|$ was inflated to 64 for all write requests under the RW-RNLP, as read requests can access any resource.

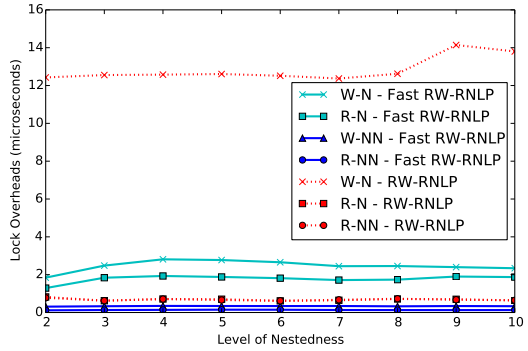

(a) Lock overhead.

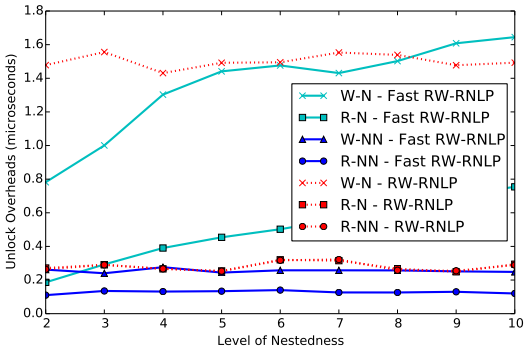

(b) Unlock overhead.

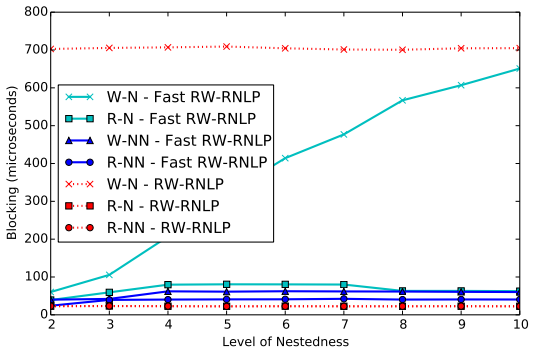

(c) Blocking.

Figure 458: (a) Lock and (b) unlock overheads and (c) blocking for nested and non-nested read and write requests under the RW-RNLP and the fast RW-RNLP. Here, for each request $\mathcal{R}_i$, $m = 18$, $L_i = 20\mu$s, $n_r = 64$, and $|D_i|$ is as shown. Each request was randomly chosen to be a read (as opposed to a write) with probability 0.8 and to be a nested request with probability 0.8. Due to write expansion, $|D_i|$ was inflated to 64 for all write requests under the RW-RNLP, as read requests can access any resource.

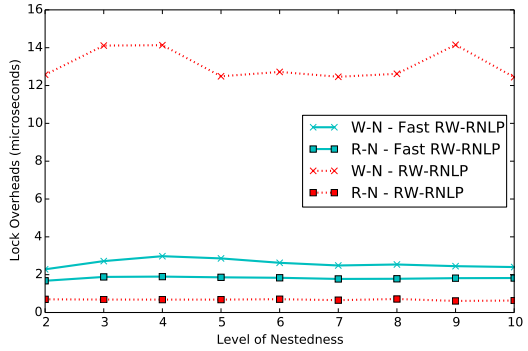

(a) Lock overhead.

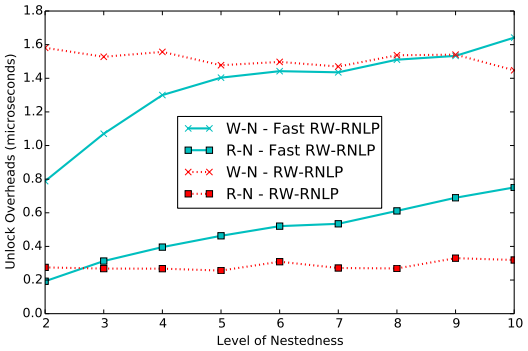

(b) Unlock overhead.

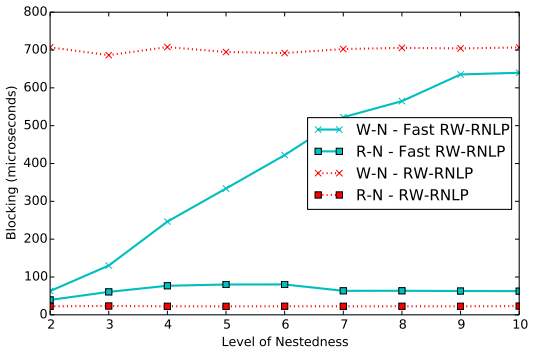

(c) Blocking.

Figure 459: (a) Lock and (b) unlock overheads and (c) blocking for nested read and write requests under the RW-RNLP and the fast RW-RNLP. Here, for each request $\mathcal{R}_i$, $m = 18$, $L_i = 20\mu$s, $n_r = 64$, and $|D_i|$ is as shown. Each request was randomly chosen to be a read (as opposed to a write) with probability 0.8 and to be a nested request with probability 1. Due to write expansion, $|D_i|$ was inflated to 64 for all write requests under the RW-RNLP, as read requests can access any resource.

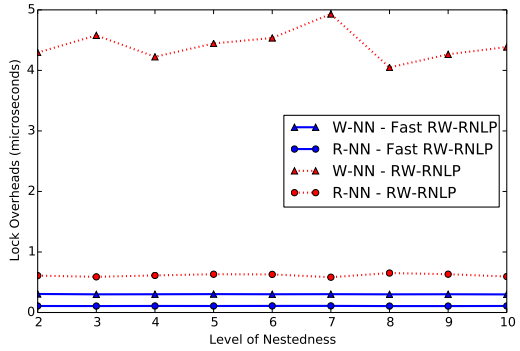

(a) Lock overhead.

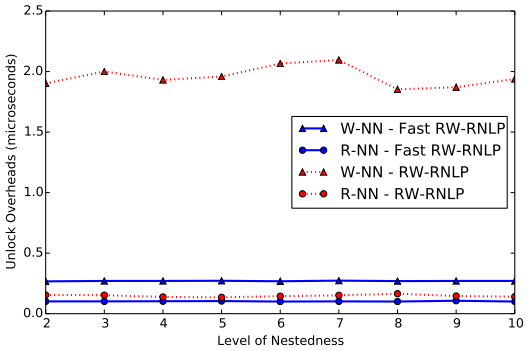

(b) Unlock overhead.

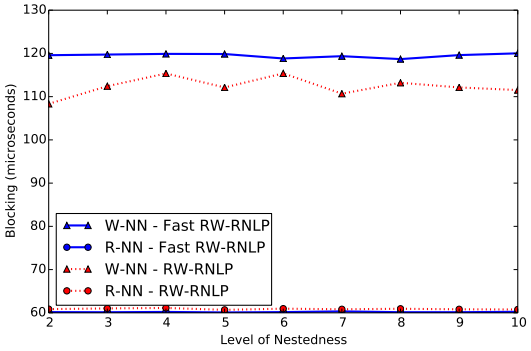

(c) Blocking.

Figure 460: (a) Lock and (b) unlock overheads and (c) blocking for non-nested read and write requests under the RW-RNLP and the fast RW-RNLP. Here, for each request $\mathcal{R}_i$, $m = 18$, $L_i = 60\mu$s, $n_r = 64$, and $|D_i|$ is as shown. Each request was randomly chosen to be a read (as opposed to a write) with probability 0.2 and to be a nested request with probability 0.

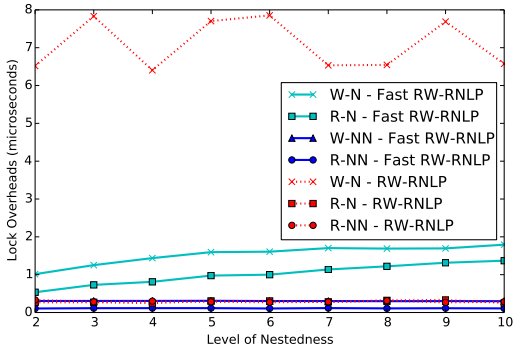

(a) Lock overhead.

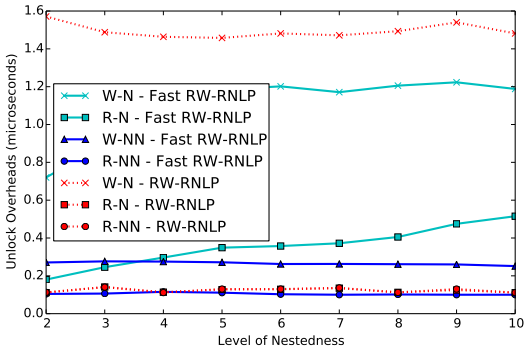

(b) Unlock overhead.

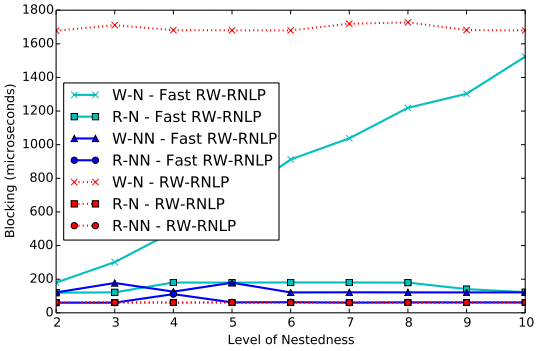

(c) Blocking.

Figure 461: (a) Lock and (b) unlock overheads and (c) blocking for nested and non-nested read and write requests under the RW-RNLP and the fast RW-RNLP. Here, for each request $\mathcal{R}_i$, $m = 18$, $L_i = 60\mu$s, $n_r = 64$, and $|D_i|$ is as shown. Each request was randomly chosen to be a read (as opposed to a write) with probability 0.2 and to be a nested request with probability 0.2. Due to write expansion, $|D_i|$ was inflated to 64 for all write requests under the RW-RNLP, as read requests can access any resource.

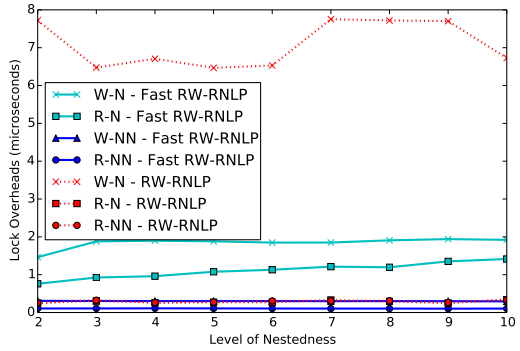

(a) Lock overhead.

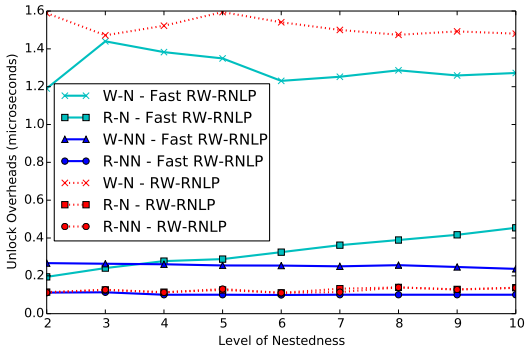

(b) Unlock overhead.

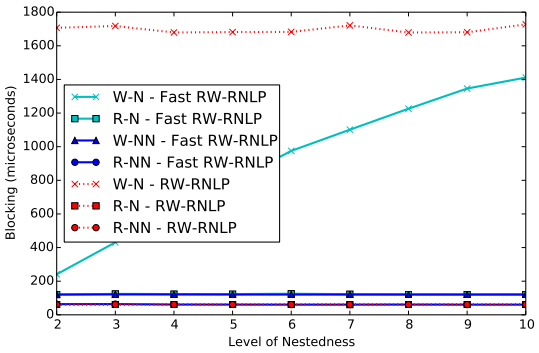

(c) Blocking.

Figure 462: (a) Lock and (b) unlock overheads and (c) blocking for nested and non-nested read and write requests under the RW-RNLP and the fast RW-RNLP. Here, for each request $\mathcal{R}_i$, $m = 18$, $L_i = 60\mu$s, $n_r = 64$, and $|D_i|$ is as shown. Each request was randomly chosen to be a read (as opposed to a write) with probability 0.2 and to be a nested request with probability 0.5. Due to write expansion, $|D_i|$ was inflated to 64 for all write requests under the RW-RNLP, as read requests can access any resource.

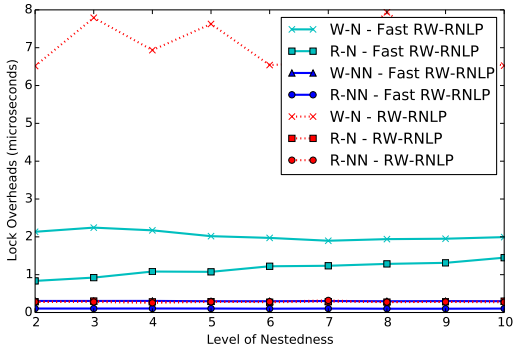

(a) Lock overhead.

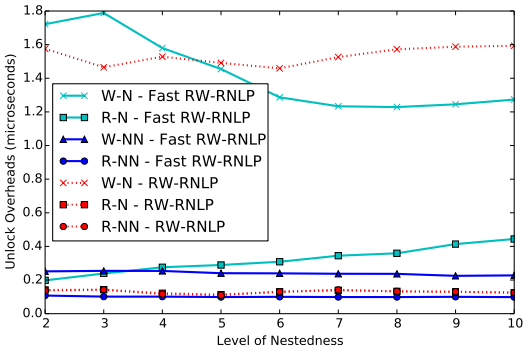

(b) Unlock overhead.

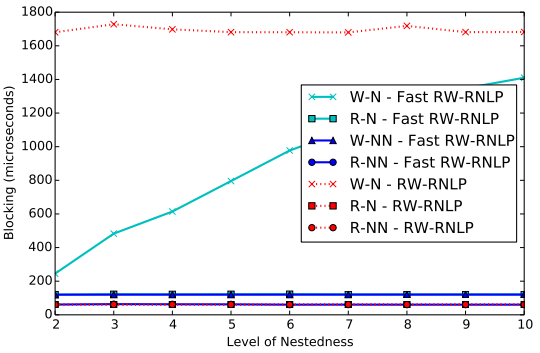

(c) Blocking.

Figure 463: (a) Lock and (b) unlock overheads and (c) blocking for nested and non-nested read and write requests under the RW-RNLP and the fast RW-RNLP. Here, for each request $\mathcal{R}_i$, $m = 18$, $L_i = 60\mu$s, $n_r = 64$, and $|D_i|$ is as shown. Each request was randomly chosen to be a read (as opposed to a write) with probability 0.2 and to be a nested request with probability 0.8. Due to write expansion, $|D_i|$ was inflated to 64 for all write requests under the RW-RNLP, as read requests can access any resource.

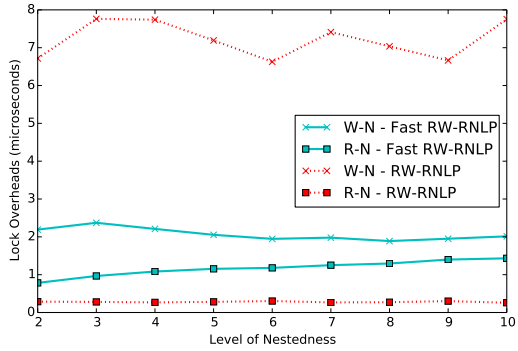

(a) Lock overhead.

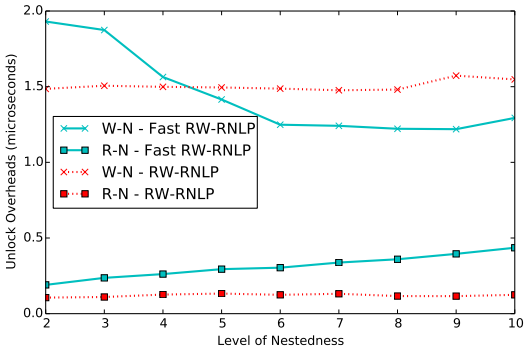

(b) Unlock overhead.

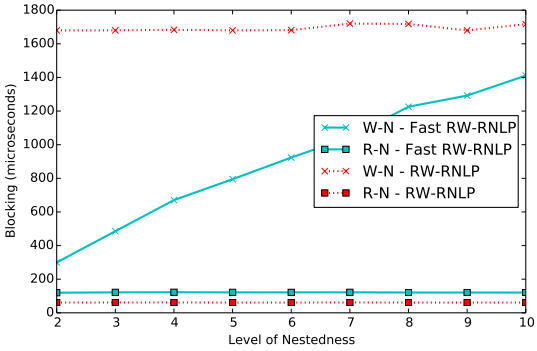

(c) Blocking.

Figure 464: (a) Lock and (b) unlock overheads and (c) blocking for nested read and write requests under the RW-RNLP and the fast RW-RNLP. Here, for each request $\mathcal{R}_i$, $m = 18$, $L_i = 60\mu$s, $n_r = 64$, and $|D_i|$ is as shown. Each request was randomly chosen to be a read (as opposed to a write) with probability 0.2 and to be a nested request with probability 1. Due to write expansion, $|D_i|$ was inflated to 64 for all write requests under the RW-RNLP, as read requests can access any resource.

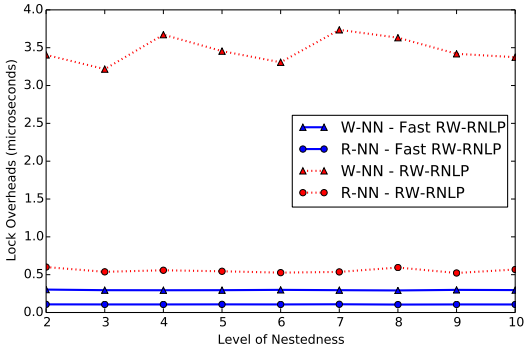

(a) Lock overhead.

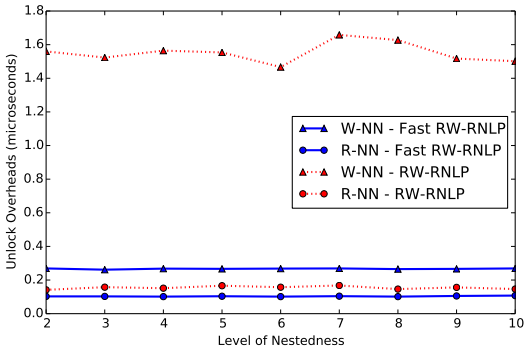

(b) Unlock overhead.

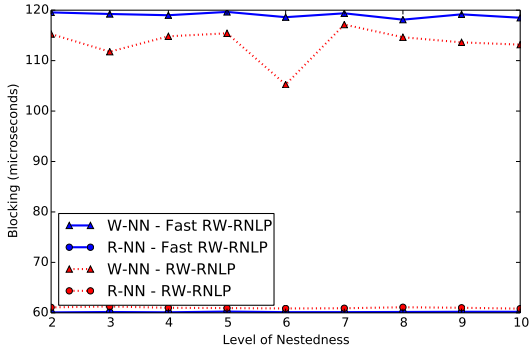

(c) Blocking.

Figure 465: (a) Lock and (b) unlock overheads and (c) blocking for non-nested read and write requests under the RW-RNLP and the fast RW-RNLP. Here, for each request $\mathcal{R}_i$, $m = 18$, $L_i = 60\mu$s, $n_r = 64$, and $|D_i|$ is as shown. Each request was randomly chosen to be a read (as opposed to a write) with probability 0.5 and to be a nested request with probability 0.

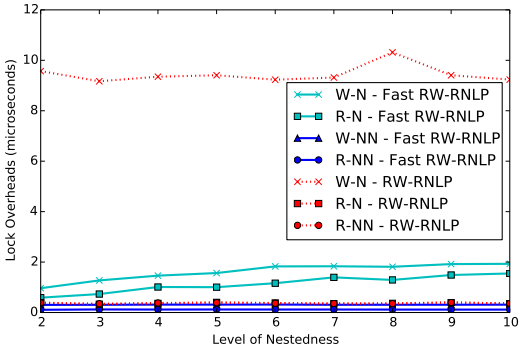

(a) Lock overhead.

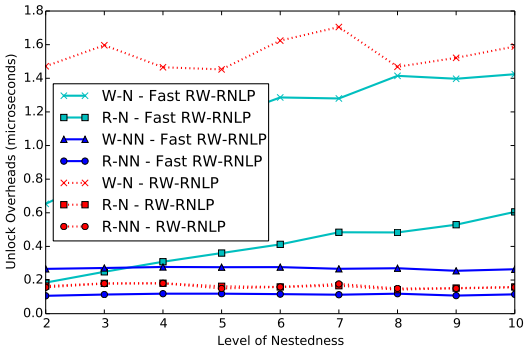

(b) Unlock overhead.

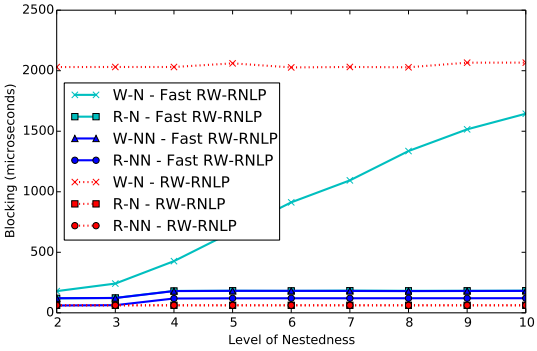

(c) Blocking.

Figure 466: (a) Lock and (b) unlock overheads and (c) blocking for nested and non-nested read and write requests under the RW-RNLP and the fast RW-RNLP. Here, for each request $\mathcal{R}_i$, $m = 18$, $L_i = 60\mu$s, $n_r = 64$, and $|D_i|$ is as shown. Each request was randomly chosen to be a read (as opposed to a write) with probability 0.5 and to be a nested request with probability 0.2. Due to write expansion, $|D_i|$ was inflated to 64 for all write requests under the RW-RNLP, as read requests can access any resource.

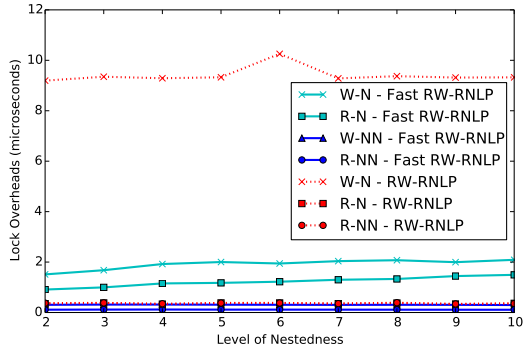

(a) Lock overhead.

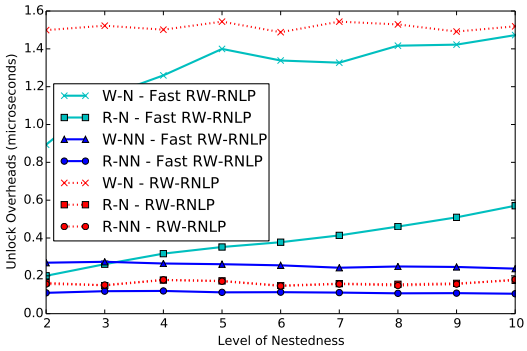

(b) Unlock overhead.

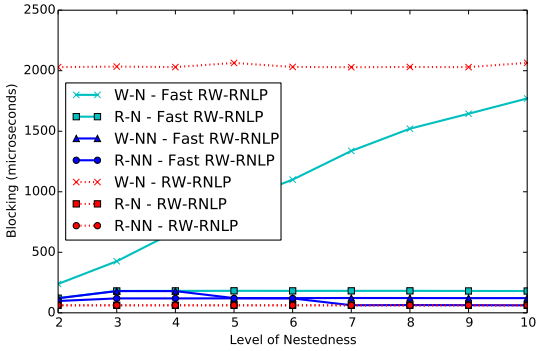

(c) Blocking.

Figure 467: (a) Lock and (b) unlock overheads and (c) blocking for nested and non-nested read and write requests under the RW-RNLP and the fast RW-RNLP. Here, for each request $\mathcal{R}_i$, $m = 18$, $L_i = 60\mu$s, $n_r = 64$, and $|D_i|$ is as shown. Each request was randomly chosen to be a read (as opposed to a write) with probability 0.5 and to be a nested request with probability 0.5. Due to write expansion, $|D_i|$ was inflated to 64 for all write requests under the RW-RNLP, as read requests can access any resource.

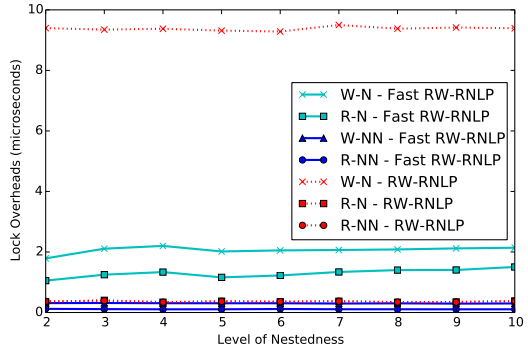

(a) Lock overhead.

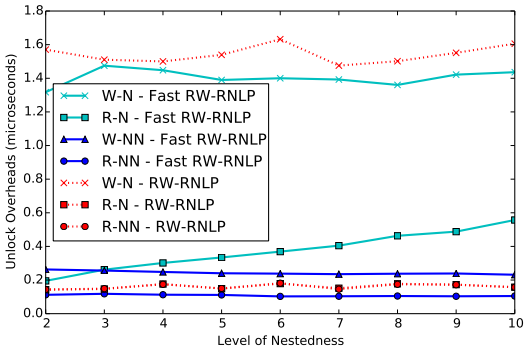

(b) Unlock overhead.

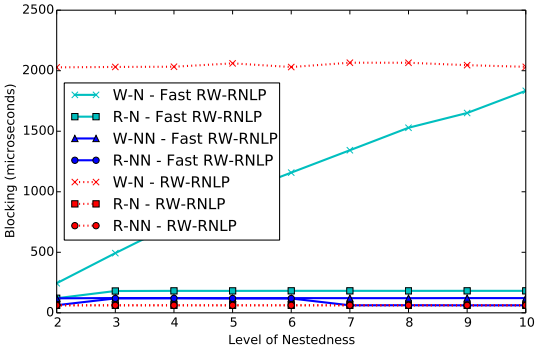

(c) Blocking.

Figure 468: (a) Lock and (b) unlock overheads and (c) blocking for nested and non-nested read and write requests under the RW-RNLP and the fast RW-RNLP. Here, for each request $\mathcal{R}_i$, $m = 18$, $L_i = 60\mu$s, $n_r = 64$, and $|D_i|$ is as shown. Each request was randomly chosen to be a read (as opposed to a write) with probability 0.5 and to be a nested request with probability 0.8. Due to write expansion, $|D_i|$ was inflated to 64 for all write requests under the RW-RNLP, as read requests can access any resource.

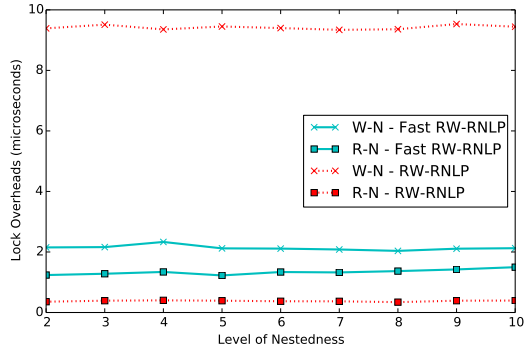

(a) Lock overhead.

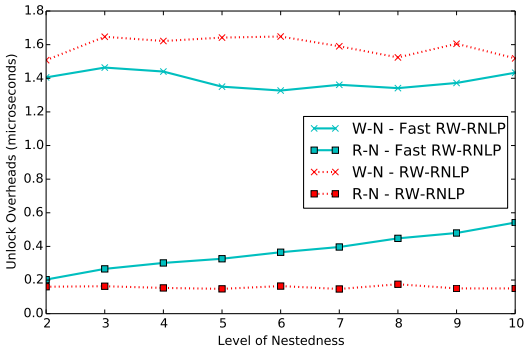

(b) Unlock overhead.

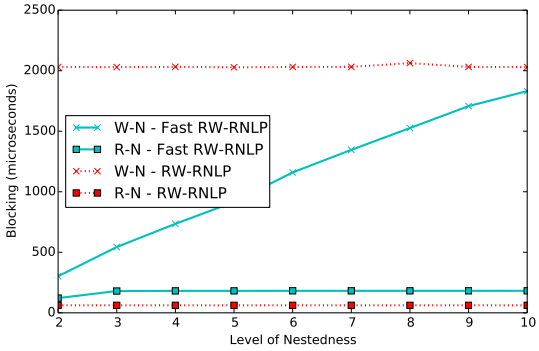

(c) Blocking.

Figure 469: (a) Lock and (b) unlock overheads and (c) blocking for nested read and write requests under the RW-RNLP and the fast RW-RNLP. Here, for each request $\mathcal{R}_i$, $m = 18$, $L_i = 60\mu$s, $n_r = 64$, and $|D_i|$ is as shown. Each request was randomly chosen to be a read (as opposed to a write) with probability 0.5 and to be a nested request with probability 1. Due to write expansion, $|D_i|$ was inflated to 64 for all write requests under the RW-RNLP, as read requests can access any resource.

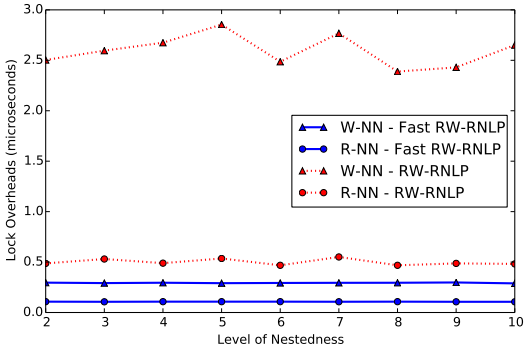

(a) Lock overhead.

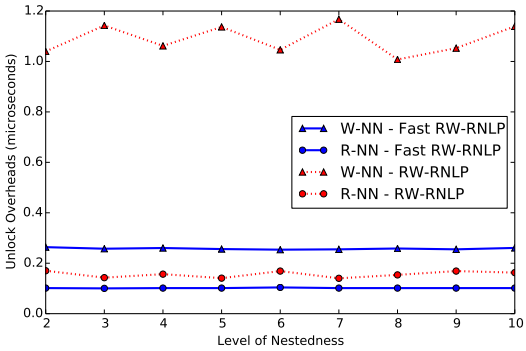

(b) Unlock overhead.

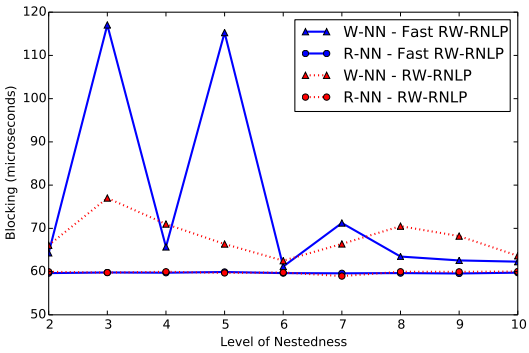

(c) Blocking.

Figure 470: (a) Lock and (b) unlock overheads and (c) blocking for non-nested read and write requests under the RW-RNLP and the fast RW-RNLP. Here, for each request $\mathcal{R}_i$, $m = 18$, $L_i = 60\mu$s, $n_r = 64$, and $|D_i|$ is as shown. Each request was randomly chosen to be a read (as opposed to a write) with probability 0.8 and to be a nested request with probability 0.

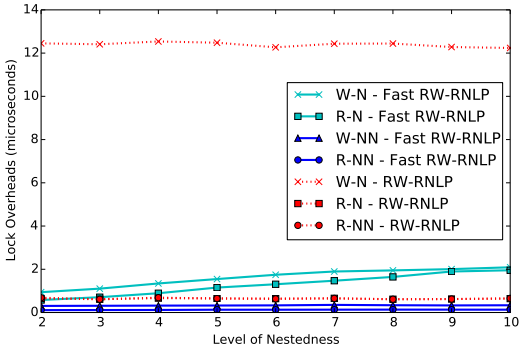

(a) Lock overhead.

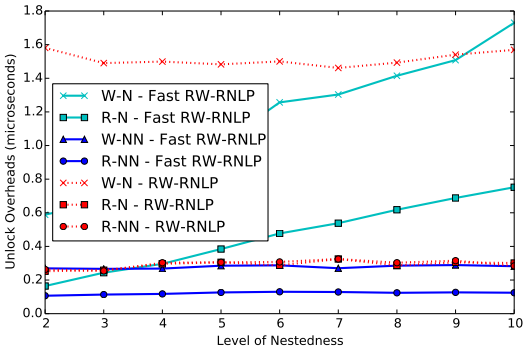

(b) Unlock overhead.

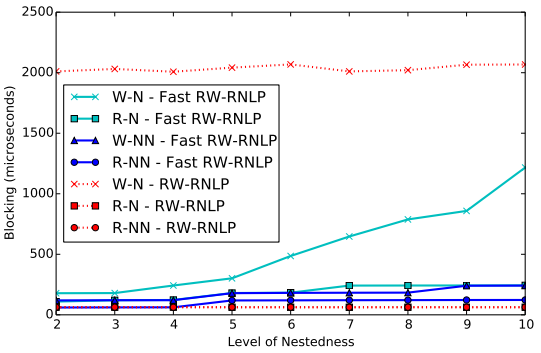

(c) Blocking.

Figure 471: (a) Lock and (b) unlock overheads and (c) blocking for nested and non-nested read and write requests under the RW-RNLP and the fast RW-RNLP. Here, for each request $\mathcal{R}_i$, $m = 18$, $L_i = 60\mu$s, $n_r = 64$, and $|D_i|$ is as shown. Each request was randomly chosen to be a read (as opposed to a write) with probability 0.8 and to be a nested request with probability 0.2. Due to write expansion, $|D_i|$ was inflated to 64 for all write requests under the RW-RNLP, as read requests can access any resource.

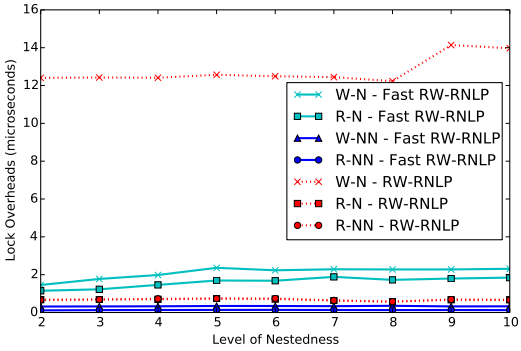

(a) Lock overhead.

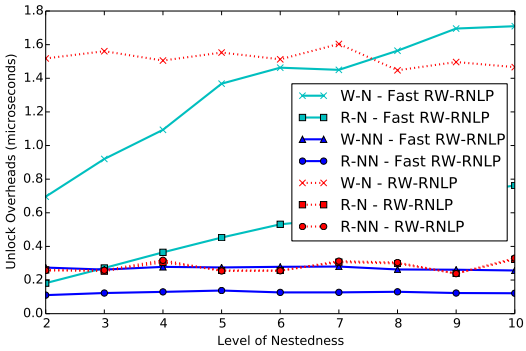

(b) Unlock overhead.

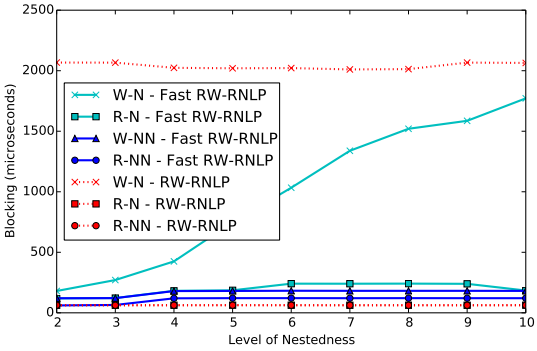

(c) Blocking.

Figure 472: (a) Lock and (b) unlock overheads and (c) blocking for nested and non-nested read and write requests under the RW-RNLP and the fast RW-RNLP. Here, for each request $\mathcal{R}_i$, $m = 18$, $L_i = 60\mu$s, $n_r = 64$, and $|D_i|$ is as shown. Each request was randomly chosen to be a read (as opposed to a write) with probability 0.8 and to be a nested request with probability 0.5. Due to write expansion, $|D_i|$ was inflated to 64 for all write requests under the RW-RNLP, as read requests can access any resource.

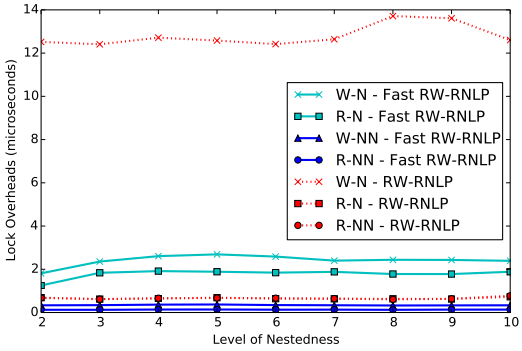

(a) Lock overhead.

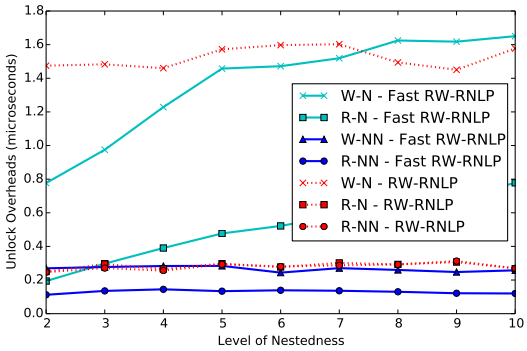

(b) Unlock overhead.

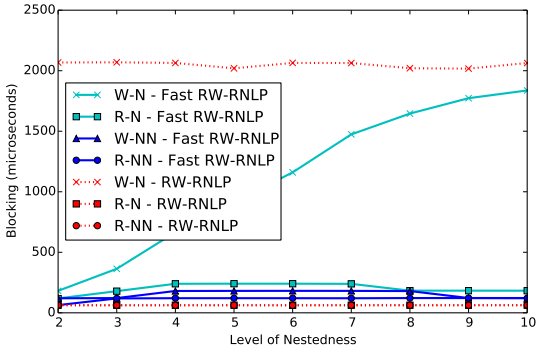

(c) Blocking.

Figure 473: (a) Lock and (b) unlock overheads and (c) blocking for nested and non-nested read and write requests under the RW-RNLP and the fast RW-RNLP. Here, for each request $\mathcal{R}_i$, $m = 18$, $L_i = 60\mu$s, $n_r = 64$, and $|D_i|$ is as shown. Each request was randomly chosen to be a read (as opposed to a write) with probability 0.8 and to be a nested request with probability 0.8. Due to write expansion, $|D_i|$ was inflated to 64 for all write requests under the RW-RNLP, as read requests can access any resource.

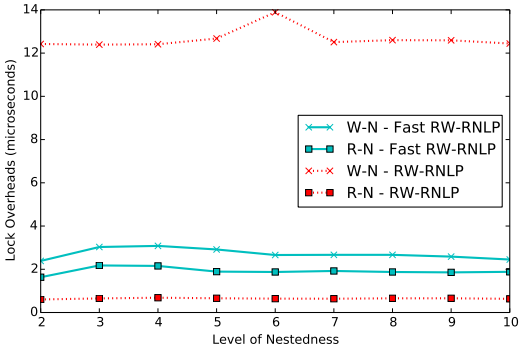

(a) Lock overhead.

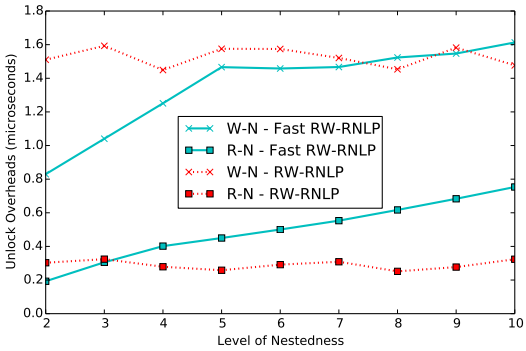

(b) Unlock overhead.

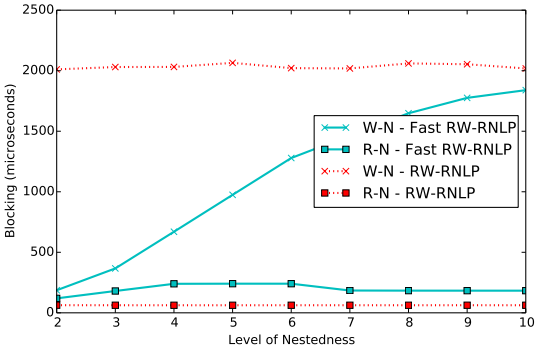

(c) Blocking.

Figure 474: (a) Lock and (b) unlock overheads and (c) blocking for nested read and write requests under the RW-RNLP and the fast RW-RNLP. Here, for each request $\mathcal{R}_i$, $m = 18$, $L_i = 60\mu$s, $n_r = 64$, and $|D_i|$ is as shown. Each request was randomly chosen to be a read (as opposed to a write) with probability 0.8 and to be a nested request with probability 1. Due to write expansion, $|D_i|$ was inflated to 64 for all write requests under the RW-RNLP, as read requests can access any resource.

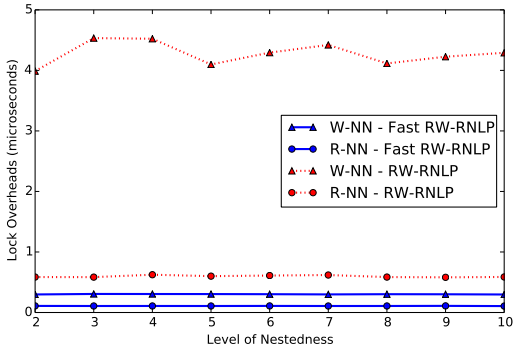

(a) Lock overhead.

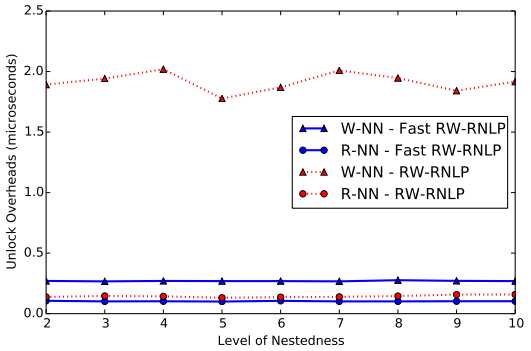

(b) Unlock overhead.

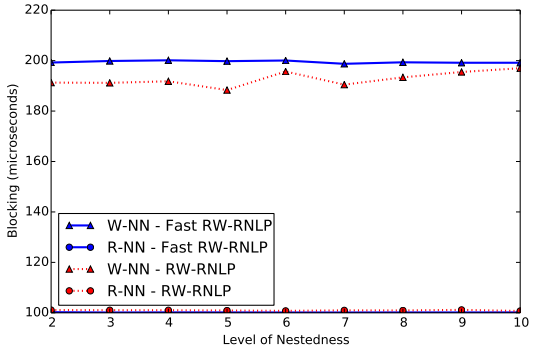

(c) Blocking.

Figure 475: (a) Lock and (b) unlock overheads and (c) blocking for non-nested read and write requests under the RW-RNLP and the fast RW-RNLP. Here, for each request $\mathcal{R}_i$, $m = 18$, $L_i = 100\mu$s, $n_r = 64$, and $|D_i|$ is as shown. Each request was randomly chosen to be a read (as opposed to a write) with probability 0.2 and to be a nested request with probability 0.

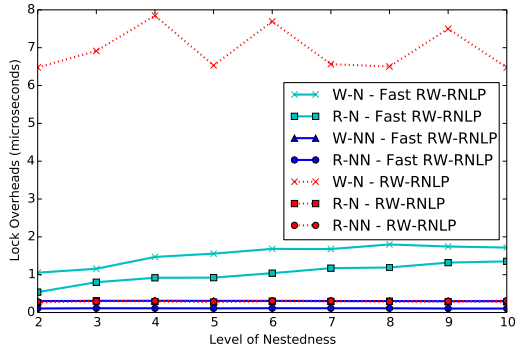

(a) Lock overhead.

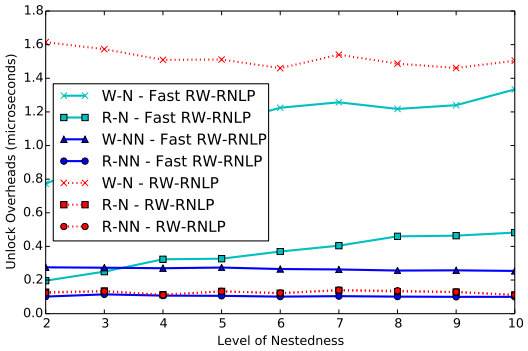

(b) Unlock overhead.

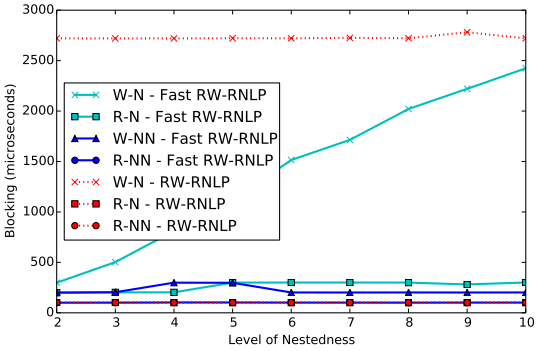

(c) Blocking.

Figure 476: (a) Lock and (b) unlock overheads and (c) blocking for nested and non-nested read and write requests under the RW-RNLP and the fast RW-RNLP. Here, for each request $\mathcal{R}_i$, $m = 18$, $L_i = 100\mu$s, $n_r = 64$, and $|D_i|$ is as shown. Each request was randomly chosen to be a read (as opposed to a write) with probability 0.2 and to be a nested request with probability 0.2. Due to write expansion, $|D_i|$ was inflated to 64 for all write requests under the RW-RNLP, as read requests can access any resource.

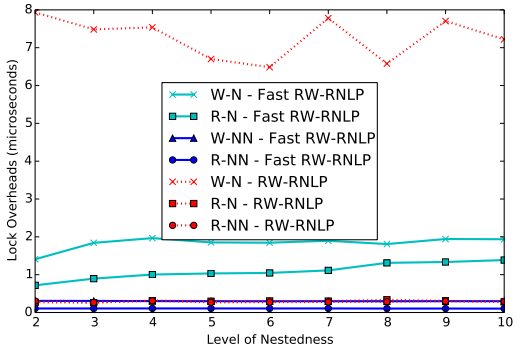

(a) Lock overhead.

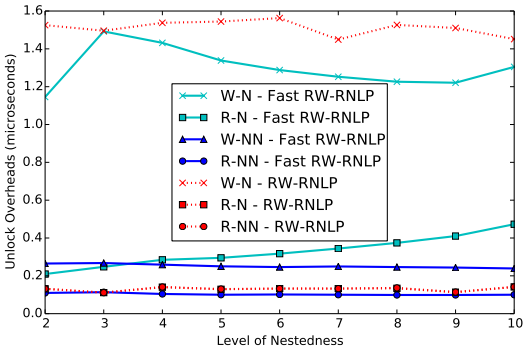

(b) Unlock overhead.

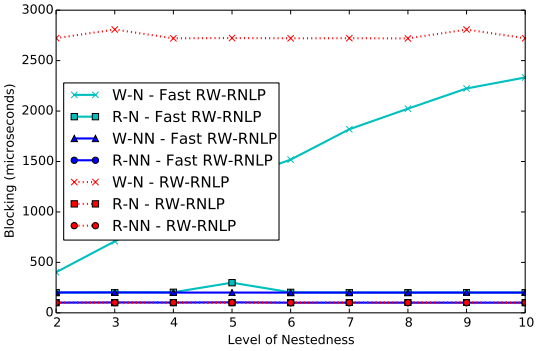

(c) Blocking.

Figure 477: (a) Lock and (b) unlock overheads and (c) blocking for nested and non-nested read and write requests under the RW-RNLP and the fast RW-RNLP. Here, for each request $\mathcal{R}_i$, $m = 18$, $L_i = 100\mu$s, $n_r = 64$, and $|D_i|$ is as shown. Each request was randomly chosen to be a read (as opposed to a write) with probability 0.2 and to be a nested request with probability 0.5. Due to write expansion, $|D_i|$ was inflated to 64 for all write requests under the RW-RNLP, as read requests can access any resource.

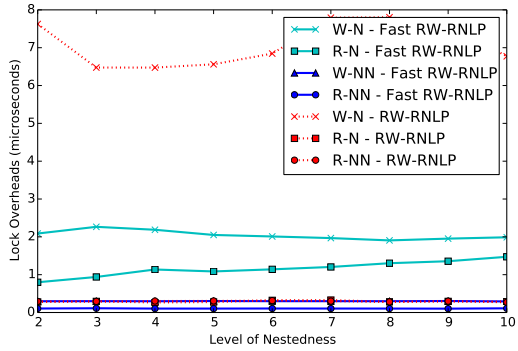

(a) Lock overhead.

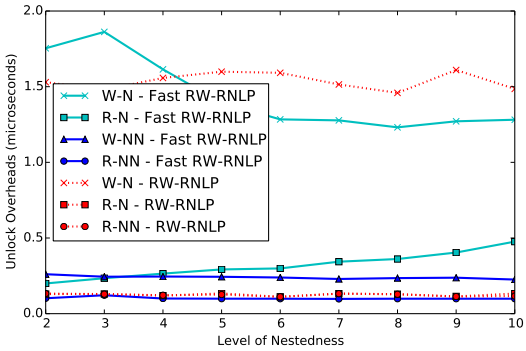

(b) Unlock overhead.

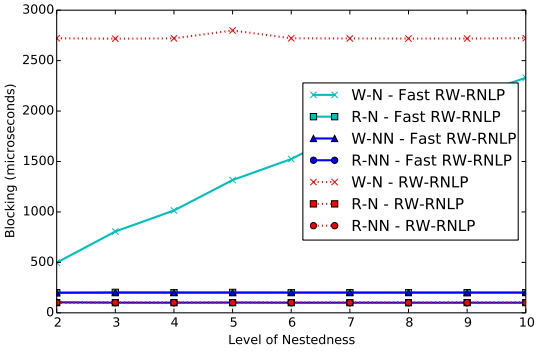

(c) Blocking.

Figure 478: (a) Lock and (b) unlock overheads and (c) blocking for nested and non-nested read and write requests under the RW-RNLP and the fast RW-RNLP. Here, for each request $\mathcal{R}_i$, $m = 18$, $L_i = 100\mu$s, $n_r = 64$, and $|D_i|$ is as shown. Each request was randomly chosen to be a read (as opposed to a write) with probability 0.2 and to be a nested request with probability 0.8. Due to write expansion, $|D_i|$ was inflated to 64 for all write requests under the RW-RNLP, as read requests can access any resource.

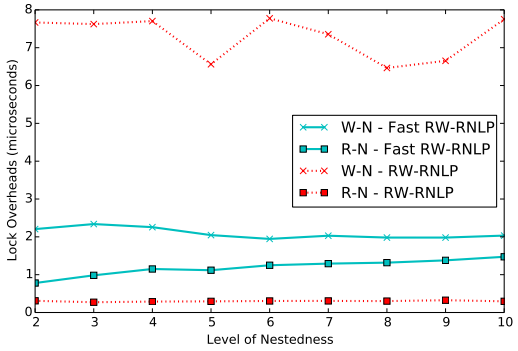

(a) Lock overhead.

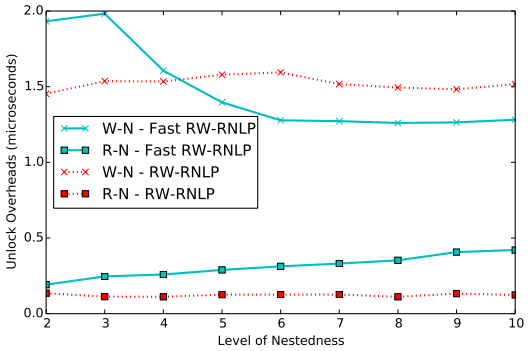

(b) Unlock overhead.

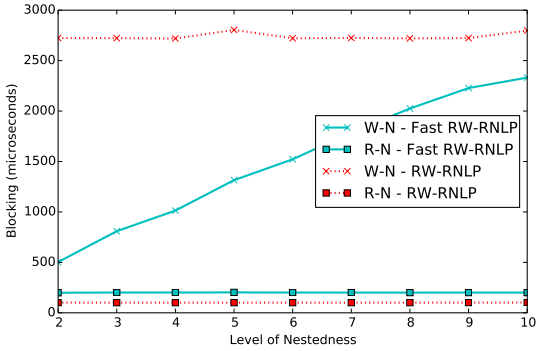

(c) Blocking.

Figure 479: (a) Lock and (b) unlock overheads and (c) blocking for nested read and write requests under the RW-RNLP and the fast RW-RNLP. Here, for each request $\mathcal{R}_i$, $m = 18$, $L_i = 100\mu$s, $n_r = 64$, and $|D_i|$ is as shown. Each request was randomly chosen to be a read (as opposed to a write) with probability 0.2 and to be a nested request with probability 1. Due to write expansion, $|D_i|$ was inflated to 64 for all write requests under the RW-RNLP, as read requests can access any resource.

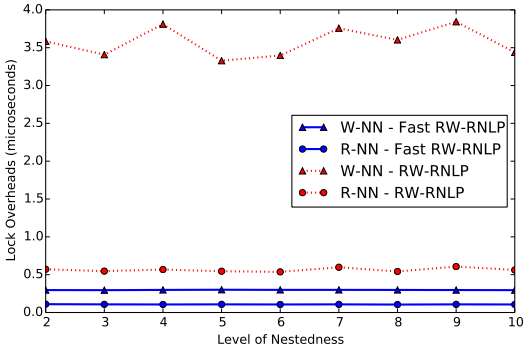

(a) Lock overhead.

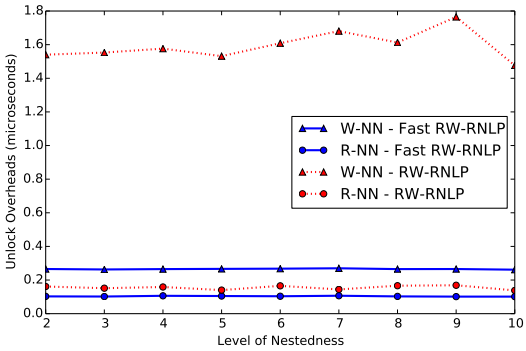

(b) Unlock overhead.

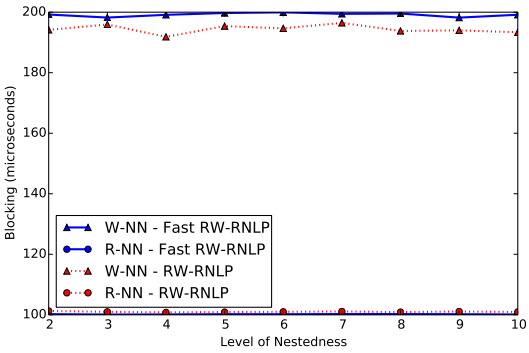

(c) Blocking.

Figure 480: (a) Lock and (b) unlock overheads and (c) blocking for non-nested read and write requests under the RW-RNLP and the fast RW-RNLP. Here, for each request $\mathcal{R}_i$, $m = 18$, $L_i = 100\mu$s, $n_r = 64$, and $|D_i|$ is as shown. Each request was randomly chosen to be a read (as opposed to a write) with probability 0.5 and to be a nested request with probability 0.

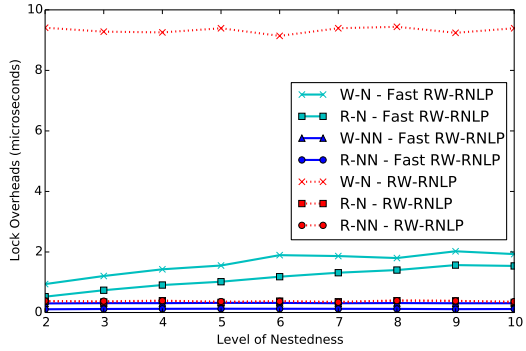

(a) Lock overhead.

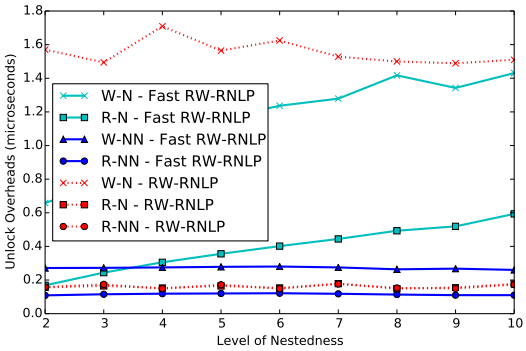

(b) Unlock overhead.

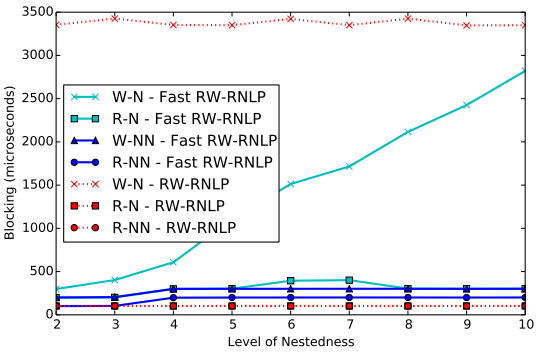

(c) Blocking.

Figure 481: (a) Lock and (b) unlock overheads and (c) blocking for nested and non-nested read and write requests under the RW-RNLP and the fast RW-RNLP. Here, for each request $\mathcal{R}_i$, $m = 18$, $L_i = 100\mu$s, $n_r = 64$, and $|D_i|$ is as shown. Each request was randomly chosen to be a read (as opposed to a write) with probability 0.5 and to be a nested request with probability 0.2. Due to write expansion, $|D_i|$ was inflated to 64 for all write requests under the RW-RNLP, as read requests can access any resource.

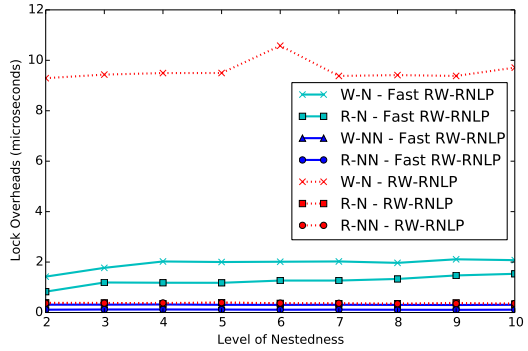

(a) Lock overhead.

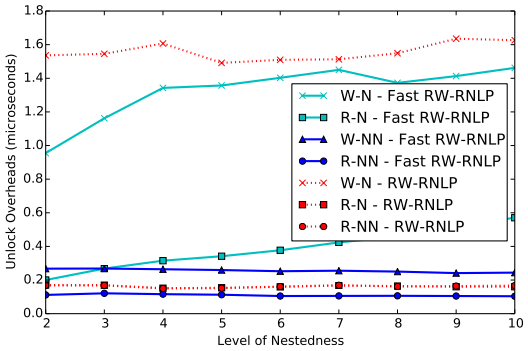

(b) Unlock overhead.

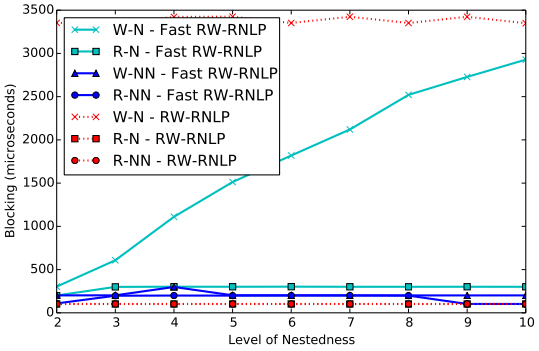

(c) Blocking.

Figure 482: (a) Lock and (b) unlock overheads and (c) blocking for nested and non-nested read and write requests under the RW-RNLP and the fast RW-RNLP. Here, for each request $\mathcal{R}_i$, $m = 18$, $L_i = 100\mu$s, $n_r = 64$, and $|D_i|$ is as shown. Each request was randomly chosen to be a read (as opposed to a write) with probability 0.5 and to be a nested request with probability 0.5. Due to write expansion, $|D_i|$ was inflated to 64 for all write requests under the RW-RNLP, as read requests can access any resource.

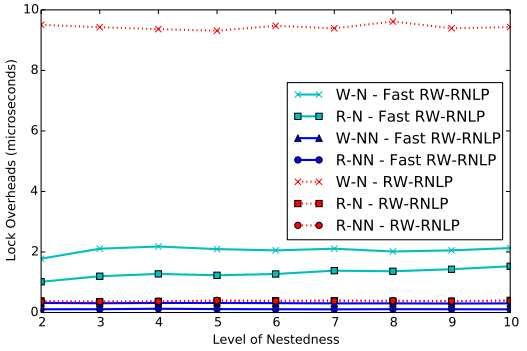

(a) Lock overhead.

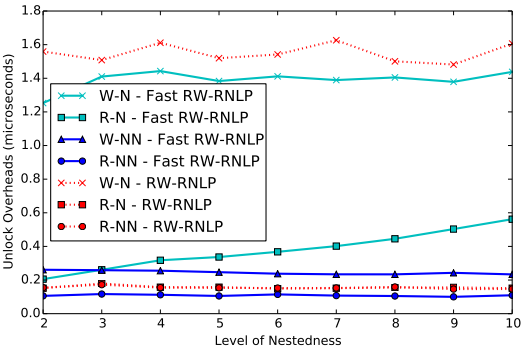

(b) Unlock overhead.

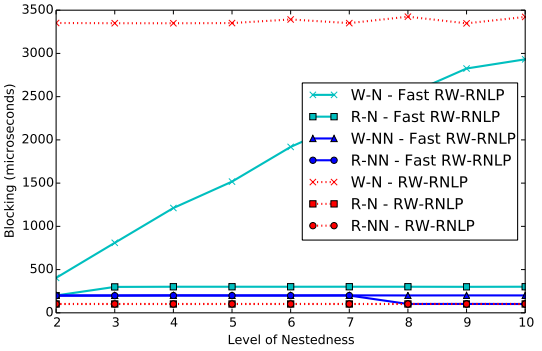

(c) Blocking.

Figure 483: (a) Lock and (b) unlock overheads and (c) blocking for nested and non-nested read and write requests under the RW-RNLP and the fast RW-RNLP. Here, for each request $\mathcal{R}_i$, $m = 18$, $L_i = 100\mu$s, $n_r = 64$, and $|D_i|$ is as shown. Each request was randomly chosen to be a read (as opposed to a write) with probability 0.5 and to be a nested request with probability 0.8. Due to write expansion, $|D_i|$ was inflated to 64 for all write requests under the RW-RNLP, as read requests can access any resource.

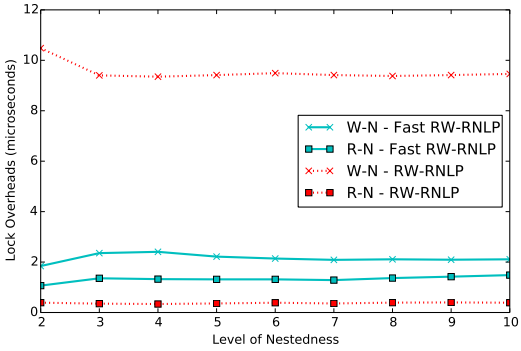

(a) Lock overhead.

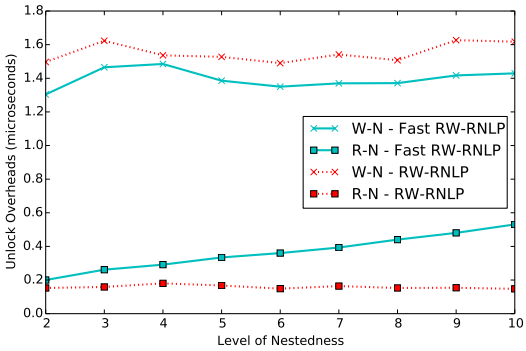

(b) Unlock overhead.

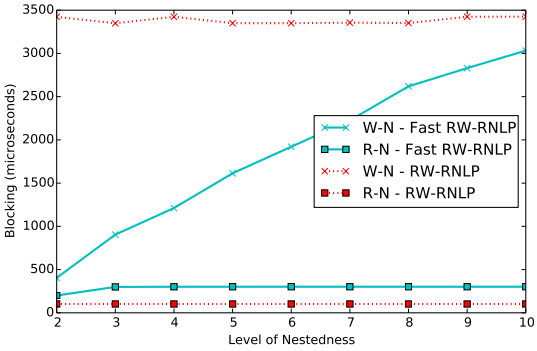

(c) Blocking.

Figure 484: (a) Lock and (b) unlock overheads and (c) blocking for nested read and write requests under the RW-RNLP and the fast RW-RNLP. Here, for each request $\mathcal{R}_i$, $m = 18$, $L_i = 100\mu$s, $n_r = 64$, and $|D_i|$ is as shown. Each request was randomly chosen to be a read (as opposed to a write) with probability 0.5 and to be a nested request with probability 1. Due to write expansion, $|D_i|$ was inflated to 64 for all write requests under the RW-RNLP, as read requests can access any resource.

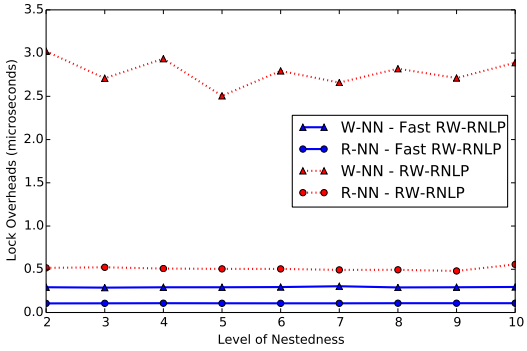

(a) Lock overhead.

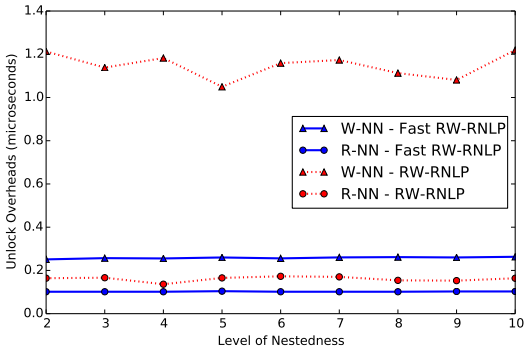

(b) Unlock overhead.

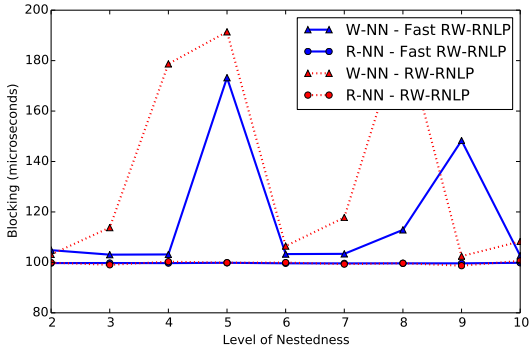

(c) Blocking.

Figure 485: (a) Lock and (b) unlock overheads and (c) blocking for non-nested read and write requests under the RW-RNLP and the fast RW-RNLP. Here, for each request $\mathcal{R}_i$, $m = 18$, $L_i = 100\mu$s, $n_r = 64$, and $|D_i|$ is as shown. Each request was randomly chosen to be a read (as opposed to a write) with probability 0.8 and to be a nested request with probability 0.

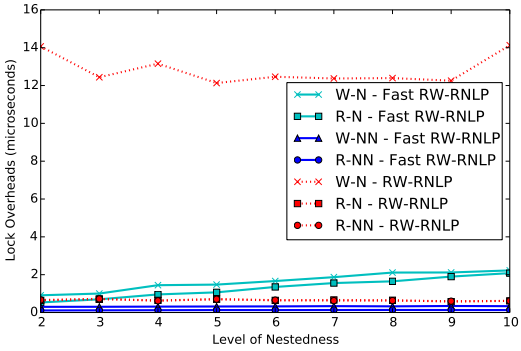

(a) Lock overhead.

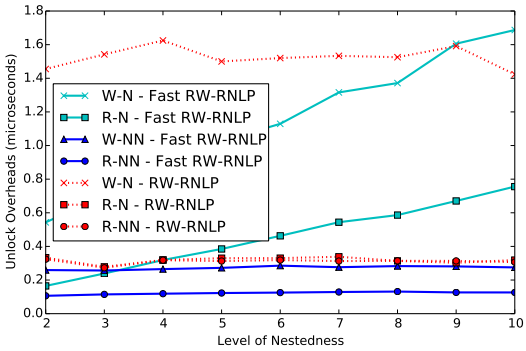

(b) Unlock overhead.

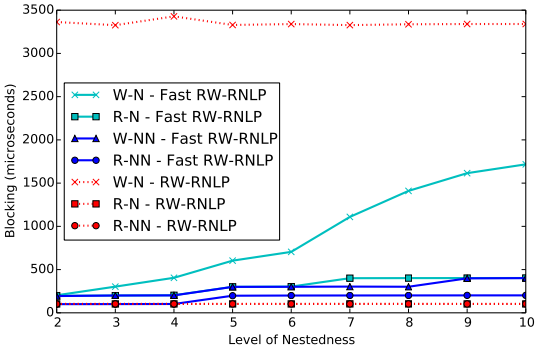

(c) Blocking.

Figure 486: (a) Lock and (b) unlock overheads and (c) blocking for nested and non-nested read and write requests under the RW-RNLP and the fast RW-RNLP. Here, for each request $\mathcal{R}_i$, $m = 18$, $L_i = 100\mu$s, $n_r = 64$, and $|D_i|$ is as shown. Each request was randomly chosen to be a read (as opposed to a write) with probability 0.8 and to be a nested request with probability 0.2. Due to write expansion, $|D_i|$ was inflated to 64 for all write requests under the RW-RNLP, as read requests can access any resource.

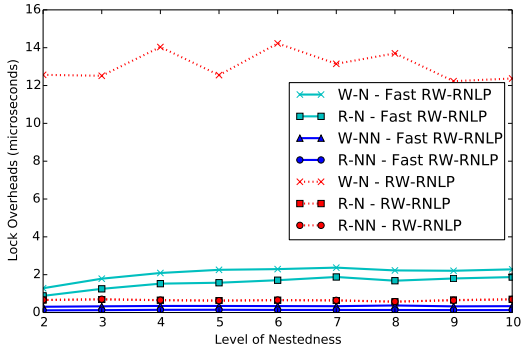

(a) Lock overhead.

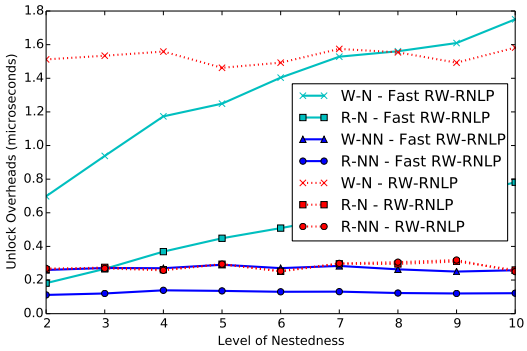

(b) Unlock overhead.

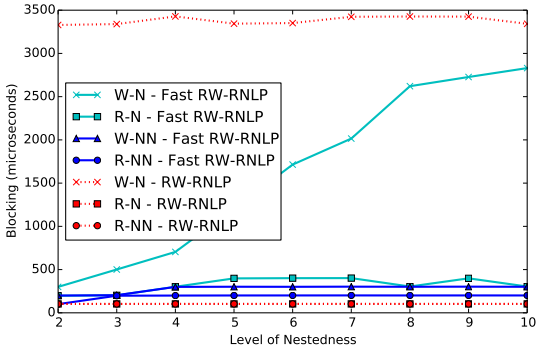

(c) Blocking.

Figure 487: (a) Lock and (b) unlock overheads and (c) blocking for nested and non-nested read and write requests under the RW-RNLP and the fast RW-RNLP. Here, for each request $\mathcal{R}_i$, $m = 18$, $L_i = 100\mu$s, $n_r = 64$, and $|D_i|$ is as shown. Each request was randomly chosen to be a read (as opposed to a write) with probability 0.8 and to be a nested request with probability 0.5. Due to write expansion, $|D_i|$ was inflated to 64 for all write requests under the RW-RNLP, as read requests can access any resource.

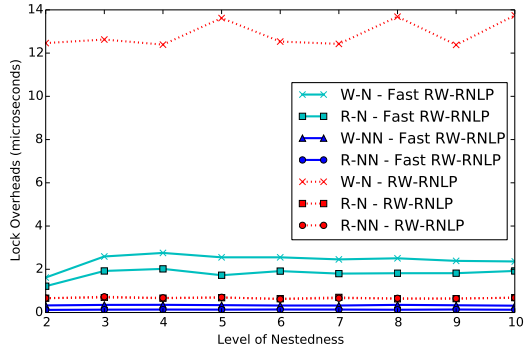

(a) Lock overhead.

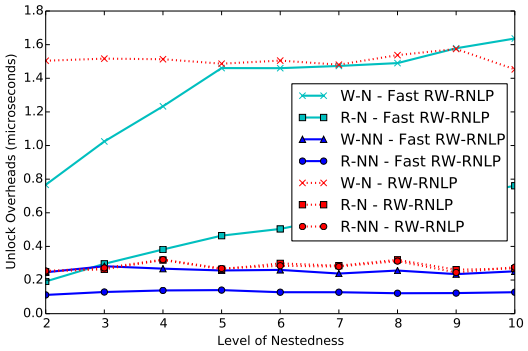

(b) Unlock overhead.

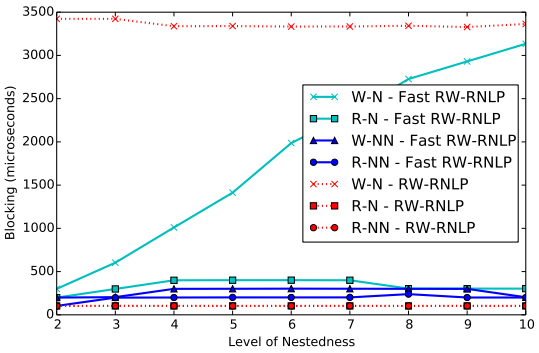

(c) Blocking.

Figure 488: (a) Lock and (b) unlock overheads and (c) blocking for nested and non-nested read and write requests under the RW-RNLP and the fast RW-RNLP. Here, for each request $\mathcal{R}_i$, $m = 18$, $L_i = 100\mu$s, $n_r = 64$, and $|D_i|$ is as shown. Each request was randomly chosen to be a read (as opposed to a write) with probability 0.8 and to be a nested request with probability 0.8. Due to write expansion, $|D_i|$ was inflated to 64 for all write requests under the RW-RNLP, as read requests can access any resource.

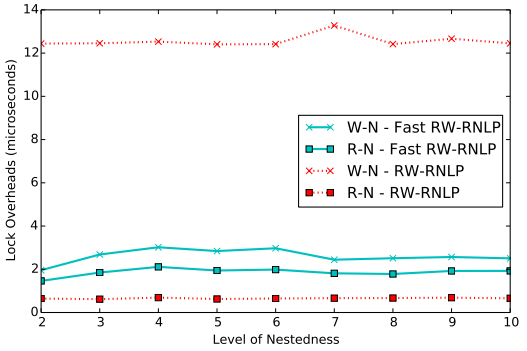

(a) Lock overhead.

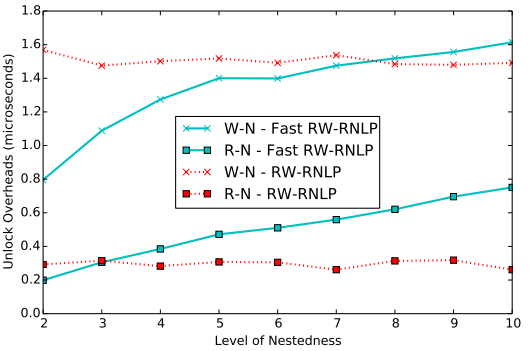

(b) Unlock overhead.

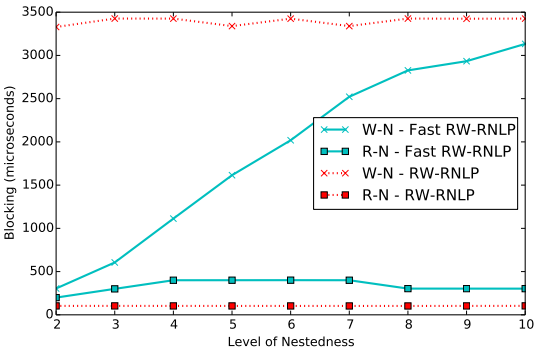

(c) Blocking.

Figure 489: (a) Lock and (b) unlock overheads and (c) blocking for nested read and write requests under the RW-RNLP and the fast RW-RNLP. Here, for each request $\mathcal{R}_i$, $m = 18$, $L_i = 100\mu$s, $n_r = 64$, and $|D_i|$ is as shown. Each request was randomly chosen to be a read (as opposed to a write) with probability 0.8 and to be a nested request with probability 1. Due to write expansion, $|D_i|$ was inflated to 64 for all write requests under the RW-RNLP, as read requests can access any resource.

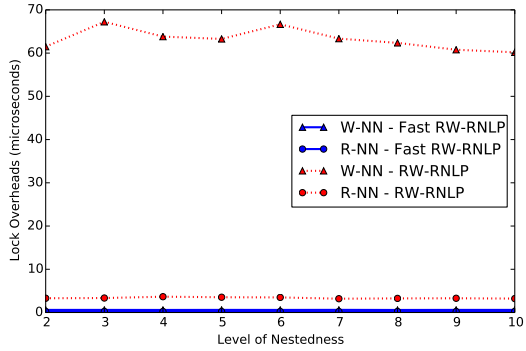

(a) Lock overhead.

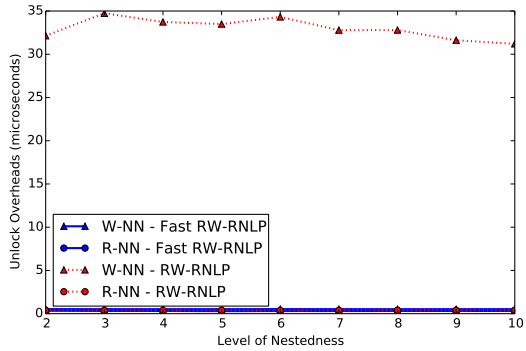

(b) Unlock overhead.

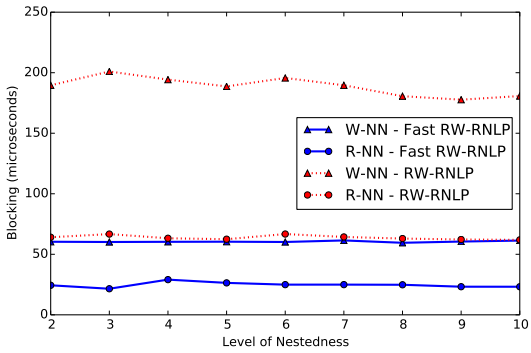

(c) Blocking.

Figure 490: (a) Lock and (b) unlock overheads and (c) blocking for non-nested read and write requests under the RW-RNLP and the fast RW-RNLP. Here, for each request $\mathcal{R}_i$, $m = 36$, $L_i = 20\mu$s, $n_r = 64$, and $|D_i|$ is as shown. Each request was randomly chosen to be a read (as opposed to a write) with probability 0.2 and to be a nested request with probability 0.

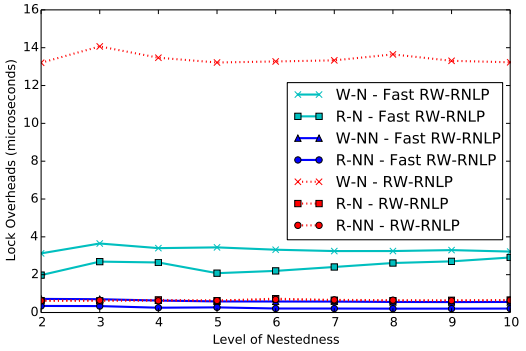

(a) Lock overhead.

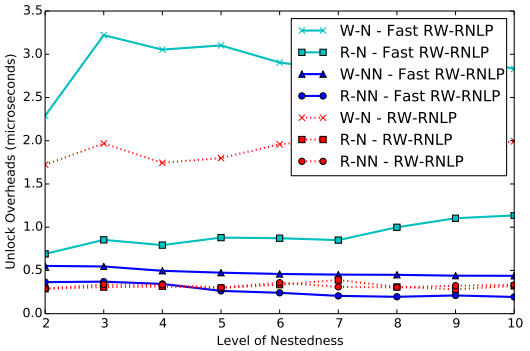

(b) Unlock overhead.

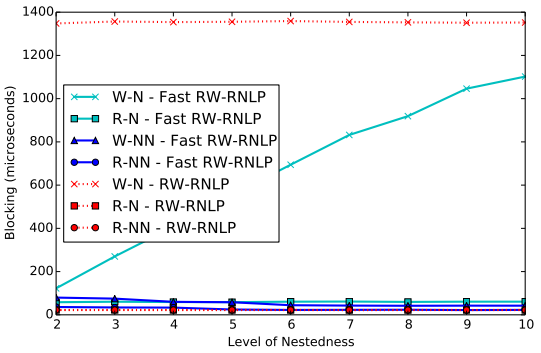

(c) Blocking.

Figure 491: (a) Lock and (b) unlock overheads and (c) blocking for nested and non-nested read and write requests under the RW-RNLP and the fast RW-RNLP. Here, for each request $\mathcal{R}_i$, $m = 36$, $L_i = 20\mu$s, $n_r = 64$, and $|D_i|$ is as shown. Each request was randomly chosen to be a read (as opposed to a write) with probability 0.2 and to be a nested request with probability 0.2. Due to write expansion, $|D_i|$ was inflated to 64 for all write requests under the RW-RNLP, as read requests can access any resource.

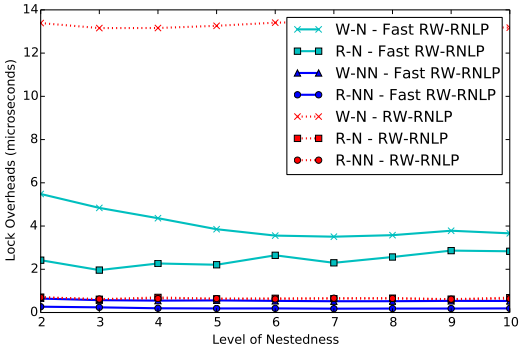

(a) Lock overhead.

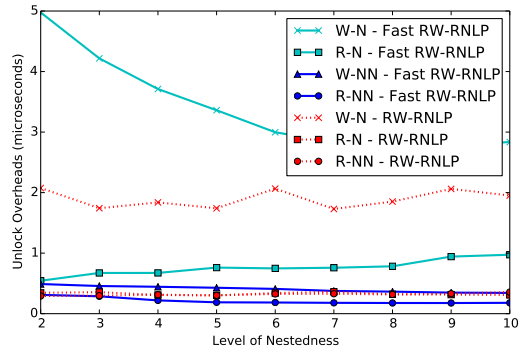

(b) Unlock overhead.

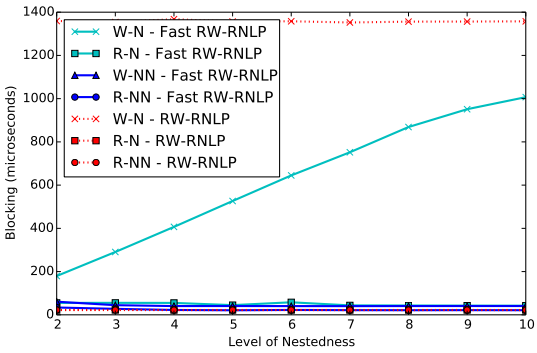

(c) Blocking.

Figure 492: (a) Lock and (b) unlock overheads and (c) blocking for nested and non-nested read and write requests under the RW-RNLP and the fast RW-RNLP. Here, for each request $\mathcal{R}_i$, $m = 36$, $L_i = 20\mu$s, $n_r = 64$, and $|D_i|$ is as shown. Each request was randomly chosen to be a read (as opposed to a write) with probability 0.2 and to be a nested request with probability 0.5. Due to write expansion, $|D_i|$ was inflated to 64 for all write requests under the RW-RNLP, as read requests can access any resource.

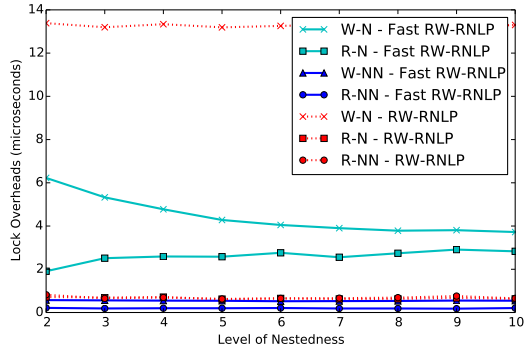

(a) Lock overhead.

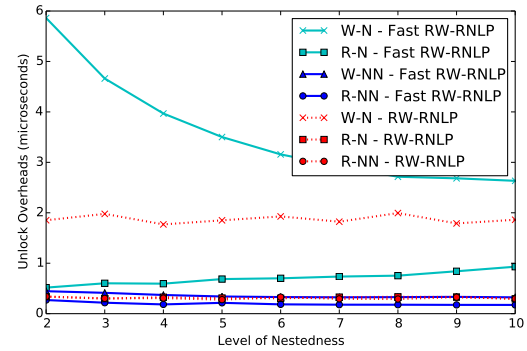

(b) Unlock overhead.

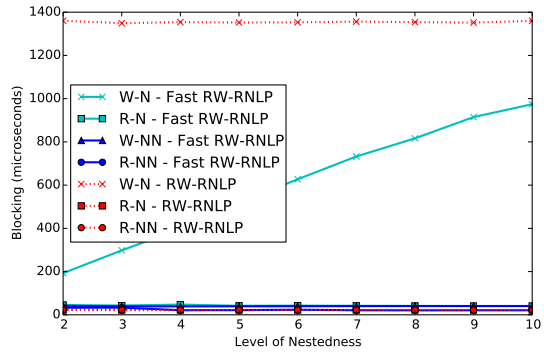

(c) Blocking.

Figure 493: (a) Lock and (b) unlock overheads and (c) blocking for nested and non-nested read and write requests under the RW-RNLP and the fast RW-RNLP. Here, for each request $\mathcal{R}_i$, $m = 36$, $L_i = 20\mu$s, $n_r = 64$, and $|D_i|$ is as shown. Each request was randomly chosen to be a read (as opposed to a write) with probability 0.2 and to be a nested request with probability 0.8. Due to write expansion, $|D_i|$ was inflated to 64 for all write requests under the RW-RNLP, as read requests can access any resource.

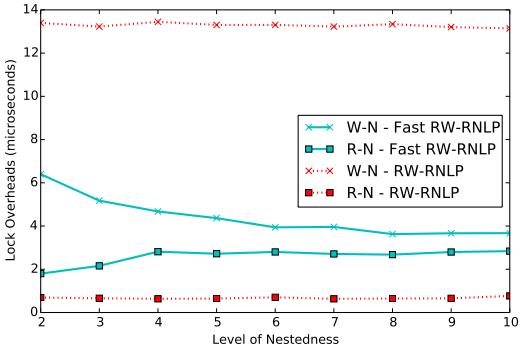

(a) Lock overhead.

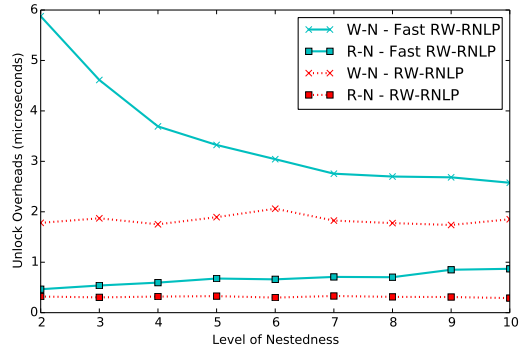

(b) Unlock overhead.

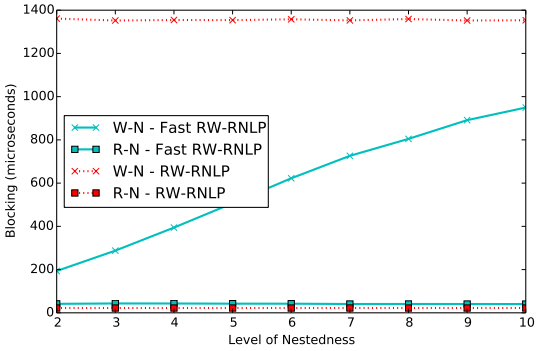

(c) Blocking.

Figure 494: (a) Lock and (b) unlock overheads and (c) blocking for nested read and write requests under the RW-RNLP and the fast RW-RNLP. Here, for each request $\mathcal{R}_i$, $m = 36$, $L_i = 20\mu$s, $n_r = 64$, and $|D_i|$ is as shown. Each request was randomly chosen to be a read (as opposed to a write) with probability 0.2 and to be a nested request with probability 1. Due to write expansion, $|D_i|$ was inflated to 64 for all write requests under the RW-RNLP, as read requests can access any resource.

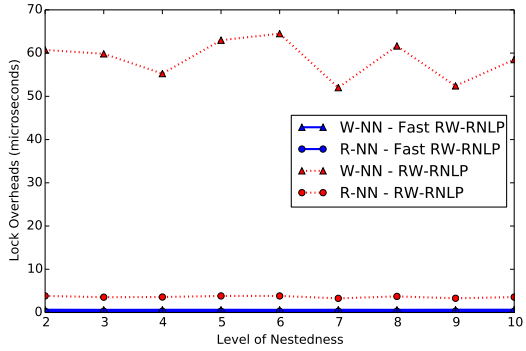

(a) Lock overhead.

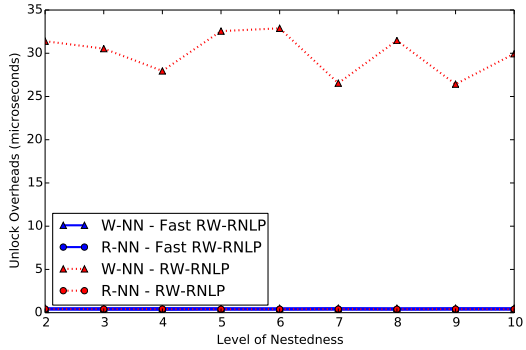

(b) Unlock overhead.

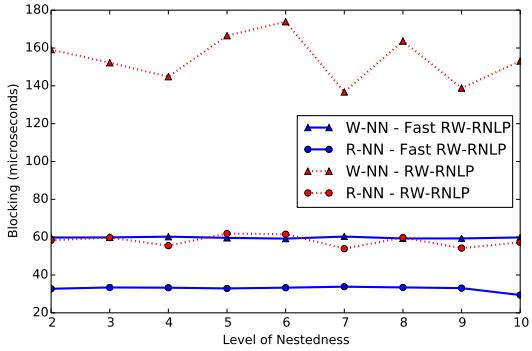

(c) Blocking.

Figure 495: (a) Lock and (b) unlock overheads and (c) blocking for non-nested read and write requests under the RW-RNLP and the fast RW-RNLP. Here, for each request $\mathcal{R}_i$, $m = 36$, $L_i = 20\mu$s, $n_r = 64$, and $|D_i|$ is as shown. Each request was randomly chosen to be a read (as opposed to a write) with probability 0.5 and to be a nested request with probability 0.

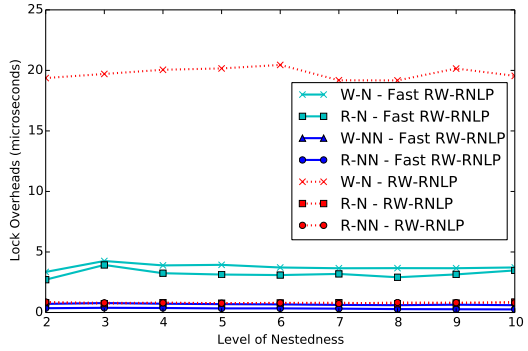

(a) Lock overhead.

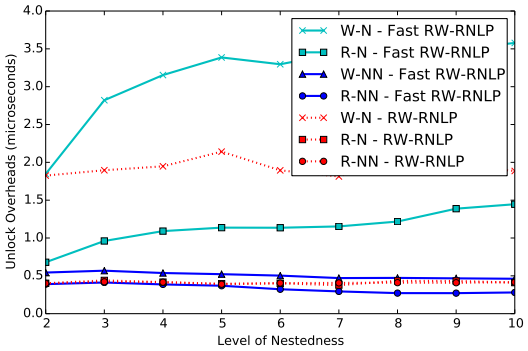

(b) Unlock overhead.

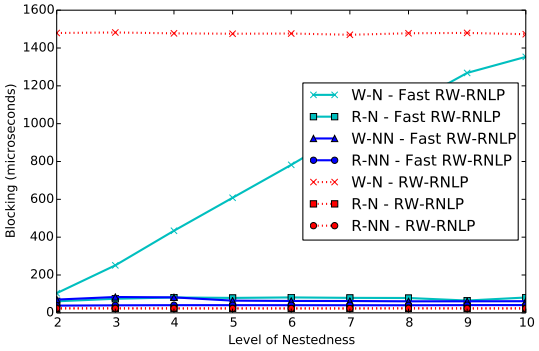

(c) Blocking.

Figure 496: (a) Lock and (b) unlock overheads and (c) blocking for nested and non-nested read and write requests under the RW-RNLP and the fast RW-RNLP. Here, for each request $\mathcal{R}_i$, $m = 36$, $L_i = 20\mu$s, $n_r = 64$, and $|D_i|$ is as shown. Each request was randomly chosen to be a read (as opposed to a write) with probability 0.5 and to be a nested request with probability 0.2. Due to write expansion, $|D_i|$ was inflated to 64 for all write requests under the RW-RNLP, as read requests can access any resource.

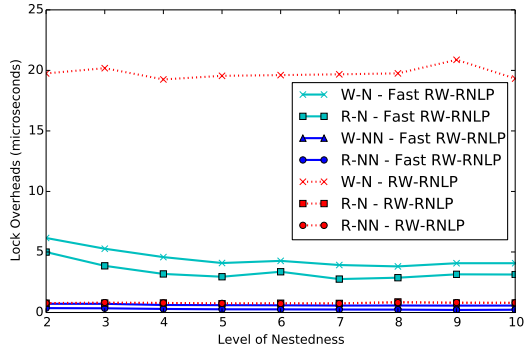

(a) Lock overhead.

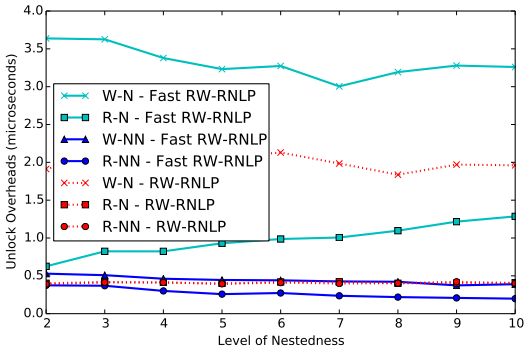

(b) Unlock overhead.

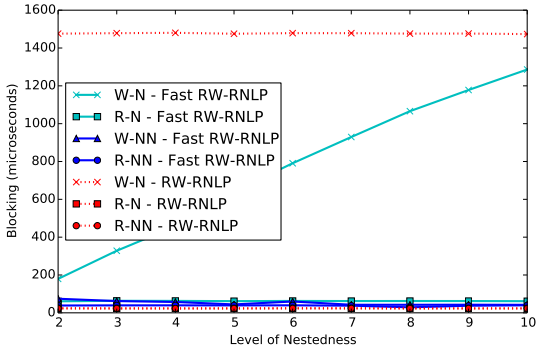

(c) Blocking.

Figure 497: (a) Lock and (b) unlock overheads and (c) blocking for nested and non-nested read and write requests under the RW-RNLP and the fast RW-RNLP. Here, for each request $\mathcal{R}_i$, $m = 36$, $L_i = 20\mu$s, $n_r = 64$, and $|D_i|$ is as shown. Each request was randomly chosen to be a read (as opposed to a write) with probability 0.5 and to be a nested request with probability 0.5. Due to write expansion, $|D_i|$ was inflated to 64 for all write requests under the RW-RNLP, as read requests can access any resource.

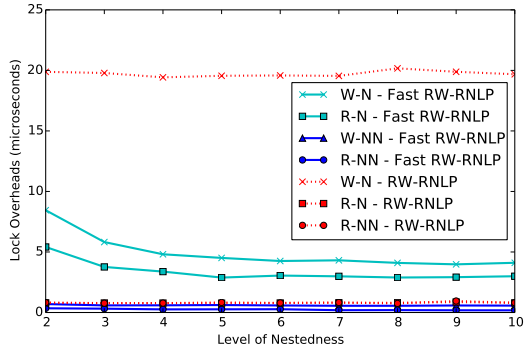

(a) Lock overhead.

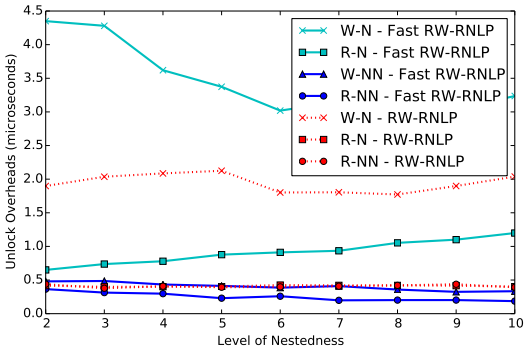

(b) Unlock overhead.

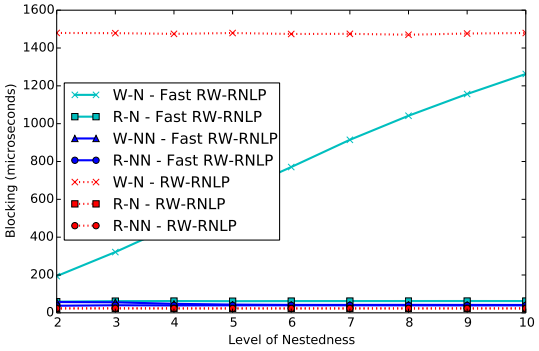

(c) Blocking.

Figure 498: (a) Lock and (b) unlock overheads and (c) blocking for nested and non-nested read and write requests under the RW-RNLP and the fast RW-RNLP. Here, for each request $\mathcal{R}_i$, $m = 36$, $L_i = 20\mu$s, $n_r = 64$, and $|D_i|$ is as shown. Each request was randomly chosen to be a read (as opposed to a write) with probability 0.5 and to be a nested request with probability 0.8. Due to write expansion, $|D_i|$ was inflated to 64 for all write requests under the RW-RNLP, as read requests can access any resource.

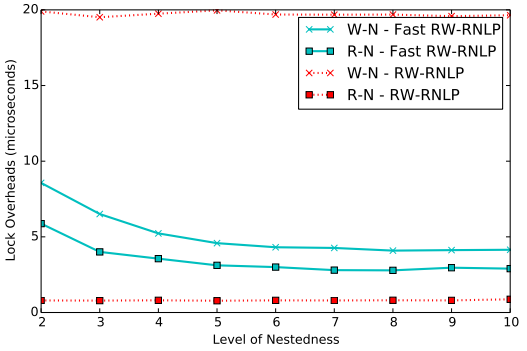

(a) Lock overhead.

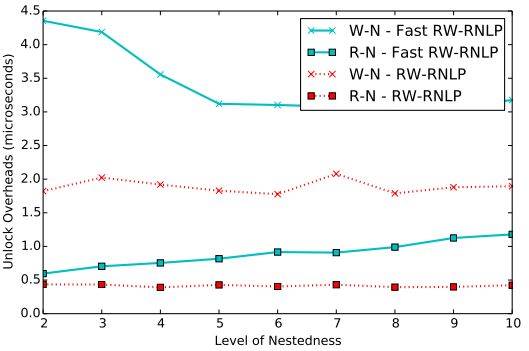

(b) Unlock overhead.

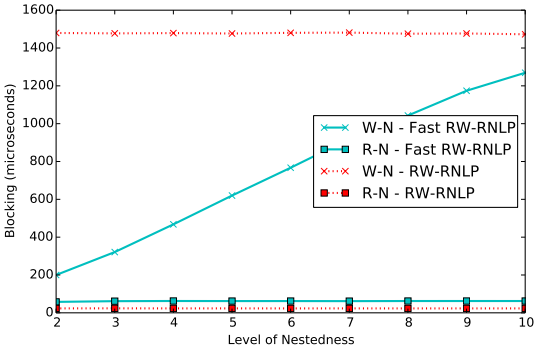

(c) Blocking.

Figure 499: (a) Lock and (b) unlock overheads and (c) blocking for nested read and write requests under the RW-RNLP and the fast RW-RNLP. Here, for each request $\mathcal{R}_i$, $m = 36$, $L_i = 20\mu$s, $n_r = 64$, and $|D_i|$ is as shown. Each request was randomly chosen to be a read (as opposed to a write) with probability 0.5 and to be a nested request with probability 1. Due to write expansion, $|D_i|$ was inflated to 64 for all write requests under the RW-RNLP, as read requests can access any resource.

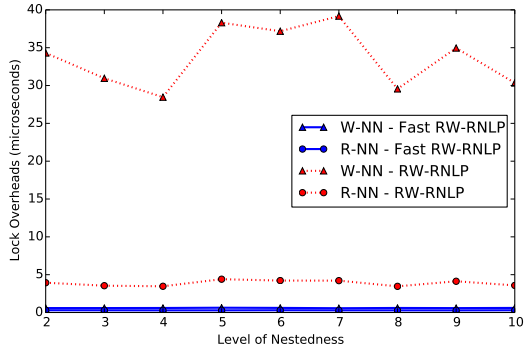

(a) Lock overhead.

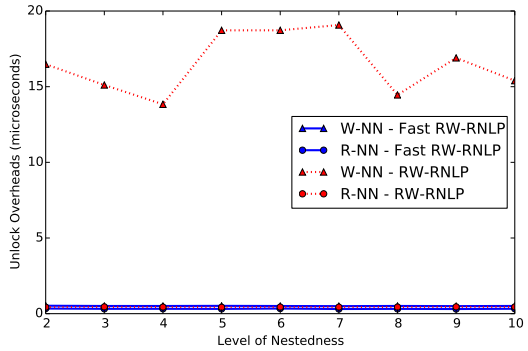

(b) Unlock overhead.

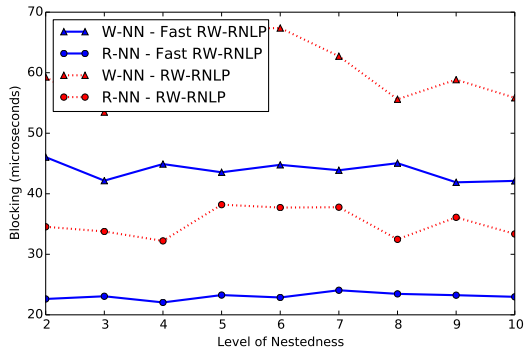

(c) Blocking.

Figure 500: (a) Lock and (b) unlock overheads and (c) blocking for non-nested read and write requests under the RW-RNLP and the fast RW-RNLP. Here, for each request $\mathcal{R}_i$, $m = 36$, $L_i = 20\mu$s, $n_r = 64$, and $|D_i|$ is as shown. Each request was randomly chosen to be a read (as opposed to a write) with probability 0.8 and to be a nested request with probability 0.

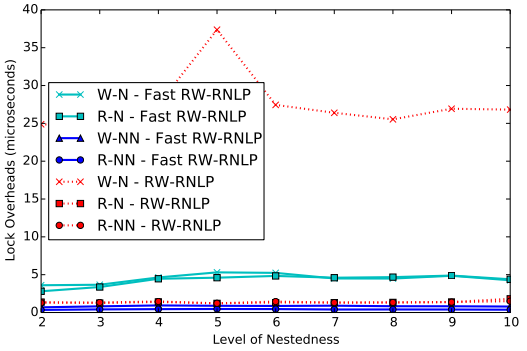

(a) Lock overhead.

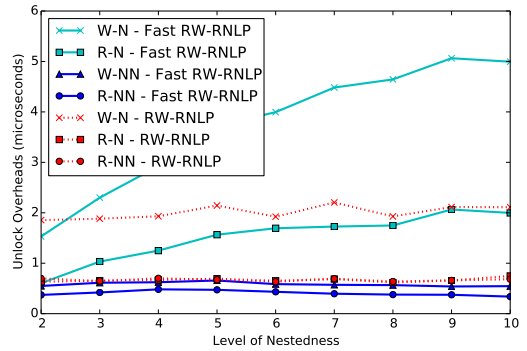

(b) Unlock overhead.

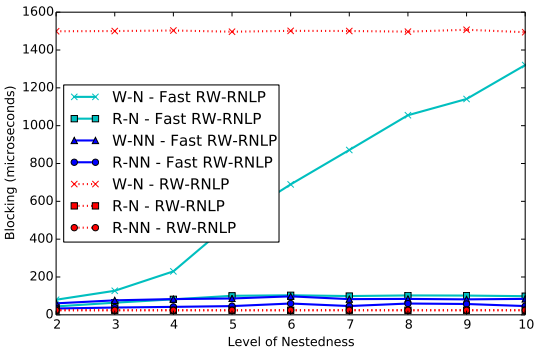

(c) Blocking.

Figure 501: (a) Lock and (b) unlock overheads and (c) blocking for nested and non-nested read and write requests under the RW-RNLP and the fast RW-RNLP. Here, for each request $\mathcal{R}_i$, $m = 36$, $L_i = 20\mu$s, $n_r = 64$, and $|D_i|$ is as shown. Each request was randomly chosen to be a read (as opposed to a write) with probability 0.8 and to be a nested request with probability 0.2. Due to write expansion, $|D_i|$ was inflated to 64 for all write requests under the RW-RNLP, as read requests can access any resource.

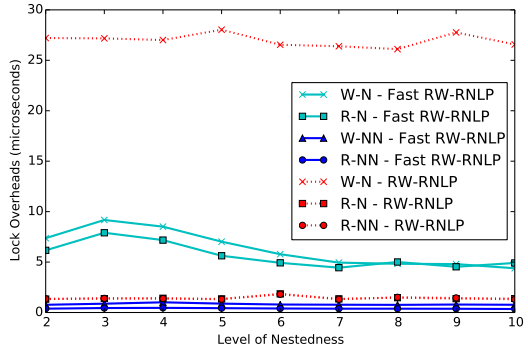

(a) Lock overhead.

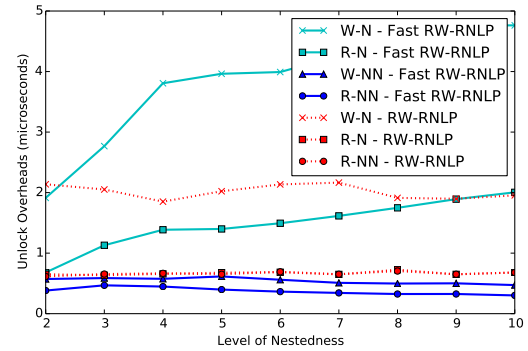

(b) Unlock overhead.

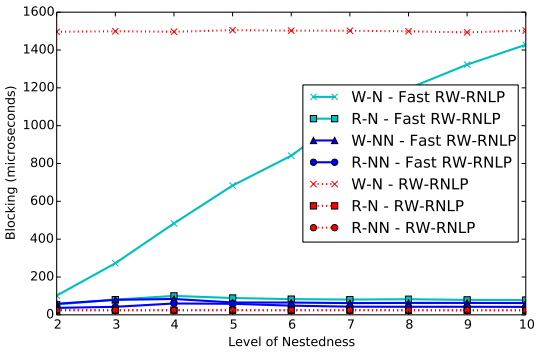

(c) Blocking.

Figure 502: (a) Lock and (b) unlock overheads and (c) blocking for nested and non-nested read and write requests under the RW-RNLP and the fast RW-RNLP. Here, for each request $\mathcal{R}_i$, $m = 36$, $L_i = 20\mu$s, $n_r = 64$, and $|D_i|$ is as shown. Each request was randomly chosen to be a read (as opposed to a write) with probability 0.8 and to be a nested request with probability 0.5. Due to write expansion, $|D_i|$ was inflated to 64 for all write requests under the RW-RNLP, as read requests can access any resource.

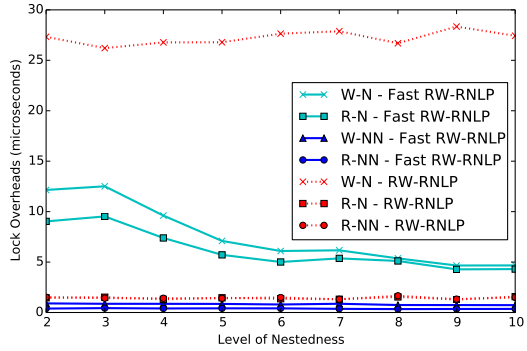

(a) Lock overhead.

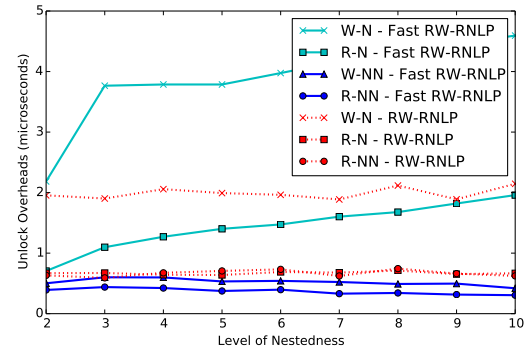

(b) Unlock overhead.

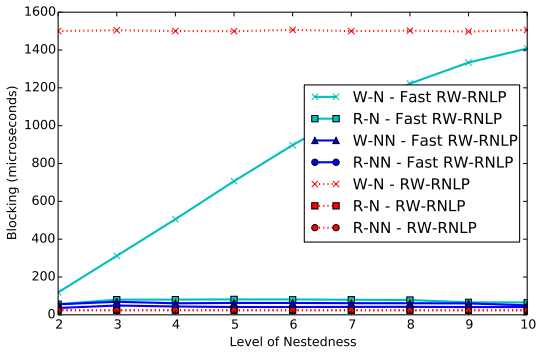

(c) Blocking.

Figure 503: (a) Lock and (b) unlock overheads and (c) blocking for nested and non-nested read and write requests under the RW-RNLP and the fast RW-RNLP. Here, for each request $\mathcal{R}_i$, $m = 36$, $L_i = 20\mu$s, $n_r = 64$, and $|D_i|$ is as shown. Each request was randomly chosen to be a read (as opposed to a write) with probability 0.8 and to be a nested request with probability 0.8. Due to write expansion, $|D_i|$ was inflated to 64 for all write requests under the RW-RNLP, as read requests can access any resource.

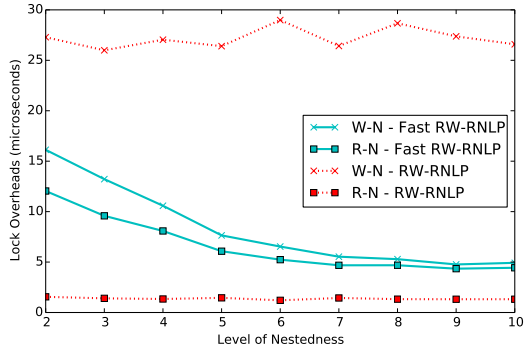

(a) Lock overhead.

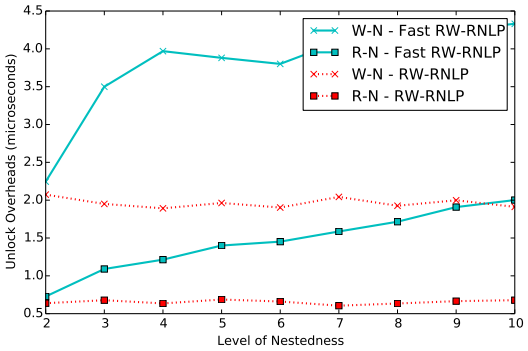

(b) Unlock overhead.

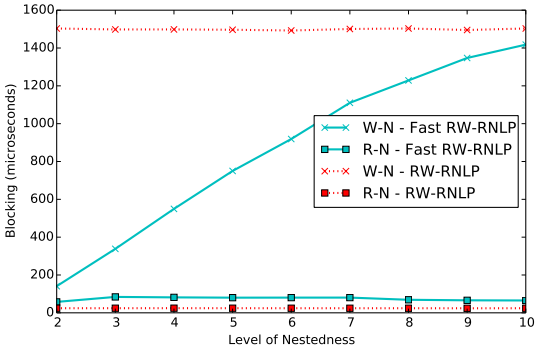

(c) Blocking.

Figure 504: (a) Lock and (b) unlock overheads and (c) blocking for nested read and write requests under the RW-RNLP and the fast RW-RNLP. Here, for each request $\mathcal{R}_i$, $m = 36$, $L_i = 20\mu$s, $n_r = 64$, and $|D_i|$ is as shown. Each request was randomly chosen to be a read (as opposed to a write) with probability 0.8 and to be a nested request with probability 1. Due to write expansion, $|D_i|$ was inflated to 64 for all write requests under the RW-RNLP, as read requests can access any resource.

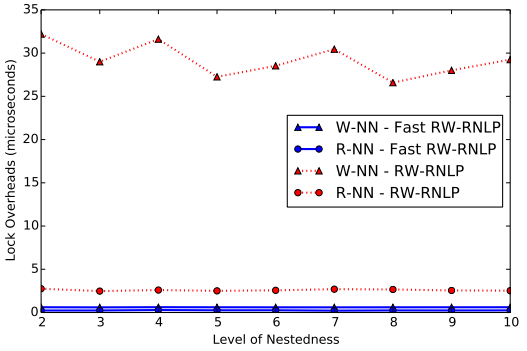

(a) Lock overhead.

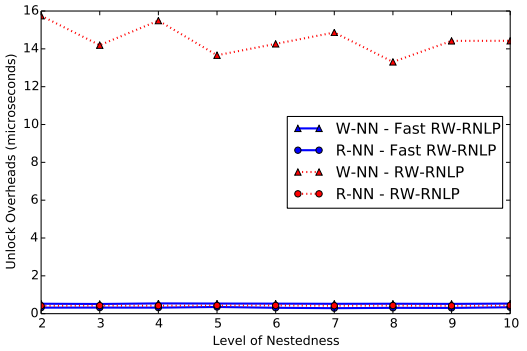

(b) Unlock overhead.

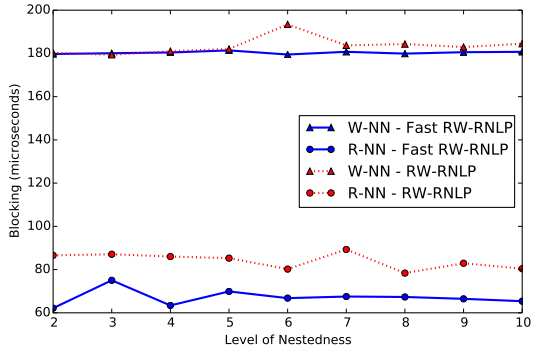

(c) Blocking.

Figure 505: (a) Lock and (b) unlock overheads and (c) blocking for non-nested read and write requests under the RW-RNLP and the fast RW-RNLP. Here, for each request $\mathcal{R}_i$, $m = 36$, $L_i = 60\mu$s, $n_r = 64$, and $|D_i|$ is as shown. Each request was randomly chosen to be a read (as opposed to a write) with probability 0.2 and to be a nested request with probability 0.

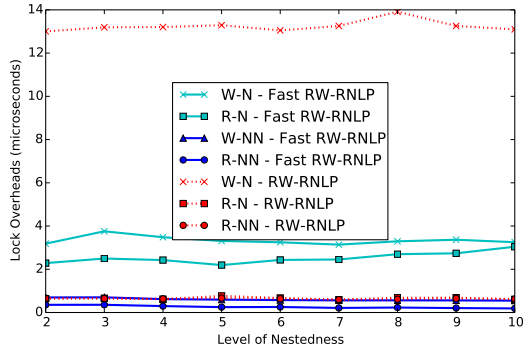

(a) Lock overhead.

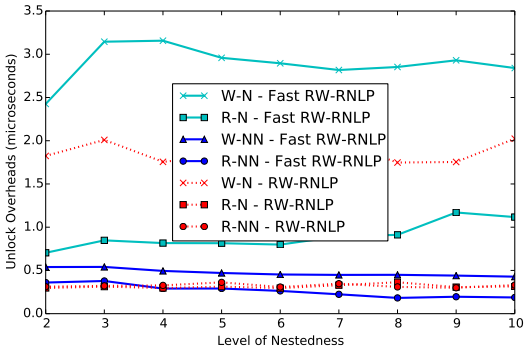

(b) Unlock overhead.

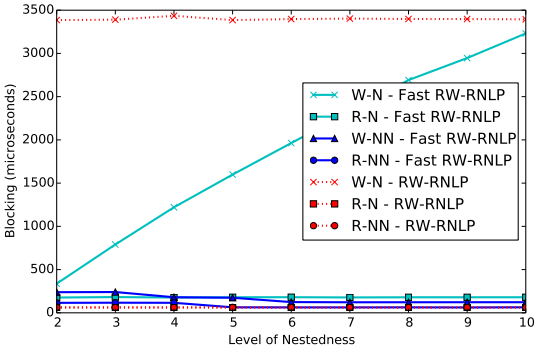

(c) Blocking.

Figure 506: (a) Lock and (b) unlock overheads and (c) blocking for nested and non-nested read and write requests under the RW-RNLP and the fast RW-RNLP. Here, for each request $\mathcal{R}_i$, $m = 36$, $L_i = 60\mu$s, $n_r = 64$, and $|D_i|$ is as shown. Each request was randomly chosen to be a read (as opposed to a write) with probability 0.2 and to be a nested request with probability 0.2. Due to write expansion, $|D_i|$ was inflated to 64 for all write requests under the RW-RNLP, as read requests can access any resource.

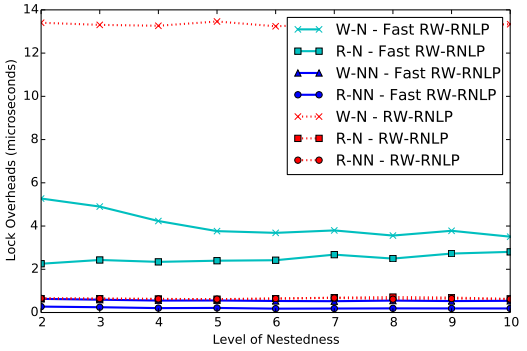

(a) Lock overhead.

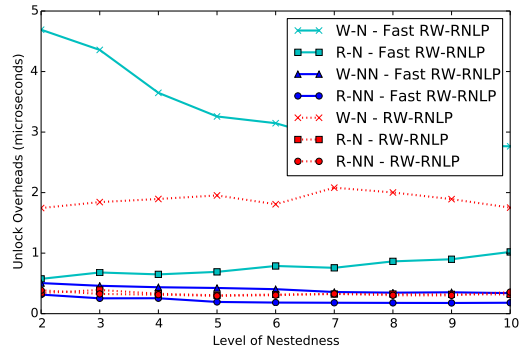

(b) Unlock overhead.

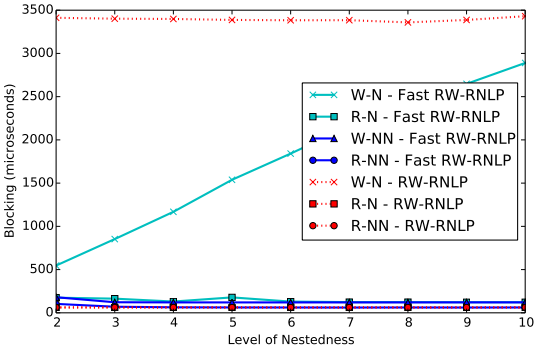

(c) Blocking.

Figure 507: (a) Lock and (b) unlock overheads and (c) blocking for nested and non-nested read and write requests under the RW-RNLP and the fast RW-RNLP. Here, for each request $\mathcal{R}_i$, $m = 36$, $L_i = 60\mu$s, $n_r = 64$, and $|D_i|$ is as shown. Each request was randomly chosen to be a read (as opposed to a write) with probability 0.2 and to be a nested request with probability 0.5. Due to write expansion, $|D_i|$ was inflated to 64 for all write requests under the RW-RNLP, as read requests can access any resource.

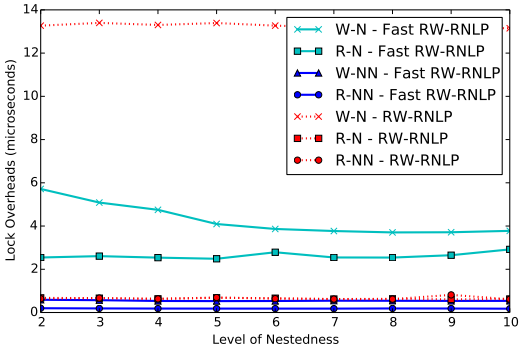

(a) Lock overhead.

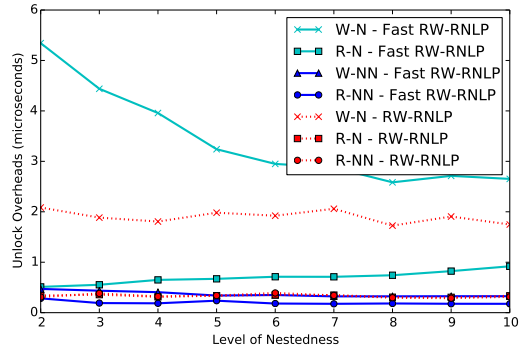

(b) Unlock overhead.

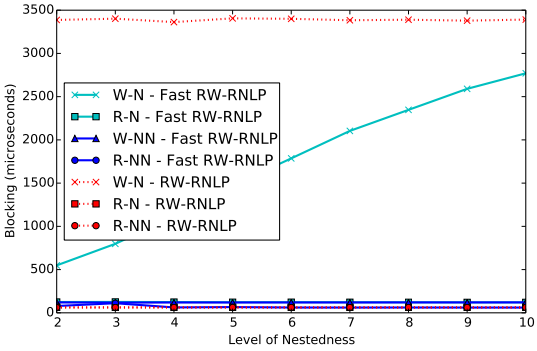

(c) Blocking.

Figure 508: (a) Lock and (b) unlock overheads and (c) blocking for nested and non-nested read and write requests under the RW-RNLP and the fast RW-RNLP. Here, for each request $\mathcal{R}_i$, $m = 36$, $L_i = 60\mu$s, $n_r = 64$, and $|D_i|$ is as shown. Each request was randomly chosen to be a read (as opposed to a write) with probability 0.2 and to be a nested request with probability 0.8. Due to write expansion, $|D_i|$ was inflated to 64 for all write requests under the RW-RNLP, as read requests can access any resource.

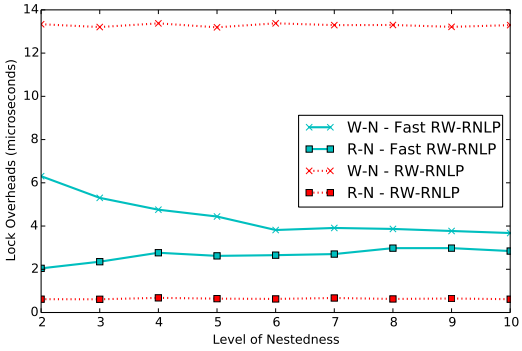

(a) Lock overhead.

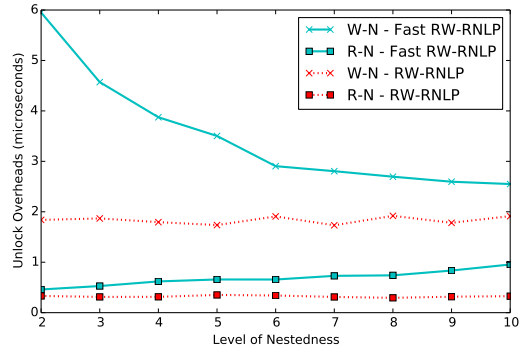

(b) Unlock overhead.

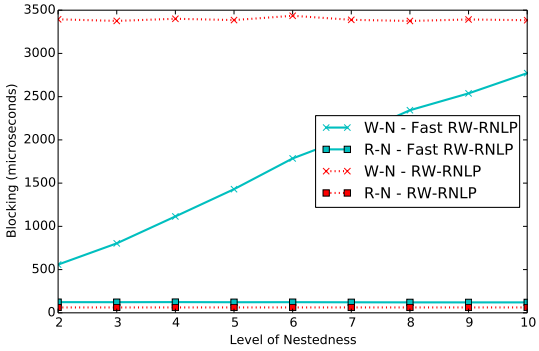

(c) Blocking.

Figure 509: (a) Lock and (b) unlock overheads and (c) blocking for nested read and write requests under the RW-RNLP and the fast RW-RNLP. Here, for each request $\mathcal{R}_i$, $m = 36$, $L_i = 60\mu$s, $n_r = 64$, and $|D_i|$ is as shown. Each request was randomly chosen to be a read (as opposed to a write) with probability 0.2 and to be a nested request with probability 1. Due to write expansion, $|D_i|$ was inflated to 64 for all write requests under the RW-RNLP, as read requests can access any resource.

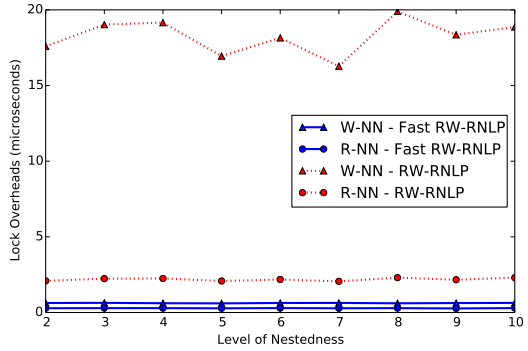

(a) Lock overhead.

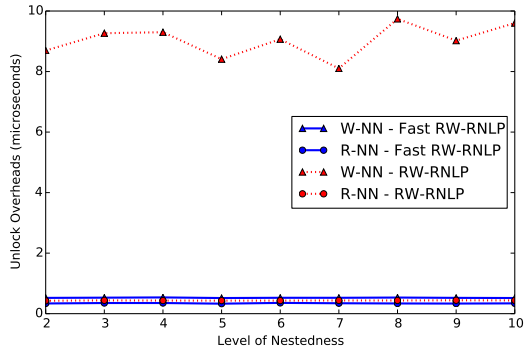

(b) Unlock overhead.

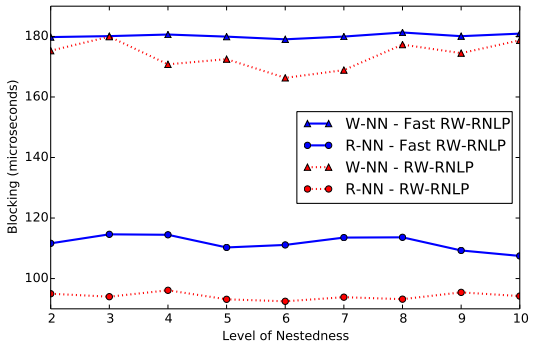

(c) Blocking.

Figure 510: (a) Lock and (b) unlock overheads and (c) blocking for non-nested read and write requests under the RW-RNLP and the fast RW-RNLP. Here, for each request $\mathcal{R}_i$, $m = 36$, $L_i = 60\mu$s, $n_r = 64$, and $|D_i|$ is as shown. Each request was randomly chosen to be a read (as opposed to a write) with probability 0.5 and to be a nested request with probability 0.

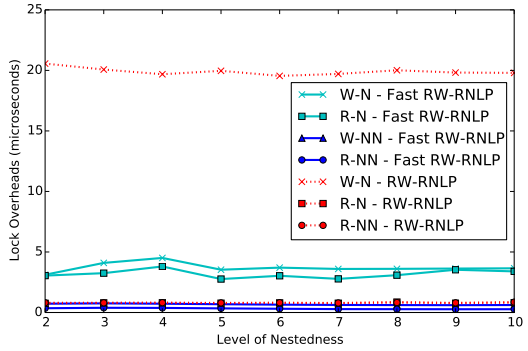

(a) Lock overhead.

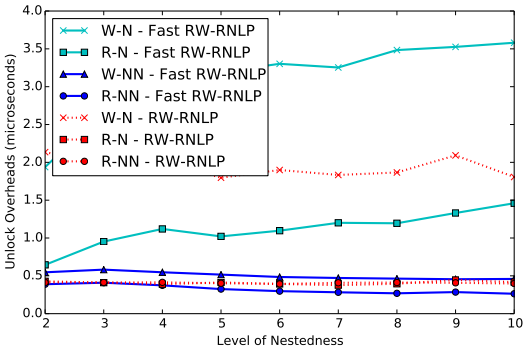

(b) Unlock overhead.

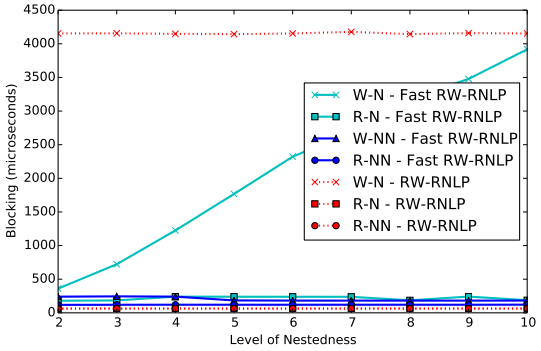

(c) Blocking.

Figure 511: (a) Lock and (b) unlock overheads and (c) blocking for nested and non-nested read and write requests under the RW-RNLP and the fast RW-RNLP. Here, for each request $\mathcal{R}_i$, $m = 36$, $L_i = 60\mu$s, $n_r = 64$, and $|D_i|$ is as shown. Each request was randomly chosen to be a read (as opposed to a write) with probability 0.5 and to be a nested request with probability 0.2. Due to write expansion, $|D_i|$ was inflated to 64 for all write requests under the RW-RNLP, as read requests can access any resource.

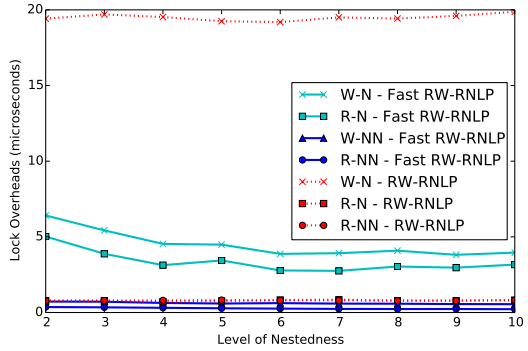

(a) Lock overhead.

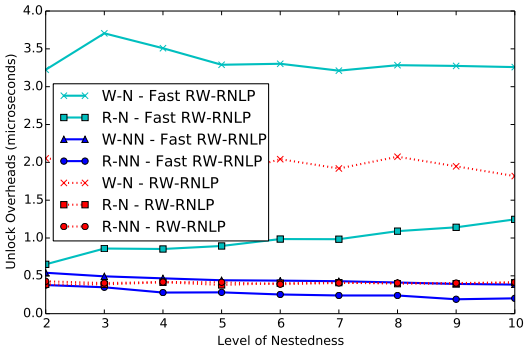

(b) Unlock overhead.

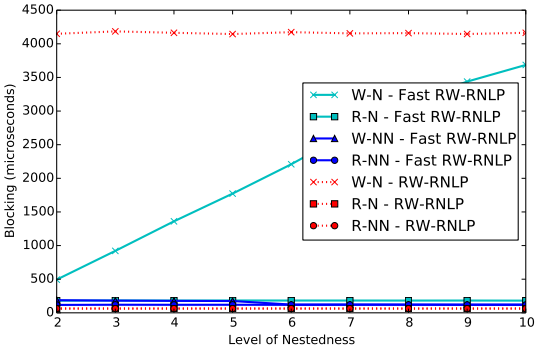

(c) Blocking.

Figure 512: (a) Lock and (b) unlock overheads and (c) blocking for nested and non-nested read and write requests under the RW-RNLP and the fast RW-RNLP. Here, for each request $\mathcal{R}_i$, $m = 36$, $L_i = 60\mu$s, $n_r = 64$, and $|D_i|$ is as shown. Each request was randomly chosen to be a read (as opposed to a write) with probability 0.5 and to be a nested request with probability 0.5. Due to write expansion, $|D_i|$ was inflated to 64 for all write requests under the RW-RNLP, as read requests can access any resource.

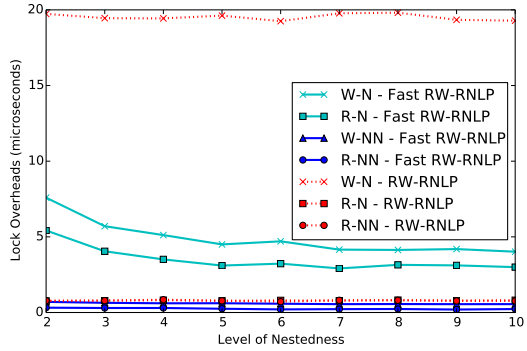

(a) Lock overhead.

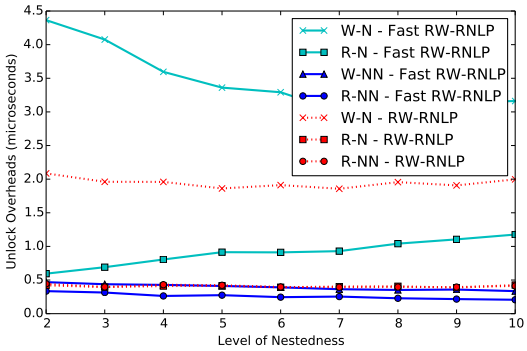

(b) Unlock overhead.

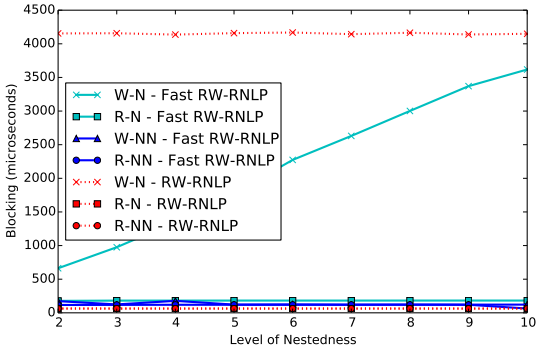

(c) Blocking.

Figure 513: (a) Lock and (b) unlock overheads and (c) blocking for nested and non-nested read and write requests under the RW-RNLP and the fast RW-RNLP. Here, for each request $\mathcal{R}_i$, $m = 36$, $L_i = 60\mu$s, $n_r = 64$, and $|D_i|$ is as shown. Each request was randomly chosen to be a read (as opposed to a write) with probability 0.5 and to be a nested request with probability 0.8. Due to write expansion, $|D_i|$ was inflated to 64 for all write requests under the RW-RNLP, as read requests can access any resource.

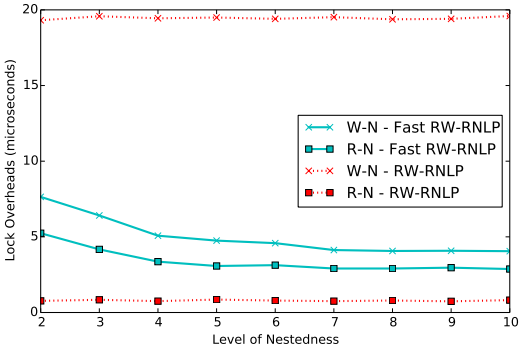

(a) Lock overhead.

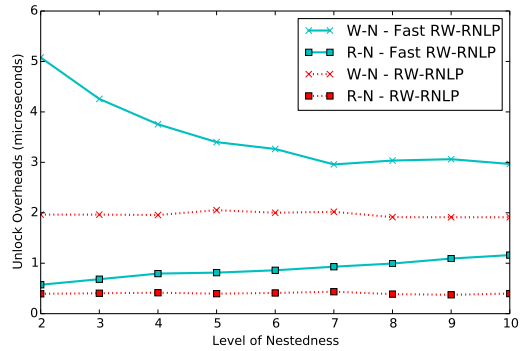

(b) Unlock overhead.

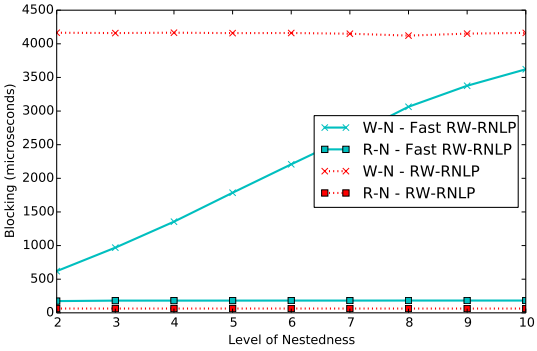

(c) Blocking.

Figure 514: (a) Lock and (b) unlock overheads and (c) blocking for nested read and write requests under the RW-RNLP and the fast RW-RNLP. Here, for each request $\mathcal{R}_i$, $m = 36$, $L_i = 60\mu$s, $n_r = 64$, and $|D_i|$ is as shown. Each request was randomly chosen to be a read (as opposed to a write) with probability 0.5 and to be a nested request with probability 1. Due to write expansion, $|D_i|$ was inflated to 64 for all write requests under the RW-RNLP, as read requests can access any resource.

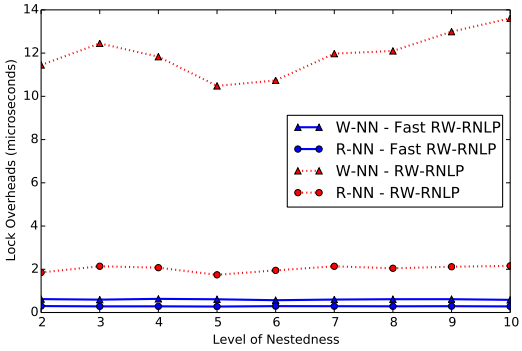

(a) Lock overhead.

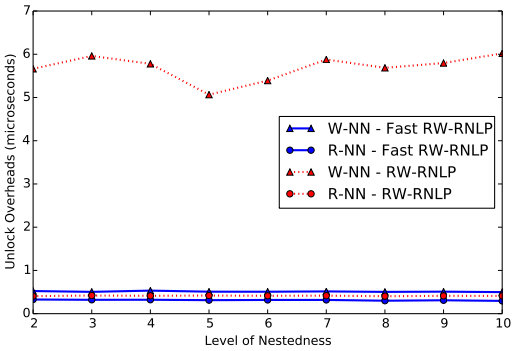

(b) Unlock overhead.

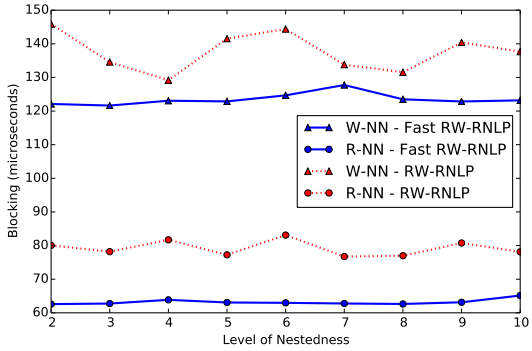

(c) Blocking.

Figure 515: (a) Lock and (b) unlock overheads and (c) blocking for non-nested read and write requests under the RW-RNLP and the fast RW-RNLP. Here, for each request $\mathcal{R}_i$, $m = 36$, $L_i = 60\mu$s, $n_r = 64$, and $|D_i|$ is as shown. Each request was randomly chosen to be a read (as opposed to a write) with probability 0.8 and to be a nested request with probability 0.

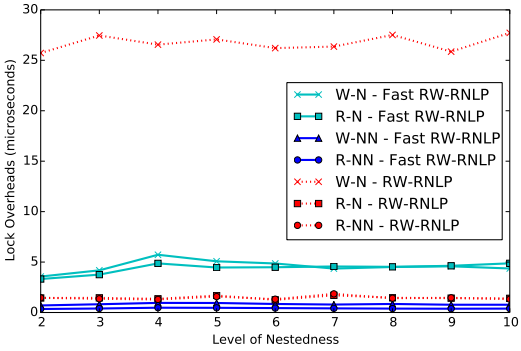

(a) Lock overhead.

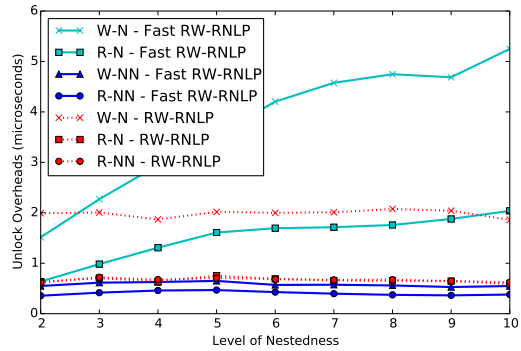

(b) Unlock overhead.

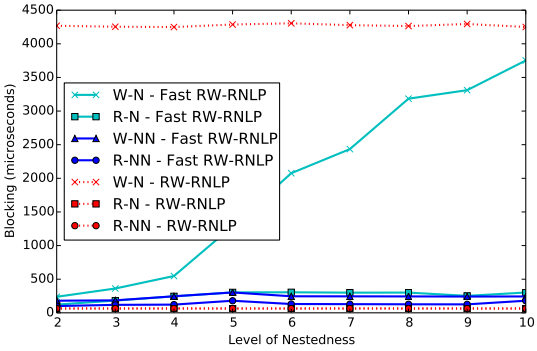

(c) Blocking.

Figure 516: (a) Lock and (b) unlock overheads and (c) blocking for nested and non-nested read and write requests under the RW-RNLP and the fast RW-RNLP. Here, for each request $\mathcal{R}_i$, $m = 36$, $L_i = 60\mu$s, $n_r = 64$, and $|D_i|$ is as shown. Each request was randomly chosen to be a read (as opposed to a write) with probability 0.8 and to be a nested request with probability 0.2. Due to write expansion, $|D_i|$ was inflated to 64 for all write requests under the RW-RNLP, as read requests can access any resource.

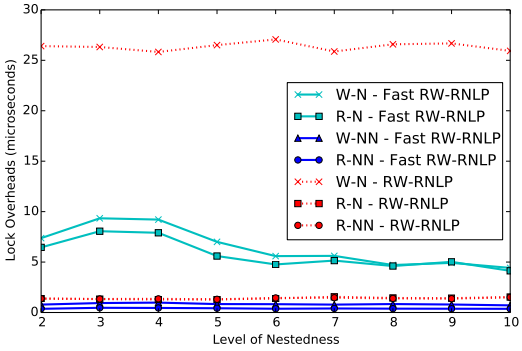

(a) Lock overhead.

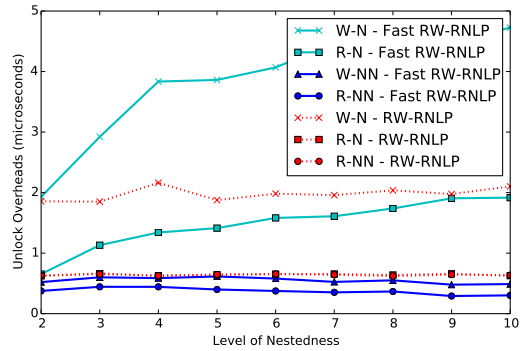

(b) Unlock overhead.

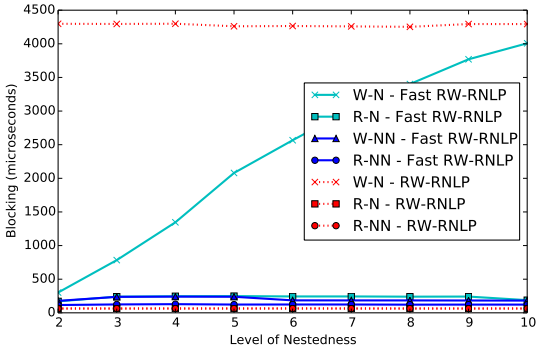

(c) Blocking.

Figure 517: (a) Lock and (b) unlock overheads and (c) blocking for nested and non-nested read and write requests under the RW-RNLP and the fast RW-RNLP. Here, for each request $\mathcal{R}_i$, $m = 36$, $L_i = 60\mu$s, $n_r = 64$, and $|D_i|$ is as shown. Each request was randomly chosen to be a read (as opposed to a write) with probability 0.8 and to be a nested request with probability 0.5. Due to write expansion, $|D_i|$ was inflated to 64 for all write requests under the RW-RNLP, as read requests can access any resource.

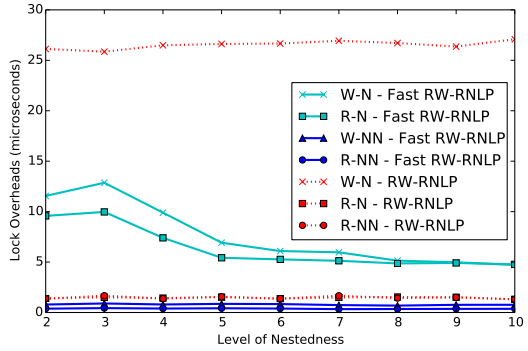

(a) Lock overhead.

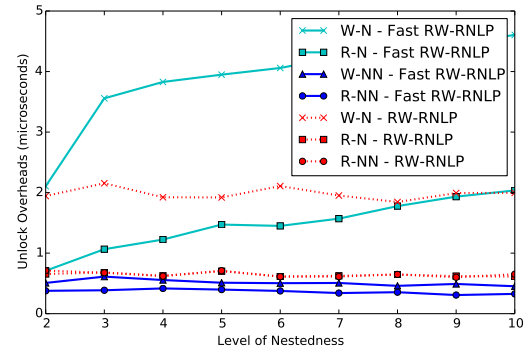

(b) Unlock overhead.

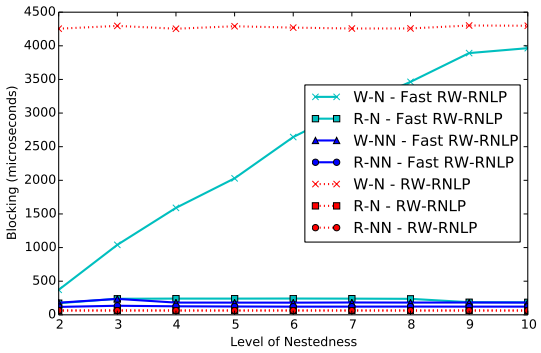

(c) Blocking.

Figure 518: (a) Lock and (b) unlock overheads and (c) blocking for nested and non-nested read and write requests under the RW-RNLP and the fast RW-RNLP. Here, for each request $\mathcal{R}_i$, $m = 36$, $L_i = 60\mu$s, $n_r = 64$, and $|D_i|$ is as shown. Each request was randomly chosen to be a read (as opposed to a write) with probability 0.8 and to be a nested request with probability 0.8. Due to write expansion, $|D_i|$ was inflated to 64 for all write requests under the RW-RNLP, as read requests can access any resource.

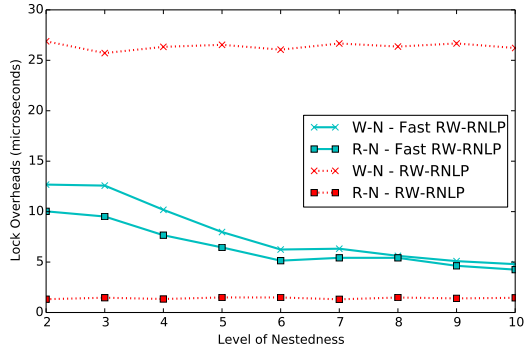

(a) Lock overhead.

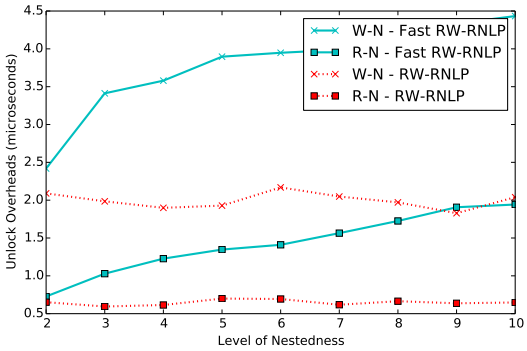

(b) Unlock overhead.

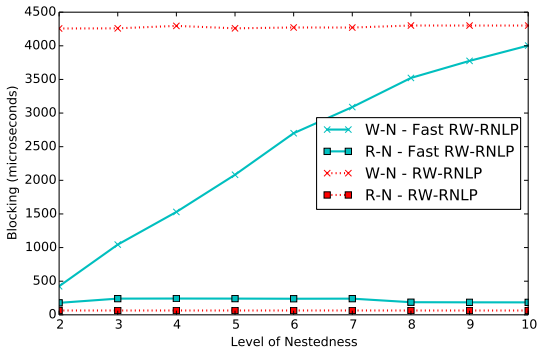

(c) Blocking.

Figure 519: (a) Lock and (b) unlock overheads and (c) blocking for nested read and write requests under the RW-RNLP and the fast RW-RNLP. Here, for each request $\mathcal{R}_i$, $m = 36$, $L_i = 60\mu$s, $n_r = 64$, and $|D_i|$ is as shown. Each request was randomly chosen to be a read (as opposed to a write) with probability 0.8 and to be a nested request with probability 1. Due to write expansion, $|D_i|$ was inflated to 64 for all write requests under the RW-RNLP, as read requests can access any resource.

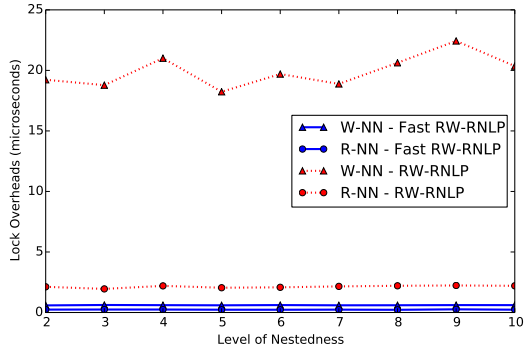

(a) Lock overhead.

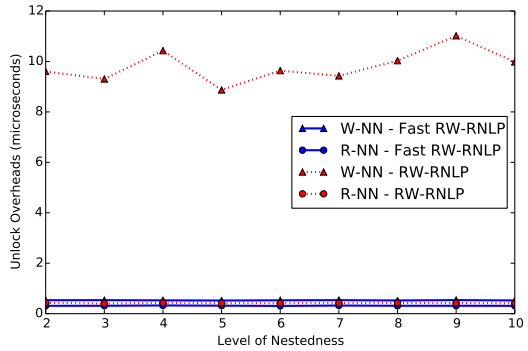

(b) Unlock overhead.

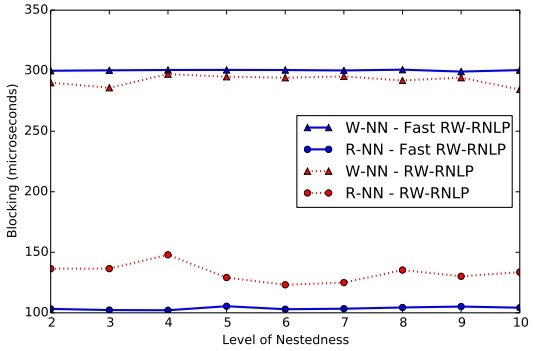

(c) Blocking.

Figure 520: (a) Lock and (b) unlock overheads and (c) blocking for non-nested read and write requests under the RW-RNLP and the fast RW-RNLP. Here, for each request $\mathcal{R}_i$, $m = 36$, $L_i = 100\mu$s, $n_r = 64$, and $|D_i|$ is as shown. Each request was randomly chosen to be a read (as opposed to a write) with probability 0.2 and to be a nested request with probability 0.

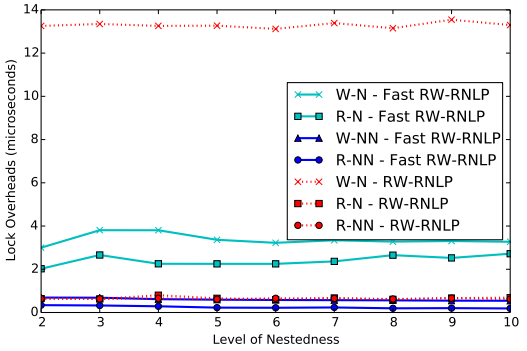

(a) Lock overhead.

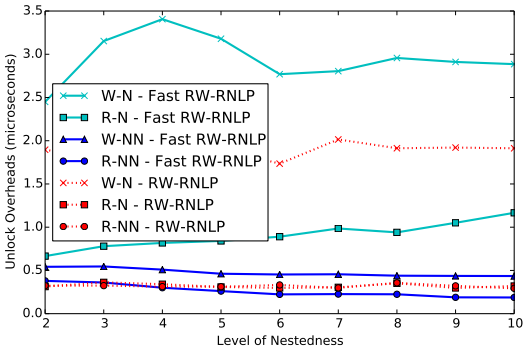

(b) Unlock overhead.

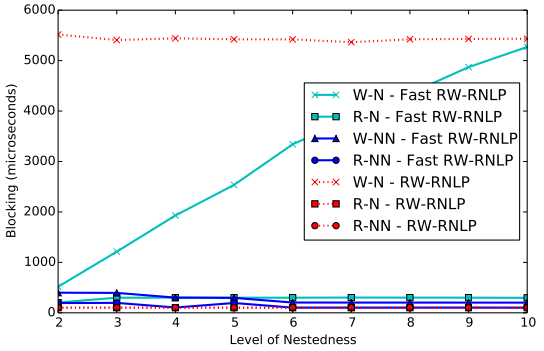

(c) Blocking.

Figure 521: (a) Lock and (b) unlock overheads and (c) blocking for nested and non-nested read and write requests under the RW-RNLP and the fast RW-RNLP. Here, for each request $\mathcal{R}_i$, $m = 36$, $L_i = 100\mu$s, $n_r = 64$, and $|D_i|$ is as shown. Each request was randomly chosen to be a read (as opposed to a write) with probability 0.2 and to be a nested request with probability 0.2. Due to write expansion, $|D_i|$ was inflated to 64 for all write requests under the RW-RNLP, as read requests can access any resource.

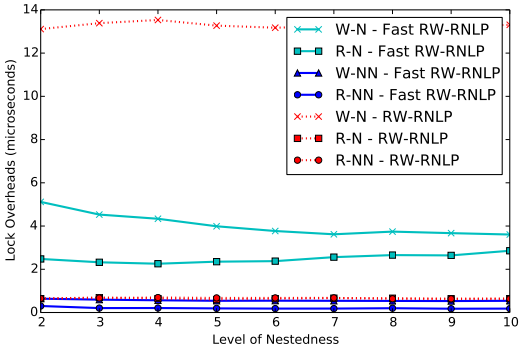

(a) Lock overhead.

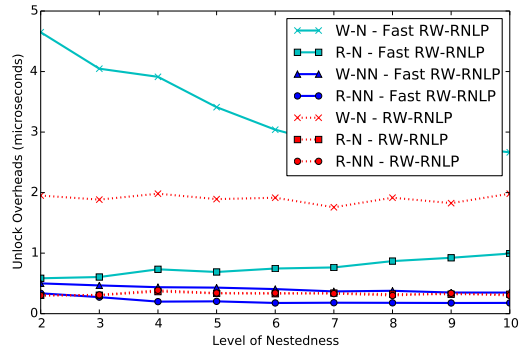

(b) Unlock overhead.

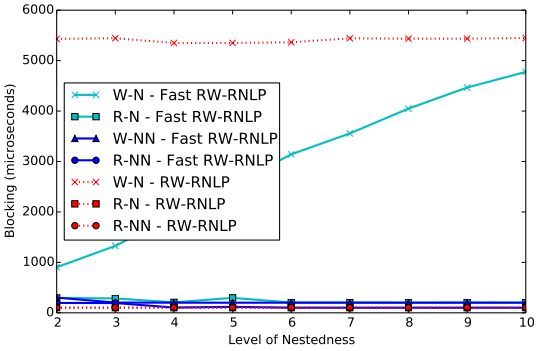

(c) Blocking.

Figure 522: (a) Lock and (b) unlock overheads and (c) blocking for nested and non-nested read and write requests under the RW-RNLP and the fast RW-RNLP. Here, for each request $\mathcal{R}_i$, $m = 36$, $L_i = 100\mu$s, $n_r = 64$, and $|D_i|$ is as shown. Each request was randomly chosen to be a read (as opposed to a write) with probability 0.2 and to be a nested request with probability 0.5. Due to write expansion, $|D_i|$ was inflated to 64 for all write requests under the RW-RNLP, as read requests can access any resource.

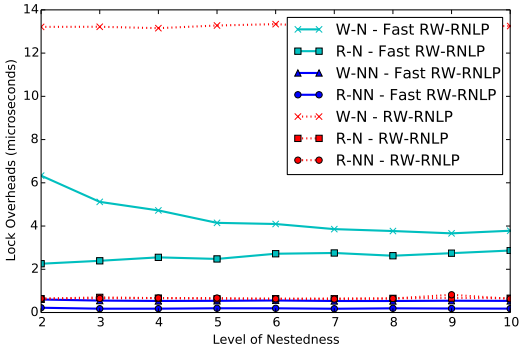

(a) Lock overhead.

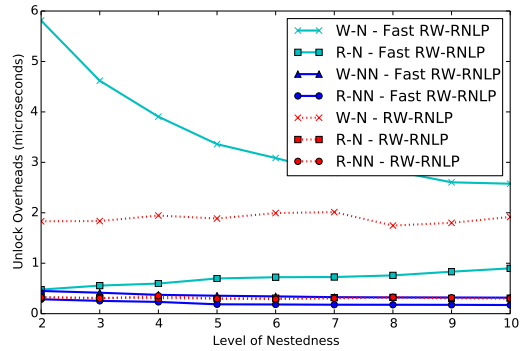

(b) Unlock overhead.

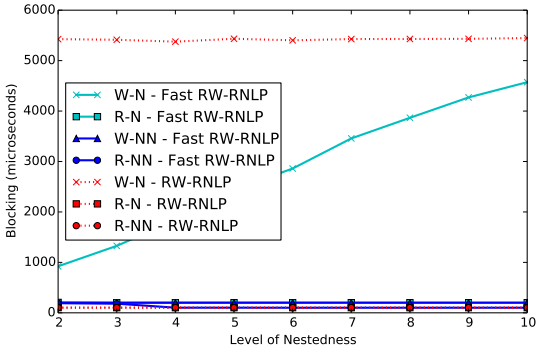

(c) Blocking.

Figure 523: (a) Lock and (b) unlock overheads and (c) blocking for nested and non-nested read and write requests under the RW-RNLP and the fast RW-RNLP. Here, for each request $\mathcal{R}_i$, $m = 36$, $L_i = 100\mu$s, $n_r = 64$, and $|D_i|$ is as shown. Each request was randomly chosen to be a read (as opposed to a write) with probability 0.2 and to be a nested request with probability 0.8. Due to write expansion, $|D_i|$ was inflated to 64 for all write requests under the RW-RNLP, as read requests can access any resource.

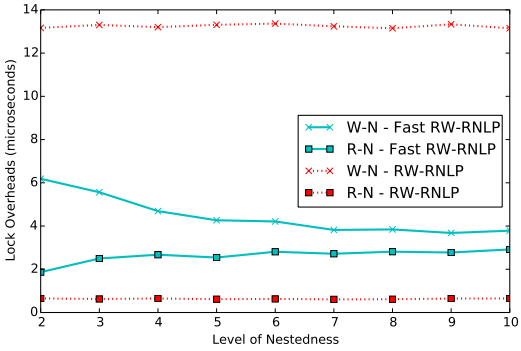

(a) Lock overhead.

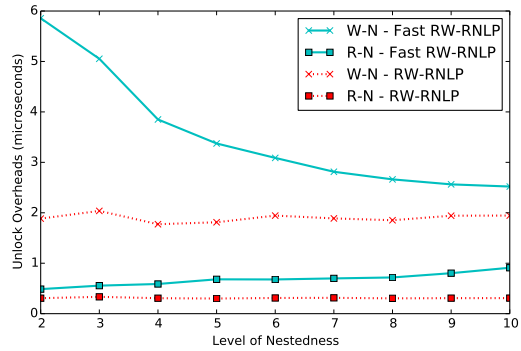

(b) Unlock overhead.

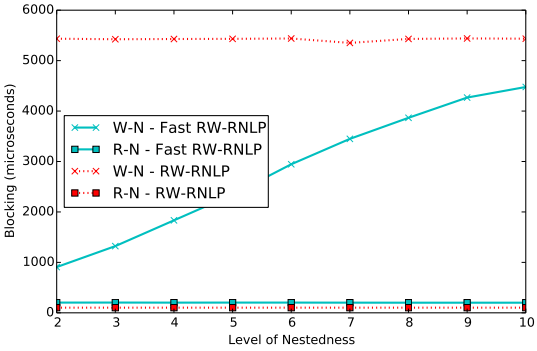

(c) Blocking.

Figure 524: (a) Lock and (b) unlock overheads and (c) blocking for nested read and write requests under the RW-RNLP and the fast RW-RNLP. Here, for each request $\mathcal{R}_i$, $m = 36$, $L_i = 100\mu$s, $n_r = 64$, and $|D_i|$ is as shown. Each request was randomly chosen to be a read (as opposed to a write) with probability 0.2 and to be a nested request with probability 1. Due to write expansion, $|D_i|$ was inflated to 64 for all write requests under the RW-RNLP, as read requests can access any resource.

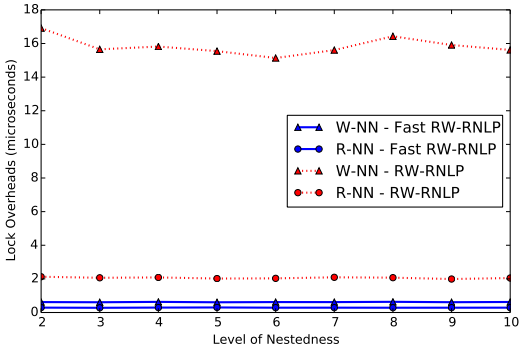

(a) Lock overhead.

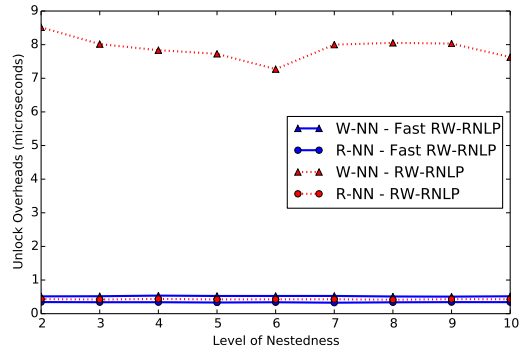

(b) Unlock overhead.

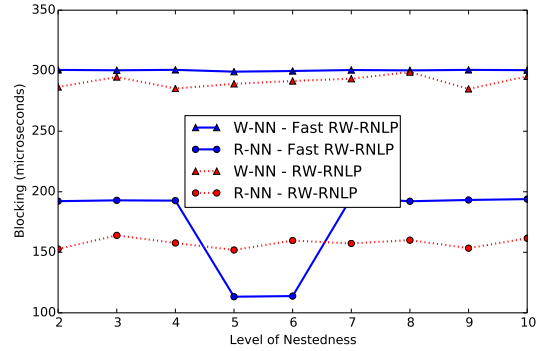

(c) Blocking.

Figure 525: (a) Lock and (b) unlock overheads and (c) blocking for non-nested read and write requests under the RW-RNLP and the fast RW-RNLP. Here, for each request $\mathcal{R}_i$, $m = 36$, $L_i = 100\mu$s, $n_r = 64$, and $|D_i|$ is as shown. Each request was randomly chosen to be a read (as opposed to a write) with probability 0.5 and to be a nested request with probability 0.

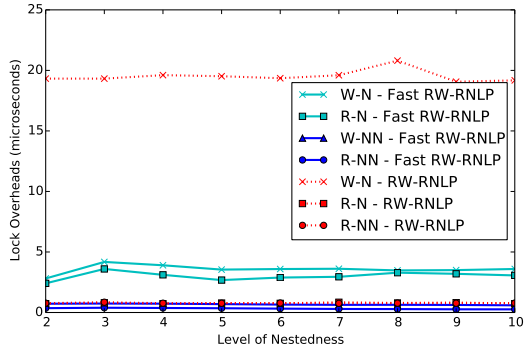

(a) Lock overhead.

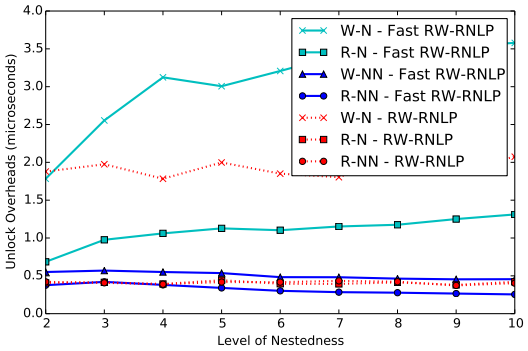

(b) Unlock overhead.

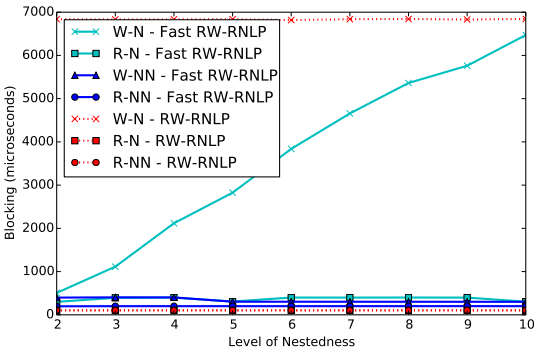

(c) Blocking.

Figure 526: (a) Lock and (b) unlock overheads and (c) blocking for nested and non-nested read and write requests under the RW-RNLP and the fast RW-RNLP. Here, for each request $\mathcal{R}_i$, $m = 36$, $L_i = 100\mu$s, $n_r = 64$, and $|D_i|$ is as shown. Each request was randomly chosen to be a read (as opposed to a write) with probability 0.5 and to be a nested request with probability 0.2. Due to write expansion, $|D_i|$ was inflated to 64 for all write requests under the RW-RNLP, as read requests can access any resource.

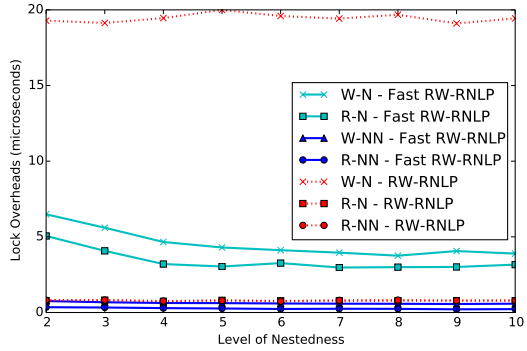

(a) Lock overhead.

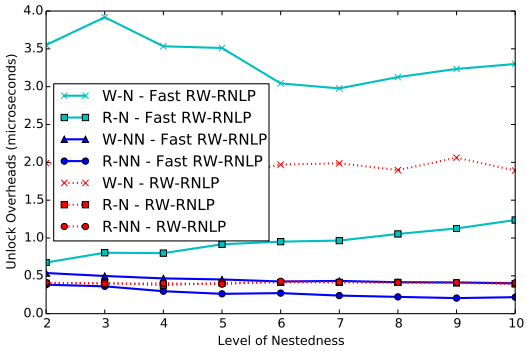

(b) Unlock overhead.

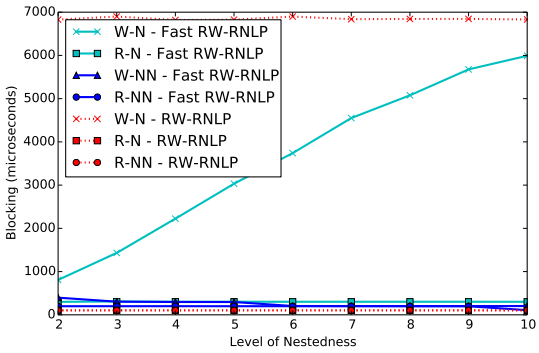

(c) Blocking.

Figure 527: (a) Lock and (b) unlock overheads and (c) blocking for nested and non-nested read and write requests under the RW-RNLP and the fast RW-RNLP. Here, for each request $\mathcal{R}_i$, $m = 36$, $L_i = 100\mu$s, $n_r = 64$, and $|D_i|$ is as shown. Each request was randomly chosen to be a read (as opposed to a write) with probability 0.5 and to be a nested request with probability 0.5. Due to write expansion, $|D_i|$ was inflated to 64 for all write requests under the RW-RNLP, as read requests can access any resource.

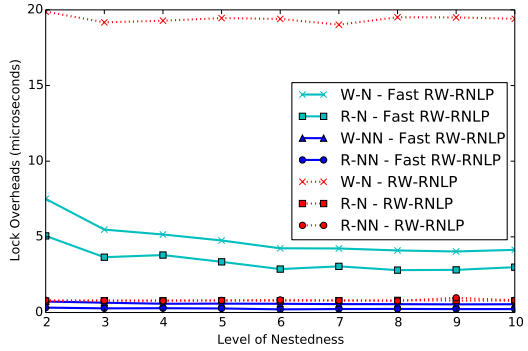

(a) Lock overhead.

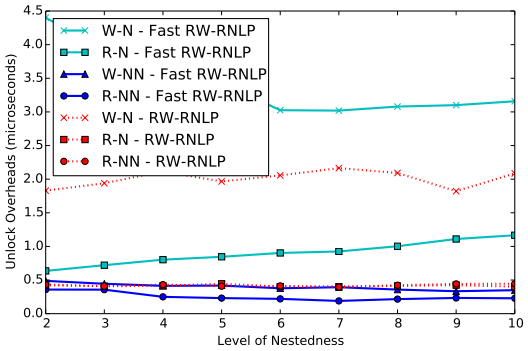

(b) Unlock overhead.

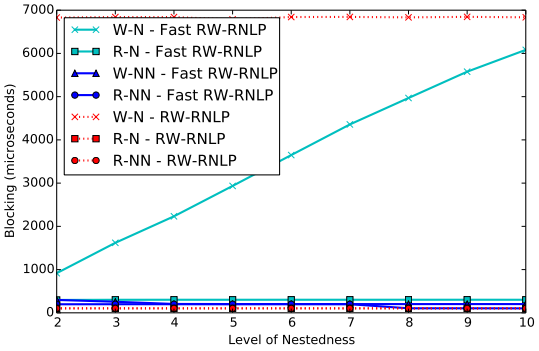

(c) Blocking.

Figure 528: (a) Lock and (b) unlock overheads and (c) blocking for nested and non-nested read and write requests under the RW-RNLP and the fast RW-RNLP. Here, for each request $\mathcal{R}_i$, $m = 36$, $L_i = 100\mu$s, $n_r = 64$, and $|D_i|$ is as shown. Each request was randomly chosen to be a read (as opposed to a write) with probability 0.5 and to be a nested request with probability 0.8. Due to write expansion, $|D_i|$ was inflated to 64 for all write requests under the RW-RNLP, as read requests can access any resource.

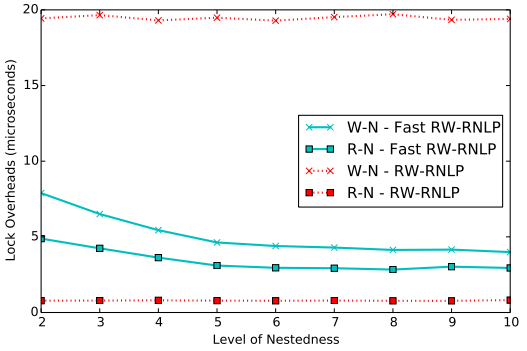

(a) Lock overhead.

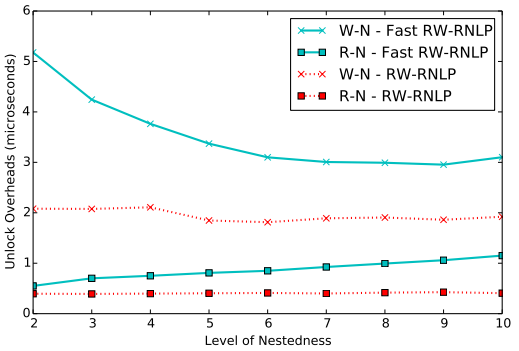

(b) Unlock overhead.

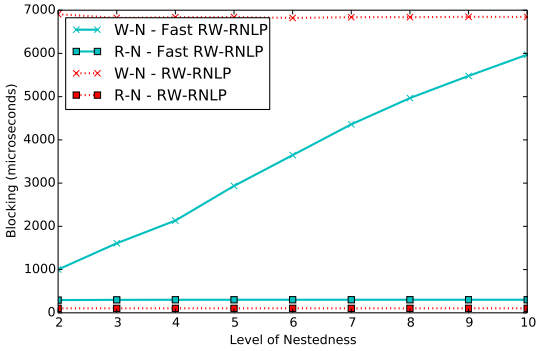

(c) Blocking.

Figure 529: (a) Lock and (b) unlock overheads and (c) blocking for nested read and write requests under the RW-RNLP and the fast RW-RNLP. Here, for each request $\mathcal{R}_i$, $m = 36$, $L_i = 100\mu$s, $n_r = 64$, and $|D_i|$ is as shown. Each request was randomly chosen to be a read (as opposed to a write) with probability 0.5 and to be a nested request with probability 1. Due to write expansion, $|D_i|$ was inflated to 64 for all write requests under the RW-RNLP, as read requests can access any resource.

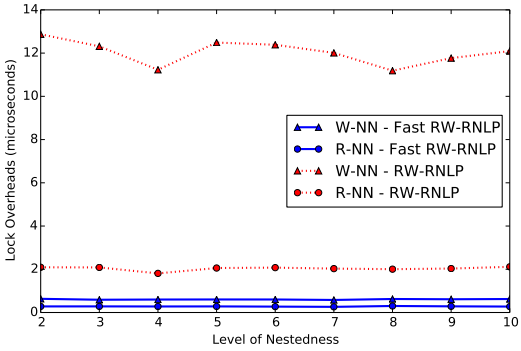

(a) Lock overhead.

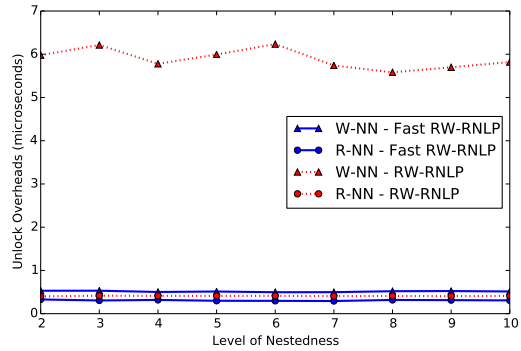

(b) Unlock overhead.

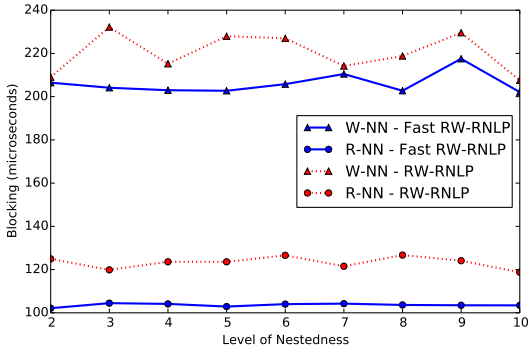

(c) Blocking.

Figure 530: (a) Lock and (b) unlock overheads and (c) blocking for non-nested read and write requests under the RW-RNLP and the fast RW-RNLP. Here, for each request $\mathcal{R}_i$, $m = 36$, $L_i = 100\mu$s, $n_r = 64$, and $|D_i|$ is as shown. Each request was randomly chosen to be a read (as opposed to a write) with probability 0.8 and to be a nested request with probability 0.

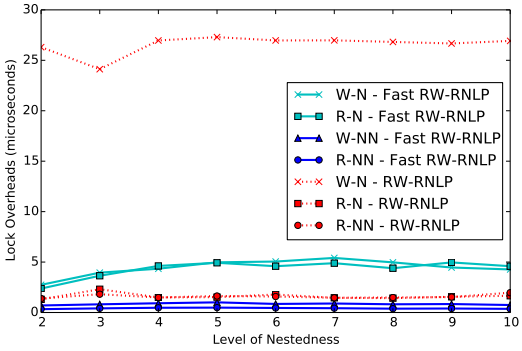

(a) Lock overhead.

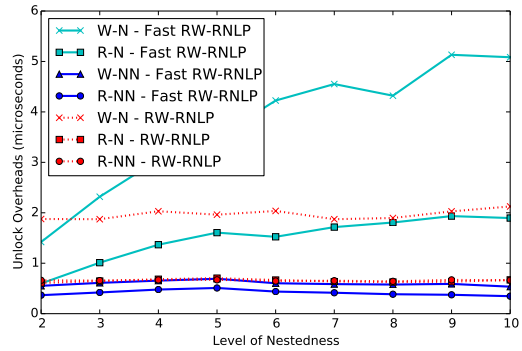

(b) Unlock overhead.

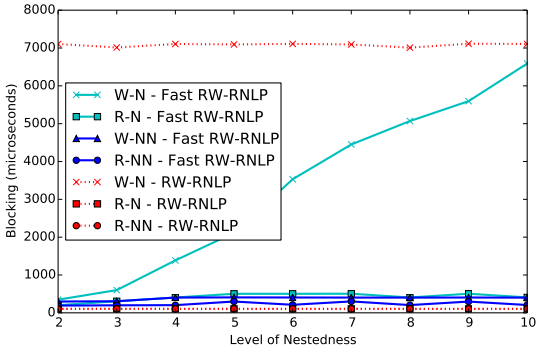

(c) Blocking.

Figure 531: (a) Lock and (b) unlock overheads and (c) blocking for nested and non-nested read and write requests under the RW-RNLP and the fast RW-RNLP. Here, for each request $\mathcal{R}_i$, $m = 36$, $L_i = 100\mu$s, $n_r = 64$, and $|D_i|$ is as shown. Each request was randomly chosen to be a read (as opposed to a write) with probability 0.8 and to be a nested request with probability 0.2. Due to write expansion, $|D_i|$ was inflated to 64 for all write requests under the RW-RNLP, as read requests can access any resource.

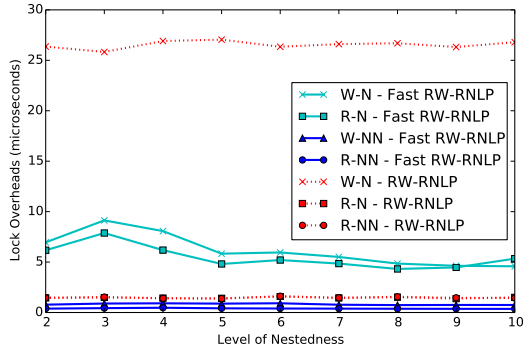

(a) Lock overhead.

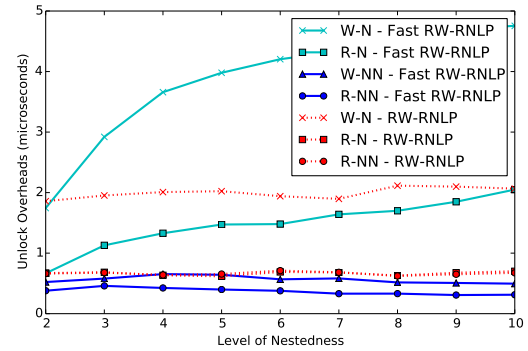

(b) Unlock overhead.

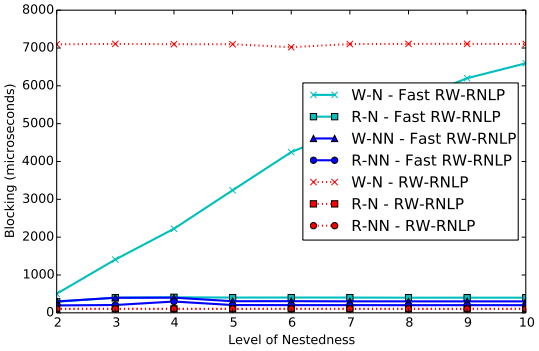

(c) Blocking.

Figure 532: (a) Lock and (b) unlock overheads and (c) blocking for nested and non-nested read and write requests under the RW-RNLP and the fast RW-RNLP. Here, for each request $\mathcal{R}_i$, $m = 36$, $L_i = 100\mu$s, $n_r = 64$, and $|D_i|$ is as shown. Each request was randomly chosen to be a read (as opposed to a write) with probability 0.8 and to be a nested request with probability 0.5. Due to write expansion, $|D_i|$ was inflated to 64 for all write requests under the RW-RNLP, as read requests can access any resource.

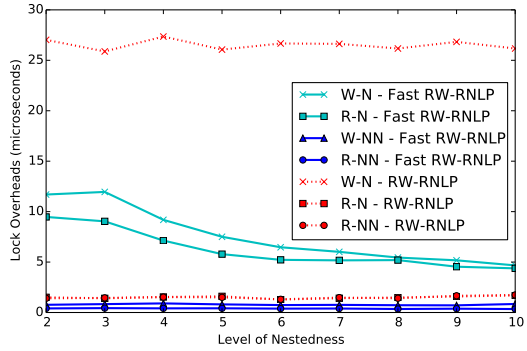

(a) Lock overhead.

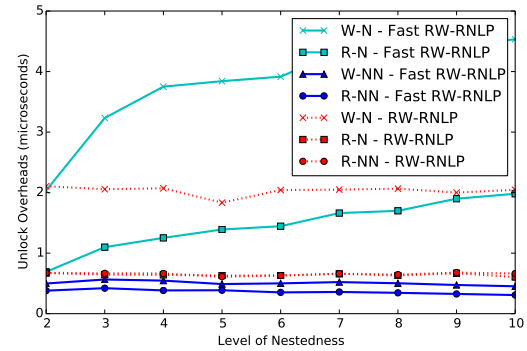

(b) Unlock overhead.

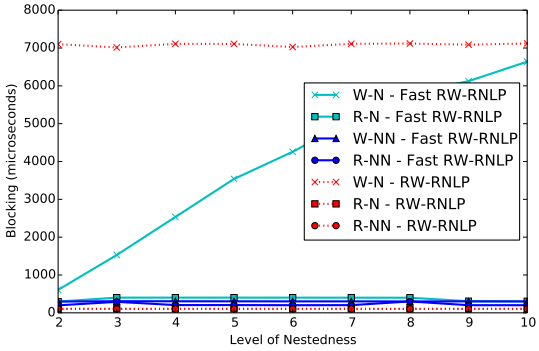

(c) Blocking.

Figure 533: (a) Lock and (b) unlock overheads and (c) blocking for nested and non-nested read and write requests under the RW-RNLP and the fast RW-RNLP. Here, for each request $\mathcal{R}_i$, $m = 36$, $L_i = 100\mu$s, $n_r = 64$, and $|D_i|$ is as shown. Each request was randomly chosen to be a read (as opposed to a write) with probability 0.8 and to be a nested request with probability 0.8. Due to write expansion, $|D_i|$ was inflated to 64 for all write requests under the RW-RNLP, as read requests can access any resource.

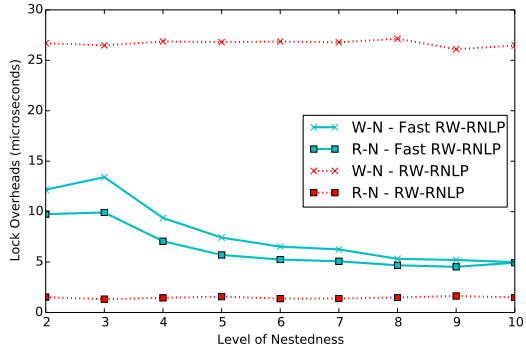

(a) Lock overhead.

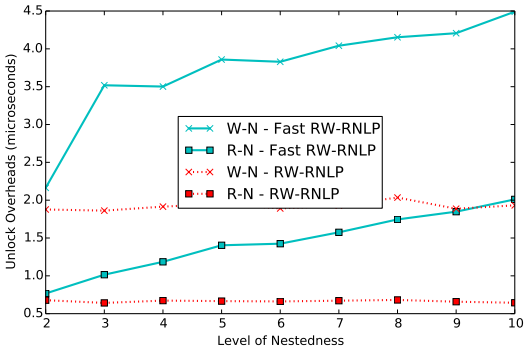

(b) Unlock overhead.

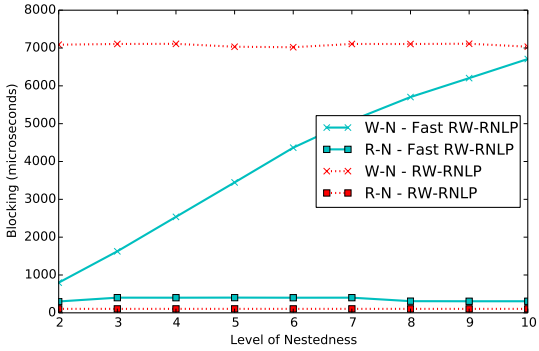

(c) Blocking.

Figure 534: (a) Lock and (b) unlock overheads and (c) blocking for nested read and write requests under the RW-RNLP and the fast RW-RNLP. Here, for each request $\mathcal{R}_i$, $m = 36$, $L_i = 100\mu$s, $n_r = 64$, and $|D_i|$ is as shown. Each request was randomly chosen to be a read (as opposed to a write) with probability 0.8 and to be a nested request with probability 1. Due to write expansion, $|D_i|$ was inflated to 64 for all write requests under the RW-RNLP, as read requests can access any resource.